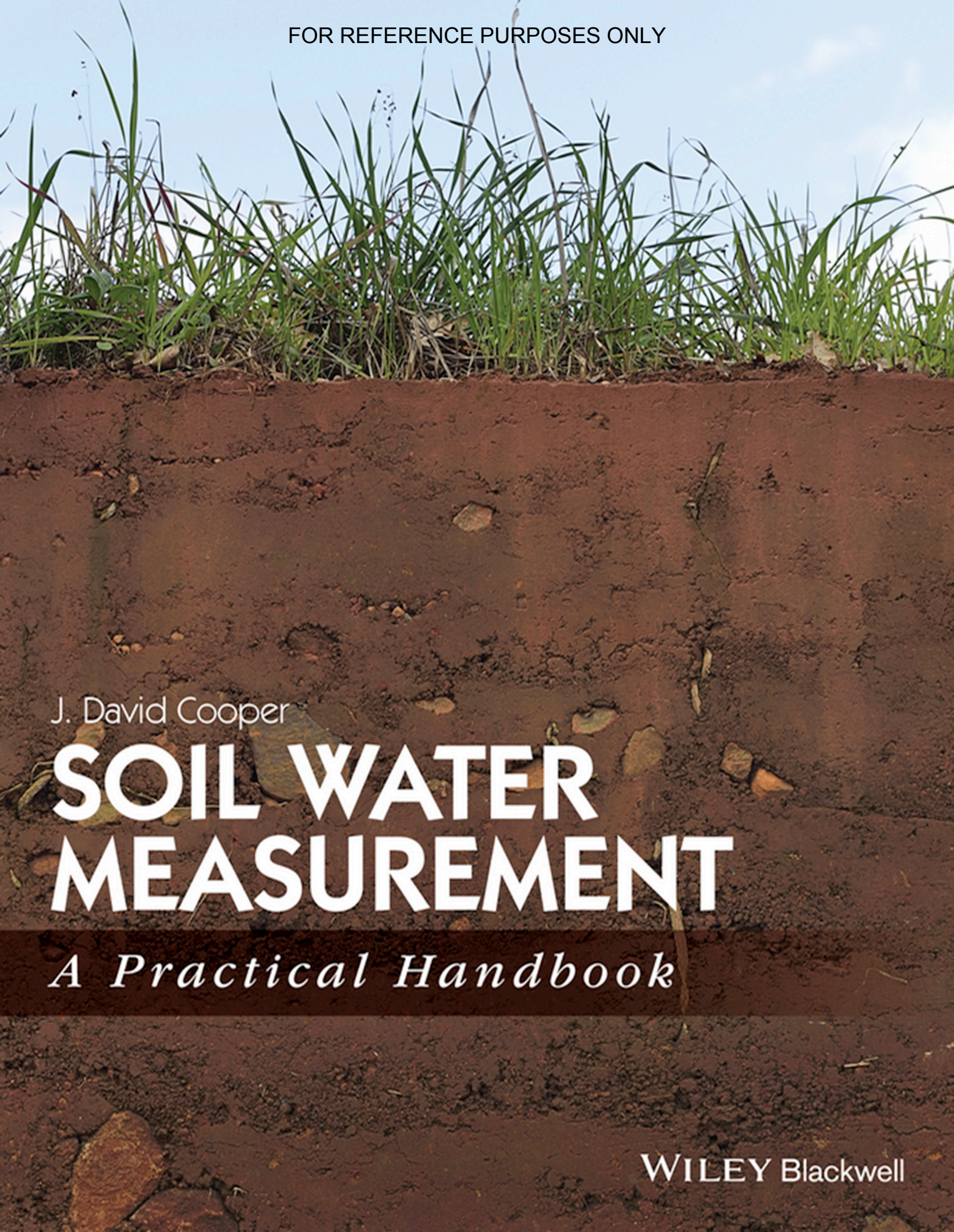

J. David Cooper

SOIL WATER MEASUREMENT

A Practical Handbook

WILEY Blackwell

SOIL WATER MEASUREMENT

Don't think, try the experiment
John Hunter, 1728–1793

I love deadlines. I love the whooshing noise they make as they go by
Douglas Adams 1952–2001

Soil Water Measurement

A Practical Handbook

J. David Cooper
Former Head of Soil Physics Group and Instrument Group
Centre for Ecology and Hydrology
Wallingford, UK

Research Fellow
University of Brighton
Brighton, UK

With a contribution from Richard H. Cuenca
Professor Emeritus
Department of Biological and Ecological Engineering
Oregon State University
Corvallis, OR, USA

WILEY Blackwell

This edition first published 2016 © 2016 by John Wiley & Sons, Ltd

Registered Office
John Wiley & Sons, Ltd, The Atrium, Southern Gate, Chichester, West Sussex, PO19 8SQ, UK

Editorial Offices
9600 Garsington Road, Oxford, OX4 2DQ, UK
The Atrium, Southern Gate, Chichester, West Sussex, PO19 8SQ, UK
111 River Street, Hoboken, NJ 07030-5774, USA

For details of our global editorial offices, for customer services and for information about how to apply for permission to reuse the copyright material in this book please see our website at www.wiley.com/wiley-blackwell.

Library of Congress Cataloging-in-Publication Data

Names: Cooper, David, 1946– author.
Title: Soil water measurement : a practical handbook / David Cooper.
Description: Hoboken, NJ : John Wiley & Sons, 2016. | Includes bibliographical references and index.
Identifiers: LCCN 2015034625 | ISBN 9781405176767 (cloth)
Subjects: LCSH: Soil moisture–Measurement–Handbooks, manuals, etc.
Classification: LCC S594 .C67 2016 | DDC 631.4/32–dc23 LC record available at http://lccn.loc.gov/2015034625

A catalogue record for this book is available from the British Library.

Wiley also publishes its books in a variety of electronic formats. Some content that appears in print may not be available in electronic books.

Cover image: © David Malan/GettyImages

Set in 9/11.5 TrumpMediaeval by SPi Global, Pondicherry, India

1 2016

Contents

Preface

The principal motivation for writing this book is that for over 35 years of measuring water in soil, I had not come across a book that brought together in one place the principles of operation of all the important methods and instruments available, together with their methods of use. This book aims to correct that.

The secondary motivation is that writing this book is a kind of penance for not having completed a PhD and written too few papers while I was working at the Institute of Hydrology/Centre for Ecology & Hydrology.

With a long career in the subject, I am indebted to many more people than there is space to identify here. It would be bordering on criminal, however, not to mention some of the more prominent ones. The late Jim McCulloch and John Bell must take pride of place for taking the chance on employing me over other, no doubt well-qualified, aspirants for a job in the Soil Physics Section of the rapidly expanding Institute of Hydrology and for guiding me towards a satisfying career in the underground. Other sometime colleagues at the Institute who both taught and helped me well beyond the call of duty include (in no particular order) the late Steve Wellings, the late Sam Boyle, Phil Holdsworth, Gareth Roberts, Richard Raynor, Paul Rosier, Cate Gardner, Alan Warwick, Ned Hewitt, Roger Wyatt, the late Pete Andrews, Jim Wallace, Atul Haria, Andy Dixon, the late Brian Smith, Tony Debney, the late Ian Calder, John Bromley, Ragab Ragab, Liz Morris, Keith Beven, Peter Germann, Jim Shuttleworth, the late John Stewart, Colin Lloyd, David Robinson, Brenda Burton, the late John Roberts, Jimmy Blackie, the late Tony Edwards, Tom Dean, Dave McNeil, Dave Harris, Richard Cross and Geoff Wicks. In the British Geological Survey, I enjoyed fruitful collaborations with David Kinniburgh, Helen Rutter, David Buckley, Brian Adams, Stephen Foster and Mike Edmunds. Outside these two organisations, David Fourt, Edward Youngs, Peter Leeds-Harrison, Declan Barraclough, Chris Young, Andree Carter, Tim Atkinson, Joseph Oisebe, Samson, Donald Laycock, Caleb Othieno, Val Mercer, John Smith, Georges Vachaud, Michel Vauclin and Tim Burt have been most helpful. Adrian Smith and Dee Galliford of the CEH library have been most helpful in providing access to both old and recent literature.

In writing this book, as well as several of those mentioned above, discussions with Gaylon Campbell, David Young and Mark Robinson have been fruitful. Aside from reviewing the early part of the manuscript, Richard Cuenca alerted me to and kindly contributed a section on COSMOS. Long-suffering staff at Wiley, particularly Kelvin Matthews, Ian Francis and Delia Sandford, have been immensely patient over my frequent missing of deadlines.

None of any of this would have been possible without the support and encouragement of my family, particularly my wife, Sue, who put up with my frequent absences working in various parts of the UK and abroad while being left to bring up six children and who has had to forego several years of my "retirement" while preparing this book.

To all of the above, my everlasting thanks.

J. David Cooper
Ewelme
Oxfordshire

Part I Introduction

1 Soil Water in Context

The interactions between water and soil are, arguably, the most fundamental relationships in the terrestrial environment. They control, in combination with other agents, such as the weather and plants, the fate of water after it falls as rain. This, in turn, determines aquifer recharge, river flow, water availability to crops and pasture for animals and the transport of nutrients and pollutants. These are critical in determining water resources, flooding, food production, the potability of water, ecology and public health. In view of these important roles, there has been and continues to be a great deal of scientific effort expended in understanding soil–water relationships. Nevertheless, many soil water specialists feel that the value of this work is not fully recognised and is underfunded by comparison with many other environmental topics. The reasons for this may include the fact that several aspects of the subject run counter to most people's intuition, that work in the field is physically hard and frequently messy, that little spectacular equipment or results are involved and that the subject rarely offers good photo opportunities.

The applications of soil physics are principally in the fields of agriculture, environmental protection and water resources. Some of the more common uses are:

- Measuring or estimating the soil bearing capacity to support agricultural operations
- Characterising the soil water status at various stages of crop growth
- Estimating irrigation requirements
- Optimising the quantity and timing of fertiliser or pesticide applications
- Estimating the water consumption of crops and other land covers
- Estimating the recharge of water to aquifers
- Estimating the rate at which pollutants travel through the unsaturated zone to groundwater bodies or watercourses
- Forecasting and mitigating the hazards of floods

Serious study of the physics involved in the relations between water and soil started in the early 20th century in the United States, driven by the need to increase food production for a rapidly expanding population. Later, important centres of research developed in the Netherlands, Australia, Israel and the United Kingdom. The motivation was usually to increase agricultural yields, focussed either on irrigation in arid areas or land drainage in humid and low-lying ones. From the 1970s, environmental concerns have accounted for an increasing proportion of the research effort, focussing on flood generation, pollution of rivers and aquifers from both natural and artificial sources, water resources assessment and effects on biodiversity. This has taken the subject into the area between what would normally be regarded as 'soil' and the zone of saturated rock, which is the province of hydrogeologists. This is often referred to as the vadose zone, particularly in America, although many hydrologists prefer to define the unsaturated zone as a composite of the soil and vadose zone. In this book, the term unsaturated zone will be used, recognising that there is, in reality, no neat subdivision between the soil, the underlying porous material of weathered or unweathered rock and, indeed, the saturated zone.

The amount of work on soil physics has produced a steady stream of books on the subject (e.g. Marshall *et al.*, 1996; Warrick, 2002, 2003; Hillel, 2004; Jury & Horton, 2004; Lal & Shukla, 2004; Rose, 2004). Some of these are highly mathematical and theoretical, while others attempt to explain the principles in relatively simple language. Few of them contain much detail explaining how it is actually *done*. There are also several books dealing with measurement methods and principles. Pride of place should probably go to the encyclopaedic work of Dane and Topp (2002), one of a series of books on all aspects of soil measurement. Over some 300 pages, it explains the principles behind most methods of soil water measurement, as well as having sections on all manner of other physical measurements in the soil. In similar mode is Mullins and Smith's (2001) book, focussed more specifically on soil water. While giving comprehensive coverage of the principles of measurement, both books tend to lack information on the practicalities of making measurements in frequently imperfect conditions. The book closest in

Soil Water Measurement: A Practical Handbook, First Edition. J. David Cooper.

spirit to the present one is that of Dirksen (1999). This book is intended to update and extend the contents of Dirksen (1999); to explain without descent into hand-waving argument, but using no more mathematics than necessary, the principles of operation of the most common instruments and methods of water measurement in the unsaturated zone and to give as much practical guidance as possible on using the methods in real-life situations. The emphasis is firmly on techniques for use in the field. Much useful research has been conducted on real and artificial soils in the laboratory, and the discovery of some principles of soil water behaviour would not have been possible without laboratory measurements. The author is not, for instance, aware of any convincing demonstration of the applicability of Darcy's law to unsaturated field soils. However, in almost all cases, laboratory measurements are intended to mimic field conditions and be applicable to that situation. It is the contention of this book that, for all the difficulties caused by distance, the weather, mud, stones, communications, power supply, spatial variability, animals and vandalism, field measurements are the final arbiter of research and monitoring work on soil–water interactions.

The limitations imposed by the nature of soil and the difficulties just mentioned mean that the accuracy achievable in any measurement is usually at best modest and in some cases extremely poor by most standards. It may come as a shock to some that, when we can measure the distance to the moon to a few cm and the value of some fundamental constants to 1 part in 10^{12}, we often do well to achieve a measurement accuracy of soil water content better than 5% by volume. It is, however, also true that astrophysicists are often happy to get within a few orders of magnitude of the 'true' figure, so soil physicists are, at least, somewhere in between. The modest level of accuracy achievable usually makes it unnecessary to take into account quantities like the variation of density of water with temperature and small variations of the acceleration due to gravity from one place to another. These will be assumed equal to 1000 $\mathrm{kg\,m^{-3}}$ and $9.8\ \mathrm{m\,s^{-2}}$, respectively, throughout this text. The reader should, however, be aware that there are circumstances when such imprecision is not warranted, although such instances in soil physics are extremely rare.

With large increases in computer power and its availability over the last few decades, numerical modelling of ever more complex environmental systems has achieved great prominence. Additionally, many of the methods described in the later chapters of this book would not be practical without the availability of cheap computer power, whether for measurement of soil hydraulic properties by inverse methods, for statistical evaluation of data collected, for controlling the recording and storage of field data automatically or for incorporation into instruments to perform the calculations which turn an electrical signal into a meaningful quantity. The Internet is making large databases of soil properties and much other environmental information available to researchers and decision makers worldwide. So whether derived from the modeller's own or their colleagues' observations, or from elsewhere, a wealth of data is easily available, although its quality may be difficult to assess.

This book is not, however, about modelling, except in so far as it can be used to help interpret experiments, but the use of soil water measurements as input to a variety of models in environmental science, management of water resources, agriculture and ecology cannot be ignored. Measurements are important for modelling of environmental systems in several ways:

- To provide a description of the properties of the various components of the system, such as soil water characteristics and hydraulic conductivity of the soil.
- To supply data to drive the model, for instance, rainfall and other meteorological information.
- To *validate* the model and evaluate how well it reproduces the observed behaviour of the system. The more aspects of the system that are successfully reproduced by a model, the more confidence can be placed in its ability to predict events, either in the future or at locations where monitoring is absent.

A prominent omission from the methods described later is that of remote sensing. I felt that not only am I not sufficiently qualified to deal with the subject adequately but also that the topic would need too much space in the present volume. There are, in any case, several good books on this rapidly developing subject that repetition here would be superfluous.

All fields of human endeavour tend to develop a language to refer to peculiar aspects of the field. This is often perceived (and sometimes intended) to exclude those outside the field from entering it. I have tried to avoid the use of this jargon, but where it would not be practical to do so, I have put the first use of such a term in italics and defined its meaning. In other cases, I have provided a definition of common jargon words in the hope that readers will be able to understand the works of others more easily.

1.1 What Is Soil Water?

At first sight, the concept of soil water seems very easy to define. However, closer inspection reveals a number of unexpected complications. These have all to do with variable interactions between the water and the substances comprising the soil. In essence, the difficulty is in knowing where physical interactions stop and chemical ones begin. Many substances common in soils bind more or less strongly to water molecules. At one end of the scale, water molecules may be held in the soil by forces sufficiently weak that the water is easily removed and its physical properties are hardly different from those of water in bulk. At the other end, water may be so tightly bound that temperatures in excess of 400°C are needed to remove it. Many clay minerals are able to accommodate layers of water molecules between and on the surface of aluminosilicate sheets. These forms of behaviour not only complicate the

assessment of whether the water is part of the soil fabric or not, but also different measurement methods respond differently with that water, making intercomparison between methods complex and difficult.

Much has been and continues to be written on this subject. While there is a real philosophical difficulty in deciding what constitutes water and what is part of the soil fabric, it is only when this 'in-between' water plays a part in some of the interactions we are studying that it becomes of practical importance. In this book, we will take a pragmatic approach. Unless there are strong reasons to consider the behaviour of 'bound' water separately, no distinction will be made between water held by capillary forces and that where chemical interactions are important.

2 How Does Water in Soil Interact with the Soil Matrix, Air, Roots, Gravity and Other Substances Present?

There are several excellent textbooks describing at various levels the concepts and practice of soil physics. The aim of this book is not to rival those. However, it is important to review the essential features to ensure that there is a common set of concepts and nomenclature and hence avoid confusion with other works which use different terminology.

2.1 Static Properties of Soil Water

The behaviour of water in the soil is generally dominated by its interaction with the surfaces that it comes into contact with. These are usually the surfaces of soil particles or pores in rock. Most often, there is an attractive force between the water molecules and the surface, which leads to an energy reduction as water is taken up by the soil. To get a picture of how this works, the pores of the material are often likened to a capillary tube, as in Fig. 2.1.

The pressure change across the interface between the water and air in a tube of radius r is

$$P = -\frac{2\gamma}{r}\cos\phi \qquad (2.1.1)$$

where

P is the pressure difference;

γ is the surface tension between water and air (about 7.3×10^{-2} N m^{-1});

r is the radius of the tube, and

ϕ is the angle at which the water surface meets the tube wall.

This is known as the angle of contact and is a measure of the attraction between the water molecules and the material of the tube wall. The negative sign indicates that the pressure in the water is usually lower than that in the air, and consequently the water will rise up a capillary tube until the weight of the water column balances the pressure reduction.

Most materials have a strong attraction for water molecules, and this is often so great that the contact angle is very close to zero. Under these circumstances, cos ϕ is equal to 1 and so Equation 2.1.1 reduces to

$$P = -\frac{2\gamma}{r}. \qquad (2.1.2)$$

Equations 2.1.1 and 2.1.2 show that as the radius of the tube decreases, that is, as soil pores become smaller, the pressure becomes more negative. This corresponds to a suction exerted by the soil on the water. The greatest suction is exerted by the smallest pores, so that, as water enters a dry soil, it enters the smallest pores first, leaving the larger ones empty. In a small volume, all the water must be at the same pressure; otherwise, it will move from one set of pores to another. As a result, high levels of suction (low pressure) are associated with low water contents held in the smallest pores, while smaller suctions (higher pressure) are linked with greater water contents, as progressively larger pores fill. Emptying of soil pores occurs in the reverse manner. The water held in the large pores can be removed most easily while the pressure is relatively high (although still below that of the atmosphere). To remove more, ever greater suctions must be exerted on the soil water to empty progressively smaller pores. There is, therefore, a relationship between the water content of the soil and the suction with which it is held. This is called the *soil water characteristic* (see Section 2.1.2) and is determined by the distribution of pore sizes within the soil.

The preceding description gives a relatively simple picture of the manner in which water is held in the soil. It is clear that, as the water content falls, the amount of suction which needs to be applied increases and corresponds with the everyday experience that plant roots have increasing difficulty in extracting water from the soil as it dries. It is not, however, the whole story.

Firstly, a straight capillary tube is only a very rough approximation to a soil pore, which normally has a very irregular shape. Nevertheless, it allows us to visualise in a qualitative way what happens inside many soils and has been used as the basis for numerous models of soil water behaviour.

Soil Water Measurement: A Practical Handbook, First Edition. J. David Cooper.

Fig. 2.1 An idealised cylindrical pore.

Secondly, water is held in the soil not only by capillary forces in tube-like structures but also as thin films on the surface of larger pores and particles.

Thirdly, some minerals are able to hold water by physico-chemical processes. Gypsum (calcium sulphate), for instance, binds weakly to water molecules. The water can be driven off by heating to moderate temperature. In most cases, this water does not participate in soil processes, but it may be measured as part of the water in the soil using the methods described in Part II. Clays, however, are the most common minerals which bind more or less weakly to water molecules. Clays are composed of layers of molecules, bound to one another by weak electrostatic forces, known as *van der Waals forces*, which affect the distribution of electric charge. In effect, a clay platelet is covered by a small negative charge, with a slight excess of positive charge inside. Water molecules, although electrically neutral, do not have a uniform distribution of charge and may be thought of as having one end slightly positively charged, with the other negatively so. This is called an *electrical dipole*. The positively charged end is attracted to the negative charge on the clay platelet surface. The effect is enhanced by the fact that the lattice structure of many clays is similar to that of common forms of ice, so the water molecules are able to settle snugly onto the clay surface in a way that not only takes advantage of the forces between the water molecules and the clay mineral but also between the water molecules themselves. In some clay minerals (e.g. bentonite or montmorillonite), the van der Waals forces holding the layers together are so weak that they can be parted very easily and a layer of water molecules, taking advantage of the similarity in lattice structure between the clay and ice, can enter (*intercalate*) inside the clay platelet. The dipoles of the water molecules shield the clay layers from one another electrically, so that once one layer has intercalated, others can do so with increasing ease. As more and more water molecules force the clay layers apart, so the platelets expand and cause the entire soil matrix to expand. Conversely, as the soil dries, the soil matrix contracts, giving rise to cracks in the soil. Some cracking under dry conditions is very common. However, some soils crack to an extreme degree, with large cracks of several centimetres width, extending to 2 or 3 m depth. These are called *vertisols*. Cracks in soils form an important class of *macropore*, which often have a profound influence on water movement within the soil (Section 2.3.2).

Fourthly, pressures less than absolute zero are predicted by Equation 2.1.2 for a tube radius, r, of less than about 1.5 μm. While there may be some difficulty in envisaging how this situation can exist, soils certainly behave as if it does, and conditions equivalent to water pressures lower than −6 MPa (−60 bars) have been measured.

Fifthly, some soil materials are water-repellent. In this case, ϕ is greater than 90°, cos ϕ is negative, and P becomes positive, that is, a positive pressure is needed to force the water into the soil. Water-repellent soils do not readily soak up water as a result, although water normally enters after a few minutes of contact. Water repellency is believed to be an important trigger for *fingering* behaviour (see Section 2.3.2).

2.1.1 Soil water potential

The previous discussion has been conducted in terms of water pressure or suction in the soil relative to atmosphere. Much of the early literature in soil physics used this concept, and the terms 'soil water suction' and 'tension' are often used today. However, it is now more usual to use the term 'soil water potential', often shortened to 'water potential' or even 'potential', to reflect the fact that while it is often convenient to think of water held in soil as subject to a physical suction, that is not always the case. More importantly, the simple physical interaction between the soil water and the soil matrix is only one factor affecting its state and behaviour. For the rest of this book, therefore, the concept of soil water potential will be used.

Soil water potential is defined as the amount of energy per unit quantity of water required to transfer, reversibly and isothermally, an infinitesimal amount of water from a pool of pure, free water at a reference location and at the prevailing atmospheric pressure into the soil at the specified position. This is a difficult statement to get to grips with. It may be easier to think of the reverse process, the amount of energy per unit quantity of water needed to extract an infinitesimal amount of water from the soil and place it into a pool of pure water at a reference location and at atmospheric pressure. Since we specified that the process should be reversible, this is just the negative of the first statement.

Units

The earlier definition is in terms of energy per unit quantity of water. There are a number of choices possible for the 'unit quantity'. In most areas of science, the natural unit would be of mass, and in the SI system, this would mean a kilogram, so soil water potential would be expressed as joules per kilogram, or J kg^{-1}.

This is not, however, a very common way to express soil water potential, and partly for convenience and partly for historical reasons, one of two other units is normally used.

Table 2.1 Conversions between common units for expressing water potential

	J kg^{-1}	Pa	hPa	kPa	MPa	mbar	bar	mm H_2O	cm H_2O	m H_2O	in. H_2O	ft H_2O
J kg^{-1}	1	10^3	10	1	10^{-3}	10	10^{-2}	102	10.2	0.102	4.02	0.335
Pa	1×10^{-3}	1	10^{-2}	10^{-3}	10^{-6}	10^{-2}	10^{-5}	0.102	1.02×10^{-2}	1.02×10^{-4}	4.02×10^{-3}	3.35×10^{-4}
hPa	0.1	100	1	0.1	1×10^{-4}	1	1×10^{-3}	10.2	1.02	1.02×10^{-2}	0.402	3.35×10^{-2}
kPa	1	1×10^3	10	1	1×10^{-3}	10	1×10^{-2}	102	10.2	0.102	4.02	0.335
MPa	1×10^3	1×10^6	1×10^4	1×10^3	1	1×10^4	10	1.02×10^5	1.02×10^4	102	4.02×10^3	335
mbar	0.1	100	1	0.1	1×10^{-4}	1	1×10^{-3}	10.2	1.02	1.02×10^{-2}	0.402	3.35×10^{-2}
bar	100	1×10^5	1×10^3	100	0.1	1×10^3	1	1.02×10^4	1.02×10^3	10.2	402	33.5
mm H_2O	9.8×10^{-3}	9.8	9.8×10^{-2}	9.8×10^{-3}	9.8×10^{-6}	9.8×10^{-2}	9.8×10^{-5}	1	0.1	1×10^{-3}	3.94×10^{-2}	3.28×10^{-3}
cm H_2O	9.8×10^{-2}	98	0.98	9.8×10^{-2}	9.8×10^{-5}	0.98	9.8×10^{-4}	10	1	1×10^{-2}	0.394	3.28×10^{-2}
m H_2O	9.8	9.8×10^3	98	9.8	9.8×10^{-3}	98	9.8×10^{-2}	10^3	100	1	39.4	3.28
in H_2O	0.249	249	2.49	0.249	2.49×10^{-4}	2.49	2.49×10^{-3}	25.4	2.54	2.54×10^{-2}	1	8.33×10^{-2}
ft H_2O	2.99	2.99×10^3	29.9	2.99	2.99×10^{-3}	29.9	2.99×10^{-2}	305	30.5	0.305	12	1

The horizontal rows show the equivalent potential for one unit at the left-hand end in units shown by the head of the column. For example, 1 J kg^{-1} is equivalent to 10^{-3} MPa or 4.02 in. of water head.

One alternative quantity for the unit amount of water would be a unit volume (cubic metre – m^3). Since water is, to all intents and purposes, incompressible with a density, ρ_w, of close to 1000 kg m^{-3}, then this is completely equivalent to a mass definition, except that it involves the density of water, so that a volume, v, has a mass of $\rho_w v$. This way of calculating potential is not usually expressed as joules per cubic metre, or J m^{-3}, however. Energy can be defined as a force (dimensions of $[MLT^{-2}]$) multiplied by a distance (dimension [L]), and a volume has dimensions $[L^3]$; hence, energy per unit volume has units of force per unit area, which is a pressure (dimensions $[ML^{-1}T^{-2}]$). When talking about capillary forces holding water in soil, this is the same pressure (or suction) that was encountered in the previous section.

The other, and less immediately obvious, way to define a unit quantity is to use its weight. Weight is a force and, in SI units, expressed in newtons (N). A weight, w, results from a mass of w/g, where g is the acceleration due to gravity and sufficiently constant at about 9.8 m s^{-1} that no problems are likely be incurred. While choosing weight as the unit to define water potential may seem perverse, it is, in fact, very commonly used. The reason is that energy (or work) can be regarded as a force times a distance, while weight is a force. Therefore, energy per unit weight has dimensions of length. In fact, it is the height of a water column equivalent to the pressure when using the energy per unit volume definition. Using length units to define potential means that all the equations which mix gravity, suction and other forces do not involve either the density of the water or the acceleration due to gravity. The gravitational force on a weight, w, of water is simply w, whereas for a mass, m, it is mg and for a volume, v, it is $v\rho_w g$. For this reason, length or 'head' units will be used in this book.

All three definitions of the unit quantity may be encountered, so that it is worth knowing their relationship to one another. The usual symbol to express soil water potential is ψ. We will use a leading subscript m for mass, v for volume and w for weight to denote these three.

Then

$$ {}_w\psi = \frac{m\psi}{g} = \frac{v\psi}{\rho_w g}. \qquad (2.1.3) $$

In this book, SI units will be used throughout, but these relations hold for any *coherent* set of units, that is, where all quantities are based on the same basic units, so that cm, g, ergs, dynes and μbar (dynes cm^{-2}) would be equally suitable units defined similarly to SI.

Table 2.1 shows conversions between commonly used units of water potential.

Meaning of the definition

An infinitesimal amount of water is specified because removing any significant quantity will alter the state of the system. If a very small amount of water in relation to that already there is added to or removed from the system and the energy change is divided by that very small amount, then the change will be in terms of a unit quantity.

Next, we need to think of the energy needed to remove the water from the soil. This was discussed earlier in terms of suction and pressure forces. To convert this to an energy, note that a suction pressure of h will support a water column of height h.

The energy, E, needed to lift a small weight, w, of water up this height is given by

$$ E = wh. \qquad (2.1.4) $$

Dividing through by the weight of water, w, to obtain energy per unit weight,

$$ \frac{E}{w} = h. \qquad (2.1.5) $$

But the potential is the negative of this, as the definition requires water to be put *into* the soil:

$$ \psi_m = -\frac{E}{w} = -h. \qquad (2.1.6) $$

ψ_m is usually referred to as the *matric potential* of the soil water, since it arises from the interaction between the water and the soil matrix.

In the saturated zone, the pressure is always positive. If there is no confining layer, this is usually equal or close to the depth below the water table. There is, therefore, continuity between the matric potential in the unsaturated zone and the (positive) head of water in the saturated zone, and there is no need to regard these two zones separately. In fact, the water table or *phreatic surface* is defined as the point at which the head is zero.

Returning now to the definition of the potential, the next thing to consider is that the water must be moved from its position in the soil to the reference location. This is normally a convenient position that we can use to compare the potential at different places. It is often taken as the soil surface, although sometimes it is more useful to use the water table (however, complications arise if this moves), mean sea level or an impermeable layer beneath the soil. On sloping ground things may become more complicated. As long as the position is fixed, it does not matter too much, since mostly we are concerned with differences of water potential between one place and another, so that the actual height of the reference location does not enter into this. In this book we will always use the local soil surface as the reference location.

The energy required to lift the water through a height h was calculated in Equation 2.1.4. Using z to denote the depth in the soil, the energy required to lift the water through this distance per unit weight is

$$ \frac{E}{wg} = \frac{wz}{w} = z. \qquad (2.1.7) $$

The potential, ψ_g, is the negative of this, since the definition requires water to be put into the soil:

$$\psi_g = -E = -z. \quad (2.1.8)$$

ψ_g is known as the *gravitational potential* because it describes the work done against gravity.

Next, the definition stipulates that the water from the soil has to be placed into a pool of pure water. The soil water may be better named soil solution, as it almost always contains solutes of some kind. To separate out these solutes and recover pure water requires energy. This energy is expressed in the term *osmotic potential*, ψ_s, and is related to the osmotic pressure between a solution and pure water separated by a semipermeable membrane. Once again, osmotic potential is a negative quantity, as energy is required to reverse the process of dissolving solute in the water.

The definition requires that the reference pool be at atmospheric pressure. The air in soil is usually at atmospheric pressure. Under these circumstances, there is no additional contribution to the potential. This is not always true, for instance, when there is a layer of saturated material separating the point of interest from the surface or where there may be sources of gas within the porous body, for instance, methane generation in a wetland or landfill. The matric potential is the part of the potential caused by the difference in pressure of the soil solution from the local atmosphere. If the gas-phase pressure in the soil is different from that at the surface, then an additional term is required to account for this and to bring the total potential of the soil water back to that of water at atmospheric pressure at the reference point. The magnitude of this term in head units is equal to the difference in pressure between that of the soil air and atmospheric pressure at the reference point. This term is called the *gas pressure potential*, ψ_a.

In some cases, the soil matrix may not be sufficiently rigid to support all of the weight of the overlying material. These are usually swelling soils, where the soil surface may go up and down as water content changes. In such cases, a part of the weight of this overburden is transmitted to the water in the soil, which helps to support that weight. Therefore, in some soils an *overburden potential*, ψ_o, can be identified as contributing to the overall water potential. We will not be much concerned with the overburden potential in this book.

Having discussed all the contributions to the soil water potential, we can now put them together to obtain an overall value for the potential:

$$\psi = \psi_m + \psi_g + \psi_s + \psi_a + \psi_o. \quad (2.1.9)$$

Osmotic, gas and overburden potentials are only rarely of sufficient magnitude to make a material difference to soil water behaviour. Moreover, the most common instruments for measuring water potential, tensiometers (Chapter 12), do not respond to osmotic potential, but indicate the sum of matric, gravitational, gas and overburden potential, collectively called *hydraulic potential*, ψ_h. In most cases, we will be concerned only with matric and gravitational potential.

2.1.2 Soil water characteristic

As explained earlier, increasing difficulty is experienced in extracting water from the soil as it dries from saturation. We expect, therefore, that there is a relation between the soil water potential and its water content and that wet soil is associated with high (i.e. less negative) water potentials and dry soil with increasingly low (more negative) ones. Laboratory studies have shown that there is a threshold value, called the *air entry potential*, above which the soil remains saturated. This can be visualised as corresponding to the size of the largest pores in the soil, which require some energy to extract water from them. We would expect that fine-textured soils (those composed of small particles – silts and clays) would have small pores and hence retain more water at low water potentials than coarse-textured soils. Lastly, some soils have a much wider range of pore size (usually associated with a large particle size distribution, for instance, loams) than others. These will lose water over a much larger range of potential than those with a narrow range of pore size. Taking all these factors into account, we expect the relation to look somewhat like that depicted in Fig. 2.2 for a range of different soils. This relationship is called the *soil water characteristic*.

Unfortunately, this is not a unique relation for any particular soil. The main cause of this is *hysteresis*, which means that there is some kind of memory in the soil water system which causes more water to remain in the soil when the conditions change from wetting to drying. The

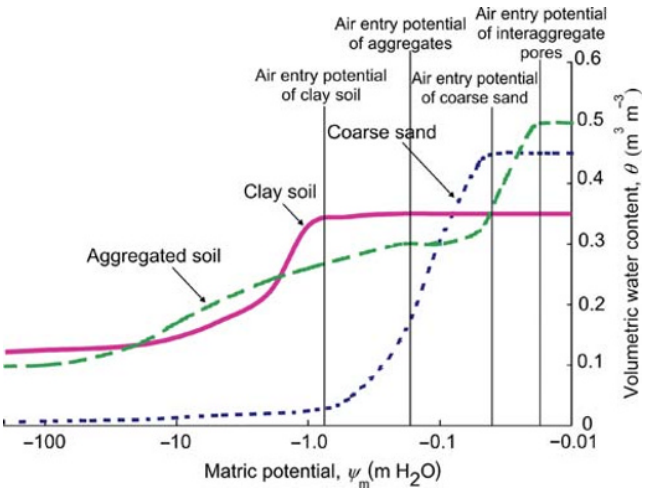

Fig. 2.2 Soil water characteristic curves for three different soils. (*See insert for colour representation of the figure.*)

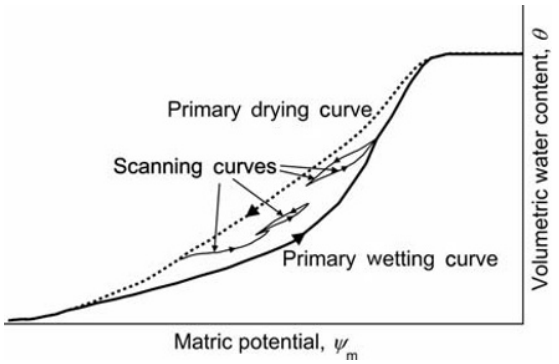

Fig. 2.3 Hysteresis in soil water characteristic.

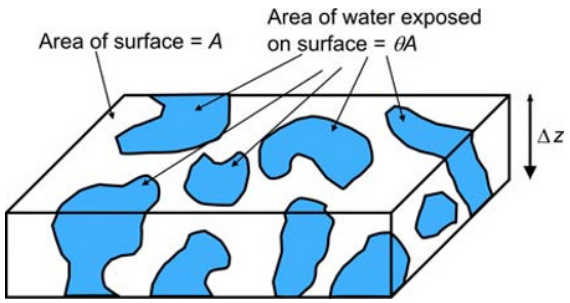

Fig. 2.4 Water-occupied areas on a slab of soil.

phenomenon is depicted in Fig. 2.3. The two outside curves are known as the *primary drying and wetting curves* and represent wetting from total dryness to saturation and back again. Usually, these are not the end points of the process in the field, and the behaviour follows intermediate *scanning curves*, which lie between the primary curves. Hysteresis is frequently ignored, mainly because of a lack of reliable data to characterise it, especially in field situations (see Section 15.5).

Intuitively, it seems reasonable that, after wetting the soil and reversing the process, the drying is likely to lag behind the wetting at the same water potential. Similarly, after drying the soil, the soil will remain drier at the same water potential as it did while wetting.

2.2 Dynamic Properties of Soil Water

The dynamic properties of soil water control the movement of water within the soil body.

2.2.1 Hydraulic conductivity

In most forms of transport, movement is caused by a force, which may be expressed as the gradient of potential energy. In the case of soil water, the forces are caused principally by gravity and matric potential, which, as explained in Section 2.1.1, may be thought of as a pressure. A volume of soil of area A and thickness Δz in the vertical direction with a volumetric water content of θ will contain water with a weight $\theta\rho_w g A \Delta z$. The pressure on the upper side of this volume will be $\psi_m(z)$ and that on the lower side is $\psi_m(z + \Delta z)$. This acts on an area of water equal to θA. The net force in the z direction is, therefore, $\theta A[\psi_m(z) - \psi_m(z + \Delta z)] + \theta\rho_w g A \Delta z$.

This is depicted in Fig. 2.4.

Darcy (1856) discovered that the rate of flow of water was proportional to this force in saturated porous media, where the water potential can be equated to a real pressure. Later, it was demonstrated that Darcy's law also holds under unsaturated conditions (Buckingham, 1907). If we write $\psi_m(z) - \psi_m(z + \Delta z)$ as $d\psi/dz\ \Delta z$, then Darcy's law can be written as

$$q = -K\frac{d\psi}{dz}, \qquad (2.2.1)$$

where q is the rate of water flow, taken as positive in the z direction.

The quantity, q, is a volume of water crossing an area, A, in a certain time, t. It therefore has dimensions of a volume [L^3] divided by an area [L^2], divided by time [T], which gives [LT^{-1}], which is the same as a velocity. For this reason, it is sometimes called the *Darcy velocity*. However, it is not the actual speed of water flow, which is, on average, equal to $q\theta$. Because we expect water to move faster in larger pores than in small ones, some of the water will be moving much faster than $q\theta$, while some will be moving much slower.

The constant of proportionality, K, is known as the *hydraulic conductivity*. Darcy's law is similar in many respects to other well-known laws of physics, in which the flow of some quantity is proportional to a gradient of a potential. Examples include Ohm's law, where current flow is proportional to electrical potential (voltage) gradient, and the law of heat conduction, in which the flow of heat is proportional to the gradient of temperature.

In most common situations, the constant of proportionality varies very little, if at all, with the other state variables. This makes it relatively easy to solve the governing equations, which are known as *linear equations*. In unsaturated materials, however, the hydraulic conductivity is strongly dependent on the water content. Because, as described previously, water content and water potential are linked, the unsaturated hydraulic conductivity is also strongly dependent on the water potential, and we also expect the relationship to be hysteretic. These complicate matters considerably and make the equations governing the behaviour of water in unsaturated porous materials highly *non-linear* and difficult to solve.

There are several reasons for this strong dependence of hydraulic conductivity on water content:

1 The area of water-filled space available to conduct flow reduces as the water content decreases.

2 To compound this, the water-filled pores reduce in size. Poiseuille's law states that flow rate reduces according to

the fourth power of the pore radius (or, approximately, as the fourth power of the matric potential).

3 Furthermore, the water-filled pathways become more convoluted or *tortuous*, so that the actual distance covered by a particle of water in getting from one point to another lengthens.

The result of these effects is that hydraulic conductivity covers a range of several orders of magnitude over the normal range of water content found under field conditions. This imposes severe constraints on the ability to measure the relationships between the variables of interest.

2.2.2 Equation of continuity

The equation of continuity is merely an expression of the principle of conservation of mass. In any volume of soil, the difference between the amount of water entering it and that leaving it must be equal to the rate of increase in water content, in the absence of any internal sources or sinks of water (e.g. roots). If we use the example of a thin slab of soil as earlier (Section 2.2.1), then if flow, q, is all in the vertical (z) direction, the amount of water entering it from the top is $Aq(z)$, while that leaving from the bottom is $Aq(z+\delta z)$, as shown in Fig. 2.5. The rate of increase in total water content, M, is, therefore,

$$\frac{\partial M}{\partial t} = Aq(z) - Aq(z+\delta z). \tag{2.2.2}$$

Now, M is equal to the volumetric water content, θ, multiplied by the volume of the slab, $A\delta z$, and $q(z+\delta z)$ may be written as $q(z) + \left(\frac{\partial q}{\partial z}\right)\delta z$. Then (2.2.2) becomes

$$A\delta z\frac{\partial \theta}{\partial t} = A\left(q(z) - q(z) - \frac{\partial q}{\partial z}\delta z\right), \tag{2.2.3}$$

which simplifies to

$$\frac{\partial \theta}{\partial t} = -\frac{\partial q}{\partial z}. \tag{2.2.4}$$

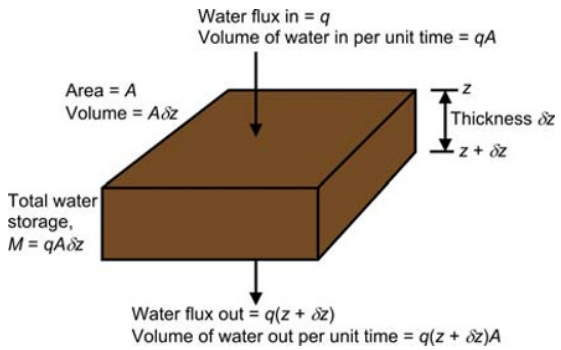

Fig. 2.5 Water entering and leaving a thin slab of soil.

The equation of continuity, therefore, relates the rate of change of water content at a point in the soil to the gradient of water flux. If the water flux increases downwards through the soil profile, then the water content must be decreasing. This may be understood intuitively. If the flow increases with depth, then the water to supply this must come from a reduction in the water content of the soil.

2.2.3 Richards equation

If we substitute q from Darcy's law, Equation 2.2.1, into the equation of continuity, Equation 2.2.4, then we obtain

$$\frac{\partial \theta}{\partial t} = -\frac{\partial}{\partial z}\left(-K\frac{\partial \psi}{\partial z}\right), \tag{2.2.5}$$

and if we write $\psi = \psi_m + \psi_g = \psi_m - z$, then we get

$$\frac{\partial \theta}{\partial t} = \frac{\partial}{\partial z}\left(K\left[\frac{\partial \psi_m}{\partial z} - 1\right]\right). \tag{2.2.6}$$

Equation 2.2.6 is known as the *Richards equation*, after L.A. Richards, who first derived it (Richards, 1931). It should be noted that it does not contain the water flux explicitly, but merely relates changes in water content to those of water potential.

2.2.4 Three-dimensional flow

For simplicity, the preceding discussion has been conducted in terms of one-dimensional (vertical) flow only. In many situations, this is perfectly adequate. Soil is, however, a three-dimensional body, and sometimes it is necessary to take horizontal movements into account, for instance, on hillslopes. Equations 2.2.1–2.2.6 are readily extended to the three-dimensional case, although their application may not be straightforward because gravity acts only in the z direction and many soils are anisotropic, with different hydraulic conductivity in different directions (usually horizontally and vertically).

2.3 Preferential Flow

The descriptions earlier suggest that the flow of water in soil is a regular, spatially uniform phenomenon, capable of neat encapsulation in a set of partial differential equations, and all that is necessary to understand soil–water interaction is an ability to solve these highly non-linear equations and a means of measuring the relevant physical properties of the soil. Solution of the equations is not straightforward, and much work has been and continues to be done on finding analytical and numerical methods of achieving this objective. It will be seen in Chapters 15–18 that measuring soil water properties is also difficult, particularly over an extended range of water status. Moreover, it turns out that water in soil often does not behave

in a way that allows it to be described as uniform. Several phenomena are responsible for this, which result in water moving up and down a soil profile very much faster in some places than in others. These come under a collective name of *preferential flow*. The importance of preferential flow has become increasingly recognised over the past three decades, and methods for describing it quantitatively at the field scale are emerging (Beven & Germann, 1982, 2013).

Although preferential flow is now known to be important in many situations, this does not completely invalidate approaches based on an assumption of a uniform medium. Preferential flow is usually an intermittent phenomenon, occurring most often under very wet conditions. For the rest of the time, the soil water system often behaves according to the more well-established principles embodied in the descriptions of Sections 2.2.1–2.2.3. Moreover, many useful and reliable applications of traditional soil water dynamics have been developed over several decades.

There are several different causes and mechanisms of preferential flow. The most important ones will be described briefly in the following.

2.3.1 Spatially variable infiltration

Infiltration of rain or irrigation water into the soil is affected by many factors. Among these are:

- *Surface cover*: Vegetation covering the ground helps shield the surface from the impact of raindrops. Where this is absent, compaction and/or sealing of the surface may occur, leading to locally reduced infiltration and runoff to other areas, where enhanced infiltration takes place.

The vegetation itself may modify the input of water to the surface. Trees, bushes and tall crops, such as maize, for instance, often channel water down their stems as *stemflow*, leading to enhanced infiltration close to the plant and consequently less elsewhere. The canopy of these plants also often modifies the input to the ground surface, as water runs on or off leaves, branches and stems to *drip points*.

- *Microtopography*: Small differences in elevation between points in an otherwise flat area can, under heavy rainfall or irrigation and, in some cases, snowmelt, cause water to run from higher places to lower ones, where it forms pools which subsequently infiltrate into the underlying soil. This is enhanced where the soil surface is hydrophobic or crusted. Schuh *et al.* (1993a, b) described in meticulous detail the degree of non-uniformity of infiltration caused by very small irregularities in the surface of a field in North Dakota.
- *Crusting*: The impact of raindrops in conjunction with the properties of the surface soil may cause the formation of a surface crust or seal, inhibiting the infiltration of water. Where the seal is broken or less effective, infiltration will be greater.

2.3.2 Non-uniform transport within the soil

- *Fingering*: Although not completely understood, fingering is a form of instability which may occur in uniform soil. It is most commonly encountered in dry, coarse-textured and hydrophobic soils; that is, in arid and semi-arid environments, and soils high in organic matter. It is closely related to the commonly observed phenomenon of a dense liquid overlying a less dense one in a jar. The dense liquid would, naturally, lie below the less dense one, and it achieves this by forming fingers, down which the dense liquid flows. In soil, a very similar behaviour is observed and wet pathways form, down which almost all of the water flows, leaving the soil between completely dry.
- *Macropores*: Macropore is a name given to a variety of different void structures encountered in the soil. The principal characteristics are that they are significantly larger than the majority of pores in the soil (usually several mm width or diameter but could be much smaller in fine-textured materials) and are usually continuous over distances of several dm, usually, but not always, in a direction close to vertical. Macropores include cracks in clay-rich soils; holes formed by worms, insects, rodents and other macrofauna; voids created by agricultural implements; and channels formed by roots, which often have decayed. The surface of the macropore may have a modified structure as a result of water running down it or be coated with organic substances or other material washed onto it. The macropore may also be partially or completely infilled with organic matter or other material originating from higher in the profile. Macropores are usually effective as conduits for water flow if they are exposed at or very close to the soil surface. Water flow within them occurs often as film flow, which requires a free water source. Where they are filled, matric potential must be high. For instance, a 1-mm-radius pore will empty at a matric potential of about –15 mm water.

3 What Do We Need to Measure?

Water content, water potential and hydraulic conductivity can be regarded as the basic variables governing the behaviour of water in soil. There are, however, combinations of these which are often more useful or which some methods yield directly. Additional information may be required to obtain estimates of the basic variables. The more important combination variables are described in this chapter.

3.1 Diffusivity

Water flows in soil in response to a potential gradient, and in many situations, the dominant gradient is that of matric potential. Combining this with the fact that there is a relationship between water potential and water content, it should be clear that, in a homogeneous soil, water flow can be thought of as occurring in response to a gradient of water content. In this case, the appropriate constant of proportionality is called the *diffusivity*, D, that is, in the absence of gravity:

$$q = -D\frac{\mathrm{d}\theta}{\mathrm{dx}}. \tag{3.1.1}$$

Comparing this with Equation 2.2.1, diffusivity is related to the basic variables by

$$D = K\frac{\mathrm{d}\psi_\mathrm{m}}{\mathrm{d}\theta}. \tag{3.1.2}$$

The inverse of the quantity $\mathrm{d}\psi_\mathrm{m}/\mathrm{d}\theta$ $(\mathrm{d}\theta/\mathrm{d}\psi_\mathrm{m})$ is called the *specific water content*. The concept of diffusivity is familiar in heat conduction situations, although usually both K and the slope of the heat content – temperature curve (the specific heat capacity) – are very nearly constant in that case, making diffusivity constant.

The Richards equation can be written in terms of diffusivity as

$$\frac{\partial\theta}{\partial t} = \frac{\partial}{\partial z}\left[D(\theta)\frac{\partial\theta}{\partial z}\right] - \frac{\mathrm{d}K}{\mathrm{d}\theta}\frac{\partial\theta}{\partial z}. \tag{3.1.3}$$

Diffusivity in the soil water sense is important for two basic reasons. One is that it varies considerably less over the range of soil water status normally encountered than does hydraulic conductivity, making its accurate measurement easier. Because of this, it reduces the non-linearity of the equations governing soil water dynamics, easing their solution. The other is that several methods for measurement of hydraulic properties yield diffusivity directly, rather than the basic properties. Set against these are limitations which result from ignoring hysteresis, gravity and spatial changes in hydraulic properties.

3.2 Matric Flux Potential

Matric flux potential is an integral hydraulic property, that is, it incorporates all the effects of soil wetting from a completely dry state to the wetness level of interest.

It is defined as

$$\phi(\psi_\mathrm{m}) = \int_{-\infty}^{\psi_\mathrm{m}} K(\psi_\mathrm{m})\mathrm{d}\psi_\mathrm{m} = \int_0^\theta D(\theta)\mathrm{d}\theta. \tag{3.2.1}$$

Like diffusivity, it has the advantage of varying much less than hydraulic conductivity, and some measurement methods yield its value directly.

3.3 Sorptivity

Sorptivity is a useful variable to describe the initial stages of wetting of soil from a dry state. It was introduced by Philip (1957), who showed that the early stages of soil wetting could be represented by a series expansion:

$$I = \int_0^t i\,\mathrm{d}t = St^{1/2} + A_2 t + A_3 t^{3/2} + \cdots + A_n t^{n/2} + \cdots \tag{3.3.1}$$

Soil Water Measurement: A Practical Handbook, First Edition. J. David Cooper.

where

S is the *sorptivity* and

the terms A_n are complex functions of the diffusivity, hydraulic conductivity, time and the distance from the surface to the wetting front

In the absence of gravity, that is, for horizontal infiltration, only the first term on the right-hand side of Equation 3.3.1 occurs:

$$I_{\text{horiz.}} = \int_0^t i_{\text{horiz.}}\,\mathrm{d}t = St^{1/2}. \qquad (3.3.2)$$

The early stages of wetting in the presence of gravity also approximate this behaviour and may persist for several hours in fine-textured soils.

Under these conditions, sorptivity is defined by

$$S = \int_{\theta_i}^{\theta_f} zt^{1/2}\mathrm{d}\theta. \qquad (3.3.3)$$

In this equation, the integration is made over the range between the initial and final water content, and $zt^{1/2}$ is the combination of depth, z, and square root of time, $t^{1/2}$, where the water content is equal to θ.

The terms involving A_n in Equation 3.1 are, essentially, corrections to account for gravity effects. By concentrating only on the early stages of infiltration, where gravity effects are small, sorptivity may be measured directly, and the other terms ignored.

Sorptivity is not an easy variable to deal with, and much effort has been expended in trying to express it in terms of more familiar variables.

Some approximate relations are

$$D(\theta_1) = \frac{\pi S^2}{4(\theta_f - \theta_i)^2}\left(\frac{\theta_f - \theta_i}{(1+\gamma)\log e}\frac{\partial}{\partial\theta_1}(\log S^2) - \frac{1-\gamma}{1+\gamma}\right) \qquad (3.3.4)$$

and, where the final water content is saturation

$$S = \left[2\int_{\theta_i}^{\theta_s}\frac{(\theta-\theta_i)D(\theta)}{F(\theta_R)}\mathrm{d}\theta\right]^{\frac{1}{2}}. \qquad (3.3.5)$$

These both contain an unknown variable. In the case of (3.3.4), the weighting parameter, γ, can be varied between 0.5 and 0.62 without much effect. A value of 0.62 is recommended (Dirksen, (1975, 1999, 2001). In (3.3.5), $F(\theta_R)$ is a shape parameter, whose value can vary only over a small range (Philip, 1973; Philip & Knight, 1974; Kutilek & Nielsen, 1994; Clothier, 2001).

If we are interested in infiltration into soil, then a directly measured value of sorptivity rather than the other more 'basic' parameters may well be of more use.

4 Spatial Variability

It is a common observation that soil and geological materials vary from place to place, often quite dramatically over very short distances. These changes generally reflect the processes that formed those materials. It is therefore hardly surprising that hydraulic and many other soil properties vary by large amounts over relatively small areas. A complicating factor is that different measurement methods involve different volumes and/or areas of ground, thus potentially exaggerating or masking the effect of spatial variability.

The degree to which spatial variability affects any results depends among other things on:

- The scale at which the measurements are valid
- The scale at which the measurements are to be used
- The degree of spatial variability
- The desired level of accuracy in the measurements
- The distance over which values of the relevant variables are correlated
- The amount of correlation between different variables

It is clear from this list that dealing with spatial variability is far from simple. In most investigations, several of the factors mentioned are either not known or can be estimated only very roughly.

4.1 Representative Elementary Volume

Some general observations may help to put the phenomenon into perspective. We will use soil water content observations as an example, as these are probably the most easy to visualise. The principles apply, however, to almost all kinds of measurement.

Firstly, any measurement of a physical quantity has an underlying implicit assumption that there is a degree of local homogeneity of that quantity, such that by moving a short distance away from one measurement location to another and making another measurement, a very similar result will be obtained. Soil water content is measured, in the simplest way, by taking a volume of soil and measuring the amount of water within it. In fact, this is true of all methods, although the boundaries of the volume may not be very well defined and some parts of it may contribute a greater or lesser amount to the final value than others. If we go to a very small scale, say, that of a molecule, then the volume will be either within a solid making up the soil fabric (zero water content), in the air phase (again zero water content if we ignore water vapour) or within the liquid water (100% water content). It is clear that we can move our measurement position by a very short distance – less than 1 mm – and go from 0 to 100%.

As the measurement volume becomes a little larger, there will still be plenty of places where it is still wholly within one of the three phases, but a few are occupied partly by two or three of solid, air and water. As the volume becomes larger still, the number of locations at which it is possible to be wholly within one phase will diminish, while those with a proportion of all three phases will increase. At some point, it will be impossible to find any location where the volume can be wholly within one or even two of the phases. And as the volume becomes larger still, it will matter less and less exactly where it is located, since the volume around each location will be almost identical in its composition of the three phases. This volume is termed the *representative elementary volume* (*REV*). Generally speaking, it is not productive to measure any quantity at a scale smaller than this one. Intuitively, it seems reasonable that the REV will be of a size to contain several of the basic units of the soil. For a granular soil, these would be individual grains, for an aggregated soil, aggregates, but for those with larger structures, for example, cracking clays, things become less clear and may well depend on the purpose for which the information is being collected. For instance, vertisols tend to crack deeply, with wide cracks, spaced typically 1 m apart. A true REV for such a soil would be many cubic metres. However, it is beyond the capability of most measurement methods to average over this volume, and there is often a need to understand what is happening at a scale much smaller than this. An REV for the soil between the cracks is likely to be of the order of cubic centimetres. Although the cracks may

Soil Water Measurement: A Practical Handbook, First Edition. J. David Cooper.

account for only a very small part of the total volume, and hence will have an almost negligible effect on total soil water content, they may, under storm conditions, conduct most of the water. This example highlights the need to understand what the processes are and how they vary spatially.

4.2 Deterministic versus Random Variation

Next, there are several types of variation of soil properties that we should be concerned with.

First, and perhaps most obviously, there are variations with depth, which are caused predominantly by soil-forming and geological processes. These may vary relatively smoothly, or there may be abrupt changes of soil from one horizon or from one lithological unit to another. Knowing where these boundaries occur is often essential in designing an instrumentation array for a site and in interpreting data from it. In soil, the boundaries between horizons tend to be relatively close together, and several kinds of instrument will integrate over a distance comparable with that, thus effectively smoothing out any abrupt variations.

Second, there are variations in the horizontal direction. Again, these may be relatively smooth, as, for instance, down a slope, or abrupt, as will happen if the parent material suddenly changes along a horizontal line. This sort of change, whether smooth or abrupt, is called *deterministic*, as it reflects some well-defined (if not always known) cause.

On top of this, there are *random* changes from place to place. It may often be difficult to distinguish between the two types, as a smooth variation from one point to another may become an essentially random variation when sampled at a wide spacing. There may also be an underlying deterministic cause to these variations, which is unknown. Deciding what is likely to be random and what is not is therefore not easy and requires a degree of subjective judgement which may prove to be wrong. It is wise, therefore, to be cautious and sometimes to consider data assuming, on the one hand, that the variations are random and, on the other, that they have a deterministic cause.

4.3 Geostatistics

The theory of *geostatistics* has been developed to deal with variations whose degree of randomness depends on the spatial relationship between measurement points. It starts from the reasonable premise that one expects that measurements of any quantity made at two different points are likely to be more similar to one another the smaller the distance between the two points. This is usually expressed in terms of a *semi-variogram*. This is a graph of half of the mean square difference between measurements made at two points separated by some distance (known as the *semi-variance*), plotted against that distance. Because the semi-variogram may be different in different directions, it is usual for the data to be collected at points along one or more lines, known as *transects*. Also, because it is necessary to calculate a mean of values, all at the same spacing, the observations should be made at regular intervals along this transect. The number of basic intervals between observations used to construct the semi-variogram is known as the *lag*.

The semi-variance at lag m is defined by

$$\gamma_m = \frac{1}{2l}\sum_{j=1}^{l}(y(j)-y(j+m))^2 \qquad (4.3.1)$$

where

γ_m is the semi-variance at lag m;
l is the number of pairs of observations used to calculate the semi-variance and
$y(j)$ is the observation at point j along the transect.

For a transect which consists of n equally spaced observation points, there will be $n-1$ values of j at lag 1, $n-2$ at lag 2, $n-m$ at lag m and only one (involving the point at each end of the transect) at lag $n-1$. Clearly, for a meaningful value of the mean, several values of the difference are needed. In practice, it is necessary to ensure that l is greater than about 6. Moreover, since we need to construct a graph of γ_m versus m, we need several values of m, say, 10, to be able to define a reasonable curve. We need, therefore, a minimum of about $10 + 6 + 1 = 17$ points along our transect to be able to construct a meaningful semi-variogram. If we need to know its form in more than one direction, then the number of points required will increase correspondingly. It often happens that there are two principal axes along which variation occurs more or less at right angles to one another. These directions may not be known in advance. If we happen to choose two transects at right angles to one another, but at 45° to each of the principal axes, then we would not detect any difference between the two transects, even if there is a substantial difference between the principal axes. It is wise, therefore, to check that the semi-variogram is the same at 45°, although this need not involve as many measurements.

The form of semi-variograms varies, but some common shapes are illustrated in Fig. 4.1.

The first of these (Fig. 4.1a) is quite common and illustrates several features. First of all, extrapolation to zero lag produces a finite value for the semi-variance, known as a *nugget*. The term derives from the origins of the methodology in the gold mining industry. Clearly, a lag of zero implies several measurements made at exactly the same place, and so one would expect a zero nugget. The fact that this is not normally obtained is partly because of inherent errors in the measurements, meaning that there is usually a small difference between two or more successive measurements of the same quantity under identical conditions. Usually more significant, however, is the fact that the true semi-variogram falls to a very small value at zero lag within the distance represented by one lag. A hypothetical curve is

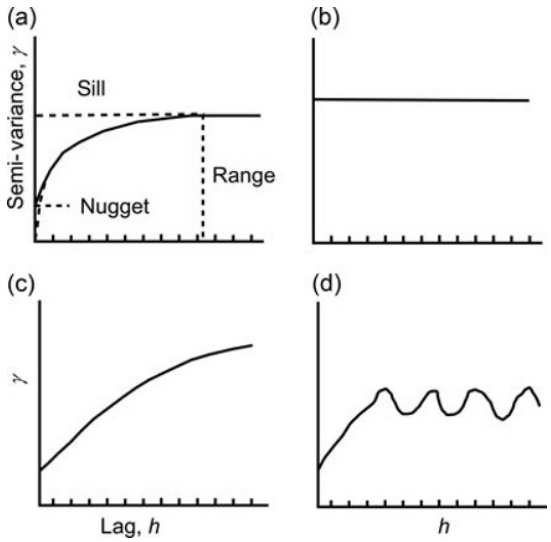

Fig. 4.1 Different forms of semi-variogram. (a) Spatially dependent with sill and nugget. (b) Spatially independent. (c) Variability increasing with no sill. (d) Periodic.

shown by the dashed line in Fig. 4.1a. Secondly, the semi-variance increases steadily with lag. This is what is expected – measurements from points close to one another are expected to differ less than those from further apart. Thirdly, the semi-variance reaches a limiting value, known as a *sill*, beyond which it does not increase any further. The distance at which the semi-variance reaches the sill is called the *range*. Measurements further apart from one another than the range can be regarded as uncorrelated with one another. This kind of behaviour will be returned to shortly.

The second form of semi-variogram (Fig. 4.1b) shows no dependence of the semi-variance on distance. It implies that no matter how close to one another we make measurements, they will be equally independent. It is likely, however, that the semi-variogram has a form similar to that of Fig. 4.1a but that the range is smaller than one lag. If we had chosen sampling points closer together, then the picture might well be different. It would be dangerous, therefore, to make measurements closer than one lag and still assume that they were not correlated.

Figure 4.1c shows a semi-variogram whose semi-variance keeps increasing, seemingly without limit. This may be the opposite case to the previous one, and our transect is shorter than the range, and so the semi-variance does not achieve the sill. It could also be caused by a monotonic change of the variable along the transect, known as a *drift*.

Lastly, Fig. 4.1d shows an oscillatory behaviour. This probably indicates some periodicity in the underlying values of the variable. These may be caused by a variety of factors, such as ploughing or planting, ancient ridge and furrow treatment of the land, periglacial action, regular changes in the underlying lithology, etc.

In both of the last two cases, it would probably be helpful to remove any underlying deterministic variation from the data first. The correlation between the random fluctuations could then be seen more easily. In any case, geostatistical theory requires that any such trends be removed. It is important to remember, however, to put these back into any estimates made on this basis. It is also difficult, as mentioned in Section 4.2, to be certain what represents a deterministic variation and what is random.

4.3.1 Uses of geostatistics

Now that we have a picture of the likely variations and their scale, we can use these for a variety of purposes. We will assume that a semi-variogram of the form of Fig. 4.1a is applicable. It has been shown that those in Fig. 4.1b and c may be special cases of this and that it may be possible to transform Fig. 4.1c and d to such a form by taking out deterministic trends.

If we need to characterise an area, therefore, we must make a series of measurements to capture all of the variability. Some of this variability will be deterministic in nature, perhaps easily identified by different crops, land uses or obvious differences in elevation or soils. Such units should be treated separately. Within a nominally 'homogeneous' unit, however, geostatistics can help decide on measurement locations, spacing, total number of points to achieve a required accuracy, likely levels of accuracy of the mean within the area and interpolation of estimates between measurement locations.

The first step is to identify the semi-variogram by laying out one or more transects. Because the range is not, at this stage, likely to be known, the transect(s) should cover as much of the complete area of interest as possible. If it is confined to just one part, a fundamental change in soil properties in another part may be missed. Measurements should be made at as many locations as economically possible along the transect(s) to provide a well-defined semi-variogram.

Next, the measurements should be examined as a plot of value against position. Obvious dubious points can then be identified. If possible, measurements at these positions may be repeated to check whether they are caused by measurement errors. In any case, any clear outliers should be omitted from the analysis. The omission of one or two data points will not invalidate the calculations. This examination should reveal any clear trends in the data or sharp boundaries within the area. If there are two or more obviously different regions, these should be analysed separately. The data should be corrected for any clear trends by drawing a smooth curve through the data and subtracting this from each reading.

The semi-variance for each lag can then be calculated according to Equation 4.3.1 and the semi-variogram constructed. With luck, this will allow the range, sill and nugget to be identified.

A sampling scheme for the area as a whole can now be designed. To get the maximum information from a limited

number of observation points, they should be spaced apart by a distance greater than the range. This will avoid losing information as a result of correlations between one point and another. It will also mean that normal statistical tests for mean, standard deviation and standard error of estimate, which assume that data points are independent of one another, can be applied. If the range is short, then there is no advantage to spreading measurement points over a wide area and they can be clustered together for convenience, so long as the initial survey covered the whole area and there is confidence that there are no deterministic changes within it.

Usually, other factors must be taken into consideration when choosing observation points, particularly for permanently installed instrumentation. This is likely particularly to be the case when instruments are installed in cropped fields. The difficulties for both farmer and experimentalist in accommodating one another's needs should not be minimised. The pressure to site instruments close to field boundaries or in islands of grass, fallow or bare soil within a field otherwise planted to an arable crop needs to be resisted strongly. A solution calls for close co-operation between the two sets of people and a degree of compromise on both sides.

4.3.2 *Interpolation and error estimation*

Geostatistics gives us a way to interpolate values of a variable at unsampled points, to calculate areal averages of a variable (e.g. soil water content over an area) and to estimate the likely error of estimation for these values.

Kriging and interpolation

Kriging allows estimates of a variable at unsampled points to be made from measured values at nearby points and a semi-variogram of the variable. This will probably involve fitting a function to the semi-variogram.

We will take as an example an area shown in Fig. 4.2. Values of a variable, for instance, water content in the upper metre of soil or matric potential at a depth of 0.5 m, have been measured at n points shown by the solid circles. Now, assume that we want to find the value of the variable at the point, X, shown by the open triangle. There are many ways of combining the known readings to obtain an estimate of the value at an unmeasured point. Kriging uses a linear combination of the values from points near to X. It can be shown that, using this basic method, kriging gives an unbiased estimate with the smallest likely error of any linear combination. For this reason, it is often referred to by the acronym *BLUE* (best linear unbiased estimator).

The value of a variable, A, at position X can be estimated from a linear combination of values of A measured at n sampling points as

$$A^*(X) = \sum_{i=1}^{n} \lambda_i A_i \qquad (4.3.2)$$

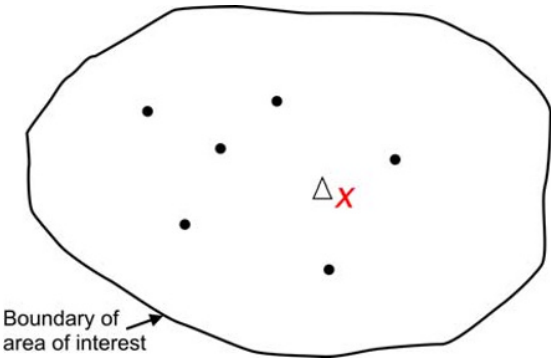

Fig. 4.2 Hypothetical area for kriging. Closed circles represent points where measurements are available. It is required to estimate the value at the open triangle, X.

where
the asterisk denotes an estimated quantity;
λ_i is the weight attached to the measured value at point x_i, and
A_i is the measured value at point x_i.

To ensure that the estimate is unbiased, all the values of λ_i must add up to one:

$$\sum_{i=1}^{n} \lambda_i = 1. \qquad (4.3.3)$$

The error associated with this estimate of A is given by

$$\varepsilon = A(X) - A^*(X) \qquad (4.3.4)$$

and, if the estimate is unbiased, the average value of this will be zero taken over all values of A in the area considered. Unfortunately, $A(X)$ (and hence ε) is not known, but, knowing the semi-variogram, the likely spread of values can be estimated. As often, the best estimation of A is taken to occur when the average of the squares of the error, ε, σ^2, has its least value. In this case, σ^2 is given by

$$\sigma^2 = \mathrm{Avg}(A - A^*)^2 = 2\sum_{i=1}^{n} \lambda_i \gamma(h_i) - \sum_{l=1}^{n}\sum_{j=1}^{n} \lambda_i \lambda_j \gamma(d_{ij}). \qquad (4.3.5)$$

Here
h_i is the distance between X and x_i and
d_{ij} is the distance between x_i and x_j

We have also used $\gamma(h_i)$ in place of γ_m to denote the semi-variance at a distance h_i, rather than for fixed lags. If a is the basic lag distance, then

$$\gamma(ma) = \gamma_m. \qquad (4.3.6)$$

To minimise σ^2, the partial derivative of Equation 4.3.5 is taken with respect to each variable λ_i and set equal to zero. This does not, unfortunately, lead to a unique set of values for the λ_s. To resolve this, an extra variable, μ, known as a Lagrange undetermined multiplier, is introduced.

We note that $\sum_{l=1}^{n}\lambda_i - 1 = 0$, so adding a quantity $\mu\left(\sum_{l=1}^{n}\lambda_i - 1\right)$ to Equation 4.3.5 will not make any difference. So this now becomes

$$\sigma^2 = 2\sum_{i=1}^{n}\lambda_i\gamma(h) - \sum_{l=1}^{n}\sum_{j=1}^{n}\lambda_i\lambda_j\gamma(d_{ij}) + \mu\left(\sum_{1}^{n}\lambda_i - 1\right). \quad (4.3.7)$$

Differentiating this equation with respect to each λ_i leads to a set of n equations of the form

$$2\gamma(h_i) - \sum_{j=1}^{n}\lambda_j\gamma(d_{ij}) + \mu = 0. \quad (4.3.8)$$

Together with Equation 4.3.3, we have $n+1$ equations and $n+1$ unknowns (μ plus n values of λ).

Note that each one contains $\gamma(d_{ii})$, which is $\gamma(0)$, the nugget semi-variance.

These $n+1$ simultaneous equations can be solved by standard techniques quite easily, provided that there are not too many of them, to give a set of values for the λs. An estimate of the error of estimation is also obtained by substituting back into Equation 4.3.5.

Usually, it is found that the weights, λ_i, are close to zero except for those of the nearest neighbours to the point at which the estimate is required. For practical purposes, the further points can be ignored, while the weights of the closest neighbours are increased slightly to ensure that they add up to one.

Other techniques

The foregoing has given an overview of the use of geostatistics to take account of expected similarities between the values of variables measured close to one another. Modifications to the basic theory would need to be made if the semi-variogram depended on orientation. Methods are also available to estimate the average value of a variable over an area or volume (known as block kriging). This would be useful to estimate rainfall input over an area from a number of scattered rain gauges, for instance. Sometimes estimates of a variable which is difficult to measure are needed, but values of another more easily measured variable which has a (spatially dependent) relationship with it are available. These can be used in a method known as co-kriging and might, for example, allow estimation of bulk density at unknown points from a sparse network of measured bulk density and a much denser one of clay content.

There are several other methods for incorporating random spatial effects into soil research. To describe these further here would not be practical, but interested readers can consult a variety of books, including those of Journel and Huijbregts (1978), Kitanidis (1997), Clark (1979), Clark and Harper (2000) and Webster and Oliver (2007).

Part II Water Content

5 Definitions

5.1 Basis for Expressing Water Content

Intuitively, the phrase 'water content' is fairly straightforward. It is the amount of water held in a unit quantity of soil. There are, however, several ways in which the unit quantity can be defined.

We may, for instance, be interested in knowing how much water is contained in a fairly large volume of soil. Normally, a 'volume of soil' means in reality a volume of space containing the soil that we are interested in. This may seem pedantic, but it is important to be clear exactly what is referred to. Many soils shrink and swell with changes in water content and sometimes other influences. In this case, by defining a fixed volume of space, the actual quantity of solid soil material that it contains will change. In such a circumstance, we might be better advised to select a defined mass of dry soil.

Alternatively, we might be interested in the storage of water over a defined depth of the soil. This is a depth in space, usually measured from the surface downwards. If the soil shrinks and swells, then similar cautionary remarks apply.

Again, we are often interested in the water content of the soil at a 'point'. A point is difficult to define exactly, but we might expect that it would be the amount of water held in a very small quantity of soil. However, we need to recall the discussion in Section 4.1 on representative elementary volume (REV). In most cases, there is little value in choosing a quantity of soil that occupies a volume smaller than the REV. We can, therefore, define the water content at a point as being the quantity of water contained within one REV of soil, centred at the point of interest, divided by the volume of the REV or mass of soil within it. In practice, it is very difficult to measure the amount of water within one REV and must be content either with that within a volume excavated from the soil or with the water contained within the volume sensed by an instrument upon or inserted into the soil. In the latter case, this volume is usually quite uncertain and varies with the water content.

To complicate matters further, a 'point' often refers to a location on the ground, and we want to know what the total water storage is over some depth of profile beneath this.

From the earlier discussion, it is clear that there are two basic ways in which the 'amount' of soil and therefore the water content can be defined.

1 The volume (or mass) of water contained within a REV per unit volume of soil. This is the most common and useful way to define it. We take the volume of water within a volume of one REV and then divide it by the volume of the REV. It is usual to express this as cubic metres of water per cubic metre of soil. This is normally written either as a fraction or as a percentage in $m^3\ m^{-3}$. This form is called the *volumetric water content* and is usually given the symbol, θ. An alternative name for θ is *moisture volume fraction* (MVF).

2 The mass (or volume) of water contained within a REV per unit mass of dry soil. This is similar, except that the quantity of water is divided by the mass of dry soil within the REV. It is normally written as $kg\ kg^{-1}$. This form is called the *mass wetness* and is usually assigned the symbol, w. Sometimes, water content according to this definition is described as gravimetric water content. However, the direct method of measuring water content by measuring the loss of mass of a soil sample on drying is usually called the *gravimetric method*. Gravimetric water content may, therefore, be interpreted as w or as that measured by the gravimetric method. To avoid this ambiguity, we will use the term 'mass wetness'.

Since both θ and w are dimensionless quantities, they are often quoted as a fraction or percentage. Hence, it is not always clear on what basis the water content is quoted. This can lead to considerable confusion and error since there are significant numerical differences between them.

If we know the dry bulk density of the soil and which version has been used to express the water content, then it can be converted to the other form quite easily.

If the volume of the REV or any other sample volume is V, then this will be made up of a volume of water, V_w, a volume of air, V_a, and a volume of solid, V_s:

Soil Water Measurement: A Practical Handbook, First Edition. J. David Cooper.

$$V_w + V_a + V_s = V. \quad (5.1.1)$$

Or, dividing by V:

$$\frac{V_w}{V} + \frac{V_a}{V} + \frac{V_s}{V} = 1. \quad (5.1.2)$$

Now $(V_w/V) = \theta$, the volumetric water content, and we can similarly define $(V_a/V) = \theta_a$, the *volumetric air content.* We could also call V_s/V the volumetric solid content, but it is more convenient to note that the space in the soil not occupied by solid constitutes the pores. Thus the *porosity*, ϕ, is defined as $1 - (V_s/V)$, giving

$$\theta + \theta_a + 1 - \phi = 1, \quad (5.1.3)$$

which reduces to

$$\theta + \theta_a = \phi, \quad (5.1.4)$$

so that the sum of the pore space occupied by water and by air adds up to the total porosity.

Since air has a negligible density compared with that of the solid and water, the total mass, M, within V is

$$M = V_w\rho_w + V_s\rho_s \quad (5.1.5)$$

where
ρ_w is the *density of water* (1000 kg m^{-3}), and
ρ_s is the *particle density*.

We can also write Equation 5.1.5 using the mass of solid per unit volume of soil, ρ_d. ρ_d is called the *dry bulk density*. Then

$$M = V_w\rho_w + V\rho_d. \quad (5.1.6)$$

Comparing Equations 5.1.5 and 5.1.6, we see that

$$V_s\rho_s = V\rho_d \quad (5.1.7)$$

and, since $1 - (V_s/V) = \phi$

$$\frac{\rho_d}{\rho_s} = 1 - \phi. \quad (5.1.8)$$

Now the mass of *dry* soil is $V\rho_d$ and that of water is $V\rho_w\theta$. So

$$w = \frac{V\rho_w\theta}{V\rho_d} = \frac{\rho_w\theta}{\rho_d}, \quad (5.1.9)$$

or

$$\theta = \frac{\rho_d w}{\rho_w}. \quad (5.1.10)$$

Because of the potential for confusion and serious error arising from different ways of expressing water content, it is recommended that the basis of calculation is always specified and/or that explicit units (e.g. m^3 m^{-3}) are used.

In most cases described in this book, volumetric water content is the most useful quantity, because we need water volumes in a particular region of space to construct water budgets. Moreover, most of the available instruments for measurement of water content are sensitive primarily to volumetric water content. The expression 'water content', therefore, will be taken to mean 'volumetric water content' unless it is explicitly stated otherwise, but we will use the units m^3 m^{-3} to reinforce this message.

5.2 Standard Definition of Soil Water

There are many methods for measuring soil water content. To compare these with one another, an agreed standard definition and methodology is needed. This will also serve as a basis for calibration. It is clearly desirable that the standard method should be as direct a determination of the water content as possible to minimise the influence of confounding factors. A standard definition should also ensure that results from different groups of workers working on related problems are comparable and that the measurement methodology is available to all who need it.

The standard method is the gravimetric method (described fully in Chapter 6). This is suitable for measuring either volumetric water content or mass wetness (Section 5.1).

Briefly, we define the water content of a sample of soil as being equal to the mass change on drying the sample at a temperature of 105°C until no further loss of mass occurs. The practicalities of doing this are discussed in Chapter 6. However, it is worth investigating some of the advantages and limitations of this definition.

The choice of temperature of 105°C seems to have been made on a naïve assumption that any water in soil would evaporate off at about the normal boiling point of water, 100°C. It is now known that water continues to be released from soil up to temperatures of at least 400°C. It also begs another question about what actually constitutes soil water, which was explored in Chapter 1. Also, some substances, most commonly organic compounds such as peat and humus, may be volatilised or oxidised at temperatures below 105°C, usually leading to a loss of mass not caused by evaporation of water.

In the face of these problems, it is clearly not possible to specify a temperature for all soils which is suitable to evaporate off all water and, at the same time, ensure that no other losses (or gains) occur.

An additional consideration is that the chosen temperature should be one at which there is little change in mass for small differences either side of that temperature. This ensures that variations in practice will have no material effect on the results from different groups of people or at different times. Unfortunately, there is no assurance that this will be the case at any temperature. However,

at temperatures just above the boiling point of free water (100°C), water loss in most soils varies little with temperature, although this is not true for every soil, in particular those with a high organic content.

Good laboratory practice – regular maintenance and calibration of instruments, and robust procedures for documentation and checking of results – is essential in obtaining reliable and reproducible results. It is also important that suitable equipment be available to carry out the necessary operations at a cost which is affordable to the organisation. The gravimetric method meets these criteria well. Laboratory ovens are relatively cheap, reliable and have low maintenance and running costs. Other standard laboratory equipment is required, such as balances and thermometers, and field sampling equipment which is inexpensive and can, in most cases, be made in a basic engineering shop,

In summary, the main reasons for adopting mass loss at 105°C as a standard for soil water content are as follows:

- In most soils, there is little change in mass loss with changes a few degrees either side of this temperature. However, it is important to be aware that this does not apply to all soils; and sometimes it may be wise to use a different temperature.
- In most soils, the great majority of water which participates in evaporation, drainage and root water uptake is removed at this temperature.
- Equipment is available at modest purchase and running costs to enable measurements to be made reliably and reproducibly by most laboratories.
- The procedures necessary do not involve any sophisticated techniques, thus ensuring that they are widely applicable.

5.3 Measurement of Water Content

Chapters 6–10 discuss various methods for measurement of water content. Some of these are the subject of national and international standards. In particular, by the International Standards Organisation (ISO, 1995, 1998a, b, 2001, 2003) and the American Society for Testing and Materials (ASTM, 2009, 2010). The large (and growing) variety of devices to measure water content means that only partial intercomparison of the available instruments is possible. The International Atomic Energy Agency has been proactive in this (e.g. Evett, 2000c).

6 Gravimetric Method

The gravimetric method is the basic reference against which all others are evaluated (Chapter 5). It is technically unsophisticated and requires only simple equipment, much of which is usually available in laboratories. Most other equipment can be purchased at relatively low cost or fabricated in a basic engineering workshop. This does not, however, mean that obtaining accurate results is completely straightforward. While a high level of technical sophistication is not required, a great deal of care and, often, physical effort is needed. We will assume that water content is needed on a volumetric basis, which usually requires samples of a predetermined volume. Obtaining a sample of known volume is usually the most difficult part of the process and the largest source of error. Alternatively, a separate measurement of the sample volume or its density can be used to convert mass wetness to volumetric water content (Section 5.1). Mass wetness is simpler to measure, since the volume of the sample is not needed. Methods for measuring sample volume or density are described in Sections 6.4 and 6.5.

The method may be divided into four stages:

1 Obtaining a sample of soil from a specified depth. This is usually of a predetermined volume (see above) collected by a special sampler.
2 Transportation to the laboratory.
3 Weighing and drying the soil.
4 Calculation of the results.

In all of stages 1–3, great care is needed to avoid loss or gain of water by the sample.

6.1 Equipment Required

The lists following are provided as a starting point for workers to develop their own requirements. These will vary according to many local circumstances, including the kind of terrain in which the investigation is conducted, weather conditions, the type of soil, local regulations, etc.

6.1.1 Soil sampling equipment

The following equipment is required to take soil samples of known volume from a given depth in the soil:

1 Large umbrella, tent, awning or portable gazebo to protect the sampling area from rain or sun, reducing the possibility of water loss or gain by the collected samples.
2 Spade for digging to the required depth and removal of the sampler.
3 Sampler for taking cores of known volume from the soil. This may not be necessary if mass wetness only is required. However, it is still important that the location and particularly the depth range of the sample are well defined and so a purpose-made sampler may be the best option.
4 Suitable impermeable containers for sealing and transporting each soil sample from the field to the laboratory. These may be plastic bags (preferably self-sealing), boxes or tins with tight-fitting lids.
5 Measuring tape.
6 Spatula or large knife for trimming soil cores.
7 Post-hole or similar auger of diameter greater than that of the sampler. This is necessary only if a spade has not been used to access the top of the soil horizon from which samples are to be taken.
8 A suitable hammer to drive the sampler into the soil if the sampler does not incorporate a sliding hammer (see Section 6.1.3). For a small sampler ($\lesssim$150 mL), this may be a 'lump' or 'club' hammer with a head mass of approximately 2 kg. For larger samplers, a long-handled sledgehammer with a head mass of up to 7 kg may be necessary, dependent on the type of soil, water status and design of sampler.
9 Tools for sampler and auger. These will vary according to the particular design of each item but will probably include spanners, screwdrivers and files or other implements for sharpening the sampler.
10 Suitable protective clothing, including waterproof outerwear, rugged footwear, leather-palm gloves and eye and head protection.

Soil Water Measurement: A Practical Handbook, First Edition. J. David Cooper.

11 Supply of forms to record details of the sampling. In many cases, it is advisable to have these printed on waterproof paper. Alternatively, a handheld computer or smartphone may be used with, for instance, a spreadsheet application, but these are often susceptible to getting wet so that a waterproof cover is advisable.
12 Labels to identify samples. Plastic bags are available having a roughened patch on them, which can be written on. Provided that this can be done legibly and indelibly, it is preferable to use these rather than separate labels, as it reduces the danger of mixing up samples or losing the label, and makes it easier to record and read the sample identification.
13 Pens, pencils, marker pens, etc. to record details of the sampling and to label samples.
14 Stout wooden or metal box to protect soil samples from mechanical disturbance during transportation to the laboratory and reduce the potential for water loss by evaporation. If possible, this should be divided into compartments for each sample.
15 Portable balance for weighing samples in the field. This is not essential but by weighing the samples immediately after collection, any loss of water from them before they reach the laboratory will not matter. The balance must, however, be accurate to 0.1 g and rugged enough to survive the journeys without loss of accuracy.

6.1.2 Laboratory equipment

1 Fan-assisted ventilated oven with thermostatic temperature control capable of controlling temperature to ±1°C
2 Thermometer to check temperature
3 Sufficient number of desiccators to hold all samples being processed in one session, with approximately 100 g dry silica gel or other drying agent in each
4 Balance capable of weighing to an accuracy of 0.1 g

6.1.3 Soil samplers

There are very many designs of sampler to gather known-volume cores of soil in common use in laboratories throughout the world. By no means all of these designs have been published. They vary in many respects from one another as a result of different local conditions and also the personal preferences of their designers. Some are available commercially, but many organisations prefer to construct their own.

The appropriate size of core collected by the sampler is a compromise between a number of factors including the purpose for which the sample is being collected. To maximise the accuracy of volume collected, the sample should be of as large an area as practicable. This reduces the relative importance of effects caused by the edge of the sample. These include stones, which are usually pushed into or outside the sampler, in either case causing an error, damage the cutting edge and make driving the sampler difficult. The height of the sample should be large enough to ensure that irregularities at each end do not cause a significant error. Obtaining an accurate length to the sample is aided by collecting slightly too much soil and then trimming the ends off with a spatula or sharp knife.

A large volume of sample reduces the effects of short-range spatial variability as well as those at the sample edges. On the other hand, it makes subsequent handling of the samples more difficult and time-consuming. It also increases the effort required to drive the sampler into the ground, making it necessary in some cases to use machinery. Long samples also increase the risk of sample compaction through friction between the sample and the retaining sleeve. This is helped, but not necessarily eliminated, by the internal diameter of the sleeve being slightly larger than that of the cutting ring. The greater the ratio of diameter to sample length, the smaller will be the chance of sample compaction.

Samples 50 mm diameter and 50 mm high are a popular choice. These have a volume of 98 mL. In general, it is recommended that the height of the sample should be close to that of its diameter.

The act of taking samples from field soils is very demanding on the sampler, and often on the operator, particularly in heavy clay, stony and hard soils. The sampler therefore needs to be constructed very ruggedly. This conflicts with the requirement to make the walls as thin as possible. The conflict can be resolved to some degree by making the sampler from strong steel. Experience shows that welded joints are a particular weakness and should be avoided if possible. The vibration from repeated impacts usually causes a weld to fail eventually.

In some cases, where sampling can be done from a flat surface – either the soil surface or the bottom of a dug pit – simple samplers made from thin metal rings, sharpened at one end, can be used. These are suitable only for soft, stone-free soils, where the ring can be pushed or gently tapped into the ground. The advantages are that little specialised equipment is needed and that the quality of the core is very easy to assess.

Most sampler designs have the basic construction shown in Fig. 6.1. Fig. 6.2 is a photograph of a typical sampler.

The key features are:
1 A sturdy body to transmit impact to the cutting edge and to contain the sample. The thinner the casing, the easier it is to drive the sampler into the soil and the more likely that the sample collected is of the correct volume. However, thin-walled samplers are less robust and may fail in use. The casing should, therefore, be made of strong steel.

Marks engraved on the body of the sampler show the position of the retaining sleeve inside and serve as a guide to aid driving the apparatus into the soil by the correct distance.
2 A removable cutting shoe with a sharp, circular edge, which is straight on the inside and bevelled on the outside, to ensure that the sample is cut from a well-defined cross-sectional area. There is a trade-off between sharpness of the cutting edge and its lifetime. A very sharp cutting edge is

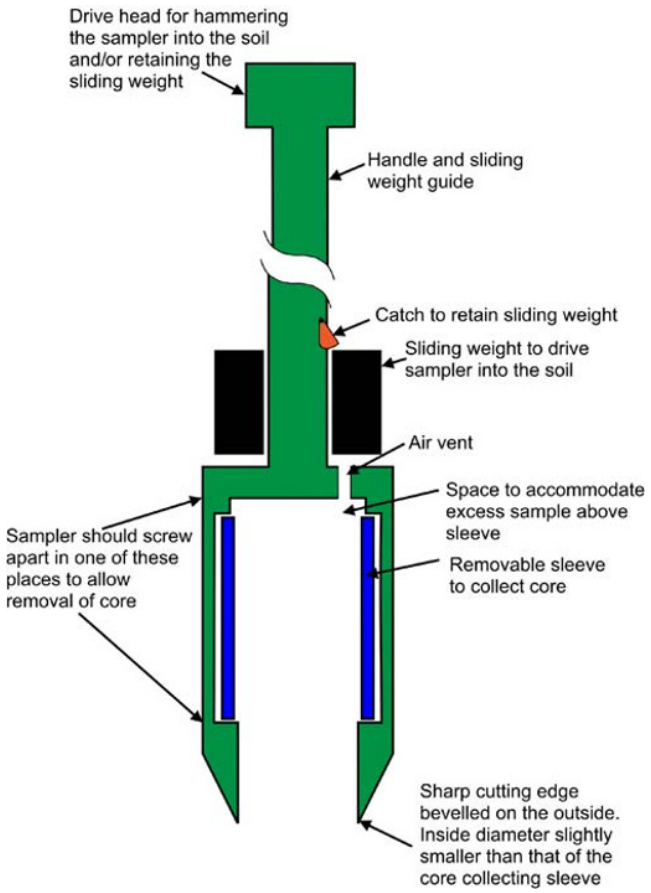

Fig. 6.1 Soil core sampler features.

easy to drive into the soil and less friction will be generated on the outside leading to better sample quality. On the other hand, stones in the soil and rough handling during transport and field operations can easily damage such an edge. Some workers have used a curved (convex) profile to the cutting edge to try to reach an acceptable compromise between sharpness and robustness. Such profiles are difficult to machine without a numerically controlled lathe and the marginal advantage gained is probably outweighed by the increased difficulty in production. The cutting shoe material needs to be selected for its wear and hardness properties. Case hardening is a tried-and-tested method to improve the hardness of the edge economically. Very hard edges chip rather than bend when encountering a stone, which may limit their life. They are also difficult to resharpen.

The cutting shoe may be fixed to the body by a variety of means. The main force when the sampler is driven into the soil is compressive. However, once the sample has been captured in the sampler body, it may be pulled out the soil, so that it needs to resist this action. Usually, the cutting shoe is secured by a screw thread, which must be screwed fully up to the limit so that the force of the impact driving the sampler is taken where the shoe butts to the body and not on the threads, which have little strength if the sampler is thin walled. A disadvantage of screw threads, especially if they are fine, is that particles of soil easily become lodged in them and prevent the shoe being tightened fully or make it difficult to unscrew. For this reason, coarse threads are preferred, especially ones with a square cross section, which will take impact well.

A removable cutting shoe makes it easy to replace a damaged cutting edge in the field as well as accommodating a separate sample sleeve.

3 A removable sample retaining sleeve. This fits inside the sampler body, behind the cutting shoe, which may have a rebate cut into to it to locate the retaining sleeve. The inside diameter of the retaining sleeve is often slightly larger (1–3 mm, dependent on the diameter of the sampler) than that of the edge of the cutting shoe. This relieves pressure on the inside of the sleeve, reducing friction between it and the soil sample as it enters. This, in turn, helps to minimise compaction of the soil sample.

The upper edge of the retaining sleeve butts against a rebate in the upper part of the soil sampler body. There is usually a space in the sampler body above the sleeve to accommodate a small amount of overdriving of the sampler into the soil. This space may be vented to prevent compression of air inside the body from restricting the free entry of soil into the sampler.

Some workers use retaining sleeves split into two or three separate rings. This allows one or both ends of the sample, which may be disturbed, to be discarded or for the sample to be divided into two or more parts. Alternatively, the retaining sleeve may be split longitudinally to ease the later removal of the sample. It is advisable to fix the parts of the sleeve together with adhesive tape or (in the case of longitudinally split sleeves) an elastic band before insertion into the sampler.

Retaining sleeves may be made of any suitable material. They are not required to be very strong but do need to be as thin walled as possible to minimise the wall thickness of the complete sampler. They should also be cheap so that a large number can be kept in store. This allows samples to be kept intact in the sleeves until they are processed, reducing field operations and the potential for loss of water or soil material when transferring the core from sampler to transport container. In some cases, the sleeve can also be used to support the sample for further experiments, for example, in a pressure membrane apparatus or for hydraulic conductivity measurement. Retaining sleeves should, therefore, be made from easily available, non-corrosive tubing cut into the correct lengths. Suitable materials are stainless steel, brass, aluminium alloy or plastic, although the latter will probably need to have thicker wall if it is to be rigid. Some samplers use thin flexible plastic membranes to retain the sample, however. The availability of suitable tubing for sleeves may well dictate most of the other dimensions of the sampler.

4 Drive head. A means of driving the sampler into the soil. If the sampler is to be used for sampling from the ground surface or a prepared surface at the bottom of a pit, then

Fig. 6.2 Soil sampler showing sharpened body, removable retaining sleeve and shaft to allow sampling at depth. This one does not have a sliding hammer. Instead, the handle is used to hold it steady, while the sampler can be driven into the soil by blows to the heavy boss at the top.

a thick top to the sampler body will suffice to allow the sample to be driven into the ground. In many cases, however, the sampler will operate below the surface, and a drive head with an extension to the surface is needed. This can have a heavy steel block on top for striking with a hammer or a fitting to mate with a hydraulic push device or mechanical hammer. A better alternative to use of a conventional hammer is incorporation of a sliding hammer in the sampler. A sliding hammer is a heavy steel cylinder, with an axial hole, which slides up and down a guiding rod. It is operated by raising the steel cylinder and dropping it onto the sampler body or an intermediate platform on the guide rod. Sliding hammers are efficient and convenient and ensure that impact is along the sampler axis, with negligible side movement. Unless they are properly designed and used, they can be hazardous, as it is easy to get fingers trapped between the hammer and the drive head or the sampler body, particularly when tipping the sampler. For this reason, it is essential that the sampler be provided with a means of locking the weight in place automatically at the end of its travel.

6.2 Procedures

6.2.1 Before setting out

1 Obtain any necessary permission from landowners.
2 Sort out access arrangements, including routes and necessary permissions.
3 Prepare location diagrams for sampling, together with target sampling depths and suitable forms for use in the field.
4 Ensure that all equipment is present and in good working order.
5 Weigh each sleeve to be used for sampling to an accuracy of 0.1 g and mark the mass on it with an indelible marker pen. Keep a separate record of these masses, as the marks often rub off or become unreadable. It helps if the sleeves have an identification number stamped on them (see Section 6.2.3).

6.2.2 Soil sampling

The first requirement for the gravimetric method is obtaining a suitable sample of soil from the desired location. It is recommended strongly that sampling be done by two or more people working together, as it is necessary to both hold the sampler steady and force it into the soil. In some cases, it is preferable to take samples from a vertical face in a pit dug in the soil, although there is some danger of the soil drying out if samples are not collected promptly and precautions against pit collapse may be necessary:
1 Dig or auger a hole of diameter greater than that of the sampler to just above (~25 mm) the top of the sampling depth.
2 Carefully clean the top of the soil to leave a clean, flat surface at the depth at which the top of the sample should be. If some soil from the top of the sample is to be discarded, allowance should be made for this.

This process is clearly much easier on a large surface, such as in a pit dug for the purpose. It is much more difficult to achieve in an augered hole. Special clearing augers with a flat end are available. It may also be possible to blow loose soil out of the hole with a tube attached to a compressed air cylinder or compressor. Overdriving of the sampler, so that the top part of the soil collected is discarded, helps to ensure that only undisturbed soil is retained. Overdriving must not, however, be to the extent that the soil becomes compacted in the sampler body.
3 Assemble the sampler and place it gently in position on the top of the soil. If the soil is sticky, it may help to grease the inside of the cutting shoe and retaining sleeve to help ease the sample into the device. A lubricant spray, such as WD-40, may also be used. Mark the sampler body or drive head where it is level with a fixed reference point, for example the soil surface. Make another mark above this at a distance equal to the depth to which the sampler must be driven into the soil. This distance should be the depth of the cutting ring, plus that of the retaining sleeve plus a little extra to be trimmed from the top of the sample. If the

retaining sleeve already has a separate ring at the top for this purpose, this would be zero, otherwise 10 mm is recommended.

4 Drive the sampler into the ground until the upper mark is level with the reference point. Do not drive it further, as there is a danger of compacting the sample. The sampler may be driven by pushing it into the ground, either manually or using a hydraulic ram or by hammering.

If the soil is soft, then pushing it in gently will normally be preferred, as this is likely to lead to less disruption to the sample and is easier to control. Mechanical pushing requires something for the ram to react against, which would normally be a heavy object, for example a motor vehicle or drill rig, although it may be possible to fix a beam above the ram, anchored into the soil by heavy-duty screw augers.

For hard and heavy soils, there is little alternative to driving by repeated blows from a hammer. A sliding hammer is recommended strongly (see Section 6.1.3). Stones may, however, upset this. Use of a conventional hammer, whether of the large, sledge, variety or a handheld one, may knock the driving head sideways, leading to the sample breaking up as it enters the sampler.

If the sample is to be used for physical measurements other than water content or bulk density determination, its structure, and hence its physical properties, are more likely to be preserved by a steady force on the sampler than by the shock of repeated impacts from a hammer.

5 If practicable, dig soil away from around the sampler, until a spade can be inserted beneath it and the sampler removed from the soil without disturbing the sample. If this is not possible, for instance because the sampler is in an auger hole well below ground surface or several samples are needed close together, rocking the sampler from side to side will normally break the soil in the sampler away from that below quite cleanly, allowing the sampler to be lifted out of the soil with an intact core.

6 Carefully remove the sampler from the soil.

7 Hold the sampler horizontal to prevent soil falling out of it. Disassemble the sampler carefully and remove the retaining sleeve. This should have some soil protruding from either end. If this is so, then trim off the excess soil from both ends and prepare immediately for transport to the laboratory. Delay may allow water to evaporate from the sample leading to an erroneous result.

In some cases, the sample may have become compacted as it entered the sleeve. This may affect only the upper part of the sample, as it will have been subjected to more accumulated frictional force as it slid further up the sleeve. Careful examination of the two ends of the sample and comparing them with the undisturbed soil may allow the degree of compaction to be assessed. If the soil is compacted, the sleeve may contain the correct amount of soil for the length of sleeve plus the overdriven distance and therefore may be usable for volumetric water content or bulk density determination. In most cases, however, compaction will extend below the cutting edge and prevent some soil entering the sampler. In this case, the sample should be rejected and another one taken. However, if one sample is compacted, it is likely that all others from the same site will be as well. The sample will still be usable to derive water content on a mass wetness basis. If independently measured bulk density values are available, mass wetness can be converted to volumetric water content (see Section 6.4).

It is essential that, if there is reason to believe that cores do not contain the correct volume of soil, this is recorded along with details of the problem.

6.2.3 Transportation to the laboratory

For the purposes of water content or bulk density measurement, any disturbance to the sample structure before or during transportation is of no consequence. Loss of water by evaporation (or gain, if it is raining at the time of sampling) and loss of sample during transfer from one container to another must be avoided by taking the following precautions:

1 Keep the core intact in its sleeve. If several samples are to be taken, enough spare sleeves for all samples will be needed.

2 Weigh the core in its sleeve as soon as possible. Portable, battery-powered digital balances, capable of weighing to 0.1 g, are readily available so that weighing the sample in the field immediately after sampling is possible. These balances are not usually designed for field use and so must be treated with care; protected from rain; used on a flat, firm and level surface and checked for accuracy frequently. Weighing the sample straight after removal from the soil reduces considerably any problems that may arise from transport. Subtracting the mass of the sample sleeve will give the mass of the wet core.

3 Commercially available sample sleeves usually come with plastic end caps. Suitable caps may be available for other sizes of sleeve and their use is recommended if at all possible. The caps should be taped onto the sleeve to secure them and to reduce evaporation. Write details of the sample – date, location, depth, sleeve identification (if one is marked on it) and operator's name(s) on the sample sleeve or an adhesive label attached firmly to it. A separate copy of this information should also be kept in, for example, a field notebook or on the form shown in Fig. 6.3 (Section 6.3.4).

4 The sleeve should then be placed into a plastic bag and sealed by tying the open end or using resealable bags. If the sample is removed from the sleeve before putting it into the bag or the ends of the sleeve are open, the bag should be placed inside a second sealed bag to protect it and prevent evaporation.

5 The samples should be placed in a stout box of wood, metal or similar. Preferably, this should be insulated to reduce evaporation and divided into compartments so that only one or two samples are in each compartment. This will

GRAVIMETRIC SAMPLING RECORD FORM

FIELD	DATE:				TIME:				OPERATORS:								
LAB	DATE:				TIME:				OPERATORS:								
A	B	C	D	E	F	G	H	I	J	K	L	M	N	O	P	Q	R
Depth	Sample no.	Sample id	Mass in field	Mass core sleeve	Mass wet sample	Mass in lab	Mass wet sample	Mass wet sample + dish	Mass dish	Mass wet sample	Mass dry sample + dish	Mass dry sample	Mass of water lost	Volume of core	Mass wetness	Volumetric water content	Dry bulk density
					= D – E		= G – E			= I – J		= L – J	= I – L		= N / M	= N / O	= M/O X1000
m			g	g	g	g	g	g	g	g	g	g	g	ml	kg kg^{-1}	m^{-3} m^{-3}	kg m^{-3}
0.2	1	AX1	566.4	392.5	173.9	566.1	173.6	781.3	607.4	173.9	757.3	149.9	24	98	0.160	0.245	1530
0.2	2	AX2	581.3	387.6	193.7	581	193.4	818.6	625.3	193.3	790.8	165.5	27.8	98	0.168	0.284	1689
0.2	3	AX3	597.7	402.8	194.9	597.9	195.1	832.9	638.1	194.8	807.4	169.3	25.5	98	0.151	0.260	1728
0.2	4	AX4	602.1	401.7	200.4	601.8	200.1	821.7	621.7	200	796.7	175	25	98	0.143	0.255	1786
0.2	5	AX5	575.8	395.2	180.6	575.5	180.3	816	635.9	180.1	791.1	155.2	24.9	98	0.160	0.254	1584
0.2	6	AX6	583.9	398.3	185.6	583.8	185.5	832.5	646.8	185.7	809.1	162.3	23.4	98	0.144	0.239	1656
														Mean	0.154	0.256	1662
														Standard deviation	0.010	0.016	94
														Standard error	0.004	0.006	38
														Correlation coefficient		0.360	
0.4	1	AX7	588.6	399.2	189.4	588.4	189.2	802.6	613.5	189.1	773.0	159.5	29.6	98	0.186	0.302	1628
0.4	2	AX8	592.5	401.3	191.2	592.4	191.1	829.5	638.2	191.3	801.0	162.8	28.5	98	0.175	0.291	1661
0.4	3	AX9	574.3	404.5	169.8	574.1	169.6	787.0	617.6	169.4	758.9	141.3	28.1	98	0.199	0.287	1442
0.4	4	AX10	523.2	396.4	126.8	523.2	126.8	751.1	624.4	126.7	731.1	106.7	20.0	98	0.187	0.204	1089
0.4	5	AX11	585.8	392.8	193.0	585.8	193.0	819.5	626.8	192.7	791.6	164.8	27.9	98	0.169	0.285	1682
0.4	6	AX12	594.3	397.1	197.2	594.2	197.1	816.5	619.5	197.0	788.8	169.3	27.7	98	0.164	0.283	1728
														Mean	0.180	0.275	1538
														Standard deviation	0.013	0.035	241
														Standard error	0.005	0.014	98
														Correlation coefficient		0.886	
								Excluding sample AX10						Mean	0.178	0.289	1628
														Standard deviation	0.014	0.008	110
														Standard error	0.006	0.003	49
														Correlation coefficient		–0.955	

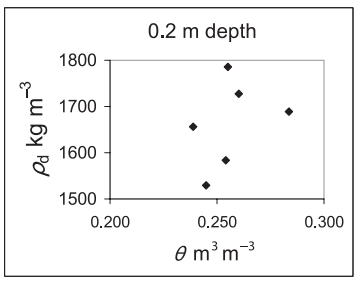

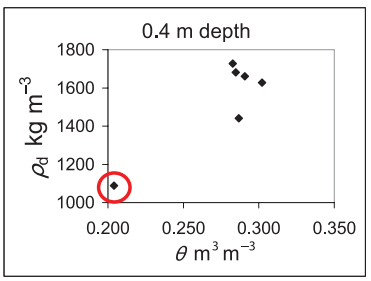

Field Notes	Lab Notes

Fig. 6.3 Suggested form for recording the collection and processing of gravimetric samples.

protect the samples and their containers, reducing the chance of loss of sample by the bag being punctured or abraded, particularly if the samples fit snugly into the compartments or are protected by some packing (e.g. rag or paper towel). Preventing the samples from moving around in transportation is particularly important if they are to be used for hydraulic properties measurements when the structure of the sample must be preserved.

6 The box should be placed in the vehicle in such a way as to minimise its movement. This may be achieved by placing it on some cushioning material or a seat and packing other items around it or using restraining straps.

7 Care should be taken when transporting the samples back to the laboratory that they are bumped around as little as possible to minimise damage and disturbance.

6.2.4 Laboratory procedures

Laboratory procedures must be equally rigorous as those in the field. The following procedures should be followed:
1 Weigh the samples in their bags and other outer containers as soon as possible after arrival at the laboratory. This will minimise the potential for loss of water from the sample. If the sample was weighed in the field, this will serve as a check on any loss of water during transportation.
2 Remove any outer container that is not in contact with the soil and reweigh. If the mass of the parts that are in contact with the soil are known, the soil can be removed from these carefully to ensure that they are completely clean of soil and all of it is in a dish. The dish needs to be sufficiently large to hold the sample without any spilling out but small enough to fit into the oven. The dish should have been weighed beforehand.

An alternative procedure is to keep all the containers that are in contact with the soil in the dish (bags, retaining sleeve and sleeve caps). This is particularly useful when the soil is very sticky and cannot easily be removed from the items. Also, for small samples, where even a small amount of sample or water lost may have a significant effect on the result, it ensures that accuracy is maintained.
3 Place the samples into a ventilated oven set at 105°C. A thermometer should be placed inside the oven to check the temperature. Some ovens have a glass door, which makes checking the thermometer without opening the oven easy. Others have a vent in the top, through which a thermometer can be mounted, with its bulb inside the oven and its stem outside.
The amount of time taken to dry the samples will depend on a number of factors. Among these are:

Number of samples
Design of oven
Size of samples
Type of soil
Water content of soil

It is important to be certain that the samples have dried out completely at the chosen temperature. This may require some samples to be removed from the oven, cooled and weighed every few hours to determine when this has occurred. The samples chosen should be those which are expected to take the longest time. With experience, a time that will suit all samples can be found, although it is wise to check this from time to time, particularly if wetter or larger than usual samples are dried.

It is also important to check that the drying temperature inside the oven is even all over. Some difference from one place to another is inevitable, but differences of more than 5°C are not acceptable.

4 When the samples are completely dried, place them immediately in a desiccator, containing fresh silica gel or other drying agent, to cool and prevent reabsorption of water. Convection currents set up by hot samples will disturb the weighing balance reading by an unacceptable amount. In warm, low humidity conditions, a desiccator may not always be necessary, particularly for soils low in clay. As always, if in doubt, check.
5 Once cool, the samples, each one in its drying dish, should be weighed.

The volumetric water content and dry bulk density can now be calculated. First, the mass of the wet field sample, m_f, should be calculated by subtracting that of its container(s). Then that of the dry sample, m_d, by the same process.

The volumetric water content is calculated, knowing the sample volume, V, as

$$\theta = \frac{m_f - m_d}{V}. \tag{6.2.1}$$

The dry bulk density is also given by

$$\rho_d = \frac{m_d}{V}. \tag{6.2.2}$$

It should be clear that volumetric water content can also be calculated from the difference in mass between the sample in its container(s) when wet and when dry. Any inaccuracy in the mass of the containers will not, therefore, have an effect on the water content determination. This is not, however, true for bulk density.

6.3 Likely Problems with Gravimetric Sampling

The simplicity of gravimetric sampling belies the difficulty in obtaining good results. There are numerous sources of error in the process, some of which are discussed in the following text.

6.3.1 Errors in the volume of the sample

This is probably the most difficult to eliminate. Errors in the volume of soil sampled may arise from several sources:
1 Compaction of the sample. This was discussed in Section 6.2.2. Recommendations for minimising it have been given and, apart from following them, little can often be done except to reject any sample, which is obviously compacted or where soil has been lost. This is difficult advice to follow when much physical effort and time have been invested in obtaining the sample in the first place!

However, even if the sample is compacted, or some soil is lost, the mass wetness will still be an accurate value. Sometimes, mass wetness measurements can be combined with values of dry bulk density measured independently to calculate volumetric water content values using Equation 5.1.10. Some methods for doing this are described in Sections 6.4 and 6.5. An alternative, related, approach is to derive a factor describing the degree of compaction for a particular sampler design, a particular soil and its degree

of wetness. This can be used, often after the original sampling date, by making independent bulk density measurements compared with those obtained using the original sampler. Some loss of accuracy is inevitable.

2 Stones. These may have several effects.

Firstly, they may compact the sample, as stones are normally not broken by the sampler's cutting shoe. Part of a stone that lies outside the volume defined by the cutting shoe and the height of the retaining sleeve will often, therefore, be included in the sample. It may also have the effect of pushing extra soil in with it. Alternatively, part of a stone may be left out of the sample, which should have been inside, resulting in too little sample material.

Secondly, stones occupy some volume in the soil. From the point of view that volumetric water content is the total water content within a volume of space, then this must include the stone fraction. However, stones are often quite large compared with the volume taken by a sampler, leading to greater variability in results. This is discussed further in Section 6.3.3.

3 Difficulty in sampling. Hard, stony, sticky, very wet or dry soils often make driving the sampler into the soil difficult. To ensure that the full volume of soil is collected, it is important to ensure that the sampler is driven the full length of the retaining sleeve plus the distance from the bottom of the sleeve to the cutting edge.

4 Sampling from depth. If samples are needed at some depth from the surface, say more than 1 m, then it is likely that access to the profile will need to be *via* a predrilled auger hole. This introduces its own difficulties, as it is impossible to see what is happening as the sampler is driven into the soil. Loose soil at the bottom of the auger hole should be removed before sampling, but it is often difficult to check that this has been done completely. Driving the sampler a little further than the desired sample height plus cutting shoe depth and discarding the top of the sample will help such a situation. Removal of the sampler from the soil at the bottom of a small hole may also be difficult, as the soil inside the sampler may not break away cleanly from that beneath, resulting in too little sample being collected. A clean break of the soil can often be achieved by rocking and rotating the stem of the sampler.

5 Non-cohesive soil. This often results in the sampler failing to retain all of the sample. Some samplers (usually those designed for sampling at great depth using a drilling rig) have a 'core catcher', which is a series of flexible or hinged flaps mounted just above the cutting edge. As the sample enters, it pushes the flaps back into an upright position allowing the sample to pass, but on removal from the soil, the weight of the sample pushes the flaps back into a horizontal position, preventing its loss.

There is no single solution to these problems, and rejection of dubious samples may be the best plan. This may lead to a bias in the results, as only data for samples having those properties suitable for sampling will be retained. Some hints for assessing the quality of samples is given in Section 6.3.4.

6.3.2 Loss or gain of water

Water may be lost from the sample by evaporation or gained by accidental contact with water at various stages of the sampling or processing procedure. Smaller and drier samples are more vulnerable to this as there is clearly less water in the sample in the first place, so water lost or gained is a greater proportion of that present. In addition, smaller samples have a greater ratio of surface area to volume than large ones, so there is proportionately more surface through which water can be exchanged. Samples of volume smaller than 100 mL are not, therefore, recommended.

To minimise the chance of water loss during and after sampling, the two most important precautions are shading and speed. Shading of the sample from direct sunlight reduces the energy available to evaporate water from the sample surface. A large umbrella or portable shelter may be the best solution in this instance. The less time that the sample is exposed to air, then the less opportunity there will be for water to be lost by evaporation. Samples should, therefore, be sealed and transferred to storage containers as quickly as possible. Sample sleeves with end caps taped on provide an excellent barrier to water loss and save time in the field. However, water may still escape from the sample, so they should be stored in a sealed plastic bag inside a cool, closed box. Water vapour diffuses through thin plastic bags surprisingly quickly so that transportation to the laboratory for weighing and processing should be done promptly.

Gain of water is most likely to occur from rainfall coming into contact with the sample. The same umbrella or portable shelter will help to prevent this happening. Very dry samples may absorb water from the atmosphere. The same precautions that prevent evaporation will also protect the samples from gain by absorption.

6.3.3 Stones

Problems caused by stones and their effect on obtaining a good, known-volume sample have been discussed in Sections 6.1.3, 6.2.2 and 6.3.1. There are, however, other aspects of stones in soil, which need to be considered.

Most stones are not porous and so will not, themselves, hold water. However, this is not always the case and some of the water in the soil may be held inside the stones. This is particularly important if stones are separated out from the fine material before drying (see the following text).

For most purposes, the stones must be regarded as forming part of the soil and included in all calculations. Some workers appear to regard only the fine fraction as constituting soil. This is erroneous and stones should be regarded as large soil particles.

In soils containing a significant fraction of stones, particularly where these are large, a statistical (as well as a practical) sampling problem may arise. If a sufficient number and variety of stones is not collected by whatever sampling method is employed, then a proper REV will not have been taken. One approach is to separate the stone fraction from

the fine material by passing it through a coarse sieve (usually 2 mm, but a larger size may be justified in many cases) and to determine the water content of the fine fraction alone (as well as the water content of the stones themselves, whose volume will also need to be measured). A separate exercise can then be mounted to take much larger samples to determine the stoniness of the soil and arrive at an average volume fraction of stones. The volumetric water content of the soil as a whole is then given by

$$\theta = f_f\theta_f + f_c\theta_c, \qquad (6.3.1)$$

where
f_f is the volumetric fraction of fine material;
θ_f is the volumetric water content of the fine material;
f_c is the volumetric fraction of stones, and
θ_c is the volumetric water content of the stones.

Measurement of the volume of an irregular stone is best done using Archimedes' principle. The stone is weighed in air and then suspended in water by a fine thread or wire. The difference in mass is the volume of the stone multiplied by the density of water (1000 kg m^{-3}). Porous stones must be coated in an impervious material, such as varnish, saran resin or a plastic resin before immersion. Provided that the water content of the stone has been measured previously and the coating has dried properly, weighing the coated stone in air and when immersed will ensure that the mass of the coating material will have no effect on the result, although the thickness of the coating will have a very small effect. The mass of the stone (dried on a paper towel or similar) should be checked after the procedure to ensure that no water has penetrated the stone through any holes in the coating.

6.3.4 End to end record keeping

Good record keeping is vital in any kind of monitoring or research activity. Because of the number of stages and possibly different personnel involved, this is particularly true of the gravimetric method. It is recommended, therefore, that a standardised record keeping procedure be adopted and that all records relating to a particular sample are kept on one sheet of paper. A suitably laid out form should also make it easy to transfer the results directly to a spreadsheet for electronic calculation and archive storage.

A suggested form is shown in Fig. 6.3. By combining all parts of the operation onto one form, the risk of samples being mixed up or data lost is reduced. Also, notes from one part of the operation, such as difficulties experienced during sample collection, are available to those conducting subsequent parts so that any concerns that may affect the interpretation of the measurements can be taken into account. For subsequent analysis, evaluation and storage, having all the information together is a big advantage, and recording it all on the one original form avoids errors in transcribing information from one piece of paper to another.

The use of a form such as that shown in Fig. 6.3 is suitable for implementation on a spreadsheet. The increasing availability of rugged portable computers and handheld devices makes it possible to enter field data directly into a spreadsheet at the time of sampling. Use of a spreadsheet allows the semi-automatic calculation of results, statistical information and display of graphs that help to evaluate the reliability of the data collected.

In Fig. 6.3, statistics of both water content and dry bulk density have been calculated, including the correlation coefficient between them. A positive correlation coefficient might point to problems with collecting the correct amount of material, since if too little were collected, this would lead to underestimation of both bulk density and volumetric water content. Similarly, too much material would lead to overestimation of both quantities. Negative correlation, on the other hand, especially at high water content, may be understood in terms of change in porosity. Higher bulk density implies lower porosity and, usually, a smaller number of larger pores, which are occupied at high water content. Both sets of data shown in Fig. 6.3 have relatively high water content, so a negative correlation may often be expected, although there are many circumstances where this would not be the case.

The graph of the second set, however, shows one point (circled), which appears to be inconsistent with the others, having both low volumetric water content and low dry bulk density, suggesting that some material was either missed by the sampler or lost from the sample during the collection procedure. Removal of this point (see the second set of statistics for this set) produces the expected negative correlation and reduces the standard deviation and standard error of both variables markedly.

In the case of the first set of data, two points appear to be inconsistent with the other four. However, there is no strong evidence to reject these two. It is not recommended that samples should be rejected purely on the basis of inconsistency unless there is strong evidence for over or under collection of sample, such as that in the second set, and it is preferably backed up by field notes documenting a loose or compacted sample or stone causing problems in taking the sample.

6.4 Direct Measurement of Bulk Density

The major problem in measuring volumetric water content accurately is ensuring that the sample volume and hence bulk density is correct. By comparison, it is quite easy to measure the mass wetness. Alternative approaches therefore centre on different ways to measure bulk density. By measuring this separately, many of the stringent conditions to ensure that samples are of known volume are unnecessary. In difficult soils, therefore, the sample could be collected by spade, trowel or auger. There may, however, be more opportunity for the sample to dry out before being put into a tight storage container.

Direct and indirect methods for measurement of bulk density exist. Both measure the wet bulk density of soil, and this must be corrected for water content to obtain dry bulk density.

There is an unavoidable loss of accuracy caused by dealing with two spatially separated measurements. There may also be additional error caused by a change in dry bulk density between two sampling occasions in a swelling soil. It is good practice, therefore, to take the samples for mass wetness and bulk density at similar states of soil wetness if it is not possible to do both at the same time and if swelling or shrinking may be a factor.

Direct methods, like the gravimetric method itself, rely on taking a known volume of soil and weighing it, or alternatively, collecting soil and determining its volume by measuring the size of the cavity left behind. Since the soil collected will not be at exactly the same place as that for the water content measurement, some inaccuracy will result from this cause. To reduce this, it should be taken as close as possible to the water content sample location and certainly at the same depth. If the soil shows strong horizon development, it is also important to ensure that both samples come from the same horizon whose depth may vary from place to place.

If many samples are being collected from the same area, the magnitude of the uncertainties can be both reduced and estimated better by making use of the methods of geostatistics (see Chapter 4).

6.4.1 Large-diameter sampler

Problems with core samplers are caused mainly by the cutting shoe not incising cleanly through the soil or by friction between the core and the retaining sleeve. These are both affected to a considerable extent by the ratio between the perimeter of the cutting shoe and the area and height of the sample. Large diameter and short cores are, therefore, less likely to suffer from problems caused by stones and friction in the retaining sleeve.

One solution to the problem of obtaining reliable bulk density samples is to conduct a separate exercise to collect short, large-diameter cores for this purpose.

All the principles of sampler design discussed in Section 6.1.3 apply to the design of large-diameter samplers.

The method also gives good quality samples for measurement of water content so that both types of data may be collected together. More work is, however, needed to collect the samples, handle them to avoid disturbance and to deal with them in the laboratory so that a smaller number can be collected and processed for the same amount of effort.

6.4.2 Soil removal methods

These are an alternative approach, particularly suited to situations where a constant volume sampler cannot be used because of high stone content, very hard or non-cohesive soil or because a suitable sampler is not available.

In essence, all methods in this class rely on excavation of a quantity of soil from the surface. The soil is collected for subsequent weighing, drying and reweighing in the same way as for core samples. The volume of the excavated cavity is then measured. This is equal to the volume of soil, which was removed. The methods differ in the way in which the volume of the cavity is measured.

Some general remarks concerning these methods are in order:

1 It is very important to ensure that all of the soil from the cavity is collected. Any soil lost will represent an error in the measurement.

2 The cavity must remain intact. If any soil collapses into it, it may reduce the volume by the introduction of 'foreign' soil, or, if it comes from the side of the cavity, the bulk density of the soil collecting at the bottom is likely to be lower than that of the surroundings. In either case, a smaller volume is likely to be measured than would otherwise be the case.

3 These methods are really suitable only for situations where a flat surface can be prepared from which the soil can be removed and so are suitable only for surface and shallow depth sampling. Measurement of both water content and dry bulk density of a known volume of the same soil sample can be obtained using these methods in some very difficult situations, although high accuracy cannot usually be achieved.

4 The sampling of soil usually involves digging with a spade or trowel. This gives more opportunity for loss of material from the trowel or by wind. To minimise this, it is important that a plastic sheet be spread on the ground around the working area to catch any spilt material. If water content is being measured, loss by evaporation (or gain in rainy conditions) is also more likely than by core sampling. Where appropriate, a wind and/or sun shield should also be used.

There are many ways of measuring the volume of the cavity. They fall, however, into two categories – measurement of the volume of material needed to fill the cavity and direct measurement.

The first of these – estimating the volume of material needed to refill the cavity – usually relies on filling the cavity with fine, dry sand or small plastic spheres. The amount of material used to fill the cavity is measured. Clearly, it is important that the material used packs easily to the same bulk density each time. Round-grained, fine sand is better for this than coarser, sharp sand. Small plastic spheres are likely to be even better, as they are smoother. However, they are more prone to being blown by the wind.

An alternative method, which is often easier to implement, is to line the hole with a flexible plastic sheet and to fill it with water. The major problem with this method is in ensuring that the plastic sheet fits snugly in the cavity, that small irregularities are not bridged over and that folds in the plastic sheet do not occupy a significant volume. Thin, flexible and elastic material performs better than thicker, stiffer and non-stretching film. However, it may be punctured too easily by sharp stones, which prevent the film from retaining the water. Some slow leakage could be difficult to detect, so great care must be taken that this does not occur. Sophisticated equipment for

making these measurements accurately is described by Evett (2007).

6.5 Indirect Measurement of Bulk Density: Gamma Ray Probes

The only indirect methods in widespread use rely on the scattering of gamma radiation by the soil. By measuring the amount of scattering or absorption of radiation by the soil from a gamma source in an access tube in the soil, the bulk density of the soil may be estimated.

The most common radiation sources are ^{241}Am and ^{137}Cs. These are isotopes of Americium, an artificial element, and Caesium, which are relatively long-lived gamma ray emitters (^{241}Am has a half-life of 432 years and ^{137}Cs of 30 years). ^{241}Am emits gamma rays with an energy of 60 keV, which penetrate into soil a few cm only, while ^{137}Cs emits rays with an energy of 660 keV, with a useful penetration of a few 10s of centimetres. ^{241}Am is, therefore, useful only for laboratory studies while most field instruments employ ^{137}Cs sources, usually of about 40 MBq. The relatively small size of the source and moderate energy of the gamma rays means that the radioactive hazard is fairly modest, although it is large enough to oblige the user to comply with radiological protection regulations. Radiological protection is dealt with in Section 7.11, which contains an explanation of some common radiological terms in Sections 7.11.1 and 7.11.4.

6.5.1 *Gamma ray scattering*

When one small object collides with another, the first object usually loses some energy and changes its direction of travel. This is known as *scattering*. The predominant scattering process for gamma rays with energy between about 0.3 and 1.02 MeV is *Compton scattering*. A gamma ray is a very high-frequency electromagnetic wave, which interacts with matter through the charged electrons. Unless the gamma ray is of extremely high energy, the electrons shield the nuclei of the atoms extremely well and so the gamma ray only 'sees' the electrons. The amount of scattering, therefore, is proportional to the total density of electrons. This is well related to the density of the material (Section 6.5.5). Compton scattering is fairly easy to understand, as it relies only on the principles of conservation of energy and momentum. This is described as *elastic scattering*. For higher-energy gamma rays, a process of *pair production* is possible, giving rise to *inelastic* scattering. At energies lower than about 0.3 MeV, photoelectric absorption becomes important, which depends very much more on soil chemistry than the Compton effect.

It is usual to use electron volts (eV) as the energy unit in dealing with radiation rather than joules used throughout most of the rest of science. One electron volt is 1.602×10^{-19} J. It is the energy acquired by an electron in moving through a potential difference of 1 V.

Although Compton scattering depends on the electromagnetic interaction of the gamma rays with electrons in the soil, for the purpose of calculating the scattering, we can treat them as particles or *photons*.

A photon has energy, E_γ, of $h\nu$, where h is Planck's constant (6.626×10^{-34} J s or 4.135×10^{-15} eV s) and ν is the frequency of the electromagnetic wave. Frequency is related to the wavelength of the electromagnetic wave, λ, by

$$\nu = \frac{c}{\lambda}, \tag{6.5.1}$$

where c is the speed of light in vacuum (3×10^8 m s^{-1}).

Although having no mass, a photon has momentum of E_γ/c. If we treat the electrons as being effectively stationary and ignore the energy required to release them from the atoms (which is small in comparison with the photon energy), then the situation before and after a collision between the gamma ray photon and the electron is as shown in Fig. 6.4. The incoming photon has energy, E_1, and momentum of E_1/c. The electron has a mass of m but no initial kinetic energy or momentum. After the collision, the photon will have energy of E_2 and momentum E_2/c and have been deflected through an angle θ. The electron will have a kinetic energy of T, a momentum of p and be travelling in a direction at an angle of ϕ relative to that of the incoming photon. Unfortunately, we cannot ignore relativistic effects, which means that the familiar relations of kinetic energy being equal to $\frac{1}{2}mv^2$ and momentum being mv do not hold.

Applying conservation of energy to this case, we obtain

$$E_1 = E_2 + T. \tag{6.5.2}$$

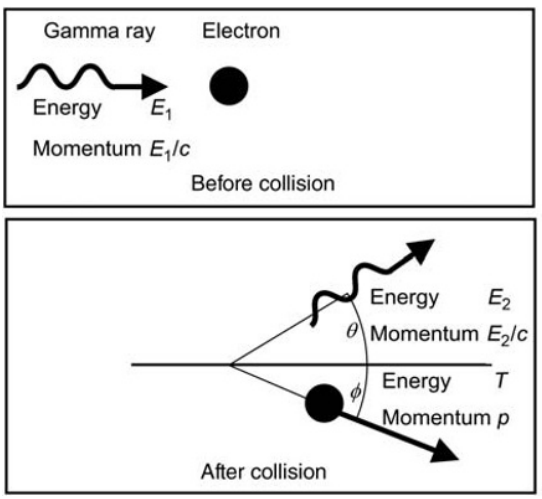

Fig. 6.4 Compton scattering between a gamma ray and an electron.

Conservation of momentum along the direction of travel of the original photon path gives

$$\frac{E_1}{c} = \frac{E_2}{c}\cos\theta + p\ \cos\phi \tag{6.5.3}$$

and similarly at right angles to this direction,

$$\frac{E_2}{c}\sin\theta - p\sin\phi = 0. \tag{6.5.4}$$

The relationship between kinetic energy, T, and momentum for a relativistic particle of rest mass, m, is

$$p^2 = \frac{T^2}{c^2} + 2Tm. \tag{6.5.5}$$

These four equations contain five unknown quantities: E_2, T, p, θ and ϕ. Any four of these can, however, be expressed in terms of the other one. For the present purpose, we will express the results in terms of θ, the angle through which the photon is scattered. Application of simple algebra then leads to

$$E_2 = \frac{E_1 mc^2}{mc^2 + E_1(1-\cos\theta)}. \tag{6.5.6}$$

The amount of energy lost by the gamma ray, therefore, depends on its initial energy and the angle through which it is scattered. This is the basis of *electronic collimation*, in which photons suffering scattering through large angles can be rejected by counting only those that retain most of their original energy without the need for mechanical barriers. For a high-energy photon, a larger proportion of its energy is lost at any particular scattering angle, θ, than for one of lower energy. Electronic collimation is, therefore, more effective for the higher-energy gamma rays of ^{137}Cs than the lower-energy ones of ^{241}Am.

6.5.2 Detectors

Two types of ionising radiation detector are in common use for gamma ray scattering in soil.

A *proportional counter* consists of a tube filled with a gas, which can be ionised by particles passing though it. A central wire is maintained at a high positive voltage (the *anode*) with respect to the outer metal case (the *cathode*). When ions are produced in the gas, the electrons are attracted towards the anode and the positively charged ions to the cathode. If the voltage is high enough, the momentum gained by these ions is enough to cause further ionisation of other atoms in the gas, which multiply in a cascade effect called an *avalanche*. By adjusting the voltage on the tube correctly, the size of each pulse as the ions and electrons reach the electrodes is proportional to the number of ion pairs produced and hence the energy of the particle.

A *scintillation detector* consists of a material that produces flashes of light when an ionising particle passes through it and a light detector to record the flashes (see Appendix 6.A).

Both proportional counters and scintillation detectors need high voltages (hundreds of volts) to work. Proportional counters are cheaper and more robust but less sensitive. They also need a longer time to recover between each pulse, leading to an appreciable *dead time*, which usually needs to be corrected for when calculating results.

6.5.3 Transmission gauges

Gamma ray density meters fall into two types: *transmission* and *backscatter*.

Transmission gauges measure the amount of radiation transmitted between a source of gamma rays (usually a small capsule containing ^{137}Cs) and a detector. In transmission mode, the detector is usually a scintillation counter, which allows the user to select the energy of gamma rays that will be detected. Because the soil must be between the source and the detector, transmission gauges for field use usually use two parallel access tubes. The source is lowered down one of these and the detector down the other, usually (but not always) to the same depth. The count rate at the detector is measured when the apparatus is in the soil and when it is out of the soil with just air between the source and detector. The ratio of the two is the amount of absorption by the soil.

The arrangement is depicted in Fig. 6.5, where the radiation passes from a radioactive source through a thickness of soil to a detector.

Figure 6.6a shows a typical intensity profile for a ^{137}Cs source and that resulting from scattering as it passes through a thickness of absorbing material. It can be seen that the intensity at the peak energy of the source is reduced, while there is much greater intensity at lower gamma ray energies. At each scattering event, the energy of the gamma ray is reduced, as explained previously, so that the number of gamma rays passing through the soil suffering no or little scattering becomes smaller, the greater the thickness of material that is traversed.

For radiation of a particular energy, the intensity, I, measured at the detector after passing through a thickness of soil, d, is given by

$$I = I_0 e^{-\mu d} \tag{6.5.7}$$

or

$$\mu = \frac{\ln(I_0/I)}{d} \tag{6.5.8}$$

where

I_0 is the intensity of gamma rays detected in air *at the same source–detector spacing* and

μ is the absorption coefficient of the soil and is very nearly proportional to its density (Section 6.5.5).

There are many difficulties associated with transmission gauges. These include:

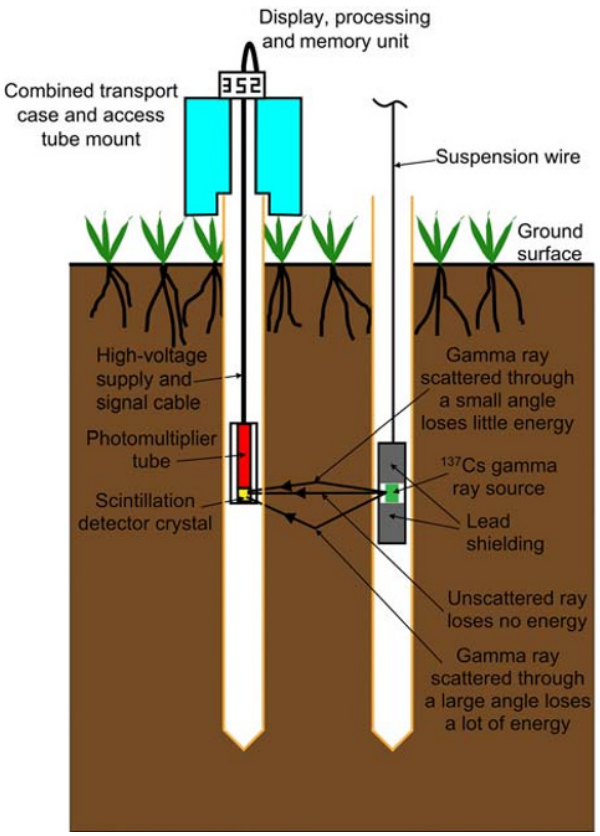

Fig. 6.5 Schematic of a gamma ray transmission gauge. (*See insert for colour representation of the figure.*)

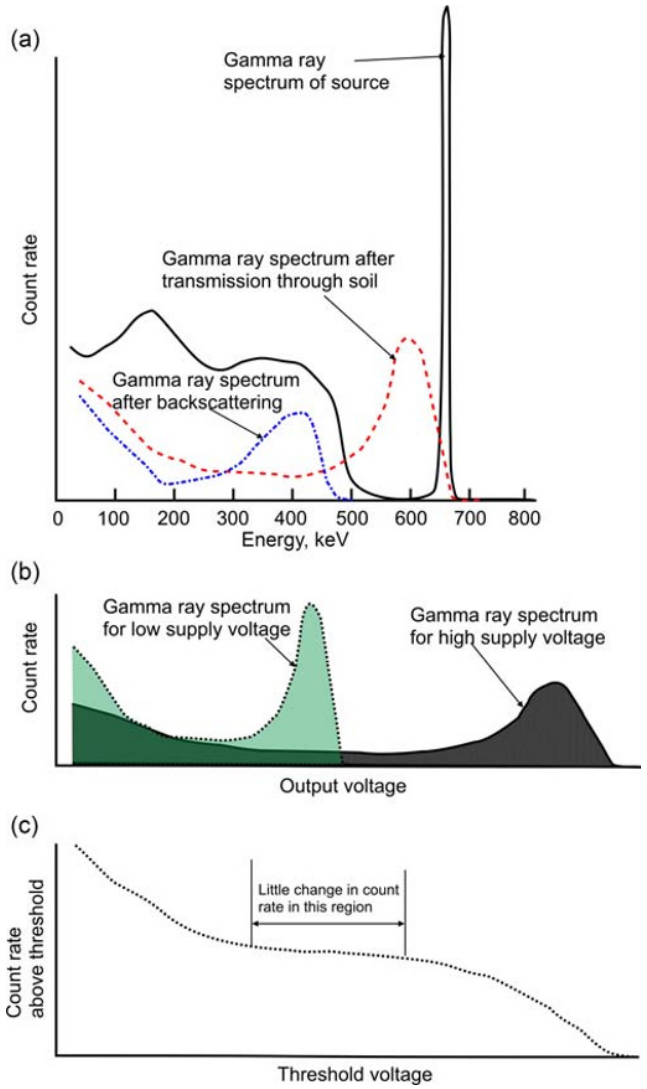

Fig. 6.6 (a) ^{137}Cs gamma ray spectrum of the source alone: after passing through a thickness of soil and after backscattering to a detector near the source. Note that the peak is both broader and lower and occurs at a lower energy for the transmitted and backscattered spectra. (b) The effect of different supply voltage to the photomultiplier. The area under both the light- and dark-shaded areas is the same. (c) Integrated count rate as a function of threshold voltage for the higher supply voltage curve in (b).

1 Temperature and voltage stability. The scintillation detector is very sensitive to temperature changes. It gives a pulse output for each gamma ray detected. The pulse voltage is proportional to the energy of the gamma ray. However, the size of the pulse also depends on the temperature of the detector and the supply voltage to the photomultiplier tube. Transmission gauges usually detect gamma rays within a very narrow energy band close to the peak energy emitted from the source. If this detection band moves relative to the peak source energy, because of temperature changes, supply voltage fluctuations, etc., then erroneous results occur. Various schemes have been tried to overcome this problem. One uses a very small auxiliary source close to the detector and a two-channel data acquisition system, one set at the auxiliary source peak and the other measuring at the energy of the main source. An automatic servo system keeps the gain of the amplifiers such that the secondary data channel is at the maximum of the auxiliary source peak, and hence the gain of the primary data channel can be kept at the correct level to track the peak of the main source.

2 An easier strategy is to set the *window* of the detector electronics fairly wide so that there is little change in count rate even if the peak moves within the window. A window is the range of gamma ray energies that the electronics records. This has two disadvantages. One is that it reduces the sensitivity of the detector. When gamma rays are scattered by soil particles, they lose energy rather than being completely absorbed (see the following section). Having a wide window on the detector means that many of these scattered rays are detected, which otherwise would have been rejected. The second problem is that, with a wider window, it becomes more difficult to define the volume of soil contributing to the observation. This is because the more energy lost in a scattering event, the greater the range of angles that the gamma ray can be scattered through. Low-energy rays may therefore come from parts

of the soil well away from that directly between the source and detector. They may also have undergone two or more scattering events on their journey.

3 Temperature stability is also clearly a problem when comparing count rates in the soil, where, once the apparatus has settled down, temperature is usually sufficiently constant over the time needed to take a reading. The outside air is, however, almost always at a different temperature from that of the soil and fluctuates much more.

4 Tube emplacement. It is important that the distance between source and detector be known. This is partly because μ is calculated according to Equation 6.5.8 so that the proportional error in measurement of μ, and hence that of the soil density, will be the same as that of d. However, the intensity when there is no absorber between the source and detector, I_0, varies according to the inverse square of the distance between the two, which compounds the error in measurement of μ.

5 For these reasons, it is important to install the tubes as nearly parallel as possible using a rigid jig to guide them. In many soils, it is very difficult to keep them parallel and so to know well enough how far apart they are, particularly at depths of 1 m or more. Excavation of the tubes at the end of the experiment would allow the parallelism to be checked and data to be corrected retrospectively if necessary.

6 Gaps around the tubes. These have a similar effect to that of non-parallel tubes in that the amount of soil between the source and detector is reduced in an unknown way.

For these reasons, the use of gamma ray transmission is almost never used for one-off measurements of soil density using two parallel tubes. It can, however, be used to track changes in bulk density or of water content over time, where the effort of installing semi-permanent tubes and the investment in overcoming the temperature problems can be justified.

Close to the surface, however, many of the difficulties described above are reduced. In road construction, gamma ray transmission density gauges are very common to check the degree of compaction of the subgrade. These gauges use a small ^{137}Cs source, which can be lowered to a maximum of about 0.3 m in a small hole in the ground. The detector, usually a Geiger counter, is contained within the housing of the gauge, which is placed on the ground surface. The measurement is made between the subsurface source and the detector at ground level. By measuring count rate with the source at a series of depths, a measurement of the variation of density in the shallow subsurface can be obtained. These gauges usually also incorporate a neutron source and detector to measure water content. Knowledge of the water content is usually needed both for its own sake and to correct the density reading. These gauges are described further in the next chapter, Section 7.2.1.

6.5.4 *Backscatter gauges*

Backscatter is a more common method for bulk density measurement at depth. This requires just one tube, which

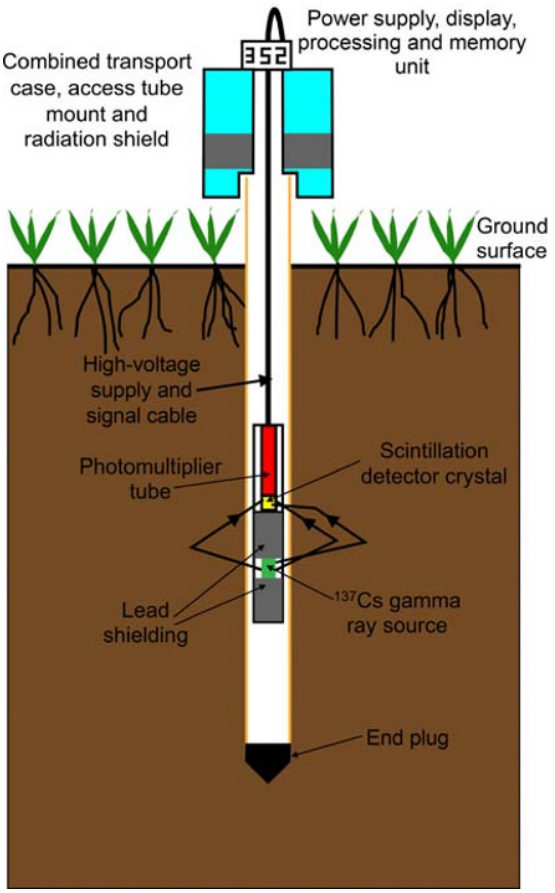

Fig. 6.7 Schematic diagram of a gamma ray backscatter gauge. (*See insert for colour representation of the figure.*)

can often also be used for measurement of water content by a neutron probe. The probe used normally has a gamma source (^{137}Cs) mounted about 150 mm beneath a detector as shown in Fig. 6.7. Lead shielding between the two minimises direct passage of gamma rays from one to the other.

The detector may be of the scintillation type or a Geiger or proportional (gas tube) counter. The mode of operation is partly by transmission and partly by scattering. Scattering is always through an appreciable angle, and so energy must be lost by the gamma rays as they pass from the source to the detector. Because of this, the location and weighting of the volume sampled by the probe is difficult to define but probably does not extend more than 75 mm from the source – detector axis, with 50% of the contribution from within 25 mm (Campbell & Henshall, 2001). Poor access tube installation, leading to gaps between the access tube and the soil, or cavities left behind by stones, are therefore likely to have a serious effect on the results. On the other hand, using a gamma backscatter gauge in association with a neutron probe (see Chapter 7) will reveal places where there may be cavities, aiding the interpretation of anomalously low readings. The location of the centre of the zone sampled is closer to the detector than the source because

high-energy photons have a longer range than lower-energy ones. Therefore rays scattered close to the detector are more likely to reach it than ones scattered close to the source.

Proportional counters and scintillation detectors give output pulses whose magnitude depends on the energy of the incoming gamma ray. The spectrum of energies looks something like that shown in Fig. 6.6a. With proportional counter-type instruments, the threshold level will probably have been set by the manufacturer. Scintillation detector-based instruments usually require the user to set up the operating conditions themselves, as the detector and power/counter unit are often bought separately.

There are two basic adjustments involved for scintillation detector instruments – the voltage applied to the photomultiplier tube (usually in the range 500–2000 V) and the window/threshold adjustment, which determines which pulses will be counted. Changing the input voltage affects the magnitude of the output pulses as shown in Fig. 6.6b. However, the two graphs shown both contain the same number of pulses in the shaded area: that for the higher input voltage is merely a stretched-out version of that for the lower input voltage.

The first decision, therefore, is to choose an input operating voltage. Photomultiplier tubes will not work below a certain minimum input voltage. Using a much higher voltage than necessary is not advised, as the risk of insulation breakdown in the cables and leakage current between terminals affected by damp increase rapidly with increasing voltage. If the manufacturer recommends a certain voltage, then it is best to adopt this. If not, then a voltage comfortably above the minimum that produces reliable operation of the photomultiplier should be chosen. If the photomultiplier will operate at a minimum voltage of 500 V, then it would be sensible to choose 550 or 600 V as the normal operating voltage. A well-designed power unit should not present any significant risk from electric shock, as the current needed to operate the photomultiplier is only a few microamps, so there is no need for the power supply to deliver any more.

The next decision is to choose the *threshold voltag*e, beneath which pulses will be rejected and above which they will be counted. It can be seen from Fig. 6.6a and b that there is a distinct valley in the graph of output pulse frequency *v* pulse height. It is found, in practice, that the number of pulses at low voltage varies greatly, as these arise from a variety of sources – multiple scattering events, circuit noise, etc. The actual shape of the graph will vary according to a number of factors, chief of which are temperature and the nature of the medium in which the probe is embedded. A threshold voltage for a given input voltage must, therefore, be chosen experimentally so that the effect of the curve shape varying in different media is minimised. Because of the effect of soil chemistry on photoelectric absorption, it is also important to exclude lower-energy photons to avoid this influence (Pirie *et al.*, 1968).

Most units for use with photomultipliers contain both an adjustable voltage power source and a *pulse height analyser*, which can be adjusted to count pulses only within a particular voltage range. Some have two or more channels, which can do this simultaneously for different ranges, but only a single channel is needed for this application. Most can be set to count all pulses above a particular level (*threshold*) or within a range of voltages (*window*). *Threshold* is the appropriate setting for use with a backscatter gauge. If the pulse height analyser does not have a *threshold* setting, then setting the upper window voltage level slightly higher than the cut-off where no more pulses are recorded, as shown in Fig. 6.6c, can simulate it.

It is worth using the *window* mode, with a fairly narrow window, to explore the shape of the output from the photomultiplier. This should be done in a variety of materials whose densities span the range expected to be encountered. The threshold can then be set to a value which minimises the error over this range. Some pulse height analysers have a setting for the lower window voltage level and one for the window width, while others require the upper and lower edge of the window to be set separately.

Using the *threshold* setting, the area under the curves in Fig. 6.6b becomes the total number of pulses above the threshold as shown in Fig. 6.6c. It can be seen that, if the actual voltage of the pulses change as a result of changes in input voltage or temperature, then there is little change in total pulse counts. There will, however, be a difference in total counts between two densities of material.

6.5.5 Calibration and density calculation

The gamma ray scattering process involves interactions with the electrons in the material through which the gamma rays pass. It therefore measures the total number of electrons in a volume of material rather than the density *per se*. Fortunately, there is a very good relationship between the two for most substances in soil.

The number of electrons in an atom is equal to the number of protons. This is called the *atomic number*. For most elements that make up soil, the number of protons is equal to the number of neutrons and, since neutrons and protons have very nearly the same mass, the atomic number is half the *atomic weight*. The electron density, therefore, is proportional to the density of the material. The main exception to this is hydrogen, which has one proton and no neutrons. The water molecule (consisting of one oxygen atom, atomic number 8 and atomic weight 16, and two hydrogen atoms, atomic number 1 and atomic weight also 1) therefore has a molecular weight of 18 and 10 electrons. It therefore appears to be about 10% heavier than would be the case if it had a 2:1 ratio of mass to electrons. This is sometimes referred to as the *Z/A ratio*. By measuring water content at the same time as using the gamma probe, a correction can be applied to take this into account.

Whereas the relation between wet and dry bulk density is

$$\rho_d = \rho - \theta, \tag{6.5.9}$$

the apparently higher density of water as detected by the gamma probe means that the appropriate equation to use is

$$\rho_d = \rho^* - 1.11\theta \tag{6.5.10}$$

where ρ^* is the apparent wet density of the soil obtained from the calibration.

Calibration can be performed in the laboratory or the field.

For laboratory calibration, a number of samples covering the range of density expected to be encountered are needed. For the backscatter gauge, these should be packed carefully into a drum, which has an access tube of the same diameter and material as used in the field installed through its centre. To avoid disturbance from surrounding objects and also to protect the operator from radiation, the size of the drum should be at least 600 mm diameter and 600 mm high. To avoid complications caused by water movement and also corrections for the hydrogen Z/A ratio, it is best to use dry materials, which need not be soils. Water, cement, sand and solid materials (e.g. plastics) may be used and can provide permanent standards to allow convenient recalibration over time to correct for the effects of radioactive decay of the source and change in sensitivity of the detector. This will normally be needed at only one density, however.

Calibration in the field has the advantage that it is performed on the same or similar materials as the calibration will be applied to. However, obtaining accurate samples of soil from the zone that the probe measures is often difficult, as has been described previously, and there will almost always be a significant amount of scatter in the results as a consequence. Apart from the Z/A effect, the interactions are generally well understood and so laboratory calibration is usually both more accurate and economical.

The exact functional relationship between count rate and density depends on the details of the geometrical arrangement of the probe construction and size and material of the access tube. Greacen and Hignett (1979) and Hignett *et al.* (1980) found that a calibration for their NEA probe could be described well by a linear equation given by

$$\rho_d + 1.11\theta = 2.60 - 1.61(\pm 0.068)\frac{R}{R_w} \tag{6.5.11}$$

where
R is the count rate recorded in the soil and
R_w is the count rate recorded in a drum of water.

For values of ρ_d of 1500 kg m^{-3} and θ of 0.3, this implies an uncertainty in the wet density of soil, ρ, of about 70 kg m^{-3}.

Cross (1983), however, working with a Nuclear Enterprises probe over a wider range of densities, found that a linear calibration curve was not adequate and that a relationship given by

$$\rho_d + 1.11\theta = 3.29\left(\frac{R}{R_w}\right)^{-1.21} \tag{6.5.12}$$

with a correlation coefficient of 0.97 explained his data, implying an uncertainty in wet density of about 100 kg m^{-3}.

It seems that over a limited range of density, a linear calibration may well be adequate, but that if the probe is required to work over a wider range of soil densities, a non-linear calibration is needed.

6.6 Conclusion

Although simple in concept, obtaining an accurate and representative value for the volumetric water content of soil presents several problems. The biggest source of error is in knowing the volume of a sample. Either a large amount of effort is needed to ensure that samples of accurately known volume are collected or bulk density must be measured separately by direct or indirect methods. An awareness of the difficulties and limitations of the various techniques available will go a long way to ensure that the reliability of results is as high as possible, while also giving a realistic assessment of the confidence that can be placed on the results.

Appendix 6.A Scintillation Detectors

Scintillation detectors consist of a *scintillating material* and a light detector. When an ionising particle enters the scintillating material, the energy lost is converted to light. Provided that the scintillator is large enough, the amount of light produced is proportional to the particle's energy. The detector records the light flashes produced as particles enter the scintillator. To ensure that as much light as possible is detected, all of the scintillator, apart from the window of the detector, is surrounded by reflective material. An *optical coupler* is also used to ensure that light is not lost by reflection at the interface between the scintillator and detector. This is a viscous liquid of similar refractive index to those of the scintillator and the window and ensures that there are no air interfaces between the two, which would reflect rather than transmit the light. The complete assembly must be enclosed in a light-tight enclosure to prevent any ambient light from reaching the detector, which would swamp the signals from the scintillator. Both the reflective material and the enclosure are made as thin as practicable to minimise absorption of the gamma rays.

Scintillation detectors used in gamma probes for soil density work usually use sodium iodide crystals doped with a small amount of thallium [NaI (Tl)] to detect the gamma rays and a *photomultiplier* as the detector. A gamma ray excites electrons in the crystal to a high-energy state. These then fall back to their ground state, emitting a pulse of light as they do so (this is scintillation). The intensity of each

flash is proportional to the energy of the original photon. A 25 mm diameter × 25 mm high crystal is usually sufficient to ensure capture of almost all gamma rays. One of the flat faces of the crystal is mounted on the end window of the photomultiplier, which is of a similar diameter.

This window has a light-sensitive coating on the inside, called a *photocathode*, which converts light into electrons by the *photoelectric effect*. These are attracted by an electrical field towards the first of a series of *dynodes* whose surface material produces several more electrons for each one impacting on it. These electrons are then attracted towards second, third, etc. dynodes, each time multiplying in numbers in a cascade. Typically, there will be about ten dynodes and the total current gain as a result of electron multiplication may be 1,000,000 or more.

In operation, a voltage of several hundred volts is applied to the last dynode, while the photocathode is maintained at ground potential. A series of resistors forms a *dynode chain* and connects successive dynodes together to maintain an accelerating potential between each one, as illustrated in Fig. 6.8, which shows both the physical and electrical arrangements of a scintillation detector.

The number of secondary electrons liberated at each dynode depends on the voltage between them in a non-linear manner so that the amplification of the photomultiplier increases faster than the voltage applied. This makes the size of pulses from the scintillation counter quite sensitive to the supply voltage, and so to measure the energy of incident gamma rays, the voltage must be very well regulated. Scintillation detectors are also very temperature sensitive, making it necessary to keep the temperature stable or to employ sophisticated methods to track an emission peak.

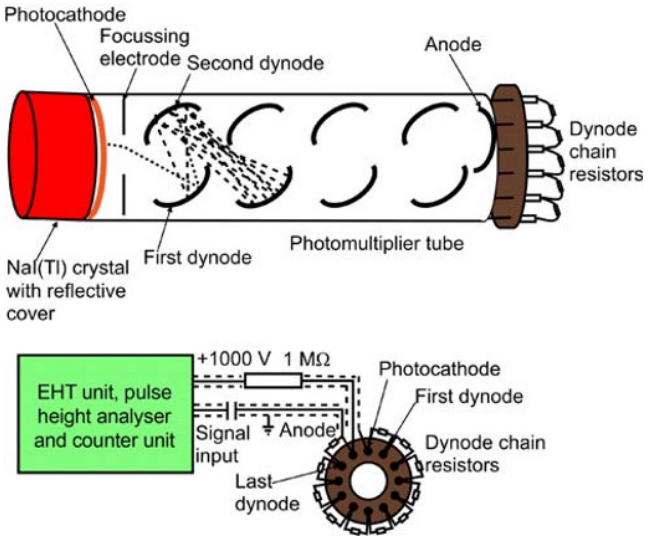

Fig. 6.8 Construction and wiring arrangement of a scintillation detector.

Scintillation detectors are very sensitive devices, capable of detecting particles with great efficiency at high repetition rates. They are, however, delicate and expensive. Great care is therefore required when transporting them to avoid damaging the photomultiplier. For this reason, some manufacturers choose to use solid-state light detectors or proportional counters, which are less efficient, as a substitute for the complete scintillation detector.

More information on photomultipliers can be found in publications by two of the major manufacturers (Burle Industries Inc., 1980; Hamamatsu, 2006).

7 Neutron Scattering

Although gravimetric water content determination is the reference method, it has many disadvantages, several of which were described in Chapter 6. The greatest disadvantage is probably that it is destructive. Not only does repetitive sampling to follow water content changes over time cause major damage to the site, it is also impossible to observe those changes at the same place. The practicalities of the sampling procedure mean that repeat samplings must be no closer than about 0.3 m apart for surface samples and at least 1 m apart for deeper samples. Spatial variability and the inherent inaccuracies in the method mean that differences from one location to another are often much larger than the change in soil water content between sampling occasions. Increasing the number of samples taken on each occasion rapidly becomes prohibitively expensive as well as more destructive.

A non-destructive method which can make measurements possible at the same point repeatedly would, therefore, offer many advantages. It would be even more valuable if the effort required were significantly less than that associated with the gravimetric method. The neutron probe method is one such non-destructive, *in situ* and relatively easy method.

Neutron probes were first used in the late 1940s (Brummer & Mardock, 1945; Pieper, 1949; Belcher *et al.*, 1950) and gained widespread use through the 1950s, 1960s and 1970s as equipment became more portable, reliable, lower power and relatively cheaper. Concerns over the use of radioactive materials and the consequent tightening of usage regulations have made many workers nervous about these devices, and they are no longer used in some countries. They are, however, still in widespread use worldwide and, for many purposes, there is no adequate alternative. Moreover, a description of neutron probe use serves as a useful introduction to other indirect methods.

7.1 Principles of the Method

The neutron probe measures, primarily, the hydrogen density of the soil by detecting the number of slow neutrons produced through collisions by fast neutrons with hydrogen nuclei. Except in a few exceptional cases, the water fraction contains almost all the hydrogen in soil. Even where significant amounts of hydrogen are found in, for instance, organic matter, this rarely changes more than a negligible amount with time; and hence changes of water content can be followed, even if the absolute quantity is uncertain. Monitoring changes over time is the most common use of the device, and so uncertainty in the absolute water content is not usually a great disadvantage.

The principal components of a neutron probe are a *source* of fast neutrons, a *detector* of slow neutrons, a *scaler* to count the number of slow neutrons detected and a means of positioning the source and detector at the required depth.

7.1.1 Basic theory of operation

When a neutron of mass m and velocity v collides with another subatomic particle of mass M, there is usually a transfer of energy from one to the other. Compared with the energy of a fast neutron, nuclei of atoms within the soil may be regarded as effectively stationary. In such a collision, the neutron loses some energy, while the other particle gains the same amount. These are called *elastic* collisions, since kinetic energy is conserved. After this, the neutron can collide with further nuclei in the soil, losing some energy each time until it is within the range of *thermal energies*. That is the range of energies characteristic of thermal motion of molecules in the material. These are generally regarded as being smaller than 1 eV, although at normal room temperature the average thermal energy is only about 0.025 eV. Thermal neutrons continue to collide with other particles, but will not lose appreciably more energy in elastic collisions, since they are colliding with particles having comparable energy. However, nuclei of most elements can absorb thermal neutrons in a process called *capture*. These collisions are called *inelastic*, since kinetic energy is not conserved. Most neutrons move well away from the source region, but a few return to it, where they can encounter a slow neutron detector and be counted.

Soil Water Measurement: A Practical Handbook, First Edition. J. David Cooper.

7.1.2 Collisions

For the present purpose, we can assume that conventional Newtonian mechanics applies in elastic collisions and that all the energy and momentum lost by the neutron are transferred to the other particle. The energies involved are much higher than that of the chemical bonds holding molecules together, which are usually a few electron volts, and so the nuclei can be regarded as free to move. Neutrons are uncharged, and so, unlike gamma rays, penetrate easily through the electron shell of an atom. The 'target' particles are, therefore, the nuclei of elements within the soil.

If the mass of the neutron is m and its initial velocity is v, then its kinetic energy before the collision, E, is $(1/2)mv^2$ and its momentum is mv. The kinetic energy and momentum of the target particle, of mass M, before the collision can be taken as zero, as explained earlier. The simplest case is a head-on collision, where the neutron's direction is along the line joining the centre of each particle, as shown in Fig. 7.1. The particles will both move along this line after the collision.

Conservation of energy gives:

$$\frac{1}{2}mv^2 = \frac{1}{2}m{v_1}^2 + \frac{1}{2}M{V_1}^2 \qquad (7.1.1)$$

and conservation of momentum gives:

$$mv = mv_1 + MV_1, \qquad (7.1.2)$$

where v_1 and V_1 are the velocity of the neutron and the target nucleus, respectively, after the collision

The solution for the velocity of the neutron after the collision is:

$$v_1 = \frac{m-M}{m+M}v \qquad (7.1.3)$$

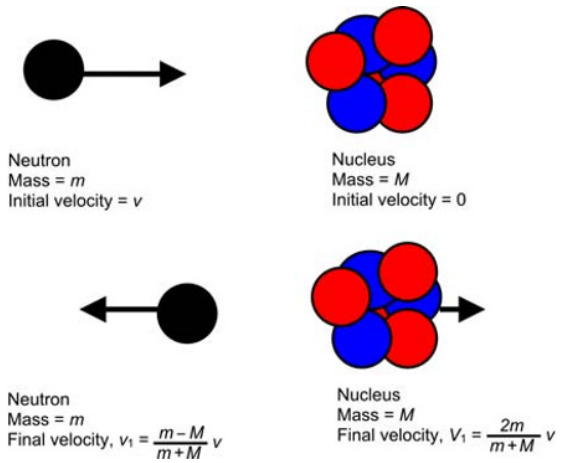

Fig. 7.1 Head-on collision between neutron and atomic nucleus.

and the loss of energy by the neutron, $(1/2)m(v^2 - v_1^2)$, is:

$$E - E_1 = 4\frac{mM}{(m+M)^2}E, \qquad (7.1.4)$$

where E_1 is the neutron's kinetic energy after the collision.

From Equation 7.1.3, it can be seen that, if the mass of the target particle, M, is larger than that of the neutron, m, which is usually the case, v_1 is negative, that is the neutron bounces backwards. This accords with common experience, where a small ball hitting a much larger one will bounce off.

Equation 7.1.3 also shows that when the two have equal mass, all of the neutron's energy is transferred to the target particle and the neutron is brought to a halt. Again, this is in accordance with common experience as, for instance, the balls in a Newton's cradle or on a snooker or pool table. Equation 7.1.4 shows that in a collision with a high mass particle, the neutron loses less energy than when the particle has a lower mass.

Of course, most collisions between a neutron and a nucleus are not head-on, but to one side. This results in the energy loss being less than for a head-on collision. Extension to this case shows that, on average, the neutron loses exactly half the energy of the head-on collision.

Figure 7.2 is a graph of the average energy lost by the neutron as a proportion of its initial energy as the mass of the target increases. It can be seen that the energy lost decreases quite rapidly as the size of the target nucleus increases. The atomic mass of common elements found in soil is indicated in the figure.

The number of collisions needed to reduce the energy of the neutron from that when it leaves the source (average about 4.5 MeV) to thermal energies depends on the energy lost on each collision. Typically, it takes about 19 collisions with hydrogen, 115 with carbon, 150 with oxygen and a much higher number with heavier nuclei. This is compounded by the fact that the *cross-section* for scattering by hydrogen nuclei is appreciably larger than for most other common soil elements. The cross-section is the equivalent area presented by a target nucleus to the incoming neutron

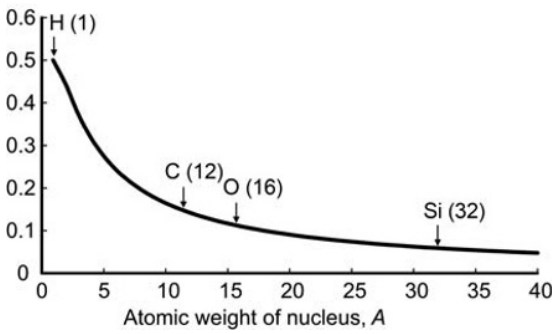

Fig. 7.2 Average fraction of neutron energy lost per collision with nuclei of different atomic mass.

and is proportional to the probability of a scattering event taking place. Although a hydrogen nucleus is expected to be physically much smaller than a multi-nucleon nucleus, in fact, it appears larger than most of these to neutrons, thereby increasing the number of interactions.

As well as these scattering events, there are other types of collision. The most important, from our point of view, are those where the neutron is absorbed by the target nucleus and so disappears from the system. Almost all elements have a certain *absorption cross-section*, defined in a similar way to the scattering cross-section, but some of these are very much larger than others. Absorption cross-sections are very much larger for slow neutrons than for fast ones.

Hydrogen itself has a moderately large absorption cross-section of 0.33 barns (1 barn is $10^{-28}\,m^2$), while that of carbon is 0.0035 barns, aluminium 0.23 barns, oxygen 0.00019 barns, silicon 0.17 barns and iron 2.6 barns. Iron is, therefore, a significant absorber of slow neutrons even in relatively small quantities. Other elements can exert a powerful influence even in trace quantities. Among those important in some soils are cadmium (2,500 barns), boron (770 barns) and gadolinium (49,000 barns) (Nicolls *et al.*, 1977).

A fast neutron emitted from a source in the soil, therefore, suffers a series of collisions with nuclei of elements forming the soil fabric and with hydrogen and oxygen nuclei in the soil water. Collisions with heavier elements slow down the neutron very little. They do, however, tend to keep it close to the source, since the distance between collisions is reduced when there are more scatterers. Thus there is a greater density of neutrons close to the source in a high bulk density soil than in a lower density one. Collisions with hydrogen nuclei cause the neutron to lose, on the average, half of its energy. As it slows down, the probability that a collision with a nucleus will result in its capture increases. Thus high bulk density increases the density of neutrons near the source, but also the higher number of absorbers reduces it. In nearly all practical cases, the former effect dominates and higher bulk density increases the slow neutron density and hence the number detected (Greacen & Schrale, 1976).

7.1.3 Neutron sources

Very few radioactive isotopes emit fast neutrons spontaneously in sufficient numbers to make a practical neutron source for field use. A possible exception to this is Californium-252. This has a rather short half-life of only 2.6 years, which means that the source rapidly becomes too weak to be useful. An ideal source would emit neutrons of a few MeV energy, with no other radiation and have a half-life of 20–40 years. This would ensure that it was as safe as possible, with neutrons the only radiological hazard, have a lifetime long enough to be useful for several years, but present only a small hazard after a century or so. Some basic information on radioactive sources and radiation are contained in Section 7.11.

In the absence of a single isotope, the almost universal choice is a mixture of two isotopes: Americium-241 (^{241}Am) and Beryllium-9 (^{9}Be). ^{241}Am is an artificial isotope, made in a nuclear reactor. It is radioactive, decaying with the production of a relatively soft gamma ray of 60 keV and an alpha particle. The alpha particles collide with Beryllium nuclei to form Carbon-12 (^{12}C) and a neutron. Neutron energies lie in the range 2–6 MeV. The half-life of ^{241}Am is 432 years and, since it contains excess Beryllium, the half-life of the source is almost as long. Therefore, the source is, for practical purposes, stable for a long time, but it is also a radiological hazard for very much longer – thousands of years.

This does not mean that the source may be used indefinitely. The decay of Americium produces gaseous products, which increase the internal pressure in the source and may, in time, rupture it. For this reason, sources in use are produced to very stringent standards, with a double stainless steel wall. Once a source is more than about 15 years old, the conditions for its use become much more stringent, such that, in practice, it cannot be used in field investigations. The source must then be disposed of and replaced. Disposal costs are becoming very expensive, often exceeding the cost of a new source. Moreover, many countries do not have disposal facilities, increasing the difficulty of arranging safe source disposal.

7.1.4 Slow neutron detectors

For field use, a compact detector of slow neutrons is required. Three types are in common use.

A scintillation detector, similar to that used for density measurement by gamma ray scattering (Section 6.7), can be used. Most commonly, the scintillator is glass, doped with a small amount of lithium. When a lithium nucleus absorbs a neutron, it becomes unstable and disintegrates, liberating an alpha particle. The alpha particle produces a scintillation in the glass. Scintillation detectors are, however, expensive and fairly delicate. Their main use is in combined neutron and gamma probes, which measure both density and water content (Section 7.2.3).

Proportional counters containing either $^{10}BF_3$ (Boron trifluoride) or ^{3}He (Helium-3) constitute the other two main types of detector. They both contain a gas, which absorbs neutrons and then emits an ionising particle. In the case of ^{10}B an alpha particle is released (as for ^{6}Li), while the neutron absorbed by ^{3}He results in a proton being ejected. The ionisation resulting from the passage of the charged particle in the detector tube allows the gas to conduct electricity when a potential of a few hundred volts is applied. ^{3}He detectors are sensitive to more energetic neutrons than $^{10}BF_3$ ones and so give higher count rates, allowing smaller neutron sources to be used, typically 37 MBq, rather than 1.85 GBq. However, the output count rate of a ^{3}He proportional counter is more sensitive to the applied voltage and discriminator level used than the $^{10}BF_3$ counter, meaning that the instrument is more likely to

drift over time and more care is needed to avoid this affecting the results. Section 7.11.4 explains the different units of radioactivity.

7.1.5 *Range of neutrons – sphere of importance*

It takes many collisions to bring neutrons down to thermal energies, where they can be detected. In the process, they can travel a significant distance from the source before returning and being counted. From the earlier discussion, it should be clear that this distance depends on the distance between collisions and that the smaller this is, the greater the density of neutrons near the source. Also, neutrons colliding with nuclei close to the source are more likely to return to the detector than those that have travelled further. In wet or high bulk density soils, there are more collisions in this region, and hence its relative contribution to the number detected is greater than in lower density or drier soil.

The result is that the counts recorded by the probe reflect an average water content over a volume which varies in size according to the bulk density of the soil and its water content. Moreover, the contribution of different regions of the soil to this average depends on their distance from the neutron source.

It is usual to define a *sphere of importance*, from which 95% of the counts emanate. Thus, if all the soil outside this sphere were removed, the count rate would still be 95% of that before this happened. The choice of 95% is clearly arbitrary, but reflects the fact that anything outside the sphere of importance will have only a small effect on the counts recorded.

Typically, the sphere of importance has a radius of 150 mm in wet soil (volumetric water content about 50%) and 500 mm or more in very dry soil. This has three consequences.

- The volume over which averaging takes place is quite large. For the sphere sizes just quoted, this is 14 and 520 L, respectively. This reduces the effect of minor gaps around the access tube, down which the probe is lowered, or of inhomogeneities in the soil and helps to make the neutron probe method robust.
- The spatial resolution of the probe is very limited. Steep gradients of water content or sharp interfaces are smeared out. As a result of this, there is little point in collecting data from depths closer together than 100 mm. Further, because the sphere of importance is much larger in dry than in wet soil, the probe responds asymmetrically to a sharp interface in water content. In a dry soil layer, the effect of a wetter layer can be detected progressively from about 500 mm away, while if the probe is in a wet layer, it will respond to the dry soil only when it gets within about 150 mm of it.
- The effective volume over which water content is averaged varies, sometimes very markedly, as the water content of the soil changes over time. See Equation 7.8.1.

7.2 Types of Neutron Probe

Two basic configurations of neutron probe are in common use, depending on whether the probe is used for surface measurements or at some depth in the soil. These are illustrated in Figs. 7.3 and 7.4.

7.2.1 *Surface neutron probes*

The *surface* measurement probe is placed on the ground, with the source and detector both as nearly at ground level as possible and separated horizontally by about 100 mm. Neutrons emitted from the source are scattered within the surface layers of the soil, and a proportion find their way to the detector. The separation distance defines, to some extent, the depths from which scattered neutrons are detected. For larger separation distances, a greater proportion of neutrons scattered deeper in the soil are measured. The region close to the surface between the source and detector positions gives rise to most of the signal, which is some kind of average of soil water content in the upper *ca.* 100 mm. An inhomogeneous distribution of water in this region may give problems in interpreting the data because of the effects described in Section 7.1.5. Usually, a surface probe is combined with a gamma source and detector to measure near-surface density as well as water content (Section 6.5.3).

The most common use for surface probes is in road construction to check on soil water conditions in the road base before applying the surface layers. They are also used in building maintenance to detect leaks in flat roofs by indicating wet areas beneath the surface covering. Surface probes are not used commonly in environmental

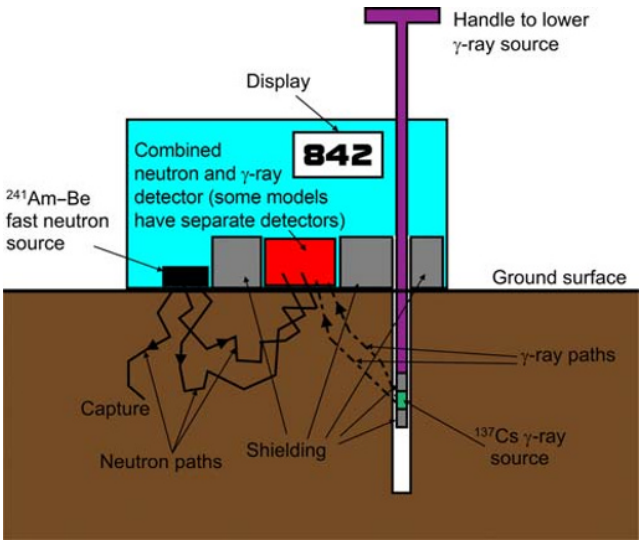

Fig. 7.3 Combined neutron water content and gamma density probe for surface measurement. (*See insert for colour representation of the figure.*)

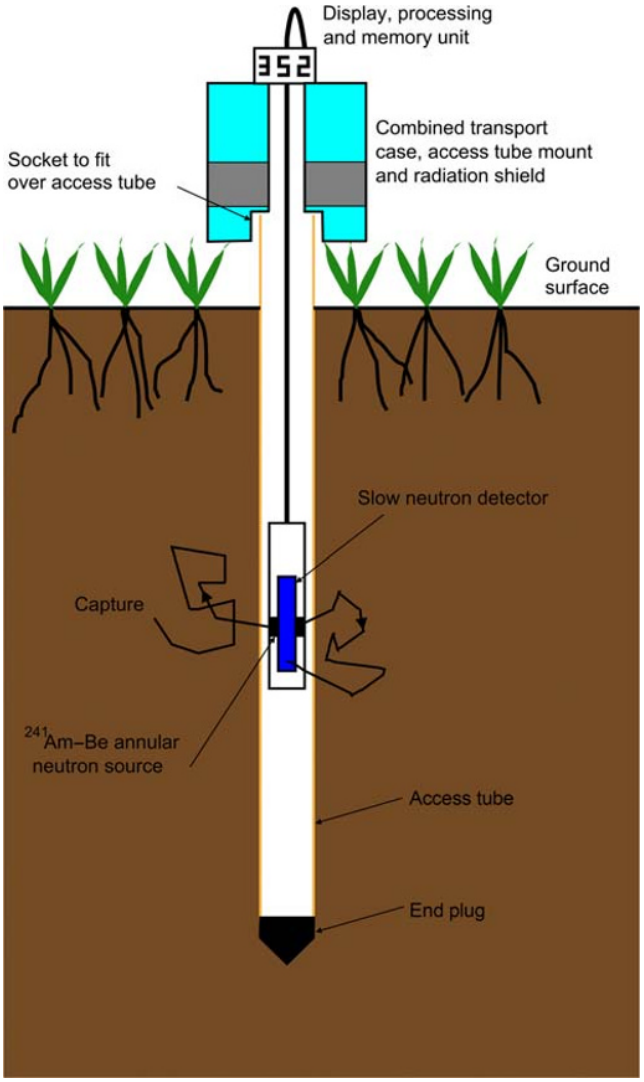

Fig. 7.4 Schematic diagram of depth neutron probe. Hypothetical paths for a neutron which returns to the detector and one captured in the soil are shown. (*See insert for colour representation of the figure.*)

and agricultural applications, which generally require measurements to some depth. The depth neutron probe is not good at making near-surface measurements and a surface probe may, therefore, be a useful complement. However, few organisations carry both types of instrument because of the extra costs of purchase, administration, maintenance and field operations. Possible damage to crops from placing a heavy piece of equipment on the ground, and problems in making good contact with the surface, as well as making repeated measurements at the same spot days, weeks or months apart are additional barriers.

For these reasons, we will not be much concerned with surface probes in the rest of this chapter, although many of the principles applying to depth probes are equally applicable to the surface version.

Fig. 7.5 A neutron probe in use in the field. © NERC (CEH). Reproduced with permission.

7.2.2 Depth neutron probes

The *depth* probe is also a backscatter device. The source and detector are lowered down an *access tube* in the ground to the desired measurement depth and returning neutrons are counted.

Depth neutron probes are, in many ways, similar to gamma ray backscatter density probes (Section 6.5.4). Apart from using a different source and detector, the principal difference is that there is no separation between these two. Ideally, the source and detector would be located at the same place and occupy only a point. In practice, the finite size of practical detectors and sources make this impossible. Some designs (e.g. Bell, 1969) use an annular source placed around the midpoint of the detector tube, as shown in Fig. 7.4, maximising the symmetry of the system and avoiding uncertainty over where the centre of the measurement region is situated. Annular sources are expensive, and the most common arrangement is a source in a much cheaper, small cylindrical capsule mounted on the bottom end of the detector tube. Fortuitously, the finite size of the source and detector, as well as the presence of an access tube, makes the relationship between count rate and soil water content very nearly linear (Couchat, 1967).

The physical arrangement of a neutron depth probe is shown schematically in Fig. 7.4, while Fig. 7.5 shows a probe in use in the field. Figure 7.4 also shows the path of two hypothetical neutrons emitted by the source. One of these undergoes several collisions, moving erratically away from the source (and detector) region. Eventually, it is captured by a nucleus in one of the soil constituents once it reaches thermal energy. The other neutron undergoes a similar series of collisions but, by chance, does not migrate as far from the detector as the first one and is captured by a nucleus in the detector and so can be counted by the probe electronics.

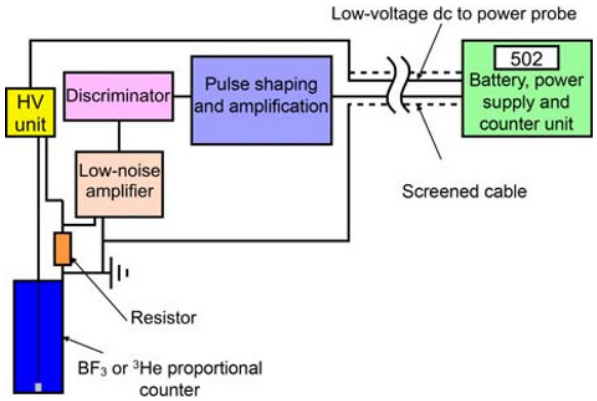

Fig. 7.6 Schematic electronic arrangement of a neutron probe.

Figure 7.6 shows a schematic of the electronic arrangement of a neutron probe. Whenever a slow neutron enters the proportional counter, which needs a few hundred volts to power it, the ionised gas within allows a current to flow briefly between the centre wire and the outside of the tube. This current is converted to a voltage by measuring the potential drop across a small resistor in the high-voltage supply line. This voltage is normally a few millivolts and lasts for about 1 μs. The pulse is amplified and passed to a discriminator, which rejects very small pulses caused by gamma rays from the source, cosmic rays and radiation from the surroundings. Those pulses which exceed the discriminator threshold are counted and divided by the time over which they have been collected by the *ratescaler* to display a count rate. Some units count the number of pulses arriving over a predetermined time; others measure the time taken to accumulate a predetermined number of pulses. Some units give a choice of time or number of pulses.

7.2.3 *Combination neutron and gamma probes*

Both surface and depth neutron probes can be bought combined with a gamma density gauge. Surface probes are normally made as a combination unit. The same detector is used for measuring both gamma rays and neutrons, but a different source is used for each kind of measurement. The arrangement for the surface gauge was described in Section 7.2.1. For the depth gauge, the gamma ray source is placed some 100–150 mm below the detector and shielded from it by lead, as shown in Fig. 7.7, just as in the normal backscatter gauge (Section 6.5.4).

Some design compromises are necessary in a combination gauge. This is principally in the choice of detector, which must be able to detect both gamma rays and neutrons efficiently. Both ^{3}He and scintillation detectors using lithium-loaded glass have been employed. The detector gives very different size pulses for gamma rays and neutrons, so that they are easily separated. The principal difficulty with combination gauges, however, is in the extra weight of two lots of radiological shielding for the sources.

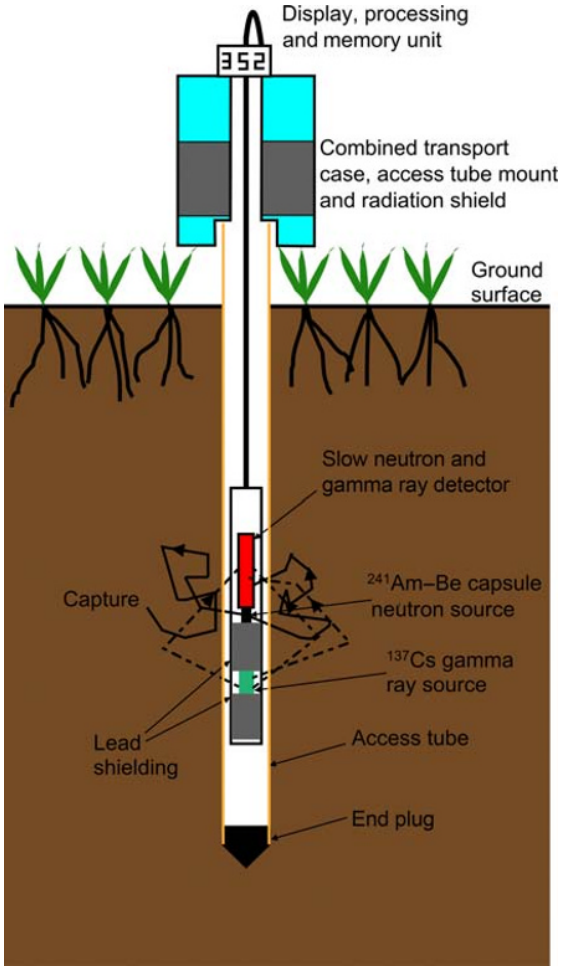

Fig. 7.7 Combined neutron and gamma density backscatter probe. (*See insert for colour representation of the figure.*)

7.3 Access Tube Installation

Depth neutron probes need an access tube installed in the soil, down which the probe can be lowered to the required depths of measurement. The neutron probe, in common with other methods for soil water and density measurement, measures a weighted average of contributions from around the centre of sensitivity of the instrument. The largest contributor to the measurement is the region closest to this point, with decreasing contributions from further distances. The soil immediately around the access tube, therefore, contributes most to the measurement. It follows that compaction of the soil, alteration of its structure or voids close to the access tube, can distort the measurements appreciably. Unfortunately, this is the region most at risk when installing the tube. A further potential problem is that a small gap around the top of the tube may be

created or developed, down which water can flow during rainfall or irrigation. This will make the soil immediately around the tube wetter than in the surrounding soil and lead to overestimation of water content. It is very important, therefore, to take maximum care during tube installation to avoid gaps around the access tube. It is also important to avoid damage to the ground surface and vegetation by, for instance, operators' feet, which will affect the soil immediately beneath differently from the rest of the area.

The ideal installation is one in which the access tube fits perfectly into a hole in the soil, which is completely undisturbed apart from the removal of material to form the hole, and is in an area of ground which is totally representative of the surrounding, untouched area. Unfortunately, this ideal is very difficult and, in many cases, impossible to achieve. Nevertheless, good planning, preparation and care while on site allow most of the problems to be avoided or at least minimised. Many likely problems are site-specific, so that it is difficult to be prescriptive about suitable installation methods to cover all eventualities. Perhaps the most useful advice is to allow plenty of time for both preparation and installation and to use at least two people to install even a shallow tube in an easy situation. The temptation to complete the job as quickly and cheaply as possible and, because the work is heavy, to employ unskilled labour without adequate training or supervision must be resisted. Although the work is undoubtedly heavy, it is also delicate. Both the soil and ground surface are fragile and any vegetation is vulnerable to damage. Any lack of representivity of the site caused by poor instrument installation will be reflected in poor (and probably unknown) quality of data for the lifetime of the study.

7.3.1 Choice of access tube material

The material chosen for the access tube is important. It must be strong enough to withstand the stresses of installation: durable, considering the time that the installation will be in use; economical, readily available locally; and minimise disturbance to neutrons.

Aluminium alloy is usually the most appropriate choice. It is reasonably cheap and widely available, has low neutron scattering and capture cross-sections, is sufficiently resistant to corrosion in most soil environments; and is strong enough to take repeated axial blows during installation down to at least 10 m in a pre-formed hole in most soils. The inside diameter of the tube should be 3–10 mm larger than the outside diameter of the probe; a larger diameter causes errors if the probe is not in the centre of the tube. A wall thickness of about 1.5 mm is sufficient in most situations. A 45 mm (1 ¾") outside diameter tube with this wall thickness is widely available and suitable for use with probes of diameter 38 mm (1 ½"). Extruded tube is considerably cheaper than drawn and quite suitable, despite less stringent manufacturing tolerances.

It is usually preferable to use locally available materials, rather than specially imported ones. For instance, 2" (50.8 mm) aluminium alloy irrigation pipe is often easily available. Using this, rather than importing other materials, saves money, time and problems if more is unexpectedly needed.

Other materials which have been used include stainless or mild steel, polythene, PVC and brass. Iron has a relatively high absorption cross-section for neutrons and so will reduce the count rate obtainable. However, steel is much stronger than aluminium, and stainless steel is highly resistant to corrosion and so may be more suitable in some applications. Plastics all have a high hydrogen content, which thermalises neutrons additional to that by the soil, producing an artificially higher count rate. However, the chlorine in PVC is a strong neutron absorber which reduces the count rate. ABS is widely available as an alternative to PVC and has similar mechanical properties, but does not contain chlorine and so appears to be a better choice. Brass is both expensive and less 'transparent' to neutrons, but may be suitable in some applications.

7.3.2 Access tube construction

Finishing of the top and bottom of the tube must be considered; and if the tube is long, lengths may be joined together.

A closure at the top end of the tube is essential in almost all cases to keep out rain, irrigation water or stray objects. A simple rubber bung is often adequate. Sometimes, greater protection is necessary, to prevent removal of the bung or objects or other substances being put into the tube. An extra sleeve covering both tube and bung usually prevents accidental removal, including by animals. A steel cap, as illustrated in Fig. 7.8a, will, in most cases, prevent deliberate tampering. Both the cap and the access tube have a hole running across a diameter, through which a pin is passed. Casual removal of the pin is prevented by a small padlock, fitted through a small hole on one end of the pin. Padlocks can be bought all having the same key to avoid field staff having to carry a number of different keys. Alternatively, a nut and bolt may be used instead of the pin and lock, although this is less secure. Higher security bolts are available, which can be unscrewed only with a special tool.

It is tempting to leave the bottom of the tube open. Experience shows that this is unwise for the following reasons:

- The water table may rise unexpectedly above the bottom of the tube. Unreliable readings will be obtained as a result. Damage to the probe may occur if it is immersed in water at the bottom of the tube.
- A cone-shaped end to the tube helps to guide the tube into the hole during installation, reducing the chance that small stones are displaced or soil is shaved from the side of the hole.
- The bottom of the tube may be slightly damaged during installation. This can grip the probe tightly at the bottom of the hole, preventing it from being withdrawn and necessitating the digging out of the tube and probe as a whole.
- Repeated placing of the probe onto the top of the access tube may drive the tube gradually further into the soil,

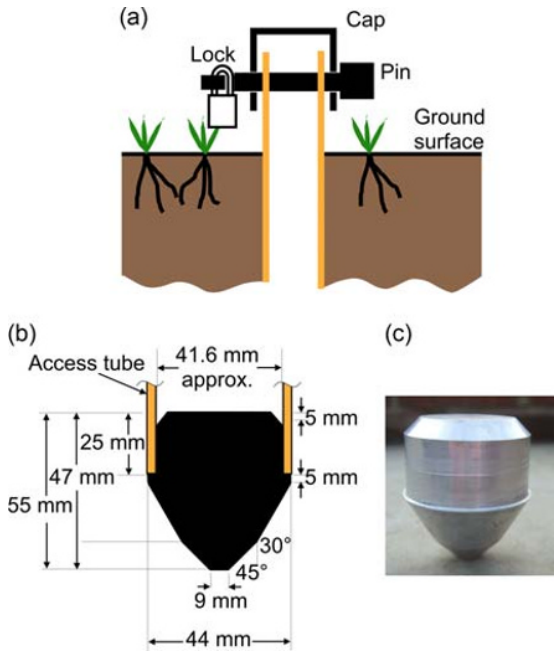

Fig. 7.8 (a) Locking cap for access tube security. (b) and (c) End plug. The plug should fit snugly inside the tube, and its outer diameter must be no larger than that of the access tube. It must be sealed onto the tube to keep water out.

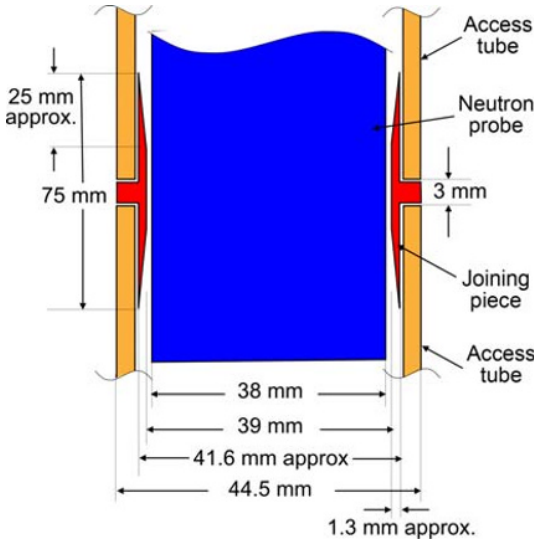

Fig. 7.9 Section through an access tube with an internal joining piece. The angle of the internal bevel is 3°.

making the reading depths progressively deeper. A large area of contact provided by the end plug will usually prevent this.

The first and third of these are not hypothetical examples.

The disadvantages of a bottom plug are that rain and other liquids which accidentally get into the tube cannot soak away easily and that sometimes air pressure builds up ahead of the tube while pushing it into the hole, preventing its insertion.

Bottom plugs are most conveniently and cheaply machined from solid aluminium alloy rod (see Fig. 7.8b). Because of the variation in tube size, they need to be manufactured to fit a particular batch of tubing – variation within a batch has been found to be very small. Fixing them to lengths of access tube with epoxy or by welding before going to the field is usually easier and quicker in the workshop than in the field, especially in poor weather. Ensure that the tube has not been enlarged when fixing the bottom plug. If it has, file it down to the same diameter as the rest of the tube.

In some applications, tubes must be inserted to depths of 10 m or more. Supply, transport and handling of a tube of this length are all difficult – 6 m is about as long as can be managed conveniently. If longer lengths are required, then it is recommended that they be joined on site as the tube is put into the hole. Since the tube should be, as far as possible, a snug fit in the hole, the tube must not be any wider at the join than elsewhere. An internal joining piece, which has been used on many occasions, is shown in Fig. 7.9. The metal is very thin and so the pieces must be stored carefully to avoid damage. Epoxy cement has been found suitable for sealing the joints, which are, in any case, under compression while inserting the tube. Again, the joining pieces should be made to fit a particular batch of tube (see also Fig. 7.18).

Access tubes should be at least 300 mm longer than the deepest reading depth required, to provide some stick-up above ground and accommodate the part of the probe below its centre of sensitivity.

7.3.3 *Site characteristics affecting access tube installation quality*

Some considerations when planning an installation are listed here. Every site is different, however, and there will almost always be additional issues.

- **Weather.** Installation in wet weather may make the soil surface easily compacted. Tools are more difficult to clean when muddy. Discomfort of operators from wet, cold or heat increases the temptation to exercise less care than usual. In heavy rain, water may run down the hole, increasing apparent water content of the soil at depth temporarily.
- **Season.** This affects the state of the ground surface and any vegetation and their vulnerability to damage. In wet and/or cool seasons, the water table and soil water content may be high, which will affect both the mechanical resistance and cohesiveness of the soil. Dry soil is often difficult to install tubes into. It is usually harder than wetter soil and often lacks cohesion, which makes removal of material with an auger difficult, as it tends to fall off.
- **Vegetation cover.** Damage to the vegetation on the site, whether natural, arable crop, forest understorey or grass, will affect the water balance and, hence, the water content

of the underlying soil, making it unrepresentative of the area as a whole. In most cases, grass is resistant to damage and will recover quickly. It is usually sufficient, in this case, to spread the weight of operators using planks or duck boards (wooden slats nailed to heavier battens). Taller or more delicate crops present greater challenges. It may be necessary to construct a platform of wooden planks, supported by scaffolding or a wooden framework, from which to work. Clearly this increases both the time for preparation and on site, with consequent increase in cost.

With arable crops, it is much easier to install tubes after sowing or soon after emergence, rather than when it has grown more than 100 or 200 mm high. In temperate climates, many autumn-sown crops are quite robust to traffic over the winter period.

- **Ground surface conditions.** The underlying soil type and surface wetness influence the vulnerability of the surface to damage. Generally speaking, a wet surface has a lower bearing capacity and is more easily compacted or scraped than a dry one. Stones or gravel lying on the surface can be pressed into it by operators' feet. A bare soil surface is usually more vulnerable to damage than one covered by vegetation.

The greatest hazard to the ground surface is compaction, causing localised ponding and runoff, sometimes towards and sometimes away from the access tube. In either case, measurements are unlikely to be representative of the surrounding area.

Particular care must be taken where there is a surface crust or loose material, such as litter or poorly decomposed humus.

- **Soil type** has several implications for the difficulty and most appropriate methods of tube installation.

Sandy soils are often poorly cohesive, particularly when dry or very wet, and soil material is difficult to remove by means of a standard auger. They often also lack the ability to relax after compression. This means that a small gap, created around the top of the tube by movement of the installation tools or subsequently by repeatedly placing a neutron probe on it, does not close up naturally, leading to water running into the gap.

Expansive clay soils are a particular problem, as the access tube may act as a focus for cracking and the soil may shatter during the installation process when dry.

Heavy clays are very sticky when wet, making it difficult to insert or remove a close-fitting tube. When dry, they are often very hard and difficult to work. Late spring in temperate climates, or early in the dry season in tropical ones, is usually the best time for installation in such soils.

Some soils and many geological materials are cemented, making it difficult to penetrate with a tool.

- **Stones** create many problems. They disrupt the passage of an auger. They may shatter when hit by a tool. Alternatively, they can be dislodged into the hole, leaving a cavity next to the access tube. Or they can be pushed into the soil, causing local compression and probably a cavity as well. There are no really satisfactory answers to this kind of problem. The best that can be done is to record the presence of the stone, making the best assessment possible of the resulting situation and to bear this in mind when interpreting results later.
- **Depth of installation.** The difficulty of installing access tubes increases rapidly with increasing depth. While the largest water content changes normally take place near to the surface, changes deeper in the profile cannot usually be ignored. Many workers confine themselves to installing monitoring tubes to no deeper than 1 m. This is usually inadequate for water balance monitoring, as most crops extract water from deeper depths. An installation depth of 2 m should usually be considered the minimum acceptable. Some crops, especially woody species, have root systems which may reach 6 m or more (e.g. Calder *et al.*, 1997).

The effort required and the dangers of gaps developing and surface or crop damage all increase with increasing depth of installation.

7.3.4 Access tube locations

The effects of spatial variability were discussed in Chapter 4. The main conclusions relevant to neutron probe use can be summarised as follows:

- Sample at as wide a range of locations within the study area as possible and, in particular, include all significant combinations of crop, soil type and landscape position. In statistical terminology, these are often called *strata*.
- Sample as many points within each stratum as practical. If the spatial variability in each stratum is expected to be similar, then having a number of access tubes roughly proportional to the area occupied by each stratum will produce the best overall average for the area. However, if an important stratum is expected to exhibit significantly higher spatial variation, then more tubes in this stratum would be justified to make the confidence limits between all important strata comparable.
- Because measurements at locations close to one another (separated by less than the range of the data) are often more similar than between those further apart, it is advisable to spread measurements evenly over each stratum (Papritz & Webster 1995a, b) unless there is other information to help make choices of location. However, practical constraints may require this to be modified heavily.
- Choose locations which are as easy as possible to access, reduce damage to soil surface and crops as much as possible and minimise the time taken to move from one to another. This should not, however, be at the expense of representivity. Locations must be typical of the area, well away from field edges, paths and other features likely to affect soil water. As a general rule, a narrow path of about 2 m width is likely to cause a disturbance for about twice its width either side, so that an access tube 4 m away from it should be acceptable. A wide road or a field boundary will have an effect much further away. This distance is likely to increase the deeper that measurements are made. A good guide is to locate the access tube at least twice as far from the boundary as its depth.

7.3.5 *Equipment required – manual and semi-manual installation*

The following should be regarded as a guide only. Different sites may require slightly different techniques and, hence, different equipment. Additionally, installation techniques vary according to individual preferences and equipment available. The equipment is most suitable for relatively shallow installations (up to 3 m), but has been used for semi-manual installations up to 12 m depth. The access tube is assumed to be 45 mm outside diameter. A different size of access tube will need some of the dimensions to be adjusted.

Ground protection

- Planks or duckboards sufficient to support the weight of two or three operators – if the soil or vegetation is particularly fragile, then material to build a framework will be needed to support a wooden platform above the surface of area about 3 m × 2 m around the access tube position.
- A ground protection plate of 6 mm thick aluminium alloy 0.5 m square, with a central hole of 46 mm. Holes of 7 mm diameter in each corner anchor the plate to the ground by four 200 mm × 6 mm diameter pegs. A further 6 mm hole 25 mm from the edge of the central hole holds a 6 mm diameter bolt to act as a locating pin for a jack to remove the guide tube (see Fig. 7.10).
- Stakes and tape to mark off zones to keep operators off most of the surrounding area.

Equipment for making the hole

- Enough 1 m lengths of AQ drill rod to reach the desired depth when assembled. This has an outside diameter of 44.5 mm and an inside diameter of 34.9 mm (4.8 mm wall thickness). The lengths screw together with square cut threads to withstand repeated blows. Also required are a head piece to take a rammer and tommy bar, made from a short (75 mm approx.) piece of AQ rod, with a male thread, as in Fig. 7.11a, and an internally bevelled short length with a female thread to act as a cutting shoe, cut from the opposite end of the same rod, as in Fig. 7.11b. If more than one or two tubes are to be installed, it is wise to have one or two spare cutting shoes and head pieces.

Or:

- Mild steel guide tubes in lengths of 1.15 m, 2.15 m, etc. 45 mm o.d., 39 mm i.d. (3 mm wall thickness). The top of the guide tube has a reinforcing ring welded to it and a hole drilled through to take a 20 mm diameter tommy bar for guide tube removal, as shown in Fig. 7.11c, while the bottom should be sharpened by an internal bevel (Fig. 7.11d).
- Screw augers of 28 mm (for AQ rod) or 35 mm (for separate guide tubes) with extension rods and handles to allow working to the maximum length of tube to be used plus 150 mm. Note this may be more than the depth of the tube to be installed. With the guide tubes mentioned earlier, a 1.5 m hole would require an auger of total length at least 2.30 m. Ensure that the auger extensions will fit inside the guide tube. Suitable screw augers have proved difficult to obtain commercially. A wood auger of the appropriate diameter, brazed to a length of auger extension has proved to be successful. Sometimes, other designs of auger (e.g. Edelman) are more successful at penetrating or retaining soil (Fig. 7.12).
- A rammer to knock the guide tube into the hole after each augering. A suitable design is shown in Fig. 7.13. An alternative would be a small diameter post hole rammer, which fits over the guide tube. These tend to be a little too light for maximum effectiveness, however, and also require that the longest guide tube be even longer than

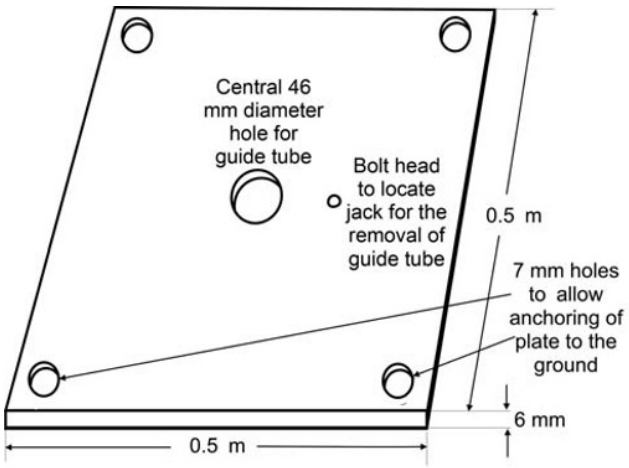

Fig. 7.10 Aluminium alloy ground protection plate.

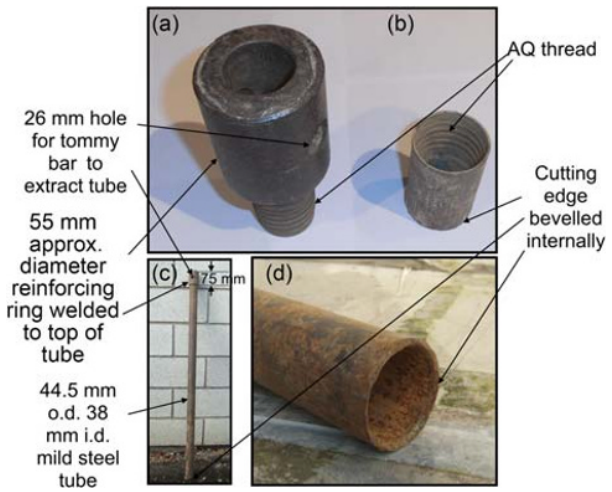

Fig. 7.11 (a) and (b) AQ drill rod ends for access tube installation made from a length of drill rod. Photographs by Andy Dixon. Reproduced with permission. (a) Head piece to allow driving into the soil. (b) Cutting edge. (c) Fixed length guide tube (d) Cutting edge of fixed length guide tube; this one has been damaged by contact with stones in the soil and needs sharpening.

Fig. 7.12 Screw and Edelman auger.

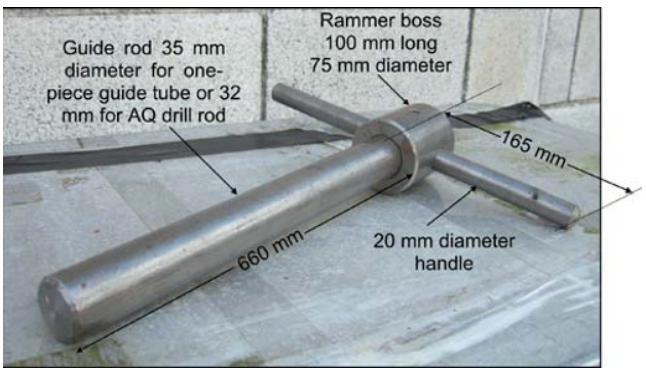

Fig. 7.13 Rammer for hammering guide tube into the soil.

the access tube, as the rammer must all be outside the guide tube and above the surface. Using one of these types of rammer ensures that the top of the guide tube is impacted along its axis, and there is no significant side force to enlarge the hole, as may happen if a sledge hammer is used.

Equipment for removal of the guide tube

- A tommy bar of mild steel, 20 mm diameter and 0.4 m long.
- A clamp to fit onto the guide tube, with a piece of box section mild steel welded to it, to take a car jack.
- A suitable car jack to lift up to 2 tonnes. The jack should be able to lift from not more than 100 mm from the ground with a lift of at least 0.5 m.

Ancillary equipment

- Spanners for auger extensions and clamps.
- Heavy hammer to shake out soil from guide tubes.
- Half-round file to repair damage to cutting shoe edge.
- Clamp wrenches, chain wrenches or stilsons to separate AQ rods and to assist guide tube removal.
- Wire brushes to clean equipment.
- Spirit level to ensure verticality of tube.
- WD-40 or similar lubricating spray to lubricate threads.
- Marker pen to mark depths on guide tube and auger stem.
- Bucket to put soil removed into.
- Tube cutter to cut access tube to the correct height after insertion.

Alternative, optional or additional equipment (see also Section 7.3.8)

- Petrol-driven, pneumatic or hydraulic hammer and adaptor to mate with the top of the guide tube to provide more power for ramming guide tubes.
- Petrol-driven, pneumatic or hydraulic drill with adaptor to enable it to drive the auger.
- Ball clamp and rod puller for guide tube removal.
- Sample bags to collect soil samples for later examination or analysis.

7.3.6 Access tube installation – manual and semi-manual method

In most cases, access tubes can be inserted by manual means, perhaps supplemented by powered, manually operated tools for deep installations or in hard and heavy soils. The following notes are intended as a guide to good practice. The availability of equipment, site conditions, etc. will influence the details of the procedure. However, the overriding consideration must be to produce a hole with a diameter all the way down equal to the outside diameter of the access tube, while leaving the ground surface and vegetation surrounding it undamaged. This is quite a demanding task, but is perfectly possible in light- to medium stone-free soils and can be achieved to an acceptable degree in almost all others provided sufficient care is taken. The biggest dangers are enlargement of the hole near the top and damage to the ground surface and/or vegetation.

Preparation

Protection of the ground surface and vegetation is the first priority. There will, inevitably, be some foot traffic around the access tube location. If there is a slope on the site, then the approach to the access tube location should always be from the downslope side. Any soil compaction occurring

during installation will then cause water to run away from the access tube. Mark off an approach route at least 5 m long and about 1 m wide using stakes and tape. Widen this out to an area of about 3 m × 2 m around the access tube.

If the soil is bare or covered with short vegetation (less than about 75 mm in height), place the ground protection plate onto the surface, with the hole at the desired location. Secure it with pegs to prevent movement. Place planks or duckboards on the ground surrounding the ground protection plate, ensuring that accidental trampling of the ground within 1 m of the plate is prevented.

If the ground surface is very soft or there is fragile or tall vegetation, then build a platform around the access tube location as low as possible without damaging the vegetation. Cover this with planks, so that the area of the platform is covered, except for a small gap over the access tube location. Secure the planks in place. It may be necessary to build a railing around the edge of the platform to stop people from falling off. Fix the ground protection plate to the planks over the access tube location.

To minimise traffic in the area surrounding the access tube, all the frequently used and smaller tools should be kept on the boards surrounding the tube.

Drilling the hole

1 Take one section of AQ drill rod, with cutting shoe and head piece fitted, or the shortest length of guide tube, and hold it vertical, with the cutting shoe on the ground through the ground protection plate. While keeping the guide tube vertical, knock it into the ground by approximately 150 mm with the rammer. Remove the rammer and insert the screw auger. Auger through the guide tube to remove the soil inside the guide tube and then drill 150 mm ahead of the cutting edge. This will take a few attempts. Clear the soil from the auger into the bucket each time. Alternatively, collect it into sample bags for later examination. Make sure to label all sample bags with the date, location and depth. Notes should be made on the type of soil as the hole is drilled, noting, in particular, the location of any boundaries.

2 Now reinsert the rammer and knock the guide tube down by another 150 mm, so that it reams out the auger hole to the correct diameter for the access tube. Do not knock the cutting edge of the guide tube beyond the depth that the auger has drilled.

3 Repeat this process, advancing the guide tube by 150 mm each time, until just 150 mm of the guide tube protrudes above the ground protection plate.

4 If using AQ drill rod, hold the length sticking out of the soil with a clamp wrench or stilson and unscrew the headpiece. Then screw on the next length of drill rod and replace the head piece, ensuring that the metal shoulders at the end of each thread are in contact with one another.

5 With separate guide tubes, the complete tube must be removed. This can often be accomplished by using the tommy bar to pull and, if necessary, twist the tube. With long guide tubes and/or difficult soils, the use of a jack or rod puller will usually be necessary. This is the part of the process when the top of the hole is most likely to be enlarged, so it is important to ensure that the tube is pulled as straight as possible. A rod puller and ball clamp has much greater lifting power than a car jack; and with two levers, the pull will be along the axis of the tube.

6 The process is repeated with the new length of tube until the desired depth is reached. Note that the bottom of the neutron probe is below its centre of sensitivity by about 100 mm (depending on the probe design). The hole must be made somewhat deeper than the deepest reading depth, therefore, to accommodate this and the bottom plug. The last augering through the guide tube should stop at the bottom of the guide tube, to remove just the soil inside it.

7 When the desired depth has been reached, remove the guide tube.

8 Insert the bottom end of the access tube into the hole and, taking care to keep it vertical, push firmly down. The first 1 or 2 m of the tube usually goes in quite easily, becoming harder as it gets further down. Tapping the top of the access tube with the rammer will usually achieve complete insertion. It is important to ensure that it is seated solidly on the bottom of the hole, to prevent repeated neutron probe use from gradually pushing the tube further into the soil over time.

9 Trim the top of the access tube to leave an amount of tube protruding (known as the *stick-up*). It is good practice to standardise on the amount of stick-up to avoid confusion later when the tube is read. This will depend on the design of the neutron probe used, as they normally have a socket in the bottom to fit over the tube. It may also be necessary to leave a length of stick-up to avoid damage to the vegetation by the neutron probe and to accommodate growth, or to gain a convenient reading height for the probe. The stick-up should not, however, be any greater than necessary to satisfy these considerations, as the lateral leverage effect of the probe on the tube can be substantial when the stick-up is large. The protruding tube will also intercept rain, which will then run down the outside of the tube to the ground immediately around it. 100, 150 or 200 mm is often a good choice for the stick-up.

10 If the installation has been done very well, there will be no gap around the tube at the top. This can often be achieved, but frequently there is a small (1 or 2 mm) gap. This is most likely caused by compression of the soil which may, in time, relax back to fit well around the tube, eliminating the gap. This process can be encouraged by using gentle foot pressure to press (*not* scrape) the soil back around the top of the tube. Some very sandy soils lack the ability to do this, and the only recourse seems to be to sift dry sand from the surroundings down the gap. While not ideal, this is certainly preferable to leaving a gap for water to run down.

7.3.7 Installation into stony soils

Stones probably cause more problems in access tube installation than anything else. The consequences in disturbing subsequent readings from the tube can be profound. There are very few situations where encountering a stone during installation will not force some departure from the ideal method, described earlier.

Very small stones, less than about 6 mm diameter, can probably be picked up by the auger along with its surrounding soil and not cause a problem. Slightly larger ones usually prevent the auger from turning and thus halt the alternate auger and ream out process. In this situation, the best course is normally to hammer the guide tube down by about 50 mm, to catch the stone and some soil in the bottom of the guide tube. The guide tube then has to be taken out of the soil, the soil removed from it and then the guide tube replaced.

In these situations, it is sometimes difficult to remove the soil from the guide tube. Tapping with a heavy hammer will often shake the soil out; but sometimes, it can take several minutes to remove soil jammed into the bottom of the guide tube using a combination of hitting the tube with a hammer, to push it out from the top with the auger and removing it from the bottom with a spatula or screwdriver.

Large stones that will not pass into the guide tube are an even bigger problem. There is little alternative in such cases to trying to break up the stone or abandoning the hole. Depending on the size of the stone and its brittleness, the guide tube cutting shoe, when used with the rammer, may break it sufficiently to allow the fragments to be caught inside the tube. The tube has to then be withdrawn, emptied as described earlier and replaced. Several attempts may be needed before the hole has been cleared of all the larger fragments of stone and augering is again possible. The surrounding soil will also not be in its natural state, with probably both compaction and cavities left behind. It is, therefore, important to record the incident and the best estimate of the depth(s) affected.

Using the guide tube to break up stones damages the cutting edge, which should be re-sharpened and any protrusions removed from the outside with a file.

Stones rarely come singly and if one is encountered, another is usually found before long. The result is that many holes have long lengths where no augering is possible and drilling is entirely a result of using the rammer. The need to remove the guide tube from the hole each time makes this a very time-consuming process. The temptation to ram the tube down by more than 150 mm at a time, however, should be resisted. Soil and stones get very tightly packed into the end of the guide tube and, rather than cutting its way through the soil, the process is closer to hammering a solid bar into the ground, compacting the surrounding soil.

Some soils are so stony that it is impossible to remove material from the hole, either by auger or inside the guide tube. In these cases, a hole can be made by hammering a sharpened rod of the same diameter as the access tube into the ground and accepting that the soil will be compacted locally. This clearly affects the accuracy of the results, but it is normally preferable to obtain some measurements of lower accuracy than none at all.

7.3.8 Use of powered tools in manual installation (semi-manual methods)

In heavy soils, situations where installation greater than 2 or 3 m is required and in stony soils, it is very difficult to complete a hole solely using manual labour. The most useful powered tool is a mechanically driven (petrol, air or hydraulically powered) hammer, which can be used in place of the rammer. An adaptor will be required so that one end fits onto and inside the guide tube and the other fits onto the hammer (see Fig. 7.14).

Drill steels, which fit inside the access tube, are available with hardened tips, which can be used with the petrol

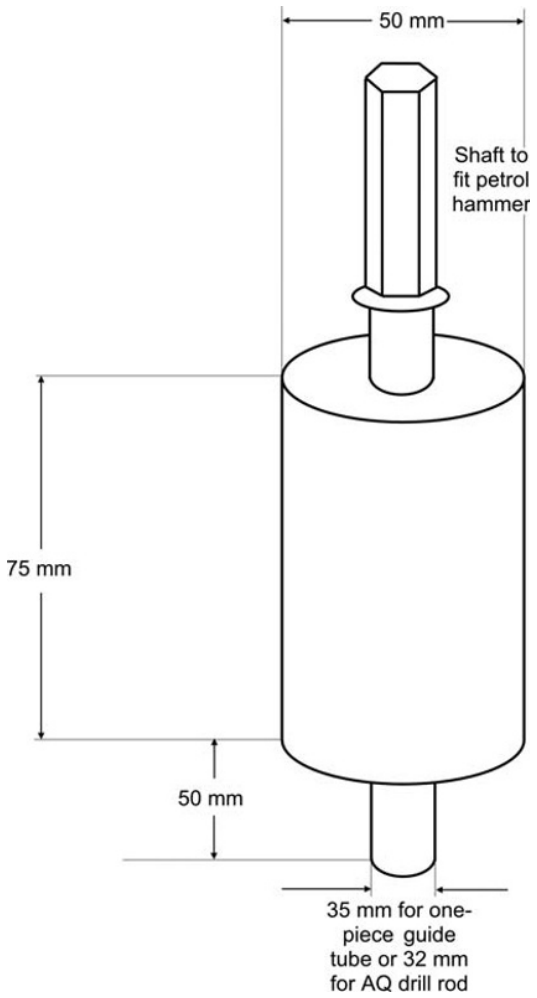

Fig. 7.14 Rammer adapted for petrol hammer.

hammer to break up stones at the bottom of the guide tube and save some damage to the edge of the cutting shoe.

The ability to power the auger is usually less valuable than having a petrol hammer. However, in cemented formations and some heavy soils, it can save a great deal of effort and time.

7.3.9 Other manual methods

There are many variations on the basic method discussed earlier, which may be more suitable for different situations or even personnel. It is not possible to go into all of these. Two possible methods, both of which avoid using a guide tube, are worth a mention.

The first method uses the access tube as its own guide tube. This can be done using aluminium alloy tubes in light, stone-free soils to shallow depths. At the beginning of the process, the auger must be inserted and removed with almost the full length of the tube sticking above the ground, thus limiting the depth to a little over 1.2 m. The end of the access tube can be sharpened and an end plug inserted at the end of the process using a rubber bung (39 mm for a 45 mm o.d. aluminium alloy tube) forced into the tube. Alternatively, an expanding elastomer closure or epoxy or other cement introduced down a tremmy pipe can be used. Figure 7.15 shows a typical expanding elastomer (silicone rubber or similar) closure.

For deeper depths or more difficult (but still stone-free) soils, thicker-walled steel or stainless steel pipe, which can be screwed together in sections, can be used for both guide and access tube, as for a guide tube made from AQ drill rod.

The advantages of not using a separate guide tube are that time taken in removing it from the soil is saved, and the likely problems associated with hole enlargement on guide tube removal and reinsertion are avoided.

The second method, is, once again, suitable only for stone-free soils and involves augering a hole directly into the soil. A bucket-type auger, which has a diameter exactly the same as the access tube, is used. Great care is needed to avoid the hole being enlarged near the surface by constant friction as the auger is removed each time for emptying.

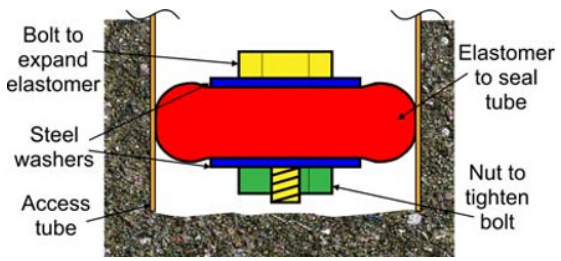

Fig. 7.15 Elastomer seal for access tube bottom. The elastomer may be cut from a rubber bung or made from a ball of suitable size. An alternative is to use several rubber washers, each separated by a smaller diameter metal washer.

However, very good quality installations have been achieved by this means to depths in excess of 6 m in deep, volcanic, stone-free soils in East Africa (Gunston & Eeles, 1979).

In the vast majority of cases, however, the use of a guide tube is essential to avoid the hole being enlarged.

7.3.10 Access tube installation – mechanical methods

When a large number of access tubes need to be installed, where installation to depths greater than about 2 m are needed or where soils are very heavy or stony, fully mechanised installation may be a viable option. The capital cost of the equipment is high, as is the ongoing maintenance; but suitable equipment may be available for other purposes, such as drilling shallow boreholes for water supply or groundwater observation. Some drilling contractors may be willing to do the work, although, unless they are specialists in this work, close supervision will be necessary to avoid unacceptable levels of ground compaction and disturbance and poorly fitting tubes.

The equipment is inevitably much heavier than for manual or semi-manual installation and brings with it attendant problems of ground compaction, spillage of fuel or lubricating oil and damage to vegetation. Thorough attention to preparation beforehand, fencing off access routes and awareness of the importance of avoiding disturbance to the natural state of the site by operators should avoid serious problems.

A successful method for installing deep (over 4 m) tubes in a variety of materials uses a light rotary drilling rig. AQ drill rod is used, with a tip as shown in Fig. 7.11b, encrusted with carborundum nuggets. This may produce a very slightly oversize hole. However, drilling too tight a hole often makes insertion of an access tube impossible. It is believed that the drilling process removes most of the soil, but some is pushed out sideways and relaxes slowly back again when the drill tool is removed, leaving a tight-fitting tube. It is important to ensure that there is no gap around the top of the access tube after installation.

Removal of the drilled material from the hole is by air flush. A central pipe, which extends to the bottom of the drill string, carries air, which then blows the material up to the top of the hole. The use of a dust mask to prevent respiratory problems is essential. In light winds, some of the arisings collect around the top of the hole, which should be caught on a rubber mat, tarpaulin or similar. Dust collectors are available, but have, in practice, proved difficult to use successfully. Water or other drilling fluids to flush out the arisings are, for obvious reasons, not acceptable.

At the end of the drilling, an access tube is inserted in the same way as for manual installation. The drilling rig, however, provides a means to press the tube with a force of a few tonnes into the soil from a greater height than can be done standing on the ground. Installation by this means has been carried out successfully at a number of sites to depths of 6 m or more.

7.3.11 Very difficult soils and use in existing boreholes

Despite the best intentions to drill close-fitting access tube holes, in very stony and heavy soils (particularly when wet), this may prove impossible. The deliberate drilling of an oversize hole may be the only option. Equally, a site may already have some existing boreholes which could be used for neutron probe logging. Ideally, the borehole should be backfilled with a grouting material around an access tube. Two approaches have been reported (see Fig. 7.16).

One uses closed-cell polyurethane foam, which can be mixed on site and dropped to the bottom of the hole via a tremmy pipe, after inserting the tube (Black, 1977). The mixture foams up, filling the void space and, if the correct quantity of mixture has been used, just filling the hole in a few minutes. If there is too little, then it is easy to have a second attempt to fill the remaining space. Too much could be embarrassing, but should not cause long-term problems. The foam is sufficiently light that its hydrogen content is extremely low, and the foam acts almost like an empty space to neutrons. Because it is closed cell, it absorbs negligible amounts of water, but prevents the hole from filling with water. The expansion of the foam normally means that a small mound of foam appears around the top of the tube, which will encourage rainwater to run away from the tube. The foam degrades in ultra-violet light and so should be protected from sunlight.

If there is no possibility of a water table within the depth of the access tube (more unlikely than it at first appears), then the same effect could be achieved by inserting the tube into an empty hole, using light, flexible arms attached to the tube at intervals to centralise it in the hole.

The other involves filling the void space with a cement and clay-based slurry. Prebble *et al.* (1981) used a cement–kaolin mixture, while Keller *et al.* (1990) investigated two types of bentonite and cement slurry. In the latter case, promising results were obtained in a laboratory test, although the stability of the results over time was not investigated.

In some situations, it may be desirable to dispense with an access tube altogether and lower the probe, with a centraliser, down the hole. It is even more important in this situation that the probe is not lowered below the water table, since most probes are not watertight and significant damage would result from immersion.

Centralisation of the probe in oversize holes is important, as there is a significant effect on count rate of the distance of the probe from the edge (Morris & Cooper, 2004).

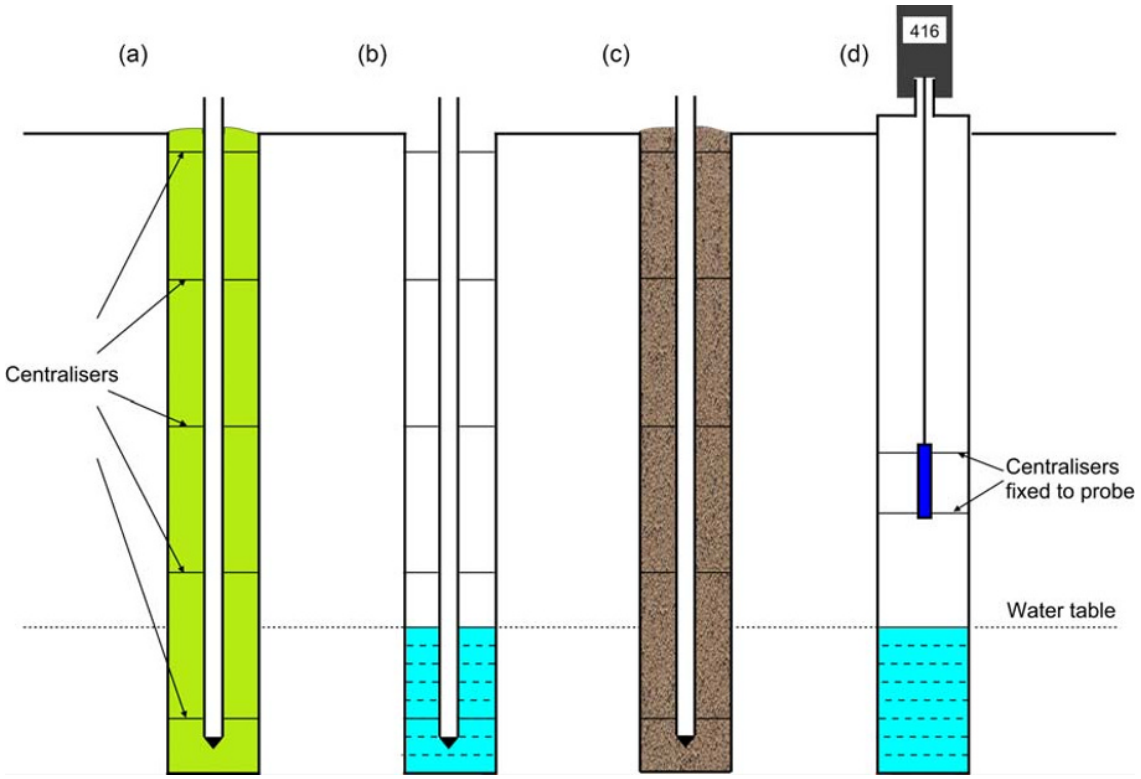

Fig. 7.16 Neutron probe in large diameter boreholes. (a) Access tube in a foam-filled grout; (b) access tube in empty borehole – note the hole is water-filled up to the water table depth; (c) access tube in cement-based grout; (d) probe in borehole with no access tube – note the use of centralisers and the possibility of damage to the probe through immersion.

7.4 Accommodating Farming Operations

Most soil water monitoring relies on permanent access from the surface, which implies some equipment both in the upper part of the soil and (usually) above ground. The latter is an obstruction for harvesting machinery and some other farming operations. Ploughing, cultivation and sowing involve penetration of the upper layers of the soil. There are, therefore, difficulties for both the farmer and experimenter in installing and operating observation equipment at the same time as normal farming operation. One solution is for the farmer to avoid the area around the instruments and to cultivate their immediate surroundings by hand to replicate as closely as possible the treatment of the rest of the field. This may be reasonable and achievable under some circumstances, but is always likely to arouse a suspicion that it may not be completely representative. What is definitely NOT acceptable is to leave a small oasis of bare ground, grass or weeds around instruments in an otherwise uniformly cultivated field.

Some agricultural operations are possible with careful siting of instruments in relation to farm machinery movements. Most farmers use a system of 'tramlines', along which the machinery's wheel tracks run. These usually persist from one year to another and minimise soil compaction and damage to the crop. Siting instruments between pairs of tramlines avoids their being run over, and ensuring that all are below the height of spray or irrigation booms minimises disruption for both the farmer and the investigator. If instruments are too tall (e.g. mercury manometer tensiometers – Section 12.5.1), then it may be possible to fold them down or remove part of them temporarily.

Where the operations involve penetration into the soil over the whole field, for example for ploughing or drilling of seed, then things are more difficult. A solution was devised by Howse (1981), and a slightly modified version is described here. It uses the same joining pieces as depicted in Fig. 7.9 (Section 7.3.2) to allow both the above-ground and upper parts of the access tube to be removed. The procedure is shown diagrammatically in Fig. 7.17.

The access tube is jointed at ground level and about 200 mm (depending on the maximum depth of cultivation) below. The joining piece in both cases should be bonded to the upper piece of access tube, so that the end pointing upwards is a plain piece of tube. The depth of the lower joint should be about 50 mm deeper than the expected maximum cultivation depth to avoid damage to the length of tube permanently in the ground. An access tube extension bonded to a joining piece is shown in Fig. 7.18.

Early in the growing season, the upper piece of access tube can be quite short (100–200 mm) as for permanently installed tubes (first picture in Fig. 7.17). Later, when the crop has grown taller than the access tube height, the upper part of the access tube can be replaced with a longer one. A temporary platform will probably be required to use the neutron probe at that height, to avoid crop damage, to allow convenient handling of the neutron probe and for radiological safety. A light, temporary platform, which can be placed onto semi-permanently installed supports, is a good solution. The supports will have to be removed for harvest, ploughing, etc.

For harvesting, the top part of the access tube is removed and a cap or rubber bung placed into it. A metal cap is more robust, but it needs to have a watertight seal. Occasionally, a rubber bung may be forced into the top of the tube by pressure from a wheel. This can usually be removed with some effort. Even less often, the top of the tube may be damaged, which usually requires that the lower extension piece be replaced.

After harvest, the upper extension piece can be replaced and readings resumed.

For ploughing and/or seed drilling, the upper and lower extensions must be removed completely. When extracting the lower extension, care must be taken to leave the hole intact. A rubber bung or waterproof cap, with a maximum diameter slightly smaller than that of the hole, is then placed on top of the permanent part of the access tube in the ground. A ring or hook firmly fixed to the top of the bung or cap will aid its removal, and a short length of string (enough to reach just above the ground surface) also helps locate the position after ploughing. The hole above the bung is lined with thin paper (80 g m^{-2} photocopying paper is quite suitable) and then filled with expanding polyurethane foam. This is available in builders' merchants and do-it-yourself stores in press-button cans. The foam comes as two components which mix as they leave the can. It expands rapidly by a very large amount, and so it is easy to produce too much foam. Some experimentation to find the right amount to use is, therefore, wise. The paper liner prevents the foam from penetrating into the soil.

The polyurethane foam is very weak and ploughing breaks it off easily, leaving the foam plug below the plough layer intact. Fears that problems may be caused by machinery catching the string and pulling the bung out have not been realised.

The access tube position after ploughing and sowing can be located by careful measurement from points at the edge of the field, aided by visual lining up of landscape features (e.g. the edge of a fence post with the corner of a distant building). Alternatively, surveying equipment can be used. With sufficient care, both before the top of the access tube is removed and after ploughing, the access tube position can be located to within about 15 mm. It then remains to dig carefully down to locate the top of the remaining polyurethane plug, making as small a hole as possible, remove the plug and bung – the string helps here, or alternatively the ring can be grabbed by a sharp-pointed hook on a short rod – and take out the rest of the paper liner. The soil and, especially, the seeds must be preserved. The hole in the undisturbed soil should be intact and the upper access tube extension can be replaced, taking care that it fits snugly down. The already disturbed soil now needs to be replaced carefully to match as nearly as possible the loosened soil around it. With care, the seeds can be replaced

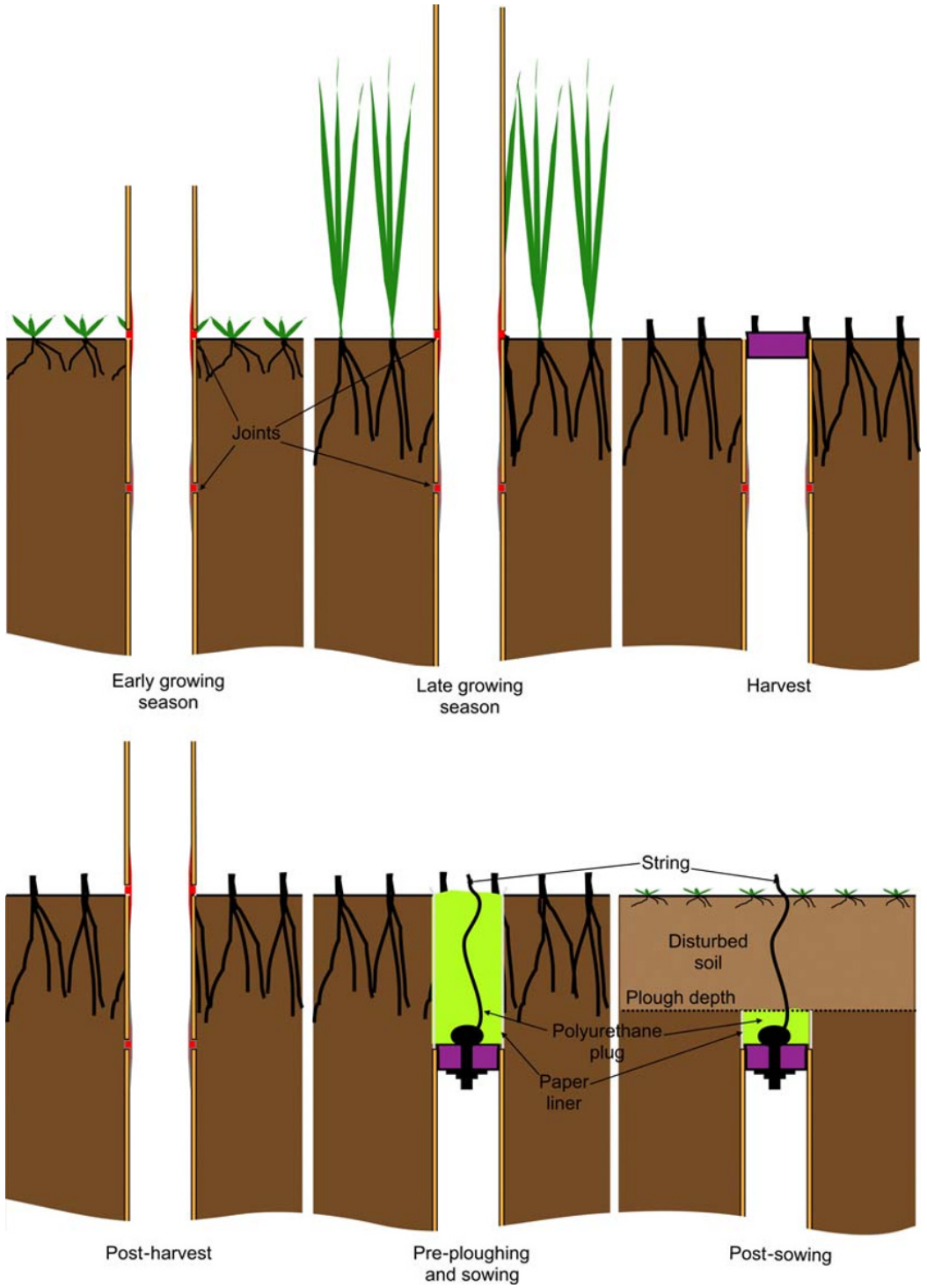

Fig. 7.17 Access tube arrangement to accommodate farming operations. (*See insert for colour representation of the figure.*)

as well and if germination has not proceeded too far, will grow as well as the rest of those in the field. Their progress should, of course, be monitored and remedial action taken if necessary.

This procedure ensures that only soil that was disturbed by ploughing needs to be dug up and replaced, so minimising the amount of artificial disturbance. Good liaison with the farmer will ensure that the access tube is out of action for the minimum time.

A similar method was used by Glenn *et al.* (1980). They attached a strong nylon cord to the bottom of the access tube, allowing the access tube and extension to be pulled

Fig. 7.18 Removable access tube extension, showing the joining piece.

up. The extension was removed, the cord wrapped around the top of the access tube a few times and the access tube capped, then pushed back into the soil, with a short length of the cord above ground. The cord had a flag on it to aid in finding it after ploughing. After cultivation, the tube could be pulled up again with the cord and the extension refitted, then pushed back into position. Glenn *et al.* (1980) reported that in the silty soil where they used it, there were no problems of hole collapse, but it would be wise to check whether this is the case for other soils.

7.5 Accuracy and Precision of Measurement

Data are collected using a neutron probe by lowering the probe to a series of depths in the access tube and recording the number of slow neutrons collected over a period of time. There are several ways in which the process affects the accuracy and precision of the measurements. Before discussing this issue, it is worth being clear about what is meant. *Precision* and *accuracy* are not the same thing. Precision relates to the reproducibility of a measurement. Thus if the same quantity is measured two or more times and the same or a very similar result is obtained on each occasion, then the measurement would be described as precise. Accuracy, however, is concerned with whether the result of the measurement conforms to some absolute standard. Measurements may be very precise; but because of some consistent defect in the method or equipment, they are not very accurate. If all measurements are in error by a similar amount in the same direction, then this is termed a *bias* and the resultant errors are described as *systematic*. Examples of systematic errors in water content measurement are discussed in Section 7.5.3. Variations between repeated measurements of the same quantity are, on the other hand, described as *random*. It follows that estimating the precision of a set of measurements is much easier than assessing their accuracy. Nevertheless, to ensure good accuracy, one precondition is that the measurements be precise.

7.5.1 Standard error of water content measurement due to random counting

This section deals with the main factor in the neutron probe method affecting precision, usually called *random counting error*. Other sources of imprecision and inaccuracy are described in Section 7.5.3.

Anyone who has heard the clicks from a Geiger counter knows that they do not come steadily, but several clicks are bunched together, then there is a short period with no clicks, then maybe one or two clicks, more silence, then perhaps a few more close together and so on. This is because the arrival of radioactive particles at the counter is random. Over a long time period, the number of counts is likely to be fairly constant, but in a short time, there may be no clicks, one, two or more. This can be characterised by saying that in any time interval the expected number of particles arriving is the same as in any other equal time interval. If the interval is very short, the number expected will be small (less than one if it is short enough) and if it is very long, then the expected number will be high. The expected number is the long-term average and so is not usually a whole number, although in any particular interval it must be an integer (i.e. a fraction of a count is not possible). If the expected number in a short time interval is 0.1, then in about 90% of intervals, no particles will be detected. In about 1 in 11, one particle will be detected and, more rarely, two. Even more rarely, three (or even more) will be detected. For an interval 1000 times as long, the expected number is 100. We expect, in this case, that 100 events will turn up quite often, but should expect 99, 102, 95, etc. almost as frequently. Numbers as low as 50 or as high as 150 will be extremely rare.

Figure 7.19 shows the frequency of different numbers of counts, when the expected number is 0.1 and 100.

This frequency is described by a *Poisson distribution*. For our purposes, the important characteristics of a Poisson distribution are that the standard deviation of the number of counts is $\sqrt{N}$, where N is the expected number of counts, and that, for large N, the distribution approximates to the more familiar Normal Distribution. So for 100 counts, the standard deviation is 10. In Fig. 7.19, a Normal Distribution curve with the same mean and standard deviation is superimposed onto the Poisson distribution. For a mean of 0.1, the Poisson distribution is very skewed and bears little relation to the Normal Distribution. However, for a number of expected events over about 100, the two are very close to one another. For a reasonable number of total events, therefore, we can use Normal statistics to characterise the uncertainty in measurements, with a standard deviation of the estimate equal to the square root of the total number detected.

For one measurement of a quantity, the standard error of measurement is the same as its standard deviation, that is

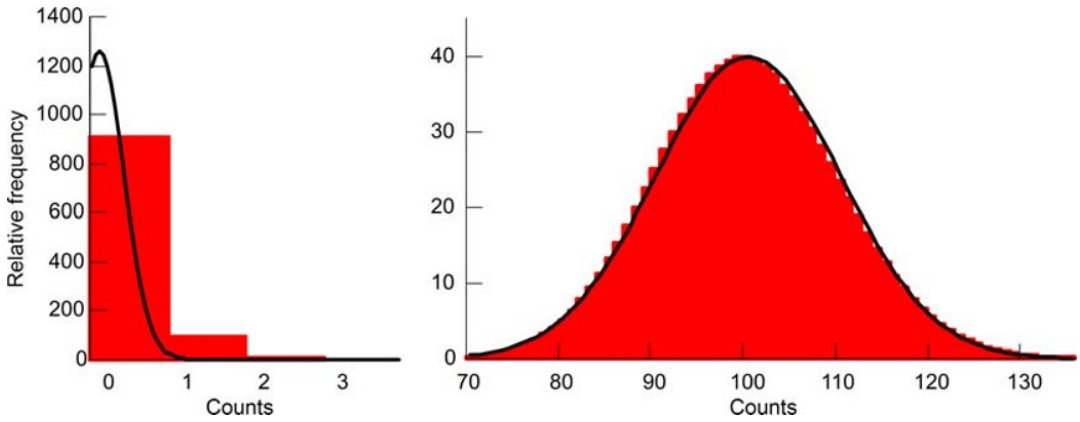

Fig. 7.19 Expected number of events for a Poisson distribution recorded over 1000 intervals when the mean number per interval is 0.1 (left-hand graph) and 100 (right-hand graph). The Normal Distribution for the same mean and standard deviation (the square root of the mean) is shown in each case as the continuous line.

on 68% of occasions the measurement will be within one standard deviation of the true value. So, if the expected count is 100, 68% of the measurements will be between 90 and 110 and 95% will be between 80 and 120.

More realistically, the total number of counts from neutron probe measurements is usually of the order of 10,000, so that the standard error is around 100 or 1% of the number of counts, as opposed to 10% when the expected number is 100.

Most modern probes give the output as a *count rate*, R, that is the total counts recorded divided by the time:

$$R = \frac{N}{t}. \tag{7.5.1}$$

To calculate the standard error of the count rate, the total number of counts must be calculated, then their standard error and finally divided by the time. So the total number of counts is:

$$N \pm \sqrt{N} = Rt \pm \sqrt{Rt}. \tag{7.5.2}$$

Dividing through by t shows that the count rate is expected to lie in the range:

$$R \pm \sqrt{\frac{R}{t}}. \tag{7.5.3}$$

$\sqrt{R/t}$ is the *standard error* of the count rate, R. Equation 7.5.3 shows, as one might expect, that the longer the counting time, the smaller the expected error in the count rate. However, because the error reduces according to the square root of the time, to halve the standard error, one must wait four times as long to accumulate the counts.

In most cases, soil water content is related to the count rate by a calibration equation of the form:

$$\theta = a\frac{R}{R_w} + b \tag{7.5.4}$$

where
a and b are calibration constants and
R_w is a standard count rate specific to a particular probe.

It follows that the standard error in θ due to random counting error is given by:

$$\sigma_\theta = \frac{a}{R_w}\sqrt{\frac{R}{t}}. \tag{7.5.5}$$

7.5.2 Standard error of change in water content

We are usually much more interested in the change of water content between two reading occasions, rather than its absolute value. This is the primary focus in any investigation concerning soil water balance, water extraction by a crop, amount of irrigation applied, infiltration by rain or irrigation, or drainage from the soil profile. In this case, the standard error, $\sigma(\theta_2 - \theta_1)$, of the change in water content is given in the usual way for Normal statistics by:

$$\sigma(\theta_2 - \theta_1) = \sqrt{\sigma_{\theta_1}^2 + \sigma_{\theta_2}^2} \tag{7.5.6}$$

where
θ_1 is the volumetric water content at the beginning of a period and
θ_2 is the volumetric water content at the end of the period.

If the counting time, t, is the same on both occasions, then, from Equation 7.5.5:

$$\sigma(\theta_2 - \theta_1) = \frac{a}{R_w}\sqrt{\frac{R_1 + R_2}{t}} \tag{7.5.7}$$

where R_1 and R_2 are the count rate on each occasion or, if R_1 and R_2 are not too different:

$$\sigma(\theta_2 - \theta_1) \approx \frac{a}{R_w}\sqrt{\frac{2R}{t}} \tag{7.5.8}$$

where R is one or the other (or ideally the mean) of R_1 and R_2. This is the same as the standard error of a single determination (Eq. 7.5.5) multiplied by the square root of 2.

7.5.3 Other sources of measurement error

So far, we have discussed only spatial variability and random counting as a source of error in water content measurement. In an ideal world, these should be the dominant mechanisms. However, several other significant causes of inaccuracy may be present, particularly in difficult soils and where installation or measurement practice is poor. An exhaustive list may not be possible, as there are often site-specific circumstances. However, the more common ones appear below.

Calibration errors

Calibration practice is described in Section 7.7. Because this depends itself on measurements sometimes made under difficult circumstances, the calibration relationship can never be perfect. Unlike random counting error, however, errors resulting from calibration are *systematic*, that is to say that they affect all measurements at that point in the same direction and the error does not reduce by using longer counting times or more measurements. An error in the slope, a, of the calibration relationship (Eq. 7.5.4.4) of, say, 2% will affect all measurements by this amount and will lead to a systematic over- or underestimate of water content changes of 2%. An error in the intercept value, b, will, however, affect absolute values of water content measurement but have no effect on changes.

Two points should be made about calibration relationships. Firstly, all soils vary spatially in many ways. The calibration curve is determined primarily by the chemical composition of the soil and its dry bulk density. It should be expected that these will vary spatially and hence there is a spatial dependence of the calibration constants a and b. It is not possible to know their precise value at any particular place and so there is always likely to be an unknown systematic error in the measurements from this cause. Secondly, describing the calibration curve itself in the form of Equation 7.5.4 is itself an approximation to reality. In practice, calibration relationships will always show some curvature, introducing an error into the measurements. In most cases, this curvature cannot be resolved from the measurements available and so straight line calibrations are almost universally adopted, except sometimes for near-surface measurements.

Standard count errors

The use of a standard count, R_w, to characterise a particular probe allows for instrumental drift and interchangeability of instruments. However, the standard count is itself a source of error, which can be minimised by good practice, but never entirely eliminated. There is a random component to it, as a result of random counting and a systematic component which results from variations in the standard count occurring over time. The random component can be reduced by using very long count times and the systematic component by making frequent standard counts. However, this does not compensate for short-term changes in R_w, to which some probes are prone. Standard counts are discussed in more detail in Section 7.7.1.

Depth location errors

As described earlier, the neutron probe measures water content integrated over a large volume of soil. This makes it relatively insensitive to small changes in position. However, where sharp interfaces occur or where there is a strong gradient in water content, even small changes in depth location can produce sufficiently different count rates that the error is comparable with or greater than that due to random counting. This is particularly true where repeated measurements are made in the same tube and where the change from one reading occasion to the next is small. If the probe is placed at different depths on successive occasions, this error may enhance or reduce the real changes significantly. Where there is a steady change in water content over a long depth range, a systematic error in probe placement, say 5 mm too deep at each depth, will have an appreciable accumulative effect on water content over the complete profile.

To illustrate this latter point, consider an idealised section of profile of 1 m depth, whose volumetric water content varies smoothly from 0.1 at the top to 0.4 at the bottom. If each measurement point is made 5 mm too deep, then the water content at the point of measurement is actually $5/1000 \times (0.4 - 0.1)$ greater than it is at the correct depth. Over the 1 m depth of profile, the accumulated difference in total water storage is, therefore, $5/1000 \times (0.4 - 0.1) \times 1000$ mm, that is 1.5 mm. Random counting error will typically be 2 mm over such a profile for a 15 s counting time and 1 mm if 60 s counting times are employed. A 5 mm error in depth placement will, therefore, produce an error in water storage comparable with that resulting from random counting.

Sharp interfaces and steep gradients

A sharp boundary between two different soil horizons is usually accompanied by an equally sharp change of water content. We have already remarked that the effect of the boundary is apparent from a greater distance away on the drier side than on the wetter one, because of the dependence of the size of the sphere of importance on water content. It might be expected from this that the total water content in the profile would be overestimated, as the depth of profile over which water content is overestimated is greater than that over which it is underestimated. In fact, the opposite is the case and sharp interfaces produce an underestimate of total water content.

Steep gradients have much the same effect: the boundary is just not as sharp.

These effects are rarely taken into account in practical field investigations. Identifying the location of the exact position of a boundary is difficult when installing access

tubes and water content either side of it is not often sufficiently homogeneous with depth to allow a reliable correction to be made. Steep gradients are even more difficult to deal with in this way. Water content changes over the year usually preserve most of the difference across boundaries and gradients, so that errors from this effect on changes of water content are usually small.

Water running down the outside of the access tube

The part of the access tube above ground is vulnerable to several hazards. It can be kicked or struck accidentally by people, animals or falling objects or it may be loosened by repeated placing of the probe on the top. The tube intercepts rainfall, which can run down a small gap between the soil and the tube, making the soil immediately around the tube wetter than it would be if there were no gap. It is, therefore, important to ensure that there is no gap between the soil surface and the tube.

Additional precautions to minimise any effect on the readings include using a small rubber or plastic drip ring to stop water running down the outside of the tube and let it drip onto the soil close to the tube, and building a very small ridge of soil a few mm high around the contact between soil and tube to ensure that water runs away from the tube.

In any case, the tube should be inspected on each visit to ensure that there is no gap and to take remedial action if there is, such as pressing the soil back around the tube or, if that is not effective, sifting a small amount of soil from close by into the gap.

7.6 Measurements in Access Tubes

Once tubes are installed, they can be used to measure water content and its variation with time at a series of depths. Travel to the site, unpacking and repacking the equipment, making the measurements and moving between one measurement location and the next all take time. Intelligent choice of locations (Section 7.3.4), measurement depths and count times as well as good experimental practice will maximise the value of the necessarily limited time available for data collection. The final choice of sampling strategy depends on the experimental objectives. For instance, a strategy to make the best estimate of the water balance over a large area differs from one comparing the water or solute balance between different crops on the same soil or from one where the focus is on transport in the deep unsaturated zone.

7.6.1 Choice of measurement depths

Choice of appropriate measurement depths is critically dependent on the objectives of the study. As a general rule, water content changes are greatest near the surface, and so it is natural to have a greater density of measurement in this zone. Where the water table may fluctuate within the depth of the access tube, however, water content may change even more than close to the surface, particularly in sands and gravels, where a change in water content between saturated (i.e. under the water table) and unsaturated of more than 25% by volume may be experienced.

As noted above, there is very little to be gained by making measurements closer together than 100 mm in depth, because of the very limited depth resolution of the neutron probe.

It is prudent to make measurements initially to the fullest depth possible. After one or two years of data have been collected, it may become clear that water content changes below a particular depth are negligible and the deepest reading depth can be reduced. Because of random counting error and other sources of random error, however, small changes in water content may be masked by the noise in the readings. Aggregating together readings from several locations in the bottom metre of the depth range will reduce the noise and reveal small seasonal trends.

7.6.2 Choice of counting time or total counts

As described in Section 7.5.1, the measurement precision resulting from random counting error is proportional to the square root of the total number of counts, which is equal to the count rate multiplied by the time over which the counts are accumulated. We are usually interested in determining water content to a particular precision, say 0.5% by volume, and so a convenient routine to achieve a result close to this is useful.

Some scalers or ratescalers give a choice of counting for a predetermined time or up to a predetermined number of counts.

For a predetermined time, t, the likely error in water content measurement is given by Equation 7.5.5.

The likely error is, therefore, proportional to the square root of the count rate.

For a predetermined count, the time, t, to accumulate N counts is given from Equation 7.5.1:

$$t = \frac{N}{R}. \tag{7.6.1}$$

Substituting this into Equation 7.5.5 gives for the likely error in θ:

$$\sigma_\theta = \frac{a}{R_w}.\frac{R}{\sqrt{N}}, \tag{7.6.2}$$

which is proportional to the count rate.

While neither method yields a constant absolute error, the change in likely error over a range of water content, is much smaller when using a predetermined counting time. If the count rate changes by a factor of two (say from 200 to 400 counts s^{-1}), then the likely error will increase by a factor of $\sqrt{2}$. For the same change in count rate, the likely error if measurements were made using a predetermined

count would increase by a factor of 2. Since volumetric water content is usually very nearly proportional to count rate, this means that the likely error is closely proportional to the square root of the water content in one case and to the water content in the other. A constant count time also has the advantage that the time required to make a measurement is predictable. It is recommended, therefore, that a predetermined count time be used.

The count time chosen is inevitably a compromise between a desire for maximum precision and the time available to make readings. Travel to the site, setting up the equipment, moving between different instrument locations, making readings of other instruments and doing maintenance jobs at the site are likely to take the majority of an operator's available time. This limits the time to make readings and, hence, the maximum count time for measurement.

Assuming that there is some flexibility in choosing count times, then the time, t, required to achieve a desired level of precision in water content, σ_θ, can be calculated by inverting Equation 7.5.5:

$$t = \frac{a^2 R}{R_w^2 \sigma_\theta^2}. \tag{7.6.3}$$

Or, using Equation 7.5.4:

$$t = \frac{a(\theta - b)}{R_w \sigma_\theta^2}. \tag{7.6.4}$$

Thus if the desired precision of measurement, σ_θ is 0.5% by volume, then for a typical probe and soil with R = 300 counts s^{-1}, R_w = 900 counts s^{-1}, a = 0.9, b = –0.01, and θ = 0.29, t turns out to be 12 s. To achieve a precision of 0.1% by volume would require a counting time of 300 s (5 minutes), which is likely to be excessive for most routine monitoring programmes. Counting times in the range of 10 s to 1 minute at each depth are usually regarded as practical, giving a precision in the range of 0.5–0.22% volumetric water content for these counting times. At a water content of 0.09, these would be 0.32–0.13% and for a water content of 0.49, the precision would be 0.7–0.3%.

These results apply to measurements at a single depth and consider only errors caused by random counting. The application to measurement of total storage over the whole profile or a range of depths will be considered in Section 7.7.2.

7.6.3 *Long count times or measure more tubes?*

As mentioned previously, there is a trade-off between making precise measurements in a single tube or a few tubes and collecting more, less precise measurements in several tubes. The total time taken depends on the count time selected, the number of depths at which counts are collected, the time taken to position the probe between depths and record the information, and the time taken to carry the probe from one tube to another and set it up for reading. As a general guideline, it will normally take about twice as long to make readings in a tube using 60 second counting times as using 15 seconds, that is twice the precision for twice the effort expended.

The relevant question is whether the uncertainty in the areal estimate is greater by following one strategy (e.g. making individual measurements with high precision by using a long counting time at each depth) or by following an alternative one (e.g. reading twice as many tubes, each with a short counting time at each depth).

The uncertainty in water content at each individual reading depth is easily calculated from Equation 7.5.5, although in reality it will be a little higher than this as a result of other factors. And the overall uncertainty as a result of the spatial variability between tubes can be estimated using the usual formula:

$$\sigma_{\theta V} = \sqrt{\frac{\sum_{i=1}^{n} (\theta_i - \bar{\theta})^2}{n-1}}, \tag{7.6.5}$$

where

$\sigma_{\theta V}$ is the standard deviation arising from spatial variability derived from a reading of θ at n different locations (access tubes);

θ_i is the value of θ at the ith location, and

$\bar{\theta}$ is the mean value of θ.

The standard error resulting from spatial variability, $SE_{\theta V}$ is then:

$$SE_{\theta V} = \frac{\sigma_{\theta V}}{\sqrt{n}} = \sqrt{\frac{\sum_{i=1}^{n} (\theta_i - \bar{\theta})^2}{n(n-1)}}. \tag{7.6.6}$$

This assumes that normal statistics can be applied and that there is no spatial correlation between the value of θ at the different locations. If this is not the case, the sampling scheme is likely to be less efficient and the standard error of the estimate will be larger (see Chapter 4).

The uncertainty in the mean value of θ at any particular depth over the area is then:

$$SE_\theta = \sqrt{\frac{\sigma_{\theta V}^2 + \sigma_{\theta R}^2}{n}} \tag{7.6.7}$$

where $\sigma_{\theta R}$ is the uncertainty arising from random counting error. We expect the value of θ to be similar at each location, so that $\sigma_{\theta R}$ will be very close to that given by using $\bar{\theta}$ for θ in Equation 7.5.4 inserted into Equation 7.5.5, with an approximation that b is zero, that is:

$$\sigma_{\theta R} \approx \sqrt{\frac{a}{R_w} \cdot \frac{\bar{\theta}}{t}}. \tag{7.6.8}$$

The overall standard error is, therefore:

$$SE_\theta = \sqrt{\frac{\sigma_{\theta v}^2 + \frac{a}{R_w}.\frac{\bar{\theta}}{t}}{n}} \quad (7.6.9)$$

In our example, with two different count times, $t_1 = 4\,t_2$ and different number of tubes read, $n_1 = (n_2/2)$, the standard error in each case is:

$$SE_{\theta 1} = \sqrt{\frac{\sigma_{\theta v}^2 + \frac{a}{R_w}.\frac{\bar{\theta}}{t_1}}{n_1}} \quad (7.6.10)$$

and:

$$SE_{\theta 2} = \sqrt{\frac{\sigma_{\theta v}^2 + \frac{a}{R_w}.\frac{4\bar{\theta}}{t_1}}{2n_1}} \quad (7.6.11)$$

The long count time/smaller number of tubes standard error, $SE_{\theta 1}$, will be greater than $SE_{\theta 2}$ if:

$$\frac{\sigma_{\theta v}^2 + \frac{a}{R_w}.\frac{\bar{\theta}}{t_1}}{n_1} > \frac{\sigma_{\theta v}^2 + \frac{a}{R_w}.\frac{4\bar{\theta}}{t_1}}{2n_1} \quad (7.6.12)$$

which simplifies to:

$$\sigma_{\theta v} > \sqrt{\frac{2a}{R_w}.\frac{\bar{\theta}}{t_1}} \quad (7.6.13)$$

Using some typical numbers of $a = 0.9$, $R_w = 900$ counts s^{-1}, $t_1 = 60$ s and a value of mean water content, $\bar{\theta}$, of 0.3 $m^3\,m^{-3}$, we have: $\sigma_{\theta v} > 0.0032$ or 0.32%.

So, in this example, if the spatial variability is expected to be greater than 0.32% by volume (in this case about 1% of the mean), the overall estimate of error will be smaller if the time available is used to read a greater number of tubes using a shorter counting time. In most cases, this is likely to be true.

This ignores the extra effort required to install the extra access tubes in the first place! It is also true that the underlying spatial variability cannot be assessed until there are measurements available. In addition, spatial variability will probably vary seasonally. For a long period monitoring programme, it may be possible to run a pilot study to establish the variability between a small number of tubes. Alternatively or additionally, gravimetric sampling on one wet and one dry occasion before the main tube installation programme will help to plan an installation and monitoring programme. As explained in Chapter 6, the uncertainties associated with volumetric sampling are likely to increase the apparent spatial variability, but this is much less likely to be true of mass wetness, which can be converted to volumetric water content by using a representative bulk density and Equation 5.1.10. This will not take into account variations in bulk density, but should be adequate as a guide both for estimating the likely spatial variability and the range over which there is spatial correlation (Cuenca *et al.*, 1997a).

Unfortunately, knowing the variability in water content is not the whole story. Usually, there is a relatively consistent difference in water content between different tube locations, with a similar pattern of changes superimposed upon this (Vachaud *et al.*, 1985). If changes in water content are of primary interest, for instance if the primary purpose of the study is to compute the water balance of a soil profile, then the calculation should be made on *changes* of water content. This can be done by comparing the likely precision of measurement of changes at a single depth, or over a depth of profile as described in Section 7.9.2, at one location with the variability of that quantity between tubes. This can be done by using $\sigma(\theta_2 - \theta_1)$ according to Equation 7.5.8 or $\sigma(W_2–W_1)$ according to Equation 7.9.7 in place of $\sigma_\theta v$ and Equation 7.6.13.

For the condition that it is favourable to use a greater number of access tubes with short count times, these lead to:

$$\sigma_{\Delta\theta v} > \sqrt{\frac{4a}{R_w}.\frac{\bar{\theta}}{t_1}} \quad (7.6.14)$$

and:

$$\sigma_{\Delta W} > \sqrt{\frac{4a}{R_w}.\frac{\bar{\theta}D^2}{Nt_1}}, \quad (7.6.15)$$

where
D is the total depth of profile, and
N is the number of depths at which it has been read.

For the values of a, R_w, t_1 and $\bar{\theta}$ used above, $D = 2$ m and $N = 10$, these work out at 0.0044 $m^3\,m^{-3}$ and 2.8 mm respectively.

Over the course of a year, there are likely to be many different time periods over which change could be computed. The best choice will depend on the objectives of the measurements, but the difference between the maximum and minimum values experienced or that between the mean summer (or dry season) and winter (or wet season) values should serve in many cases.

As shown earlier, it will be unusual for random counting error of absolute water content, even for relatively short counting times of 15 seconds, to be larger than spatial variability. This is also likely to be true for most sites where water content changes, either at a single depth or over a profile, are needed. However, it may not be so in homogeneous soils with small inter-plant spacings.

7.6.4 Good measurement practice

Good measurement practice aims to minimise all controllable sources of error and to ensure that the readings are as

close as possible to what would be measured in a totally undisturbed soil. In pursuit of this, the following precautions must be taken. In some situations, additional or modified measures will be required.

Crop and ground protection

As with access tube installation, protection of the natural state of the site is of paramount importance and many of the same precautions apply. On grassed sites, with soil that is not easily compacted, no special measures may be needed, especially if the site is not visited frequently. It may be advisable to stand in a different place on each reading occasion to avoid wear and compaction if visits are more frequent than once per week or during very wet or dry periods. Alternatively, a small platform, placed a few centimetres above the ground, with an open surface (e.g. a mesh or slats) will avoid pressure on the ground, let rain through and shade the surface only very slightly (see Fig. 7.5). The platform should not, however, be larger than necessary.

Tall crops and rough vegetation are harder to protect and may need permanent platforms for operators to stand on. Shading of the ground surface from rain and sun presents additional problems, which may be avoided by leaving a permanent framework in place, onto which a portable platform can be placed when readings are taken. Working above the ground surface may introduce a danger of falling from the platform and make a light handrail necessary. If the crop rows are separated widely enough, it may be possible to walk between the rows and use the neutron probe without damaging the crop and avoid a raised platform.

Depth placement

As discussed earlier, accurate depth placement to better than 5 mm is important. This is crucial where repeated measurements are made, so that the measurement at each depth on each occasion is truly comparable with those on other occasions.

The way in which the probe is positioned at each depth varies between different models of probe. In some, locating pieces are clamped to the cable. These are held by a support on the transport shield of the probe. Provided that the socket on the bottom of the transport shield is seated properly onto the top of the access tube, this is a robust system. Almost the only ways that error can occur are if the cable should stretch over time (a not unknown occurrence); if the top of the tube is damaged, preventing it fitting completely into the transport shield socket; if the tube should move up or down in the soil; or if the clamps are not tight enough. The system is, however, rather inflexible and cannot cope with using different depths in different tubes.

Others use a plastic spring clamp, rather like a large clothes peg, which is clipped onto the cable at appropriate places and sits on a support on the transport shield or directly on the top of the access tube. Marks on the cable may be used to indicate places to locate the clamp. This is a less robust system, as it depends on accurate placing of the clamp, and there is always a danger that it may slip on the cable, particularly in cold weather. A marked cable is also at risk of stretching.

The most flexible and, arguably, convenient method is to use a knurled wheel attached to a mechanical or electronic indicator. The wheel is driven by the cable as it is fed into the access tube. A spring-loaded pulley maintains pressure between wheel and cable and a hand-operated, spring-loaded clamp holds the cable at the desired depth. High-quality components are necessary, but the system has proved itself in many parts of the world. Problems can occur if the probe needs to be moved up and down to get past a slight obstruction in the tube, and backlash in the mechanism needs to be watched. It is best to make measurements from the top to the bottom of the tube, to avoid reversing the direction of cable travel and ensure that the cable always approaches the measurement depth from above. With these precautions, depth location is normally sufficiently accurate, although it is good practice to record the indicated depth as the probe reaches the bottom of the tube. In very cold weather, the cable may slip, either against the knurled wheel or through the clamp if the spring is not strong enough to hold the stiff and possibly slippery cable.

7.6.5 Recording measurements

It may seem obvious, but proper recording of data is at least as important as collecting it in the first place. In particular, it is important to record sufficient information to allow users at some time (possibly a few decades) in the future to interpret it. This means that the following information should be recorded along with the raw count rates: the location, date, time, observer's name, instrumentation identification and depth of observations. There are many possible variations in the way that data are collected and recorded. It may be written manually onto paper forms, entered directly into a portable computing device or recorded automatically in the internal memory of the ratescaler. In the last case, not all of the relevant information may be entered easily into the memory, requiring an auxiliary paper record to be kept with the field data. This introduces the danger that the two will become separated.

Whatever the recording medium, work is needed to set up the recording system before any data are collected. The principles of this are the same for all methods of recording, but the actual mechanics will be different.

In most cases, a number of different access tubes will be logged at a series of dates. For recording onto paper forms, it may be more suitable to record all readings for one particular tube over a period of time on the same form or, alternatively, to record all tubes read on one date together. This is less of an issue with data being recorded automatically by the ratescaler, since all readings should be date- and time-stamped. Entering the location and other auxiliary information and ensuring that the internal clock is set correctly must, of course, be done manually.

Figure 7.20 is an example of a form suitable for manual recording of data in which several access tubes are read at

NEUTRON PROBE FIELD READING FORM

DATE	(dd/mm/yy)	**SITE**	
PROBE		**RATESCALER**	
CROP		**GROUND COND**	
OBSERVER		**Standard Count**	cps

TUBE		A1		A2		A3		B1		B2	
TIME (GMT)											
DEPTH	**Tube ht**	**15**		**20**		**10**		**20**		**25**	
cm		**Gauge**	**Rdg**	**Gauge**	**Rdg**	**Gauge**	**Rdg**	**Gauge**	**Rdg**	**Gauge**	**Rdg**
10											
20											
30											
40											
50											
60											
70											
80											
90											
100											
120											
140											
160											
180											
200											
220											
240											
260											
280											
300											
Sum of Readings											
Depth Gauge Start											
Depth Gauge Bottom											
Depth Gauge End											

NOTES

Fig. 7.20 Example of a form for manual recording of neutron probe readings from several tubes on the same date.

the same site on the same occasion. It can be adapted easily to record data for the same tube on a number of different occasions.

It is written for a neutron probe having a wheel-driven depth indicator. These are normally set to a reading when locked in the transport shield of 9994, so that when it is lowered to a position where the centre of sensitivity is level with the top of the access tube, it reads 0000 (this example is for the Didcot Instruments IH II Probe, whose centre of sensitivity is 60 mm above the access tube top – 100 mm above the probe bottom with a 40 mm deep socket in the bottom of the transport shield which fits over the access tube (see Fig. 7.4). The indicator displays in centimetres). With this procedure, the indicator shows the desired depth plus the height of the access tube above ground. An alternative strategy would be for the depth indicator to be reset to a different value for each tube height, so that the reading was zero when the centre of sensitivity was level with the ground surface. At this site, each access tube has a different stickup ('tube ht'), and so the depth indicator readings will be different for the same depth of observation in each tube. It is strongly recommended that the actual indicator readings be entered onto the field sheet as they are set, rather than having them prefilled onto the form. Then, if an error is made in setting the depth, this will be recorded, aiding subsequent quality control of the data. For the same reasons, the depth indicator reading with the probe locked in its transport shield (Depth Gauge Start), resting on the bottom of the access tube (Depth Gauge Bottom) and on return to the transport shield (Depth Gauge End) should be recorded. The latter two will detect any slippage in the transport mechanism, allowing the reliability of depth setting to be assessed. Similar considerations apply to probes having marked or clamped cables.

The form has space for the standard count to be written. This may be entered after the readings have been taken or, alternatively, the standard counts may be stored elsewhere in the data processing system used.

The time is recorded as Greenwich Mean Time (GMT) to accord with British conditions. Local time will normally be appropriate, but in countries which use daylight saving, the local time changes according to the season. To ensure that there is compatibility with other data sources (e.g. meteorological), there needs to be a fixed relation between the time recorded on the form and solar time. It is recommended that the time be the same as that used by the meteorological service in the local area.

There is space at the bottom of each set of readings to record the sum of all the readings. This may be done in the field, if there is time, or subsequently. It is an important check to ensure that data are transcribed correctly from the form to the processing system (see Section 7.9.3).

The form also contains a generous area for writing notes. Observers should be encouraged to make full use of this to record any unusual situation or conditions.

The form can also be implemented as a spreadsheet on a handheld personal digital assistant (PDA), smartphone, or on a laptop or tablet computer. In this case, data may be transferred directly into a processing system or the spreadsheet may be the processing system itself. In the latter case, the field operator could see instantly the data displayed in graphical format and identify and correct probable reading errors.

7.7 Calibration

There are two aspects to calibration—Instrument and soil. *Instrument calibration* relates to a particular neutron probe. It takes into account differences between different probes. *Soil calibration* relates to differences in the relationship between the count rate of a particular design of probe in a range of soils.

7.7.1 Instrument calibration

Different examples of the same probe design often display a markedly different count rate in the same soil at the same water content. This is a consequence of differences in source strength, detector sensitivity and electronic characteristics, such as the voltage applied to the detector and the threshold level of the discriminator between probes. Over time, a probe's count rate will change somewhat. This may be a consequence of decay of the source (^{241}Am–Be sources have a half-life of about 432 years, so this is very slow), conversion of the gas in the detector tube (again a very slow process), or changes in electronic components.

Provided that the change is fairly slow and regular, then this can be accommodated by using a count rate in a standard medium to normalise the count rate.

Various materials have been used for a standard medium. Some workers use a large block of plastic, into which an access tube is inserted. Others use the moderator of the transport shield. Another choice might be the soil at a particular depth in an access tube, which was known not to change its water content over time. Such a case would occur at a depth of more than about 300 mm below the deepest occurrence of the water table, provided that no chemical change in the water accompanied the seasonal fluctuations. In many ways, the simplest choice is a large drum of water with an access tube in its centre.

The essential characteristics of a standard are as follows:

- It should be large enough to contain the neutron cloud. This ensures that there is no influence on the count rate by, for instance the floor or ground surface, or objects nearby. It also protects operators from radiation emanating from the source. If the standard is not large enough to meet this criterion, then particular attention must be given to ensure that the surroundings are always exactly the same. This can be difficult to realise in practice.

• It should be high in hydrogenous material. This ensures a high count rate and minimises errors resulting from random counting. Also, the greater the hydrogen content, the smaller the sphere of importance.
• It should have a low coefficient of thermal expansion. The effective water content of the standard is proportional to its density, and so the count rate is expected to be similarly related. Thus count rate will vary inversely with temperature and the coefficient of expansion of the material of the standard. Most plastics have a relatively high thermal expansion coefficient.
• It should be chemically stable and not absorb water from the atmosphere. If it does the latter, then count rates will vary as atmospheric humidity changes.

As a result of these considerations, it is recommended that the standard adopted is a large drum of water. Water is easily available, and so reproducible standards can be constructed easily and cheaply at almost any location. It has one of the densest hydrogen concentrations available, so that, provided there is at least 200 mm of water surrounding the probe on all sides, the effect of any change to the surroundings is negligible. Its thermal expansion coefficient is quite small, typically $2.1 \times 10^{-4}\,^{\circ}C^{-1}$, ensuring a change of only about 0.4% over a 20°C range of temperature. This, however, assumes that the water does not freeze, which would produce a 9% change in volume, so that the water drum should not be left outside in seasonally cold climates. 0.4% equates to 4 mm of water in a soil profile containing 1000 mm (2 m depth at 50% by volume, 5 m at 20% by volume), so that for accurate work, it is advisable either to keep the water standard in a reasonably constant temperature environment or to monitor the water temperature (which may be quite different from the local air temperature) and to make a correction to the standard count rate for this. This consideration is even more important for plastic standards, most of which have a coefficient of thermal expansion larger than water. The appropriate calculation is:

$$R_w(T_0) = (T - T_0)R_w(T)\beta \qquad (7.7.1)$$

where
$R_w(T)$ is the count rate in the standard at temperature T;
β is the coefficient of volume expansion of the standard material (for solids, this is three times the linear coefficient of expansion, usually designated α); and
T_0 is the reference temperature at which the standard count rate is expressed (e.g. 20°C).

A water standard may be constructed from any suitable water-holding container, provided that it is large enough. Old oil drums or waste bins have been used very successfully. The biggest problem encountered is usually in holding an access tube in position. A 45 mm diameter access tube has a buoyancy of about 15 N m^{-1} length. A 1.2 m immersed length of tube, therefore, will require a downward force of 18 N (about 1.8 kg weight) to keep it in place. A suitable design for a water drum standard is shown in Fig. 7.21 and a photograph of one is in Fig. 7.22. If any components are made of steel, they should be protected from corrosion by galvanising or another coating to avoid iron species gradually dissolving into the water. Growth of algae can be inhibited by using an opaque container.

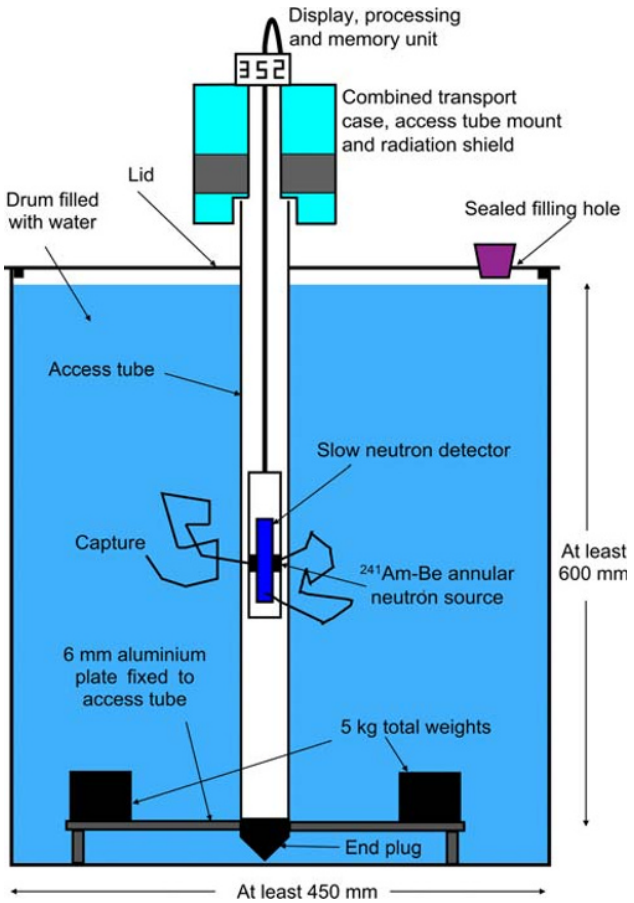

Fig. 7.21 Water drum standard.

A further advantage of using an easily reproducible standard is that it allows different neutron probes of the same design to be interchanged easily, without significant loss of measurement accuracy. It is expected that, in any situation, the count rate between two similar probes or the same probe at different times will be affected proportionally by the same amount. Normalising the reading according to a standard count should, therefore, produce an identical figure. This was tested by Hodnett and Bell (1991) and found to lead to an error in water content of less than 0.3% by volume. This was superior to the practice of using a different calibration for each probe in each soil and that of using a plastic block as a standard.

Even when only one probe is in use, frequent measurements in a standard allow any change in the probe's characteristics to be identified. A well-designed and well-made probe may prove to be very stable over long periods of time,

Fig. 7.22 Water drum. The transparent cover allows the water level and clarity to be monitored. To prevent growth of algae, the drum should be covered with an opaque lid when not in use.

but unexpected changes to the standard count sometimes occur for no apparent reason. This may be indicative of an impending failure, but often there is no other symptom other than a change in count rate. If the probe does fail and needs repair, then usually a different count rate is found after the repair than before. Hence the use of a standard count allows readings from before the change to be compared with those from afterwards.

Using standard counts

The usual method for using standard counts is to express all measurements of count rate recorded in the soil as a ratio to that of the standard count rate. This is usually termed the *count rate ratio*, R/R_w, where R is the count rate in the soil and R_w is that in the standard. The subscript, w, is used to indicate that water is the preferred standard.

Random counting error affects standard counts in the same way as counts within the soil. To avoid this having an appreciable effect on the accuracy of measurements, it should itself be as accurate as possible. The use of water as the standard helps, since count rates are high, and this reduces the proportional error (see Eq. 7.5.3). Using a long counting time, or several successive shorter counts, reduces the error further. If counts in the soil are made for a time t and those in the standard for a time t_w, then the combined error as a result of random counting is:

$$\frac{R \pm \sigma_R}{R_w \pm \sigma_{R_w}} \tag{7.7.2}$$

This can be written as follows:

$$\frac{(R/R_w) \pm (\sigma_R/R_w)}{1 \pm (\sigma_{R_w}/R_w)} \tag{7.7.3}$$

giving approximately:

$$\frac{R}{R_w} \pm \frac{\sigma_R}{R_w} \pm \frac{R\sigma_{R_w}}{R_w^2}. \tag{7.7.4}$$

Combining the uncertainties in the usual way by adding the squares and taking the square root, gives:

$$\sigma_{\frac{R}{R_w}} = \frac{1}{R_w}\sqrt{\sigma_R^2 + \frac{R^2\sigma_{R_w}^2}{R_w^2}}. \tag{7.7.5}$$

Using $\sigma_R^2 = (R/t)$ from Equation 7.5.3, this gives:

$$\sigma_{\frac{R}{R_w}} = \frac{\sqrt{R}}{R_w\sqrt{t}}\sqrt{1 + \frac{Rt}{R_w t_w}}. \tag{7.7.6}$$

If Rt is small by comparison with $R_w t_w$, this is approximately:

$$\sigma_{\frac{R}{R_w}} = \frac{\sqrt{R}}{R_w\sqrt{t}}\left(1 + \frac{Rt}{2R_w t_w}\right). \tag{7.7.7}$$

So if $R_w t_w$ is much greater than Rt, the error resulting from random counting on the water count is small. Using a water standard, R_w is usually at least twice R and quite commonly three or four times as large. If we take $R_w = 4R$ and $t_w = 25t$, then the additional error resulting from the standard count is only 0.5% of that resulting from random counting on the count in the soil. However, if we are interested in calculating the storage of water in the profile and the storage is calculated from 10 measurements, then the error resulting from random counting on the standard count becomes 5% of that from counting in the soil; and for 25 measurements, it is 12%, still acceptably low for most purposes. For most routine use, therefore, standard counts in a water drum should be at least 25 times longer than counting times in the soil. This will ensure that errors from the water count do not contribute significantly to the resultant error from counting in the soil.

Some makes of neutron probe allow long count times to be selected. It is easy, therefore, to set the probe on a water drum and leave it to count for perhaps 30 or 60 minutes,

while the operator gets on with other jobs. Alternatively, 25 separate counts may be taken at the same count time as used in the field and the average used. This has the advantage that a check can be made that the standard deviation is approximately as expected from Equation 7.5.3. If this is not the case, then a malfunction of the probe should be suspected and further investigations carried out, perhaps making repair of the probe necessary before reliable data can be collected. An easy way to check on the statistics is to use some of the characteristics of the normal distribution. From this, we expect that 68% (about 2/3) of the readings will be within one standard deviation of the mean, and only about 5% will be more than two standard deviations from it. For 25 readings, this would mean that about 7 are expected to be more than one standard deviation away and only 1 would be more than two standard deviations from the mean.

7.7.2 Soil calibration

Several methods have been proposed to make soil calibrations. They fall into three main categories: laboratory methods, field methods and theoretical calculations. The objective of calibration is to obtain as good an estimate of the value of a and b in Equation 7.5.4 as possible. A number of points should be recognised in this task.

- Equation 7.5.4 is an approximation to the real relationship relating count rate ratio to volumetric water content. In most instances, it is a very close approximation, but it may fail over a very wide range of water content.
- Values of a and b are likely to vary from place to place within nominally homogeneous soil. In particular, the intercept value, b, is usually much more sensitive to the dry bulk density of the soil than the slope value, a (Couchat, 1967).
- Care must be exercised when dealing with soils having distinctly different horizons. Each of these may need a different calibration (Greacen & Hignett, 1979). The use of a common calibration for mineralogically different horizons may produce highly misleading results. Sufficient data should be collected and analysed for each horizon to determine whether a separate calibration should be applied. This can involve some difficult judgements.
- It is unusual to obtain very high accuracy in soil calibration. An accuracy of 5% or better for the slope value, a, is regarded as good.

Laboratory methods

In essence, laboratory calibrations rely on transporting a large quantity of soil to the laboratory, packing it into a suitable container, taking readings with a neutron probe and then determining the water content. The water content is changed and a second set of neutron probe and water content measurements made. This may be repeated several times. Variations occur with the methods used for packing, the way in which water content is measured or calculated and whether the soil is repacked in the container for each water content.

The advantages of laboratory calibration are as follows:

- The same soil is used for each water content.
- Laboratory conditions are easier to control than those in the field.
- Soil can be mixed to give a homogeneous medium, which is representative of the field, but avoids spurious differences as a result of unexpected variations.
- The range of water content over which the calibration is made can be controlled.
- Stony soils can be much more easily dealt with.

Disadvantages of laboratory calibration include the following:

- A large mass and volume of soil is required (at least 1200 kg or 0.7 m^3, often much more).
- packing and repacking this amount of soil is very time consuming and heavy work.
- It is difficult to repack soil to the same bulk density as occurs in the field.
- Maintaining a uniform water content in the soil for long enough to perform the calibration may be impossible, particularly when wet.

A typical procedure would be as follows:

1 Identify in the field the soil horizon(s) to be calibrated.

2 Measure the dry bulk density of the horizon(s) and estimate the range of water content over which the calibration is required. This latter can be difficult, and it is probably best to slightly overestimate, rather than underestimate the range.

3 Collect sufficient soil from the field site to fill the container to be used for calibration. This should have a minimum dimension in any direction of 0.8 m (1 m if very dry soil is to be used). The mass of soil will be at least 500 kg and may be 1000 kg.

4 Spread the soil over a large area, so that it is no more than 100 mm thick and leave to dry. Mix daily to ensure even drying.

5 When the soil is air dry, or at a uniform water content at or below that at which the driest calibration point is required, it is ready to be packed into the container. If the soil is drier than is required, take small amounts (approximately 10 kg at a time) of soil and mix with sufficient water to bring it to the desired wetness. A small concrete mixer is useful for this operation. Spread the soil in an even layer into the container and compact to the desired bulk density. Then repeat for the next layer and so on until the container is filled to the desired level. To minimise water loss by evaporation, keep the soil (both in the container and waiting to be put into it), covered as much as possible. Compaction can be most efficiently and reliably done by using a stiff metal or wooden plate which will just fit easily into the container. A heavy weight impacting the centre of the plate will compact the soil. Alternatively, a vibrating hammer can be used. Careful measurement of the mass of soil put into the

container and the level of the surface will allow the bulk density to be monitored.

If the soil contains stones, these should be incorporated at the same time as the soil in as uniform way as possible. Small stones are best mixed into the soil before it goes into the container, while large ones can be incorporated by hand into each layer of soil.

Sub-samples of soil should be taken at intervals to check on water content, bulk density and their uniformity.

6 It is usually most convenient to place an access tube into the correct position in the container before packing soil into it. If this was not done beforehand, then install the access tube now using the methods described in Section 7.3.

7 Now neutron probe measurements can be taken in the access tube. Depending on the depth of soil in the container, it may be possible to do this at more than one depth. It is good practice to make measurements down the access tube from close to the surface to near the bottom. This will provide assurance that measurements are not affected by proximity to the surface or the bottom of the container. There should be a section of stable count rate of at least 400 mm depth. If this is not the case, then more soil should be added until this condition is met. Counts should be taken for as long as practical, so that the random counting error is as small as possible. In any case, the count rate should be determined to give a standard deviation of the count rate ratio, $^{R}/_{R_w}$, better than 0.001 (0.1%). Provided that R_w is known sufficiently well that we can ignore any uncertainty in its value, compared with that of R, the standard deviation of the count rate ratio is, using Equation 7.5.3:

$$\sigma\left(\frac{R}{R_w}\right) = \frac{\sigma_R}{R_w} = \frac{1}{R_w}\sqrt{\frac{R}{t}}. \qquad (7.7.8)$$

The counting time to achieve a given precision of $\sigma(R/R_w)$ is then:

$$t = \frac{R}{\left[R_w \sigma\left(\frac{R}{R_w}\right)\right]^2}. \qquad (7.7.9)$$

So the time required is proportional to R. If R_w is 1000 counts s^{-1} and the desired value of $\sigma(^{R}/_{R_w})$ is 0.001, then t in seconds is numerically equal to R in counts s^{-1}. So for R = 100 counts s^{-1}, t = 100 s; and if R = 400 counts s^{-1}, the counting time would need to be 400 s. It is recommended that all counts be taken at the same count time, which should be chosen to be that needed at the highest expected count rate encountered during the calibration.

8 Four to six soil samples should be taken from immediately around the access tube at the depth(s) at which neutron probe measurements have been made. These are most conveniently taken using rings of about 50 mm diameter and 50 mm high, sharpened at one end, as described in Chapter 6. They can be taken while removing the soil from the container, ensuring that the soil to be sampled has not been disturbed during this operation.

9 A measurement needs now to be taken at one or more higher water contents. This may cause some problems.

The simplest water content to achieve is at effective saturation. This may not be true saturation, as there is usually a few percent by volume of entrapped air. However, it is likely to approximate quite well to the situation in the field when the soil is at saturation. Although the soil may rarely or never reach this point, it has several advantages:

- The need for repacking of the soil again is avoided, since water can be introduced into the already packed container.
- The increase in water content can be measured accurately simply by measuring the amount of water added to achieve saturation.
- Provided that the container was packed well in the first place, so that it does not slump or otherwise change its structure on wetting, the change in count rate recorded by the neutron probe can be assigned fairly unambiguously to a change in water content of the soil, as the dry bulk density will not change. It is very difficult to achieve the same dry bulk density when attempting to repack soil at a different water content.

To saturate the soil evenly, it is best to introduce it at the bottom of the container. This is facilitated if there is a shallow layer of gravel in the bottom, separated from the overlying soil by a geotextile or layer of coarse sand to stop the soil penetrating the gravel. A sight tube on the side of the container allows progress of the water level to be monitored and corrections to be made for the amount of water needed to saturate the gravel and sand layers. By making a plot of cumulative water introduced against water level in the sight tube, any inhomogeneities in the packing should become apparent. To avoid disruption of the soil and excessive air entrapment, it is recommended that the container be filled over a period of about 1 hour.

For some soils, it is possible to drain the container and make another measurement at 'field capacity'. There needs, however, to be a sufficient depth of soil beneath the measurement depth that this can be achieved over a reasonable length of profile, since the base of the soil will be at saturation when drainage stops. In practice, this limits the use of a field capacity point to coarse-textured soils. Determination of the water content must be done by gravimetric sampling as in Step 8.

To make measurements at other water contents, the container must be repacked again. At water contents higher than 'field capacity', the soil drains rapidly, and so a uniform water content cannot be maintained. Samples for gravimetric determination of water content must, in any case, be taken as close to the time that the neutron probe measurements were made as possible.

While very time-consuming, this method usually produces very accurate results, at least for the particular sample of soil in the container. As long as this is

representative of the field soil, the method has much to recommend it.

Field methods

Most workers use field methods of calibration, which avoid the difficulties of digging and transporting large quantities of soil and handling them in the laboratory. In essence, the procedure consists of taking neutron probe counts in an access tube, followed by gravimetric sampling of the soil at the same depth around the tube.

The advantages of field calibration are as follows:

- The calibration is performed on soil in its natural state *in situ*.
- Water contents outside the natural range of variation are not used in the calibration.
- Large amounts of soil need not be removed from the site.
- A large amount of effort need not be concentrated over a short time period, but can be spread over a much longer time.

The disadvantages are as follows:

- A good calibration relies on getting the full natural range of water content over a year and so takes a long time to collect enough information.
- The difficulties attending the collection of good quality known volume samples (Section 6.3) mean that the gravimetric water content data are frequently very noisy.
- A suitable calibration for the soil is often not available until well into a study because of the need to collect data over a long time period.

There are several variants of the methodology in use.

Temporary access tube method In this method, an access tube is installed in the ground specifically for calibration. Once installed, a profile is measured with a neutron probe to identify the most suitable depths for calibration. It is usually not wise to measure close to interfaces or where there are large gradients of water content. Depending on the length of the tube, more than one depth may be selected. A long count (or several shorter counts) is made at each selected depth, as described for laboratory calibration, to ensure that random counting errors are negligible compared with those resulting from the sampling procedure. Making the counts will take only a short time compared with the rest of the procedure.

Once counts have been taken, gravimetric samples are collected from the soil surrounding the access tube as described in Section 6.2. These should be from as close as possible to the access tube and have a diameter and half-height similar to that of the radius of the sphere of importance. This will ensure that the calibration samples contain a large proportion of the actual soil that was measured by the neutron probe. Large samples also minimise likely errors (Section 6.4.1). More than one depth can be sampled if the shallowest one is done first.

Removal of soil from guide tube method When an access tube is installed, soil is removed from the guide tube and, usually, discarded. This soil is expected to have a water content very similar to that surrounding the tube and so should be suitable to use as a calibration sample. The access tube can be used for routine monitoring after installation. The main problems are that the volume of soil is quite small – 238 mL for a 150 mm length of a 45 mm diameter tube – and it is very difficult to collect the soil occupying a well-defined length exactly, particularly if the soil contains stones.

Two approaches have been used.

1 Collection of an accurately measured volume of soil This method aims to collect an accurately measured volume of soil by ensuring that all the soil from a very well defined depth range is captured. It uses a screw auger, which has had two holes drilled in the stem, through which a peg can be inserted, as shown in Fig. 7.23. The lower hole is positioned so that the end of the auger is exactly level with the end of the access tube, while the other is a short distance, say 150 mm, above this. The end of the auger bit is ground flat, so as to leave a flat surface at the bottom of the access tube.

The technique is to insert a guide tube in the normal way to 75 mm above the depth at which the first calibration is required. Then, using the auger with the peg in the lower hole, all the soil from within the guide tube is removed and discarded (Fig. 7.23a). At this point, the empty guide tube is positioned above undisturbed soil. Then, soil is augered from below the guide tube, with the peg in the upper hole, so that a hole of exactly 150 mm depth is made with the same diameter as the auger (Fig. 7.23b). This soil is kept and placed immediately in a plastic bag to prevent loss of water. The guide tube must then be knocked down by exactly 150 mm (Fig. 7.23c) and the soil from within it augered out, with the peg in the lower hole again, and added to that in the bag (Fig. 7.23d). This should ensure that the soil in the bag is that from a 150 mm depth of soil of diameter equal to the outer diameter of the guide tube.

The next 150 mm depth can be sampled in the same way, and the process is repeated to as great a depth as required. After reaching the desired installation depth, the guide tube is removed and an access tube inserted. It is important then to make measurements with the neutron probe immediately, so that the water content of the soil does not change after sampling.

With care, the technique is capable of gathering samples of well-defined volume. The likely problems are as follows:

- Loss of soil. It is important to be sure that no soil falls off the auger while removing it from the guide tube and is lost. Bell *et al.* (1987) used the method to take 40 mm length samples and fitted a bowl around the tube to catch soil. The bowl is an insurance against losing soil.
- Drying out of the soil. The volume collected is fairly small and has a large surface area, so that it is easily dried

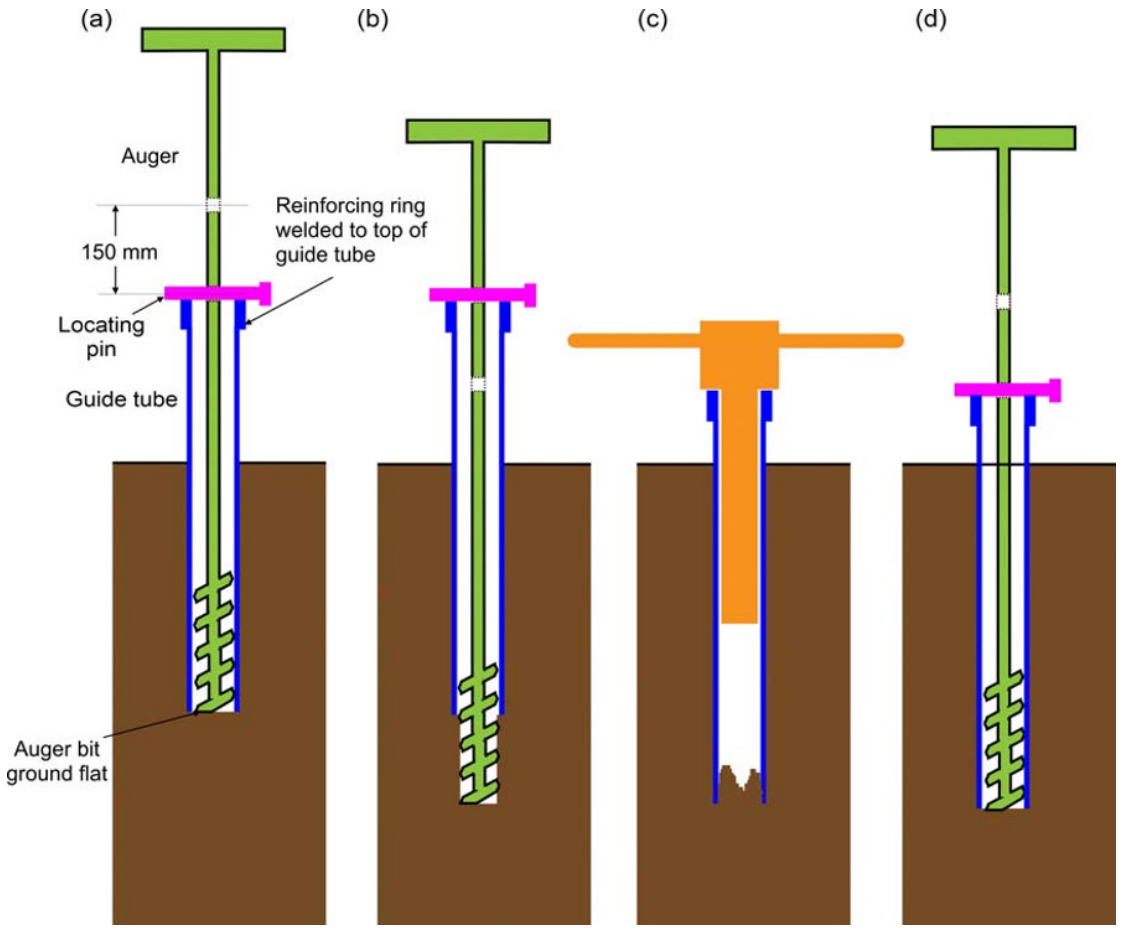

Fig. 7.23 Calibration by removing constant volume samples during access tube installation. (a) The hole is cleared to the bottom of the guide tube using an auger ground to have a flat bottom surface. A pin through a hole in the auger stem locates the bottom of the auger with the bottom of the guide tube. (b) The hole is deepened by 150 mm, using the pin in a second hole in the auger stem to define it. The soil removed is collected. (c) The guide tube is knocked to the bottom of the pre-drilled hole, collecting the soil shaved from the sides inside it. Marks on the guide tube indicate the correct depth. (d) The auger again clears the hole to the bottom of the guide tube and the soil from the bottom is collected. (*See insert for colour representation of the figure.*)

out. Shading the area from direct sunlight, transferring soil quickly from the auger to the plastic bag and making sure that collecting bags are kept sealed, except when putting soil into them will help. If it is raining, the samples could, of course, get wetter.

- Inaccurate volume of soil collected. Compaction of the soil may occur if too large a depth of soil is excavated at once. This may be avoided by taking the sample in two tranches, each of 75 mm.

To ensure that the guide tube is knocked down exactly by the correct depth, it helps if rings are machined on its outside, which will be level with the top of the ground protection plate. The ground protection plate must also be secured firmly and operators avoid stepping on it, so that it remains stable during the operation.

2 Use of a gamma density backscatter depth gauge (see Section 6.5.4) This approach is simpler, but requires a gamma probe. The technique has been described by Haverkamp *et al.* (1984) and involves sampling the soil from within the access tube, as for the method just described. However, there is no need for accurate volumetric sampling. The samples are used simply to measure gravimetric water content, which is then converted to a volumetric basis by using a density measurement made with the backscatter gauge, using Equation 5.1.10.

Normally, either of these two approaches will give only a few points (often very close together) on a calibration curve on each occasion. However, Haverkamp *et al.* (1984) installed a lot of tubes at the same time and measured each one at several depths. This allowed them to produce a calibration curve from just one installation/calibration session. The range of water content can be maximised by choosing the right time of year, usually early in a dry season or spring, when soil near the surface may be dry, but that at depth is still wet. Care is needed to make sure that all depths used have the same mineralogy (Greacen & Hignett, 1979).

Single access tube – multiple sampling method Van Vuuren (1984) developed a technique for calibration which required only one access tube, but neutron probe measurements were made at different times and related to gravimetric measurements at those times. To achieve this, the gravimetric samples were taken from around a circle of radius about 2 m from the tube. The advantage is that only one tube need be installed; but on the other hand, spatial variability may introduce substantial noise into the calibration relationship. Further, the repeated gravimetric samplings must be done without appreciable damage to the vegetation or soil surface close by, so that soil water conditions at the tube or future gravimetric sampling points are unaffected by the sampling operation.

Accelerated calibration The calibration process can be accelerated by starting with a dry soil, taking neutron counts and collecting gravimetric samples, then repeating the process after irrigating the soil. Sharp wetting fronts should be avoided, but calibration samples can be collected when the soil has wetted and after initial drainage over an hour or two has taken place and then again after several days or weeks, when the soil has dried some more.

Steady irrigation method Carneiro and de Jong (1985) introduced a calibration technique which did not involve destructive sampling. They irrigated three confined soil plots, 1.5 m square, with 20 mm increments of water and made neutron probe measurements from a centrally installed access tube. By plotting cumulative depth of water applied against count ratio integrated down the profile, they obtained a good estimate of the slope, a, in Equation 7.5.4. Integration of this equation down to a depth Z (1.2 m in this case) gives:

$$\int_0^Z \theta \, dz = \int_0^Z a \frac{R}{R_w} dz + bZ. \qquad (7.7.10)$$

The plot is initially curved, as wetting occurs only close to the surface and is thus affected by neutron escape to the air, but then straightens out with a slope of a and flattens off when the wetting front reaches the bottom of the profile and water drains below depth Z. If there is a change in soil properties at some depth, affecting the value of a, then this would show up as a change in the slope of the graph. Figure 7.24 shows the curves obtained by Carneiro and de Jong (1985). Note that a and b in Carneiro and de Jong's (1985) paper represent b and a, respectively, as used here.

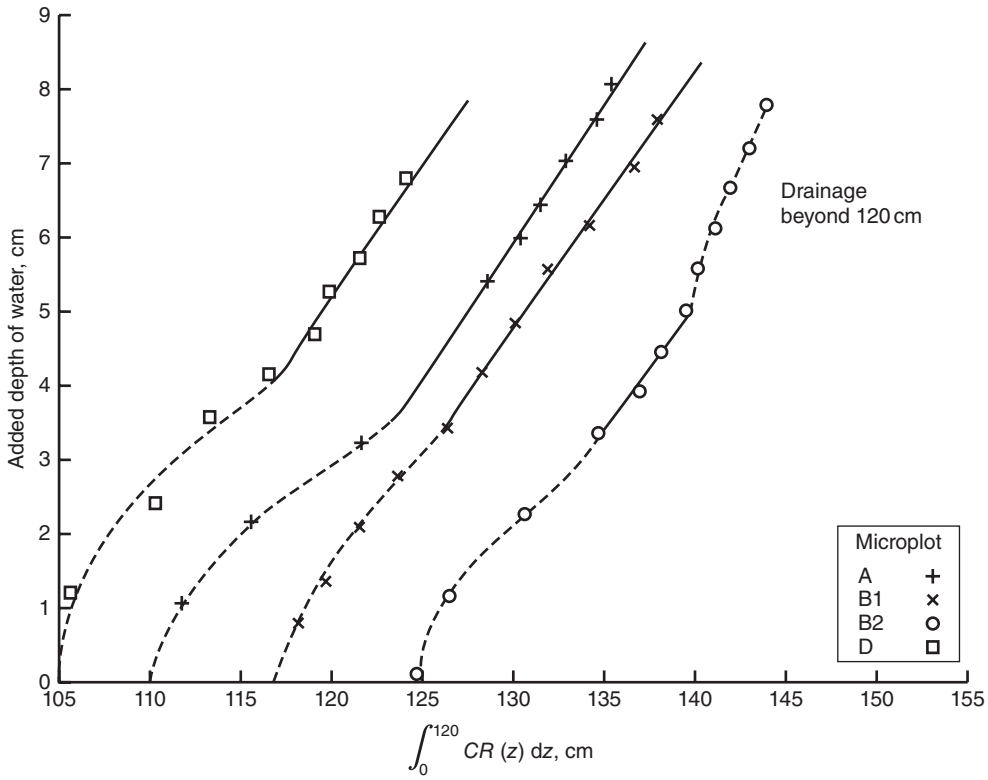

Fig. 7.24 Depth of water added to the profile plotted against count ratio integrated down the profile in three microplots reported by Carneiro & de Jong (1985), figure 2. Note that for Plot B, the experiment was repeated with a higher initial water content in the microplot (B2). Carneiro & de Jong (1985). Reproduced with permission of Lippincott Williams & Wilkins/Wolters Kluwer Health.

If the area irrigated is sufficiently large, there is no need for a confined plot, which makes the method much easier to implement. As a rule of thumb, the smallest distance from the access tube to the edge of the plot should be at least equal to the deepest depth monitored, Z. The method can also be used with continuous irrigation, provided that it is evenly distributed and its rate can be monitored accurately, so that the cumulative amount of water applied at any time is known.

Calculation of calibration constants

Usually, the result of either laboratory or field calibration experiments is a set of pairs of values of volumetric water content and count ratio. These are normally converted to a calibration curve using linear regression. The relationship obtained by regressing a series of y values upon their corresponding x values usually yields a different relationship from that when x is regressed on y. The variable upon which the other is regressed (i.e. x when y is regressed on x) is often called the *independent variable*. The implicit assumption is that this variable is free of error and that all uncertainties in the data are contained in the y or *dependent variable*. The use of the terms independent and dependent can cause a lot of confusion. In the present case, one might regard the independent variable as being the soil water content and count ratio as the dependent one since changing water content will lead to a change in count rate, whereas it is not possible to do it the other way round. However, we can reduce the error in count ratio to as small a value as we like, whereas measurement of volumetric water content using the gravimetric method is usually prone to considerable uncertainty. It seems appropriate, therefore, to calculate the calibration curve by regressing volumetric water content on count ratio and making this latter quantity as accurate as practical.

Greacen (1981), however, believed that this was incorrect and argued that there was likely to be more error in values of count ratio because this quantity is influenced by variations in the chemical composition of the soil which are unknown. It is the contention in this book, however, that, usually, the dominant errors are those in determining water content and, therefore, that the calculation should be made by regressing water content on count ratio.

Haverkamp *et al.* (1984) used short counting times when obtaining a calibration in a large number of access tubes and took likely errors in both water content and count ratio into account in a modified regression procedure. It is also possible to include dry bulk density in the regression procedure (e.g. Vachaud *et al.*, 1977).

Theoretical methods

Ølgaard (1965) first explained the neutron probe calibration relationship using neutron diffusion theory with three energy groups. This was built on by Couchat (1967, 1983), Couchat *et al.* (1975), McCulloch and Wall (1976), Elder and Rasmussen (1994) and Li *et al.* (2003a). The latter two sets of authors used seven energy groups for greater accuracy. By assuming that the soil is a homogenous mixture of the atoms making up its composition, the relationship between count rate and water content can be predicted quite well. Hence if the chemical composition of the soil is known, a calibration curve can be calculated. Unfortunately, several elements which are expensive to measure and usually found only in trace quantities in soil (e.g. boron, cadmium and gadolinium) have a large slow neutron absorption cross-section. So even at low concentration, one of these elements can have a large effect on the calibration equation. Couchat *et al.* (1975) circumvented this by measuring the transport and absorption cross-section of the dry soil directly. They used a large neutron source in a 1 m^3 graphite block. The method measures the change in neutron flux at the surface and inside the block, when soil is introduced into a cavity. This allows an estimate of the cross-sections to be obtained, which can then be used to produce theoretical calibrations for different probe designs, of the form:

$$\frac{R}{R_w} = (\alpha + \beta\rho_d)\theta + \gamma + \delta\rho_d \qquad (7.7.11)$$

where α, β, γ and δ are parameters derived from the theoretical model.

In terms of the more familiar relationship (Eq. 7.5.4), the calibration parameters are:

$$a = \frac{1}{\alpha + \beta\rho_d} \qquad (7.7.12)$$

$$b = -\frac{\gamma + \delta\rho_d}{\alpha + \beta\rho_d}. \qquad (7.7.13)$$

Vachaud *et al.* (1977) tested the method against field-measured calibrations and obtained good agreement between them, lending confidence to the method and providing a workable methodology for neutron probe calibration in soils in which *in situ* calibration is difficult. For several years, the French nuclear research centre at Cadarache provided calibrations for soils from samples submitted. Unfortunately, this facility is no longer available. However, measurements of transport and absorption cross-sections can be made by many organisations across the world, and there seems no reason why these cannot be used in much the same way. Elder and Rasmussen (1994) compared calibration by chemical analysis of the soil with measurement of neutron cross-sections using a graphite block. Although the cross-sections using each method differed substantially, there was little difference in the calculated calibration curves, which agreed well with experimental data.

The model of Li *et al.* (2003a) was used by Li *et al.* (2003b) to investigate the effect of air gaps around an access tube on the calibration relationship and to explore the effect of different access tube diameters. For the clay soil properties fed

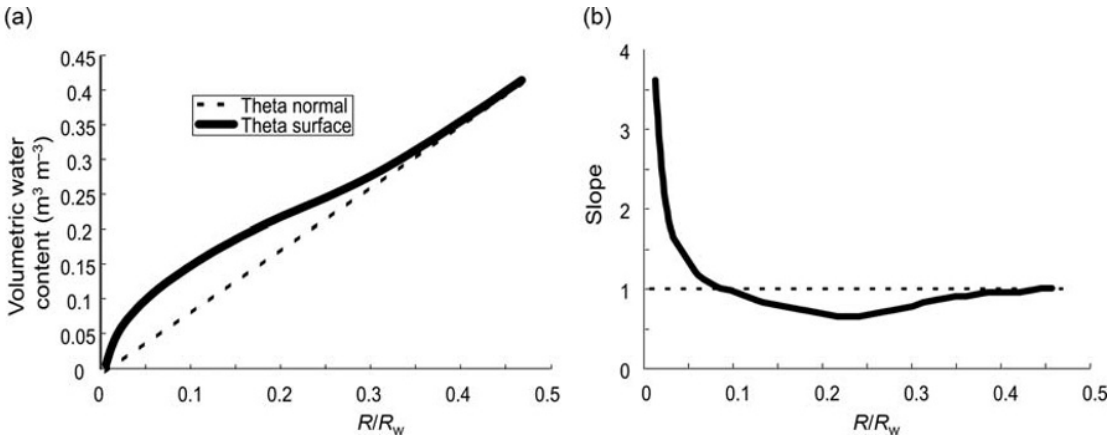

Fig. 7.25 Effect of the surface on neutron probe readings (a), and slope of the calibration curve (b).

into the model, a 5 mm air gap reduced count rate at 0.05 $m^3 m^{-3}$ by about 13%, increasing to about 37% at 0.35 $m^3 m^{-3}$. Larger gaps had a greater effect, although the rate of reduction in count rate reduced. Water-filled gaps had the opposite effect.

The Li *et al*. (2003a) model was also used by Huang and Fityus (2008) and Fityus *et al*. (2011) to investigate the effect of soil shrinking and swelling on the calibration curve. The change in bulk density was found to preserve a linear relationship, but the presence of cracks caused it to be highly non-linear and complex.

7.8 Measurements near the Surface

Problems caused by a sharp interface between two horizons with different water content have been mentioned several times earlier. Possibly, the most extreme case of a sharp interface is the soil surface. The seasonal pattern of changes is usually greatest in this region, making measurements close to the surface important. However, spatial variability is often maximised as well, meaning that a single measurement or only a few may not be adequate to characterise an area. Soil near the surface is usually richer in organic matter and may be different chemically in other ways from that deeper in the profile, which presents yet another challenge to accurate measurement.

Unlike at a sharp boundary deep in the soil, neutrons crossing the soil–air interface cannot return, but will escape into the atmosphere. Several solutions have been proposed to combat this and to improve the accuracy of near-surface measurements, although none are completely satisfactory.

To understand the likely effect of measurement close to the soil surface, a hypothetical pair of calibration curves, comparing one for soil deep in the profile with one close to the surface, is shown in Fig. 7.25. For dry soil, count rate is very small for both surface and depth locations, hence the difference between the two is small, even though proportionally one may be much greater than the other. As the soil becomes wetter, the difference increases initially and then decreases. The ratio between the near-surface measurements and the deeper ones becomes progressively closer to one as the size of the sphere of importance reduces. At some point, the sphere of importance becomes small enough that there is no significant difference between the two count rates. At moderate depths, say 150 mm, this will be achieved at realistic water contents of 35–40%, but at shallower depth may not be observed in practice.

The overall effect is that, although a straight line calibration curve is a sufficiently good approximation to the true relationship at depth, this is not the case close to the soil surface and the relationship is distinctly curvilinear.

A number of strategies have been used to cater for the special situation of making measurements close to the surface. Some of the more common ones are described in the following.

7.8.1 Objects placed on the ground

Three methods reduce loss of neutrons from the surface and increase the count rate by placing an object on the ground surface. Because of the weight of the object, these are suitable only for bare soil or very short, robust vegetation, such as short grass.

Surface extension unit

The surface extension unit (Hanna & Siam, 1980; Parkes & Siam, 1979; Bell, 1987) is depicted in Fig. 7.26. It is a cylinder of soil, about 150 mm thick and 500 mm diameter, contained within a circular tray, perforated at its base and kept in a lined hole near the access tube. A central hole allows the tray to be placed over the access tube, effectively increasing the surface layer thickness. A reading at 100 mm depth, therefore, becomes effectively one at 250 mm, which is usually negligibly affected by the surface effect.

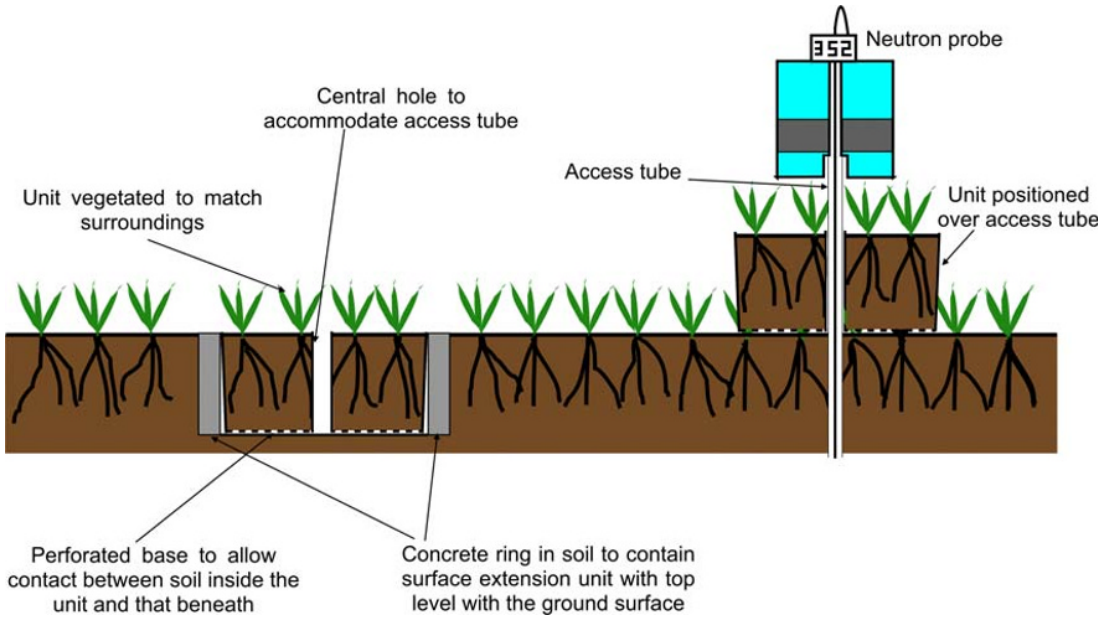

Fig. 7.26 Surface extension unit. Left – in the ground between reading occasions. Right – in use over an access tube. (*See insert for colour representation of the figure.*)

The soil in the tray is subject to all the same influences as its surroundings, having the same vegetation, exposed to the same weather conditions and being in contact with the soil below through the perforated base. By these means, the use of a surface extension unit should avoid the need to make a special calibration for the surface layers.

The surface extension unit is suitable only for crops whose roots do not extend below the depth of the tray.

Heavy metal reflector

Rather than use an extra layer of soil, the two other methods place a standard object on the ground surface around the access tube. The heavy metal reflector is a cylinder of cast iron or other heavy metal, which scatters neutrons escaping from the ground surface, without their losing much energy. Many return to the soil and hence are available for thermalisation, thus increasing the count rate (Marcesse, 1967).

Plastic reflector

Similar in use to the heavy metal reflector, the plastic version thermalises neutrons as well as providing the opportunity for them to return to the detector (Pierpont, 1966; Arslan *et al.*, 1997). Some workers use the plastic shield of the neutron probe transport case in direct contact with the ground as a convenient way to achieve this without requiring any other special equipment. The shield is, however, quite small in diameter compared with the size of most purpose-made reflectors and, in some designs, contains a slow neutron absorber.

An alternative way to measure near-surface water content using a depth neutron probe is to lay the probe on the ground surface beneath a plastic block (Chanasyk & Naith, 1988). This mimics, to some extent, the surface neutron probe.

7.8.2 Special calibration

Most workers use either a special calibration for the surface layers or a means of adjusting the count rate to take account of the loss of neutrons. Development of a calibration relationship between probe count rate and gravimetrically measured water content over a wide range is the most straightforward approach. The procedure is almost identical to that used for calibration at depth (Section 7.7.2). Three points are more important in the near-surface situation. The first two points stem from the fact that gravimetric samples are, by necessity, of a size comparable to the dimension of the sphere of importance.

Water content gradients are often much steeper and variable in time close to the surface than deeper in the soil profile. The same average water content over the depth of soil captured by the sampler and within the sphere of importance may, therefore, be achieved by a range of different distributions of water content. For instance, the same average water content may be achieved by a more or less homogeneous distribution of water or by half of it being very wet and the other half very dry, such as may happen when a sharp wetting front penetrates into an initially dry soil. These are quite different situations, and the neutron probe is likely to produce a different count rate in each. There is, therefore, a limit to the accuracy with which a single calibration curve can represent the relationship.

Most commonly, neutron probe measurements are used to measure the total water storage (or changes in it) over a depth of profile, rather than to provide measurements at individual 'points'. A near-surface measurement, therefore, is usually required to provide an estimate of water storage within the surface layer, from the ground surface to a depth of a few centimetres. For instance, a reading at 100 mm depth may represent the water content from 0 to 150 mm depth (van Bavel & Stirk, 1967; Haverkamp *et al.*, 1984). The gravimetric samples, therefore, should cover the whole of this depth range.

The presence of the transport shield close to the surface may also affect the neutron probe reading, particularly if it contains hydrogen-rich material at its base, where it will act to some extent as a plastic reflector – see Section 'Plastic Reflector'. The calibration must, therefore, be done under the same conditions as readings are to be made later. A calibration developed for tubes with a stick-up of 100 mm may not be valid for one with a stick-up of 200 mm in the same soil.

7.8.3 *Corrections to the normal (depth) calibration curve*

An alternative to developing a near-surface calibration curve for each soil is to start with the normal calibration curve, valid for measurement at depth, and to apply a correction to account for the surface effect.

Grant (1975) made measurements through the profile, starting at the surface, down to 0.6 m depth, which is sufficiently deep to be unaffected by the surface. He then removed the upper 100 mm of soil and made a second set of measurements at the same points. This produced a series of ratios of count rate at each depth and at 100 mm more shallow. By multiplying these together, he could compute the count rate that would have been obtained had the soil been at 0.6 m depth. He also made an approximate calculation of the dependence of these factors on water content by using dry, coarse sand and water to represent very dry and very wet soil. At 100 mm, for example, the correction factor for his soil fell from about 3.3 at 2.5% water content by volume to 1.25 at 25% and 1.048 at 100%. At 200 mm depth, the corresponding correction factors were 1.8, 1.02 and 1.00.

Harris (1973) developed a set of corrections based on a relationship between the radius of a 'sphere of integration', r, and volumetric water content, such that:

$$r = r_w \theta^{-0.33} \tag{7.8.1}$$

where r_w is the radius of the sphere of integration in water (Glubrecht & Kühn, 1971). The sphere of integration is taken as the depth at which there is no effect of the surface (i.e. the correction factor becomes 1). Harris measured r_w as 90 mm for his neutron probe. He also found that an empirical relationship between the correction factor, C, depth of measurement, z, and the radius of the sphere of integration, r, of:

$$C = \left(\frac{r}{z}\right)^{0.4} \tag{7.8.2}$$

worked well.

This leads to a relationship between the correction factor, measurement depth and water content of:

$$C = \left(\frac{r_w}{z}\right)^{0.4} \theta^{-0.132}. \tag{7.8.3}$$

The correction factors are different from those derived by Grant (1975). At 100 mm depth, Harris's were 1.56 at 2.5% volumetric water content and 1.15 at 25%; while at 200 mm depth, they were 1.18 and 1.0 at the same water contents. Both Grant and Harris's relationship for the soils they used are shown in Fig. 7.27. Grant's neutron probe may have had a longer detector tube than Harris's, and Harris's readings were taken with the plastic shield 150 mm above the soil surface. Both of these factors would be expected to reduce the effect of the surface on the readings. Note that

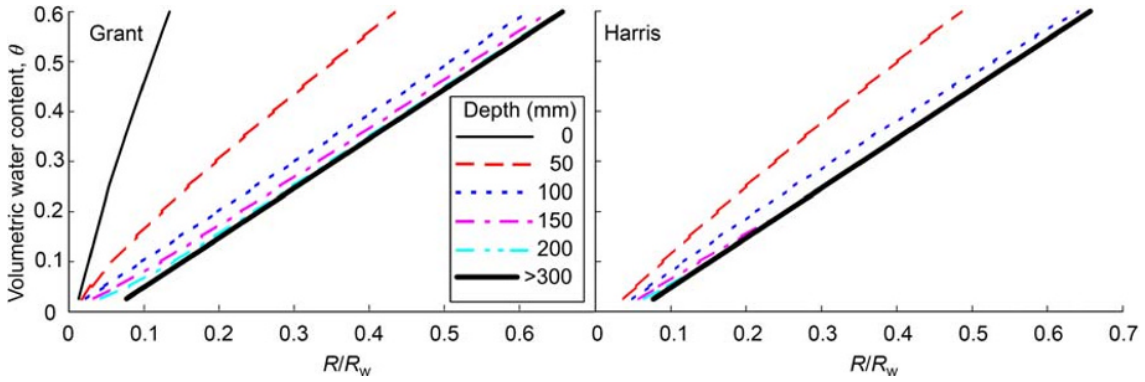

Fig. 7.27 Calibration curves for near-surface neutron probe readings using the correction factors calculated by Grant (1975) and Harris (1973).

both sets of curves are reasonably straight, although the form depicted in Fig. 7.25a is just discernible. Different soil and neutron probe designs produce different corrections for each method (see Parkes & Siam, 1979).

7.9 Processing and Use of Data

The basic data collected from a neutron probe are pairs of depth and count rate values taken at a particular place (access tube location) and time. Some designs of neutron probe allow a calibration to be input to the counting unit and to display and store values directly as volumetric water content. **It is strongly recommended that data should not be stored in this way.** The reason for this is that should either the standard count or the calibration parameters need to be revised, it will be difficult or even impossible to return to the raw data values and hence recalculate revised values. Manipulation of data by computer is such an easy task that very little effort is required to calculate values of water content from raw data when they are required, using the most up to date information. Reliable standard counts for a probe are, in any case, often not available until some time after collection of the field data.

7.9.1 Standard counts

Standard counts are expected to vary very little over short periods (Section 7.7.1), but cannot be ignored completely. Handling it depends on the frequency with which both standard counts and field measurements are made.

If frequent standard counts are measured, then it should be possible to construct a smooth relationship of standard count against time over a period. The appropriate value of the standard count for any particular occasion can then be calculated from this. Usually, a simple linear regression will suffice, but inspection of the data graphically will reveal whether this is adequate. This procedure is preferable when the change over time is smaller than the precision of measurement of individual standard counts. Using the value closest in time to that of the field measurement may result in moderate jumps in the standard count and hence in water content, particularly when aggregated over a profile and/or averaged over several access tube locations. The random counting error (standard deviation) for a typical standard count in water of 900 counts s^{-1} taken over 30 minutes is 0.7 counts s^{-1} or the equivalent of 0.5 mm of water in a 2 m soil profile with an average water content of 0.3 m^3 m^{-3}.

On the other hand, if field measurements are made infrequently, it is probably more sensible to use a standard count determined close to the time of the field readings and to ensure that this count is made with high precision.

7.9.2 Calculation of profile water storage

One of the most important applications of the neutron probe is to measure the amount of water stored within the soil profile, either over a limited depth range or between the surface and a specified depth. Since measurements are made at discrete depths, these must be integrated over the depth range required. Changes of storage over time are usually of more interest than a single measurement.

The neutron probe already measures water content integrated over a fairly large volume (Section 7.1.5), and so a sophisticated method to estimate the integrated water storage is not justified. For most purposes, it is sufficient to assume that the soil comprises layers, each having a uniform water content equal to that at the measurement depth within that layer. Each layer extends from midway between the measurement depth and the one above and the one below. Figure 7.28 shows this. It can also be seen from Fig. 7.28 that the method yields an identical value to that obtained by assuming a linear variation of water content between adjacent depths, provided that the upper and lower limits of the range are coincident with reading depths. This is because the layer method alternatively under- and over-estimates water storage in each half-layer and these cancel one another out. The shaded triangles shown in Fig. 7.28 demonstrate this. Integration assuming a linear variation from one measurement point to the next is called *trapezoidal integration*.

In practice, there is a difficulty associated with this method, since integration right up to the soil surface is usually required. It is usual to assume that all of the soil above the shallowest measurement depth is characterised by that measurement. If the probe has been calibrated for the shallowest depth assuming that it characterises the soil right up to the surface (Section 7.8.2), then this should reduce any error from this cause. Similarly, estimates of water storage

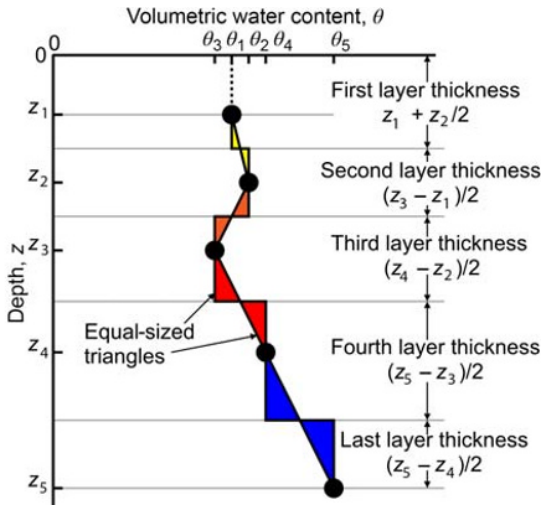

Fig. 7.28 Equivalence between layer and trapezoidal integration.

to a depth not coincident with a measurement may be needed. It is recommended that, if possible, measurement depths should be chosen such that one coincides with the bottom boundary of the range required; but if that cannot be done, no great error is likely to arise by extending the bottom layer below the deepest reading depth by a modest amount.

More sophisticated integration schemes, such as Simpson's rule (Haverkamp *et al.*, 1984) can be used. It is very questionable whether there is any advantage in this.

Errors in estimating profile water storage and its change over time

The only reasonably quantifiable source of random error in measuring water content at an individual depth is random counting error. To apply this to profile water storage, we will use the integration method described above, with N layers, labelled from 1 to N.

The ith layer has a thickness of d_i, a volumetric water content of θ_i and, therefore, a water storage, W_i of $\theta_I d_i$. Assuming no error in the layer thickness, d_i, the likely error in W_i is:

$$\sigma_{W_i} = \sigma_{\theta_i} d_i = \frac{a d_i}{R_w}\sqrt{\frac{R_i}{t_i}}, \tag{7.9.1}$$

where $\sigma_{\theta i}$ is taken from Equation 7.5.5.

Now for all N layers, the total water storage, W, is the sum of that in all the individual layers:

$$W = \sum_{i=1}^{N} W_i = \sum_{i=1}^{N} \theta_i d_i = \sum_{i=1}^{N} \left(a\frac{R_i}{R_w} + b \right) d_i, \tag{7.9.2}$$

but the likely error is calculated by taking the square root of the sum of squares of the individual errors:

$$\sigma_W = \sqrt{\sum_{i=1}^{N} \sigma_{W_i}^2} = \frac{a}{R_w}\sqrt{\sum_{i=1}^{N} \frac{R_i {d_i}^2}{t_i}}. \tag{7.9.3}$$

Equation 7.9.3 allows for different count times and layer depths through the profile. It is quite common practice to have different layer depths in a profile, spacing them further apart at greater depth, but the counting time usually remains constant. To understand this equation, we will, for simplicity, assume that all counting times and layer depths are equal, given by t and d respectively. Equation 7.9.3 then becomes:

$$\sigma_W = \frac{ad}{R_w}\sqrt{\frac{\sum_{i=1}^{N} R_i}{t}}. \tag{7.9.4}$$

As we found for an individual reading, the likely error is proportional to the square root of the total number of counts and inversely proportional to the square root of the count time. Equation 7.9.4 can also be written as follows:

$$\sigma_W = \frac{ad}{R_w}\sqrt{\frac{N\bar{R}}{t}} = d\sigma_{\bar{\theta}}\sqrt{N}. \tag{7.9.5}$$

where

$\bar{R}$ is the average count rate down the profile and

$\sigma_{\bar{\theta}}$ is the standard deviation of the average water content in the profile, according to Equation 7.5.5.

The total profile depth, $D = Nd$, so:

$$\sigma_W = \frac{\sigma_{\bar{\theta}}}{\sqrt{N}} D. \tag{7.9.6}$$

Therefore, the likely error in total water storage as a result of random counting error is proportional to the total profile depth and the random counting error of the average water content, but inversely proportional to the square root of the number of depths measured. Closely spaced readings, therefore, (large N) reduce the contribution of random counting error to the overall total.

As an illustration, take as an example a profile of depth 2 m, an average reading, $\bar{R}$, at each depth of 300 counts s^{-1}, R_w = 900 counts s^{-1}, a = 0.9, b = –0.01 with a count time of 60 s, giving $\bar{\theta}$ = 0.29 and $\sigma_{\bar{\theta}}$ = 0.0022 (from Eqs.7.5.4 and 7.5.5). The total water storage over this 2 m (2000 mm) is, therefore, 2000 × 0.29 = 580 mm. If the profile is read at 200 mm intervals, then 10 measurements will be needed, so that the overall uncertainty in total water storage, σ_W, as a result of random counting error is, from Equation 7.9.6, $\frac{0.0022 \times 2000}{\sqrt{10}} = 1.4$ mm. For more closely spaced readings, say 100 mm, N = 20, and σ_W reduces to 1.0 mm and at 50 mm spacing, σ_W becomes 0.7 mm (i.e. half the value at 200 mm spacing for four times as many readings).

We can extend this analysis to estimate the likely error in estimating changes of water storage between two reading occasions, similarly to Section 7.5.2. The standard deviation of estimate of changes in water content at a single depth is given by Equation 7.5.8. This is the same as the standard deviation of a single determination multiplied by the square root of two. It follows that the standard deviation of estimates of change of water storage over a depth, D, can be derived from Equation 7.9.6 as follows:

$$\sigma(W_2 - W_1) = \sqrt{2}\frac{\sigma_{\bar{\theta}}}{\sqrt{N}} D. \tag{7.9.7}$$

Effect of profile depth Equation 7.9.6 shows that increasing the depth of profile measured increases the uncertainty

in total water storage. If the number of reading depths, N, remains the same for different profile depths, D, then σ_W increases in proportion to D (and W). If, on the other hand, different depth profiles are measured at the same spacing, then N will increase in proportion to D and the overall value of σ_W increases proportionally to $\sqrt{D}$ or $\sqrt{W}$. In this latter case, however, the proportional uncertainty reduces approximately as $1/\sqrt{D}$ or $1/\sqrt{W}$.

Often, readings are made with increasing spacing for deeper depths. This ensures that the much larger changes near the surface are measured with better depth resolution, yielding not only better detail in this region but also smaller errors arising from under-sampling within this depth range. A typical set of measurement depths, as used by Cuenca *et al.* (1997a), is a depth spacing of 100 mm for measurement depths from 0.1 to 1.0 m and 200 mm below this to a total depth of 3.6 m.

The use of unequal depth spacings produces a small increase in the likely random counting error for the water content of the whole profile. Typically, this will be a few percent compared with using the same depth spacing over the entire profile and the same total number of reading depths. In most cases, this is likely to be outweighed by the increased accuracy resulting from better resolution of water content (and its change) in the depth range where it varies most.

Effect on change in water storage The likely error in the change of profile water storage between two occasions is given by Equation 7.9.7. If the approximation used in the expression (7.5.8) is acceptable, that is water content is similar on each occasion, then the likely error in assessing the change in water storage between two occasions, in the more general case of a non-uniform profile, is just $\sqrt{2}$ times that of the likely error in a single determination.

In many profiles, changes in water content over time become very small below a certain depth. Indeed, if there is a water table within the depth range of the access tube, it should not change below the deepest depth that the water table reaches. In such cases, the random counting (and other) errors below the maximum water table depth contribute to the overall noise in measurements of water storage change and degrade the precision of those measurements. There is, however, a balance to be struck here. In some profiles, small water content changes over a large (several metres) depth range contribute a significant proportion of the change in total water storage. Depending on the application, this may or may not be important and a too hasty decision to discontinue deep readings may lead to significant underestimation of water content change in the profile as a whole (e.g. Calder *et al.*, 1997).

7.9.3 Data processing

If only small quantities of data are being collected, data may be processed efficiently on paper using hand calculations or a simple calculator. The equations are simple and the most complicated function required is the square root. Most workers, however, use a computer and many ratescalers incorporate memory to store the readings, which can be transferred easily into a computer, saving time and, perhaps more importantly, reducing the chance of errors caused by transcribing numbers from field sheets.

Data can be processed easily on a computer using a spreadsheet program. This provides a flexible way to enter data; perform checks for data integrity; transform the raw data into water content and water storage, together with their changes and likely errors; combine the neutron probe data with other measurements, for example rainfall and tensiometer measurements; and display the results graphically in a variety of ways, including variation by depth and time.

The use of formulae and simple macros allows the spreadsheet to be customised to suit almost any application and for changes to be made to accommodate new demands.

Whatever the method used to process the data, good practice demands that the following information be recorded:

In the field

- Location of the access tube
- Date and time of reading
- Person making the readings
- The integration time used
- Ground conditions (e.g. wet, dry and snow-covered)
- Any special relevant information which would aid in interpretation of the data (e.g. height of crop or damage to the site or equipment)
- The sum of all the readings made (see the following text)

In the office

- Date of data entry
- Person entering the data and/or making the calculations
- The sum of the readings (see the following text).

A table suitable for processing data for one access tube is shown in Fig. 7.29. This can be implemented either as a paper form for manual processing or as a spreadsheet. It can be extended easily to accommodate either readings of multiple tubes on the same occasion or readings of the same tube on different occasions. If processing is done by hand, then the same form can be used to record the field readings and the result of calculations, thus avoiding laborious copying and transcription errors.

Much of the information can be pre-filled onto the form; and if the processing is done on a spreadsheet, formulae can be stored in protected cells for all calculated quantities. Data entered are the site, tube, date, time, probe, ratescaler, crop, ground condition, observer, standard count, the depth gauge readings, the neutron probe readings, the sum of readings (see the following text) and notes, both from the field form and subsequent information. The basic data applying to each tube (reading depths and calibration codes) and the calibration constants can be obtained from look-up tables. Each calibration code refers to a pair of slope (a) and intercept (b) values. For instance, in Fig. 7.29, the 10 cm

NEUTRON PROBE DATA PROCESSING FORM

SITE	West Field		TUBE	A1	STICKUP 15 cm
READING DATE	21/09/2011 (dd/mm/yy)		READING TIME	15 sec	
PROBE	155		RATESCALER	336	
CROP	Grass		GROUND COND	Wet	
OBSERVER	Joe Bloggs		Standard Count	924 cps	

Depth cm	Gauge Rdg cm	Rdg cps	R/R_w	Calib. Curve	Slope a	Intcpt b	VWC θ $m^3\ m^{-3}$	+/– $m^3\ m^{-3}$	Layer Depth mm	Layer WC mm	+/– mm	Cum WC mm	+/– mm	To Depth m
10	25	203	0.220	8	0.851	–0.004	0.183	0.003	150	27.4	0.5	27.4	0.5	0.150
20	35	191	0.207	1	0.790	–0.024	0.139	0.003	100	13.9	0.3	41.4	0.6	0.250
30	45	170	0.184	1	0.790	–0.024	0.121	0.003	100	12.1	0.3	53.5	0.7	0.350
40	55	145	0.157	1	0.790	–0.024	0.100	0.003	100	10.0	0.3	63.5	0.7	0.450
50	65	150	0.162	1	0.790	–0.024	0.104	0.003	100	10.4	0.3	73.9	0.8	0.550
60	75	157	0.170	1	0.790	–0.024	0.110	0.003	100	11.0	0.3	85.0	0.8	0.650
70	85	212	0.229	1	0.790	–0.024	0.157	0.003	100	15.7	0.3	100.7	0.9	0.750
80	95	287	0.311	3	0.915	–0.062	0.222	0.004	100	22.2	0.4	122.9	1.0	0.850
90	105	346	0.374	3	0.915	–0.062	0.281	0.005	100	28.1	0.5	151.0	1.1	0.950
100	115	342	0.370	3	0.915	–0.062	0.277	0.005	150	41.5	0.7	192.5	1.3	1.100
120	135	335	0.363	3	0.915	–0.062	0.270	0.005	200	53.9	0.9	246.4	1.6	1.300
140	155	369	0.399	3	0.915	–0.062	0.303	0.005	200	60.7	1.0	307.1	1.9	1.500
160	175	354	0.383	3	0.915	–0.062	0.289	0.005	200	57.7	1.0	364.8	2.1	1.700
180	195	387	0.419	3	0.915	–0.062	0.321	0.005	200	64.2	1.0	429.0	2.3	1.900
200	215	371	0.402	3	0.915	–0.062	0.305	0.005	200	61.1	1.0	490.1	2.5	2.100
220	235	385	0.417	3	0.915	–0.062	0.319	0.005	200	63.9	1.0	554.0	2.7	2.300
240	255	402	0.435	3	0.915	–0.062	0.336	0.005	200	67.2	1.0	621.2	2.9	2.500
260	275	422	0.457	3	0.915	–0.062	0.356	0.005	200	71.2	1.1	692.4	3.1	2.700
280	295	416	0.450	3	0.915	–0.062	0.350	0.005	200	70.0	1.0	762.4	3.3	2.900
300	315	432	0.468	3	0.915	–0.062	0.366	0.005	100	36.6	0.5	798.9	3.3	3.000

Sum of Readings	6076	OK			
Depth Gauge Start	9994	Water in upper 1 m	164.8 mm	+/–1.1 mm	
Depth Gauge Bottom	318	Water in upper 2 m	459.59 mm	+/–2.4 mm	
Depth Gauge End	9993	Water in upper 3 m	798.94 mm	+/–3.3 mm	
Processed on	23/09/2011	By	Alice Smith		

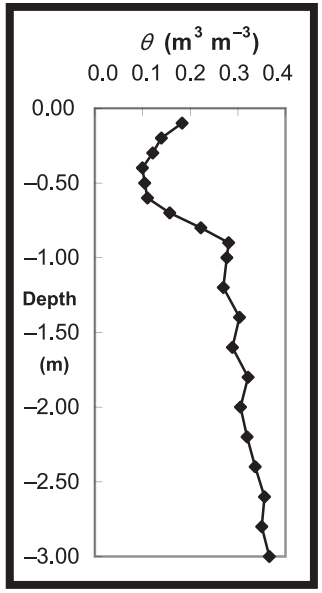

NOTES

Recent rain after dry spell. Cattle have poached the ground around the access tube.

Fig. 7.29 Example neutron probe data processing form.

depth uses a specific near-surface equation for the soil, referred to as 8, with a slope of 0.851 and intercept value of –0.004, while the soil down to 70 cm has a calibration code of 1 with different constants. Below this, there is a change in soil composition and the calibration line changes to one with a code of 3.

Data integrity

Whenever data are recorded, it is important to check for plausibility (i.e. do I believe this?) and to be aware of ways in which errors may creep in. One of the most common errors is in writing down a number. It is very easy, for instance, to write down 563 as 536. The more times that numbers are copied, the more likely that this sort of error will occur. It is, therefore, advisable to minimise the number of times that numbers are copied from one piece of paper to another (or entered into a calculator or computer). When this is unavoidable, a simple safeguard is to add up all the figures in a column. Adding up the same column in the transcribed data, the two can be compared and will be different if an error has occurred. It is, of course, essential that the two sets of additions are done independently of one another. For this reason, the sum of readings should be entered into the appropriate cell on the form. The computer calculates the same sum and, if the two match, then it displays 'OK' in the next cell. If not, a message can be displayed, asking the user to check the adding up on the field sheet (NOT that entered onto the data processing form!) and/or the data entered from the field sheet. This method is not entirely foolproof – for instance if 563 had been written as 536 and 447 had been written as 474, the two would cancel out, but this will happen extremely rarely.

Other problems can arise from recording the wrong access tube identity, recording the depth(s) incorrectly and from equipment malfunctions.

The most powerful checks to reveal data problems are graphical display of the data, both by depth and time. The example form, shown in Fig. 7.29, has a space for plotting the calculated water content as a function of depth. This is usually quite similar from one reading occasion to another. Plotting water content at a particular depth against time is expected to show a relatively smooth variation. Sudden jumps in the data, either up or down, particularly when they revert to the expected pattern on later reading occasions, suggest a reading error. It is important not to dismiss such discrepancies too quickly, however, as they may reflect real variations of water content resulting from a variety of causes. There may be several of these. Preferential flow phenomena can cause rainwater to penetrate deep into the soil, bypassing the upper layers. Water table movements may also cause large and rapid changes of water content deep in the profile, unrelated to behaviour near to the surface. A poorly-fitting access tube may allow water to run down the gap when it rains, leading to a real, but spurious, increase in water content where there is better contact with the tube.

There are too many other possible causes of unexpected change in water content to list here. Some of these reflect real hydrological processes, while others result from less than ideal experimental conditions. Experience shows that checking for data integrity, usually known as *quality control*, is an ongoing process, extending throughout the time that the data is used. New ways of looking at the data often reveal unexpected discrepancies, which frequently require checking against the original records or notes written when the readings were made.

For this reason, it should be a cardinal rule of any environmental investigation NEVER to destroy the original data, whether these be handwritten or automatically recorded by some form of logger, and to keep all notebooks and field records.

7.10 Cosmic-Ray Soil Moisture Observing System[1]

Cosmic-Ray Soil Moisture Observing System (COSMOS) also relies on neutron thermalisation to provide measurements of soil water content in the upper 0.1–0.7 m of soil. There are significant differences from the use of a neutron probe, however:

- The fast neutrons arise naturally from cosmic rays arriving in the Earth's atmosphere.
- The method is non-invasive, with monitoring taking place above the ground surface and no equipment installed beneath the surface.
- Neutrons detected by the system *decrease* with higher soil water content.
- Continuous, unattended monitoring is not only possible, but at the heart of the system.
- No artificial radioactive source, and so no burdensome radiological protection regulations are needed.
- The signal arises from an area of a few hundred metres around the monitoring station.

At the time of writing (Autumn 2014), the COSMOS system consists of an array of over 100 soil water monitoring stations distributed principally throughout the continental United States, with at least one each in Canada, Austria and France, and a network of 14 stations in Australia (http://cosmos.hwr.arizona.edu/). There is a rapidly expanding network in the United Kingdom with currently 20 monitoring stations managed by the Centre for Ecology and Hydrology (www.ceh.ac.uk/cosmos/). There is a growing network of COSMOS probes associated with the Terrestrial Environmental Observatories (TERENO) network in Germany (http://teodoor.icg.kfa-juelich.de/overview-de).

The principle of operation of the cosmic ray probe is similar to that of the neutron probe, but the originating source of high-energy neutrons is cosmic rays. The footprint of the signal of reflected neutrons is much more extensive than any other soil moisture measurement system discussed in this text and is dependent on soil moisture conditions, particularly in the vertical direction. It is

[1] This section is a contribution of Professor Richard Cuenca of Oregon State University.

envisaged that output from the COSMOS network will be integrated with Critical Zone Observatories (CZOs) (http://criticalzone.org/national/), atmospheric boundary layer simulation models, AmeriFlux network sites (http://ameriflux.ornl.gov/), and with test sites for related projects, for example the NASA AirMOSS remotely sensed soil moisture sensor development project (http://airmoss.jpl.nasa.gov/).

7.10.1 Theory of application of cosmic rays

The top of the Earth's atmosphere is continuously bombarded by high energy cosmic rays which produce secondary cascades of energized particles. The Hadronic Cascade gives rise to high energy neutrons and protons which can penetrate the Earth's atmosphere and continue to the surface. The actual number of particles reaching the ground surface depends on the energy and type of incident cosmic ray and elevation of the site. The number of high energy particles reaching the ground fluctuates widely which must be accounted for in the probe design.

Of the fast neutrons that reach the ground surface, those which collide with a particle of similar mass lose energy in the collision and can be counted by a detector for slow neutrons, as described in Section 7.1 for the standard neutron probe. As will be described later, this is not the same case for the COSMOS probe system. The major source of hydrogen ions on the Earth's surface is that associated with water molecules. It should be noted that the number of water molecules detected by the cosmic probe is all of the molecules in the probe zone of influence including those in vegetation, surface water, ice and snow. So the neutrons detected by the cosmic probe are not just those associated with soil water content. We will see that there are advantages and disadvantages to this phenomenon.

The spatial extent of soil (and vegetation) moisture monitored by a cosmic probe is much more extensive than any other method discussed in this text and depends on the probe height above the ground. In the typical design for a COSMOS probe discussed in the next section, the zone of influence is a circle 335 m in radius (Zreda *et al.*, 2008; Desilets and Zreda, 2013). The depth of the zone of influence is basically dependent on the soil water content and to a lesser extent on soil organic carbon and soil bulk density. Drier soils have a greater depth monitored at the centre of the sample volume due to there being fewer water molecules to slow down the neutrons. Typical depths monitored by the COSMOS probe at the centre of the zone of influence range from 0.1 to 0.7 m (Desilets *et al.*, 2010; Zreda *et al.*, 2008, 2012; Franz *et al.*, 2012). The depth monitored goes to zero at the edge of the zone of influence.

7.10.2 Design and components of the COSMOS probes

A COSMOS probe is shown in the centre foreground of Fig. 7.30 at a NASA AirMOSS project site, Tonzi Ranch,

Fig. 7.30 COSMOS probe in centre foreground at Tonzi Ranch, California (USA). AmeriFlux eddy covariance tower is seen in background at left and NASA AirMOSS soil profile monitoring station is shown in background at right. Photograph by Richard Cuenca. (*See insert for colour representation of the figure.*)

where an AmeriFlux eddy covariance flux tower (see Section 24.3.2) and an AirMOSS soil profile monitoring installation are also located. As seen in the photo, the COSMOS installation includes a solar panel and enclosure for a micrologger, additional sensors and electronics. Additional sensors are needed to adjust for environmental conditions including barometric pressure, atmospheric humidity and temperature (Rosolem *et al.*, 2013). The datalogger can normally support other sensors such as precipitation gauges and other types of localised soil water sensors. Other adjustments must be made for variations in the incoming neutron flux due to changes in solar activity and elevation of the site. Remote data retrieval options include satellite and cell phone network downloads.

The two vertical cylinders shown in the photo house the neutron detectors. In one configuration, neutrons are recorded with ^{3}He-filled proportional counters with different energy sensitivities. Neutrons in the fast to epithermal range can be recorded with a detector surrounded by 25 mm of low-density polyethylene and a 0.5 mm thick outer layer of Cd shielding. Epithermal neutrons can be recorded by detectors with 0.5 mm of Cd shielding, while slow neutrons are recorded using an unshielded detector. A calibration curve for soil water content determined by fitting ground-level fluxes generated by the MCNPX simulation code (Pelowitz, 2005) was derived as follows:

$$\theta(N) = \frac{a_0}{\left(\frac{N}{N_0}\right) - a_1} - a_2. \qquad (7.10.1)$$

where

$\theta(N)$ is the volumetric soil water content;

N is the neutron count rate normalized to a reference atmospheric pressure and solar activity level;

N_0 is the neutron count rate over dry soil under the same reference conditions and
a_0–a_2 are fitting parameters.

Note that, unlike the neutron probe, there is an inverse relationship between the neutron count rate and the soil water content (or in fact total hydrogen present) for the COSMOS probe. This is because the COSMOS probe sensor measures the faster neutrons which have not been slowed down by collision with the hydrogen molecules.

The effective depth measured is a strong function of the volumetric soil water content and is given by Franz *et al.* (2012, 2013) as follows:

$$z_{\text{eff}} = \frac{0.058}{\frac{\rho_{\text{d}}}{\rho_{\text{w}}}(\tau + \text{SOC}) + \theta + 0.0829}, \qquad (7.10.2)$$

where
z_{eff} is the effective measurement depth (m);
ρ_{d} is the soil dry bulk density (kg m^{-3});
ρ_{w} is the density of liquid water (kg m^{-3});
τ is the weight fraction of lattice water in the mineral grains and bound water and
SOC represents the soil organic content (kg of water per kg dry minerals).

The 0.058 (m) represents the 86% cumulative sensitivity depth of low energy neutrons in liquid water and 0.0829 is controlled by the nuclear cross-section of SiO_2.

7.10.3 In situ *COSMOS probe calibration*

A major difficulty in application of the COSMOS probe is obtaining calibration data to convert the neutron count rate to volumetric soil water content. Collection of samples for measuring volumetric water content by the gravimetric method is covered in Chapter 6, and the principles of calibration are similar to those described in Section 7.7.2 for the neutron probe.

Franz (2012) has put together a calibration manual for the COSMOS probe based on his experience in making installations at 35 sites. The key concept is that the sampling grid must be representative of the volume monitored by the COSMOS probe, which decreases exponentially with distance from the counter. This has been accomplished using the sampling grid indicated in Fig. 7.31. A total of 18 sample locations are monitored in 50 mm increments over a total depth of 300 mm (a total of 108 samples). As indicated in the figure, the sample locations are every 60° and at radii of 25-, 75- and 200 m. Using this set-up, each sample location is given equal weight within the volume sampled by the probe. Each sample is analysed for gravimetric soil water content, bulk density and, finally, volumetric soil water content. The results are then applied in Equation 7.10.1 to determine the regression coefficients, a_0, a_1 and a_2.

Since the COSMOS probe measures all the water within the footprint of the probe, Franz (2012) indicated

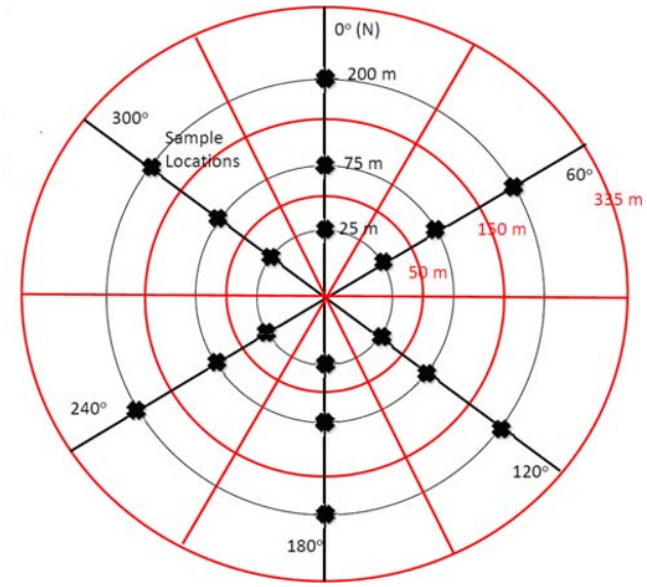

Fig. 7.31 Sampling grid for calibration of COSMOS probe (Franz, 2012). Gravimetric sample locations are shown as bold black ✱, six 5-cm deep samples per location. From Franz (2012). Reproduced with permission of T. Franz.

that samples should be taken to determine the lattice water content contained in the mineral structure of the soil. The analysis must be done in a laboratory. Since the lattice water content does not vary significantly within the footprint of the COSMOS probe, it is recommended to take four samples. The first three are taken at three different radii and in three different directions, and the fourth is a composite sample. The recommended procedure is described in Franz (2012).

7.10.4 *Sample results*

The data from the COSMOS sensor are normally displayed as two graphs, one for the volumetric soil water content over time and the other for the effective measurement depth over time. These two parameters are inversely related as shown in Equation 7.10.2, the higher the soil water content, the shallower the effective measurement depth. An example for the Metolius, Oregon AmeriFlux and NASA AirMOSS site for 2013 is shown in Fig. 7.32. Note that the soil water content values (Fig. 7.32a) early in the year appear to be too high for this highly volcanic soil and do not agree with the AirMOSS soil water sensors which indicate a maximum value of approximately 0.32 m^3 m^{-3} early in the year (Fig. 7.33). This may be due to the fact that the COSMOS sensor captures all of the water within the footprint of the sensor, including snow. The soil temperature data plots indicate a suppressed diurnal soil temperature signal, which is characteristic of snow cover until approximately DOY 074 when this plot indicates that the snow melts off (Fig. 7.34).

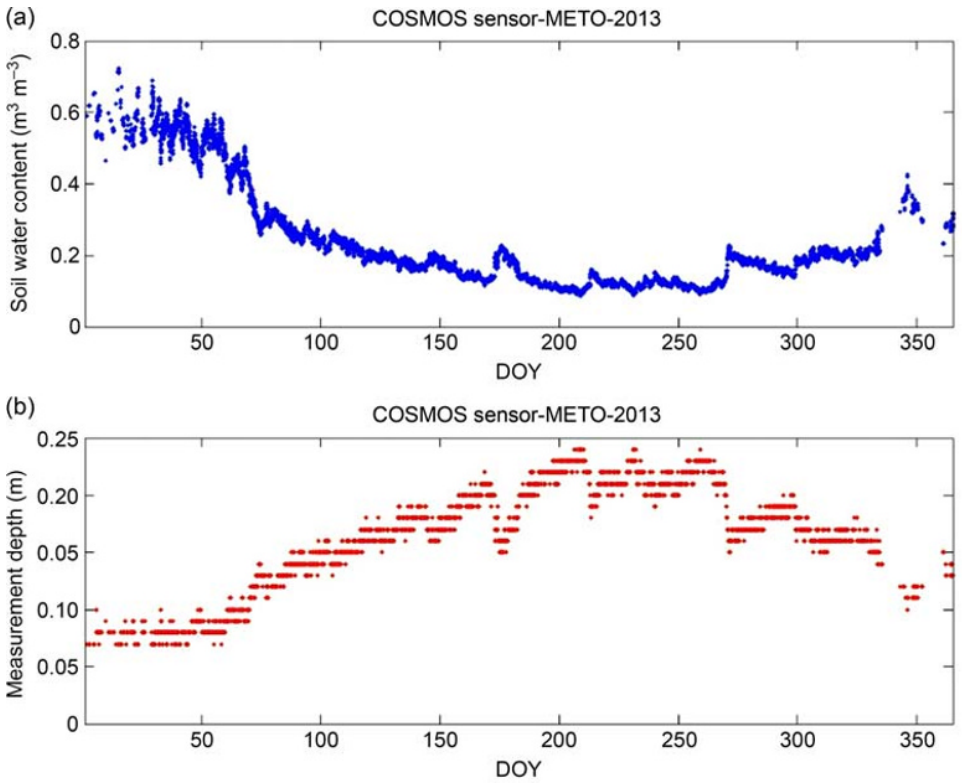

Fig. 7.32 (a) Retrieved volumetric soil water content from COSMOS probe at AmeriFlux Metolius site, Oregon (USA) for 2013. (b) Effective measurement depth for COSMOS probe at same site for 2013.

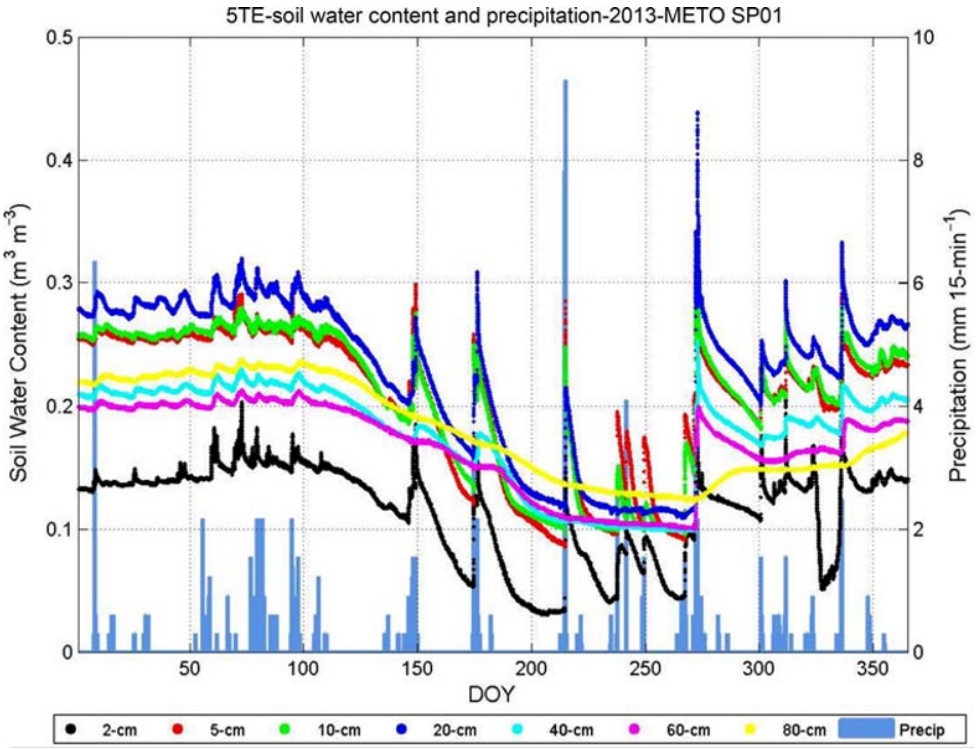

Fig. 7.33 Volumetric soil water content for seven depth layers from NASA AirMOSS soil profile monitoring station (using Decagon 5-TE dielectric probe) at AmeriFlux Metolius site, Oregon (USA) for 2013. Precipitation captured in 15-min intervals on right-hand side *y*-axis. (*See insert for colour representation of the figure.*)

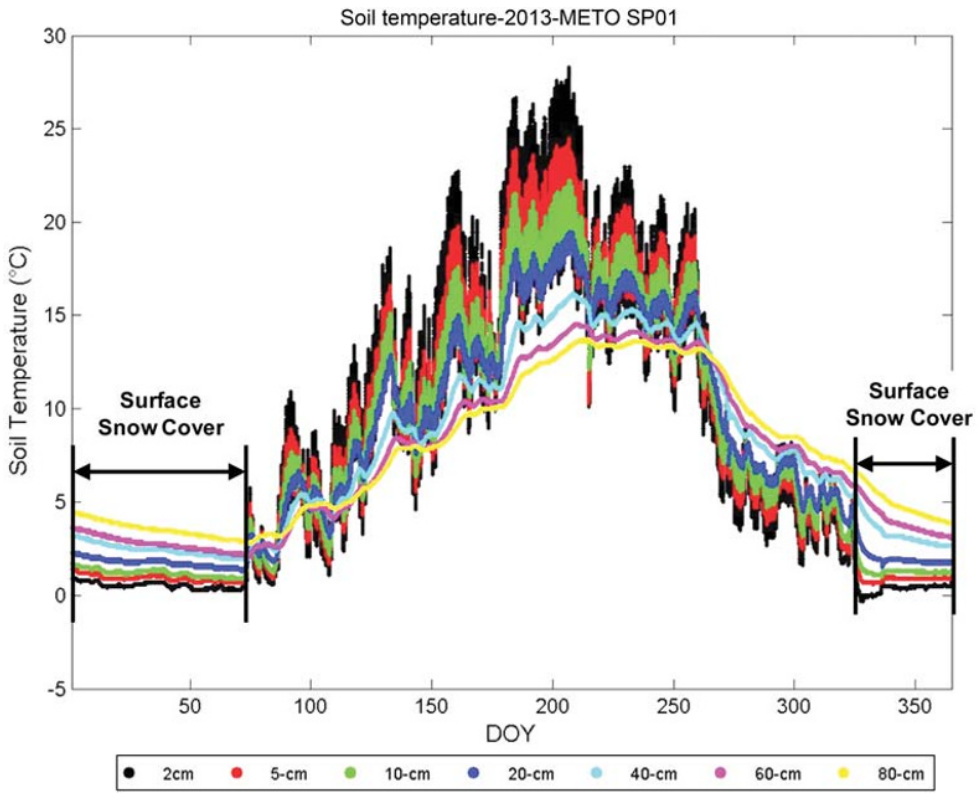

Fig. 7.34 Soil temperature for seven depth layers from NASA AirMOSS soil profile monitoring station (using Decagon 5-TE dielectric probe) at AmeriFlux Metolius site, Oregon (USA) for 2013. Periods of dampened diurnal fluctuation are evidence of snow cover over the soil profile. (*See insert for colour representation of the figure.*)

The effective measurement depth (Fig. 7.32b) is seen to vary from a low value of approximately 0.07 m to a high value of approximately 0.25 m throughout the year, based on the values of soil bulk density, soil organic content, lattice water content and soil water content (in fact, total water content) as shown in Equation 7.10.2. The range of the effective measurement depth over limited time steps is surprising but is basically the effect of the variation in soil water content with time, since the other parameters in Equation 7.10.2 are assumed constant. The results, in fact, demonstrate a moving range of effective measurement depth with time.

The key point to recall is that the COSMOS sensor has a footprint in the range of 300 m in radius and 0.3 m deep. No other soil water content sensor system currently deployed has such an extensive footprint.

7.10.5 Issues requiring further attention

One of the major difficulties, and surprisingly advantages, in application of the COSMOS data was indicated in the previous section. The COSMOS sensor picks up all of the water within its footprint, including intercepted water on leaves after rainfall or, as discussed earlier, the water in snow on the soil surface. This confuses the soil water content signal, but at the same time can be advantageous when considering intercepted rainfall or snow on the soil surface. To explain, before a rainfall event there is a signal for stored water content in the COSMOS sensor footprint which does not include interception. After the rainfall event, the signal includes interception. But after a relatively short amount of time, the intercepted rainfall will evaporate and the COSMOS signal will be more stable. Therefore, the equivalent depth of intercepted rainfall can be quantified from the COSMOS data. A similar case can be made for the effects of snow seen in the previous section. It is clear from the diurnal soil temperature signal in Fig. 7.34 when there is snow on the soil surface and when it melts off. The difference in the COSMOS total water signal between these conditions can be used to determine the snow water equivalent (SWE) depth over the soil surface. Limited work has been done to exploit these aspects of the COSMOS data series.

The use of the COSMOS sensor in agricultural fields is more problematic, since the water stored in plant tissue during the growing season is detected by the COSMOS sensor as soil water (Hornbuckle *et al.*, 2012). Hornbuckle *et al.* (2012) show a potential correction to the neutron

count rate over dry soil, N_0, in Equation 7.10.1, to account for this significant effect. However, this correction is non-linear over the growing season, and there appear to be hysteresis effects late in the growing season. Baatz *et al*. (2014) carried out calibration of ten cosmic-ray probes of the TERENO network under humid climate conditions in the Rur catchment in western Germany. Three calibration methods were tested; and while they performed similarly well in validation, there were distinct differences in the results in this humid climate with various degrees of vegetation density. No doubt additional work will be carried out on this topic and perhaps, as indicated for intercepted rainfall and snow cover, advantages will be found for applications of the COSMOS data signal. An example of developments in this direction is the direct relation of neutron flux density to aboveground biomass observed by Franz *et al*. (2013).

7.11 Radiological Safety

Neutron and gamma ray probes contain small radioactive sources, which are a hazard to operators and other persons close by. The size of the sources used is sufficient that measures must almost always be taken to comply with radiological safety legislation in whatever country the apparatus is used. These vary across the world, but the general principles are almost universally the same and are based on a few internationally recognised sets of regulations and principles. A fairly recent development takes account of the international terrorist threat, with increasing emphasis on security of the material alongside protection of individuals.

Everyone is exposed to radiation in everyday life, from natural and artificial sources in the environment and from other activities not normally associated with a radiation hazard. The earth is constantly bombarded by cosmic rays from space. This exposure is greater at higher altitudes, where the earth's atmosphere is thinner, and at higher latitudes, where the earth's magnetic field deflects charged particles less easily. Steady background radiation also emanates from rocks beneath the ground surface. In some areas, particularly where granite predominates, this can be quite significant and the natural dose experienced by inhabitants can be at least as high as many workers in the nuclear industry receive. In the late 1950s and early 1960s, atmospheric testing of nuclear bombs caused significant radioactive 'fallout', to which all inhabitants on earth were exposed. Fallout is now very much reduced, although not entirely eliminated. Civil nuclear power stations emit small amounts of radioactive material into the atmosphere, as do some other industrial, medical and research activities. The Chernobyl accident in Ukraine in 1986 contaminated not only extensive areas of Ukraine, Belarus and Russia, but large parts of western Europe, albeit much less heavily. Many everyday activities, not generally associated with carrying a radiation risk, can result in significant radiation doses. These include mountain climbing and aircraft travel as well as medical exposures, such as X-ray examinations or radiotherapy.

Radiation exposure from using neutron or gamma probes is additional to that received from these other sources.

7.11.1 Nature of radiation

The term *radiation* covers any kind of energy transmitted without a physical connection between the transmitter and receiver. The main forms are electromagnetic radiation and moving (usually subatomic) particles.

Electromagnetic radiation occurs over an extremely wide range of frequencies and wavelengths, from below that at which alternating current power is distributed (50 or 60 Hz; 6000 or 5000 km), through radio waves (100 kHz to 3 GHz; 3000 m to 100 mm), microwaves (3–300 GHz; 100–1 mm), infrared (300 GHz to 400 THz; 1 mm to 700 nm), visible light (400–750 THz; 70–400 nm), ultraviolet light (750 THz to 30 PHz [30×10^{15} Hz]; 400–10 nm), X-rays (30 PHz to 30 EHz [30×10^{18} Hz];10 nm to 10 pm [10×10^{-12} m]) and gamma rays (above 30 EHz – below 10 pm). Although there are possible health hazards associated with very low-frequency waves and higher frequency radio waves (as used in mobile phones, for instance), health risks are associated mainly with exposure to higher frequency ultra-violet radiation and beyond. The relation between photon energy, E, and frequency, ν, is as follows:

$$E = h\nu, \tag{7.11.1}$$

where h is Planck's constant, 4.135×10^{-16} eV s.

Thus, the higher the frequency (or smaller the wavelength) of the wave, the more energetic the photons and the greater the potential for causing damage in biological tissues.

There are several types of *particle radiation*. *Alpha radiation* is composed of helium nuclei (two protons and two neutrons), which are particularly stable and released in many nuclear disintegration events. Alpha radiation penetrates material very poorly, so that shielding it is easy. The main biological hazard is through internal exposure as a result of inhalation or ingestion.

Beta radiation is composed of energetic electrons, another common product of nuclear disintegrations. Beta particles penetrate more deeply than alpha particles, but are still relatively easy to shield. They are not commonly encountered in soil water work.

Gamma rays are electromagnetic radiation of high energy ($\gtrsim$50 keV). Because of their high energy, they are usually treated more conveniently as particles than as waves. Gamma rays are highly penetrating; the higher the energy, the greater their penetrating power.

Neutrons are uncharged particles found in atomic nuclei. Because they are uncharged, they can penetrate

deeply into material, as they do not interact with electrons in the material.

Other forms of particle radiation are protons and heavy particles – fragments of atomic nuclei.

7.11.2 Biological interactions

Radiation can damage biological systems in various ways, not all of which are fully understood. The main ones, however, are as follows:

- Burns – very similar to burns from heat. The principal cause is the energy deposited into the body. This occurs only at doses much higher than are likely to be encountered in the use of small sources, unless there is extremely close contact.
- Disruption of cell functions. Cell walls are delicate membranes and easily damaged. This can cause the cell contents to leak out and result in death of the cell. Similar damage can be caused to other structures within cells, leading to similar results. Damage to the cell nucleus can cause it to start to divide uncontrollably, leading to cancer.
- DNA damage. This can cause abnormalities in organs as well as genetic mutations, if cells in the reproductive organs are damaged.

The effect on humans has been studied extensively from the medical history of people exposed to radiation, usually accidentally. As a result, there is a large body of evidence, which is added to and reviewed about every 10 years by the International Commission for Radiation Protection (ICRP). Based on this evidence, the ICRP makes recommendations on exposure limits for people exposed to radiation from artificial sources. This results in a strong similarity of the permissible exposure limits in different countries, although the details and the way that the regulations are enforced differ.

7.11.3 Measurement of radiation dose

To assess the likelihood of harm from radiation exposure, a system has been developed to convert the amount of radiation received by a person into units which relate to the damage which may be caused.

The starting point is the amount of energy deposited per unit mass into the receiving body. This is called the *specific absorbed dose* and is measured by the *gray* (Gy), which is equal to one joule per kilogram ($J\,kg^{-1}$). Thus if a person of mass 64 kg were exposed to radiation consisting of 1 MeV particles and, over their body, they intercepted 4×10^{11} particles, they would have received an absorbed dose of $\frac{10^6 \times 1.6 \times 10^{-19} \times 4 \times 10^{11}}{64} = 1$ mGy ($1\ eV = 1.6 \times 10^{-19}$ J). However, the energy deposited in the body by radiation does not tell the whole story, and it has been found that different types of radiation vary in their ability to cause harm. To take this into account, *quality factors* are used, which are roughly proportional to the potential of each type of radiation to harm humans. Quality factors, Q, are 1 for X-, γ- and β-radiation; 20 for α particles, multiple-charged particles, fission fragments and heavy particles of unknown charge; 10 for neutrons and high energy protons. The quantity obtained by multiplying the specific absorbed dose by the quality factor gives an adjusted *dose equivalent*, measured in *sieverts* (Sv). Quality factors are clearly only rough indicators of the required adjustment, reflecting uncertainties in a number of factors. Amongst these are

- the effects of different forms of radiation;
- the actual amounts received by those whose medical history has been used to compile the dose limits. These people were mainly victims of accidental exposure, and hence the dose rate must usually be estimated;
- the necessity to have a small number of categories making up each quality factor.

Nevertheless, they are sufficiently accurate to make useful calculations of the effect of different working practices. These are also usually subject to considerable uncertainty in the likely dose received.

Older units are still in use in some places. There are two older units for specific absorbed dose. The *roentgen* (R) is actually a measure of ionising potential of the radiation. 1 R = 9.33 mGy. The *rad* is directly comparable to the gray, being equal to 0.01 Gy. The older equivalent of the Sievert is the *rem* (actually an acronym of 'rad equivalent man') and equal to 0.01 Sv.

7.11.4 Units of radioactivity

The activity of a sample of radioactive material is measured primarily by the number of radioactive disintegrations per unit of time occurring within it. This unit is the *becquerel* (Bq). One Bq is one disintegration per second and so a very small quantity. Most sources are measured in kBq, MBq or GBq. Note that the Bq takes no account of the number, energy or type of particles released in the disintegration, and so the same number of Bq of different substances can cover a very wide range of hazard.

An older unit of radioactivity is still quite common. This is the *curie* (Ci). One Ci = 3.7×10^{10} Bq, so that common sources were normally measured in μCi or mCi.

Another common measure connected with radioactivity is the *half-life* of radioactive material. This is the time taken for half of a quantity of material to disappear through disintegrations. It is believed that every atom of a radioactive isotope has exactly the same probability of disintegrating in any particular time period as every other atom of that isotope. Because of the enormous number of atoms in even a small amount of matter ($\sim 10^{23}$ in 1 mL), disintegrations usually occur in sufficient numbers that the decay is indistinguishable from a continuous process. From this it follows that, no matter what amount of isotope is present at any given time, after one half-life, exactly half of the isotope will be left. After a second half-life, half of that (i.e. a quarter of the original amount) will be left and so on. This is illustrated in Fig. 7.35.

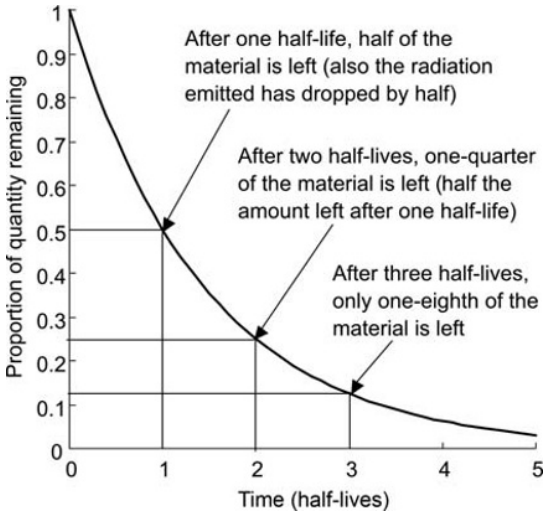

Fig. 7.35 Radioactive decay of a source.

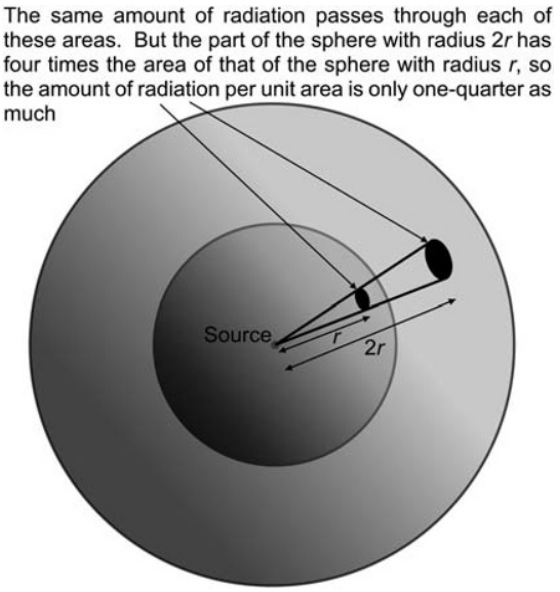

Fig. 7.36 Distance shielding as a consequence of the inverse square law.

Half-lives vary enormously, from minute fractions of a second to very many years (the half-life of ^{238}U is 4.5 billion years). Isotopes used commonly in soil physics are ^{137}Cs, which has a half-life of 13.7 years and ^{241}Am, with a half-life of 432 years. A half-life much shorter than 10 years would not be useful as a source in an instrument, since its activity would decline too quickly and need replacing after a relatively short time.

The activity of a source and its half-life are related, as the higher the number of disintegrations, the faster the atoms of the isotope will disappear, so that after one half-life the amount of radiation emitted will also be halved.

7.11.5 Principles of radiological protection

Various legal limits of exposure have been set for different aspects of dealing with radiation and radioactive materials, covering different classes of people, transport, use, disposal, etc. These are, however, very much maximum levels and the whole philosophy of radiation safety revolves around the principle of 'as low as reasonably achievable' known more commonly by its acronym, *ALARA*. Sometimes, this is changed to 'as low as reasonably practicable' or *ALARP*, which is essentially the same thing.

ALARA requires that, notwithstanding the regulatory limits on exposure, all reasonable steps be taken to reduce exposure of individuals to the lowest level achievable. This reflects, to some extent, continuing uncertainty over the long-term effects of radiation exposure, particularly at low levels. However, the inclusion of the word 'reasonably' indicates that, provided the levels are comfortably below the regulatory limits, extraordinary measures are not necessary. Measures to reduce exposure must, however, be taken that are achievable without major cost or disruption.

Reduction of exposure

The amount of radiation to which an individual is exposed is given by the rate at which (s)he is exposed, measured in Sv hour^{-1} multiplied by the time over which (s)he is exposed. To keep exposure as low as possible, therefore, the radiation level should be kept low and the time of exposure limited as much as practical.

Reduction of radiation level

The easiest, and often most effective, way to reduce the exposure level is to increase the distance from the source of radiation. Radiation levels obey the *inverse-square law*, so that by doubling the distance from the source, the amount of radiation received over the same area of body drops by a factor of four. Similarly if the distance increases by ten times, then the radiation level drops to only 1%.

To appreciate the inverse-square law, imagine a sphere of radius, r, as shown in Fig. 7.36, drawn around the source. All the particles emitted from this, say n per unit of time, will, in the absence of any absorbers, pass through the surface of the sphere, which has an area of $4\pi r^2$. So the number of particles passing through a unit area of the sphere's surface will be $n/4\pi r^2$. Thus, the radiation intensity decreases as the square of the distance from the source. Clearly, this is only strictly true if the size of both the source and the receiver are small compared with the distance between them, but the principle still holds.

The inverse-square law is a powerful means to reduce exposure levels, sometimes called *distance shielding*. For instance, to halve the exposure level requires only a 40% increase in distance from the source.

Practical steps to increase distance include carrying an instrument containing a radioactive source so as to

maintain the maximum distance between the source and the bearer's body (even better if the device is on a small portable trolley); packing a vehicle in such a way as to keep the source as far away as possible from the driver and passengers; storing the source well away from where people congregate or work, or where casual passers-by may be exposed; keeping the source as far away from the body, particularly the most sensitive areas, as practical during use; and keeping any persons not directly involved in use of the device well away from it.

The most important consideration in making distance shielding effective is to ensure that all those concerned, not just the operators, are aware through training of the location of the source and the need to maintain as much distance as possible from it (and for the least time).

The second way to reduce radiation levels is to use *shielding*. Most substances absorb radiation, but some are much more effective than others. Gamma rays, for instance, are absorbed primarily by interaction with the electrons within a substance, and so the number of these per unit volume (which is closely related to the density of the substance) is very nearly proportional to its absorbing power. The consequence is that doubling the thickness of a light absorber would have almost the same effect as using the original thickness of one whose density is twice as much. The shielding power, as a consequence, is often expressed in terms of kg m^{-2}, that is the mass per unit area normal to a line between the source and the target. For a small source, ideally a 'point', this favours using the heaviest substances available. If the shielding is in the form of a sphere of radius r and density ρ, with the source at its centre, the mass-weighted thickness, S, of shielding material between the source and a target outside the shield is ρr. The mass of the shield, M, however, is equal to $4\pi\rho r^3/3$. For a given shielding level, then, M is related to S as follows:

$$M \propto \frac{S^3}{\rho^2}. \qquad (7.11.2)$$

So to achieve the same level of shielding, the required mass is inversely proportional to the square of the density. Hence, lead (ρ = 11,340 kg m^{-3}) is a common shielding material and, where the expense can be justified, depleted uranium (ρ = 18,900 kg m^{-3}) may be used. The mass of a depleted uranium shield, therefore, need be only a little over 1/3 that of a lead one with the same shielding power. Since the mass of shielding is often the dominant factor in the overall mass of the device, this is an important consideration. The use of high density shielding also makes for a more compact device, although this reduces the benefit of distance shielding.

A given thickness of shielding will produce a reduction of the radiation by a factor of, say, x. A second layer of the same thickness will reduce the amount of radiation by a further factor x, to give an overall reduction of x^2, each succeeding layer reducing the radiation by another factor of x. So if x is 2, then each layer reduces the radiation by a half and successive layers produce reductions of ½, ¼, 1/8, and so on. Mathematically, this can be expressed as follows:

$$I = I_0 e^{-\alpha t} \qquad (7.11.3)$$

where

I is the radiation intensity emerging from shielding of thickness t;
I_0 is the radiation intensity entering the shielding and
α is an *attenuation coefficient*, expressing the effectiveness of the shielding material.

For gamma rays, α is expected to be proportional to the density of the material, although its value will depend on the energy of the gamma rays, decreasing with increasing energy for photon energies of less than 4 MeV. In other words, the higher the gamma ray energy, the smaller the attenuation and the greater the penetration.

For neutrons, which do not interact with electrons in the material, the situation is somewhat different. Lighter nuclei (particularly hydrogen) are better at slowing fast neutrons. Hydrogen-rich materials are therefore used. The slow neutrons are readily captured by many elements. Water is a very efficient material for shielding and for portable shields plastics are often used. The addition of boron, which is a very efficient slow neutron absorber, to the shield material increases the efficiency of shielding markedly and the addition of a thin lead shield will reduce the hazard caused by gamma rays, which are a by-product of the capture process.

Time of exposure

With modern equipment used in the correct manner, the rate of exposure to radiation is low. Nevertheless, the ALARA principle requires keeping oneself (and others) near to a radioactive source for the least time necessary to perform the task in hand. It is very important to remember that, even though equipment may be switched off, the radioactive source is still decaying and emitting radiation. A little forethought and planning will help to ensure that operators are exposed to the source for as short a time as possible. In most cases, the measures required are fairly obvious, but a few general points may help to achieve minimum exposure.

The most important point is to ensure that no one is exposed to a significant level of radiation when the equipment is not being used. This means that it should be stored well away from any people except when it is in use or being transported. This applies both to the laboratory situation, where the equipment should be kept in a safe, secure and permanent store, and to the field, where people should not be allowed near to a source during breaks or when performing tasks not involving the radioactive equipment. Similarly, only those people who are actively using the radioactive equipment should be allowed near the source. If other people have tasks to perform close to where the radioactive source is used, it can usually be arranged for them to do these before or after work with the equipment.

It is often difficult to arrange separate transport for personnel and the equipment. However, as far as possible, this should be adhered to. If it is necessary for others to travel in the same vehicle, then:

- the vehicle must be packed to ensure that the radioactive source is as far away from the occupants as possible and that appropriate shielding is placed in between;
- people who are not essential for the task must not be allowed to travel in the vehicle.

7.11.6 The legal framework

In most countries, laws have been adopted based on recommendations and regulations framed by international bodies. While each country is responsible for passing its own laws, these documents ensure that the practices are similar in different countries.

The regulations in most countries cover four main areas of activity:

1 Protection of persons from radiation during use and storage of the equipment
2 Transport
3 Environmental protection
4 Security of the radioactive material.

Radiation protection during use and storage

These regulations are based on limits recommended by the ICRP for human exposure. They normally distinguish between exposure of those working professionally with radioactive sources and the general public, for whom there is a lower dose limit. The ICRP's latest (2007) recommendations (ICRP103) set a limit of 1 mSv per annum for members of the general public and 20 mSv per annum, averaged over 5 years, for occupational users. The recommendations also incorporate the ALARA principle and advise that zones around radioactive sources be designated as *controlled* and *supervised areas*. Controlled areas are ones in which only designated people may enter, while supervised areas enjoy a lower level of protection, while still having the potential for members of the public to receive a dose above the recommended limit if they remain within it for a significant proportion of the time.

To put these recommendations into practice, it is usual to take the annual dose limit and divide it by the working time over the year. This will yield the maximum allowable dose rate. For some working environments, this is not practical, but for the type of work discussed here, is perfectly feasible. Often the law will insist that workers wear personal dosimetry monitors. These are usually either photographic films encased in a light-proof covering and partially shielded or more modern photoluminescent detectors. These are sent to a testing house on a regular (usually monthly or three-monthly) schedule and the dose received by the wearer over that time assessed. Neutron monitors are more complex and expensive, partly because of a lower demand for such monitoring. Strict recording procedures are necessary to ensure that annual doses are calculated correctly and that records are passed from one employer to another. Provided that sensible procedures to achieve ALARA are in place, it is rare for such monitors to record any measurable dose with the use of neutron and gamma soil probes.

Transport

Because transport is an international industry, regulations for the movement of radioactive materials are similar for different modes of transport and standardised between different countries. Recommendations for the transport of radioactive materials are published by the International Atomic Energy Agency (IAEA, 2012) and cover packaging, labelling and handling of the materials. The International Air Transport Association (IATA) and International Maritime Organisation (IMO) have their own (very similar) regulations for transport of hazardous goods, which incorporate the IAEA recommendations and also cover documentation.

The main relevant elements of the transport regulations are as follows.

Special form sources These are manufactured to very stringent standards to ensure that the radioactive contents will stay within the source capsule even under very severe conditions, for instance a mechanical accident or serious fire. Special Form Certificates are issued by national accreditation bodies and are valid for a few years at a time. They can be renewed, but are often valid for a limited time from the date of manufacture to reflect deterioration of the capsule's construction, pressure build up within it from evolved gases, changing standards, etc. Thus, although the half-life of a neutron source may be 432 years, the Special Form Certificate may be renewable only for 15 years. A Special Form Certificate exempts the consignor of the package from many of the transport regulations, since there is a very high level of confidence that, no matter what may happen to the package, the source will remain intact. Without a Special Form Certificate, routine transport of neutron and gamma ray probes would be almost impossible.

Containers The outer packaging of the equipment containing a radioactive source should conform to certain standards, which ensure that it is sufficiently robust to stay intact during transport and that the radiation level at the surface will not endanger handlers. The most common container for Special Form sources is known as *Type A*. A Type A container must be capable, when it has the equipment inside it, of withstanding: dropping onto a hard surface from 1 m height on any corner and of being penetrated by a 20 kg iron bar dropped from 1 m and retain this ability when soaked in water.

Labelling All vehicles carrying hazardous goods, of which radioactive materials are an example, must display

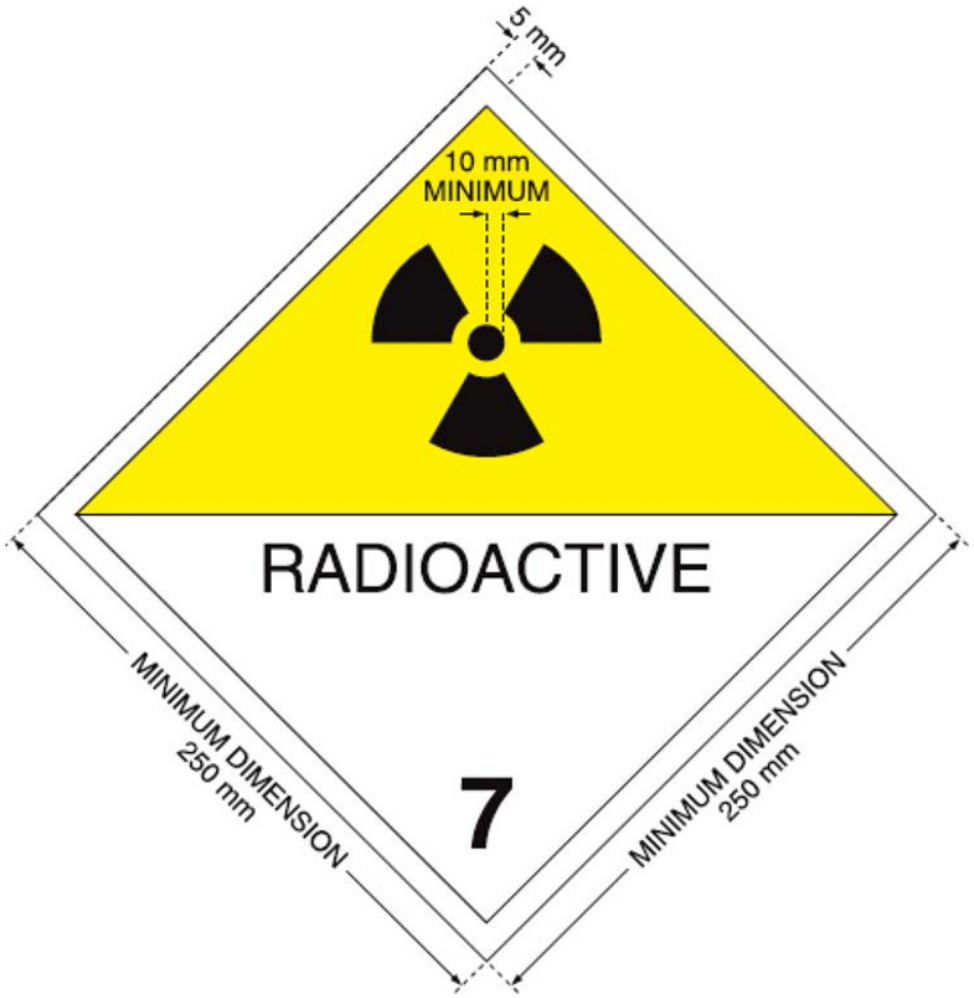

Fig. 7.37 Placard to be displayed on the outside of a vehicle carrying radioactive materials. The upper part has a yellow background. From IAEA (2012). Reproduced with permission of IAEA.

appropriate signage. These comprise three diamond-shaped half yellow, half white signs, similar to Fig. 7.37, with a radioactive trefoil sign. These must be displayed on each side and the back of the vehicle.

In some countries, an orange rectangle, edged in black, must also be displayed on the front and back of the vehicle, to indicate hazardous goods. In others, there must be either or additionally a fireproof plate in the cab, visible to the driver, warning of radioactive materials on board. The box containing the source must also display signage. This is quite tightly prescribed. The examples given here apply to a Type A container, since these are used almost universally for portable equipment. The first requirement is for a small diamond radioactive trefoil label, similar to that used on the outside of the vehicle. This label, however, must carry some details of the source and the dose rate at the surface of the box, in the form of a *Transport Index*. The Transport Index is the dose rate in mSv hour^{-1} at 1 m from the outside of the container multiplied by 100 and rounded up to the nearest 0.1. There are three forms of this label, depending on the Transport Index. Category I labels are used for transport indices lower than 0.1, Category II for those between 0.1 and 1 and Category III for those higher than this. Figure 7.38 shows an example of a Type II label, which is most likely to be appropriate for portable soil water equipment. The box must have at least two of these labels on opposite sides. The container must also have labels similar to those illustrated in Figs. 7.39 and 7.40. Again, the wording is tightly prescribed. Lastly, the box must have a label showing the consignor's and/or consignee's details.

Documentation For road transport, each radioactive package must be accompanied by a Consignment Note. This contains details of the radioactive content of the package, the origin and destination of the journey, etc. An

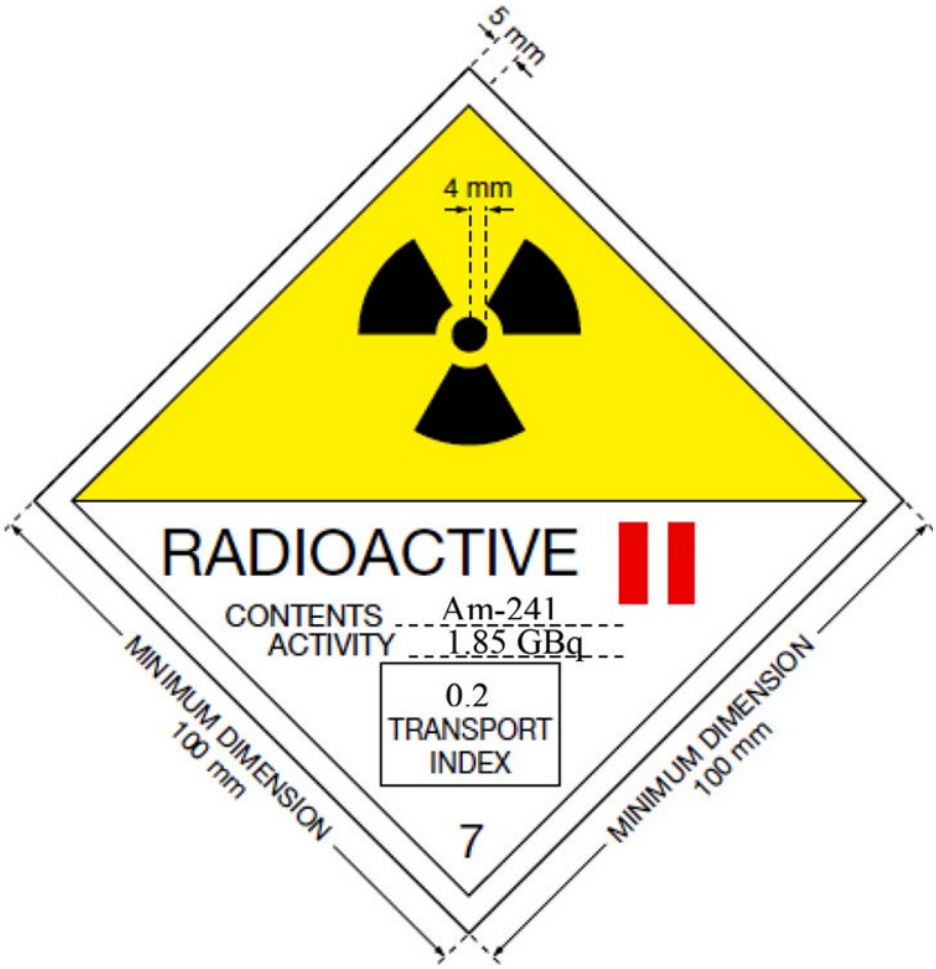

Fig. 7.38 Category II label to be affixed to a transport container. The upper half of the label is yellow, and the lower half of the label is white. The trefoil and printing is black and the Category II bars are red. From IAEA (2012). Reproduced with permission of IAEA.

UN3332

RADIOACTIVE MATERIAL,
TYPE A PACKAGE,
SPECIAL FORM

Fig. 7.39 Package label identifying the UN marking and proper shipping name.

example of a Consignment Note is shown in Fig. 7.41. The Consignment Note should be accompanied by a Special Form Certificate and may require other documents, such as a copy of Local Rules. For air and sea transport, an IATA or IMO Hazardous Goods Certificate is required. An

TYPE A

Fig. 7.40 Package label identifying a Type A container.

example copy of an IATA form is shown in Fig. 7.42. The IMO version is very similar. Only original copies of this form are acceptable and many carriers will not accept any corrections on the form. Other documentation may be required, in particular for international transfers, customs documents and permission from the authorities in the receiving country.

Transport across administrative boundaries Journeys that cross administrative boundaries often require permission from the authorities in the destination area. These are not necessarily international borders. Different states of the

Consignment Certificate for the Transport of Radioactive Materials

The Radioactive Material (Road Transport) Regulations 2009

Date	
Name & Address of Consignor:	
Tel:	
Radionuclide Group for Transport Purposes:	RADIOACTIVE MATERIAL, TYPE A PACKAGE, SPECIAL FORM UN 3332, UN Class 7
Type & Category of Packaging:	Type A. Category II Yellow
Transport Index:	0.2
Radioactive Material:	^{241}Am–Be
Source No.:	
Source Activity:	1.85 GBq
Special Form Certificate No.:	USA/0659/S
Special Form Certificate Expiry Date:	31 December 2008
Name & Address to whom package is consigned:	
Tel:	

I hereby declare that the contents of this consignment are fully and accurately described above by the proper shipping name and are classified, packed, marked and labelled, and are in all respects in proper condition for transport by road according to the applicable international and national governmental regulations.

It is declared that the packing of the goods into the vehicle has been carried out in accordance with the applicable provisions.

Signed: Name in capitals:

Fig. 7.41 Example of a transport document complying with the IAEA (2012) Transport Regulations. Note that information must be entered into all the grey areas and that some of the other information will not be applicable in all cases. © NERC (CEH). Reproduced with permission.

SHIPPER'S DECLARATION FOR DANGEROUS GOODS

Shipper

Air Waybill No.

Page of Pages

Shipper's Reference Number *(optional)*

Consignee

For optional use for Company logo name and address

Two completed and signed copies of this Declaration must be handed to the operator.

WARNING

Failure to comply in all respects with the applicable Dangerous Goods Regulations may be in breach of the applicable law, subject to legal penalties.

TRANSPORT DETAILS

This shipment is within the limitations prescribed for: *(delete non-applicable)*

PASSENGER AND CARGO AIRCRAFT | ~~CARGO AIRCRAFT ONLY~~

Airport of Departure:

Airport of Destination:

Shipment type: *(delete non-applicable)*

~~NON-RADIOACTIVE~~ | RADIOACTIVE

NATURE AND QUANTITY OF DANGEROUS GOODS

Dangerous Goods Identification						
UN or ID No.	Proper Shipping Name	Class or Division (Subsidiary Risk)	Packing Group	Quantity and type of packing	Packing Inst.	Authorization
UN3332	RADIOACTIVE MATERIAL, TYPE A PACKAGE, SPECIAL FORM UN3332, UN CLASS 7	7		Am-241 One package 1.85 GBq Activity within limits for Type A Package	Category II Yellow TI 0.2 II x ww x hh cm	Special Form Certificate USA/0659/S

Additional Handling Information

I hereby declare that the contents of this consignment are fully and accurately described above by the proper shipping name, and are classified, packaged, marked and labelled/placarded, and are in all respects in proper condition for transport according to applicable international and national governmental regulations. I declare that all of the applicable air transport requirements have been met.

Name/Title of Signatory

Place and Date

Signature *(see warning above)*

Fig. 7.42 IATA Shippers declaration form. © 2014, IATA. Used by permission of IATA. All rights reserved. The IATA Dangerous Goods Manual is available at http://www.iata.org/publications/dgr/Pages/index.aspx

United States, for example, require such permission. Permission is also required for transport between different countries of the European Union, although it may not be needed (depending on the receiving country) if the package originates from outside the EU. Transport (and other) rules within different administrative areas often differ, so that it is essential to establish these in advance.

Transport by road Users often transport radioactive devices themselves as part of their regular monitoring activity. Many of the same requirements concerning placarding of vehicles, transport documents, etc. apply equally to these people as to commercial carriers. However, commercial carriers usually have a well-established set of operating procedures, whereas the neutron or gamma probe user needs to produce their own in consultation with their advisers.

The principal areas to cover are limitation of radiation exposure to occupants of the vehicle and those outside, emergency procedures in case of accident or breakdown of the vehicle and security of the radioactive materials.

Exposure to vehicle occupants can be minimised by ensuring that no one not directly involved in the work travels in the vehicle and that the radioactive device(s) are packed as far away from the occupants as possible. There may be an appreciable level of radiation outside the vehicle, so that if it is parked for more than a very short time, it should be well away from other vehicles or where other people pass or congregate.

Emergencies should be catered for by establishing procedures for notifying a responsible person of accidents or breakdown, for securing the vehicle and its contents in such a situation and by signalling the presence of a disabled vehicle carrying hazardous goods to other road users by, for instance, marker cones or lights. A fire extinguisher in the vehicle will help prevent problems in case of a fire.

Security of the radioactive contents clearly depends on individual circumstances, but should include measures to lock the device in its transport container, to prevent theft of the device in its container by securing it in the vehicle (this will also help keep it secure in case of a serious accident) and by ensuring that the vehicle is not left unattended or out of surveillance.

Environmental protection

The use of sealed, Special Form sources should prevent the possibility of contamination of the environment by radioactive material in the source. Loss of a source would create a minor environmental hazard, but a much greater one to individual members of the public, who might come into contact with it. For this reason, loss of a radioactive source is taken very seriously indeed. It is essential to formulate emergency procedures to deal with such an eventuality (see later).

The main environmental hazard relating to radioactive materials comes from the use of unsealed sources. In soil water investigations, their use is almost always as tracers (see Sections 19.2.4 and 24.4). These are mostly confined to laboratory experiments, but have been applied in the field. Permission to use a radioactive tracer in the field is extremely difficult to obtain and is likely to be granted only if no other methods are possible and if the need for the investigation is regarded as of sufficient importance that it outweighs the public health hazard resulting from possible exposure of members of the public. Stringent safeguards must be in place for either laboratory or field use, to reduce releases of radioactivity to the air, water bodies or the soil. Licensing is normally required, specifying limits for disposal by each of these routes and the measures required both to comply with ALARA principles and with the stated disposal limits.

Security

For many reasons, security of radioactive material is important. Recent concerns over global terrorism have increased the prominence of the security aspects of the use and storage of radioactive materials, resulting in more stringent regulations in many countries. The sources used for the work described here are relatively small and, therefore, unlikely to pose a significant public health hazard, whether lost accidentally or stolen deliberately. There is, however, potential for very significant levels of public concern over the loss of even a small quantity of radioactive material, which can be exploited by those seeking to cause civil unrest. To ensure an adequate level of security, the following steps should be taken:

- All radioactive materials must be stored in a secure store. Particular attention should be paid to the security of windows, rooflights or other potential weak points. The door to the store must be strong enough to withstand attempts at forced entry. It must also be marked clearly with radioactive trefoil signs to signal that there is a hazard within. The objective is to ensure that, even if the building in which the store is sited is entered illegally, the radioactive material will remain secure.
- The materials within the store must be placed so that the dose rate on the surface of its walls is below that which would give rise to a supervised area. This ensures negligible hazard to people passing close to the store.
- Entry to the store should be controlled, so that only those who need access to the radioactive materials can do so. This may be by ensuring that only authorised people possess a key to the store. Alternatively, there may be only two keys to the store, which are kept in a locked key cabinet. Keys to the key cabinet may be held by each person requiring access, but not by others. This latter arrangement often works better where there are several people needing access to the store. Higher levels of security may be achieved by using various electronic access arrangements.

• Only equipment connected directly with use of the radioactive materials should be kept in the store. This helps to ensure that access is restricted only to those people with a direct need to use the radioactive equipment.
• All movements of radioactive sources into and out of the store must be recorded in a book kept within the store. As a minimum, this should record the identification of the source, the date and time of its removal and replacement, the destination and the person who takes it out or returns it. It also helps if the amount of time that the source is in transport, being carried and in use is recorded, as this helps to give a semi-quantitative picture of the amount of exposure to individuals.
• When not in the store, the radioactive material should be kept under surveillance at all times. This is not normally difficult to arrange, since it will usually be in a vehicle with the driver or in use. Breaks can usually be arranged so that the vehicle or the instrument container can be kept in sight. If it is necessary to take the instrument out of its store overnight, then a temporary arrangement must be made to ensure the security of the source, which is no less stringent than that of its permanent storage. Commercial facilities exist in some places, while many research stations or academic institutions may provide suitable accommodation. If overnight storage is needed frequently, it may be worthwhile constructing a suitable store.

A store need not be particularly elaborate. For a single neutron probe, a large steel cabinet, about 1 m square and high enough to accommodate the probe will often suffice. The construction must be robust enough to withstand attempts to break into it, as does the lock. On its own, this is probably not sufficiently secure, but security may be enhanced by locating the store inside a building or a secure compound. Another solution is the use of a ground safe. This is a watertight steel box about 400 × 400 mm and deep enough to accommodate the probe, buried in the ground, so that its top just protrudes above the ground surface. An overlapping, lockable lid secures the contents and prevents rain getting in. Security is increased by the unobtrusive nature of the installation, although this is clearly not a suitable option where surface flooding is possible. Once again, the ground safe should be located in a secure compound. An added advantage of a ground safe is that very little radiation is likely to be experienced at or above ground level.

7.11.7 Practical compliance with radiological protection regulations

The foregoing discussion may seem bewilderingly complicated. However, advice is often available to help devise arrangements which are both practical and fulfil the legal requirements. Large commercial and research organisations and universities usually employ people experienced in using radioactive materials and who are familiar with many of the regulations, although this is often from a laboratory viewpoint and use in the field may be beyond their experience. In the United Kingdom and some other countries, each registered organisation must have a radiological protection advisor. This may be someone within the organisation or, for smaller establishments, an employee of a specialist advisory service. Regular contact with such people ensures that practicality is compatible with rigorous compliance, that experience is shared among different groups with similar problems and that changes in the regulations are dealt with in a timely fashion.

The heart of good radiological protection is a set of *local rules*. These should embody all the aforementioned principles in a form specific to the organisation and the work undertaken. The local rules form part of the overall working regime and may be incorporated into an observer's handbook or set of instructions, or may be a standalone document. They need to be clearly written and no longer than absolutely necessary, so that everyone involved understands and complies with them.

The local rules should include the following:
• A brief description of the hazard from each radioactive source used;
• Advice on minimising exposure;
• The storage requirements, including safe emplacement in the store and security measures needed;
• The rules for transporting the sources, including the containers which must be used, which vehicles may be used, measures to protect occupants of the vehicle, the signs to be displayed on the vehicle and on the containers;
• The procedures to be followed when using the devices to minimise exposure;
• All documentation which must be carried and/or completed when moving or using the radioactive materials; and,
• Emergency procedures in the event of unexpected events; for instance, vehicle breakdown, accident, jamming of a device below ground, theft or fire. Contact details for emergency services and a responsible person (who may not necessarily be a member of the employing organisation but, for instance, of a specialist radiological protection organisation).

Formulating contingency procedures for these events is, in itself, a useful exercise in focusing on the important issues surrounding particular activities and will often prompt changes in working practice to make the events less likely.

Local rules should be revised regularly and at least annually. It is surprising how quickly procedures become out of date as circumstances, personnel and working patterns change. Frequent revision of the rules also allows improvements to be incorporated into working practices. For this reason, the people actually carrying out the work should be fully involved in writing and revising the rules.

The local rules must be complemented by regular training of all staff involved. All those who use the devices should attend a training session before being allowed to

work with any radioactive source. This should contain the kind of information described in this chapter, followed by a full description of the organisation's procedures, as set out in the local rules. It should also include hands-on training in each phase of the work, concentrating on practices to reduce exposure to oneself and others during storage, transport (including loading) and use of the devices. Some training will often also be necessary for staff indirectly involved in the work, including managers.

Good practice would provide refresher training about once every 2 years and a full repeat training session after 5 years.

8 Dielectric Methods

Neutron probes proved to be very successful in enabling field observations of soil water content in sufficient detail to follow changes in water storage as a function of both depth and time. This allowed major progress to be made in both scientific studies of soil water dynamics and practical applications. The latter included irrigation scheduling, estimation of pollution of groundwater via the unsaturated zone, estimation of recharge to groundwater and clogging of sewage filter beds.

However, neutron probes suffer a number of disadvantages. Chief amongst these are the following:

- The need to install access tubes, which is very time-consuming and laborious. Moreover, it carries dangers of excessive disturbance to vegetation, the ground surface and the subsurface environment. Additionally, any gap around the access tube may allow water to bypass the upper soil matrix to deeper depths.
- Radiological protection regulations impose significant overheads on their use. Over time, these have become increasingly burdensome.
- The equipment is heavy and data acquisition is slow, requiring manual operation of the instrument.
- Automatic, unattended data acquisition is not possible except in very rare circumstances.
- The equipment is expensive.
- Some operators and landowners are resistant to the use of radioactive equipment.

These difficulties led to a search for alternative methods to measure soil water content, which would avoid some or all of these problems.

A good basis for such a method is to exploit the very high permittivity of water, relative to that of almost all other materials. This had been recognised for several decades, but practical techniques were not developed until the late 1970s, when sufficiently robust high-frequency electronic devices became available.

Techniques for using this property to measure soil water content use different ways in which permittivity variations affect high-frequency electromagnetic waves. These include their velocity in the soil medium (the basis of time domain reflectometry (TDR) and time domain transmission (TDT)), the characteristic impedance of the medium to wave propagation (used in the *Theta Probe*) and the capacitance between two electrodes embedded in the soil (used in various ways in capacitance probes, the ECH2O probe and others).

Much of the theory behind the use of these devices is quite complex. It is described in some detail, starting with the concept of permittivity and why it varies from one substance to another, then onto the particular dielectric properties of water. This is followed by a description of the fundamental principles of electrical circuits and their response to time-varying voltages. Many readers may find this very familiar, while others may not. It is included to provide the theoretical basis for all the techniques described later in the chapter.

Section 8.4 discusses the relationship between permittivity and soil water content, which underpins all of these techniques. Following this, Section 8.5 develops the theory behind transmission lines and how permittivity affects the velocity of an electromagnetic wave along such a line, the concept of characteristic impedance and how electrical conductivity of the medium between the conductors affects the wave. Many capacitance-based instruments are, in reality, short transmission lines embedded in the soil. Part of Section 8.5 describes how the capacitance of these short lines depends on their length, the oscillation frequency and the electrical conductivity of the medium. This section presents the fundamental physics behind most dielectric methods. It may, however, be both mathematically and conceptually challenging for many readers. In view of its importance, the key concepts are brought together in a short summary at the end of this section.

Section 8.6 describes how the dependence of electromagnetic wave velocity on medium permittivity may be used to measure the permittivity of soil, and hence its water content, in practical field situations through TDR and TDT.

Sections 8.7 through 8.10 describe the conceptually simpler capacitance-based methods for measurement of soil water content and compare different methods used to

Soil Water Measurement: A Practical Handbook, First Edition. J. David Cooper.

measure the capacitance between electrodes embedded in the soil. These include measuring the frequency of an oscillator in which the capacitor formed by the electrodes is part of the circuit (capacitance probes) and three different methods by which the capacitance may be deduced at a fixed frequency – by its effect as the termination of a transmission line (*Theta Probe*), the charging of a resistor – capacitance circuit (*ECH2O Probe*) or a full measurement of real and imaginary parts of the permittivity (*Hydra Probe*).

8.1 Dielectrics – Basic Principles

When an electric field is applied to an insulating material, the negatively charged electrons and the positively charged nuclei which compose it are pulled in opposite directions. The mutual attraction between the electrons and nuclei opposes this, so that the two sets of electric charges can separate by only a small distance. For small electric fields, the separation is proportional to the field strength. This transforms each molecule into a tiny *dipole*, which can be envisaged as having a positive charge at one end and a negative one at the other. The process is called *polarisation* and is conceptually similar to the stretching of a spring, in which the force applied (the electric field) is opposed by the stiffness of the spring (the attraction between positive and negative charges). To achieve the charge separation (as in stretching a spring) work must be done, which is stored as potential energy. This energy is released when the field is turned off or the force on the spring removed.

A device for storing energy in this way is called a *capacitor*. This is usually thought of as two parallel metal plates, separated by a small distance, d. When a voltage, V, is applied to the capacitor, a current flows from the voltage source and opposing charges collect on each plate. The electric field between the plates is V/d and the work done to achieve this charge storage is $\frac{1}{2}CV^2$, where C is called the *capacitance* of the capacitor. It is measured in farads (F), although the farad is a very large quantity and most practical capacitors are measured in μF (10^{-6} F) or pF (10^{-9} F).

Even with no material between its plates, the capacitor can store electric charge and energy. However, if there is a dielectric (i.e. an insulator) present, extra energy goes into separating the charges, which means that the capacitor stores both more charge and more energy. Figure 8.1 shows the way in which an electric field separates the charges of molecules in a solid (Fig. 8.1a and b) and in a liquid (Fig. 8.1c and d). Thus the presence of the dielectric increases the capacitance. For the flat plate capacitor, the capacitance is given by

$$C = \varepsilon \frac{A}{d}, \tag{8.1.1}$$

where
A is the area of the plates and
ε is called the *permittivity* of the material between them.

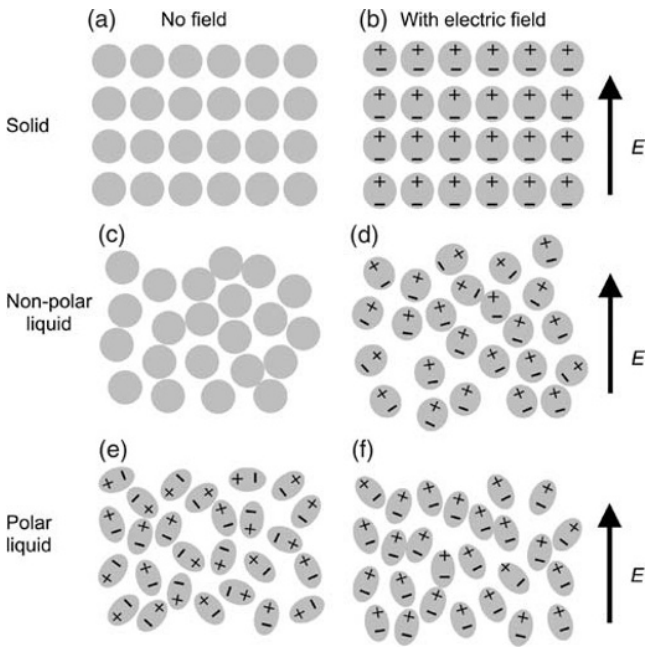

Fig. 8.1 Polarisation of a solid (a and b), non-polar liquid (c and d) and a polar liquid (e and f) by an electric field. The amount of alignment in liquids is much exaggerated.

The *electrodes* of the capacitor do not have to be parallel plates, however. Any pair of conductors will form a capacitor. For other configurations, the relationship is defined as follows:

$$C = g\varepsilon, \tag{8.1.2}$$

where g is called a *geometric factor*. In the case of the flat plate capacitor,

$$g = \frac{A}{d}. \tag{8.1.3}$$

Since the capacitor can store charge and energy when there is a vacuum between the plates, ε for the vacuum is not zero and is equal to 8.854×10^{-12} F m^{-1}. This is known as the *permittivity of free space* and given the symbol ε_0. ε_0 is sometimes called the *electric constant* or *vacuum permittivity*. For almost all practical purposes, air, because of its very low density, can be treated as having the same permittivity as that of free space. Solid and liquid dielectrics have higher values of permittivity. It is usual to use the ratio of the permittivity of the material to that of free space when discussing the properties of materials. This is called the *relative permittivity*, ε_r:

$$\varepsilon = \varepsilon_r \varepsilon_0. \tag{8.1.4}$$

A frequently used alternative, but more old-fashioned, name for relative permittivity is *dielectric constant*. Values of ε_r for most common materials are in the region of 3–6.

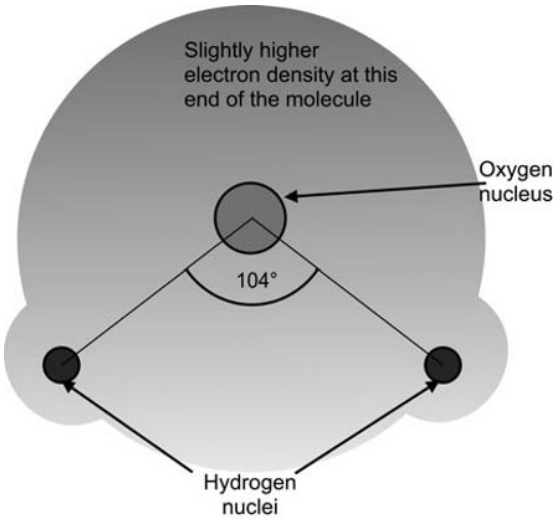

Fig. 8.2 Electron distribution in a water molecule.

Some substances, however, exhibit much larger values. Water, in particular, has a relative permittivity of about 80.

The reason for such a high permittivity is that the water molecule is itself a dipole, even when there is no electrical field present. That is, the charge within the molecule is distributed with a small net positive charge at one end and a small net negative charge at the opposite end (see Fig. 8.2). Such materials are known as *polar* substances. Applying an electric field to a polar substance not only causes the charges to separate a little more but also allows the existing dipoles to align with the field. More energy is stored by this process than by polarisation alone, and hence polar substances have a higher permittivity than non-polar ones. For the molecules to align with the field, however, they must be free to move. This is not normally possible in a solid, where the atoms are held tightly in a lattice; but in liquids and gases, where the molecules can rotate freely, there are no such constraints. The density of gases is very low, and hence there are few molecules per unit volume so that the permittivity of a gas is always very close to that of free space. Polar liquids, however, have very many molecules per unit volume and so exhibit a high value of permittivity. In water, this is around 80. Figure 8.1e and f shows the effect of an electric field on a polar liquid. When there is no electric field, the dipoles have a random orientation, but when a field is applied, they tend to line up with the field, although frequent collisions between molecules means that they are often knocked out of orientation.

8.2 Factors Affecting Permittivity of Water

The permittivity of water is not completely constant. The most important influences are temperature, electromagnetic frequency, the presence of electrically charged surfaces and dissolved solutes.

8.2.1 Temperature

Since the high permittivity of water depends on the molecules lining up in the electric field, anything which affects this will affect the permittivity. As described earlier, collisions knock them out of orientation. The more often collisions occur, the smaller the number aligned with the field at any moment. As temperature increases, the molecules move faster and so undergo more collisions. The result is that permittivity decreases as the temperature increases.

Additionally, thermal expansion means that there are fewer molecules per unit volume at higher temperatures, which also contributes slightly to the reduction of permittivity. The temperature coefficient of the relative permittivity of pure water resulting from these processes is about $-0.3^{\circ}C^{-1}$, that is it declines by about 0.3 for each increase in temperature of 1°C.

Freezing traps the water molecules in a rigid lattice structure and prevents them from reorienting in the field, except at frequencies of less than a few kilohertz. The relative permittivity of ice is, therefore, only about 3.2, a value typical of many other solids. This phenomenon can be used to detect when water freezes or, in association with a neutron probe or other means of measuring total water content, to assess the proportion of frozen to unfrozen water.

8.2.2 Frequency

An alternating electric field causes the electric dipoles to first orient themselves in the field in one direction, then in the opposite one a short time later. As the frequency increases, the dipoles' inertia inhibits their response to the field reversals, a phenomenon known as *relaxation*. The dipole orientation lags further behind the field, and the degree of alignment is less strong so that the permittivity reduces. Less obviously, the lag between the stimulus and the response means that energy is dissipated in the process. Relaxation is discussed further in Section 8.3.8.

8.2.3 Solid surfaces

Clay minerals have a similar crystal structure to ice. This explains in part why water is attracted to clay surfaces and often binds tightly to them. The consequent immobilisation of the first few molecular layers of water would be expected to reduce the permittivity of these layers, perhaps with the first layer having a value close to that of ice, with layers successively further from the surface becoming closer to free water. The precise details are not yet known and some of the data appear to conflict, but the qualitative picture is believed to be correct.

8.2.4 Solutes

Solutes in water are charged ions, which can screen water molecules from the electric field. Most soil solutions are quite dilute and the effect is, consequently, small.

A bigger effect is that solutes enhance the electrical conductivity of the solution very markedly. This affects various methods for measuring the permittivity in different ways and is described in each method's relevant section.

8.3 Fundamentals of Electrical Circuits

There are four kinds of passive circuit elements (i.e. those which do not need an external power source). These are resistors, capacitors, inductors and diodes.

8.3.1 Resistors

Resistors, as the name suggests, resist the flow of electric current. The basic equation governing the current through a resistor is the familiar Ohm's law:

$$V_R = IR \tag{8.3.1}$$

where
V_R is the voltage across the resistor;
I is the current passing through it, and
R is the *resistance* of the resistor.

Current passing through a resistor causes it to heat up, as energy is dissipated inside it. The rate at which energy (W) is dissipated is given by

$$\frac{dW}{dt} = IV_R = I^2R = \frac{V_R^2}{R}. \tag{8.3.2}$$

Electrical circuits are usually depicted by showing the various elements as symbols, with lines showing wire or printed circuit board connections between them. A resistor is usually depicted by this symbol: 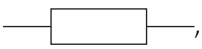 , although in older texts it may be shown as:  .

8.3.2 Capacitors

As described in Section 8.1, capacitors store electric charge and energy. The amount stored depends on the physical arrangement of the parts of the capacitor and on the permittivity of the dielectric.

The relationship between charge stored and voltage is given by

$$Q = CV_C, \tag{8.3.3}$$

where
Q is the charge stored by the capacitor;
C is the *capacitance* and
V_C is the voltage across the capacitor.

The energy, W, stored in the capacitor is given by

$$W = \frac{1}{2}QV_C = \frac{1}{2}CV_C^2 = \frac{1}{2}\frac{Q^2}{V_C} \tag{8.3.4}$$

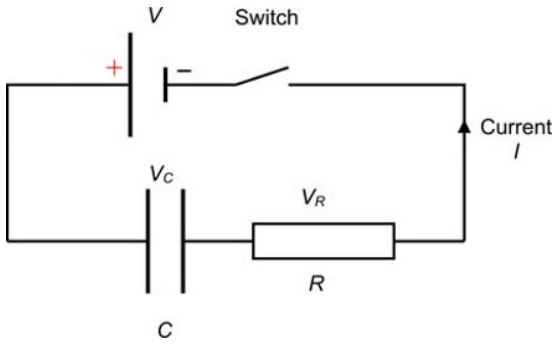

Fig. 8.3 Capacitor charging through a resistor.

A steady voltage applied to the capacitor initially causes current to flow in the circuit as it stores charge. Once the capacitor voltage reaches that of the power source, no further current will flow, making the capacitor a complete barrier to current flow.

A capacitor is usually indicated on a circuit diagram by this symbol:  .

To illustrate this, Fig. 8.3 shows a circuit in which a capacitor is charged from a steady voltage source, V, through a resistor. At time $t = 0$, the switch is closed and a current, I, starts to flow in the circuit. Electric current is a flow of charge, and so the rate at which charge is accumulated on the capacitor is given by:

$$\frac{dQ}{dt} = I. \tag{8.3.5}$$

Using Equations 8.3.1, 8.3.3 and 8.3.5, the voltage across the resistor, V_R, and the capacitor, V_C, are as follows:

$$V_R = IR \tag{8.3.6}$$

$$I = \frac{dQ}{dt} = C\frac{dV_C}{dt}. \tag{8.3.7}$$

Since

$$V = V_R + V_C = \text{constant}, \tag{8.3.8}$$

$$\frac{dV_R}{dt} + \frac{dV_C}{dt} = 0. \tag{8.3.9}$$

Differentiating Equation 8.3.6 and using (8.3.9) yields:

$$\frac{dV_C}{dt} = -R\frac{dI}{dt}, \tag{8.3.10}$$

which can be substituted into (8.3.7) and rearranged to obtain:

$$\frac{1}{I}\frac{dI}{dt} = -\frac{1}{RC}. \tag{8.3.11}$$

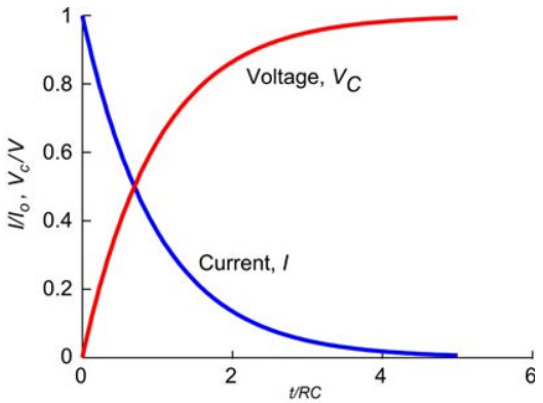

Fig. 8.4 Variation of current and voltage with time during capacitor charging.

Integrating both sides with respect to t gives

$$\int_{I_0}^{I} \frac{\mathrm{d}I}{I} = -\frac{1}{RC}\int_0^t \mathrm{d}t, \tag{8.3.12}$$

where I_0 is the current at $t = 0$, which must be equal to V/R since there is no voltage across the capacitor initially.

The solution of (8.3.12) is:

$$\ln\left(\frac{I}{I_0}\right) = -\frac{t}{RC}. \tag{8.3.13}$$

Or

$$I = \frac{V}{R}e^{-\frac{t}{RC}}. \tag{8.3.14}$$

The result is shown graphically in Fig. 8.4. The quantity RC is often called a *time constant*, as it defines a characteristic time over which the current falls to $1/e$ (about 37%) of its final value and is usually given a symbol τ.

The voltage on the capacitor is found by using Equations 8.3.6 and 8.3.8:

$$V_C = V\left(1 - e^{-\frac{t}{RC}}\right). \tag{8.3.15}$$

This is also shown in Fig. 8.4, and indicates that the voltage rises up to a steady value of V with the same time constant.

8.3.3 Inductors

Sometimes referred to as a *solenoid* or *coil*, these are usually in the form of a coiled piece of wire. When current flows through the coil, it creates a magnetic field, the build-up of which resists the flow of current. In contrast with a capacitor, the maximum resistance occurs when voltage is first applied to the inductor, as it produces an opposing voltage proportional to the rate of change of current. Once the current becomes steady, an inductor provides no barrier to the current. An inductor is characterised by its *inductance*, which is usually given a symbol L and is measured in henries (H).

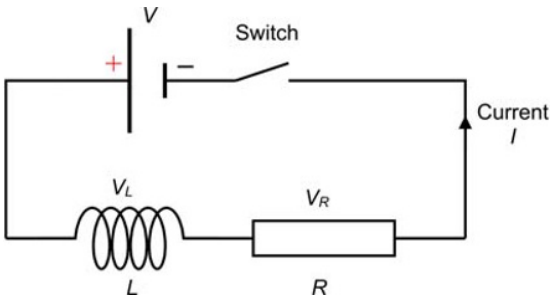

Fig. 8.5 Inductor circuit.

In circuit diagrams, an inductor is usually denoted by this symbol: 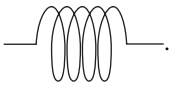 .

The relationship between current through the inductor and the voltage, V_L, across it is given by

$$V_L = -L\frac{dI}{dt}, \tag{8.3.16}$$

where the negative sign signifies that the voltage is directed in the opposite direction to the current flow.

The energy, W, is stored in the magnetic field of the coil and is given, similarly to Equation 8.3.4, by

$$W = \frac{1}{2}LI^2. \tag{8.3.17}$$

The behaviour of an inductor can be illustrated in a similar way to that of a capacitor, as shown in Fig. 8.5, by replacing the capacitor with an inductor.

Initially, there is no current in the circuit when the switch is closed, and so all applied voltage, V, appears across the inductor.

Equation 8.3.16 gives the voltage across the inductor, and the voltage across the resistor, V_R, is given by Equation 8.3.6:

Then, the total voltage, $V_R + V_L = V$, which is constant, so

$$IR - L\frac{\mathrm{d}I}{\mathrm{d}t} = V. \tag{8.3.18}$$

The method of solution is very similar to that for the capacitor and leads to

$$I = \frac{V}{R}\left(1 - e^{-\frac{tR}{L}}\right). \tag{8.3.19}$$

This is shown graphically in Fig. 8.6. In this case, the current increases from zero to a steady maximum value

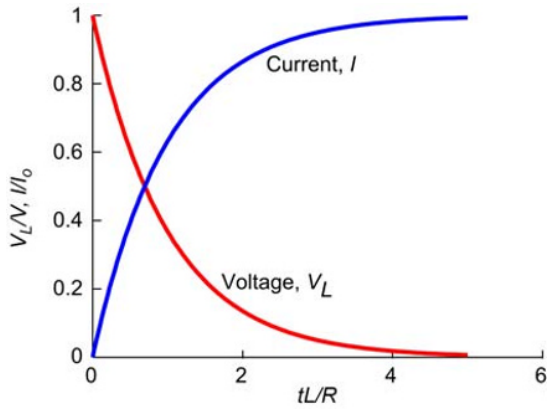

Fig. 8.6 Voltage drop and current build-up through an inductor.

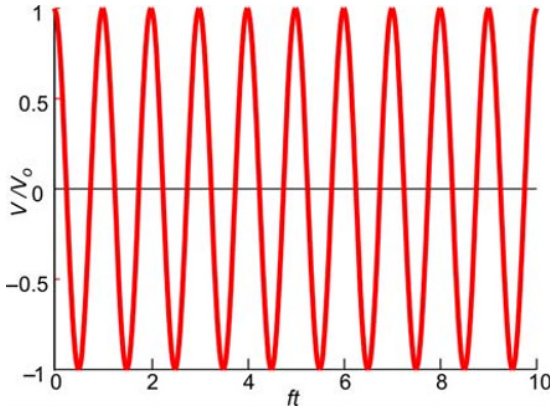

Fig. 8.7 Oscillatory voltage described by $V = V_0\cos(2\pi ft)$.

of (V/R), and the time constant is equal to (L/R). Figure 8.6 also shows the voltage across the inductor falling with the same time constant to reach zero eventually, when the current becomes steady. Figures 8.4 and 8.6 are, in fact, identical except that the time constant in one case is RC and in the other, (L/R) with the current and voltage curves being exchanged.

Similarly to a capacitor, the value of the inductance can be enhanced by a material, usually iron or ferrite, which has a large *magnetic permeability*.

Inductors do not have to be coils of wire. Even a straight length of wire has an inductance, as a current produces a magnetic field around it. A pair of conductors or electrodes has an inductance that can be expressed by the same geometric constant, g, as that for a capacitor, except that L is inversely related to g (see Eq. 8.1.2):

$$L = \frac{\mu}{g}, \tag{8.3.20}$$

where μ is the magnetic permeability.

The main use of capacitors and inductors is in alternating current applications, where they regulate current without dissipating energy. This is described in Section 8.3.5.

8.3.4 Diodes

A diode is effectively a one-way valve, allowing current to flow through it in one direction, but not in the other. Ideally, it will have zero resistance when current flows in the "forward" direction and infinite resistance in the other direction; but, in practice, these are not quite realised. A diode is depicted in circuit diagrams thus:  . The arrow indicates the direction in which current is allowed to flow.

8.3.5 Alternating currents and voltages

When the strength of the voltage source varies in a regular manner, the behaviour of capacitors and inductors is qualitatively different from the dc case. The basic equations remain the same, but since the voltage is always changing, the average current through the circuit is quite different.

A fundamental property of any variable waveform, even a non-periodic one, is that it can be made up by adding together many different sinusoidal waveforms. These are called the *Fourier components*. The behaviour of any circuit can be analysed by calculating the response to each of these components and then adding them together at the end in the proportions that were present in the original waveform. This has proved to be a powerful method in many applications and one we shall follow here.

Firstly, we will take the simple case that was used for a steady source voltage of a capacitor and resistor shown in Fig. 8.3. Instead of imposing a steady voltage on the system, though, the voltage, V, varies with time according to

$$V = V_0\cos 2\pi ft. \tag{8.3.21}$$

This describes a sinusoidally varying voltage with *amplitude* V_0 and frequency f, as shown in Fig. 8.7. Thus the pattern repeats itself f times every second. Alternatively, the time between one complete cycle and the next is $1/f$. The unit of frequency is the *hertz* (symbol Hz) or, sometimes, s^{-1}. To simplify matters, we will not, however, use the frequency as described earlier, but a quantity designated $\omega = 2\pi f$. ω is called the *angular frequency* and is, in fact, radians per second. The advantage of using it is that it saves writing 2π each time. ω is about 6.3 times larger than f, so for $f = 100$ MHz, $\omega = 6.3 \times 10^8$ rad s^{-1}. Using this convention, Equation 8.3.21 becomes:

$$V = V_0\cos\omega t. \tag{8.3.22}$$

We will not worry about the transient case a short time after the source voltage is turned on, but concentrate on the

steady-state solutions. Applying Equation 8.3.22 for V to the circuit in Fig. 8.3, Equations 8.3.6–8.3.8 still apply. However, V is no longer constant, so that:

$$\frac{dV}{dt} = \frac{dV_R}{dt} + \frac{dV_C}{dt} = -V_0\omega\sin\omega t \tag{8.3.23}$$

in place of Equation 8.3.9 and so, using Equation 8.3.7:

$$R\frac{dI}{dt} + \frac{I}{C} = -V_0\omega\sin\omega t. \tag{8.3.24}$$

To solve this, we will try a solution of

$$I = I_0\cos(\omega t + \varphi), \tag{8.3.25}$$

where ϕ allows for a possible phase difference between V and I.

Substituting this into Equation 8.3.24 gives

$$-I_0\omega R\sin(\omega t + \varphi) + \frac{I_0\cos(\omega t + \varphi)}{C} = -V_0\omega\sin\omega t. \tag{8.3.26}$$

Expanding the functions of summed angles leads to

$$I_0\left[\omega R\cos\omega t\sin\phi + \omega R\sin\omega t\cos\phi - \frac{\cos\omega t\cos\phi - \sin\omega t\sin\phi}{C}\right] = V_0\omega\sin\omega t. \tag{8.3.27}$$

At steady state, this must be valid for all values of t, so that for $t = 0$, $\sin\omega t = 0$ and $\cos\omega t = 1$ so:

$$\omega R\sin\phi - \frac{\cos\phi}{C} = 0. \tag{8.3.28}$$

That is,

$$\cot\phi = \omega CR, \tag{8.3.29}$$

giving

$$\cos\phi = \omega CR\sqrt{\frac{1}{1+\omega^2C^2R^2}} \tag{8.3.30}$$

and

$$\sin\phi = \sqrt{\frac{1}{1+\omega^2C^2R^2}}. \tag{8.3.31}$$

Substituting these into Equation 8.3.27 for a value of t where $\sin\omega t = 1$ and $\cos\omega t = 0$, yields

$$I_0 = \frac{V_0\omega C}{\sqrt{1+\omega^2C^2R^2}}, \tag{8.3.32}$$

and, using Equation 8.3.25,

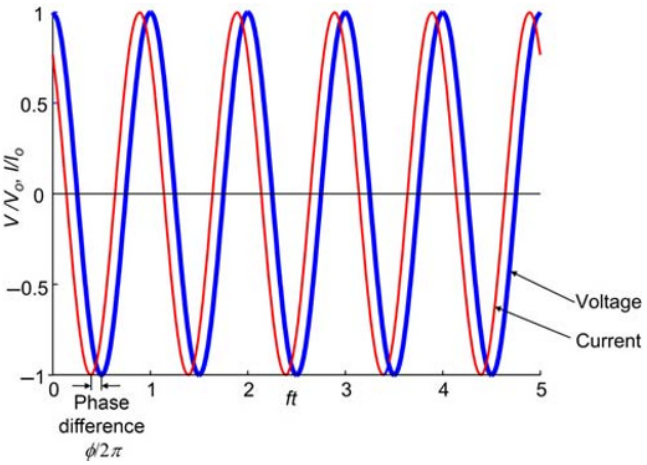

Fig. 8.8 Current and voltage through a capacitor in series with a resistor, showing phase shift.

$$I = \frac{V_0\omega C\cos(\omega t + \phi)}{\sqrt{1+\omega^2C^2R^2}}. \tag{8.3.33}$$

This shows that the current varies at the same frequency as the applied voltage, with an amplitude given by Equation 8.3.32. The current, however, is not in synchronism with the applied voltage – there is a *phase difference* between them. This means that the variation in current actually comes before the equivalent point in the cycle of the voltage. This is illustrated in Fig. 8.8, where the variation of voltage and current is shown. It may, at first sight, appear strange that the current actually seems to rise before the voltage does, since we expect voltage to drive the current, but we are considering only the steady-state case and a *lead* of the voltage by the current of an angle ϕ could just as easily be a *lag* of $2\pi - \phi$. This is shown in Fig. 8.8. In mathematical terms, 2π is a full circle measured in radians and is the same as 360° in more familiar terms.

There are a few things worth noting about this solution. First, the quantity ωCR keeps coming up. This is the angular frequency of the applied voltage multiplied by the time constant that appeared earlier in the dc case. So, if the frequency were doubled and the capacitance halved, ωCR would remain the same and the behaviour of the circuit would also be the same. Equally, the resistance could be halved, except that this would affect the amplitude of the current, I_0.

Secondly, for very high frequencies (large values of ωCR), the circuit behaves as if the capacitor were not there at all. The phase angle approaches zero ($\tan\phi = 0$) and the current amplitude, I_0 becomes V_0/R. This is best seen by dividing both top and bottom of the fraction in Equation 8.3.32 by ωCR:

$$I_0 = \frac{V_0}{R\sqrt{\frac{1}{\omega^2C^2R^2}+1}}, \tag{8.3.34}$$

when it can be seen that the term $1/(\omega^2C^2R^2)$ becomes negligibly small compared to 1 for large values of ωCR.

At low frequencies, where ωCR is small, the current is very low, as only a small current gets through the capacitor. The phase angle also becomes large, approaching $(\pi/2)$ $(90°)$.

Lastly, the power consumed can be calculated using Equation 8.3.2, as the product of the current and voltage (IV). From Equations 8.3.22 and 8.3.25, this is

$$\frac{dW}{dt} = I_0V_0\cos\omega t\cos(\omega t+\phi), \tag{8.3.35}$$

which is

$$\frac{dW}{dt} = I_0V_0\left(\cos^2\omega t\cos\phi - \frac{\sin 2\omega t}{2}\sin\phi\right). \tag{8.3.36}$$

This function varies periodically over time, but the average value over one or more complete cycles is normally relevant. The second term in brackets alternates between positive and negative values and so will average out as zero. The first term can be written:

$$\cos^2\omega t\cos\phi = \frac{1}{2}(\cos 2\omega t+1)\cos\phi. \tag{8.3.37}$$

Taking the steady part of this, the power consumption is

$$\frac{dW}{dt} = \frac{1}{2}I_0V_0\cos\phi. \tag{8.3.38}$$

Substituting for I_0 from Equation 8.3.32 and for cos ϕ from Equation 8.3.30 gives

$$\frac{dW}{dt} = \frac{\omega^2C^2R}{2(1+\omega^2C^2R^2)}V_0^2. \tag{8.3.39}$$

For small values of ω, that is low frequencies, the power consumption is small because the capacitor blocks most of the current. At high frequency, current is maximised and power is dissipated in the resistor.

This is quite a complex calculation for a very simple circuit, and more complicated circuits become even more difficult to anlayse. Help is, however, at hand in the form of complex number theory.

8.3.6 *Complex numbers*

By employing the imaginary number j, defined as $j=\sqrt{-1}$, much of the complexity in handling oscillatory functions can be avoided, allowing much more compact equations. j is often designated i, especially in scientific and mathematical applications; j avoids confusion with electric current, for which i is also often used.

Using j, the square root of other negative numbers can be defined. So, for instance, the square root of –4 is equal to $j2$ and, in general, the square root of $-x$ is $j\sqrt{x}$. It is usual to write an imaginary number by preceding it with j.

A useful property of j is that

$$\frac{1}{j} = -j. \tag{8.3.40}$$

Complex numbers have both a real and an imaginary part and make the invention of j really useful. The complex number is defined as the sum of each part, so that a number with a real part, a, and an imaginary part, b, is written as $a + jb$.

Complex numbers are often represented as the x- (abscissa) and y- (ordinate) values on a Cartesian graph as shown in Fig. 8.9. This allows fairly simple algebraic manipulation of two-dimensional data, so that a point at (a,b) on a graph can be written as $a + jb$. The distance of this point from the origin of the graph is $\sqrt{a^2+b^2}$ and this can also be calculated using

$$\sqrt{(a+jb)(a-jb)} = \sqrt{a^2-j^2b^2} = \sqrt{a^2+b^2}, \tag{8.3.41}$$

since $-j^2 = +1$.

The quantity $\sqrt{a^2+b^2}$ is referred to as the magnitude or *modulus* of the complex number and may be written $|a+jb|$.

For the purposes of analysing high-frequency electrical circuits, the advantage of using complex numbers stems from the following relation:

$$e^{j\theta} = \cos\theta + j\sin\theta, \tag{8.3.42}$$

where θ is an angle expressed in radians.

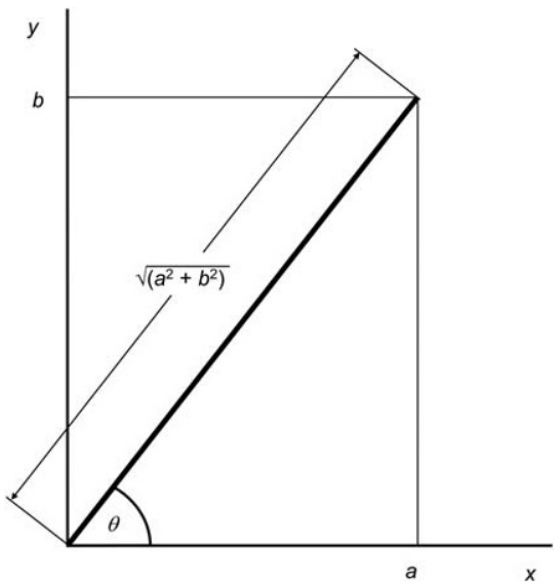

Fig. 8.9 Complex numbers represented on an x–y graph.

This property also means that any complex number can be expressed in terms of a magnitude and an angle. So, $a + jb$ can be written as follows:

$$|a + jb|e^{j\theta} = \sqrt{a^2 + b^2}(\cos\theta + j\sin\theta), \tag{8.3.43}$$

where $\tan\theta = (b/a)$. This is also illustrated in Fig. 8.9.

This allows simple combination of oscillating functions using the rules of power multiplication (e.g. $x^a \times x^b = x^{a+b}$). At the end of the calculation, the real part of the solution is used. Circuit elements like capacitors and inductors can be treated in this representation as having an *imaginary impedance* and then combined in the usual way for resistor networks. A capacitor has an impedance of $1/j\omega C$ and an inductor $j\omega L$.

For the simple case of a capacitor and resistor in series, treated earlier, the pair will have a *complex impedance*, Z, given by

$$Z = R + \frac{1}{j\omega C}. \tag{8.3.44}$$

The voltage source can be represented as follows:

$$V = V_0 e^{jwt}, \tag{8.3.45}$$

and so the analogue of Ohm's law becomes:

$$I = \frac{V}{Z} = \frac{V_0 e^{j\omega t}}{R + \frac{1}{j\omega C}} = \frac{V_0 e^{j\omega t}}{R^2 + \frac{1}{\omega^2 C^2}}\left(R - \frac{1}{j\omega C}\right), \tag{8.3.46}$$

where both top and bottom of the fraction were multiplied by $\left(R - \frac{1}{j\omega C}\right)$.

Using the definition in Equation 8.3.43,

$$R - \frac{1}{j\omega C} = e^{j\phi}\sqrt{R^2 + \frac{1}{\omega^2 C^2}}, \tag{8.3.47}$$

where

$$\tan\phi = \frac{1}{\omega CR} \quad \text{or} \quad \cot\phi = \omega CR. \tag{8.3.48}$$

Then Equation 8.3.46 becomes

$$I = \frac{V_0 e^{j(wt+\phi)}}{\sqrt{R^2 + \frac{1}{\omega^2 C^2}}}, \tag{8.3.49}$$

or, expanding $e^{i(\omega t+\phi)}$ and multiplying top and bottom of the fraction by ωC,

$$I = \frac{V_0 \omega C[\cos(\omega t + \phi) + j\sin(\omega t + \phi)]}{\sqrt{1 + \omega^2 C^2 R^2}}, \tag{8.3.50}$$

and taking the real part of the solution only, we obtain

$$I = \frac{V_0 \omega C\cos(\omega t + \phi)}{\sqrt{1 + \omega^2 C^2 R^2}}, \tag{8.3.51}$$

which is the same as Equation 8.3.33.

This is slightly simpler than the process used to derive the solution leading to Equation 8.3.33.

Note also that the phase difference between current and voltage arises naturally in this formulation, rather than having to be introduced as a trial function and justified afterwards.

The use of complex numbers has several advantages. The process of solution becomes relatively much simpler with increasingly complex circuits than with the kind of methodology first used. It also allows for the combination of different circuit elements according to their complex impedance, and it extends easily to wave transmission.

8.3.7 Lossy dielectrics

So far, we have considered only perfect capacitors and, by implication, dielectrics. While pure water is a good insulator, soil solution is not and wet soil has appreciable conductivity, making it a far from perfect dielectric. Such a medium is often called a *lossy dielectric*. This violates one of the basic assumptions underlying capacitors – that they are filled with insulating material. The way to handle this is to think of the lossy capacitor as a perfect capacitor in parallel with a resistor, as shown in Fig. 8.10.

The impedance of this combination is calculated similarly to the resistance of two resistors in parallel:

$$\frac{1}{Z} = \frac{1}{R} + j\omega C. \tag{8.3.52}$$

It is usually easier to think of this parallel resistor in terms of its *conductance*, $G(= 1/R)$, the reciprocal of its

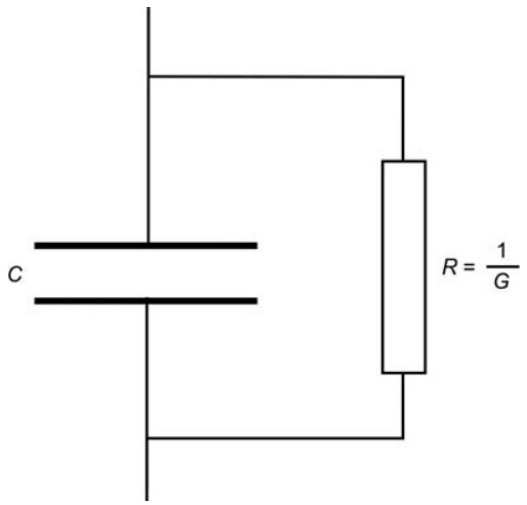

Fig. 8.10 Capacitor with a lossy dielectric modelled as a perfect capacitor in parallel with a resistor.

resistance, and the capacitor by its *susceptance* ($j\omega C$) to give an overall *admittance*, $Y(=1/Z)$, of the combination in Fig. 8.10 of $G + j\omega C$. As we might expect from the analysis of a resistor in series with a capacitor, the conductance will start to have an appreciable effect on the behaviour of the circuit when G becomes comparable with ωC. This means that the higher the frequency, the less influence G will have. This is a very important issue in measurement of water content by dielectric devices and causes different kinds of device to behave differently with changing conductivity of the soil.

8.3.8 Complex permittivity

The literature on dielectric measurements frequently refers to complex permittivity and its imaginary part. In reality, there is nothing imaginary at all about permittivity, but the language is borrowed from the theory of imaginary numbers and the complex representation of circuit components in ac circuits, as described in the previous section.

To understand this, think about a conventional parallel-plate capacitor in parallel with a conductance, G (or resistance, R), as shown in Fig. 8.10. As stated before, this has a capacitance of $C = (\varepsilon A/d)$, and a conductance $G = (\sigma A/d)$, where σ is the *conductivity* of the medium. Note that the geometric factor for capacitance and conductance is the same. σ is usually measured in siemens per metre (S m^{-1}). A *siemen* is the reciprocal of an ohm (i.e. 1 S $= (1/1\ \Omega)$). Thus the admittance of the lossy capacitor is

$$Y = G + j\omega C = \frac{A}{d}(\sigma + j\omega\varepsilon). \tag{8.3.53}$$

We could equally well represent this as the admittance of a single capacitor with a complex permittivity:

$$Y = j\omega\frac{A}{d}\varepsilon^*, \tag{8.3.54}$$

where

$$\varepsilon^* = \varepsilon + \frac{\sigma}{j\omega}. \tag{8.3.55}$$

Or, since $(1/j) = -j$

$$\varepsilon^* = \varepsilon - \frac{j\sigma}{\omega}. \tag{8.3.56}$$

In this way of looking at it, ε is the real part of the complex permittivity and $-(\sigma/\omega)$ is the imaginary part. It is more usual, however, to designate the complex permittivity as ε, with real and imaginary parts ε' and ε'', that is,

$$\varepsilon = \varepsilon' - j\varepsilon''. \tag{8.3.57}$$

Relaxation processes may also contribute to the imaginary part of the permittivity, so that

$$\varepsilon'' = \frac{\sigma}{\omega} + \varepsilon''_{\text{relax}}. \tag{8.3.58}$$

Relaxation occurs when the dipoles are unable to keep up with variations of the electric field and the response lags behind the field changes. At low frequency, the dipoles can easily align with the field variations and so the permittivity will be the same as in a static field, ε_s. At very high frequencies, the dipoles are hardly able to respond at all to variations of the field and so contribute very little to the permittivity, which has a value designated ε_∞. In between these two, as the frequency increases from a low value, the dipoles start to lag slightly behind the field variations and their amplitude of movement will be slightly less than in the low frequency case since the field reverses before they attain complete alignment. As the frequency increases further, the dipole alignment lags further behind the field and the amplitude reduces further. In many ways, this mirrors the response of the resistor – capacitor combination, described in Section 8.3.5, where the resistor both reduced the amplitude of the current and caused it to become more out of phase with the voltage. In a similar way, we can characterize the response of the dielectric to frequency by using a *relaxation time*, τ_r, as a measure of the time taken for the dipoles to come into alignment with the field.

The simplest model is called *Debye relaxation*, in which the permittivity can be expressed as follows:

$$\varepsilon = \varepsilon_\infty + \frac{\varepsilon_s - \varepsilon_\infty}{1 - j\omega\tau_r}. \tag{8.3.59}$$

Or

$$\varepsilon = \varepsilon_\infty + \frac{\varepsilon_s - \varepsilon_\infty}{1 + \omega^2\tau_r^2} + j\frac{(\varepsilon_s - \varepsilon_\infty)\omega\tau_r}{1 + \omega^2\tau_r^2}. \tag{8.3.60}$$

For small values of ω, this reduces to ε_s and for large ω to ε_∞. In both cases, the imaginary part of the permittivity tends to zero. However, at intermediate values of ω, there is a transition between ε_s and ε_∞. The imaginary part of ε also becomes appreciable, reaching a maximum at the point where $\omega = (1/\tau_r)$.

This is illustrated in Fig. 8.11, where it can be seen that the imaginary permittivity extends over a frequency range from about $\omega = 0.1/\tau$ to $\omega = 10/\tau$. The peak value of the imaginary permittivity is $(\varepsilon_s - \varepsilon_\infty)/2$.

It might be expected that the permittivity at high frequency, ε_∞, would be equal to the permittivity of free space. This is not the case because there are other interactions between the electromagnetic wave and atoms in both the soil fabric and the water with very much higher relaxation frequencies. Other relaxation mechanisms also operate to produce imaginary components of the permittivity and so the situation is more complicated than described here and only partially understood for a complex system like soil.

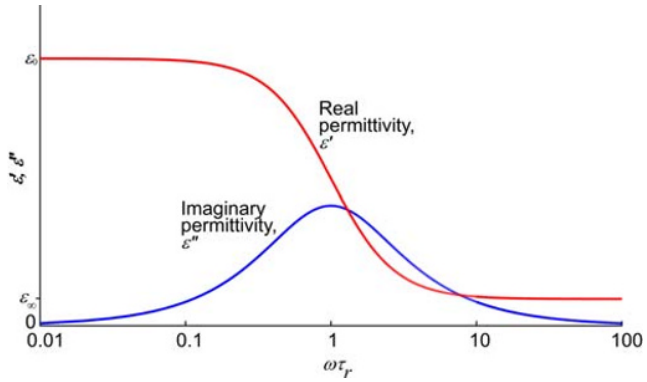

Fig. 8.11 Real and imaginary permittivity variation with frequency with Debye relaxation.

8.4 The Relationship between Soil Water Content and Permittivity

Soil is a complex substance, consisting of many materials, having different shapes, sizes and degrees of organisation. Some materials, for example clay platelets and some organic molecules, are either inherently polarised or easily so. The soil itself, therefore, may have a high permittivity. Fortunately, most of these substances are physically quite large by molecular standards and cannot, therefore, easily respond to the field reversals of high frequency electromagnetic fields (i.e. they have a low relaxation frequency), so that at frequencies above about 10 MHz they contribute little more to the overall relative permittivity of the soil fabric, which is usually in the region of 4 or 5. This phenomenon does, however, reinforce the case for working at high frequency to make reliable measurements of permittivity.

Water in soil may behave differently from bulk liquid water when exposed to electromagnetic radiation. It is usually present in relatively small pores where the interfacial area, whether with solid substances or air is large compared with the total volume. Because the structure of water in these zones differs from that of the bulk liquid, we can expect that this has an appreciable influence on the dielectric properties of the medium as a whole. As mentioned in Section 8.2, clays are believed to immobilise the first few layers of water and produce a dielectric behaviour similar to that of ice, while the top skin of water in contact with air is denser than that of the bulk liquid and hence is also expected to have different physical properties, including permittivity.

The shape and arrangement of soil particles and water will also have an effect. As a consequence, the permittivity of a mixture of a number of components of dissimilar permittivity is not a simple weighted mean value of that of the individual components. A material of high permittivity embedded in one of lower permittivity and subject to an electric field will tend to steer the lines of electrical force towards and inside it. Figure 8.12 shows the effect of a high-permittivity sphere in a low permittivity medium on the lines of the electrical field. The field, therefore, is not uniform at the scale of particles and pores and is concentrated in some parts while other parts are partially shielded from it.

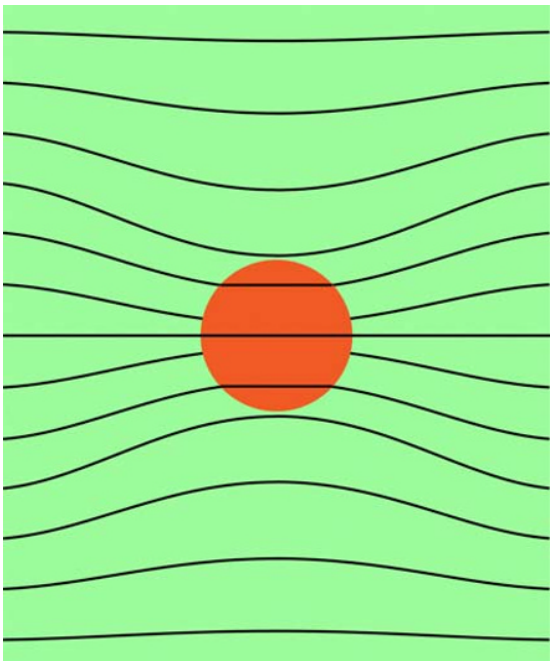

Fig. 8.12 Electric field lines around a sphere of higher permittivity in a low permittivity medium subjected to an initially uniform electric field.

Several theories have been developed to calculate the effective permittivity of mixtures of dielectrics. These are, generally, applicable only to two-component systems, where one component is quite dilute, and to simple shapes (e.g. ellipsoids) of the embedded component. By contrast, soil is an at least three-component system; the shape of all components is almost never regular; their size and orientation, while not necessarily random, is not easily described in a simple way, and the proportion of most components is rarely so small that it can be described as dilute. Nevertheless, the results of such theories help in understanding some of the behaviour found.

It is clear from this discussion that there is unlikely to be a simple way to predict the permittivity of a medium such as soil from first principles and that a pragmatic approach to finding a relationship between permittivity and water content is necessary. The following observations provide a guide:

- The permittivity of soil water is likely to be close to that of bulk water in coarse-textured soils, which have a relatively small interfacial area, and in soils low in clay and/or organic matter, which are believed to restrict the mobility of water molecules.

• The permittivity of the solid portion of soil does not vary greatly, leading to only small differences between soils caused by their mineralogy.
• The disordered nature of most soils is likely to act as a homogenising factor between the relationships for different soils.

We expect, therefore, that, while the relationship between permittivity and water content will not be the same for all soils, there is unlikely to be a large spread of different relationships. We shall see later that this is mostly realised in practice.

8.4.1 Measured calibration curves

In the absence of a firm theoretical basis for relating permittivity to water content, most researchers use empirical calibrations. The general principles are much the same as has already been described for neutron probe calibrations (Section 7.7). The investigator should, however, be aware of some additional points:
• The volume sampled by most dielectric devices is much smaller than that for the neutron probe. This is likely to increase the difficulty of field calibration, since it is usually necessary to sample a volume of soil comparable to that which contributes to the measurement. Smaller volumes mean greater difficulty in ensuring an accurate volume for the sample and demand greater precision in most other aspects of the measurement. On the other hand, the smaller range of measurement makes laboratory calibration much easier than for a neutron probe, as the quantity of soil needed is very much smaller. Calibration can often be performed in a large beaker, rather than a large drum.

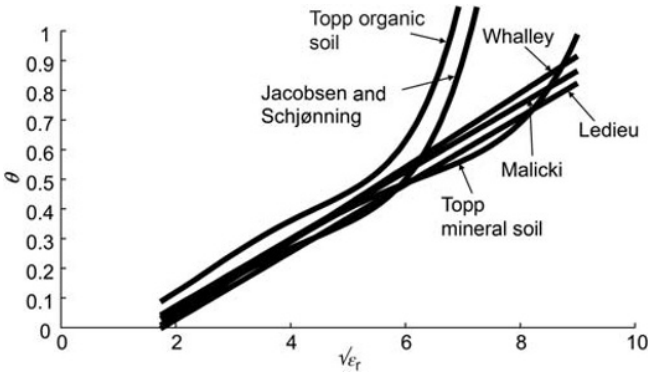

Fig. 8.13 A selection of published calibration equations relating volumetric water content to apparent relative permittivity. Topp Mineral Soil & Topp Organic Soil (Topp *et al.*, 1980) and Jacobsen & Schjønning (Jacobsen & Schjønning, 1993) are polynomial equations in apparent relative permittivity, while Ledieu (Ledieu *et al.*, 1986), Malicki (Malicki *et al.*, 1996) and Whalley (Whalley, 1993) are all linear in $\sqrt{\varepsilon_r}$ with different ways of accounting for variations in dry bulk density. All equations calculated for a dry bulk density of 1400 kg m^{-3}.

A possible exception to this advantage is TDR, which usually integrates over an approximately cylindrical volume of length 150–500 mm, but a diameter of about 100 mm.
• The small volume sampled by the device means that there is often a large spatial variability attached to the measurements, as the volume is not as large as the Representative Elementary Volume (see Sections 4.1 and 5.1).
• All the common methods for dielectric measurement of soil water content are affected in different ways by the imaginary part of the permittivity (electrical conductivity and relaxation effects). Additionally, some devices work at a single frequency, while others employ a wide range of frequencies. Taken together, these mean that the permittivity measured by one device may well be different from that indicated by another for the same sample of soil. In most cases, therefore, it is not possible to transfer the relationship between permittivity and water content found by one method to a different type of instrument. For this reason, it has long been recognised that each method yields an apparent permittivity (Topp *et al.*, 1980), rather than a true value.

There are two basic approaches to calibration.

The first is purely pragmatic, with the primary objective to obtain a good estimate of the water content, expressed as a function of apparent permittivity (or, in some cases, of some less well-defined instrument output). A very common example is that of Topp *et al.* (1980), who found that the expression

$$\theta = -0.0530 + 0.0292\varepsilon_r - 0.00055\varepsilon_r^2 + 0.0000043\varepsilon_r^3 \quad (8.4.1)$$

described the relationship very well for four mineral soils using TDR.

The other approach uses a relationship in terms of $\sqrt{\varepsilon_r}$ and may also incorporate terms in dry bulk density and clay content (e.g. Ledieu *et al.*, 1986; Malicki *et al.*, 1996).

While an expression like that of Equation 8.4.1 provides a convenient calibration relation, it is valid only for the range of water content over which data were collected. It is not always possible to obtain calibration data over the complete range of water content experienced, so that if the expression has unexpected behaviour outside the range of the calibration data, gross errors may occur. This is illustrated in Fig. 8.13, in which six calibration equations have been plotted. It is seen that, for two of them, predicted water content increases rapidly above θ = ~0.45 m^3 m^{-3}. This does not appear plausible, especially when values of more than 1 are predicted. Water content above 0.45 m^3 m^{-3} may be unusual, but is by no means impossible, especially in soils of low bulk density.

Figure 8.13 also illustrates fairly wide variations in predicted water content at more common water contents. All data shown in Fig. 8.13 were obtained using TDR, although

the equipment and experimental methodology varied slightly between investigators.

A fairly naïve argument suggests that the square root of the composite relative permittivity, ε_r, of a mixture, such as soil, should be the sum of the square root of the relative permittivity of each individual component weighted by the proportion of each component. This is sometimes known as the *refractive index model* (Whalley, 1993). Thus this model predicts

$$\sqrt{\varepsilon_r} = f_s\sqrt{\varepsilon_{sr}} + \theta\sqrt{\varepsilon_{wr}} + (1 - f_s - \theta)\sqrt{\varepsilon_{ar}}, \tag{8.4.2}$$

where
f_s is the proportion of solid material by volume;
ε_{sr} is the relative permittivity of the solids;
θ is the proportion of water by volume;
ε_{wr} is the relative permittivity of the water;
$1 - f_s - \theta$ is the proportion of air by volume (since all proportions must add up to 1) and
ε_{ar} is the relative permittivity of air.

The relative permittivity of water is close to 81, and so $\sqrt{\varepsilon_{wr}} \approx 9$ and $\sqrt{\varepsilon_{ar}} \approx 1$. If we also assume a particle density, ρ_s of 2.56, $f_s = \frac{\rho_d}{\rho_s}$. Using these figures, Equation 8.4.2 becomes

$$\sqrt{\varepsilon_r} = \frac{\rho_d}{2.56}(\sqrt{\varepsilon_{sr}} - 1)) + 8\theta + 1. \tag{8.4.3}$$

Alternatively,

$$\theta = 0.125\left(\sqrt{\varepsilon_r} - \frac{\rho_d}{2.56}[\sqrt{\varepsilon_{sr}} - 1] - 1\right). \tag{8.4.4}$$

ε_{sr} is usually in the region of 5 or 6, so that $\sqrt{\varepsilon_{sr}} - 1$ is about 1.28, leading to the following:

$$\theta \approx 0.125\sqrt{\varepsilon_r} - 0.063\rho_d - 0.125. \tag{8.4.5}$$

This has been found to be reasonably close to experimental measurements in sandy soils, with low surface area, which have a slope in the range 0.111–0.125 (Whalley, 1993); but in clayey soils, the slope may be much smaller (White *et al.*, 1994), suggesting that the effective relative permittivity is smaller than 81. Over the range of volumetric water content up to 0.4 $m^3\ m^{-3}$, the Topp curve approximates very closely to this form, with a slope 0.111–0.118 (White *et al.*, 1994; Ferré *et al.*, 1996).

8.5 Transmission Lines

Most dielectric methods for measurement of soil water content rely on the properties of *transmission lines*. These are usually envisaged as two parallel metal rods embedded in a dielectric medium, which is the simplest practical arrangement to relate the speed of travel to permittivity.

Figure 8.14 shows schematically a transmission line embedded in a medium with permittivity, ε and a magnetic

Fig. 8.14 Schematic transmission line embedded in a medium, connected to an alternating voltage source, V.

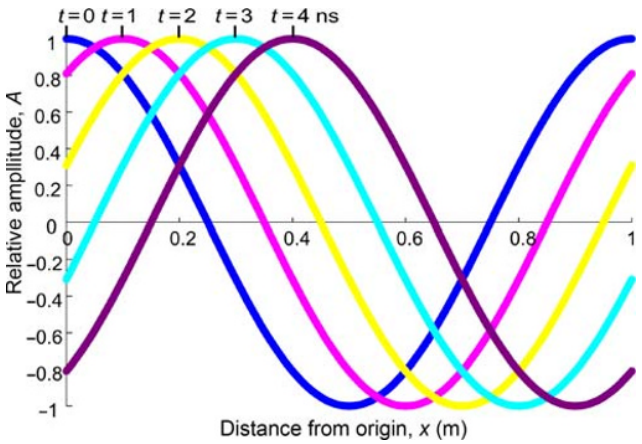

Fig. 8.15 Wave propagation along a 1 m length of transmission line. The wave has a frequency of 100 MHz and a speed, v, of 10^8 m s^{-1}, so that it travels 0.1 m in 1 ns. The curves have the equation $A = \cos\omega(t - {}^{x}/_{v})$, where $\omega = 2\pi \times 10^8\ s^{-1}$. (*See insert for colour representation of the figure.*)

permeability μ. Each unit length of the line has a capacitance, $g\varepsilon$ and an inductance, μ/g. g is the geometric factor introduced in Section 8.1, although here it refers to a unit length of line, rather than the whole electrode combination. It is a function of the size and arrangement of the rods. For two parallel rods of diameter, a, separated by a distance d, g is given by:

$$g = \frac{\pi}{\ln\left[\frac{d}{a} + \sqrt{\left(\frac{d}{a}\right)^2 - 1}\right]}. \tag{8.5.1}$$

To progress further, we imagine an electrical wave travelling along the line with velocity, v as shown in Fig. 8.15.

The variation of the voltage and current at one point, say $x = 0$, can be represented by

$$V(x = 0) = V_0 e^{j\omega t}, \tag{8.5.2}$$

and

$$I(x = 0) = I_0 e^{j(\omega t + \varphi)}, \tag{8.5.3}$$

where there is phase difference of ϕ between them.

The wave will take a time x/v to travel a short distance, x, along the line, so we expect the same conditions there to be experienced at time $t + x/v$. To put it another way, the conditions at point x at time t are the same as at $x = 0$ when $t = t - x/v$ (see Fig. 8.15). A wave travelling along the line can, therefore, be represented as follows:

$$V = V_0 e^{j\omega\left(t-\frac{x}{v}\right)}. \tag{8.5.4}$$

And

$$I = I_0 e^{j\omega\left(t-\frac{x}{v}\right)+j\phi}. \tag{8.5.5}$$

We also consider the electrical conditions on one small segment of line of length δx as shown in Fig. 8.16a. This has a capacitance, $C\delta x = g\varepsilon\delta x$ and an inductance, $L\delta x = (\mu/g)\delta x$. Here, C and L are the capacitance and inductance of the line per unit length. The whole line can be envisaged as a very large number of these short segments joined end to end as shown in Fig. 8.16b.

The rate at which charge is accumulated in this small capacitance is given by the difference in current flowing in at one end and out at the other, that is $I(x) - I(x + \delta x)$. So, as in Equation 8.3.7 and using $C\delta x$ in place of C, we obtain the following:

$$C\delta x\frac{\partial V}{\partial t} = I(x) - I(x+\delta x). \tag{8.5.6}$$

And as in (8.3.16) for the voltage,

$$L\delta x\frac{\partial I}{\partial t} = V(x) - V(x+\delta x), \tag{8.5.7}$$

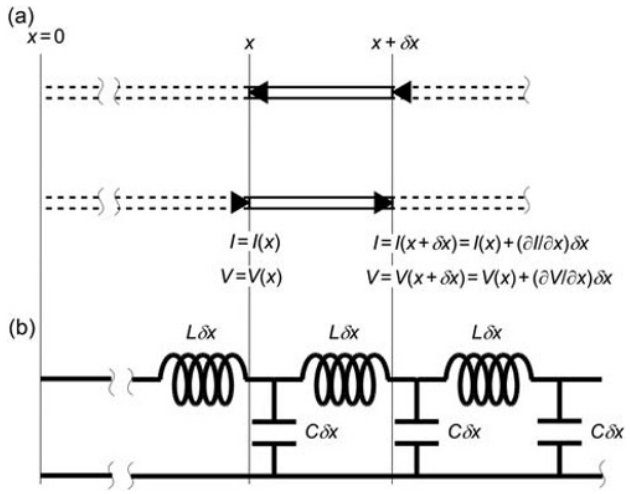

Fig. 8.16 (a) Current and voltage at each end of a segment of transmission line of length δx. (b) The line envisaged as a series of inductors and capacitors.

where the partial differentials signify that x does not vary when considering the variation with time.

Now, Equation 8.5.6 can be written as follows:

$$C\frac{\partial V}{\partial t} = \frac{I(x) - I(x+\delta x)}{\delta x}. \tag{8.5.8}$$

And as δx becomes very small:

$$\frac{I(x) - I(x+\delta x)}{\delta x} \to -\frac{\partial I}{\partial x}. \tag{8.5.9}$$

So

$$C\frac{\partial V}{\partial t} = -\frac{\partial I}{\partial x} \tag{8.5.10}$$

Similarly, Equation 8.5.7 gives

$$L\frac{\partial I}{\partial t} = -\frac{\partial V}{\partial x}. \tag{8.5.11}$$

Now, using Equations 8.5.4 and 8.5.5 to describe the current and voltage at position x, the partial differentials of V and I with respect to time can be written as follows:

$$\frac{\partial V}{\partial t} = j\omega V_0 e^{j\omega\left(t-\frac{x}{v}\right)+j\phi} = j\omega V. \tag{8.5.12}$$

And similarly,

$$\frac{\partial I}{\partial t} = j\omega I. \tag{8.5.13}$$

Substituting these into Equations 8.5.10 and 8.5.11 leads to

$$-j\omega CV = \frac{\partial I}{\partial x} \tag{8.5.14}$$

and

$$-j\omega LI = \frac{\partial V}{\partial x}. \tag{8.5.15}$$

Differentiating Equation 8.5.15 with respect to x and substituting for $(\partial I/\partial x)$ from (8.5.14) into it leads to

$$\frac{\partial^2 V}{\partial x^2} = -\omega^2 LCV. \tag{8.5.16}$$

This has a solution:

$$V = \left(V_1 e^{-j\frac{\omega x}{v}} + V_2 e^{j\frac{\omega x}{v}}\right)e^{j\omega t}, \tag{8.5.17}$$

with

$$v^2 = \frac{1}{LC} = \frac{1}{\frac{\mu}{g}g\varepsilon} = \frac{1}{\mu\varepsilon}. \tag{8.5.18}$$

To see what this means, we can write the first term on the right hand side of Equation 8.5.17 as $V_1 e^{-j\omega(x/v - t)}$.

This expression is similar to Equation 8.5.4 and so describes a wave travelling in the x direction with a speed of v.

Using the same argument, the second term describes a wave travelling in the opposite direction with the same speed.

So the waves travel with speed $1/\sqrt{\mu\varepsilon}$. The speed of light in free space, c, is $1/\sqrt{\mu_0\varepsilon_0}$, hence the speed in the medium is

$$v = \frac{c}{\sqrt{\mu_r\varepsilon_r}}. \tag{8.5.19}$$

And, since μ_r is very close to 1 in almost all cases in which we are interested:

$$v = \frac{c}{\sqrt{\varepsilon_r}}. \tag{8.5.20}$$

The speed of the wave, therefore, is equal to the speed of light in free space divided by the square root of the relative permittivity of the medium.

This is independent of the geometrical details of the system, for instance the diameter or spacing of the rods, embodied in the parameter, g. In practice, this means that the wave speed is not sensitive to minor – or even major – departures from parallelism of the rods. For instance, Stein & Kane (1983) investigated line configurations in which the rods converged and diverged from one another, including one where they were not in the same plane, and found no effect on travel time. In stony soils, in particular, it is very likely that rods will not stay parallel to one another.

8.5.1 Characteristic impedance

The current in the line can be found by substituting V from Equation 8.5.17 into Equation 8.5.15:

$$I = \frac{1}{vL}\left(V_1 e^{-j\frac{\omega x}{v}} - V_2 e^{j\frac{\omega x}{v}}\right)e^{j\omega t}. \tag{8.5.21}$$

Or, using Equation 8.5.18 for v,

$$I = \sqrt{\frac{C}{L}}\left(V_1 e^{-j\frac{\omega x}{v}} - V_2 e^{j\frac{\omega x}{v}}\right)e^{j\omega t}. \tag{8.5.22}$$

This describes a relationship between the current and voltage in which $\sqrt{L/C}$ has the form of an impedance and is a real quantity, that is it appears to be resistive. However, in our perfect transmission line, there are only capacitors and inductors, neither of which dissipates energy. This seems, therefore to be paradoxical. If, however, we think of the wave travelling down a long transmission line some short while after switching on the alternating voltage at one end, the wave has travelled a distance determined by the speed of the wave, v. Beyond that point, there is no current or voltage, and hence no energy is stored in the inductance or capacitance of the line. As the wave reaches this point, energy starts to be stored in the line. So although the line appears to be a resistor to an alternating voltage source at the end, it is actually carrying energy down the line to ever-increasing distance from the source end.

The value of this apparent resistor is called the *characteristic impedance* of the line, Z_0. Its value is

$$Z_0 = \sqrt{\frac{L}{C}} = \sqrt{\frac{\mu}{g^2\varepsilon}}. \tag{8.5.23}$$

This is not independent of either the medium or the geometrical arrangement of the line. It can be expressed in relative permittivity terms as

$$Z_0 = \frac{1}{g}\sqrt{\frac{\mu_r}{\varepsilon_r}}\sqrt{\frac{\mu_0}{\varepsilon_0}}, \tag{8.5.24}$$

where $\sqrt{\mu_0/\varepsilon_0}$ is the *characteristic impedance of free space* and equal to approximately $120\pi\ \Omega$ or 377 Ω.

8.5.2 Finite length line

In practice, transmission lines are never infinitely long and, in the applications we are concerned with, quite short – usually less than, and often much less than, 1 m. This has a strong effect on the behaviour of the line.

Consider the situation depicted in Fig. 8.17, where the transmission line is terminated at position $x = l$ by a load, Z_L, with real and imaginary parts R_L and X_L. The voltage and current at $x = l$ are given by Equations 8.5.17 and 8.5.22

$$V(l) = \left(V_1 e^{-j\frac{\omega l}{v}} + V_2 e^{j\frac{\omega l}{v}}\right)e^{j\omega t} \tag{8.5.25}$$

Fig. 8.17 Transmission line terminated with a load, Z_L.

and

$$I(l) = \sqrt{\frac{C}{L}}\left(V_1 e^{-j\frac{\omega l}{v}} - V_2 e^{j\frac{\omega l}{v}}\right)e^{j\omega t} = \frac{1}{Z_0}\left(V_1 e^{-j\frac{\omega l}{v}} - V_2 e^{j\frac{\omega l}{v}}\right)e^{j\omega t} \tag{8.5.26}$$

since $Z_0 = \sqrt{L/C}$ (Eq. 8.5.23).

But the voltage and current at $x = l$ must also be related to the load impedance, Z_L:

$$I(l) = \frac{V(l)}{Z_L}. \tag{8.5.27}$$

So

$$\frac{V_1 e^{-j\frac{\omega l}{v}} - V_2 e^{j\frac{\omega l}{v}}}{Z_0} = \frac{V_1 e^{-j\frac{\omega l}{v}} + V_2 e^{j\frac{\omega l}{v}}}{Z_L}. \tag{8.5.28}$$

This can be rearranged to give

$$\frac{V_2}{V_1} = \frac{Z_L - Z_0}{Z_L + Z_0} e^{-j\frac{2\omega l}{v}}. \tag{8.5.29}$$

The term $e^{-j\frac{2\omega l}{v}}$ determines the phase difference between the outgoing and incoming wave. It does not affect the magnitude of V_1 and V_2, since

$$\left|e^{-j\frac{2\omega l}{v}}\right| = 1. \tag{8.5.30}$$

V_2/V_1 is called the *reflection coefficient*. It is the ratio of the voltage of the reflected wave (i.e. the one coming back) to that of the outgoing wave.

Four situations are of interest for measurements in soil.

- The first of these occurs where the load impedance is equal to the characteristic impedance of the line. In that case, Z_0 is equal to Z_L and, according to Equation 8.5.29, the reflection coefficient and, hence, the amplitude of the reflected wave is zero and all of the voltage from the source is transmitted to the load. The line and load are said to be *matched*. Voltage sources have an *output impedance*, that is they behave as though they are an alternating voltage in series with an impedance, as shown in Fig. 8.17. The same principle applies whether the signal goes from a transmission line to a load or from a source to a transmission line. TDR instruments usually have an output impedance of 50 Ω, with no imaginary part, so that feeding the signal into a coaxial transmission line cable with a characteristic impedance of 50 Ω *via* a high-quality connector ensures that almost all of the signal is fed to the cable.
- In the second situation, the line has no termination. It is said to be *open circuit*. In this case, Z_L is infinite and the reflection coefficient, from Equation 8.5.29 is 1, and there is no phase difference between the two waves at the end. This is the most common situation encountered in soils.
- The third situation is that of a *short circuit* of the line, with Z_L equal to zero. In this case, Equation 8.5.29 shows that the reflection coefficient equals –1, which is, again, complete reflection, with, in this case, a phase change of π.
- Lastly, we have seen that a long length of line appears as a resistance with a value equal to the characteristic impedance of that piece of line. A junction between two transmission lines of different characteristic impedance, therefore, also produces a reflection of the same magnitude as that between one line and a load equal to the characteristic impedance of the second line, as given by Equation 8.5.29. In this case, Z_L would be the characteristic impedance of the second section of line. If the reflection coefficient is too large, then very little of the original voltage wave will be transmitted to the second length of line, which may cause problems where, for instance, a connecting cable is joined to a transmission line. The returning signal will also be reflected at this junction (with the same magnitude of reflection coefficient – Equation 8.5.29), meaning that even less of this gets through.

8.5.3 Short lines

The previous section described the conditions at one end of the line ($x = l$), where it is terminated by a load. But how does this affect conditions seen from the other end ($x = 0$), particularly if the line is a short one? This is particularly important for capacitance and other devices, which are often short transmission lines.

Equation 8.5.29 describes the relationship between V_1 and V_2 as a function of the line characteristic impedance, Z_0 and the load impedance, Z_L. These were derived for a position on the line designated as $x = l$. Equations 8.5.17 and 8.5.22 are expressions for the voltage and current at any point, x. Inserting a value for the voltage of the reflected wave, V_2, from Equation 8.5.29 into these two equations gives

$$V(x) = V_1\left(e^{-j\frac{\omega x}{v}} + \frac{Z_L - Z_0}{Z_L + Z_0} e^{j\frac{\omega(x-2l)}{v}}\right)e^{j\omega t} \tag{8.5.31}$$

and

$$I(x) = \frac{V_1}{Z_0}\left(e^{-j\frac{\omega x}{v}} - \frac{Z_L - Z_0}{Z_L + Z_0} e^{j\frac{\omega(x-2l)}{v}}\right)e^{j\omega t}, \tag{8.5.32}$$

where Z_0 has again been substituted for $\sqrt{L/C}$.

V and I at the input end of the line is given by these equations with $x = 0$. The line of length l appears from this point as an impedance, $Z(l)$, of value

$$Z(l) = \frac{V(0)}{I(0)} = Z_0\left(\frac{(Z_L + Z_0)e^{j\frac{\omega l}{v}} + (Z_L - Z_0)e^{-j\frac{\omega l}{v}}}{(Z_L + Z_0)e^{j\frac{\omega l}{v}} - (Z_L - Z_0)e^{-j\frac{\omega l}{v}}}\right). \tag{8.5.33}$$

Using the definition of $e^{j\theta}$ from Equation 8.3.42, this can be expressed as follows:

$$Z(l) = Z_0 \left(\frac{Z_L \cos\left(\frac{\omega l}{v}\right) + jZ_0 \sin\left(\frac{\omega l}{v}\right)}{Z_0 \cos\left(\frac{\omega l}{v}\right) + jZ_L \sin\left(\frac{\omega l}{v}\right)} \right). \tag{8.5.34}$$

For the open-circuit case, $Z_L \to \infty$ and $(Z_0/Z_L) \to 0$, so dividing both top and bottom of the right hand side by Z_L, this becomes:

$$Z(l) = \frac{Z_0}{j\tan\left(\frac{\omega l}{v}\right)}. \tag{8.5.35}$$

The line therefore behaves as an imaginary load for all values of l, in marked contrast with the infinite line. However, its character changes as l increases or decreases. For small values of $\frac{\omega l}{v}$, $\tan\left(\frac{\omega l}{v}\right) \approx \frac{\omega l}{v}$. Substituting for Z_0 from Equation 8.5.23 and v from (8.5.18), we obtain

$$Z(l) \approx \frac{1}{j\omega Cl}, \tag{8.5.36}$$

that is the line behaves as a capacitor of value Cl. This is what would be expected for two short rods and is the basis for treating the short, parallel electrodes of several dielectric devices as a simple capacitor, when in reality they are short transmission lines.

It is convenient to express the length of the line in terms of the *wavelength* of the wave. This is the length of line occupied by one oscillation (see Fig. 8.15, where the wavelength is 1 m). In the time taken for one complete oscillation $\frac{1}{f} = \frac{2\pi}{\omega}$, the wave travels a distance equal to one wavelength, λ, so that

$$\lambda = \frac{v}{f} = \frac{2\pi v}{\omega}. \tag{8.5.37}$$

Equation 8.5.35 can therefore also be written as follows:

$$Z(l) = \frac{Z_0}{j\tan\left(\frac{2\pi l}{\lambda}\right)}. \tag{8.5.38}$$

And Equation 8.5.36 is valid when the line is short compared with the wavelength.

The approximation of Equation 8.5.36 is correct within 1% for values of l/λ up to 0.027 (rod lengths of 81 mm in air, 16 mm in a medium with $\varepsilon_r = 25$ and 9 mm in water at a frequency of 100 MHz), within 5% for values of l/λ up to 0.060 (rod lengths of 181 mm in air, 36 mm in a medium with $\varepsilon_r = 25$ and 20 mm in water) and within 10% for values of l/λ up to 0.083 (rod lengths of 250 mm in air, 50 mm in a medium with $\varepsilon_r = 25$ and 28 mm in water).

Longer lines still have a capacitive character (i.e. the relationship between current and voltage is such that the phase of the current is $\pi/2$ ahead of the voltage). However, the apparent value of the capacitance increases faster as the line gets longer, until it tends to infinity as the line length approaches $\lambda/4$, that is the line behaves as a short circuit. Figure 8.18 illustrates the behaviour for three different lengths of line. At even longer lengths, the line becomes inductive, initially with small values of the apparent inductance, but increasing as the line becomes longer.

For lines that are shorter than $\lambda/4$, Equation 8.3.35, together with Equation 8.5.24, leads to an *apparent* capacitance, C^*, of

$$C^* = \frac{1}{j\omega Z(l)} = \sqrt{\frac{C}{L}} \frac{\tan\left(\omega l\sqrt{\varepsilon_r \varepsilon_0 \mu_0}\right)}{\omega} = \frac{g}{\omega}\sqrt{\frac{\varepsilon_r \varepsilon_0}{\mu_0}} \tan\left(\omega l\sqrt{\varepsilon_r \varepsilon_0 \mu_0}\right). \tag{8.5.39}$$

Alternatively, the apparent relative permittivity, ε_r^* is as follows:

$$\varepsilon_r^* = \frac{C^*}{\varepsilon_0 gl} = \frac{1}{l\omega}\sqrt{\frac{\varepsilon_r}{\varepsilon_0 \mu_0}} \tan\left(\omega l\sqrt{\varepsilon_r \varepsilon_0 \mu_0}\right). \tag{8.5.40}$$

The effect of this is to make the capacitance apparently larger than its true value, by an amount equal to that shown in Fig. 8.18, and hence increase the sensitivity of the probe.

It can be seen from Fig. 8.18 that for ε_r of 25 with a 100 mm long transmission line at a frequency of 100 MHz, the apparent ε_r, ε_r^*, is 41% higher than ε_r, while at

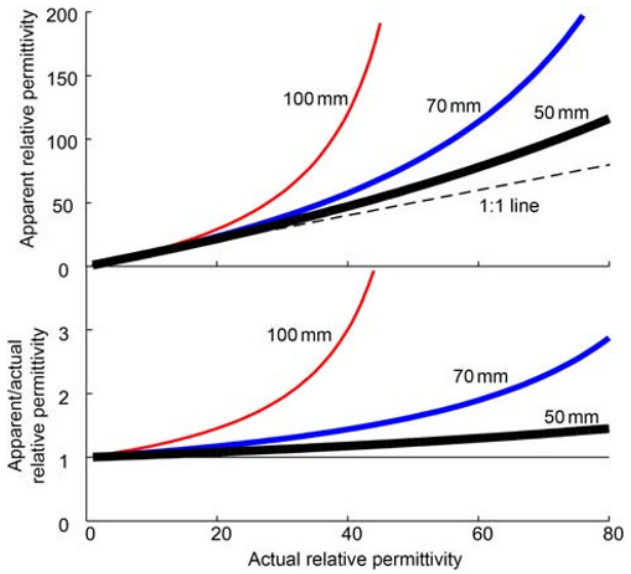

Fig. 8.18 Relationship of the apparent to the actual permittivity for a dielectric calculated from the capacitance of a short transmission line embedded in the medium at 100 MHz frequency.

70 MHz it is overestimated by 23% and at 50 MHz by only 10%. Because Equation 8.5.40 involves ωl, having a shorter line has the same effect as using a lower frequency; so keeping the frequency at 100 MHz, the overestimation would be 23% for a 70 mm line and 10% for a 50 mm one.

8.5.4 Transmission lines in conductive and dispersive media

As discussed in Section 8.3.7, soils are not perfect dielectrics, having conductivity as well as permittivity and magnetic permeability. The conductors forming the transmission line will also have some resistance. We will, however, confine ourselves to the situation of the dielectric being lossy. The justification for neglecting the resistance of the conductors is described later in Section 8.6.1. The analysis is relatively straightforward and will not be described in detail. As in Section 8.3.8, we replace the capacitance, C, per unit length of the line in Equation 8.5.6 and subsequent equations by a complex quantity, $C + (G^*/j\omega)$, where G^* is a combination of the conductance per unit length, G (= $g\sigma$ where σ is the electrical conductivity of the medium) and the relaxation effects, ($g\omega\varepsilon''_{\text{relax}}$).

The schematic equivalent circuit diagram of Fig. 8.16 is modified in this case, as shown in Fig. 8.19.

Equations 8.5.14 and 8.5.15 become thus:

$$-j\omega\left(C + \frac{G^*}{j\omega}\right)V = \frac{\partial I}{\partial x} \tag{8.5.41}$$

and

$$-j\omega LI = \frac{\partial V}{\partial x}. \tag{8.5.42}$$

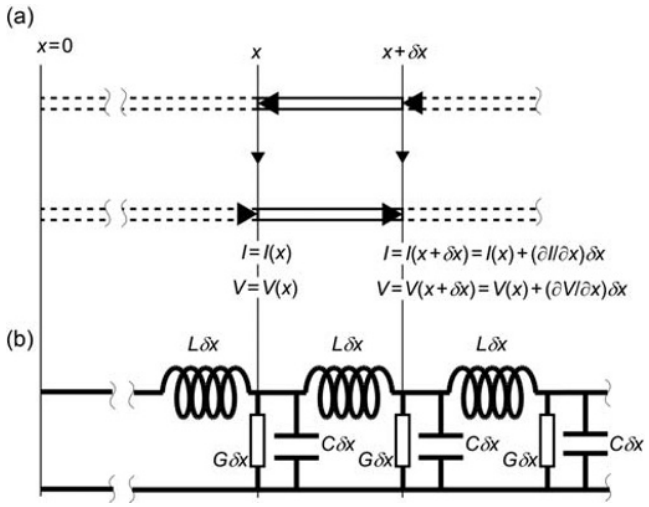

Fig. 8.19 Equivalent circuit diagram for a transmission line in a conductive medium.

Note that Equation 8.5.15 is unchanged, although if we took into account the resistance of the conductors forming the line, this would not be the case.

The speed of propagation of the wave is calculated in the same way, giving

$$v = \frac{1}{\sqrt{LC - j\frac{LG^*}{\omega}}} = \frac{1}{\sqrt{\mu(\varepsilon' - j\varepsilon'')}} = \frac{c}{\sqrt{\varepsilon'_r - j\varepsilon''_r}}, \tag{8.5.43}$$

which is complex. This can be interpreted by noting that the propagation equations (8.5.17) involve $e^{j\omega x/v}$. The square root of a complex number, $a + jb$, is

$$\sqrt{a+jb} = \sqrt{\frac{\sqrt{a^2+b^2}+a}{2}} + j\,\text{sgn}b\sqrt{\frac{\sqrt{a^2+b^2}-a}{2}}, \tag{8.5.44}$$

where sgn b is +1 if b is positive and –1 if b is negative.

Equation 8.5.17 becomes

$$V = \left(V_1 e^{-\alpha x} e^{-j\omega\frac{x}{v}} - V_2 e^{\alpha x} e^{j\omega\frac{x}{v}}\right) e^{j\omega t} \tag{8.5.45}$$

with

$$\alpha = \frac{\omega}{c}\sqrt{\frac{\sqrt{\varepsilon'^2_r + \varepsilon''^2_r} - \varepsilon'_r}{2}} \tag{8.5.46}$$

and

$$v^* = \frac{c}{\sqrt{\frac{\sqrt{\varepsilon'^2_r + \varepsilon''^2_r} + \varepsilon'_r}{2}}}. \tag{8.5.47}$$

α is known as the *attenuation coefficient*, as it describes a reduction in amplitude of the voltage wave with distance along the line, by conduction between the two conductors, and v^* is now the velocity of the wave. It can be seen that attenuation increases as ω increases. However, if the imaginary part of the permittivity is dominated by electrical conductivity, then $\varepsilon''_r \approx \frac{\sigma}{\omega\varepsilon_0}$, which makes α less frequency dependent, but also means that v^* increases with frequency. For instance, if we take $\varepsilon_r = 20$ and $\sigma = 1$ dS m^{-1}, α is 4.06 m^{-1} at $\omega = 10^9$ Hz (f = 160 MHz), $v^* = 6.47 \times 10^7$ m s^{-1} and $v^*/v = 0.96$. At $\omega = 10^{10}$ Hz (f = 1.6 GHz), α = 4.21 m^{-1}, $v^* = 6.71 \times 10^7$ m s^{-1} and $v^*/v = 0.9996$.

An imaginary component of the medium permittivity will also affect the value of the equivalent component of a short length of transmission line, described in Section 8.5.3. The modification to take this into account is in principle quite straightforward, involving the replacement of ε_r in Equation 8.5.40 by a complex quantity, $\varepsilon_r = \varepsilon'_r - j\varepsilon''_r$. The mathematics is a little involved, but leads to an expression for ε_r^* of

$$\varepsilon_r^* = \frac{c}{l\omega}\left(\frac{\sqrt{\frac{|\varepsilon_r|+\varepsilon'_r}{2}}\sin\left(\frac{\omega l}{c}\sqrt{2(|\varepsilon_r|+\varepsilon'_r)}\right)-\sqrt{\frac{|\varepsilon_r|-\varepsilon'_r}{2}}\sinh\left(\frac{\omega l}{c}\sqrt{2(|\varepsilon_r|-\varepsilon'_r)}\right)}{\cos\left(\frac{\omega l}{c}\sqrt{2(|\varepsilon_r|+\varepsilon'_r)}\right)+\cosh\left(\frac{\omega l}{c}\sqrt{2(|\varepsilon_r|-\varepsilon'_r)}\right)} - j\frac{\sqrt{\frac{|\varepsilon_r|-\varepsilon'_r}{2}}\sin\left(\frac{\omega l}{c}\sqrt{2(|\varepsilon_r|+\varepsilon'_r)}\right)+\sqrt{\frac{|\varepsilon_r|+\varepsilon'_r}{2}}\sinh\left(\frac{\omega l}{c}\sqrt{2(|\varepsilon_r|-\varepsilon'_r)}\right)}{\cos\left(\frac{\omega l}{c}\sqrt{2(|\varepsilon_r|+\varepsilon'_r)}\right)+\cosh\left(\frac{\omega l}{c}\sqrt{2(|\varepsilon_r|-\varepsilon'_r)}\right)}\right), \quad (8.5.48)$$

where $|\varepsilon_r|$ has been used in place of $\sqrt{\varepsilon_r'^2+\varepsilon_r''^2}$.

The effect of this is illustrated in Fig. 8.20.

It can be seen from these figures that the effect of introducing an imaginary part of the permittivity is to reduce slightly the apparent real part of the permittivity for a short transmission line.

8.5.5 *Summary of transmission line behaviour*

Any smooth time-varying quantity can be represented mathematically as the sum of a number of sinusoidal waves of different frequency. These are known as Fourier components.

- The speed at which an electromagnetic wave travels along a transmission line is given by

$$v = \frac{c}{\sqrt{\varepsilon_r}}, \quad (8.5.20)$$

where
c is the speed of light in vacuum and
ε_r is the relative permittivity of the medium in which the line is embedded.

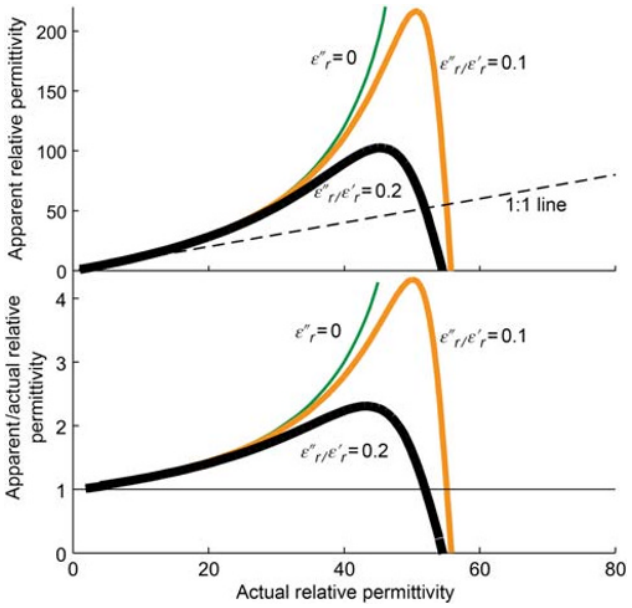

Fig. 8.20 Relationship of the apparent to the actual real part of the permittivity of a dielectric calculated from the capacitance of a 100 mm transmission line at 100 MHz frequency embedded in a medium with different imaginary parts.

- A long transmission line appears as a resistance of value:

$$Z_0 = \sqrt{\frac{\mu}{g^2\varepsilon}} \quad (8.5.23)$$

- Junctions between transmission lines, between a transmission line and a load or between a transmission line and a short- or open-circuit, produce reflections of a wave travelling along the line. If the impedance of each is very different from one another, then little signal is transmitted from one portion to the next.
- A short transmission line acts like a capacitor. If it is short enough, the capacitance is equal to Cl, where C is the capacitance per unit length of the line and l is its length (Eq. 8.5.36). For longer lines, the apparent capacitance or relative permittivity increases faster than l.
- The effect of increasing line length is the same as increasing frequency.
- Electrical conductivity or relaxation effects introduce an imaginary component to the medium permittivity. This has the effect of attenuating a wave travelling along the line and slowing it down a little, leading to an apparent increase in the permittivity.

8.6 Practical Realisation of a Transmission Line System – Time Domain Reflectometry

The concept behind this daunting name is quite simple. The speed at which an electromagnetic wave travels (or *propagates*) through a medium, such as soil, depends mainly on the permittivity of the medium. By measuring this speed, the permittivity may be inferred.

TDR is usually conducted by inserting two or more parallel metal rods into the soil and measuring the time taken for an electrical pulse to travel the length of the transmission line so formed, reflect from the end, and return to the beginning.

TDR is used extensively in the telecommunications industry for detecting faults in electrical cables, which are often buried in the ground. A telecommunications cable is a transmission line, whose speed of transmission is usually known quite accurately. Metallic cable testers contain a fast rise time pulse generator, which switches the voltage applied to the transmission line from zero to a few hundred mV in a few hundred picoseconds (ps). 1 ps = 10^{-12} s. It then monitors the voltage over the next few microseconds to detect a reflection from the point at which the fault lies. The time taken for this to return is equal to twice the distance to the fault divided by the speed of travel. The position of the fault can then be pinpointed accurately without the need for expensive exploratory excavation.

Early research into the use of TDR for measurement of soil water content used these cable testers and many researchers still do so. The principle is almost identical to fault testing, except that the pulse return time is used to estimate the speed of travel along a known length of line.

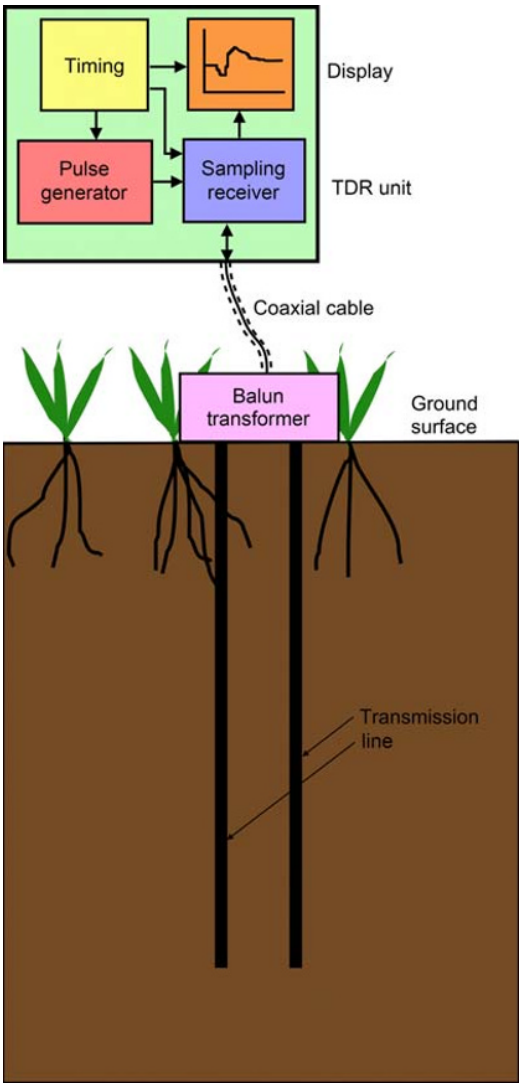

Fig. 8.21 Schematic diagram of TDR instrument connected to a transmission line embedded in the soil.

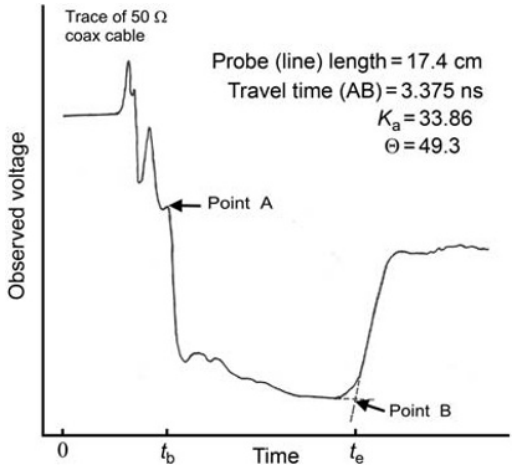

Fig. 8.22 Typical TDR trace in wet soil from parallel transmission lines (Patterson & Smith, 1981). Point A is the reflection from the start of the transmission line in the soil, while Point B is that from the end. © 2008 Canadian Science Publishing or its licensors. Reproduced with permission.

Figure 8.21 is a schematic diagram of the components of a TDR system.

A timer controls a pulse generator to produce a fast rise-time pulse, which is fed, via a coaxial cable and often a *balun* transformer, to the transmission line, embedded in the soil. The voltage at the terminals of the instrument is displayed as a function of time, so that both the outgoing and returning pulse can be detected. In practice, the process is so fast that many pulses are launched into the line, and the displayed graph is a composite of the voltage detected at a different time following each pulse.

This output graph is similar to that shown in Fig. 8.22. To interpret this, it should be borne in mind that the voltage is measured at the terminals of the instrument and not at any point on the transmission line.

At time $t = 0$, the fast rise-time pulse is applied. The voltage remains constant for a short time. However, after a time $t_b/2$, the pulse encounters the start of the transmission line (Point *A*). Some manufacturers put a small component here to provide a marker. Even if this is not present, there is usually a sufficient impedance mismatch to cause a reflection at that point, which allows the start of the line to be identified. The reflection propagates back along the connecting cable, again taking a time $t_b/2$ to reach the instrument and so is detected at time t_b. As the remainder of the pulse travels along the line, it may undergo a few partial reflections caused by discontinuities in the soil or more diffuse reflections as a result of gradients of permittivity. When it reaches the end of the line at time $t_e/2$ (Point *B*), the pulse reflects back, reaching the detector at time t_e. The total travel time along the rods is $t_e - t_b$, but this is for the double trip from the start of the line to the end and back again. The average speed of travel, v, therefore, is given by

$$v = \frac{2l}{t_e - t_b}, \tag{8.6.1}$$

where l is the length of the rods.

Because of attenuation, relaxation and partial reflections along the line, the originally sharp pulse generally becomes more indistinct as it travels to the end and back along the line, so that identification of t_e becomes more difficult with longer lines and in conductive or dispersive media. The usual way to identify the end point is to construct tangents to the curve as shown in Fig. 8.22. The end point is taken as the intersection of the two tangent lines. However, the more indistinct the end point, the less confidence that can be placed on the estimate of t_e. In nearly all applications, software is used to analyse the TDR curves automatically. Commercial systems usually have in-built proprietary software, and the details of exactly how the

Fig. 8.23 Tektronix 1502C cable tester.

analysis is performed are often not readily available. It is, however, usually possible to save the raw waveform and analysis of this can be done manually or using one of a few public domain programs. Examples are TDRANA (Heimovaara & de Water, 1993), WINTDR (Or *et al.*, 1998) and TACQ (Evett, 2000a, b). Putting together a system by oneself is not difficult, although a cable tester is expensive. The output from this can be used with one of the public domain programs.

The theory in Section 8.5 was written in terms of a single-frequency sinusoidal waveform. A pulse as described here, where the voltage goes from zero to a steady value almost instantaneously is clearly not sinusoidal. However, any waveform can be decomposed by using *Fourier analysis* into a sum of sinusoidal waves of different frequency. So the step from zero to a steady value can be treated as being composed of a large number of single-frequency waves. The upper frequency can be estimated from the rise time of the pulse. The popular 1502B and 1502C cable testers (Fig. 8.23) have a quoted rise time from 10 to 90% of full voltage of 200 ps. This corresponds to a frequency, f, of about 1.75 GHz (Robinson *et al.*, 2005). Fourier analysis gives a theoretical power at each frequency varying as $1/f^2$, so that most of the power available is at lower frequencies. Friel and Or (1999) measured the power spectrum of a TDR cable tester and confirmed that this was true when the rods were in air. In deionised water and an electrolyte solution, there was less power at all frequencies, but especially at higher ones. The lower frequencies, however, are suppressed and the effective frequency bandwidth is from about 20 kHz to 1.5 GHz (Heimovaara, 1994).

In many mineral soils, the permittivity is effectively constant over this range of frequency (Jones *et al.*, 2002), and so a reliable measurement of permittivity can be obtained by the method described earlier.

8.6.1 Probe design and construction

A number of features of a TDR probe can be varied to suit different situations. Chief amongst these are the length, arrangement, shape, material, cross-section, spacing and coating of the rods. As in most other aspects of experimental design, the choice depends on compromises between practicality and the ideal situation. Personal preference is often an important, but little acknowledged, factor.

Length of probe

The length of probe depends on several factors, some related to the objectives of the measurement programme, while others to more practical aspects.

The orientation of installation is likely to be important. In most cases, the output obtained from TDR gives a very close approximation to the average water content of the soil over the length of the probe. This is because the time taken for the pulse to travel a set distance is proportional to $\sqrt{\varepsilon}$ and water content is also usually close to a linear function of $\sqrt{\varepsilon}$. The use of more sophisticated calibration equations is unlikely to make any material difference to this fact.

The speed of the TDR pulse is extremely fast, even in very wet soil, when it may be down to 5×10^7 m s^{-1}. For very short probes (<100 mm), the pulse will travel the length of the probe and back in less than 4 ns; in dry soil, it may be less than 2 ns. The rise time of the pulse is usually about 200 ps, which suggests that resolution of the travel time is likely to be around this value at best. This translates to about 4% by volume of water content. Longer probes offer a proportionately longer travel time and, potentially, a resolution almost inversely related to probe length. So a 200 mm probe should allow about 2% by volume measurement precision and 500 mm about 1%. However, attenuation, partial reflection and dispersion effects make the returning pulse both smaller in size and longer in duration for long probes. It is difficult to generalise, but a measurement precision of between 1 and 3% water content by volume is a reasonable working estimate for 500 mm probes.

In clay, organic-rich and high electrical conductivity soils, it may not be possible to obtain measurable reflections even for very short probes. For instance, Dalton and van Genuchten (1986) and Robinson *et al.* (2003) found that the maximum length of rod at which reflections could be measured with a soil solution conductivity of 6 dS m^{-1}, corresponding to a bulk soil electrical conductivity of about 2 ds m^{-1}, and near-saturated water content of 0.4 m^3 m^{-3} was 200 mm.

Arrangement of the rods

Early experiments with TDR in the laboratory (Topp *et al.*, 1980) used coaxial cells, with the soil sample in a cylindrical metal container, which formed one of the conductors or 'rods', the other being a central rod in the centre. This is clearly an impractical arrangement for use in the field, and so nearly all early work used a configuration with two parallel rods of a few millimetres diameter spaced about 50 mm apart.

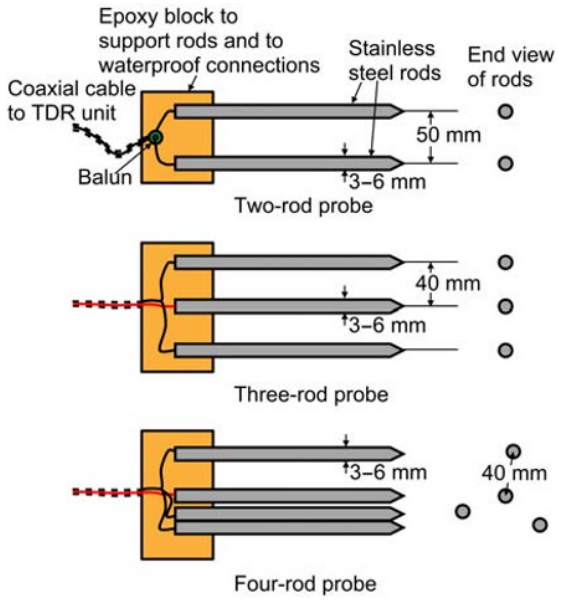

Fig. 8.24 Popular arrangements for TDR probes. Actual dimensions vary.

For field use, the most popular arrangements are either as two parallel rods or three placed in a row, as shown in Fig. 8.24. Sometimes, four or even more rods are used, arranged as a ring around a central conductor (Fig. 8.24). In almost all cases where more than two rods are used, the central rod is connected to the central conductor of the coaxial cable from the TDR instrument and the outer rods are all connected together and to the outer (shield) conductor of the cable. For two-rod probes, the rods are connected one each to the central conductor and to the shield (however, see the following text).

The principal advantage of using three or more rods is that the characteristic impedance of the arrangement is much closer to that of the coaxial cable used (50 Ω). The characteristic impedance varies with the water content of the soil, but typical values for a two-rod probe with 5 mm diameter rods with their centres 50 mm apart, are 5–15 Ω. The corresponding reflection coefficients (Eq. 8.5.29) at the junction with the coaxial cable are 0.82 and 0.54, indicating that only 18–46% of the voltage signal penetrates into the medium. For a three-rod probe with the same diameter and spacing between the conductors, the characteristic impedance is between 10 and 30 Ω, leading to a reflection coefficient between 0.67–0.25 and 33–75% of the signal penetrating the medium.

A two-rod probe arrangement is often referred to as *balanced*, since both conductors are entirely equivalent to one another and may be exchanged with no effect. A coaxial arrangement is called *unbalanced* as there is a fundamental difference between the centre and the outer conductor, which usually has a second function as a shield for stray electromagnetic radiation. This outer conductor is normally connected to earth or ground to enhance its shielding ability, although in modern electronics this is becoming less common. In the case of soils, however, the concept of balanced and unbalanced appears to be irrelevant, as all conductors are in contact with the ground and the method relies on there being a voltage wave travelling along both sets of conductors. By extension, there must be a difference in voltage between the conductors and the "ground" and within the "ground" itself. The important distinction is the impedance mismatch between the instrument and those conductors connected to it. Nissen *et al.* (2003a) and Robinson *et al.* (2003) found no difference in travel time using a two-rod probe, whichever conductor was connected to the coaxial cable screen. However, both sets of authors found some increase in noise when the rod connected to the screen was immersed in water and the other in air, compared with when they were the other way around.

Most instruments are manufactured with an output impedance of 50 Ω and a 50 Ω connecting cable and *BNC* connectors are used to ensure minimal reflections at that point. Connecting this cable to a three- or more- rod probe produces an acceptable match in most cases. However, this may not be the case for a two-rod probe. The difficulty can be dealt with by use of a *balun*, which is a word coined from 'balanced–unbalanced' and is a small transformer which has the effect of changing the apparent characteristic impedance of a line to which it is connected according to the ratio of the square of the number of turns on each side of the transformer. Baluns are used extensively in electronic and radio applications and are easily and cheaply available from electronic suppliers. They can also be made easily using ferrite rings and lacquered wire. Instructions are given by Spaans and Baker (1993).

In many instances, however, the use of a balun causes more problems than it solves. The balun changes the frequency content of the signal, attenuating higher frequencies more than lower ones and increasing the effect of imaginary components of permittivity. This is important for estimation of electrical conductivity using TDR, which relies on the low-frequency measurement (see Chapter 21). It also increases both the complexity and cost of producing TDR probes.

Shape of rods

Other forms of probe use two parallel strips of metal facing one another, rather than rods, which ensure that the field is distributed fairly evenly between the strips (Robinson and Friedman, 2000). Others use two parallel metal strips side by side on a piece of printed circuit board (Hook *et al.*, 1992; Selker *et al.*, 1993; Nissen *et al.*, 1999, 2003b). This is not the most efficient arrangement electrically, but produces a robust and convenient single-piece probe that can be slid into the ground with little fear of distortion. Selker *et al.* (1993) and Nissen *et al.* (1999, 2003b) constructed probes with a relatively small sampling length by folding the waveguide onto a printed circuit board as shown in Fig. 8.25. This allowed the length of the transmission line

to be long enough to resolve the reflections adequately, while occupying a much shorter physical length in the soil. Nissen *et al*. (1998) also solved this same problem by wrapping one conductor of a transmission line in a spiral around a cylindrical insulating rod, with the other conductor consisting of four straight rods on its periphery, as shown in Fig. 8.26. Unfortunately, this sensor is sensitive only to soil within about 2 mm of the cylinder.

A version for use in pre-installed access tubes is produced by IMKO of Germany. The arrangement is depicted in Fig. 8.27. The rods are spring-loaded, so that they press against the side of the access tube. A penetration depth of up to 150 mm into the soil is claimed (IMKO, 2013a). The probe can be used in a very similar way to other profiling probes, such as depth capacitance probes (Section 8.7) and neutron probes (Chapter 7). With this type of probe, much of the field lies between the two strips and within the access tube. Its operation depends on part of the field passing through the soil and taking the long way around from one set of plates to the other, as shown in Fig. 8.28.

IMKO also produce TDR probes of more conventional design using rods inserted into the soil. The method of

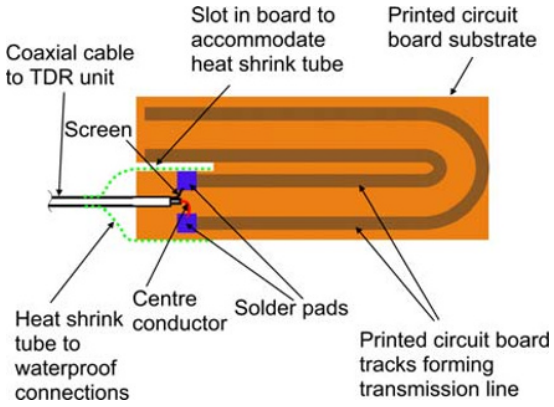

Fig. 8.25 Transmission line on printed circuit board.

Fig. 8.27 IMKO Trime IPH depth probe showing the four spring-loaded plates on one side to ensure good contact with the inside of the access tube. Photograph reproduced with permission of IMKO GmbH.

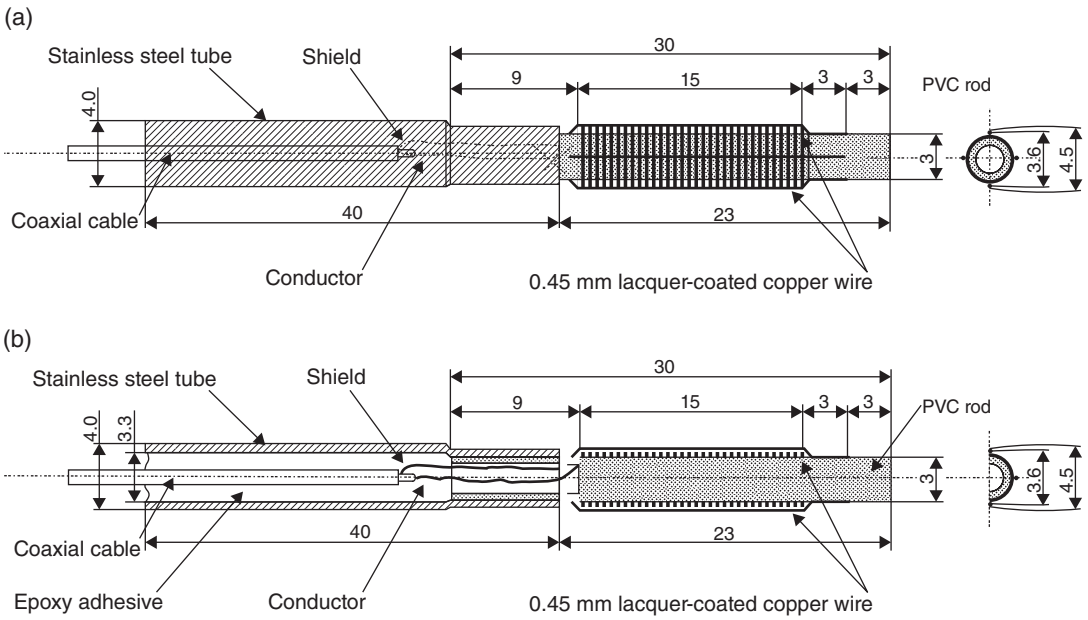

Fig. 8.26 TDR wrapped in a spiral around a cylinder (Nissen *et al*., 1998). Reprinted by Permission, ASA, CSSA, SSSA.

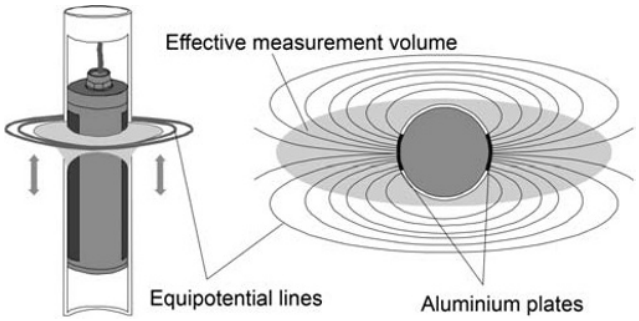

Fig. 8.28 Equipotential lines around an IMKO Trime IHP depth probe. Reproduced by permission of IMKO GmbH.

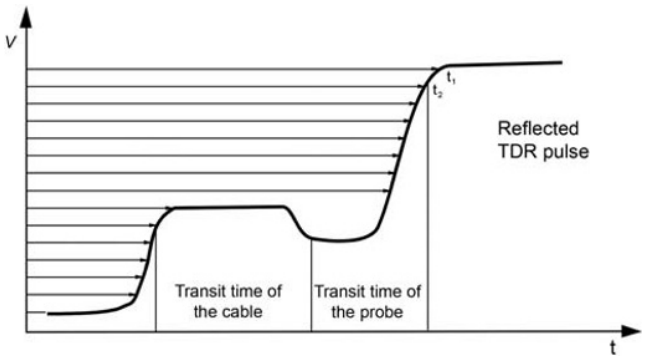

Fig. 8.29 TRIME method for waveform analysis. Reproduced with permission of IMKO GmbH.

estimating travel time is different and illustrated in Fig. 8.29. Instead of taking equal time slices and identifying the voltage corresponding to each one, the TRIME method identifies the time at which the critical voltage levels are achieved. To improve the resolution of voltage, TRIME probes use coated rods (see below), which filter out the lower frequencies and lead to a greater amplitude of the reflected wave. The height of the reflected pulse varies, however, with bulk electrical conductivity of the soil, and so an iterative algorithm is used to detect the time of the reflected wave. Nevertheless, IMKO claim that this method requires simpler, cheaper and more compact electronics than conventional TDR systems based on cable tester principles.

The Environmental Sensors Inc. (ESI) TDR also can be installed in an access tube, but is designed for permanent installation. The conductors are built into a solid plastic rod, with radio frequency diodes at intervals along it (see the following text).

Material of rods

The most important characteristics for the rod material are that it should be a good electrical conductor and be strong enough to withstand being pushed into the soil without distortion. High-frequency electrical signals travel almost entirely in the outer skin of a conductor, leaving the central portion effectively non-conducting, thus reducing the effective conductivity considerably. The effective resistance, R, per unit length of a cylindrical rod of radius r at high frequency is given by:

$$R = \frac{1}{2\pi r}\sqrt{\frac{\mu_0 \omega}{2\sigma}}. \qquad (8.6.2)$$

For $\omega = 10^9$ Hz ($f = 160$ MHz) and a typical stainless steel TDR rod of diameter 6 mm with electrical conductivity of 1.35×10^6 S m^{-1}, R is 1.14 Ω m^{-1} and at $\omega = 10^{10}$ Hz ($f = 1.6$ GHz), R is 3.6 Ω m^{-1}. This compares with a dc resistance for the same rod of 0.026 Ω m^{-1}. Stainless steel is a relatively poor conductor compared with most metals. To put this into context, the resistance needs to be compared with the inductive part of the impedance of the line per unit length. Typical values for L can be calculated from

$$L = \frac{\mu_0}{g}, \qquad (8.6.3)$$

which gives, from Equation 8.5.1, a value for ωL of 292 Ω m^{-1} at $\omega = 10^9$ Hz and 2920 Ω m^{-1} at $\omega = 10^{10}$ Hz, so the imaginary part of the rod impedance will always dominate at typical TDR frequencies, and we can expect to be able to neglect the skin effect without introducing any significant error.

Cross-section and spacing of rods

The geometric factor, g, that controls both the capacitance and inductance per unit length of the rods depends only on the ratio of the key dimensions. For a simple two-rod probe, as depicted in Fig. 8.24, Equation 8.5.1 shows that g is a function of the ratio of the rod spacing to the rod diameter, d/a. Large values of g are associated with small values of d/a, that is small spacing and/or large-diameter rods. However, beyond a spacing:diameter ratio of about 8, the change in g is relatively small, so that for most realistic arrangements, g is likely to be in the range of 0.75–1.25.

Changing the size and spacing of the rods affects the volume of soil contributing to the measurement of water content. There are two aspects to this:

1 The overall volume measured

2 The relative contribution of different parts of the volume to the measurement

Figure 8.30 shows the volume of soil contributing different proportions to the measurement for two-rod and three-rod probes with different spacing to diameter ratios. The energy density, W, of the electric field is given by

$$W = \frac{\varepsilon E^2}{2}, \qquad (8.6.4)$$

so that areas with densely packed field lines (large electric field) contribute more to the overall measurement than those where they are further apart (Knight, 1992). Field lines must converge onto the rods, and so soil close to

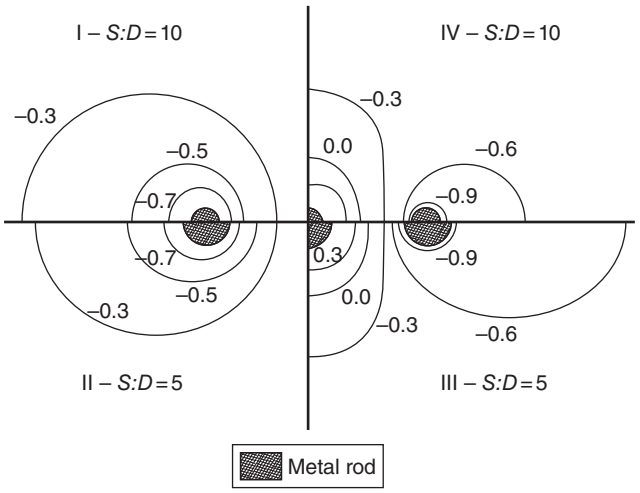

Fig. 8.30 Areas of soil around the conductors contributing to the reading with two different spacing to diameter ratios of two- (left-hand) and three-rod (right-hand) probes. The areas contributing 50, 70 and 90% of the reading are shown. From Ferré *et al.* (1998). Reproduced with permission of John Wiley & Sons. © American Geophysical Union.

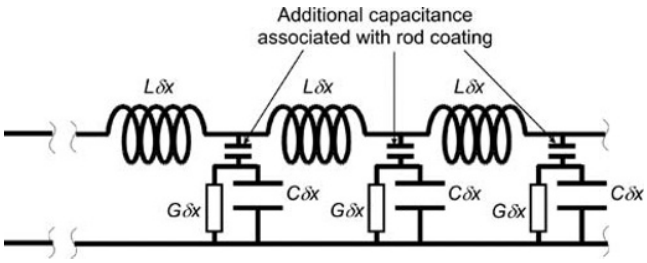

Fig. 8.31 Equivalent circuit for a transmission line with rods coated with insulating material.

the rods has more influence than that between them. This can be seen in Fig. 8.30. The cross-sectional area of soil contributing 70% of the reading is concentrated quite closely around the conductors, while that contributing the next 20% is considerably larger.

Small-diameter conductors have a larger concentration of field lines near their surface than ones of greater diameter. Large-diameter conductors in relation to the spacing improve the distribution of sensitivity between the rods. However, they are more likely to disturb the soil structure around them and provide a barrier to soil water flow, making this region atypical of the soil as a whole. For these reasons, Knight (1992) suggested that the ratio of rod spacing to diameter should not exceed 10. Most users have found very little effect of this disturbance on water content measurement for rods of diameter up to about 6 mm, but that to avoid problems with larger diameter rods, it is advisable to drill pilot holes a little smaller than the rod diameter and then insert the rods (Topp & Davis, 1985; IMKO, 2013b). Clearly, the soil from the holes should be removed and not pushed to the side.

Three-rod probes weight the reading to the area around the central conductor much more than two-rod probes (Fig. 8.30).

Coating of rods

Rods can be coated with a low-permittivity insulator (e.g. polyolefin or PVC) to reduce transmission losses in conducting materials. This effectively introduces an extra capacitor in the equivalent circuit diagram of the transmission line, as shown in Fig. 8.31. This provides more impedance for the lower frequencies across the two conductors, while leaving the high frequencies (which are, in any case, less affected by the electrical conduction) relatively unaffected. Only one of the rods needs to be coated. Ferré *et al.* (1996) found that coating the rods both reduced the sensitivity of the sensor, particularly at higher water content, and reduced the volume contributing to the measurement. The available data suggest that the higher the permittivity of the insulating material and the thinner the coating, the smaller the effect on sample size and the calibration relationship (Ferré *et al.*, 1996). Nichol *et al.* (2002) found that a coating improved the identifiability of the reflection from the end of the rods quite markedly, although each probe had to be calibrated individually. This is because the coating introduces a non-linear relationship between the travel time and the square root of the soil permittivity (Nichol *et al.*, 2002).

Diode shorting

Hook *et al.* (1992) suggested using PIN diodes at the end of the rods to provide a better-defined end-point to the probe. A 3 V dc voltage applied to the line turns the diode on and makes a short circuit at that point. By taking the difference between a trace with the diode turned off and one with it turned on, the diode position can be detected very easily. Using a diode at or close to where the probe enters the soil makes identifying this reflection much easier and eliminates the need for a balun. Alternatively, identification of the start of the line can be helped by inserting an impedance mismatch into the probe head (Robinson *et al.*, 2003), although it must be small enough so as not to reduce the signal passing into the soil significantly. The marker is often not exactly where the rods enter the soil and so this extra distance, which is usually constant, must be accounted for.

The reflection at the end of the rods is usually easier to detect as it is an open circuit. In electrically conductive or layered soils, the reflection may be obscured by noise from multiple reflections or attenuated severely. Taking the difference between the signal from the rods terminated by an open- and a short circuit can make identification of the end point possible. The arrangement is shown diagrammatically in Fig. 8.32.

Figure 8.33 gives an example of the improvement in identification of the signal by a diode situated near the

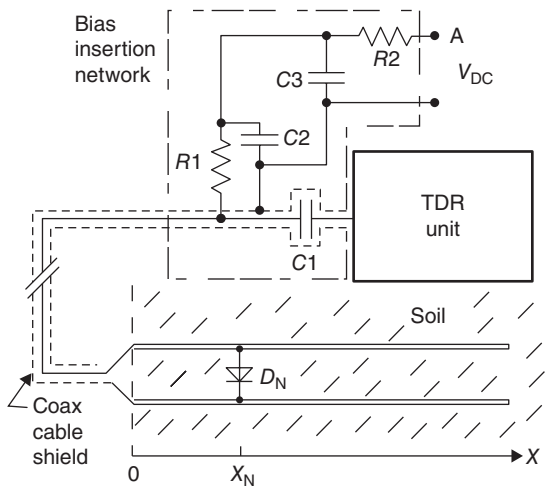

Fig. 8.32 Use of PIN diodes to define each end of the transmission line. By applying +3 V as a bias voltage, the diode near the beginning of the line is turned on, creating effectively a short circuit. 0 or –3 V voltage has no effect on the transmission line. The bias insertion network supplies the bias voltage and protects the TDR unit. Adapted from Hook *et al*. (1992). Reprinted with Permission of ASA, CSSA, SSSA.

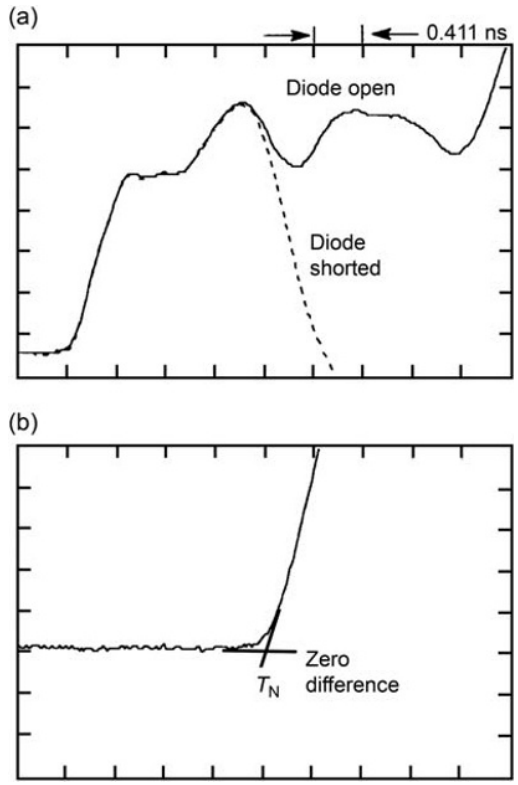

Fig. 8.33 (a) TDR traces in soil with a diode at the beginning of the line open and closed. (b) Difference between the two curves in (a), illustrating the ease of diode position location. Adapted from Hook *et al*. (1992). Reprinted with Permission of ASA, CSSA, SSSA.

point of entry to the soil. The upper diagram (A) shows the waveform obtained with the diode acting as a short circuit (bias voltage applied) and with it inactive (no bias voltage). At short times, the signal records reflections produced before the voltage pulse reaches the rods and is identical in both cases. A strong reflection is produced when the pulse reaches the diode in its shorted state and the trace diverges from that recorded when the diode is open. The lower diagram (B) shows the difference between the waveforms. The two traces are identical up to the point where the pulse reaches the diode, with zero difference. After this point, the two diverge strongly, making identification of the diode location very easy.

The principle can be extended to make one set of rods behave as a set of different length probes by stationing diodes at various positions along the rods, as shown in Fig. 8.34. Each diode is connected to one of the rods via a capacitor and a separate control wire provides the bias voltage for two diodes. Other diodes further up the line must be disconnected from the bias voltage, so that they are not turned on by the pulse.

An obvious problem with using diodes within the soil is that it is not practical for field use with probes made from separate rods, as the diodes act as obstructions to installation of the probe. This may not be such a barrier in laboratory use, where soil can be packed around the rods after emplacement. EIS produce a TDR probe in which the rods, diodes and their control wires are encased in a single epoxy bar, which can be inserted into the soil.

Nichol *et al*. (2002) found diodes at the end of the rods to be effective in relatively low conductivity media, but not in solutions of 2 dS m^{-1}. The reason for this appears to be that the diodes used (MPN3404) are not perfect short circuits, having a quoted impedance at 100 MHz of 0.8 Ω. Using copper wire to create a near-ideal short circuit improved the performance markedly.

Construction considerations

Apart from the earlier remarks, good performance of TDR probes depends on reasonable care in their construction. The use of high-quality electrical cables and connectors, ensuring that cables are not frayed and that all electrical joints are secure or firmly soldered, helps prevent spurious reflections and poor signal transmission. The head end of the rods must also be solidly embedded into a plastic block to protect the connections from moisture, prevent the rods from moving relative to one another and keep the electrical connections secure. They are simple enough that many people prefer to make their own probes, although several manufacturers produce them commercially.

8.6.2 Installation of probes

Installation requires many of the same precautions and considerations as for other instruments to ensure that gaps around the probe do not provide water pathways for rain or irrigation water to penetrate more easily into the soil than

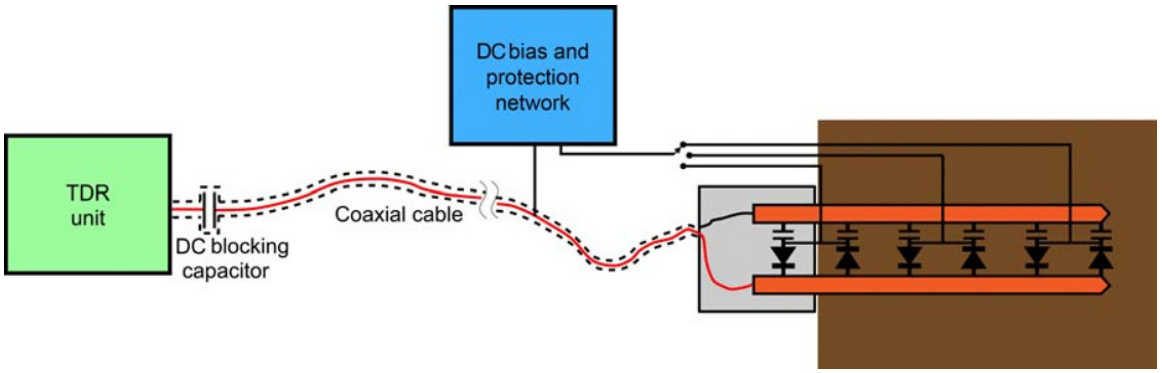

Fig. 8.34 Schematic diagram of an arrangement to allow a transmission line to be segmented to allow different lengths of the line to be sampled using one TDR unit. By connecting one pair of diodes to the dc bias voltage with different polarities, each one can be shorted separately.

in the surrounding area, that the ground surface and vegetation cover are not disturbed and that stones in the soil do not cause more than the minimum disturbance to the readings obtained.

There are two principal ways in which TDR probes can be installed. They may be installed from the soil surface, either vertically or at an angle, or horizontally from the face of a trench or pit dug in the soil. The former method gives readings of total or average water content along the depth range of the probe, while the latter gives a measurement of water content at a specific depth, averaged in an approximately cylindrical volume of length equal to that of the probe and diameter defined by the rods.

Vertically installed probes, therefore, give a very good measurement of the total water storage over the depth of soil profile that they cover. This is clearly very good if total water storage is needed, but less so if the distribution of water content with depth is desired. A series of probes of different length may be a better choice in this case. The water content of the depth interval from l to $(l + d)$ can then be calculated by taking the difference between the total water storage over these two lengths.

Horizontally installed probes have good depth resolution, and long probes may be desirable to minimise the effects of short-range spatial variability. However, it may be very difficult to ensure that long rods remain at the same depth, especially if there are large roots or the soil is hard or stony. Installation of probes horizontally in the field is also difficult without causing an unacceptable amount of disturbance to both the site and the measurements.

Vertical installation is clearly the simpler and quicker method. In many cases, an integrated measure of water storage over the upper few decimetres of soil is desired, and so this would be preferred in any case. As described earlier, more depth-specific information can be obtained by using diode shorting, markers placed on the rods in the form of notches (which may be filled with dielectric material) (Topp & Davis, 1985) or by using a set of probes, all of different length, installed close together. In the case of diode shorting and different length probes, water content in an interval of depth is calculated by difference between the total water content to one depth and that to the other. This limits the overall accuracy obtainable, especially where different length probes are installed, as spatial variability between the two locations introduces extra uncertainty. Vertical installation also introduces an additional hazard that small gaps around the probes can act as water conduits through the soil. In addition, the maximum depth achievable is limited by the length of probe which can return a reliable signal for that soil and by the depth to which rods can be inserted.

Horizontal installation is more labour intensive, as it requires access from a vertical face. This may be a pit or trench dug in the soil to the required depth. Unless this is very shallow (less than about 0.7 m), the walls will usually require support to prevent collapse and possible injury or death. The excavation may offer a suitable place to house data acquisition equipment and exposing a vertical face offers the opportunity to study the soil profile in some detail. However, an exposed soil face may allow it to dry out, leading to unrepresentative measurements close to the face. To reduce this, it is advisable to cover the face with a plastic sheet and to place all instruments some way into the soil by drilling holes up to 1 m horizontally and then inserting the probes from the end of these. More information on installation of instruments from the side of a pit is given in Section 12.11.1. The advantages of horizontal installation are good depth resolution of measurements, the ability to make measurements in two dimensions (horizontal and vertical) and the possibility of deep measurements (6 m or more).

Another method of achieving horizontal installation, which is less labour intensive and intrusive, is to drill a large (100–200 mm diameter) hole with a bucket auger, or possibly two overlapping ones to give an approximately elliptical hole. Probes can be installed to the length of an arm (about 0.7 m) from the surface. The method can presumably be extended to deeper installation by using

suitable mechanical devices. Using hand-installation, it is difficult to ensure very accurate depth placement or horizontal alignment. After installation, the hole may be backfilled with the same soil, although this risks creating a pathway for faster water infiltration than in the surroundings. Alternatives include leaving it covered and unfilled (so long as there is no risk of throughflow along an impeding horizon) and filling with low hydraulic conductivity material such as concrete or expanding closed-cell foam cast *in situ*.

Horizontally installed two- and three-rod probes should be emplaced so that the plane of the rods is horizontal. This will maximise the depth resolution. Also, if the rods are arranged vertically above one another, the sensitive volume is biased heavily towards the rod in the lower permittivity medium, which may cause problems where there is a sharp wetting front (Nissen *et al.*, 2003a).

TDR rods are often pushed or hammered directly into the soil. For small diameter rods, this appears not to cause an unacceptable disturbance around them (Topp & Davis, 1985; IMKO, 2013b). A possibly better way is to drill a pilot hole, slightly smaller than the diameter of the rods using a portable electric drill and then to insert the rods into the predrilled holes. It may, however, be difficult to ensure that the holes are sufficiently parallel to one another and a suitable jig should, therefore, be used to guide the drill bit.

8.6.3 Data acquisition

Early TDR equipment for soil water measurement used commercial cable testers, such as the Model 1502B. This produced a waveform image on a cathode ray tube, which could be photographed and the waveform analysed later manually. Later equipment was able to output and store the waveforms digitally. This increased the ability to acquire a large number of waveforms, often under automatic control, and opened up the automatic processing of waveform data to recognise the point of entry into the soil and the end reflection. Most modern equipment can acquire data, store and analyse the resulting waveforms completely automatically. This is usually based on 256 data points, which are arranged to cover the time range of most interest. Some systems consist of a commercial cable tester, a multiplexer unit (see Section 8.6.4), TDR probes, a portable computer and some dedicated software to control the process and perform analysis and storage. Most commercial systems have all of these elements, but are integrated into a single package.

8.6.4 Multiplexers

Automatic storage and analysis of data from a TDR probe was a significant step towards a usable instrument for routine soil water observation. However, most users need to measure several probes. The electronics involved in TDR are expensive, and having a dedicated control unit for each probe would be prohibitive. The answer is to use a *multiplexer*. This is a switch that can connect each of several probes sequentially to the control, storage and data analysis unit. TDR probes are very much cheaper than the electronic units, so this is a very cost-effective way to acquire data from multiple probes. The first report of the use of probes multiplexed in this way was by Baker and Allmaras (1990), who used a manual rotary switch to swap between probes, while Heimovaara & Bouten (1990) used a computer-controlled system. Later equipment uses electronic switches to perform the multiplexing.

Both multiplexers and long connecting cables filter out some of the higher frequency components of the signal. This reduces the quality of the data and may not make the measurements from one set of probes comparable with another. High-quality cables and multiplexers are, therefore, essential and where multiple multiplexers are used, they should be connected in a 'star', rather than a 'daisy-chain' arrangement, so that all probe signals traverse the same number of multiplexers (Evett *et al.*, 2008).

8.6.5 Waveform analysis

Figure 8.22 shows an example TDR waveform. Analysis of this consists of the following steps:

- Identification of the point at which the pulse enters the soil
- Identification of the reflection from the end of the line
- Calculation of the time taken for the pulse to travel through the soil
- Application of an appropriate calibration to convert travel time into soil water content

With multiplexed probes, in particular, there will often be a fairly long cable between the pulse generating unit and the probe. This part of the waveform is usually ignored when acquiring the data, so that only the more interesting part of the waveform is actually stored. It should also be noted that, for each probe, the point along the waveform at which the pulse enters the soil will always be the same. Therefore, after this has been identified for each probe, it need not be done again.

As described earlier, identification of reflections is usually performed by drawing tangents to the waveform around the point where the reflection lies. This tends to bias the distribution of frequencies which make up the waveform towards the higher frequencies, which are less affected by electrical conductivity effects. Differentiation of the waveform is performed easily by software where the data points are automatically spread evenly in time and a tangent can be identified by searching for several consecutive points where the voltage difference from one to another is very nearly the same. The tangent either side of the reflection point can then be calculated and the intersection point identified by solution of two simultaneous equations.

Most software allows the user to enter a custom calibration equation or to use one of a set of standard equations. It usually allows storage of the waveform and records the

time for the pulse to traverse the probe, the calculated relative permittivity and bulk electrical conductivity of the soil (see Chapter 21).

Waveform analysis software can be obtained from a variety of sources. Popular public domain programs are TDRANA (Heimovaara & de Water, 1993), WINTDR (Or *et al.*, 1998) and TACQ (Evett, 2000a, b).

8.6.6 Operation of TDR under field conditions

TDR measurements are a complex electronic and computational process. As such, they use significant amounts of electrical power, and the equipment is not necessarily suitable for use in harsh environments. Large batteries, solar panels and/or wind generators will usually be needed to run the equipment where mains electrical power is not available. Likewise, protection against rain, solar radiation and dust is essential. Electrical connections must be protected against damp and corrosion.

8.6.7 Advanced analysis techniques

The TDR waveform contains a great deal of information which has previously been ignored and which complicated the traditional analysis techniques. Two approaches for extracting this information have been followed.

1 Fast Fourier transform techniques have been used to extract the frequency spectrum of the signal. This allows the identification of relaxation processes and attenuation of the signal by electrical conductivity. It also allows the use of shorter probes, whose signals have proved difficult to analyse accurately using conventional tangent-fitting (Heimovaara, 1994; Heimovaara *et al.*, 2004; Friel & Or, 1999; Jones & Or, 2001; Lin, 2003).

2 Reconstructing the waveform from an assumed model of the soil water distribution, soil characteristics and electrical conductivity, which is described by a number of adjustable parameters. Inverse modelling techniques (see Section 17.13) are employed to find the best set of parameters which fit the observed waveform (Yanuka *et al.*, 1988; Feng *et al.*, 1999; Heimovaara, 2001; Robinson *et al.*, 2003; Schaap *et al.*, 2003).

Both of these methods require significant amounts of computer processing; but as this becomes more cheaply available on portable computers, they may soon become a standard part of TDR methodology.

8.6.8 TDR – Conclusion

TDR has become the leading methodology for measurement of water content in soil. This is despite a number of theoretical difficulties in interpreting waveforms and the expense of the electronics involved. Its popularity has ensured that both scientific and commercial organisations have invested heavily in overcoming the inherent problems and to extract much more information from the TDR signal. It can be expected that this process will continue, with increasing ability not only to measure average water content reliably over the length of the probe but also to extract the distribution of water along it.

Electrical conductivity and its use to estimate solute concentration is dealt with in Chapter 21. However, this has a profound effect on the TDR signal and cannot be ignored. Advances in measurement of conductivity are necessary to interpret TDR waveforms reliably as well as being of interest in their own right.

For field use, however, TDR is likely to be limited to the relatively near surface for practical reasons of installation of rods and causing unacceptable disturbance to the site.

8.6.9 TDR-related methods

Time domain transmission

TDR measures the time taken for a pulse to travel the length of the rods and back again. This introduces a number of complications in interpretation of the signal, arising mainly from multiple reflections at the various discontinuities. These mean that the signal bounces back and forth along the line and makes interpretation of the trace difficult and, in some cases, impossible. A simpler, closely related method is TDT. In TDT, the signal travels just once through the medium and is collected at the opposite end of the line from where the pulse is injected. Unfortunately, the need to have access to both ends of the line limits its use to laboratory studies, where this is easily arranged, and to the very near-surface in the field. A device known as *Aquaflex* is manufactured by Streat Instruments in New Zealand. It is in the form of a 3 m long flexible ribbon, which is buried just below the ground surface. There are two pairs of conductors, joined at one end of the ribbon, so that the signal travels out along one pair and back along the other. This makes it relatively easy to detect the signal arriving after travelling twice the length of the device without involving a reflection. The volume of soil sampled is also large – about 6 L (Streat Instruments, http://www.streatsahead.com/products). However, the sensed volume is confined to about 22 mm from the sensor cable. Assuming burial just below the ground surface, this would account for about the upper 50 mm soil.

Acclima in the United States also manufactures a TDT, illustrated in Fig. 8.35. The primary market for this instrument is irrigation control. The device is installed at a shallow depth by burying beneath the roots of a crop or lawn. Because of the loop shape of the electrodes, it is difficult to envisage how it could be installed at depth without soil disturbance, but it may be possible to install it in a slit from the side of a pit without unacceptable disturbance. Blonquist *et al.* (2005b) reported good accuracy of measurement of permittivity in liquids simulating non-dispersive, non-conducting soil; non-dispersive, conductive soil and dispersive, non-conducting soil. Blonquist *et al.* (2005a, 2006) tested a device installed beneath the root zone of a grass sward as an aid to irrigation scheduling. They found that there was a small saving when compared with using meteorological

Fig. 8.35 Acclima TDT.

evaporation estimates to predict irrigation need, but a very large saving against a regular irrigation regime.

Water content reflectometer

Campbell & Anderson (1998) proposed an oscillator method, usually called a *water content reflectometer*, or a *transmission line oscillator*, as a cheaper alternative to full TDR, but retaining many TDR characteristics. The principles of this device are embodied in the CS616 reflectometer, manufactured by Campbell Scientific Inc. The CS616 has two 300 mm long rods of 3.2 mm diameter, separated by 32 mm. The electronics are contained in a small plastic block, which also holds the two rods. A photograph of the CS616 is shown in Fig. 8.36. In use, the rods are pushed into the soil, either from the surface or the side of a pit in the same way as for other rod-based instruments; 3.2 mm rods of this length are easily bent, and so Campbell Scientific recommend that, for soils which exhibit significant resistance to insertion, a tool having stronger rods of the same dimensions as the reflectomer rods be used to make pilot holes. A block of rigid plastic or metal with two parallel holes that guides them into the soil is also recommended.

Operation of the instrument is described by Campbell & Anderson (1998) and Kelleners *et al.* (2005). A fast rise-time pulse is applied to the two rods as for TDR. The pulse travels along the rods, is reflected from the end and arrives back at the starting point. The electronics recognises this as an increase in the voltage and switches the voltage on the rods to a low level, sending a second pulse along the transmission line of the opposite sign from the first one. A complete cycle, therefore, consists of four traverses of the length of the rods. There is a small delay, t_d, of around 1 ns between one pulse arriving at the start end of the rods and the next pulse being applied. The time, t, taken for one complete cycle is, therefore

$$t = \frac{4L\sqrt{\varepsilon_r}}{c} + 2t_d, \qquad (8.6.5)$$

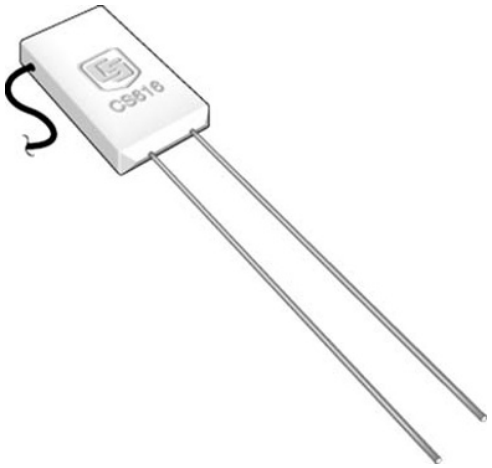

Fig. 8.36 CS616 water content reflectometer. Reproduced with permission of Campbell Scientific, Inc.

where L is the length of the rods. The time, t, is output as a square wave voltage with a period of $1024t$, which allows for common data loggers to record it as pulses or as a frequency.

The rise time of the pulse used in the CS616 is about 2 ns (Kelleners *et al.*, 2005), much longer than the typical 300 ps of a full-blown TDR, giving a maximum frequency in the signal in the region of 175 MHz, compared with about 1 GHz for a TDR. Instead of tangent-fitting, the arrival time is determined by the attainment of a fixed voltage level. Different amounts of pulse attenuation, therefore, feed into differences in travel time detected. An earlier version of the instrument, the CS615, used an 8 ns rise-time pulse (corresponding to a maximum frequency of 44 MHz) and multiplied the value of t by 32,768.

Seyfried & Murdock (2001), Chandler *et al.* (2004), Kelleners *et al.* (2005), Blonquist *et al.* (2005b) and Logsdon (2009) have all evaluated the CS615 and/or the CS616 against other devices. In general, they conclude that inter-sensor variability can be accounted for satisfactorily by

subtracting the period obtained from a simple measurement in air from all readings made with that sensor; that the manufacturer's calibration is satisfactory in some soils, but not in all, so that soil-specific calibration is usually required; that the primary limitation is that they are sensitive to electrical conductivity of the soil solution and/or relaxation effects resulting from the relatively low effective frequency of the measurement. Logsdon (2009) compared field calibrations of the CS616, using neutron probe measurements, with those obtained in the laboratory from undisturbed cores of the same high specific charge clay soils. The results did not agree well. Logsdon suggested that this may be because water in the field soil was distributed less evenly through the sensing volume than in the laboratory columns. In these circumstances, field lines would be more concentrated in the higher electrical conductivity (and therefore higher permittivity and higher water content) areas than in the drier parts, leading to higher detected permittivity for the same average water content.

Two newer models, the CS650 and CS655, have been introduced more recently that aim to overcome some of the limitations caused by attenuation of the signal by electrical conductivity of the bulk soil. They also provide a measure of electrical conductivity and temperature.

8.7 Capacitance Methods

The principle of capacitance methods is relatively simple. The soil forms the dielectric in a capacitor and the value of the capacitance is measured. There are a variety of ways in which the capacitance is measured. However, the term 'capacitance probe' is usually reserved for an instrument that incorporates the capacitor into an oscillator circuit and measures the oscillation frequency. For this reason, capacitance probes are often referred to as *frequency domain* devices.

At its simplest, an oscillator can be regarded as shown in Fig. 8.37, where the oscillator is formed of a capacitor and inductor. The impedance of the two components in series, according to Section 8.3.6 is

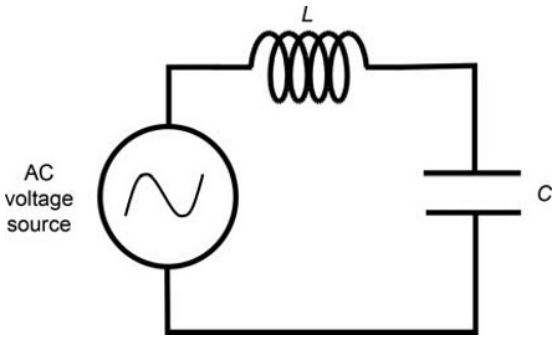

Fig. 8.37 Oscillator circuit composed of an inductance, *L*, and a capacitance, *C*.

$$Z = \frac{1}{j\omega C} + j\omega L. \tag{8.7.1}$$

The magnitude of this is given by

$$|Z| = \left|\frac{1-\omega^2 LC}{\omega C}\right|. \tag{8.7.2}$$

This is zero at an angular frequency of

$$\omega = \frac{1}{\sqrt{LC}} \tag{8.7.3}$$

or a normal frequency of

$$f = \frac{1}{2\pi\sqrt{LC}}. \tag{8.7.4}$$

In the absence of any resistance in the circuit, therefore, a current at a frequency of f would carry on for ever and not die away. This is called *resonance* and f the *resonant frequency*. As the alternating current surges round the circuit, it charges up the capacitor, first in one direction and then the other. The same current flowing through the inductor creates a magnetic field within and around it. When the capacitor is at maximum charge, the current is just starting to change direction, that is it is momentarily zero, and so there is no magnetic field and hence no energy stored in it. Conversely, when the current is maximum, the capacitor voltage is zero; there is no charge or energy stored in the capacitor, and all the energy is stored in the inductor's magnetic field. The energy in the system therefore swaps between the capacitor and the inductor.

The situation is similar to that of a swinging pendulum. Here, energy swaps back and forth between the kinetic energy of the moving bob and its potential energy. At the bottom point of the swing, the potential energy is lowest, but its velocity and hence kinetic energy is greatest. At either end of the swing, the bob is at its highest point and its potential energy is maximum, but its velocity is momentarily zero, and so it has no kinetic energy. The angular frequency of oscillation of a pendulum of length l is

$$\omega = \sqrt{\frac{g}{l}}. \tag{8.7.5}$$

where g is the acceleration due to gravity.

In a pendulum, the energy is dissipated through friction in the pivot and air resistance. In the electronic oscillator, there is always some resistance in the circuit and this dissipates the energy associated with the oscillation. To make

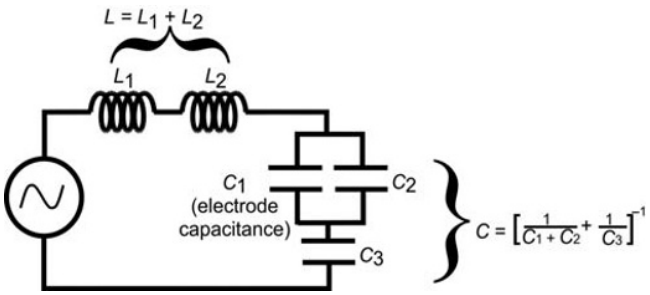

Fig. 8.38 Equivalent circuit of a practical capacitance probe. L_1 is the inductor on the circuit board, while L_2 arises from interaction between circuit components and tracks. C_1 is the capacitance between the probe electrodes, C_2 is capacitance resulting from interaction between circuit components and tracks and C_3 is the sum of capacitors on the printed circuit board.

practical use of either of these devices, as, for instance, in a clock or a capacitance probe, this lost energy must be replaced and the frequency measured.

In a clock, the solution is usually an escapement, which both feeds energy into the pendulum from a spring or weight and allows each swing of the pendulum to control the rotation of the hands via a gear train. Similarly, the oscillations in a capacitance probe are maintained by a transistor, which feeds energy into the circuit from a battery to replenish that lost, mainly through resistance in the circuitry or leakage through the capacitor dielectric – that is the soil. The oscillation frequency is measured by counting the voltage oscillations.

In a practical probe, the circuit is more complex than that depicted in Fig. 8.37, both because of the need for a transistor to maintain the oscillation and because of the capacitance and inductance of the components and the circuit wiring

The equivalent circuit of the probe can be represented approximately as shown in Fig. 8.38. Here, the circuit inductance, L, is formed of a small air-cored inductor, L_1, as well as stray inductances, L_2, on and around the circuit board (Dean, 1994). The capacitance between the electrodes of the probe, C_1, is both in parallel and in series with other capacitances in the circuit, which has the effect of diluting any variations of C_1. The parallel capacitance, C_2, is caused by stray electric field outside the printed circuit board. This varies from one instrument to another, and so C_2 must be measured for each probe. C_1 and C_2 are in series with the sum of the capacitors on the printed circuit board, C_3, including that between the electrodes of the transistors, which also vary between probes.

With these circuit components, the combined capacitance of C_1, C_2 and C_3 is given by

$$\frac{1}{C} = \frac{1}{C_1 + C_2} + \frac{1}{C_3}, \tag{8.7.6}$$

leading to an angular oscillation frequency of

$$\omega = \sqrt{\frac{1}{L}\left(\frac{1}{C_1 + C_2} + \frac{1}{C_3}\right)}. \tag{8.7.7}$$

The electrode capacitance, C_1, is then

$$C_1 = \frac{C_3}{\omega^2 L C_3 - 1} - C_2. \tag{8.7.8}$$

This contains three parameters which may be instrument-dependent: C_2, C_3 and L. C_1 depends on the design of the probe and electrodes. It should not vary between probes of the same design and electrode configuration.

8.7.1 Probe configurations

An advantage of the capacitance probe is that a wide range of electrode configurations is possible, although only the depth probe arrangement is in common use.

Depth probes

Dean *et al.* (1987) designed a probe for use at different depths within an access tube, in a similar way to a neutron probe. The electrodes were two cylinders mounted on a plastic former one above the other and separated by a small gap. This arrangement can be inserted into an access tube and readings made at different depths, utilising the 'fringing field' between the two cylinders. Enough of this passes through the soil outside the tube to make it very sensitive to changes in water content, and hence permittivity, of the soil. Because the high frequency oscillatory electromagnetic field needs to penetrate into the soil, the access tube must be made of a non-conducting, non-magnetic material, usually PVC. Figures 8.39 and 8.40 show the arrangement.

Depth probes are suitable both for permanent installation and as a portable instrument which can be carried between permanently installed access tubes. Both types are available commercially, the principal manufacturer being Sentek of Australia.

The *EnviroScan* is designed for permanent installation in an access tube, connected to a field data logger. A number of units, similar to that of Dean *et al.* (1987), are mounted at different depths on a plastic frame inside the PVC access tube. A ribbon cable running the length of the frame powers the units and transmits frequency information to the data logger. Figure 8.39 is a photograph of the device, while Fig. 8.40 shows diagrammatically the field lines associated with each sensor.

Sentek also produce the *Diviner*, which has essentially the same circuitry as the *EnviroScan*, but is packaged inside a robust casing for manual insertion into one or more pre-installed access tubes, in a similar manner to the use of a neutron depth probe. The *Diviner* incorporates a data logger and magnetic switches set at different depths to record automatically probe frequency at preset depths. Data acquisition with a *Diviner* is very fast, as the probe needs only to

Fig. 8.39 Sentek *EnviroScan* capacitance probe system showing the two cylindrical electrodes of each sensor unit. The printed circuit board of each unit is located inside the rings, with the main control board at the top. The ribbon cable connecting each sensor's printed circuit board to the main control board runs behind the plastic partition between the sensors. In operation, the complete assembly is placed inside the plastic access tube, the top of which can be seen protruding above the ground surface. Photograph reproduced with permission of Sentek Pty, Australia. (*See insert for colour representation of the figure.*)

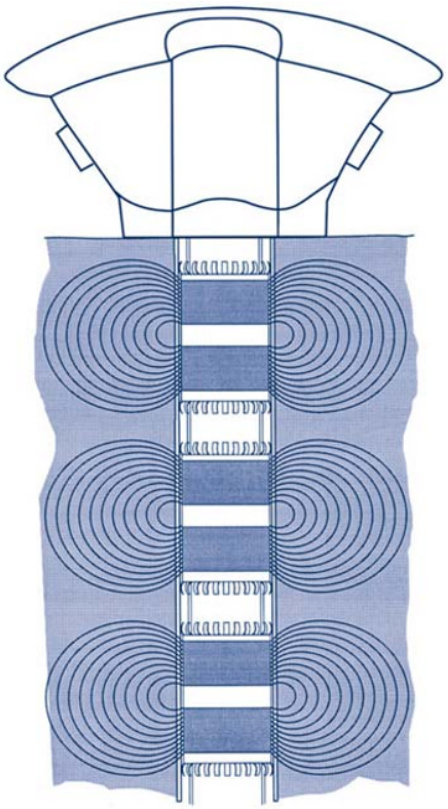

Fig. 8.40 Diagrammatic representation of a multiple sensor depth capacitance probe system, showing field lines between the ring electrodes. Reproduced with permission of Sentek Pty, Australia.

be inserted into the access tube to its maximum extent and all the recording of position and frequency is taken care of for downloading later.

Less sophisticated devices produced by Troxler in the United States, the Sentry 200 & 2000, and by Didcot Instruments in the United Kingdom are no longer in production, although a number may still be in use.

Surface probes

An arrangement with parallel rods embedded in the soil is probably the simplest electrode arrangement, as shown in Figs. 8.41 and 8.42. In contrast with the depth probe, the electrodes are in direct contact with the soil and the majority of the field passes directly through the soil. The arrangement is suitable for both portable use and permanent installations. In the former, as shown in Fig. 8.41, the probe electronics, display and electrodes form a single unit, which is lightweight and suitable for repeated insertion into the soil. Permanent installations have the probe electronics and electrodes in a single unit, with a connection via cable or optical fibre to a remote reader, which may be a data logger or a portable unit, connected when a reading is needed. An intermediate solution is to leave the electrodes permanently embedded in the soil and to connect to them with a unit containing the main electronics and a reader when required. This minimises the expense of having many permanently installed devices, while keeping the advantages of repeated measurements at one spot. Care is obviously required to make sure that the electrodes are not disturbed when connecting the electronic unit to them. A schematic of these methods of installation is shown in Fig. 8.43.

This type of probe need not necessarily be used from the soil surface. The surface in question may be a vertical face of a trench or pit dug for the purpose or the end of a hole excavated vertically, horizontally or at some angle into the ground (see Fig. 8.43).

While parallel rods are the most common arrangement for a surface probe, other configurations may be used. Two parallel plates have the advantage that the field between them is almost uniform, ensuring a more even and predictable weighting of the contribution from different parts of the soil between the electrodes. This needs to be weighed against the difficulty of and possible disturbance to the soil from inserting the electrodes.

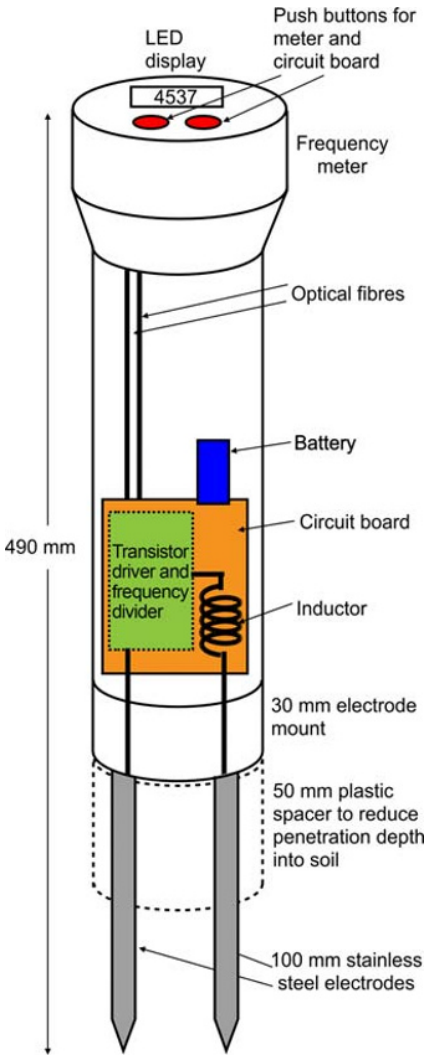

Fig. 8.41 Parallel rod capacitance probe configured for use as a portable instrument to measure water content of the upper 50 or 100 mm of soil.

Fig. 8.42 Photograph of parallel rod capacitance probe depicted in Fig. 8.41.

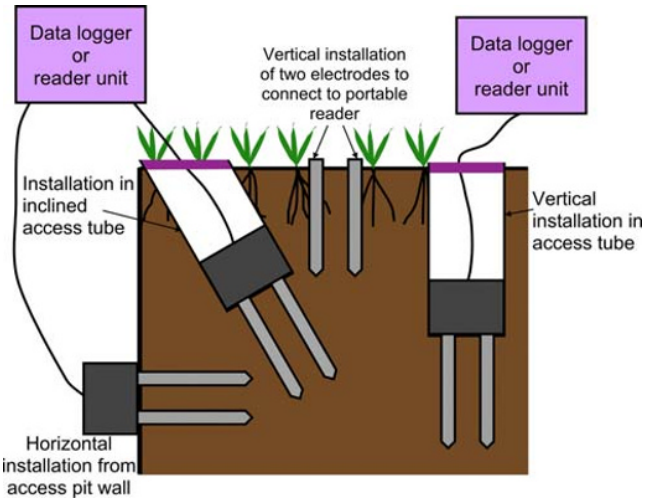

Fig. 8.43 Options for permanent installation of twin-rod capacitance probes.

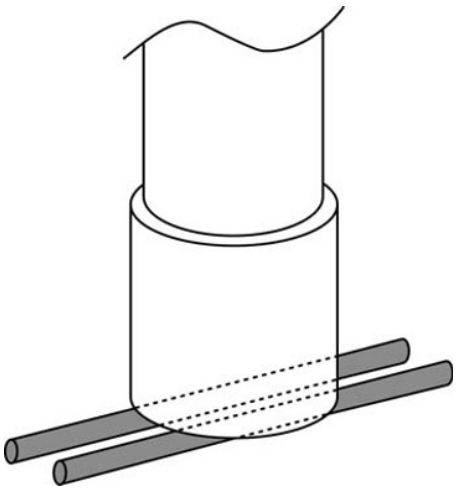

Fig. 8.44 Non-invasive parallel rod capacitance probe suitable for surface measurements in masonry or hard soils. Redrawn from Dean (1994). Reproduced with permission of © NERC (CEH).

Capacitance probes can accommodate a wide variety of electrode arrangements. Whalley *et al.* (1992) incorporated electrodes into the tine of a cultivator, which was dragged through the soil, giving a continuous reading of soil water content as it went. Another arrangement, described by Dean (1994), had two parallel rods mounted at right angles to the probe body as shown in Fig. 8.44. These can be laid on the surface of soil or porous rock to give a reading sensitive to a shallow layer. This is useful for both very near-surface measurement and where penetration with vertical rods is impossible or causes unacceptable disturbance.

8.7.2 Probe calibration

Two approaches have been proposed to convert frequency to permittivity for capacitance probes.

Scaled frequency

The first is an empirical approach, recommended by Sentek for *EnviroScan* probes (Sentek, 2011) and described by Paltineanu & Starr (1997) and Baumhardt *et al.* (2000). It is an extension of the philosophy for inter-calibrating neutron probes in which the count rate in soil is divided by a standard count to give a count ratio (Section 7.7.1). That depended on the assumption that all count rates are proportional to the strength of the neutron source and the efficiency of the detector and its associated circuitry. Things are not so simple with capacitance probes. Each unit displays a different frequency in air, f_a, and in water, f_w. The Sentek (2011) procedure reduces the measured frequency, f, to a *scaled frequency*, F:

$$F = \frac{f - f_w}{f_a - f_w}. \tag{8.7.9}$$

The procedure works well for *EnviroScan* sensors, which exhibit only a small range of values of f_a and f_w between different examples.

Most workers have calibrated directly between scaled frequency and water content of the soil.

A frequency-response model approach

Robinson *et al.* (1998) and Kelleners *et al.* (2004a) took a different approach. Robinson *et al.* (1998) took the theoretical model developed by Dean (1994), which predicts the form of the frequency v electrode capacitance, C_1, relationship for the instrument (Eq. 8.7.7). The model has three sensor-dependent parameters: C_2, C_3 and L. By assuming a common value for C_3 for all instruments, the number of unknowns is reduced to two and so a measurement of frequency in air and water allows both to be calculated. Note that the notation used here, which is that of Robinson *et al.* (1998), is different from that of Dean (1994).

To use this approach, the geometric factor, g, for the electrodes must be known, so that their capacitance in air and water can be calculated. These values are then inserted, along with the appropriate frequency measurements, into Equation 8.7.7 to solve for C_2 and L.

For electrodes designed to be in direct contact with the soil, Robinson *et al.* (1998) used the similarity between electrical conductance and capacitance to estimate g. The electrical conductance, G, between a pair of electrodes immersed in a medium of conductivity σ is given by

$$G = g\sigma \tag{8.7.10}$$

and the capacitance, C_1, of the electrode pair is

$$C_1 = g\varepsilon. \tag{8.7.11}$$

So, knowing σ and measuring G, the capacitance of the electrodes when embedded in a medium of permittivity ε will be

$$C_1 = \frac{\varepsilon}{\sigma} G. \tag{8.7.12}$$

Measurement of conductance is generally more straightforward than that of capacitance, requiring only a cheap ac conductivity meter and a solution of known conductivity. The meter should operate at a frequency above about 1 kHz to avoid polarisation effects resulting from electrolysis of the solution. For electrode configurations which are not in direct contact with the medium, such as that of the *EnviroScan*, then a direct measure of the capacitance can be made using a 'universal' bridge.

The procedure took no account of the change of apparent permittivity with frequency when the length of the probe rods is comparable with the wavelength of the oscillation (Fig. 8.18). It must therefore be regarded as being at least semi-empirical, but produced very good results when tested against the frequency obtained in liquids of known permittivity.

Kelleners *et al.* (2004a) used a similar philosophy to calibrate a depth probe configuration. They envisaged the equivalent circuit of Fig. 8.45, in which C_3 does not appear. However, an additional capacitor, C_p, is introduced to take account of the electrodes not being in direct contact with

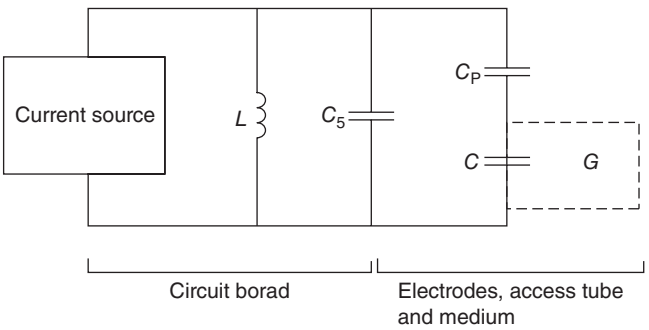

Fig. 8.45 Equivalent circuit for depth capacitance probe (Kelleners *et al.*, 2004a). Reprinted with Permission of ASA, CSSA, SSSA.

the soil, but via a small air gap and plastic access tube. They found that the probe could be calibrated successfully with the access tube in air and water by fixing the value of L and g_m (equivalent to the geometric factor, g, in Robinson *et al.*'s (1998) formulation) and solving for C_p and C_s (equivalent to C_2 of Robinson *et al.* (1998)).

Although the conceptual circuitry used by Robinson *et al.* (1998) and Kelleners *et al.* (2004a) was different, they both achieved good agreement with experimental results. This suggests that the approach is largely empirical and that particular values for the 'components' of the circuit cannot necessarily be identified with physical features.

The actual variation of frequencies recorded in air and water between different examples of the same probe design (J D Cooper, unpublished data; Baumhardt *et al.*, 2000; Paltineanu & Starr, 1997) differ by only a modest amount, typically less than 1%. There is, therefore, very little scope for a material difference in estimates of ε_r obtained by either the scaled frequency or frequency-response model approach, although there do not appear to be any published comparisons. The frequency-response model approach provides a framework for taking into account dielectric losses, arising from either electrical conductivity or relaxation effects (Robinson *et al.*, 1998; Kelleners *et al.*, 2004a). In liquid media with known electrical conductivity, these are successful.

Kelleners *et al.* (2004b) used a hybrid approach in a saline silty clay soil, using the scaled frequency approach to standardise between probes, while retaining the frequency response model of Kelleners *et al.* (2004a) to incorporate independently measured electrical conductivity and obtain ε_r, and hence θ. This was partially successful, although it was found that the predicted electrical conductivity of field soil overestimated considerably that measured by conventional methods, possibly because the electrical conductivity is anisotropic as a result of soil layering.

8.8 Theta and Profile Probes

The *Theta Probe* was invented by Gaskin & Miller (1996). It uses a transmission line approach to measure a fixed frequency voltage resulting from an impedance mismatch between a coaxial cable and rods in the soil. The arrangement is as shown in Fig. 8.46.

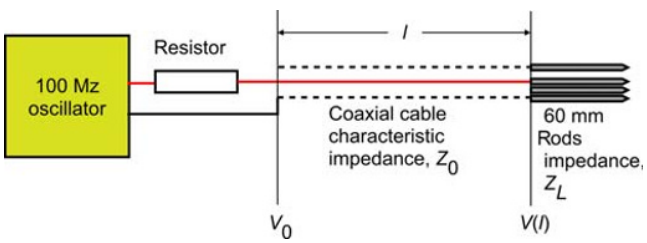

Fig. 8.46 Schematic construction of a Theta Probe.

To understand the probe's operation, some further development of transmission line theory is needed. Gaskin & Miller (1996) presented the theory in terms of two transmission lines, the second one being that formed by the rods of the probe. However, it may be better to regard this second, short, line as a capacitor. To understand this, we use Equation 8.5.31 to give the voltage at each end of the coaxial line. The voltage, $V(l)$, at the junction of the transmission line and the rods is given by

$$V(l) = V_1\left(1 + \frac{Z_L - Z_0}{Z_L + Z_0}\right)e^{-j\frac{\omega l}{v}}e^{j\omega t}, \tag{8.8.1}$$

and the voltage at the beginning of the line, where $x = 0$, is

$$V_0 = V(0) = V_1\left(1 + \frac{Z_L - Z_0}{Z_L + Z_0}e^{-j\frac{2\omega l}{v}}\right)e^{j\omega t}. \tag{8.8.2}$$

In the *Theta Probe*, the length of the transmission line, l, is equal to one quarter wavelength of the oscillation, that is $l = \frac{\pi v}{2\omega}$ so $e^{-j\omega\frac{l}{v}} = e^{-j\frac{\pi}{2}} = -j$ since, using Equation 8.3.42, $\cos\left(-\frac{\pi}{2}\right) = 0$ and $\sin\left(-\frac{\pi}{2}\right) = -1$. Similarly, $e^{-2j\omega\frac{l}{v}} = e^{-j\pi} = -1$. Substituting this into Equations 8.8.1 and 8.8.2, we get

$$V(l) = -jV_1e^{j\omega t}\left(1 + \frac{Z_L - Z_0}{Z_L + Z_0}\right), \tag{8.8.3}$$

and

$$V_0 = V_1e^{j\omega t}\left(1 - \frac{Z_L - Z_0}{Z_L + Z_0}\right). \tag{8.8.4}$$

The factor $-j$ in Equation 8.8.3 signifies that the voltage at one end of the line is $(\pi/2)$ out of phase with that at the other end.

The *Theta Probe* measures the difference between the magnitude of these two voltages:

$$|V(l)| - |V_0| = 2V_1\frac{Z_L - Z_0}{Z_L + Z_0}. \tag{8.8.5}$$

Knowing the voltage difference between each end of the transmission line, therefore, the impedance of the rods, Z_L, can be calculated, since Z_0 is a characteristic of the line. This in turn allows computation of the permittivity of the medium in which the rods are immersed. Assuming that Equation 8.5.36 applies, then Z_L is linearly related to the permittivity of the medium, although the value of the capacitance is not easily predicted by simple means as a consequence of end effects and the rod arrangement. Calibration is therefore necessary. This also takes into account the non-linear nature of the effective capacitance discussed in Section 8.5.3.

The optimum length for the rods at the *Theta Probe* frequency of 100 MHz is 83 mm (Gaskin & Miller, 1996),

Fig. 8.47 Photograph of an ML3 Theta Probe. Image courtesy of Delta-T Devices Ltd.

since this is one-quarter wavelength in water. In this case, the rods would appear to be a short circuit on the end of the transmission line and the range of voltage between air and water would be maximised. In practice, a length of 60 mm is used, as 83 mm rods may be too delicate for use in many soils.

Figure 8.47 shows a photograph of a *Theta Probe*.

The probe circuitry transforms the voltage across the transmission line, V_i–V_0, into a zero dc output voltage when the rods are in air and about 1.1 V when in water. The output is very nearly linear in $\sqrt{\varepsilon_r}$ up to values of ε_r of about 36, which includes most of the permittivity range found in mineral soils.

The relationship is close to (Miller & Gaskin, 1999):

$$\sqrt{\varepsilon_r} = 4.4V + 1.10, \tag{8.8.6}$$

where V is the probe output in volts.

Since in most cases, $\sqrt{\varepsilon_r}$ of soil is approximately a linear function of water content, the *Theta Probe* output is almost linear in volumetric water content.

A more accurate representation of the Probe voltage output with relative permittivity is (Miller & Gaskin, 1999)

$$\sqrt{\varepsilon_r} = 4.70V^3 - 6.40V^2 + 6.40V + 1.07. \tag{8.8.7}$$

These expressions relate to the ML2x version of the probe. The original ML1 and newer ML3 versions have slightly different expressions.

Water content can be derived by combining this expression with one for the variation of water content with permittivity. It is important to use a relationship appropriate to the probe's 100 MHz frequency. This can be accomplished by inserting the probe rods into a sample of soil, taking a reading and then sampling a cylinder of soil of length equal to that of the rods (60 mm) and including all the soil between and just outside the rods (see Section 8.14).

Effect of electrical conductivity and relaxation effects

The imaginary part of the soil permittivity is expected to influence the *Theta Probe* output, since it will affect the impedance represented by the rods embedded in the soil (Eq. 8.5.48 and Fig. 8.20). As both the *Theta Probe* and Profile Probe operate at a fixed frequency of 100 MHz, the effect of medium conductivity and relaxation effects cannot be distinguished.

Robinson *et al.* (1999) found no effect of electrical conductivity on *Theta Probe* output in sandy soils in the laboratory, although in ionic solutions increasing electrical conductivity decreased the probe output (i.e. reduced the apparent water content). Robinson *et al.* (1999) suggested that this might be a consequence of the concentration of probe sensitivity around the central conductor, although they gave no more detailed explanation.

Three versions of the *Theta Probe* have been produced – designated ML1x, ML2x and ML3. Differences are fairly minor, but include the following:

- A better oscillator source in the ML2x giving a more pure sinusoidal waveform with lower harmonic content.
- Replacement of the original coaxial transmission line by a chain of discrete capacitors and inductors, which is more compact and further suppresses harmonics.
- The ability to dismantle the ML2x for maintenance and repair.
- The ML3 is claimed to have less sensitivity to temperature and electrical conductivity of the soil.
- The ML3 has a detachable cable and a mount for extension rods.
- There is a small difference in response to medium permittivity and electrical conductivity between the three designs (Miller & Gaskin, 1999; Delta-T, 2013).

The *Theta Probe* is manufactured by Delta-T Devices, Cambridge, UK.

The *Theta Probe* is also used as a component of the *Equitensiometer*, manufactured by the same company for measurement of water potential and described in Section 13.3.

The Profile Probe

The principles of the *Theta Probe* have been applied to a depth probe, known as a *Profile Probe*, which can measure at a series of depths from a glass fibre-reinforced epoxy access tube of 28 mm diameter (Fig. 8.48). The uniformity and thickness of the tube wall is critical to the probe's calibration, and so only tubes obtained from the manufacturer which have been checked for consistency should be used.

The electrodes are similar to those of capacitance depth probes, such as the Sentek *EnviroScan*, being two rings around a plastic tube, which forms the body of the probe (Fig. 8.39). However, the rings do not extend all the way around the body as in other devices, but have a small gap. This probably increases the axial asymmetry of the device, making it more important to ensure that it is placed in exactly the same orientation each time it is replaced into the soil. The tubes have an alignment mark on them to aid in this, but no particular mark on the body of the probe. There are, however, three screws holding the cap of the probe to the body and choosing the one of these closest to the manufacturer's label will ensure consistent

positioning (Fig. 8.48). Two versions are available: a short one with electrodes at 100, 200, 300 and 400 mm depth and a longer one with two extra electrode pairs at 600 and 1000 mm depth.

Fig. 8.48 Delta-T PR2 Profile Probe (upper part) in epoxy access tube. Image courtesy of Delta-T Devices Ltd.

The *Profile Probe* has also been produced in two versions, the original was designated PR1, with later versions as PR2. It is suitable for use both for manual data collection in a network of tubes and as a permanently installed device. In the latter application, it can be connected to a data logger for unattended monitoring of water content over time at several depths. Care must be taken when placing the probe onto an access tube. There is a groove and retained 'O'-ring in the underside of the top cap, which must be pressed down to seat firmly onto the top of the access tube. And the orientation must be correct. For mobile application, Delta-T produces a small handheld reader (the HH2), which can also be used with *Theta Probes* and *Equitensiometers*. Alternatively, it is not too difficult to provide power from a small battery pack and use a portable digital voltmeter to read the output.

One possible strategy is to place a *Profile Probe* in an access tube connected to a data logger and then periodically, say weekly, to remove it from that tube and take manual readings from a network of nearby tubes using a handheld reader, replacing the *Profile Probe* in its 'permanent' position afterwards.

For some applications, the depth limitation of 1 m is a disadvantage. No easy solution exists for this, although it may be possible to place an access tube at the bottom of a deeper and wider lined hole, in a similar manner to that described for tensiometer placement (Section 12.6 and Fig. 12.14).

8.9 ECH2O Probe

The *ECH2O Probe*, developed and manufactured by Decagon Devices, uses another approach to measure the medium permittivity. Early versions (EC20) used a relatively low-frequency 5 MHz square-wave oscillator and 200 mm long electrodes. Later ones (EC5) have 50 mm long electrodes and a 70 MHz oscillator. The basic circuit arrangement is shown in Fig. 8.49. An oscillator feeds a square-wave voltage signal through a resistor, R, to the probe electrodes, which in this case are flat copper conductors encased in a plastic insulator. The electrodes, with capacitance, C_e, plus any stray capacitance, C_s, in the circuit form a capacitor of capacitance, C. This capacitor is

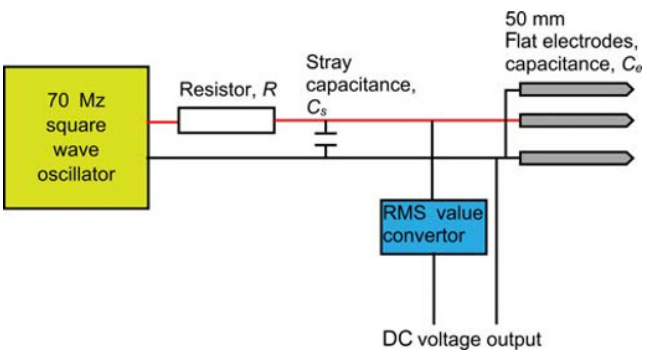

Fig. 8.49 Schematic diagram of an ECH2O PROBE.

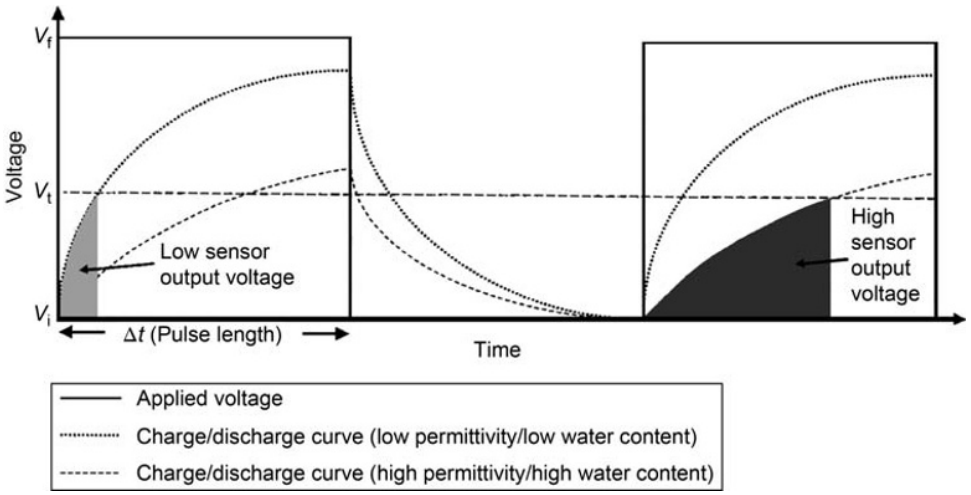

Fig. 8.50 Voltage variation on capacitors of large and small value in response to a square-wave input voltage. The average voltage on the larger capacitor is greater while below the threshold, V_t, (darker shaded area) than that of the smaller capacitor(lighter shaded area). From Bogena *et al.* (2007). Reproduced with permission of Elsevier Science Publishers B.V.

measured by repeatedly charging and discharging it as the voltage applied to resistor, R, switches between two fixed voltages. If the voltage, V, on the capacitor immediately after the supply voltage switches from zero to a voltage V_f, is V_i, then according to the analysis in Section 8.3.2 and Equation 8.3.14, V will be after a time t:

$$V = V_i + (V_f - V_i)\left(1 - e^{-\frac{t}{RC}}\right). \qquad (8.9.1)$$

The larger the value of C, the greater the time constant, RC, and so the smaller the voltage on the capacitor at any time. However, since it takes a longer time to reach a threshold value, V_t, the average voltage during which it is less than this value, will be greater, as shown in Fig. 8.50. Taking the root-mean-square voltage below the threshold voltage and rejecting that above it gives a dc output approximately linear in $\sqrt{\varepsilon}$.

Bogena *et al.* (2007) and Kizito *et al.* (2008) both presented laboratory comparisons of the performance of the EC5 version of the *ECH2O* probe against known liquid dielectrics of different electrical conductivity and temperature. They found only limited sensitivity to both variables. The TE version of the probe incorporates both temperature and electrical conductivity sensors, allowing the readings to be corrected for both, as well as providing measurement of these important variables. Laboratory tests in soil gave calibration curves that differed from the conventional TDR equations, but varied little between soils. Field tests also gave encouraging results.

8.10 Hydra Probe

The *Hydra Probe* shares some similarities with the *Theta Probe* in having a very similar electrode configuration and relying on a fixed frequency measurement (in this case 50 MHz), which relates to the characteristic impedance of the electrodes. The permittivity of the soil in which the sensor electrodes are embedded is calculated from this. Unlike the *Theta Probe*, however, the *Hydra Probe* measures both the real and imaginary parts of the permittivity, allowing for separate estimation of the electrical conductivity of the medium. The rods of the *Hydra Probe* are 57 mm long in a circle of diameter 30 mm.

Fig. 8.51 The Hydra Probe. Photo courtesy of Stevens Water Monitoring Systems Inc.

The *Hydra Probe* (Fig. 8.51) has evolved from the work of Campbell (1990), who devised a simple way to measure both real and imaginary parts of the electrode array.

8.11 Installation of Access Tubes for Dielectric Probes

Most of the earlier discussion about field measurements, particularly that related to neutron probes (Section 7.3) and TDR (Section 8.6.2), applies to all dielectric probes. The general principles will not, therefore, be repeated. All dielectric devices have a smaller measurement volume than the neutron probe, and so even greater care is needed to avoid soil and ground disturbance.

Different manufacturers and commentators advocate various ways to achieve this (e.g. Bell *et al.*, 1987; Sentek,

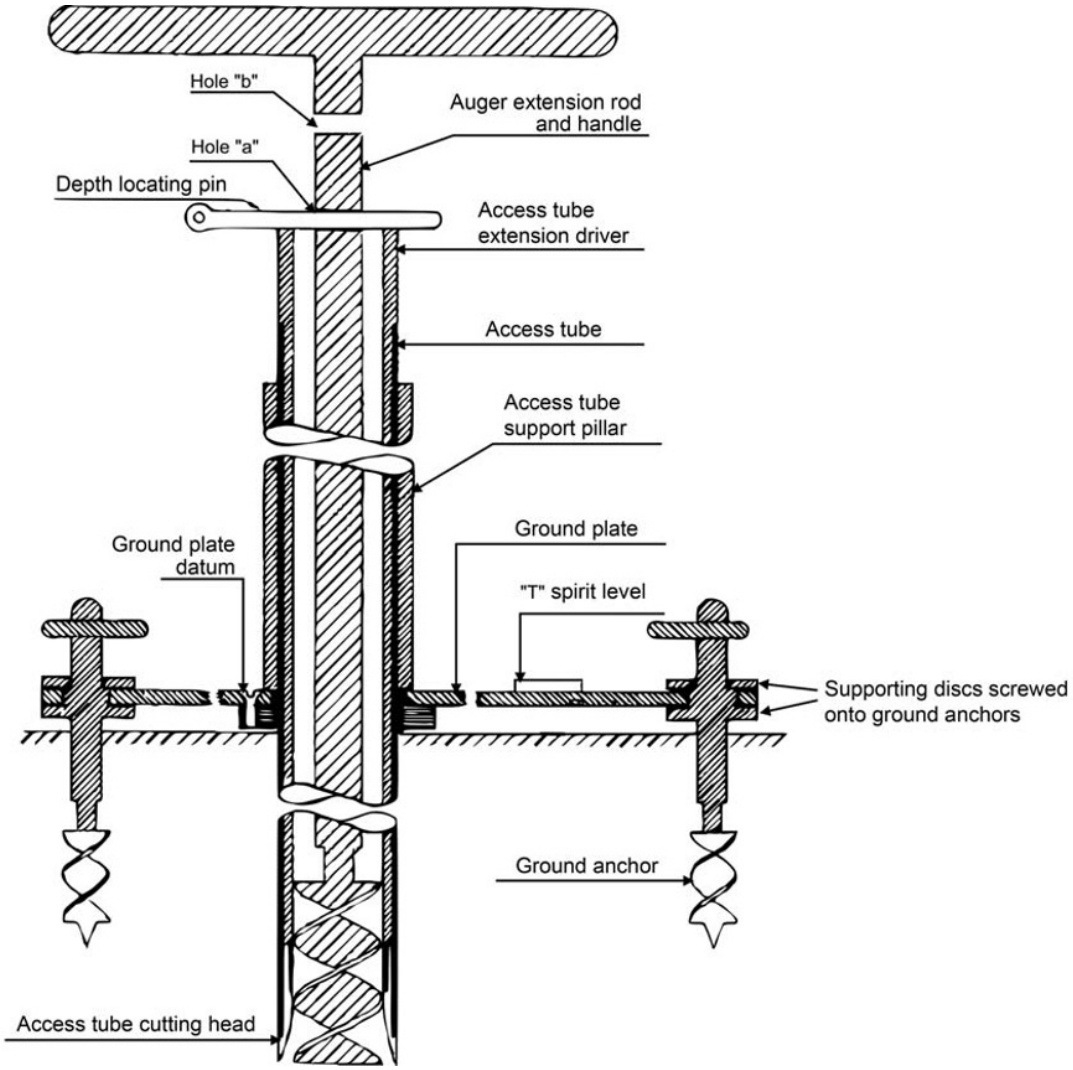

Fig. 8.52 Installation equipment for plastic access tubes. The equipment includes ground anchors to hold the baseplate rigid, a plastic pillar to support the access tube and prevent lateral movement and a steel inner guide tube to drive a steel cutting shoe fixed to the bottom of the access tube. For recovery of known volume soil samples from inside the access tube for soil calibration, the bottom of the auger is ground flat and holes are drilled in the auger stem for a locating pin. From Bell *et al.* (1987). Reproduced with permission of Elsevier Science Publishers B.V.

2003; Delta-T, 2005), but all employ similar principles to protect the ground surface and crop and to support the access tube and/or boring equipment to avoid enlargement of the hole near the surface.

The ground surface and crop are protected by a metal plate or tripod, which is anchored to the soil by sturdy metal stakes or screw augers. Keeping most of the assembly above the soil surface helps to prevent crop damage and avoids surface compaction.

An extended support, fixed to the ground protection plate, for the access tube or the shaft of an auger minimises the danger of hole enlargement by lateral movement of the equipment during installation.

As an illustration, the method described by Bell *et al.* (1987) will be used. As noted earlier, the access tube must be made of plastic and so does not possess the strength or rigidity of most metals. The equipment and procedure is a development of that used for installing neutron probe access tubes, incorporating additional measures to minimise disturbance to the soil around the tube.

Bell *et al.* (1987) devised a rigid aluminium baseplate (Fig. 8.52), which could be anchored firmly to the ground using short (~200 mm) screw augers which locked to the baseplate. This enables the baseplate to be mounted level, with its centre 40 mm above the ground surface, thus avoiding pressure on the surface. A 640 mm long plastic sleeve screws into a boss in the centre of the baseplate. The plastic sleeve is a sliding fit for the plastic access tube (50 mm outside diameter in their case), keeping it vertical and avoiding a gap forming around the top of the tube in the soil.

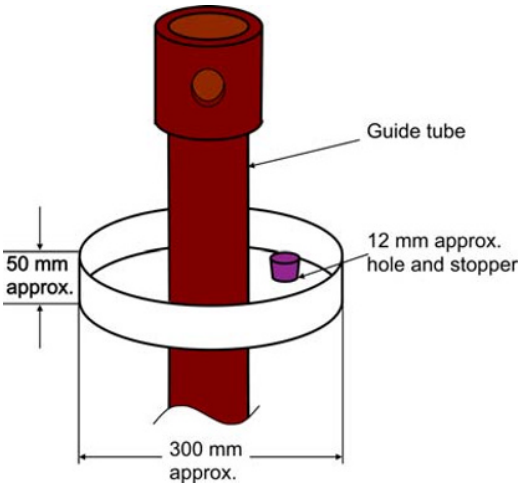

Fig. 8.53 Collecting tray to avoid soil loss from the top of the guide tube.

The access tube is fitted with a steel cutting edge of the same outer diameter and bevelled on the inside. A steel tube, a few millimetres longer than the access tube, fits into the cutting head. A steel driver head, similar to that depicted in Fig. 7.11a, screws to the top of this tube to take the impact of driving the tube into the ground.

Bell *et al.* (1987) also devised a procedure for recovering known volume samples of soil during installation of the access tube for subsequent calibration of the capacitance probe. To collect accurate volume samples, a screw auger with a flat bottom is needed, of diameter slightly smaller than the inner diameter of the steel guide tube. The stem of the auger has two holes drilled through it to take a locating peg. One hole is positioned so that when the end of the auger bit is level with the bottom end of the cutting shoe, a locating peg through that hole rests on the top of the steel guide tube. The other hole is 40 mm above this, so that when a locating peg in this hole rests on the top of the steel tube, the end of the auger protrudes exactly 40 mm beyond the end of the cutting shoe. Also to aid accurate depth location, the access tube should be marked at 40 mm intervals.

A shallow plastic tray of diameter about 300 mm, with a circular hole in the centre of diameter equal to the outside diameter of the access tube, is valuable to catch loose soil. The tray should have a hole of about 25 mm diameter in its base near the outside edge, which can be sealed with a rubber bung, to make emptying soil from the tray simple (see Fig. 8.53).

The procedure is as follows. Steps 7–11 are almost identical to those described for obtaining samples for neutron probe calibration, described in Section 7.7.2. Figure 7.20 gives further information.

1 Set up the baseplate at the chosen spot by placing it on the ground and screwing the three ground anchor augers into the soil through the holes in the corner of the baseplate, leaving sufficient protruding to allow the baseplate to sit the correct distance above the surface. This should be so that the top of the boss in the baseplate is the same distance above the ground as the desired stick-up (the amount of access tube protruding above the surface – usually about 40 mm).

2 Fix the screw augers to the baseplate using the threaded discs to hold the baseplate rigid and level.

3 Screw the plastic sleeve into the boss in the centre of the baseplate.

4 Fit the steel guide tube into the cutting shoe through the plastic access tube and gently lower the assembly into the plastic sleeve so that the cutting shoe rests on the ground surface.

5 Using the rammer, gently tap the top of the steel tube 80 mm into the soil. Markings on the access tube should align with the top of the plastic sleeve to achieve this.

6 Place the locating peg in the lower hole of the auger stem and auger out soil from the tube and discard. Repeat until no more soil is removed. This ensures that the tube is empty and the hole reaches 80 mm below the surface. Reliable measurements in the upper 80 mm of the soil are difficult to achieve, as the field between the probe electrodes is partly in air.

7 Now transfer the locating peg to the upper hole of the auger stem and auger until the peg reaches the top of the guide tube. Remove the auger from the steel tube and shake the soil into a small polythene bag. The plastic tray around the access tube should ensure that no soil is lost. It is important to put this soil into the plastic bag immediately to prevent loss of water from it. This is most conveniently done by sweeping the soil with a small brush through the hole in the tray and into the plastic bag. Repeat this until no more soil is recovered, as some soil often falls off the auger and back into the hole. The hole should now extend 40 mm beyond the end of the cutting shoe.

8 Gently tap the top of the steel tube with the rammer until it advances by 40 mm (i.e. to the bottom of the prebored hole).

9 Replace the locating peg in the lower hole of the auger stem and auger out the loose soil that has been shaved from the side of the hole. Transfer the soil to the plastic bag. Repeat as many times as necessary to remove all of the loose soil. Seal the bag and label it with a marker pen with date, site and hole identification and depth range. Seal inside another bag to minimise evaporation and place inside a covered container or, preferably, a cooled box, in a shady place.

10 Repeat steps 8–10 until the top of the access tube is level with the top of the boss in the baseplate. The access tube should now protrude 40 mm above the ground.

11 Seal the bottom of the access tube. This may be done with a close-fitting rubber bung or an expanding silicone rubber sealing device (Fig. 7.14). Depending on the soil, a rubber bung may be difficult to insert against air pressure in the tube (or water pressure if the hole penetrates below the water table). In some situations, a rubber bung has a

tendency to work its way up the tube and so an expanding seal, albeit more expensive, is a safer option.

NOTES

- This procedure envisages installing the tube as a single length. For a tube longer than about 1.5 m, a stable platform for the installer to stand on above the ground is needed. An alternative procedure is to machine the access tube before installation into approximately 1.5 m lengths, with a socket on one part and spigot on the other. The tube is usually quite thin-walled, so the ends are easily damaged. The two parts can be joined using PVC glue as they are installed. There is a danger that glue will intrude into the access tube, making it impossible to insert the probe, so it is important to apply glue only to the spigot (i.e. the male part). This will ensure that excess glue is extruded only on the outside of the joint, allowing it to be wiped off. The steel guide tube will also need to be sectional and screwed together.
- Friction between the plastic tube and the formation can be very considerable, especially in clay soils. The method of installation described requires that the plastic tube be pulled into the soil by the cutting shoe. Failure of the plastic around grub screws used to fix the cutting shoe to the tube is commonly experienced. When this occurs, some progress may be made by driving the top of the plastic tube directly and pushing the plastic tube, rather than pulling it. However, plastics are generally good at absorbing impact, rather than transmitting it. This is, however, the method recommended by Sentek for installation of *EnviroScan* tubes (Sentek, 2003). High-performance adhesives may offer a better way to bond the cutting shoe to the access tube. Lubrication of the tube as it goes into the soil with small amounts of water from a spray gun may help.
- Because of friction between the tube and its surroundings, it is difficult to install tubes to a depth greater than 2 m using this technique (shallower in some instances), although 3 m depth can be achieved in some situations. If the soil is sufficiently cohesive, installation in a predrilled hole the same diameter as the access tube has been used successfully for installation of deep (6 m) tubes. This is almost certainly necessary in cemented porous rock such as sandstone or chalk.
- Small stones do not present too large a problem and can often be removed from the tube using a screw auger with a large pitch or a gouge auger. Larger stones are much more difficult. Because the capacitance probe is much more sensitive to the conditions immediately around the tube than is a neutron probe, disturbance caused by a large stone is potentially fatal to the chance of achieving an acceptable installation. The usually larger diameter of the access tube, however, helps to cope with larger stones, especially if the steel inner tube is removed temporarily to provide more room for the auger to pick up the stone. If there are particularly difficult sections of the profile where stones are a problem, accurate recording of these during installation helps future interpretation of the measurements.
- Slightly different installation methods are recommended by different manufacturers (e.g. Sentek, 2003; Delta-T, 2005; IMKO, 2013a). In particular, different augers (e.g. gouge or Edelman) or screw augers of different pitch may work better in some soils, particularly where they are stony, loose, sticky or very hard. The access tubes for Delta-T profile probes are supplied with an end cap fitted, and so must be inserted into a pre-bored hole. Their small diameter (28 mm) precludes the use of a steel guide tube and so holes must be augered directly into the ground. Great care is required to achieve a clean hole. Delta-T recommends boring a pilot hole first, then a slightly larger one before inserting the access tube.

8.12 Permanent Installation of Rod-Type Probes

The same considerations as described in Section 8.6.2 for TDR probes and in Section 8.6.9 for the CS616 sensor apply to installation of capacitance-type rod probes. Rod-type capacitance-based probes are, however, usually shorter than these instruments, and so it is even more important that they are installed into soil that is not disturbed at its surface and that they are inserted fully. In particular, if the sensor is installed in the bottom of a predrilled, hole, great care is needed to ensure that there is no loose soil in the bottom and that the bottom of the hole is flat. A flat-bottomed auger can achieve this if the soil is sufficiently cohesive. A motor-driven vacuum cleaner, as used in garden management, can be used for removal of loose soil at the bottom of a hole.

8.13 Field Monitoring

The same considerations apply to field monitoring with dielectric probes as to other devices – avoidance of damage to the soil surface and surrounding vegetation, care in recording the readings and ensuring that locations are representative of the surrounding area. It should also be remembered that these devices have a small measurement volume, which usually means that spatial variability is relatively high, and so requires a fairly large number of replicates to obtain a good estimate of the average value of either water content or its change. Because of the small measurement volume, measurements can also be seriously biased by disturbance to the soil close to the instrument, demanding that extra care be taken not to disturb it.

8.13.1 Depth probes

The small depth resolution makes accurate and consistent vertical placement of the probe very important for obtaining good quality data. Most commercial instrumentation has features to aid in this, either having positive, pre-set positions built into the lowering mechanism, or, in the case of the *Diviner 2000* from Sentek, automatic depth sensing.

This triggers a reading every 100 mm depth as the probe is inserted into the access tube. Whichever system is in use, however, the top of the access tube is usually the reference level; and if the instrument is not placed correctly on that, there will be an error of the same amount in each reading. This type of probe is also sensitive to rotational orientation in the tube, and so the devices usually incorporate a mechanical means to ensure that it will always be in the same orientation when inserted.

In the field, checks should be made frequently that the probe reads consistently when in the air and well away from any objects. The electronics have proved to be very stable over time, so any departure of this air count by more than 0.1% from that normally experienced would be indicative of either a fault or a low battery.

8.13.2 Rod-type probes

The most important considerations are to ensure that the rods are inserted straight into the ground and not using a rocking motion and that they are fully inserted. In some soils, especially when dry, it may be impossible to insert the rods into the soil to their full length using hand pressure only. In this case, insertion to, say, 50 mm may be the only option. To ensure consistent depth placement, the upper part of the rods should be covered with a plastic sleeve, as shown in Fig. 8.41, so that the rods can be inserted until the sleeve contacts the ground surface. To ensure consistent results, the same depth of insertion must be used on all occasions.

The pointed rods of portable probes compress the soil around them, which is the most sensitive part of the region to which the probe reacts. This has the effect of increasing the water content locally, and water will often start to migrate away from the region immediately next to the rods. This will be seen as a slowly falling water content. To ensure standardisation of methodology, it is suggested that the reading on first insertion be recorded. The disturbance to the water regime will then have to be accounted for in the soil calibration.

Rod-type probes are often not installed permanently. Measurements will, therefore, be subject to spatial variability, which reduces the precision of measurements considerably when comparing readings from one measurement occasion to another. To minimise this, if sequential measurements are required, the following procedures should be adopted:

- Choose a small area of approximately 1 m square in which measurements are to be made. To obtain a good areal average, it may be necessary to have a number of such squares (see Chapter 4).
- Make at least three replicate measurements on each occasion, all within this area and distributed fairly evenly within it. Avoid any places where the marks from previous measurements are visible.

Experience will show whether the number of replicate squares and/or the number of measurements made in each square should be increased or decreased. It is best to start with a high number of each and reduce one or both once the sampling programme has been operating for some time, preferably at least 1 year.

8.14 Soil Calibration

8.14.1 Depth probes

Calibration for a depth probe may be done in the same way as for the neutron probe (Section 7.7.2), either in the laboratory or field. In either case, the fact that the measuring volume is smaller changes some of the requirements.

In laboratory calibration, the volume of soil needed is considerably less, making it much easier to obtain well-controlled water content and bulk density profiles in a container, which need be no larger than 300 mm diameter. Paltineanu and Starr (1997) used a square wooden box of 355 mm side and 405 mm deep, while Baumhardt *et al.* (2000) used 500 mm diameter plastic barrels.

For field calibration, the same approaches may be used as for the neutron probe, similar to those described in Section 7.7.2. Because dielectric probes measure a smaller volume than the neutron probe, samples should be no more than 100 mm high. When a temporary access tube is used, the samples should be taken as close as possible to it to ensure that they come from within the volume of soil recorded by the probe.

The steady irrigation method (Carneiro & de Jong, 1985) as described in Section 7.7.2 may be used if one assumes that water content is linear in $\sqrt{\varepsilon}$. So plotting cumulative infiltration against $\int_0^Z \sqrt{\varepsilon} dz$ is expected to yield a straight line. The slope of this line will determine the slope of the θ v $\sqrt{\varepsilon_r}$ relation. From the discussion in Section 8.4.1, this is expected to be close to and a little less than 0.125. The same principle can be applied even if the exponent of ε differs from 0.5.

Samples from within the access tube would be expected to give the closest correspondence to the soil actually encountered by the probe, while leaving a tube that can be used *in situ* for later monitoring, as described in Section 8.11. However, the volume of soil is smaller than can be obtained by using a separate sampler, the soil removed from the tube is not actually the same soil as sampled by the probe and soil conditions relate only to one occasion, so the spread of water content may be limited. Good results have, however, been obtained by this method (Bell *et al.*, 1987).

8.14.2 Rod-type probes

Samples for calibration of rod-type probes may be taken from the soil immediately surrounding the rods. A cylinder of diameter about twice as large as the distance between the rods and centred on the holes made by them, as in Fig. 8.54, should be taken. The height of the cylinder

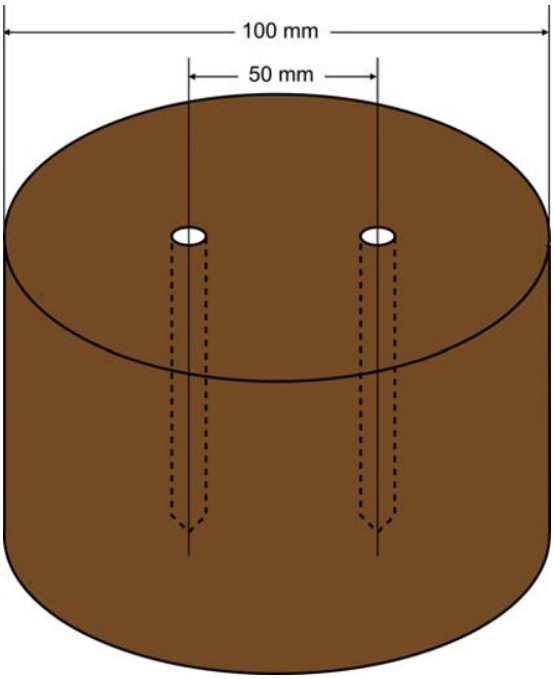

Fig. 8.54 Calibration scheme for a rod-type probe. A reading is first taken using the probe and then a cylinder of soil containing that sampled by the probe is removed for gravimetric water content determination. The height of the cylinder is equal to the length of the probe rods and its diameter is approximately double that of the rod separation.

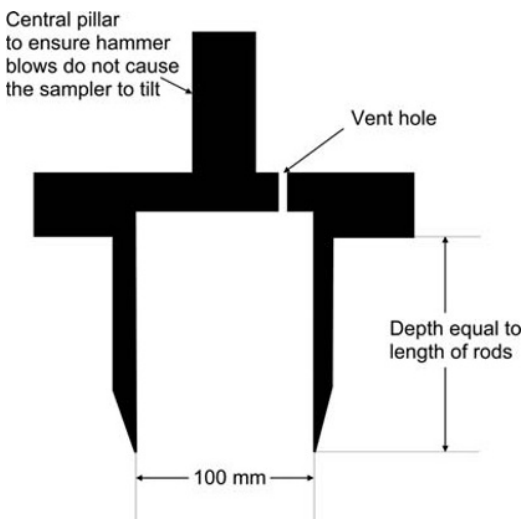

Fig. 8.55 Sampler for taking soil samples at the soil surface. Note the headroom above the level of the bottom of the flange to prevent compression.

should be the same as the length of the rods. The sampling equipment should preferably be thin-walled ($\lesssim$1 mm) metal cylinders. If the soil is not sufficiently soft, thicker steel cylinders with a sharp external bevel as shown in Fig. 8.55 can be used. A flange on the outside of the sampler indicates when the sampler has penetrated the correct distance into the soil. The sampler should, in either case, be dug out of the soil and excess soil trimmed with a sharp knife or spatula level with the bottom. In some cases, the soil will compress in the sampler as a result of friction on the wall of the sampler. Unless this has become solidly stuck in the sampler and the soil beneath has become compressed, the correct amount of soil should have been collected, and so no compensation need be made. This should, however, be recorded, as should any other problems, such as those caused by stones.

8.15 Ground-Penetrating Radar

8.15.1 Introduction

Ground-penetrating radar (GPR) has been used for a few decades for investigations in the shallow (a few metres) subsurface to identify objects and anomalies without the need for excavation. The approach was largely empirical. More recently, a quantitative approach has been taken to hydrological and hydrogeological investigations to provide rapid measurements of water content, electrical conductivity and identification of preferential flow paths.

GPR has strong links to the other dielectric methods discussed earlier in this chapter and with remote sensing methods used for measurements of large areas from satellites or aeroplanes.

In general, GPR can provide measurements of soil water over larger areas and volumes of soil than the 'point' methods described earlier in this book. At the same time, the actual volume measured is less well defined and, in common with most methods, varies with the water status of the soil. The equipment is expensive, but usually portable and so can be used at a large number of locations. Repeated measurements at the same spot are aided by the incorporation of Geophysical Positioning System (GPS) equipment into most commercial instruments.

There are three basic ways in which GPR can be used for soil water measurements: on the surface, from a borehole or boreholes and from above the surface.

8.15.2 Principles of operation

The equipment comprises essentially a transmitter of microwave radiation, a transmitting antenna, a receiving antenna, a receiver and a timer connected to both transmitter and receiver to measure the travel time between the two, as shown in Fig. 8.56. In operation, a short (few nanosecond) pulse of electromagnetic waves is generated by the transmitter, sent to the transmitting antenna and picked up by the receiving antenna. The frequency range is controlled mainly by the length of the antennae, l. Usually, the centre frequency, f_c, is quoted. This is the midpoint between the upper and lower frequency at which

the power is 10 dB lower than (i.e. one-tenth of) the maximum power transmitted. This is close to the frequency corresponding to a wavelength four times the length, l, of the antenna; that is $f_c = (c/4l)$, where c is the speed of light in air (3×10^8 m s^{-1}). In practice, the effective frequencies occupy a range between 0.5 and 1.5 times f_c. The receiver records the signal detected by the receiving antenna at time intervals of <1 ns to a few nanoseconds, depending on the antenna used.

The radar pulse is transmitted in all directions, but most strongly perpendicular to the antenna. For this reason the antennae will normally be placed parallel with the ground surface. Part of the signal travels directly from the transmitting to the receiving antenna through the air. This is called the *air wave*. The distance, and hence the travel time, between them is known, which then allows the amount of delay within the electronics to be calculated and a correction applied to all other times.

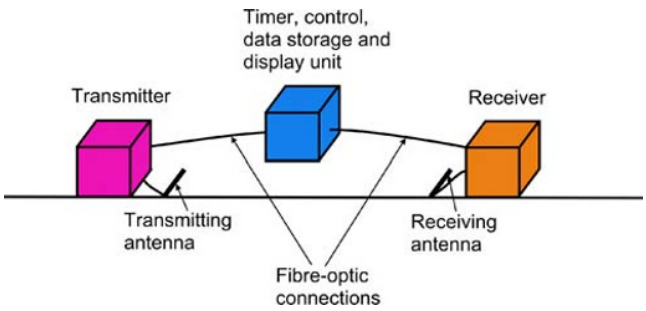

Fig. 8.56 Components of a GPR system. Fibre-optic connections between the different units are used to avoid electrical interference caused by metal-cored cables.

The most interesting part of the pulse is that which travels through the ground. One part travels directly from one antenna to the other, called the *ground* wave, but at a much slower speed of $(c/\sqrt{\varepsilon_r})$ than the air wave. Other portions of the signal are reflected from electrical discontinuities beneath the ground. These may be buried objects, boundaries between soil layers of contrasting dielectric properties or the water table (actually the top of the capillary fringe). In some coarse-textured soils, the wetting front after rain or irrigation may be detectable.

For soil hydrological purposes, the main interest is that, like TDR, the time taken for the pulse to travel from transmitter to receiver depends on the path length and the relative permittivity of the material. For the ground wave, therefore, the transit time will allow a measurement of the near-surface soil water content to be computed.

Some possible path lengths for the signal are shown in Fig. 8.57. In complex situations, there are obviously many different paths possible, which can make interpretation of the received signals difficult. For instance, one would expect that the ground wave would be the first to arrive at the receiving antenna after the air wave. This is not always so, however. If the layering is such that the speed of travel in an upper layer is slower than in an underlying one, then the wave will be refracted at the interface to make a shallower angle with the interface. At the *critical angle* of incidence, the refracted wave will be parallel to the interface and travel faster than the ground wave in the lower layer. A portion of this wave can then be refracted back through the interface to the receiving antenna and may

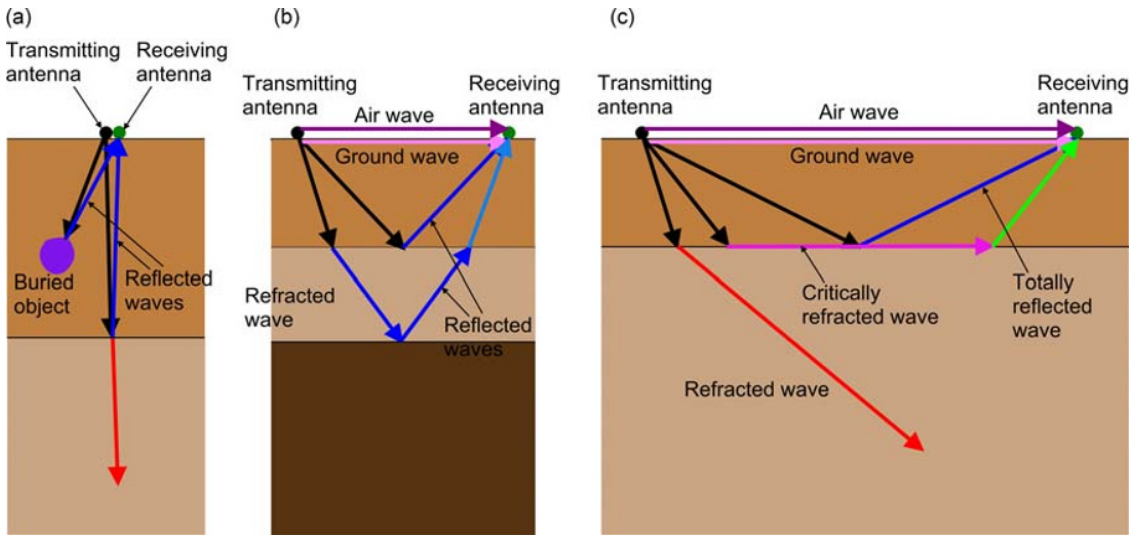

Fig. 8.57 Ray paths for GPR-generated waves in a layered medium. (a) Reflection from an interface and a buried object with no separation between antennae. (b) Reflections and refractions at interfaces with separated antennae The permittivity of the lighter-coloured layer is lower than that of the darker one, and so the speed of the wave is greater and it is refracted towards the interface in the lighter-coloured material. (c) At greater antenna separation, a critically refracted wave can travel through the faster medium and may reach the receiving antenna before the ground wave. (*See insert for colour representation of the figure.*)

well arrive earlier than the ground wave. At even shallower angles of incidence, total internal reflection occurs. This is identical to the more familiar optical phenomenon, where the speed of light is inversely proportional to the refractive index and total internal reflection occurs at an interface when light travels at a sufficiently shallow angle from, say, glass towards air.

The time taken between transmission and reception of the pulse is determined by the average speed of the radio wave and the path length. Where there are multiple paths for the wave to exploit, as in Fig. 8.57b and c, several different arrival times will be recorded. Interpreting these depends on a knowledge of the important aspects of the subsurface environment. For instance, in the configuration of Fig. 8.57a, if the distance between the antennae and either the interface or buried object is known, then the speed of travel, and hence the average permittivity of the medium can be calculated in a very similar manner to TDR. On the other hand, if the objective is to measure the depth of either of these, the medium permittivity must be known. In most cases of interest, neither is known at the outset with sufficient accuracy. However, by varying the position(s) of the antennae, this can often be resolved.

8.15.3 Antenna configurations

The most common arrangements are shown in Figs. 8.57a and 8.58. Where the antennae are effectively coincident, as in Fig. 8.57a, the same antenna can, in some cases, be used for both transmission and reception, although this is not common. More commonly, the two antennae are separated by some distance, as shown in Fig. 8.58.

The set-up shown in Fig. 8.58a is normally used for surveying large areas to investigate variations of depth to an interface or to find buried objects. The transmitting and receiving antennae are kept the same distance apart, usually in the same housing. The survey is normally performed over a number of transects, usually parallel to one another, forming a grid pattern, so that a mapping of the subsurface is obtained. Data acquisition can be very rapid in this mode. The antennae are pulled along the ground surface by hand for small areas or by a vehicle driving at slow speed (a few kilometres per hour) or even by a boat on the surface of a lake. Where a vehicle or boat is used, the antennae are towed on several metres of rope to avoid metal parts disturbing the readings. Reading events are triggered by a timer, by a GPS or by a wheel attached to the sled carrying the antennae to record data at regular distance intervals.

The wide-angle reflection and refraction (WARR) configuration (Fig. 8.58b) uses a fixed transmitting antenna and a movable receiving antenna to investigate conditions over a small area. Often the symmetrical common midpoint (CMP) configuration (Fig. 8.58c) is preferred as data are more easily interpreted. However, it is more time-consuming than WARR, since both antennae must be moved for each measurement.

Multiple measurements allow both depth of a buried object and average permittivity of the medium to be resolved. Figure 8.59 shows how this works for a fixed separation moving antenna. The object is located at a distance, z, below the surface. The horizontal distance between the transmitting antenna and the object is, successively, x_1, x_1, x_3, … and the transmit – receive antenna separation is d. The path length from T_1 to the object is $\sqrt{\left(x_1 - \frac{d}{2}\right)^2 + z^2}$, and the time taken for a pulse to travel from the antenna to the object is therefore $\frac{\varepsilon_r\sqrt{\left(x_1 - \frac{d}{2}\right)^2 + z^2}}{c}$. Similarly, the time taken for the pulse to return to the receiving antenna, $R1$, is $\frac{\varepsilon_r\sqrt{\left(x_1 + \frac{d}{2}\right)^2 + z^2}}{c}$. The total pulse travel time, t, is, therefore

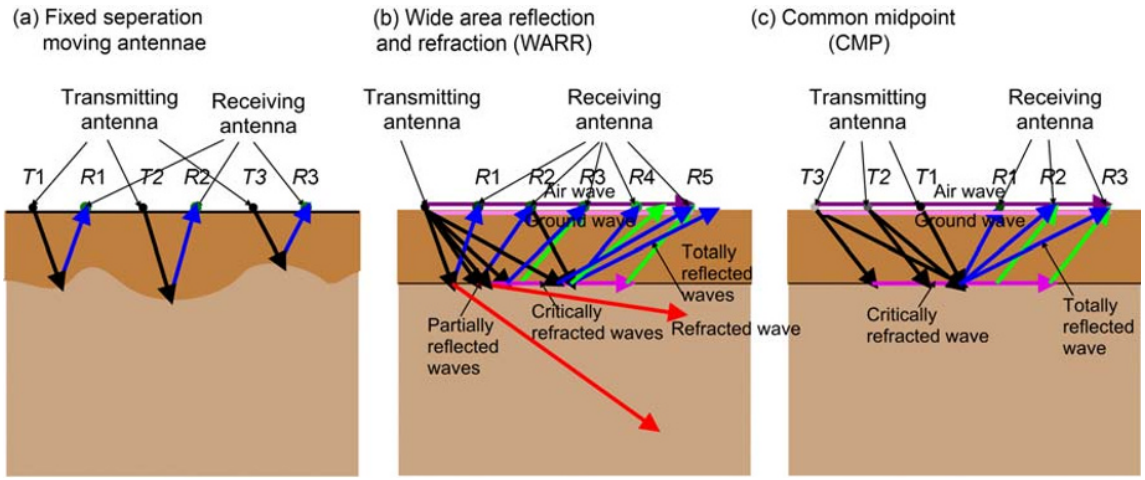

Fig. 8.58 Common configurations for separated antenna measurements using GPR at the ground surface. (*See insert for colour representation of the figure.*)

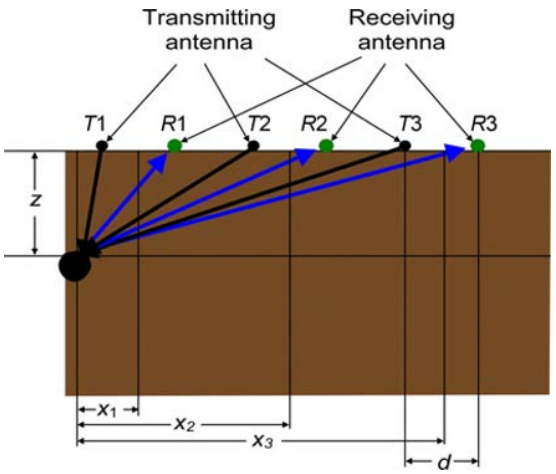

Fig. 8.59 Estimating depth of a buried object and permittivity using moving antennae. (*See insert for colour representation of the figure.*)

$$t = \frac{\varepsilon_r \left(\sqrt{\left(x_1 - \frac{d}{2}\right)^2 + z^2} + \sqrt{\left(x_1 + \frac{d}{2}\right)^2 + z^2} \right)}{c}. \qquad (8.15.1)$$

If the antennae are coincident, that is the separation, d, is zero, this reduces to

$$t = \frac{2\varepsilon_r \sqrt{x_1^2 + z^2}}{c}. \qquad (8.15.2)$$

This is the equation of a hyperbola and, by plotting t^2 against x^2, a straight line should be obtained with a slope of $\frac{4{\varepsilon_r}^2}{c^2}$ and intercept $\frac{4{\varepsilon_r}^2}{c^2}z^2$. Thus both the average permittivity and depth of the object can be found. If d is relatively small compared with z, these relations can be used to give acceptably accurate values for ε_r and z, particularly bearing in mind that the object is of finite size, which has been ignored in the above, and that ε_r is unlikely to be constant along the transect.

For WARR or CMP, the same kind of analysis can be applied to determine the depth to a reflecting layer. In the case of CMP, the reflection occurs at $x = 0$, that is the midpoint between the antennae, and so by varying the separation between the antennae, d, Equation 8.15.2 becomes

$$t = \frac{\varepsilon_r \sqrt{d^2 + 4z^2}}{c}. \qquad (8.15.3)$$

Again, plotting t^2 against d^2 yields a straight line with slope $\left(\varepsilon_r^2/c^2\right)$ and intercept $\frac{4\varepsilon_r^2}{c^2}z^2$, where in this case, z is the depth to the interface.

Further information can be obtained from the arrival times of other reflected and refracted waves. The methods are very closely related to seismic surveys, much used in geological surveying, which use sound waves to reconstruct the properties of the subsurface environment. Many of the methods of analysis and data presentation are taken directly from this older-established technology.

8.15.4 Antennae

The choice of antennae principally determines the range of frequencies in the transmitted signal, as described earlier. Higher frequency signals have a shorter wavelength and enable higher resolution images to be obtained. On the other hand, higher frequencies are more easily attenuated, reducing the penetration depth and require faster sampling by the receiver. Penetration depth varies not only with frequency but also depends on the type of material encountered. It may vary from less than 0.5 m with 1.5 GHz antennae to 100 m or more in ice or dry sand at 100 MHz, but only a few m at 900 MHz. In clay soils, penetration depths may be only 1% of these.

The size of the antenna determines the frequency, which means that lower frequency antennae are physically large. For instance, a 100 MHz antenna is about 1 m long, while a 900 MHz one can be only about 100 mm.

Some antennae incorporate shielding to improve directionality and reduce power radiated to (or picked up from) the surroundings. Most antennae, however, are simple dipoles, which radiate in all directions with a polarisation parallel to the dipole axis. For specialised applications, antennae which generate circularly polarised radiation are available.

8.15.5 Borehole GPR

Measurements of soil water using GPR at the surface are limited in depth mainly by attenuation of the radar signal, but also interpretation of the signals is difficult, with many different factors contributing to the images. The least ambiguous signal is from the ground wave, whose travel path and arrival time is known almost unambiguously. But even here, there may be problems in identifying the ground wave from critically refracted and reflected waves and the ground wave is attenuated more than other waves (Huisman *et al.*, 2003). Defining the effective depth of measurement is a further difficulty. Theoretically, it depends on the wavelength of the radiation, which, in common with the effective measurement volume for most other water content measurement methods, depends on the water content. In practice, it appears that for frequencies in the 225–900 MHz range, the measurements effectively average over the upper 200 mm of soil (Huisman *et al.*, 2003). Except where there is a sharp wetting front within the measurement volume, there are normally strong correlations between water content at nearby depths, so this result may not be surprising.

An alternative and, in some ways, more productive approach is to transmit the signal from an antenna in one borehole to another one in a nearby borehole. This means that the radio wave travels through the entire thickness

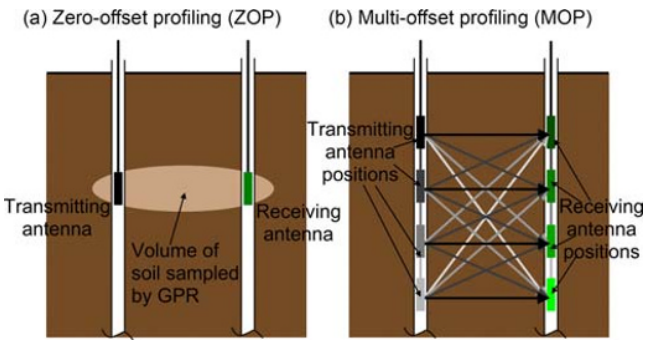

Fig. 8.60 Borehole GPR configurations. (*See insert for colour representation of the figure.*)

of soil or rock between the two holes and, therefore, produces an average measurement of permittivity, and hence water content, from a large volume of soil over a relatively narrow path.

Two arrangements are possible, as shown in Fig. 8.60. In zero-offset profiling, the transmitting and receiving antennae are kept at the same depth and measurements made at a series of depths. If the ground between the boreholes were homogeneous, the volume of measurement would be a narrow ellipsoid as shown in the figure. Heterogeneous conditions distort this. Multi-offset profiling (MOP) makes measurements between pairs of antennae at both the same and different depths. This is obviously a much slower process and may be useful only where conditions remain stable over several hours. It is not, therefore, suitable for observing the penetration of a wetting front after rain or irrigation. A two-dimensional representation of water content distribution between the two boreholes may be constructed by inversion of MOP data. This is done by dividing the domain into a number of pixels and modelling the transit times between all the antenna positions. The water content of each pixel is adjusted until the predicted and measured times match as closely as possible (see Section 17.13). The method can be extended to produce a three-dimensional image if measurements are made in several boreholes. Obviously, both the time required to make the measurements and the computing requirements rise rapidly as the number of boreholes and depths increase.

8.15.6 Surface Reflection Measurements

These are sometimes known as *air-launched measurements*. Both the transmitting and receiving antenna are positioned above the ground surface, usually coincident with one another. The amplitude of the reflected pulse is dependent on the permittivity of the near-surface soil, and so a measurement of surface soil water content can be calculated.

The reflection coefficient, R, of the air–soil interface is given by (Huisman *et al.*, 2003)

$$R = \frac{1 - \sqrt{\varepsilon_r}}{1 + \sqrt{\varepsilon_r}}, \tag{8.15.4}$$

where ε_r is the relative permittivity of the near-surface soil. In practice, the amplitude, A_0, of signal received from a 'perfect' reflector, usually a metal plate larger than the footprint of the radar is needed to calculate the reflection coefficient. R is then A_r/A_0, where A_r is the amplitude of the signal reflected from the soil and Equation 8.15.4 can be rearranged to give (Davis & Annan, 2002; Redman *et al.*, 2002; Huisman *et al.*, 2003):

$$\varepsilon_r = \left(\frac{1 + (A_r/A_0)}{1 - (A_r/A_0)}\right)^2. \tag{8.15.5}$$

The footprint of the signal varies with both wavelength, λ, of the signal and (more obviously) the height, h, of the antennae above the ground surface and is given approximately by the diameter, D, of the *first Fresnel zone* (Huisman *et al.*, 2003):

$$D = \sqrt{\left(\frac{\lambda^2}{4} + 2h\lambda\right)}. \tag{8.15.6}$$

8.15.7 Licensing

GPR involves a radio transmitter and so has the possibility to cause serious interference to other radio signals and many kinds of electrical and electronic equipment. In many countries electronic goods must pass tests to ensure that they are immune from malfunction caused by normal levels of radio wave activity in the environment and also radiate less than an acceptable amount of radiation at frequencies up to those of very short microwaves. In most cases, failure to stay within these levels may cause serious annoyance; but in others, such as emergency service radios, air bag activators in cars or some medical equipment, the results could be very serious. Hence, the regulations are very strict. Proper design eliminates problems in most cases. However, with a GPR transmitter, radiating radio waves over a broad spectrum is its principal function, and so compliance with regulations for ordinary electronic equipment is not an option. Instead, licensing is required in most countries. The details vary from one country to another, but the principle is that the equipment may be used only at well-defined places (and possibly also times) and several other conditions may be stipulated to avoid unacceptable effects. In remote areas, the conditions may be less stringent than in densely populated areas. Guidance is available from national communications regulators as well as GPR manufacturers and their trade associations.

8.15.8 GPR – Conclusion

Applications and the technology of GPR are developing rapidly. It has been possible only to provide a brief overview of its scope here. Good reviews of applications to measurement of soil water have been published by Davis & Annan

(2002) and Huisman *et al.* (2003). Books describing the theory and applications of GPR generally are those by Daniels (2004) and Jol (2009), while recent chapters on the use of the methodology for soil water measurement can be found in books by Rubin & Hubbard (2005), Vereecken *et al.* (2006) and Kirsch (2009).

8.16 Dielectric Methods – Conclusion

Since early attempts to measure water content in soil, the use of dielectric methods has advanced considerably. The seminal work of Topp *et al.* (1980) paved the way for its practical use in laboratory and field investigations. Topp *et al.* (1980)'s method relied on measuring the speed of propagation of an electromagnetic wave in the soil guided by two parallel electrodes, known as TDR.

More recently, many devices have been introduced based on measuring the capacitance between small (less than 100 mm in extent) electrodes. The first practical instrument was described by Dean *et al.* (1987) and Bell *et al.* (1987). These devices use a variety of means for measuring the capacitance between the electrodes. So-called capacitance probes incorporate the electrodes into an oscillator circuit and use the oscillation frequency (in the region of 100 MHz) to calculate the capacitance of the electrodes. Others, such as the Theta, Hydra and ECH2O Probes use a fixed frequency oscillator and different means to calculate the capacitance. Capacitance-based devices usually use either rod-shaped electrodes inserted directly into the soil or two ring electrodes placed one above the other with a small gap between them inside an access tube.

Almost all dielectric devices are capable of unattended, remote operation, allowing the collection of data with fine time resolution over extended periods.

TDR has been the subject of most effort to improve performance and reliability. Several companies produce commercial devices, and it is perfectly possible to construct a system using a commercial cable tester and rods made from easily available materials. TDR appears to be the dielectric technology least affected by electrical conductivity of the soil, while at the same time allowing this to be measured independently (Chapter 21). On the other hand, it gives a measurement of total water content over the length of the rods. In some situations, this is useful if the stock of water within a significant depth of soil is needed, or if rods are installed horizontally to give a good average water content at that depth. However, if the depth distribution of water content is needed with vertical rods, this can be estimated only by difference between rods of different length (which may be the same rods if diode switching or notched rods are used). Because electrical conductivity and relaxation effects attenuate the signal, TDR may fail to provide a measurable signal in highly conductive media or some heavy clay soils. Because of the complexity of the electronics and the very high-frequency signals involved, the measuring system is expensive, although individual sensors can be quite cheap, especially if home made. Where many sensors are multiplexed to one measurement unit, the total cost of an installation may be less than that of a similar number of discrete capacitance-based sensors. In many mineral soils, a standard calibration curve, such as Equation 8.4.1 or 8.4.5 can be used with confidence, but is not adequate where the soil is rich in organic matter or high surface area clays.

Capacitance-based sensors are usually much cheaper than TDR for small installations. However, they mostly suffer from a greater sensitivity to electrical conductivity of the soil than TDR because of operating at a lower effective frequency. As a result, a soil-specific calibration is required for most soils. The volume of soil sampled is also small. This lies in the region most prone to disturbance caused during installation or insertion of the sensor into the soil. Because of this, great care must be taken to avoid soil disturbance during this process. The small volume sampled also increases spatial variability of the measurements, meaning that, to achieve a similar precision of measurement to other methods, a much larger number of sample locations are needed. Comparative studies have generally found the results from these devices to be less reliable than those from TDR (e.g. Evett *et al.*, 2006a). Nevertheless, with great care and attention during installation and monitoring the quality of data produced, good results can be obtained from these devices. For applications requiring relatively low accuracy, such as irrigation scheduling, the cheaper devices are normally capable of providing information of an appropriate quality.

The methods described earlier measure only a small volume of soil, essentially a point. Wider area methods are being developed. GPR has been described briefly, which is portable and non-invasive. The trade-off between these different methodologies is of precision of measurement and a well-defined location against a larger volume of soil being measured. The choice depends very much on the objectives of any measurement programme; and in many cases, a combination of manual, automatic, point and wide area methods may be the most appropriate, although this will very often be beyond all but the best-funded research groups.

9 Dual-Probe Heat-Pulse Sensors

9.1 Introduction

Water content affects several physical properties of soil. Amongst these are thermal properties. It is relatively easy and cheap to power a small heat source in soil and to measure resultant temperature changes. This is therefore an attractive method for the measurement of soil water content, requiring only simple equipment to make the sensors. Because both the excitation (heat source) and detection (temperature measurement using either thermocouples or thermistors) are electrical, the method lends itself to unattended, automatic data acquisition. A further attractive feature is that the system requires very little routine maintenance, with no moving parts involved. The drawbacks are that the need for a heater makes the system relatively power hungry, implying heavy batteries and/or large solar panels or wind generators for field use; fairly complex control and data analysis requirements need a sophisticated data logger, and the volume of soil measured is much smaller than that of most other soil water content measurement methods.

The relevant thermal properties are the *thermal conductivity*, the *specific heat* and the *thermal diffusivity*, which is a combination of the other two properties. These are directly analogous to the hydraulic conductivity, the specific water content and diffusivity introduced in Chapters 2 and 3.

All three quantities vary with water content, but specific heat (symbol c) exhibits a particularly simple relationship. It is defined as the amount of heat required to raise the temperature of unit mass of the medium (soil) by one degree. It is more convenient for the present purpose to work with the *volumetric specific heat*, that is, the amount of heat required to heat a unit volume of soil by one degree. This is designated ρc, where ρ is the density of the wet soil. Adding a volume of water, θ, to the soil is expected to increase the volumetric specific heat by an amount $\theta\rho_w c_w$, where ρ_w is the density of water ($1000\,\mathrm{kg\,m^{-3}}$) and c_w is the specific heat of water ($4.18\,\mathrm{J\,kg^{-1}{}^\circ C^{-1}}$), so the volumetric specific heat of the soil is

$$\rho c = \rho_d c_s + \theta\rho_w c_w, \tag{9.1.1}$$

where
$\rho_d c_s$ is the volumetric specific heat of the soil fabric;
ρ_d is the dry bulk density of the soil, and
c_s is the specific heat of the soil solids.

The volumetric water content, θ, can then be calculated from the volumetric specific heat of the soil as

$$\theta = \frac{\rho c - \rho_d c_s}{\rho_w c_w}. \tag{9.1.2}$$

This requires knowledge of the dry bulk density and the specific heat of the soil solids. However, changes in water content do not involve these quantities.

9.2 Principles of Operation

A dual-probe heat-pulse (DPHP) sensor usually consists of two thin (about 1 mm diameter), parallel, hollow stainless steel needles of hypodermic tube, 30–40 mm long, set about 6 mm apart, embedded in the soil. One of these contains an electrical heater made from about four thicknesses of lacquered resistance wire. Nichrome (an alloy of nickel and chromium) and constantan (an alloy of copper and nickel) are the most commonly used materials. Nichrome has much higher resistance for the same gauge, but unlike constantan cannot be soldered. The other tube contains at its midpoint a thermocouple or thermistor to measure temperature. The arrangement is depicted in Fig. 9.1.

In operation, the heater is switched on for a short time (ideally it supplies an instantaneous heat pulse, but in practice this takes a few seconds), and the temperature at the midpoint of the other tube is monitored. In the ideal case of an instantaneous heat pulse, the temperature rise, ΔT, at a distance r from an infinitely long line after a time t is given by (Carslaw & Jaeger, 1959, p. 258)

Soil Water Measurement: A Practical Handbook, First Edition. J. David Cooper.

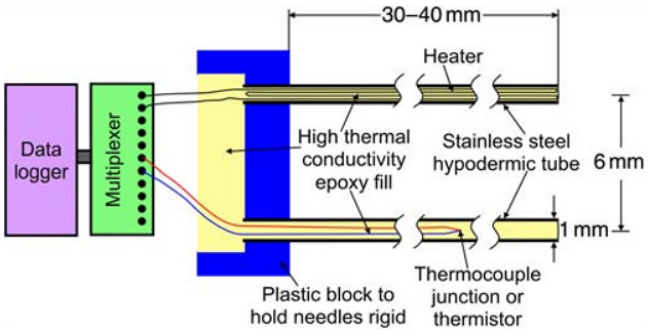

Fig. 9.1 Schematic diagram of a dual-probe heat-pulse sensor.

$$\Delta T = \frac{E}{4\pi k t} e^{-\left(r^2/4\alpha t\right)}, \tag{9.2.1}$$

where
E is the heat energy released per unit length of line;
k is the thermal conductivity of the soil, and
α is the thermal diffusivity of the soil ($k/\rho c$).

Differentiating Equation 9.2.1 with respect to t gives

$$\frac{\partial \Delta T}{\partial t} = \frac{E}{4\pi k t^2} e^{-\left(r^2/4\alpha t\right)} \left(\frac{r^2}{4\alpha t} - 1\right). \tag{9.2.2}$$

The maximum temperature rise occurs when $(\partial \Delta T/\partial t) = 0$, when

$$t_{\max} = \frac{r^2}{4\alpha}. \tag{9.2.3}$$

Substituting this value for t in Equation 9.2.1 gives the maximum temperature rise, $\Delta T_{\max}$:

$$\Delta T_{\max} = \frac{E\alpha}{e\pi k r^2}. \tag{9.2.4}$$

Using the definition of thermal diffusivity given above, the volumetric specific heat is given by

$$\rho c = \frac{E}{e\pi r^2 \Delta T_{\max}}. \tag{9.2.5}$$

DPHP sensors were first proposed by Campbell *et al.* (1991). Since then, several workers have examined the effect of various design features on measurement accuracy (Bristow *et al.*, 1993, 1994a, b, 1995, 2001; Kluitenberg *et al.*, 1993, 1995; Tarara & Ham, 1997; Bilskie *et al.*, 1998; Bristow, 1998; Song *et al.*, 1998, 1999, 2000; Kluitenberg & Philip, 1999; Philip & Kluitenberg, 1999; Ren *et al.*, 1999, 2003a, b; Abu-Hamdeh, 2001; Campbell *et al.*, 2002; Hopmans *et al.*, 2002a; Basinger *et al.*, 2003; Bremer, 2003; Heitman *et al.*, 2003; Mori *et al.*, 2003, 2005; Oschner *et al.*, 2003; Ham & Benson, 2004; Knight & Kluitenberg, 2004; Norikane *et al.*, 2005; Knight *et al.*, 2007).

These studies have shown that the approximations involved in assuming an instantaneous heat pulse from an infinitely long and thin line source cause only small errors in the measurement (Kluitenberg *et al.*, 1993); that thermal and water content gradients within the sensed volume also cause only small errors (Kluitenberg & Philip, 1999; Philip & Kluitenberg, 1999); that the main source of error appears to be in estimating the inter-tube spacing; and that the sensed area around the probes (99% of the contribution) is about 168 mm^2 for tubes separated by 6 mm (Knight *et al.*, 2007). Temperature is measured only at the midpoint of an approximately 30 mm tube, and so if an effective length of one third of this (10 mm in this example) is assumed, the sensed volume would be about 1700 mm^3 or 1.7 mL. This is equivalent to the volume of a cube of 12 mm side and compares with typical volumes of $3 - 28 \times 10^4$ L for a neutron probe, 320 mL for a 200 mm long TDR probe and 200–400 mL for capacitance sensors (Evett *et al.*, 2008). Spatial variability is, therefore, expected to be very high. On the other hand, the technique has high spatial resolution.

Temperature changes at the sensor are quite small for practical designs. Tarara and Ham (1997) calculated the temperature response of a probe with $E = 600$ J m^{-1} and $r = 6$ mm with a typical value of $\rho_d c_s$ of 1.04 MJ m^{-3}°C^{-1}. $T_{\max}$ varied from about 0.8°C for $\theta = 0.3$ to 1.4°C for $\theta = 0.1$. To obtain a sensitivity of 1% by volume water content, therefore, requires resolving temperature changes to better than about 0.03°C. For a copper–constantan thermocouple, this translates to about 1 μV, and to ensure some resilience, the measurement sensitivity should be rather better than this, perhaps 0.25 μV. Thermistors are more temperature sensitive, with a typical sensitivity of 4.5% change in resistance °C^{-1}. Using a 2.5 V supply and a resistor of the same resistance as the thermistor in series with it, the voltage across the fixed resistor changes by about 840 μV for the same 0.03°C and 1% change in volumetric water content.

For field use, the problems are the very small volume sensed by the probes and the need to bury them in as undisturbed environment as possible or insert them without deflecting the thin needles. For these reasons, the main advantage, apart from the low cost of the sensors, is the ability to measure water content changes near the soil surface and sometimes in the vicinity of individual roots, where good spatial resolution is important.

Because the method involves heating the soil, the heat injected must be allowed to dissipate and the soil temperature to recover to its ambient value before repeating a measurement. This normally takes only a few minutes and so does not cause many problems in practice.

10 Electrical Resistivity Imaging

10.1 Introduction

Often shortened to 'ERI' and alternatively called resistivity surveying or electrical resistance tomography (ERT), electrical resistivity imaging has been in use for several decades, but found little application outside the geophysical community until quite recently. Traditionally, it has been used for survey work in mapping the extent of shallow formations and depth to the water table. Until recently, the method relied on manual swapping of connections and acquisition of data, as well as graphical data interpretation. The first two limited the amount of data that could be acquired, as they required inserting electrodes into the ground and changing the connections from a power source to a measurement device for each measurement. The relatively small amounts of data collected provided little incentive to develop sophisticated data interpretation methods, which, in any case, require significant computing power. Coupled with some prejudice within the soil physics community that electrical resistivity measurements could not be expected to produce reliable water content measurements, the methodology took some considerable time for acceptance as a useful technique for this purpose.

While significant effort must still be needed to install electrodes and connect cables to them, reliable multi-way switching equipment now allows data to be acquired much more rapidly, in some instances automatically, and to make repetitive measurements of the same electrode array over a period of time. And, as for ground-penetrating radar (GPR) (Section 8.15), the development of software and data inversion methods to handle, analyse and visualise significant amounts of data has moved ERI into the mainstream. The other main recent development of ERI has been in extending it, again similar to GPR, to cross-borehole measurements.

10.2 Theoretical Basis of ERI

10.2.1 Electrical conductivity of a formation

The use of electrical resistivity to measure soil water content relies on the fact that as water content of the soil increases, so does its electrical conductivity (the inverse of resistivity). This is primarily a result of increasing number and cross-sectional area of pathways for current to flow and reduction of tortuosity as water content increases. This is similar to the increase in soil hydraulic conductivity as a function of water content. For electrical conductivity, the most commonly used relationship is *Archie's Law* (Archie, 1942). Archie recognised that the electrical conductivity of a partially saturated formation depends on both the electrical conductivity of the fluid and the water content of the formation and proposed a relation:

$$\sigma_b = \frac{\sigma_w}{F}, \tag{10.2.1}$$

where
σ_b is the bulk conductivity of the formation;
σ_w is the fluid conductivity, and
F is known as the *formation factor*.

For a saturated formation, Archie found that F could be expressed well by

$$F = \frac{a}{\theta_s{}^m}. \tag{10.2.2}$$

Here
a and m are empirical constants and
θ_s is the saturated water content (the term porosity is often used instead of saturated water content).

If the relationship represented the behaviour perfectly, then a would be equal to 1. m is known as the *cementation*

Soil Water Measurement: A Practical Handbook, First Edition. J. David Cooper.

exponent and its value is determined by the details of the pore space in the formation. It is usually in the range 1.3–2.0, although Cassiani *et al.* (2006) quote a range of 1.0–2.5.

Inserting the formation factor expression (10.2.2) into Equation 10.2.1, we obtain

$$\sigma_b = \frac{\sigma_w \theta_s^{\,m}}{a} \tag{10.2.3}$$

Archie (1942) extended Equation 10.2.3 to the unsaturated situation by introducing a *saturation exponent*, n, whose value is often close to 2, so that this equation becomes

$$\sigma_b = \frac{\sigma_w \theta_s^{\,m}}{a}\left(\frac{\theta}{\theta_s}\right)^n \tag{10.2.4}$$

or

$$\sigma_b = \frac{\sigma_w \theta_s^{\,m-n}}{a}\theta^n \tag{10.2.5}$$

Archie (1942) developed his equations for 'clean' sands and sandstones, where the only electrically conducting pathways are *via* the fluid phase. Many soils, particularly those containing significant amounts of clay, conduct electricity through the matrix as well. By assuming that this acts in parallel with the water in the pore space, Rhoades *et al.* (1976) extended Equation 10.2.1 to

$$\sigma_b = \frac{\sigma_w}{F} + \sigma_s, \tag{10.2.6}$$

where σ_s is the conductivity of the soil matrix.

Waxman and Smits (1968) recognised that electric current could be transmitted in the clays by migration of *counterions* – in their case, Na^+ loosely bound to clay surfaces. The number of ions involved in this transfer, Q_v, is proportional to the *cation exchange capacity* per unit volume of the soil as well as to an additional factor, B, which accounts for the counterion mobility:

$$B \propto 1 - be^{-(\sigma_w/\gamma)}, \tag{10.2.7}$$

where b and γ depend on the type of clay mineral, the particular counterion and temperature. Waxman and Smits (1968) assumed that the transport of the counterions was limited by the same tortuosity factors as that of transport in the normal liquid phase and so the same exponents m and n applied. However, the number of counterions participating in this form of transport would be constant, equal to Q_v. As the water content decreases, so the concentration of these in the solution would increase in inverse proportion. This leads to the *Waxman and Smits equation*:

$$\sigma_b = \frac{\sigma_w \theta^n}{a\theta_s^{\,n-m}} + \frac{BQ_v\theta^{n-1}}{a\theta_s^{\,n-m-1}}. \tag{10.2.8}$$

Both the Archie equation and Waxman and Smits equation were developed to help in oil exploration, where the oil-bearing formation is very often sandstone, unconsolidated sand or shaly sand. The nonaqueous phase is oil, rather than air, and the electrical conductivity is usually caused by NaCl. In addition, the electrical conductivity of the solution is constant in time as a result of its depth and time since formation. In near-surface soils and unsaturated rock, many of these conditions are not fulfilled. Nevertheless, the equations appear to have general validity (Cassiani *et al.*, 2006). The most important limitation to the use of the equations is that the electrical conductivity of the soil solution, σ_w, may vary with time as a result of changes in soil solution concentration and composition and temperature. Temperature correction is relatively straightforward and, in nonagricultural soils, the soil solution is often sufficiently stable that the equations can be used with reasonable confidence.

10.2.2 Current paths and electrical potentials in the subsurface

ERI is most commonly conducted using measurements made at the surface. A pair of electrodes imposes a current flow in the ground, while another pair of electrodes measures the potential difference set up by this current. In an electrically homogeneous and isotropic formation, current flow and the associated voltage distribution can be calculated by considering first a single electrode at the surface through which current flows into the ground. The other electrode (at zero potential) is considered to be sufficiently far away that it does not interfere with the current or the voltage distribution. In this case, the current and voltage distribution in the ground will be as shown in Fig. 10.1a. Fig. 10.1b shows the complementary case in which the current flow is reversed.

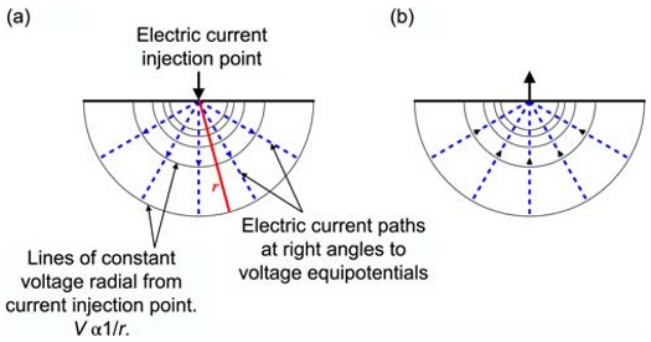

Fig. 10.1 Electrical current and potential in homogeneous ground from a single electrode at the surface. The current flows radially outwards from the electrode in (a), and surfaces of equal voltage (equipotentials) are hemispheres of increasing radius and separation as the voltage decreases. (b) The complementary case of current being extracted via the electrode. In this case, current flow is reversed and the voltages are all negative, but of the same magnitude.

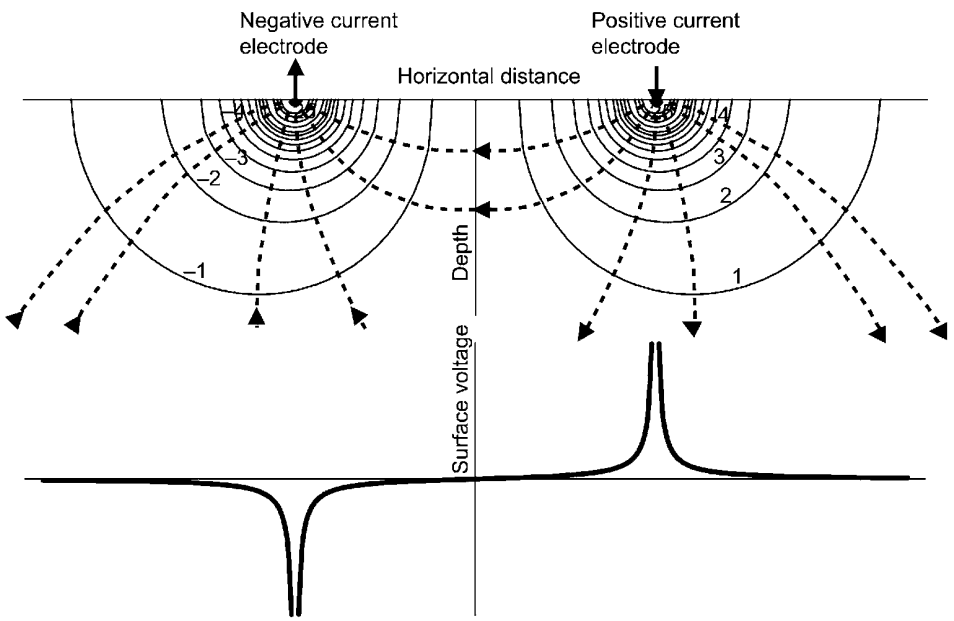

Fig. 10.2 Voltage and current paths in homogeneous ground for two electrodes (top) calculated from the sum of those for a single electrode, as in Fig. 10.1. The bottom figure shows the voltage distribution at the surface. Horizontal distances, depth and voltage are in arbitrary units.

Where there are two electrodes, which in practice are needed to complete the circuit, the voltage and current at each point are the sum of those in Fig. 10.1a and b. This is shown in Fig. 10.2 (top). Close to each electrode, the distributions are very similar to those for the single electrode case, but the distributions become increasingly distorted from those as the distance from the electrodes increases. This is because the current must pass from one electrode to the other. Figure 10.2 shows the current and voltage distribution for an ideal case of an electrically homogeneous and isotropic medium. Soils and geological materials are usually neither. They exhibit layering, often contain inclusions of markedly different electrical properties and have conductivity gradients or sharp boundaries resulting from water content or solute concentration changes. These change the current flow paths and, with them, the voltage distribution. ERI aims to interpret these differences of voltage from the ideal homogeneous and isotropic case, measured usually at the ground surface, to form an image of the electrical conductivity distribution below the surface. Using the Archie equation or the Waxman and Smits equation, or similar ones, the electrical conductivity distribution can be turned into an image of water content distribution in two or three dimensions.

10.3 Measurement Methods

ERI is most commonly used to obtain an image of the subsurface by measurements made at the soil surface. It may also be performed by measuring the resistivity between electrodes placed inside boreholes, either within the same borehole or between two or more different boreholes. It may also be performed between electrodes placed on the surface and ones inside a borehole.

In most cases, whatever the mode of measurement, four electrodes are used at one time. This is shown schematically in Fig. 10.3. Two of the electrodes are used to inject a current into the soil, while a different pair measures the voltage. The advantage of using two of each is that it minimises the effect of poor contact between the electrodes and the ground. This can be seen in Fig. 10.4, which shows a simplified one-dimensional arrangement. In this model, the resistance between the two inner electrodes is R, while there is an extra resistance of r between each electrode and R. The current in the circuit is given by

$$I = \frac{V_0}{R + r_3 + r_4}, \tag{10.3.1}$$

and the voltage, V, across the resistance, R, is

$$V = IR. \tag{10.3.2}$$

Dividing V by I leads to the correct identification of the resistance R. If the same electrodes had been used for both the current and voltage measurements, then the voltage measured would have been V_0 and the resistance would have been calculated as $R + r_3 + r_4$.

Note that by using separated current and voltage electrodes, the array will return the same value of R whichever pair of electrodes is used for the current and the voltage and whether all the rs are the same or not.

In practice, the four-electrode array does not operate perfectly, since to measure the voltage, some current must be drawn through the voltage electrodes and so there will be a

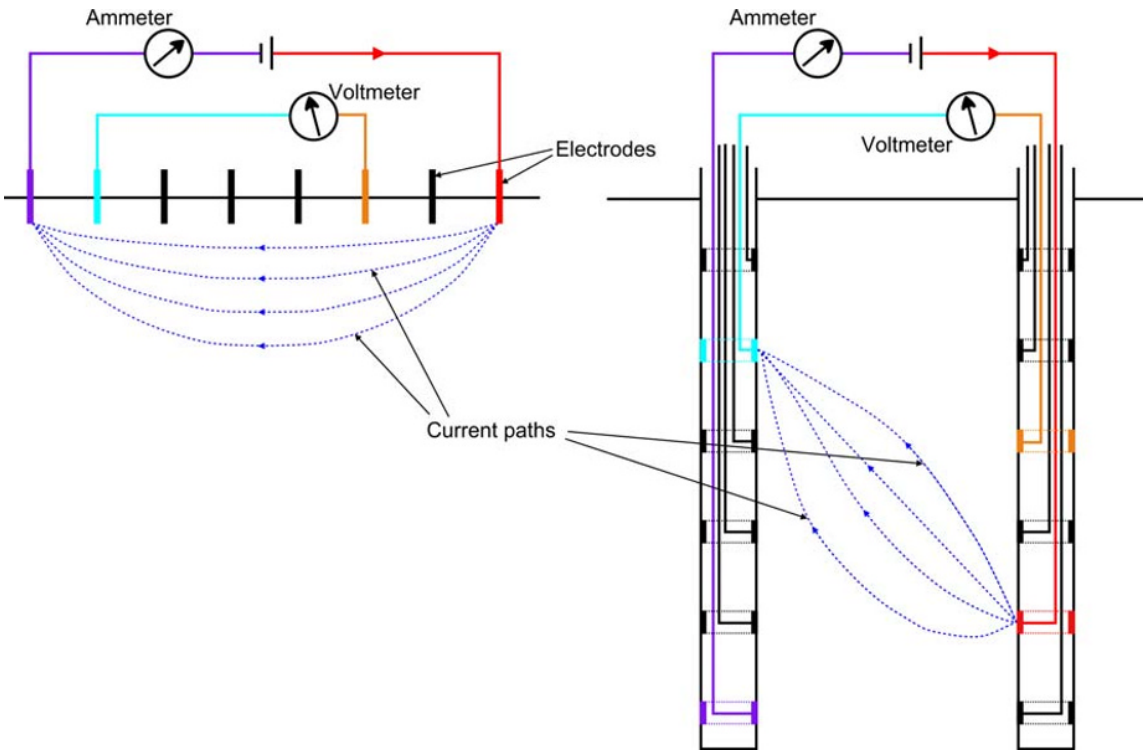

Fig. 10.3 Two possible arrays of electrodes for performing ERI measurements, one set measuring from the surface, whereas the other between two boreholes. The four-electrode array with separate current and voltage electrodes minimises errors resulting from poor contact between the electrodes and the ground. (*See insert for colour representation of the figure.*)

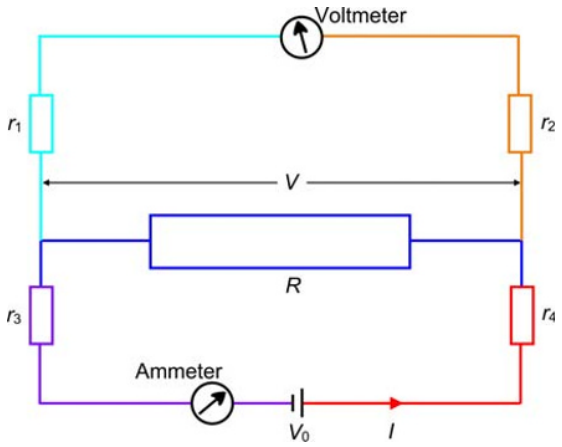

Fig. 10.4 Illustration of the elimination of contact resistance by a four-electrode array. The resistor whose value is to be measured has a resistance of R and the contact resistances are represented as resistors of value r_i. R represents the soil between the two voltage electrodes, r_1 and r_2 are contact resistances between the voltage electrodes and the ground, and r_3 and r_4 are contact resistances between the current electrodes and the ground as well as the ground resistance between the current and voltage electrodes.

small voltage drop across the contact resistances, represented by r. This can usually be made negligible by using a meter with a sufficiently high input impedance. If this is not the case, then a correction can usually be applied.

In the case of soil measurements, the current paths are not as simple as in the idealised picture in Fig. 10.3, but, nevertheless, the same principles apply.

The three most common electrode arrangements are the *Wenner*, *Schlumberger* and *dipole–dipole arrays*, illustrated in Fig. 10.5. The Wenner array is characterised by equal spacings between electrodes, while the Schlumberger one aims to measure the local gradient of voltage by having a small spacing between the inner voltage-measuring electrodes.

Electrical resistivity measurements are often analysed by calculating the *apparent resistivity* of the formation from an observation. This is the resistivity of a homogeneous medium that would produce the same voltage measurement between a pair of electrodes for the same injected current. By considering just a single electrode as in Fig. 10.1, the current spreads out radially from the injection point and is distributed equally across the surface of a hemisphere. At a radial distance, r, the *current density*, J, is the total current, I, divided by the surface area of the hemisphere, $2\pi r^2$, that is:

$$J = \frac{I}{2\pi r^2}. \tag{10.3.3}$$

This is related to the voltage gradient by a form of Ohm's Law:

$$\frac{\mathrm{d}V}{\mathrm{d}r} = \rho J, \tag{10.3.4}$$

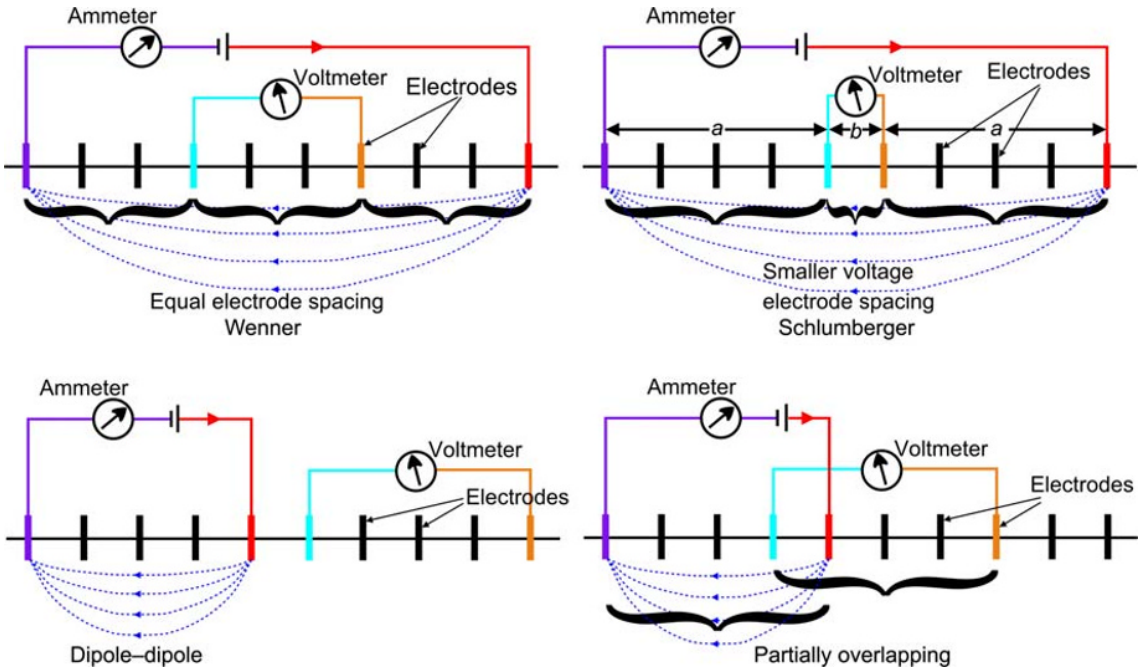

Fig. 10.5 Common electrode arrangements for surface electrical resistivity surveys.

where ρ is the resistivity of the medium.

Substituting for J into this equation and integrating and setting $V = 0$ as $r \to \infty$ give

$$V = \frac{I\rho}{2\pi r}. \tag{10.3.5}$$

This is valid both at the surface and beneath the ground. This solution is shown in Fig. 10.1 and, for two electrodes, in Fig. 10.2.

The voltage distribution produced by a particular current through any pair of electrodes in this medium can be calculated and, therefore, the resistivity of the homogeneous medium producing any observed voltage can be calculated. This is the apparent resistivity of the medium.

As an illustration, consider a symmetrical array, such as the Schlumberger or Wenner, with a distance between each current electrode and the nearer voltage one of a and between the two voltage electrodes of b, as shown in Fig. 10.5. The distance between the voltage and current electrodes is a and $a + b$, respectively. These are the relevant values of r for each voltage electrode, so that the voltage difference, ΔV, between them is

$$\Delta V = \frac{I\rho}{2\pi a} - \frac{I\rho}{2\pi(a+b)} - \left[-\frac{I\rho}{2\pi a} + \frac{I\rho}{2\pi(a+b)}\right], \tag{10.3.6}$$

giving

$$\Delta V = \frac{I\rho b}{\pi a(a+b)}. \tag{10.3.7}$$

Or

$$\rho = \frac{\pi a(a+b)\Delta V}{bI}. \tag{10.3.8}$$

The factor $(\pi a(a+b)/b)$ is called the *geometric factor*. It reduces to $2\pi a$ for the Wenner array $(a = b)$. Geometric factors for other arrays can be derived in a similar manner. Multiplying $\Delta V/I$ by the appropriate geometric factor yields the apparent resistivity of the formation.

10.4 Measurements in Practice

For measurement from the surface, it should be clear in Fig. 10.3 that the further apart the electrodes are, the deeper the penetration of the measurement. Some current will always reach a great depth and this will be reflected in the voltage across the measurement electrodes, but its contribution will be small compared with that from shallower depths. In all cases, whether measurements are made from the surface or between boreholes, the shortest current path is likely to contribute the most to the measurement, although layers or regions of greater conductivity may modify this.

A simple application is in estimating the depth to a layer of different resistivity from that close to the surface. If this has a lower resistivity than the overlying material (perhaps because it is below the water table and therefore saturated), using a Wenner or Schlumberger array with progressively

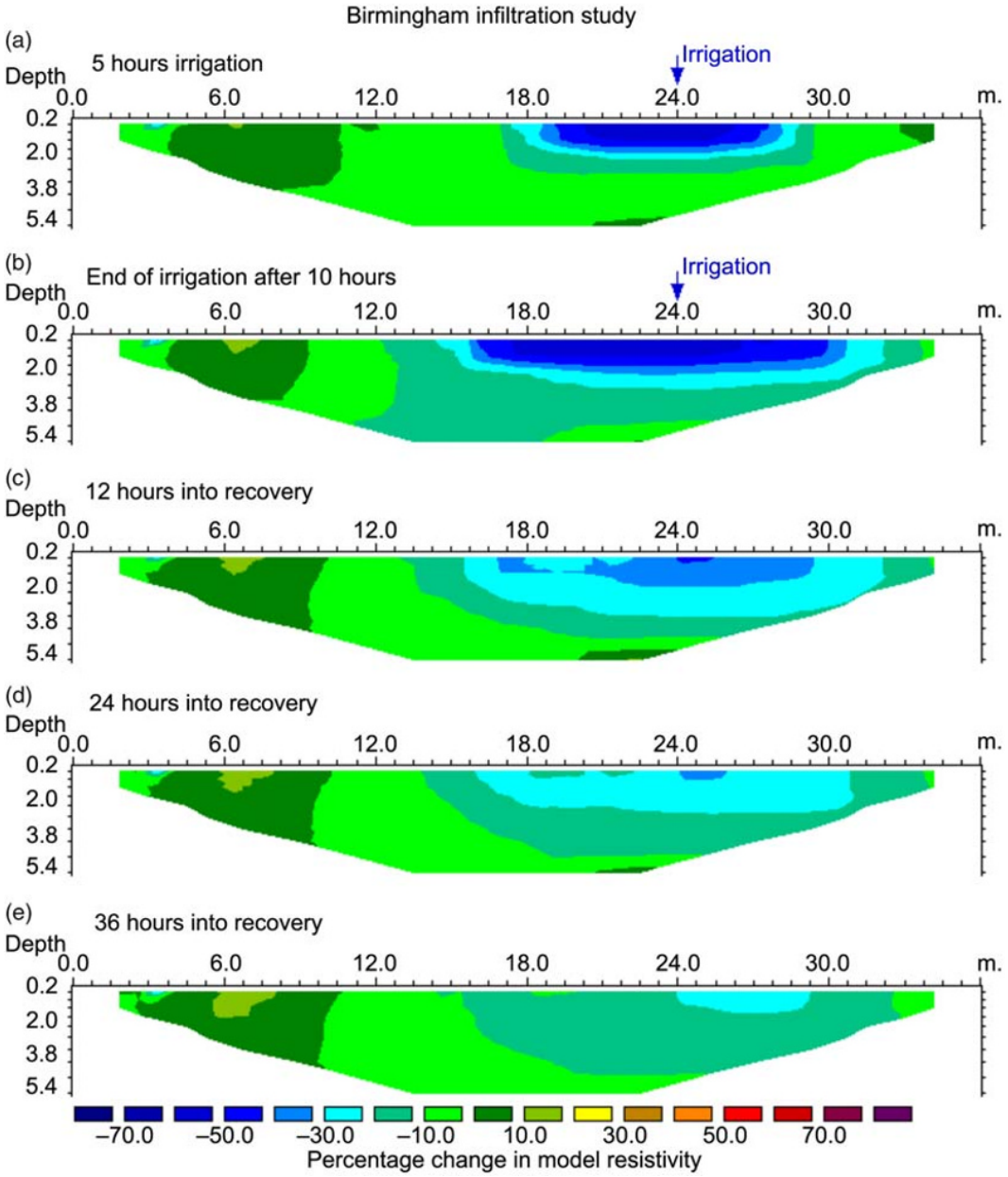

Fig. 10.6 Example of a two-dimensional resistivity survey tracking irrigation from a hosepipe in one section of the area and the subsequent redistribution (Loke, 2012 from data of Barker and Moore, 1998). Reproduced with permission of Dr. M H Loke. (*See insert for colour representation of the figure.*)

increasing distance between the electrodes will show a decreasing apparent resistivity of the formation as more of the current flow takes place in the deeper, lower-resistivity layer. This is known as *vertical electrical sounding*. By moving the entire array horizontally, lateral variations can be similarly detected. With computer-controlled electrode switching and large arrays of electrodes, much more sophisticated subsurface imaging is possible by using inverse modelling techniques (Section 17.13) to adjust a model of the subsurface environment to match the data acquired. Data acquisition does, however, take some time, perhaps a few hours for a large electrode array, making the method of limited use for transient events, such as following infiltration into the ground. Considerable labour is also involved in emplacing the electrodes, setting up the data acquisition system and, especially, connecting cables to all of them.

Although the measurements are described as dc, to avoid polarisation effects at the current electrodes and spurious effects from naturally occurring ground (telluric) currents, self-potentials and streaming potentials, in practice the power source is usually a very low-frequency

(<~20 Hz) voltage. Nevertheless, electrical noise is often a problem and this can be reduced by *stacking* readings. Stacking is another name for averaging over several readings taken in close succession. Measurement accuracy is usually better if the voltage signal is relatively large. For this reason, the potential applied to the current electrodes is often several hundred volts, since the observed voltages will be proportional to this. This introduces an obvious safety hazard and requires careful management of procedures to avoid connecting the equipment to the current source while handling of the electrodes is taking place. With modern equipment and computer-controlled electrode switching, each measurement takes of the order of 15 s. Although this appears very short, the number of possible combinations is such that it may take several hours to cycle through them all.

If the array consists of n electrodes, there are, in principle, $n(n-1)$ ways in which the voltage electrodes can be configured. However, of these, most can be calculated by difference from measurements between other pairs. For instance, knowing the voltage between electrodes 1 and 2 and between electrodes 1 and 3, the voltage between electrodes 2 and 3 is obtained by subtracting one from the other. So keeping one voltage electrode fixed and measuring the voltage between this one and each of the $n-1$ other electrodes in turn, the voltage of all of the other combinations can be calculated. That leaves $n-2$ electrodes for current injection. The same principle applies for the current electrodes and there will be $n-3$ independent ways in which these can be connected for each of the $n-1$ voltage combinations. This gives $(n-1)(n-3)$ independent possibilities. Interchanging the current electrodes for the voltage ones should also make no difference – these are known as *reciprocal* measurements (see Fig. 10.4). This halves the number of independent possibilities again, leading to $(n-1)(n-3)/2$ combinations. The inclusion of some reciprocal measurements is often valuable as a check on data quality, however. Some electrode combinations will give only a very small measurement. For instance, if the current is injected between two electrodes at one end of the array and the voltage measurement is taken between another pair at the other end, then one would expect only a negligible voltage.

One strategy is to use one fixed electrode for the current injection and another for voltage measurements, with all combinations of the remaining electrodes being used for the other current and voltage measurement point (Daily *et al.*, 2004). This reduces the number of combinations to $(n-2)(n-3)$.

Considerable effort has been expended on devising efficient sampling strategies for electrical resistivity surveys (see, for instance, Furman *et al.*, 2002, 2003, 2004). These aim to abstract the maximum information from a survey under constraints, for instance, of the number of electrode combinations that can be sampled. Much work has also been put into computer software for interpreting the information from a survey (usually termed *inverting* the measurements, since the basic technique is to use *inverse methods* to produce an image of the subsurface environment). The basic procedure is to start with an assumed electrical conductivity distribution in the subsurface, which at its simplest may be a homogeneous one, and then to adjust the electrical conductivity of different areas of the model until a good fit between the observations and the predicted measurements is obtained, such as shown in Fig. 10.6.

Electrodes used may be metallic or, often, graphite. Good contact between the formation and the electrodes is important. For surface-based measurements, this means driving the electrodes into the ground a little way, say, 300 mm (e.g. Jayawickreme *et al.*, 2008). If contact with the ground is a problem, it may be enhanced by pouring a little salt solution around the electrodes. Contact may be more difficult to ensure when the electrodes are on the side of a borehole. Borehole casings are often installed inside a somewhat larger diameter hole and the space occupied by a backfill, which may be much more or less conductive than its surroundings. Using the ratio of measurements between different sampling times can often reduce the distortions markedly or eliminate them entirely (Daily *et al.*, 2004).

10.5 Conclusion

The advantages of ERI are that it allows measurements to be made of subsurface water content of a large area (up to about 1 km in extent) and to considerable depth (several tens of metres). It does, however, require that the electrical conductivity of the soil solution be known and remain effectively constant over time if repeated measurements are needed. It is also a powerful way to track a pollutant of contrasting electrical conductivity in both the saturated and unsaturated zones (e.g. Slater *et al.*, 1997).

There are a number of similarities between GPR and ERI. Both methods are nonintrusive or at least minimally intrusive and can be used to reconstruct an image of the subsurface environment from either surface measurements or boreholes, and both use inversion techniques by adjusting the parameters of an assumed model of the subsurface to derive a 'snapshot' of the below-ground environment in two or three dimensions. In addition, both methods have application far beyond soil water monitoring. Archaeological and forensic investigations have been a major beneficiary of GPR for some time, while ERI finds employment in mineral prospecting, landfill, contaminated ground and mineshaft investigations. ERI is generally able to penetrate much deeper into the soil than GPR, except in very favourable conditions, but ERI is subject to considerable uncertainty as a result of its dependence on a good knowledge of the electrical resistivity of different strata.

A number of studies have used both methods in combination to benefit from these different characteristics, for example, Garambois *et al.* (2002), Binley *et al.* (2002a, b), and Day-Lewis *et al.* (2005).

Telford *et al.* (1990) gives a good general introduction to ERI.

Part III Water Potential

11 Water Potential Measurement

11.1 Introduction

The basic concepts of water potential were introduced in Section 2.1.1, where it was argued that the most appropriate units for hydrological purposes were in terms of equivalent head of water (i.e. m water).

In contrast to water content, the idea of some physical reality to an average water potential over a region of space is rather difficult to envisage. Nevertheless, any method to make a measurement of water potential involves some kind of averaging, either over a small volume around the sensor or over a surface in contact with the soil. A little thought leads to the conclusion that the presence of a finite size sensor causes some disturbance to the potential and/or flow distribution. Clearly, the smaller the sensor, the less this disturbance is likely to be. On the other hand, larger sensors are less susceptible to local inhomogeneities and often react more quickly to changes (Hendrickx *et al.*, 1994).

All sensors must exchange a certain amount of water with their surroundings, so that this quantity is an important factor in determining the *response time* of the sensor. The other major factor controlling the response time is the ease with which water can pass between the interior of the sensor and the bulk soil surrounding it. This involves the hydraulic characteristics of the soil, the sensor materials, the size and shape of the sensor and the degree of contact between the soil and the sensor.

As a general rule, fast response is associated with sensors that require a small amount of water exchange with the soil; have high internal hydraulic conductivity, large surface area and good contact with the soil; and are in soil with high soil water diffusivity. This last characteristic is not under the control of investigators.

11.2 Types of Sensor

Soil water potential sensors can be grouped in different ways. One is according to whether they transfer water *via* the liquid or vapour phase. Another is whether the measurement is a direct one or relies on an intermediate property, usually the water content of a block of some substance with known properties in contact with the soil.

11.2.1 Sensors communicating via the liquid phase

Most water potential sensors are in direct hydraulic contact with the soil. Water is transferred between soil and sensor until the water potential in each is the same.

The most common instrument of this type is the *tensiometer*. A space inside the device contains a reservoir of water, which is in pressure equilibrium with the matric potential outside, and this pressure is measured directly. This is the most accurate type of device, but is usually limited to potentials down to about –8.5 m water (–0.85 bar). Tensiometers are described in Chapter 12.

Various sensors essentially measure the water content of a block of porous material whose matric potential is in equilibrium with the soil in which it is embedded. These differ according to the method by which the water content is measured. Such sensors are not limited to any particular range of water potential, but it is difficult to obtain high accuracy, not only because of the large range over which they are sensitive but also because of hysteresis in the water content–water potential relationship of the porous material. Indirect sensors are described in Chapter 13.

11.2.2 Sensors communicating via the vapour phase

Vapour phase sensors measure the vapour pressure of water in the soil, which is a function of the thermodynamic potential of the water and thus is principally affected by matric and osmotic potentials. The most common type of sensor is the *soil psychrometer*. Because the vapour pressure of water varies very little from its saturated value at modest water potentials, these sensors are most suitable for use at low water potentials. Soil psychrometers are described in Section 14.2.

Soil Water Measurement: A Practical Handbook, First Edition. J. David Cooper.

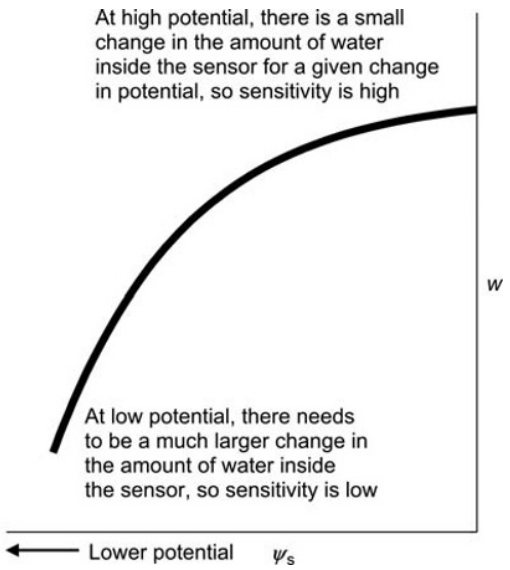

Fig. 11.1 Schematic of water contained in a water potential sensor versus indicated water potential for a sensor that communicates via the liquid phase.

11.3 Sensitivity

All water potential measurement devices rely on the exchange of a quantity of water between the soil and the sensor. Clearly, the smaller the amount of water needed to change the reading from one potential level to another, the less disturbance will be caused to the soil water potential distribution and the faster the device will reach equilibrium with its surroundings. A sensitive device, therefore, is one which requires only a small quantity of water to be exchanged for a given change of water potential.

We define the *sensitivity*, S, of a water potential sensor, therefore, as the change in indicated water potential, $\Delta\psi_s$, divided by the quantity of water, ΔW, exchanged with its surroundings to make that change in indicated potential:

$$S = \frac{\Delta\psi_s}{\Delta W}. \tag{11.3.1}$$

Or, as the change of water potential and water quantity becomes very small,

$$S = \frac{d\psi_s}{dW}. \tag{11.3.2}$$

The subscript s for the water potential indicates that it is the sensor reading and not the soil water potential that is referred to. This latter formulation accommodates those cases where the amount of water needed to cause a given change in the indicated potential varies across the potential range. It is the reciprocal of the local slope of the W versus ψ_s curve. See Fig. 11.1, which shows a typical relation between water contained in a sensor and the indicated potential for a sensor that communicates *via* the liquid phase.

11.4 Response Time

The response time is calculated in a similar way to that of the time constant of an electrical circuit (Section 8.3.2). If the potential outside the device were to change suddenly from a value of ψ to $\psi + \Delta\psi$, then the time for the potential indicated by the sensor to change by $(1-(1/e))\Delta\psi$ would be the response time of the sensor. If the resistance to exchange of water between the sensor and the bulk soil and the quantity of water required to make a given change in the device's reading were both constant, then the response time would be the same throughout the range of the instrument and the term *time constant* would be justified. However, we have already seen that the amount of water transfer needed to produce a given change in indicated potential (i.e. the reciprocal of the sensitivity) is often not constant. As soil dries, its diffusivity usually falls very significantly, making it harder for water to be exchanged with the bulk soil. The two factors combine to increase the response time very considerably as the soil dries. Changes in soil water potential, however, are usually much slower when the soil is drying than when it is wetting, when responses to rainfall or irrigation are rapid. So the situation is not as serious as it might at first appear. Nevertheless, indicated readings by some sensors can lag behind the true value by several days and, in most cases, will lag behind by increasing amounts of both time and potential as the soil dries, only to recover very quickly once it wets up.

The response time may be calculated by considering the time required for a small quantity of water, ΔW, to move from the sensor into the bulk soil. The change in potential indicated by this can be calculated from the definition of sensitivity given above:

$$\Delta\psi_s = S\Delta W. \tag{11.4.1}$$

If we can characterise the restriction to flow between the sensor and the bulk soil by a resistance, r, which we will assume for the present to be constant, then the flow of water between the device and the bulk soil can be expressed as

$$\frac{dW}{dt} = \frac{\psi - \psi_s}{r}, \tag{11.4.2}$$

where ψ is the potential of the bulk soil.

From (11.4.1),

$$\frac{dW}{dt} = \frac{1}{S}\frac{d\psi_s}{dt}. \tag{11.4.3}$$

Substituting this into (11.4.2),

$$\frac{d\psi_s}{dt} = \frac{S}{r}(\psi - \psi_s). \tag{11.4.4}$$

This is similar to the situation depicted in Fig. 8.3 for the charging of a capacitor through a resistor. So, similar to Equation 8.3.12, we expect the indicated potential to approach the true value according to

$$\psi_s = \psi_s(0) + (\psi - \psi_s(0))\left(1 - e^{-(S/r)t}\right). \qquad (11.4.5)$$

If both S and r are constant, then this would imply a time constant of r/S. Neither S nor r is usually constant, but Equation 11.4.5 gives a flavour of the behaviour and shows that the approach to indicating the true reading is often quite slow. Since a proper time constant cannot be defined, the term *response time* is used as a somewhat looser definition of the characteristic time over which equilibrium is achieved. In particular, the response time is shorter if the sensitivity of the tensiometer is high (i.e. if only a small amount of water needs to be exchanged with the soil to change the indicated reading by a given amount) and if the resistance to flow of water between the sensor and the surrounding soil is low. This condition will usually be true when the soil matric potential is high (i.e. wet soil) and diffusivity is high. Factors in the design of the sensor are also involved in r; for instance, the conductance of a tensiometer cup or the diffusivity of the material of a porous medium sensor (see Chapters 12 and 13).

12 Tensiometers

12.1 Components of a Tensiometer

In essence, a tensiometer consists of a porous barrier, allowing water but not air to flow between its interior and the soil outside; a chamber filled with water and a means of measuring the pressure of that water, as shown diagrammatically in Fig. 12.1.

In operation, water flows between the soil and the interior of the tensiometer until hydraulic equilibrium is achieved between the water in the soil and that inside the tensiometer. Measurement of the water pressure in the chamber then yields the hydraulic potential of the soil water. If air from the soil were allowed to enter the tensiometer *via* the porous barrier, this would cause all the water in the tensiometer to flow out of the chamber and the internal pressure in the chamber would be that of the air in the soil (usually the same as atmospheric pressure).

12.2 The Porous Barrier

The requirements for the porous barrier are:

- It should have sufficiently small pore size that the pores remain water-saturated over the entire range of matric potential that the tensiometer is required to operate.
- It should possess good hydraulic conductivity so that water flow is not significantly restricted.
- It must be sufficiently robust that it remains intact under the conditions of use. For field applications, installation often imposes considerable mechanical stresses on the porous barrier.

The most common material for porous barriers is unglazed ceramic. This material is readily available; fairly cheap, especially in quantity, and can be made in a wide variety of different pore sizes, hydraulic conductivity, shapes and sizes.

Some specialist suppliers, for instance Soil Moisture Equipment Corp., produce a range of ceramic *tensiometer cups* especially for the purpose. Specialist ceramics manufacturers can also supply porous ceramics tailored for different requirements. Porous ceramic is used extensively in filtration applications so that suitable material can often be purchased from suppliers to industries using these processes. An equivalent pore diameter of 1 μm is suitable for matric potentials to below –10 m water (–100 kPa or –1 bar), which is comfortably beyond the range of the tensiometer. If matric potentials are unlikely to fall below fairly modest values, then larger pore size material can be used, with consequent benefits in higher hydraulic conductivity.

The relation between pore diameter and air entry potential is given by Equation 2.1.2. Manufacturers often quote pore diameters in terms like '90% of pores smaller than' the specified value so that it is necessary to use a material with a nominal pore size about a factor of two smaller than implied by Equation 2.1.2. For instance, inserting –100 kPa for P into Equation 2.1.2 yields a pore diameter of about 3 μm so that using a material with a nominal pore diameter of 1 μm satisfies this requirement.

The air entry potential of a cup can be tested by firstly saturating it slowly by wetting from one side only. Then, with the empty cup immersed in water, increasing the air pressure inside slowly and watching until bubbles appear. The experimental setup is shown diagrammatically in Fig. 12.2. Use of high air pressure is dangerous, so it is essential to test that all joints are secure and to use a safety screen in case of an unexpected explosion caused by failure of the ceramic or other parts.

Often, suitably shaped cups may be available in the manufacturer's range. If not, it will be necessary to pay for production of a suitable mould. There is also normally a moderately substantial charge for each order, with the price of each item being very cheap. It makes sense, therefore, to keep costs down by ordering as large a number of cups as are likely to be needed in the foreseeable future.

Alternatives to ceramic include sintered glass, bronze and plastics and semipermeable membranes. Sintered materials usually exhibit high hydraulic conductivity but are often restricted to a fairly small air entry potential. Membranes, on the other hand, are easily damaged while

Soil Water Measurement: A Practical Handbook, First Edition. J. David Cooper.

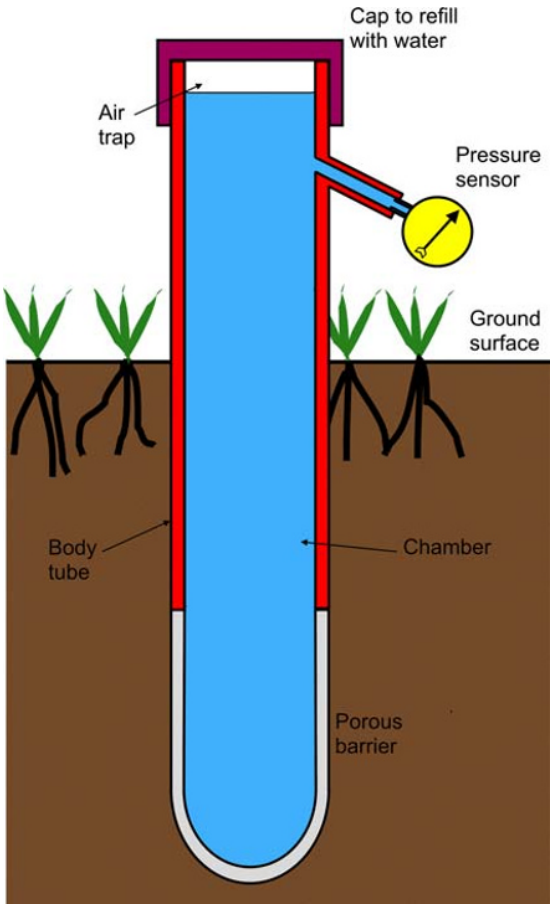

Fig. 12.1 Components of a tensiometer.

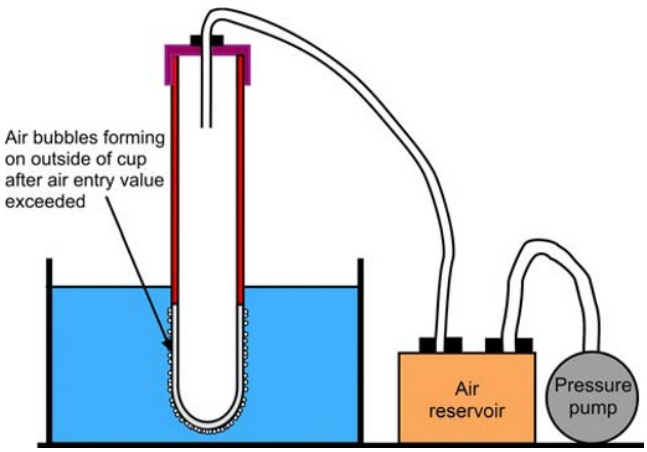

Fig. 12.2 Testing the air entry pressure of a tensiometer cup by applying air pressure to the inside. The point at which small air bubbles just start to appear on the surface of the cup is the air entry value. Note that a shield around the apparatus is essential to avoid injury from explosion of the apparatus resulting from failure of one component or a joint.

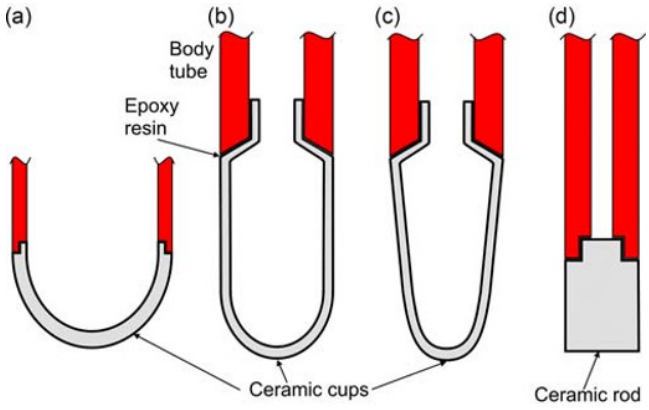

Fig. 12.3 Some common shapes of tensiometer cups. (a) Hemispherical; (b) straight-sided; (c) tapered; and (d) solid.

inserting the tensiometer into the soil and are, therefore, best suited to laboratory conditions. For these reasons, porous ceramic remains the best overall choice for general-purpose tensiometer construction.

The size and shape of the porous barrier is determined mainly by the needs to maximise the area of contact with the soil, to encourage efficient transfer of water between the tensiometer and the surrounding soil, to minimise the length of the water path across the porous barrier, to reduce resistance to flow, to have adequate strength to minimise the risk of breakage during installation and to be compatible with the other components of the tensiometer.

For these reasons, tensiometer cups are usually shaped as shown in Fig. 12.3a or b. The hemispherical end ensures good strength and will often bed into loose material at the bottom of the hole. The straight sides shown in Fig. 12.3b increase contact area provided it fits tightly into the hole.

Many other shapes are possible but rarely used in practice. A slight conical shape, as shown in Fig. 12.3c, should improve contact but requires a special tool to produce the correct shaped hole. A solid rod of porous ceramic may also be used instead of a hollow 'cup' as shown in Fig. 12.3d. This latter arrangement is suitable only where the soil is poorly conductive or where a slow response time can be tolerated.

12.3 The Body Tube

The tensiometer body is a support for the cup, a water reservoir and a means of transmitting, *via* the water column, the pressure inside the cup to the pressure sensor.

It often also provides a seal against the soil, preventing rain or irrigation water from bypassing the soil and reaching the cup. In most tensiometers, the body has the same diameter as the cup so that the two form a smooth cylindrical object. However, there is no reason why this has to be so, and tensiometers with body tubes both smaller and larger

than the cup diameter can be used, although installation may not be quite so straightforward.

12.4 The Air Trap

At the top of the body tube, there is usually an *air trap*. This collects air bubbles, which form within the cup and the body of the tensiometer. These can then be expelled easily and replaced by water. The air trap is usually made of transparent plastic, often acrylic, so that it is easy to see how much air has collected and whether the tensiometer needs to be *purged*. The air trap is either bonded to the body tube or, often, forms part of it, so that the body tube is made from a single piece of transparent acrylic plastic, PVC or polycarbonate.

The air trap is also used for refilling the tensiometer with water. This is done through a removable cap, usually a neoprene bung, although other arrangements, for instance a screw cap with rubber sealing washer, can be used. It is also the route for connecting the pressure sensor, which may be through the cap or *via* a sidearm, similar to the one depicted in Fig. 12.1.

12.5 The Pressure Sensor

To measure water potential at the position of the cup, the water pressure in the body tube must be measured. This can be done in a variety of ways. In practical terms, three types of pressure sensor are in common use – manometers, bourdon gauges and pressure transducers.

12.5.1 The manometer

A manometer measures pressure by balancing the weight of a column of liquid against the pressure in much the same way as in a barometer. In principle, many liquids could be used, but in practice, virtually all tensiometers use water or mercury.

Water manometers

A water manometer is attractive, since it is the same fluid as in the tensiometer body and is also very readily available. The principal disadvantage is that the water level in the manometer must be below the cup position if the soil is unsaturated and therefore the internal pressure inside the tensiometer is below atmospheric pressure. This is illustrated in Fig. 12.4. Even if the soil is saturated, in which case the tensiometer will act as a *piezometer*, the water level is likely to be above the soil surface only under very exceptional circumstances.

A further feature of the water manometer is that the reading is very sensitive to changes in water potential. Where very accurate measurements are required, this is clearly a very good thing. However, over the full range that the tensiometer is able to record, about 8.5 m water head, this is also the range of water levels in the manometer!

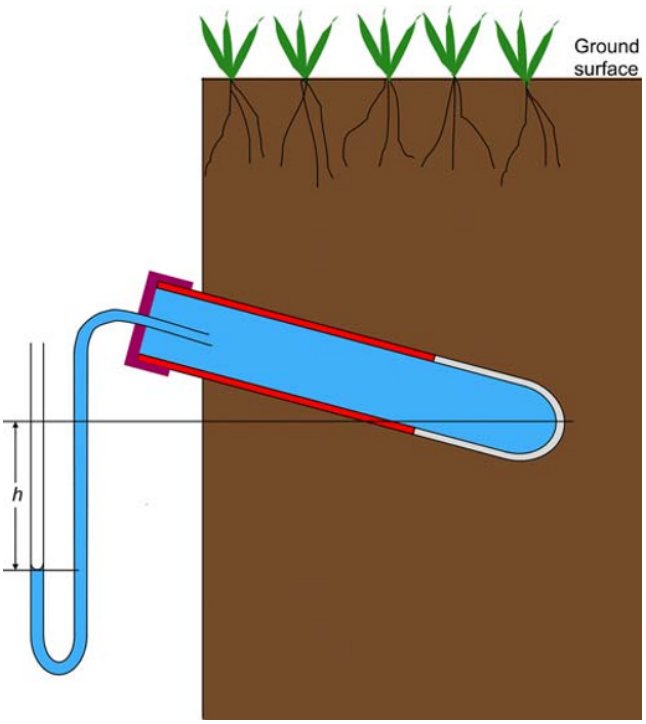

Fig. 12.4 A water manometer tensiometer used with a tensiometer.

In practical terms, this means that a water manometer can be used only where the range of water potential expected is relatively small, say 1 m.

In cold weather, freezing of the water in the manometer not only makes it unusable but may lead to serious damage, depending on the materials used.

Water manometers, therefore, have only very limited application but can be useful where suitable access is possible, such as on the side of a ditch or pit or a laboratory column, and where water potential is expected to remain close to zero.

Mercury manometers

For most practical purposes, mercury is the almost universal choice as the indicating fluid. It is very much denser than water (13.6 times), which allows the manometer to be above ground. It also allows the complete range of water potential to be accommodated on a physical scale of about 0.75 m, which is convenient for most operators. A schematic diagram of a mercury manometer is shown in Fig. 12.5.

To simplify understanding the operation of the mercury manometer, it will be assumed that the water potential in the soil is in equilibrium with that inside the tensiometer cup and that the local air pressure in the soil is the same as that in the atmosphere, A. The water pressure inside the cup is $A + \psi_m$, which in unsaturated soil is less than atmospheric pressure, since ψ_m is negative. The pressure in the water at the interface with the mercury column is therefore $A + \psi_m - z - d - h - s$, where z is the depth of the cup below

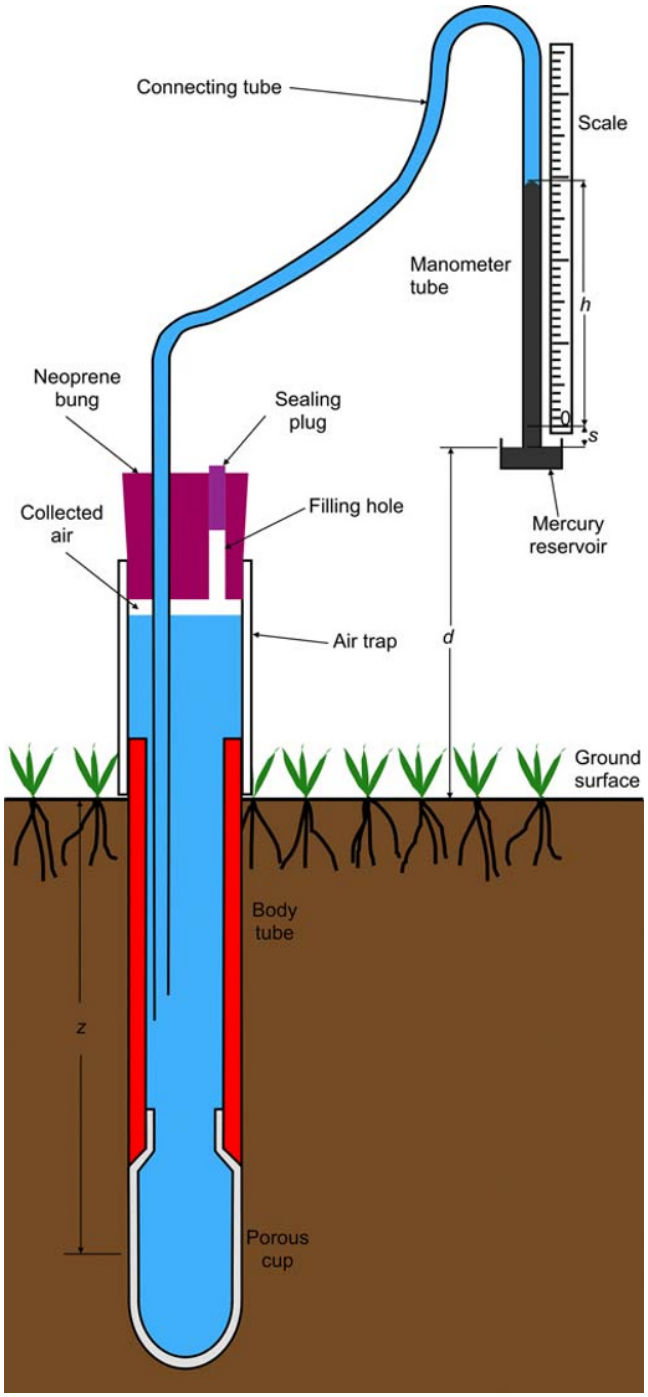

Fig. 12.5 Tensiometer with a mercury manometer.

ground level, d is the height of the top surface of the mercury in the reservoir above ground, h is the height of the mercury column above the scale zero mark and s is the distance of the scale zero above the mercury in the reservoir. The total height of mercury in the manometer above that in the reservoir is $h + s$.

Looking now at the pressure inside the mercury, that at the interface with the water is $A - (\rho_{Hg}/\rho_w)(h+s)$, where ρ_{Hg} is the density of mercury and ρ_w is the density of water. The pressure in the water and that in the mercury are not quite equal, as there is a small interfacial pressure between them, dependent on the surface tension between the two fluids, the diameter of the manometer tube and the contact angle. There is also a very small interfacial pressure difference at the mercury surface in the reservoir. We will designate the combined effect of these two as δ. So equating the pressures across the mercury – water interface:

$$A + \psi_m - z - d - h - s + \delta = A - \frac{\rho_{Hg}}{\rho_w}(h+s). \qquad (12.5.1)$$

The height of the mercury column is therefore

$$h = \frac{z + d - \delta - \psi_m}{((\rho_{Hg}/\rho_w) - 1)} - s. \qquad (12.5.2)$$

Ignoring δ and s for a moment, we see that h will always be positive, since we expect ψ_m to be negative. Indeed, even if ψ_m is positive (i.e. positive water pressure), then h will still be positive provided that $\psi_m < z + d$. That is, provided the water table is below the level of mercury in the reservoir.

δ and s are usually very small and so make very little difference to this argument.

In terms of total hydraulic potential, $\psi_h = \psi_m - z$, and so from Equation 12.5.2:

$$h = \frac{d - \delta - \psi_h}{((\rho_{Hg}/\rho_w) - 1)} - s. \qquad (12.5.3)$$

12.5.2 Bourdon gauge tensiometers

The usual arrangement for a tensiometer using a Bourdon gauge to measure the pressure is shown in Fig. 12.1. The inclined sidearm ensures that air bubbles are not trapped in it. As pressure inside the tensiometer falls, the air inside the Bourdon gauge expands and forms bubbles, which rise into the air trap. Bourdon gauges are usually fitted with a screw connector, which can be fitted to the tensiometer and sealed with an 'O'-ring, or by sealing the thread with plumbers' PTFE tape. The air trap usually has a screw-on cap sealed by a rubber washer.

Bourdon gauge tensiometers are usually bought as complete units but can be constructed easily in much the same way as a mercury manometer tensiometer.

Bourdon gauges are inherently less accurate than mercury manometers, partly because the scale is relatively small to cover the whole range from 0 to –10 m water, partly because of mechanical linkages in the mechanism and partly because the Bourdon tube is likely to creep over time causing the zero point to move. This latter can be corrected by testing the gauge periodically and either the readings adjusted to suit or by a zero-point adjustment built into the gauge.

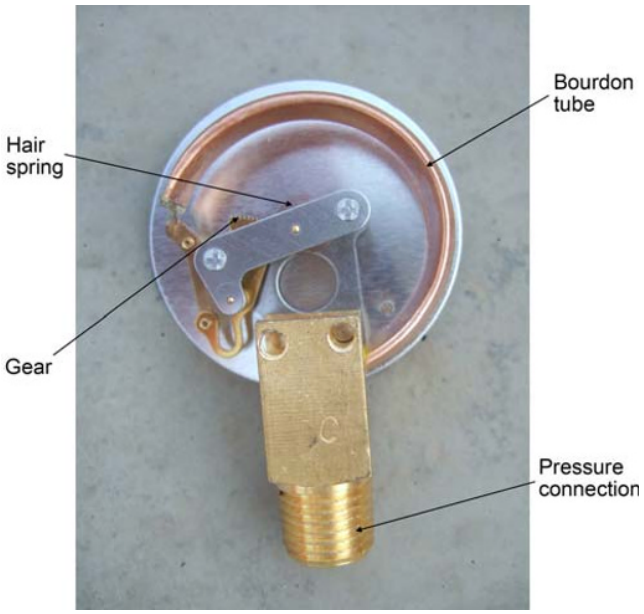

Fig. 12.6 Bourdon gauge operating mechanism.

Figure 12.6 shows a schematic diagram of the workings of a Bourdon gauge. Changes in the pressure inside the *Bourdon tube* – a sealed, flattened tube bent into a curve – cause it to change shape, either to straighten (increase in pressure) or curl more (decrease in pressure). The small movement of the tip of the tube is amplified by levers and gears, which convert it to a rotation of a needle on a scale.

Bourdon gauges are easily damaged by frost, when water inside the Bourdon tube freezes and expands, distorting the tube. These tensiometers are also quite sensitive to solar radiation and temperature changes (see Section 12.5.4) and so radiation shielding is recommended.

12.5.3 Pressure transducer tensiometers

Electrical pressure transducers have been available for several decades, and cheap transducers of sufficiently good quality to match the accuracy of mercury manometers are easily available. Compared with these, transducers need less maintenance and setup is simpler. They can also be read using a simple handheld reader with a digital output, which reduces errors. Perhaps the greatest advantage over other pressure sensors is that they can be connected to a field data logger and readings recorded automatically at frequent intervals over periods of a few weeks unattended. In conjunction with dielectric soil water sensors (Chapter 8), this provides a powerful capability to record variations of both water content and potential at several depths almost continuously. The addition of a tipping bucket or other form of recording raingauge allows infiltration events to be followed in considerable detail.

Automatic recording of environmental data poses dangers of misinterpretation through events that are not recorded nor suspected. These include human intervention, disturbance by animals, rock and tree falls, landslides and other natural processes. Tensiometer data is more prone to this than many other types of data because of incorrect readings caused by air collecting in the tensiometer. This can result in errors both from the lack of a continuous water column between the tensiometer cup and the sensor and because the tensiometer readings lag significantly behind the actual changes in the surrounding soil.

As in any other field of environmental investigation, there is no substitute for frequent visits to field sites, particularly during events of interest. The ability to record data automatically is a powerful addition to frequent personal visits, not a substitute for them.

The principles of operation of pressure transducers and some of their operating requirements are outlined in an appendix to this chapter (Appendix 12.A).

12.5.4 Tensiometers with fixed pressure transducers

A fixed pressure transducer may be attached in the same way as a Bourdon gauge as shown in Fig. 12.1. With compatible fittings on each, the transducer may be a direct replacement for the Bourdon gauge. Alternatively, it can be mounted on top of the tensiometer as shown in Fig. 12.7. In this configuration, the tensiometer may be refilled through a filling hole next to the transducer if there is room. Otherwise, the transducer must be removed each time to refill the tensiometer. With the transducer above ground, the system may be very sensitive to air temperature changes and especially to heating by solar radiation. This is particularly true if the tensiometer is completely full of water and so has very high sensitivity. A small volume change of the water in the tensiometer caused by a temperature variation can then cause a large change in the internal pressure as a result of the small compressibility of the various components. The actual size of the pressure response will depend not only on the sensitivity of the system but also on the rate at which the temperature changes and the resistance to water exchange between the tensiometer and the surrounding soil.

To reduce the sensitivity to these effects, the tensiometer should be shielded from direct sunlight and insulated. Aluminium-coated melamine film is an efficient and cheap solar radiation shielding material. It is, however, very important to mount the film with the aluminium side on the inside. Aluminium is an efficient reflector at most wavelengths, but melamine is transparent only in the optical range. At infrared wavelengths, it is no longer transparent and so radiates heat. If the melamine is on the inside, this heat is radiated into the object that it is designed to protect. In some situations, it can get hotter than if there were no shielding. Beneath the solar shield, foam insulation should be used to reduce temperature changes at the tensiometer body further. In some situations, several centimetres of insulation may be necessary. The bulk of the insulation required may create

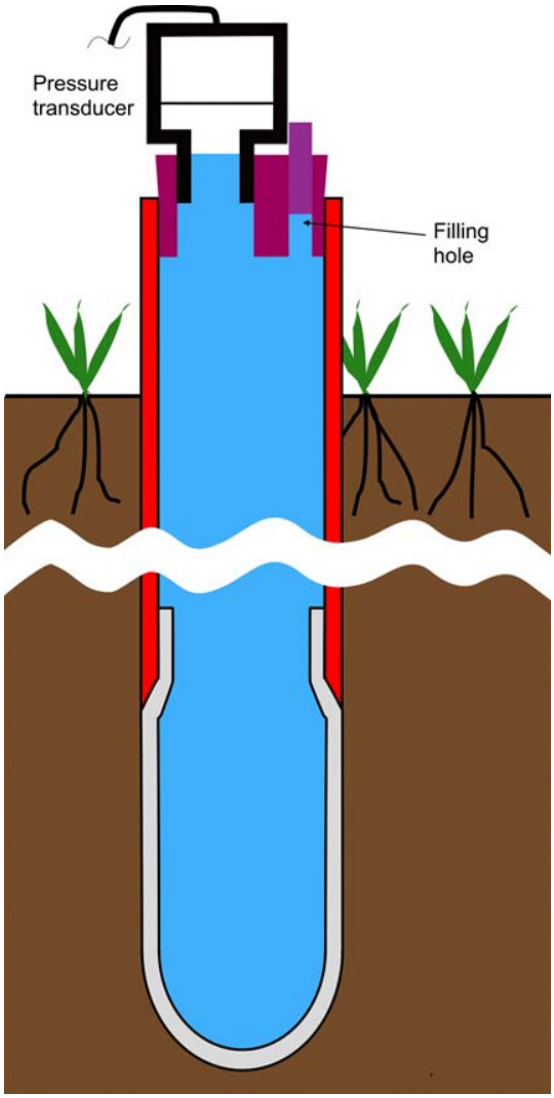

Fig. 12.7 Pressure transducer mounted on top of tensiometer.

its own problems in shielding the soil beneath from rain and sunlight. As a result, tensiometers with above-ground pressure transducers are not generally recommended.

While there may be some added complication to siting a pressure transducer close to the tensiometer cup, there are several advantages:

- All, or almost all, of the water-filled parts of the tensiometer are not subject to direct sunlight.
- Temperature changes in the soil are considerably less than those of the air.
- There is no long water column between the tensiometer cup and the pressure sensor.

The first two factors make the tensiometer almost completely immune from temperature effects, while the last one means that the range of matric potential that can be measured is extended by the length of a water column between the ground surface and the tensiometer cup. Put another way, the tensiometer with a transducer mounted close to the cup measures matric potential, while one with a transducer above the ground surface measures hydraulic potential. Small, economic transducers, some in plastic housings, are available from several manufacturers. An example of the reduction in sensitivity to air temperature changes and exposure to sunlight is shown in Fig. 12.8. The 'conventional' tensiometer was well insulated but still showed marked fluctuations in reading as air temperature changed.

The simplest design for a tensiometer with a pressure transducer mounted close to the cup is shown in Fig. 12.9a. In this design, the only connection to the ground surface is an electrical cable to supply power to the transducer and carry the signal back up. The principal difficulty with this design is that it must be removed from the soil to refill with water and remove any air which has collected. Not only is this inconvenient but repeated removal and insertion of the tensiometer will reduce contact between the cup and the soil over time, slowing the tensiometer response and in some cases, leading to seriously inaccurate readings. Removal from the soil may not be necessary in situations where matric potential is always fairly high (above about –5 m water), but at lower potentials, experience suggests that air collects in the tensiometer frequently, reducing the sensitivity of the instrument markedly. A small error also occurs when there is an air gap above the water because the water column is not continuous from the transducer.

UMS GmbH produces an ingenious design of tensiometer, which has a small pressure transducer mounted just above the cup with sufficient room around it to accommodate two fine stainless steel hypodermic tubes. One of these penetrates well inside the porous cup. The other one terminates at the topmost part of the tensiometer chamber so that any air collecting is removed when water is flushed through the instrument. The two tubes are sealed simply by joining them together at the top by means of a short length of flexible plastic 'Tygon' tube as shown in Figs. 12.9b and 12.10. If the tensiometer is long enough and the matric potential is low enough, the pressure in the top part of the tubes will fall to the saturation vapour pressure of water causing cavitation. The top part of the tubes will be effectively empty, and the volume of water involved will have to pass through the porous cup. The use of very small diameter (~0.5 mm) tubes minimises this, but the response time must, nevertheless, increase once the tubes start to empty.

Hubbell and Sisson (1998) designed an 'advanced tensiometer', which could also be refilled *in situ* (Fig. 12.9c). A plastic 'gasket throat', bonded to the neck of the porous cup and bevelled on the inside at the top, mates with a rubber gasket fixed to the bottom end of the transducer *via* a connector. The weight of the transducer and the suction inside the tensiometer cup ensures a good seal. When refilling is required, the transducer and gasket can be lifted out of the gasket throat, allowing water held in the outer tube to displace the air.

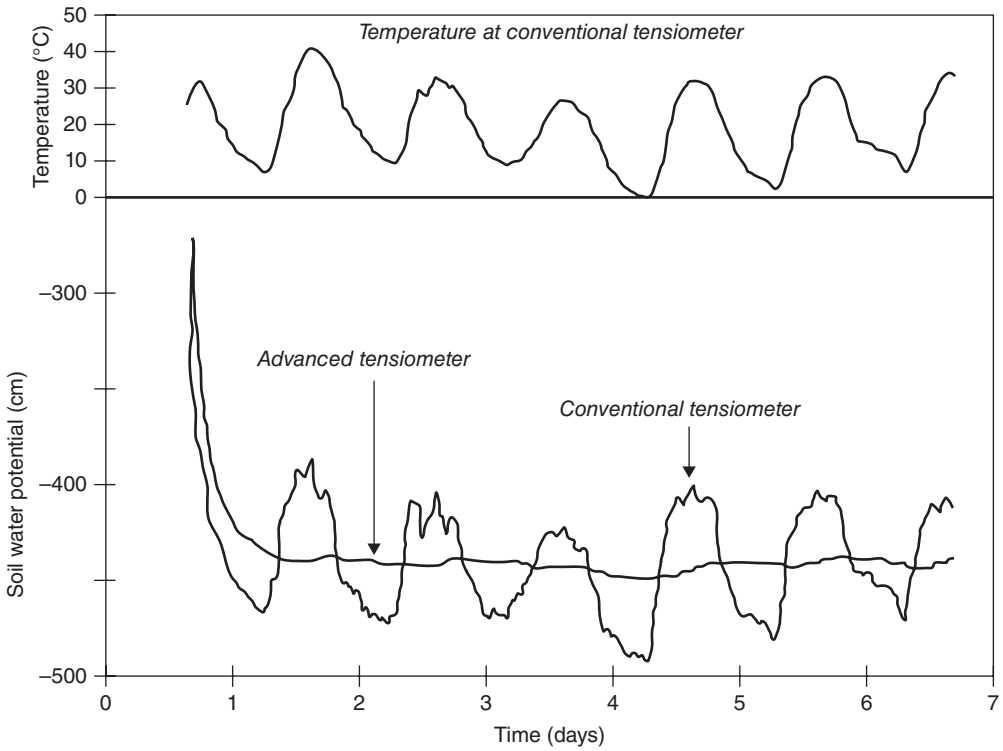

Fig. 12.8 Example of the reduction in sensitivity to air temperature and exposure to sunlight by a tensiometer with a pressure transducer below ground level compared with one with a transducer above ground. From Hubbell and Sisson (1998). Reproduced with permission of Lippincott Williams and Wilkins/Wolters Kluwer Health.

A further design, introduced also by UMS, contains a small pump in the support tube above the tensiometer cup. An infrared sensor detects air inside the upper part of the ceramic cup and turns on the pump to remove the air and suck water in through the cup to replenish the water reservoir. UMS claims that after a dry period when the tensiometer may be in soil too dry for it to operate, it can fill itself again and begin operation when the soil once again becomes wet enough.

Flush diaphragm or pressure port?

Most pressure transducers are supplied with a pressure port to connect to the system whose pressure is to be measured. Some are available with a flush diaphragm – often by special order and at extra cost – where the diaphragm forms the end of the transducer as shown in Fig. 12.11. This makes it quite easy to flush all of the air out of the tensiometer. The diaphragm is relatively delicate, though, so extra care is needed in handling and storing the transducer.

A pressure port type is less of a problem than it may appear at first sight. To understand this, we need to consider the relative volume inside the tensiometer and inside the pressure port. Assume that the volume of water held in the tensiometer is V and that in the pressure port is ν. Also assume that the tensiometer, apart from the volume of the pressure port, is full of water when the system is at atmospheric pressure, A, and the pressure port is full of air at the same pressure. For this purpose, we can ignore any vertical pressure gradient inside the tensiometer.

At an indicated matric potential of ψ_s, the internal pressure inside the tensiometer is $A + \psi_s$ (this is less than A since ψ_s is negative under unsaturated conditions). According to Boyle's Law, the air originally in the pressure port will expand to a volume ν_ψ given by

$$A\nu = (A + \psi_s)\nu_\psi. \tag{12.5.4}$$

The limiting value of matric potential that the tensiometer can indicate occurs when the air expands to fill the entire volume of the tensiometer, that is, when ν_ψ becomes equal to $V + \nu$:

Substituting this into Equation 12.5.4, the air bubble fills the tensiometer cavity when

$$\nu_\psi = V + \nu = \frac{A\nu}{A + \psi_s}, \tag{12.5.5}$$

or

$$\psi_s = -\frac{AV}{V + \nu}. \tag{12.5.6}$$

Typically, the pressure port has a diameter of 6 mm and a depth of 10 mm, so the volume, ν, is around 0.3 mL. A typical internal diameter of a tensiometer cup is about

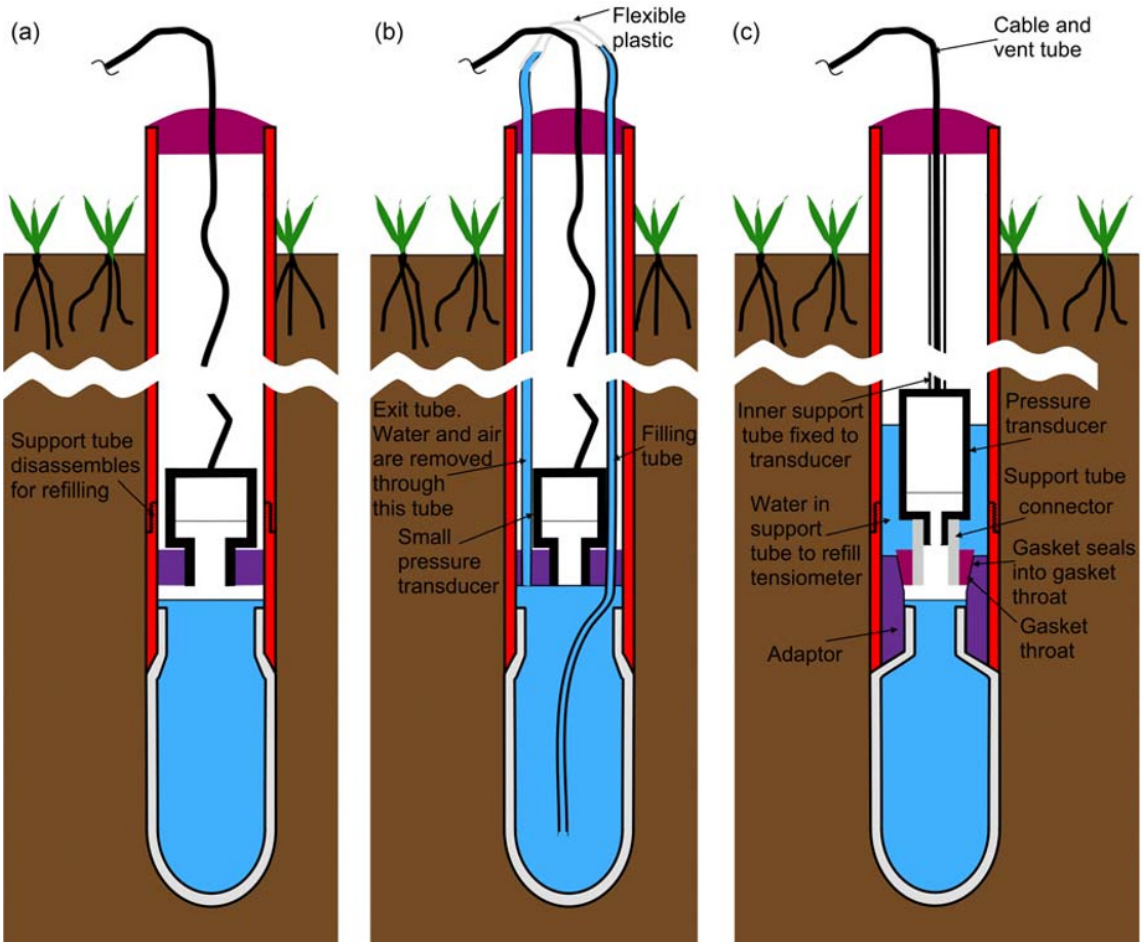

Fig. 12.9 Three designs of tensiometer with the pressure transducer mounted close to the porous cup below ground level. (a) A simple design that must be removed and disassembled to refill. (b) A design devised by UMS GmbH, which can be purged and refilled *in situ* using two hypodermic tubes. (c) A design incorporating the principles of the 'advanced tensiometer' (Hubbell & Sisson, 1998). The transducer and gasket can be lifted out of the gasket throat by the inner support tube, allowing water in the outer support tube to refill the tensiometer. (*See insert for colour representation of the figure.*)

15 mm and a length of about 40 mm, giving a volume of 7 mL. Even without any extra volume in a body tube, which is difficult to avoid, using this value for V in Equation 12.5.6 gives the minimum potential that the tensiometer can indicate of –9.6 m water for an atmospheric pressure, A, of 10 m water. So the pressure port reduces the theoretically available range of the tensiometer by only 4%. The additional air will, however, increase the response time of the tensiometer and reduce its sensitivity (Section 12.8.1). Nevertheless, these values are likely still to be favourable compared with those of a mercury manometer.

Tensiometers for use at depths of many metres using fixed pressure transducers are described in Section 12.12.

12.5.5 Puncture tensiometers

Puncture tensiometers are very simple tensiometers consisting of only a porous cup, body tube and air trap sealed by a *septum*. A portable device records manual readings of the internal pressure by penetrating the septum with a hypodermic needle attached to a pressure transducer and readout unit. A device was first introduced by Marthaler *et al.* (1983), and instruments using this principle have since become very popular owing to their economy, ease of construction and low maintenance requirements.

The essentials of the system are shown in Fig. 12.12.

Septa

The only component part of the tensiometer itself, different from other types of tensiometer, is a septum. These are used commonly in medical and gas chromatography applications as a means of sealing a vessel while allowing the insertion of a hypodermic needle, either to withdraw a liquid, for example, a vaccine, or to inject a test sample. Septa are available in many different forms. Some are similar to that in Fig. 12.12 consisting of a hollow elastomer cylinder, often ribbed, and closed at the top. The top often has a flange to aid removal. Some manufacturers recommend

Fig. 12.10 UMS T4e tensiometer showing the filling tubes connected by a flexible plastic tube at the top.

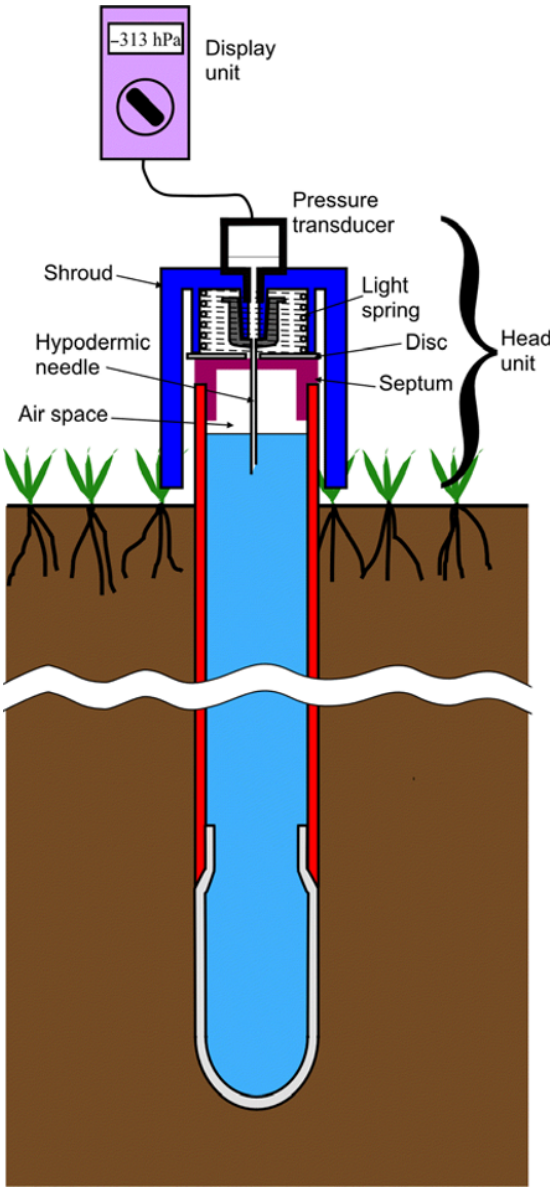

Fig. 12.12 Components of a puncture tensiometer and reader unit.

Fig. 12.11 Pressure transducers. The one on the left has a pressure port, while the other two are flush diaphragm transducers. The one on the right has a protective cap over the diaphragm for water level monitoring applications.

filling the hollow part of the cylinder with silicone rubber to prolong the life of the septum and reduce the likelihood of leaks during needle insertion. Another septum type is a small disc, which is clamped on top of the air trap by a screwed ring. These may be a simple rubber disc or consist of a stiff elastomer sandwiched between softer layers to seal to the top of the air trap. The choice depends also on the needle used in the reader unit, as the combination of the two is critical to preventing air leakage into the tensiometer when the needle is inserted.

As with other tensiometers, the upper part of the body tube or air trap should be of transparent material so that the amount of air in the top of the tensiometer can be ascertained. This is particularly critical for puncture tensiometers, as they need a small amount of air in the top of the air trap, but

the position of the internal air–water interface must also be known (see Section 12.9.3).

Reader units

The reader unit can be used with a large number of tensiometers and consists of two main parts – the *head unit* and a *display unit.* The head unit is placed on top of the tensiometer and the hypodermic needle penetrates the septum, allowing a pressure transducer to sample the pressure inside the tensiometer. Most units incorporate a *shroud* to guide the head unit onto the top of the tensiometer, protect the hypodermic needle and provide some protection for operators from accidentally penetrating themselves with the needle. The shroud should, therefore, be longer than the needle. The inner diameter of the shroud should be only slightly larger than the widest part of the top of the tensiometer to prevent the head unit from tipping while making a measurement. Some head units have a disc with a small hole for the needle to pass through, attached to a light spring, as shown in Fig. 12.12. This protects the needle from being bent and makes inserting the needle through the septum smoother. Some head units have an off-centre needle so that the needle can puncture a fresh piece of the septum each time, increasing the septum's life. One design incorporates a small syringe with a locking ring into the head unit so that as much of the space inside the needle and its connection to the pressure transducer can be filled with water, thereby reducing the compressibility of this part of the system markedly (Frede *et al.*, 1984).

Successful operation of puncture tensiometers depends critically on matching the characteristics of the needle and septum. With some combinations, the needle tends to remove a small core of septum material, which blocks the needle and can cause the septum to leak. To combat this, some manufacturers use needles with a side hole, although it is usually possible to find a suitable conventional needle to suit a particular septum. The other main pitfall is leakage of air into the tensiometer, either during insertion of the needle or while a reading is taking place. This latter is more likely if the head unit is not well stabilised by the shroud during a reading.

To improve the stability of the head unit during a reading, it should be sufficiently heavy to overcome the force of the spring and to sit securely and stably on top of the tensiometer without the need to hold it.

In view of the uncertainties surrounding manual readings of tensiometers, high accuracy is unlikely to be achieved. The pressure transducer should, however, be well protected from damp and be selected to have a low temperature coefficient (<0.025% $^{\circ}C^{-1}$) since it is likely to be used over a wide temperature range.

The display unit is usually separate from the head unit, although some manufacturers combine the two, which can make reading the output difficult. It may consist simply of a portable digital voltmeter and a stabilised battery power supply. Commercial units usually have an internal calibration to convert the voltage output from the pressure transducer to water potential units (either water head or hectopascals) and may have a memory to keep the readings. A push-button switch will ensure that the unit is switched on only when a reading is required and so conserve battery life. If the cable connecting the head and display unit is too stiff, small movements of the handheld display unit can be transmitted to the head unit, disturbing the measurements and possibly causing air leakage around the needle.

12.6 Construction of Tensiometers

Figure 12.1 shows the components of a tensiometer. Several manufacturers produce these instruments, but they are not difficult to make using simple tools and readily available materials.

12.6.1 Bonding the porous cup to the body tube

The body tube must be wide enough to allow air bubbles forming near the bottom to rise and collect in the air trap. An inner diameter of about 10 mm or more is suitable. To avoid misalignment of the cup and tube, the end of the body tube must be cut square. Porous cups vary a little in size from one to another as a result of the firing process. The tubing for the body tube may, therefore, need to be reamed out a little to accommodate the neck. Similarly, it is good practice to shape the end of the body tube to fit the profile of the cup shoulder. These two processes can be performed on a lathe or by use of a handheld reamer and a countersink. The inside of the body tube should be roughened with emery paper before bonding the cup to it to provide a key for the adhesive.

The porous cup should be bonded to the body tube using epoxy cement. A wide variety of epoxy adhesives is available and not all are suitable for tensiometers. Most types absorb some water, which causes them to swell a little. This is not a problem with a construction as shown in Fig. 12.3, where the porous cup has a neck that fits inside the body tube. The ceramic is strong enough to withstand the swelling pressure in this configuration as it is under compression. If the end of the body tube is inside the porous cup neck, however, the swelling pressure usually cracks the brittle ceramic. Special epoxy adhesives are available, which do not swell, but the configuration shown is recommended. Some epoxies absorb so much water that they become extremely weak and form a gel-like substance. The problem may not be discovered until the tensiometer is removed from the soil when the adhesive seal fails and leaves the cup in the ground. It is wise, therefore, to test the epoxy by soaking a joint for a few days and making sure that the strength is still adequate.

When bonding the cup to the body tube, it is important that there is no air path through the joint. This is best accomplished by coating the neck and shoulder of the cup liberally with adhesive and then inserting it into the body tube with a twisting motion. Excess adhesive should be wiped off carefully so that the main part of the cup is free of adhesive. The small gap between the shoulder of the cup

and the bottom of the body tube should be inspected to ensure that it is filled completely with adhesive. Before using the tensiometer, the epoxy must be fully cured. Some types of epoxy are usable within an hour, which is useful for repairs in the field, while others need 24 hours or more. The tensiometer should be kept in a vertical position during curing of the adhesive, either standing on the cup in a clean, dry place, or upside down, so that gravity keeps the joint from coming apart and the cup is aligned with the tube.

12.6.2 Fixing the air trap

The air trap may be a separate piece, as shown in Fig. 12.13, or integral with the body tube, as in Fig. 12.1. The former arrangement has the advantage that cheap and readily available material such as PVC or ABS water pipe can be used. However, it requires a separate transparent air trap (usually acrylic) with attendant potential problems of joints and extra work in construction. To avoid cracking of the air trap over time, it should have a wall thickness of at least 2.5 mm. If a neoprene bung is used to seal it, as in Fig. 12.13, the air trap should be bevelled internally at the top to avoid damaging the rubber. The air trap may be fixed to the body tube by epoxy adhesive. Similar remarks apply to the choice of epoxy adhesive as for fixing the porous cup to the body tube. Both the outside of the body tube and the inside of the air trap must be roughened before assembly and adhesive applied to the upper 15 mm of the body tube. This ensures that excess adhesive is not carried into the air trap. The adhesive that is pushed down can be used to form a fillet around the bottom of the air trap, ensuring a complete seal. A small 'O'-ring or elastic band can be placed on the body tube about 15 mm from the top to support the air trap during curing. This should be encased completely in the fillet at the bottom of the air trap. A photo of a tensiometer constructed in this way is shown in Fig. 12.14.

If machining facilities exist, the air trap may be fixed by two 'O'-rings as shown in Fig. 12.13. Grooves are machined into the top of the body tube about 10 mm apart to accommodate the 'O'-rings. A small bevel on the inside bottom edge of the air trap ensures that it does not cut the 'O'-ring, which is smeared with a very thin coating of silicone grease before assembly. Provided that the air trap is a tight fit over the 'O'-rings, the whole assembly is extremely rigid after a few days.

12.6.3 Mercury manometers

Figure 12.13 shows the components of a practical mercury manometer tensiometer. Tensiometers are usually installed in 'banks' or 'nests' of several instruments close together most often at different depths to measure the hydraulic potential profile. Several manometers are, therefore, normally mounted together on one manometer board.

The cap and connecting tube

In the design shown in Fig. 12.13, the cap to the air trap is a neoprene bung, through which the connecting tube

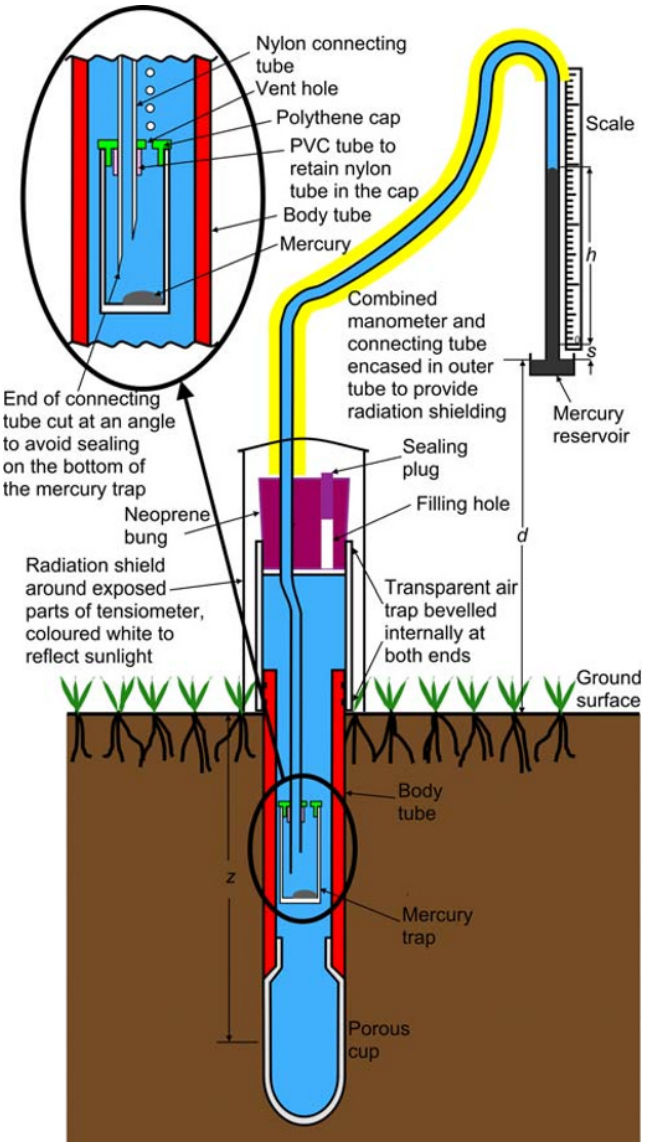

Fig. 12.13 A mercury manometer tensiometer. (*See insert for colour representation of the figure.*)

enters the tensiometer, although in some designs, this is routed *via* a sidearm as shown in Fig. 12.1. An extra hole in the neoprene bung allows a syringe nozzle to be inserted to flush water through the connecting and manometer tubes (see Section 12.7.3). Neoprene is the preferred material for the bung as natural rubber cracks after some time under field conditions. Drilling holes in bungs is a laborious process but many laboratory suppliers supply bungs pre-bored with two holes, although they are normally available only with the two holes of the same size. A 2.5-mm hole is suitable for making a tight seal to a 3-mm outer diameter connecting tube and is also suitable to accommodate the Luer fitting on a standard hypodermic syringe for flushing the connecting tube. It can be

Fig. 12.14 Tensiometer with separate air trap bonded to the body tube with epoxy.

sealed with a small piece of plastic rod or another small rubber bung.

The connecting tube to the manometer should be of semi-rigid plastic of a low permeability to air. Three millimetre outer diameter nylon 66 is suitable for this.

The mercury trap

Prolonged dry periods often cause the mercury column to break up, with short lengths of air or water between lengths of mercury. In some cases, the total column extends sufficiently that some mercury can reach the end of the connecting tube and fall into the porous cup. A trap for this mercury can be made easily from a small glass or plastic specimen bottle as shown in Fig. 12.13. A hole drilled in the top of the specimen tube cap takes the end of the connecting tube, while another hole allows water and air to be flushed out. A short piece of flexible plastic tube that is a tight fit onto the connecting tube or a small 'O'-ring is enough to retain the air trap on the connecting tube.

Manometer board support

The manometer board is usually most conveniently fixed onto a round metal pole or tube, although a bar of another shape or a wooden post can be used. Over time, a wooden post may rot, leaving the installation insecure, so this choice should be made with caution. A round post, to which the manometer board is fixed by 'U'-bolts, allows easy adjustment of the height of the board after installation, which is useful for adjusting the zero potential point on the scale.

The manometer tube, manometer board and measuring scale

The manometer tube may be made from glass capillary tube, which is durable and requires only a small volume displacement to change the mercury level. It can be joined to the connecting tube with silicone rubber tube. This should, however, *not* be lubricated with silicone grease, which degrades the rubber. Alternatively, the connecting tube and manometer tube may be one continuous piece of nylon 66 tube as shown in Fig. 12.13. This material is reasonably transparent and of low gas permeability. An outer diameter of 3 mm and an inner one of about 1 mm is suitable, although some workers prefer narrower tube.

The manometer tubes are mounted on a stable vertical board (e.g. 6 mm varnished or painted exterior grade plywood or rigid PVC sheet) with a scale attached. Suitable

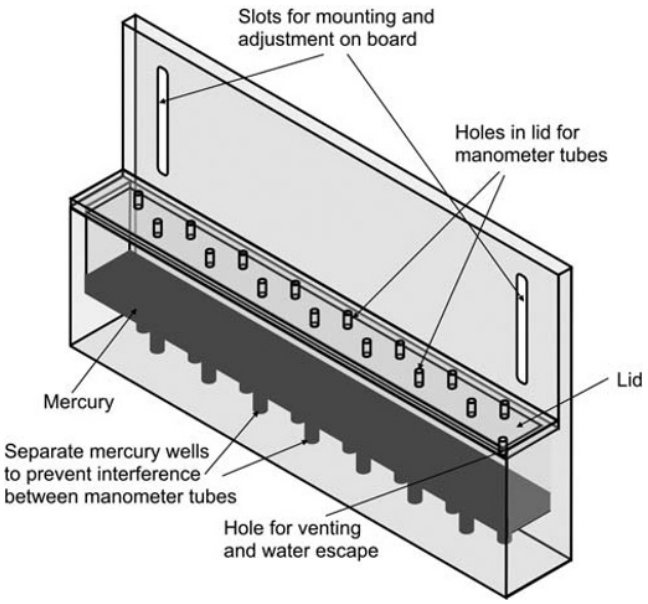

Fig. 12.15 An adjustable mercury reservoir with separate wells for each manometer tube.

scales can be made from the inside of a flexible steel rule, a laboratory ruler or printed on paper. If the last named are used, precautions to protect them from the weather are necessary. The use of waterproof glue to fix them onto the manometer board and a self-adhesive transparent waterproof film to cover the scale is recommended.

The mercury reservoir

The mercury reservoir is, at its simplest, a shallow dish, which can be fixed on the bottom of the manometer board so that each manometer tube dips into it. Three modifications to this simple design are advised (Fig. 12.15):

- A lid to the reservoir. This prevents splashing of mercury out of the reservoir during purging operations. Mercury is an environmental pollutant and all reasonable steps to prevent its spilling onto the ground must be taken. The most vigorous splashing occurs when air bubbles through the mercury and there is no water overlying the mercury surface. This occurs, for instance, when setting up a new installation. Water bubbling through the mercury produces less splash and the viscosity of water overlying it slows the small splash droplets of mercury quite effectively.

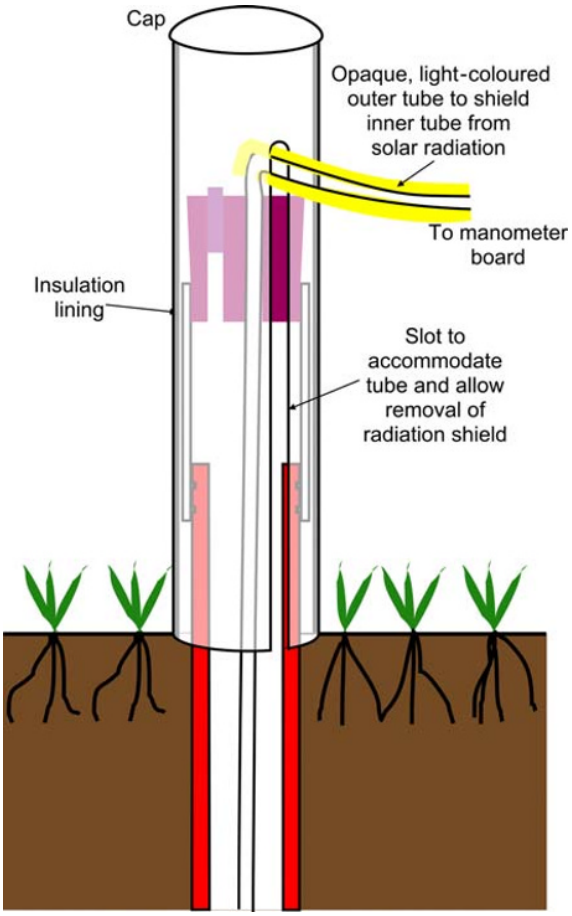

Fig. 12.16 Tensiometer radiation shield incorporating insulation.

The lid should fit tightly and have holes drilled in it to accommodate the manometer tubes, which should, again, be a tight fit. Spare holes can be sealed with a small rubber or plastic stopper. There must be one vent hole to ensure that the mercury surface is at atmospheric pressure and to allow water from purging the tensiometers to escape. This should be positioned as far away from the manometer tubes as practical to reduce the possibility of mercury splashing through this.

- Separate wells for the manometer tubes. This keeps each manometer tube separated from its neighbours so that when water is injected through one tube, water is not forced into an adjacent one. This is particularly a problem when using flexible nylon tubes. The use of wells also economises on mercury to fill the reservoir. However, there must be enough mercury to ensure that its upper surface is always above the level of the top of the wells.
- Adjustment slots to mount the reservoir. This aids setting up the tensiometers and provides some zero adjustment (see Section 12.7.3).

Radiation shielding

The transparent plastic components are susceptible to degradation by ultraviolet radiation in sunlight. This usually causes them to become opaque after a few months, depending on the amount of sunlight experienced. Nylon tube becomes brittle and may disintegrate after a few weeks in strong sunlight. In addition, solar heating expands fluids, depressing the reading.

To protect from this, all the above-ground parts should be shielded from sunlight. A successful method is as follows:

The body and air trap of the tensiometer should protrude above the ground surface as little as possible – about 100 mm is the practical minimum. These parts should be protected by a capped, metal or plastic tube coloured white to reflect sunlight. A layer of insulation glued inside the tube further reduces thermal disturbance (see Fig. 12.16).

The connecting tube can be encased in opaque silicone rubber tubing with an internal diameter of about 4 mm and wall thickness of about 3 mm.

A white-painted wooden box with a lockable door at the front over the manometer board will protect the complete manometer assembly from sunlight and tampering. Runners inside the box allow it to be slotted over the manometer board and to be held in place.

12.7 Tensiometer Installation

Tensiometers are usually installed in 'banks' or 'nests' of several instruments close together, most often at different depths to measure the hydraulic potential profile. In such a case, since it is not normally possible to install the instruments vertically above one another, it is sensible to minimise the lateral separation between instruments at adjacent depths and to keep the area occupied by the nest as small as possible.

A suggested layout for a set of 12 tensiometers in a 4×3 array is shown in Fig. 12.17. The tensiometers should be mounted as close to one another horizontally as practical. A spacing of 150 or 200 mm is usually achievable while still allowing access for maintenance.

12.7.1 Preparing the hole

Disturbance to the soil structure is less of a problem for water potential measurement than for water content measurement because water potential equilibrates regardless of soil structure. Disturbance may affect the rate at which this occurs and indirect effects can result from changes to flow patterns caused by different hydraulic properties.

The most important considerations for tensiometer installation are:

- To ensure good contact between the sensor and the soil to minimise the delay between a change of soil water potential and that indicated by the sensor. Poor contact can result from the tensiometer cup touching the soil in only a few places, sometimes as a result of soil shrinking or swelling or a hole that has been bored too large. Poor contact may also result from smearing of clay soil by the drilling tool.

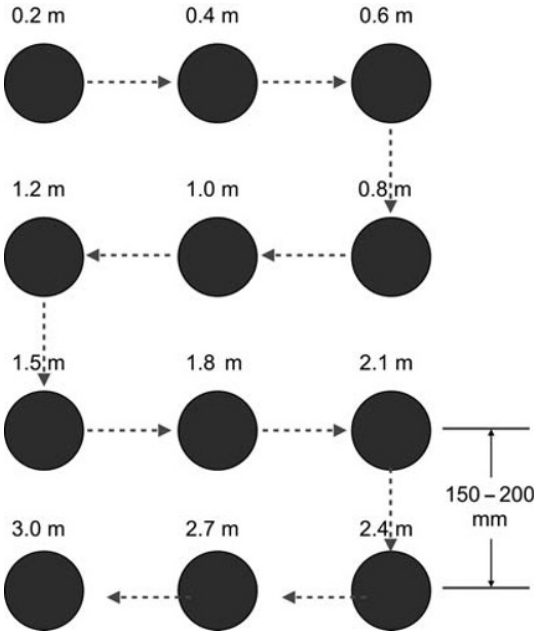

Fig. 12.17 Suggested layout for 12 tensiometers installed to represent a vertical profile from 0.2 to 3.0 m depth. Arrows show the lateral relationship between tensiometers at adjacent depths.

Smearing aligns the clay platelets along the wall of the hole. Hydraulic conductivity is very low perpendicular to this direction, providing an effective barrier to water flow. The film may be disrupted by using a stiff brush, but the problem is less likely to arise when installation happens under dry conditions.

- To avoid creating rapid water flow paths that lead to unrepresentative readings, such flow paths are most likely to result from a gap between the tensiometer stem and the soil. This is very similar to the situation for installation of access tubes for water content measurement.

To avoid a gap, it is strongly recommended that tensiometers be installed within a larger diameter sleeve as shown in Fig. 12.18. The advantages of this are:

- Any water running down the outside of the access tube can go no further than the bottom of the sleeving tube, which is sufficiently far above the tensiometer cup not to affect the reading;
- Stones in the profile can often be removed easily by an auger drilling a large (ca. 45–50 mm) diameter hole, whereas it is much more difficult using a smaller diameter auger (usually 20–25 mm). Usually, the hole below the bottom of the sleeving tube is made with an auger of the same diameter as the cup. However, if a clean hole of this diameter cannot be made, a hole of the full width of the sleeving tube should be bored to the depth of the bottom of the tensiometer cup. After insertion of the access tube, the soil from the lower part of the hole is sieved and poured back into the hole, tamping every few cm, to ensure a stable medium without voids. A hole of the correct size for the tensiometer cup should then be easy to auger in this stone-free soil.

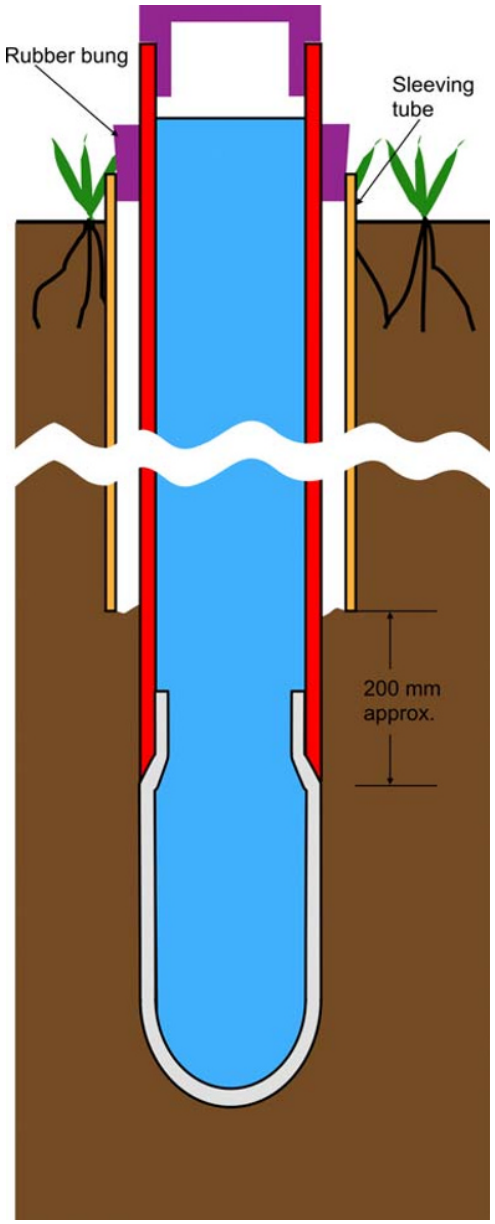

Fig. 12.18 Tensiometer installation inside a sleeving tube.

An alternative method, described by Baker *et al.* (1974), is to drill an oversize hole but to partially fill the hole with soil slurry. Pushing the tensiometer into the hole displaces slurry and forms a cap at the surface, which sheds water.

12.7.2 Installation in the hole

Before placing the tensiometer in the hole, the cup should be thoroughly wetted. To avoid air entrapment within the ceramic, the cup must be wetted from one side only, either by standing the tensiometer in a container of water for a few minutes or by pouring water into the tensiometer body. The latter is usually easier as wetting is accelerated by

the greater head of water that can be imposed. It is also obvious when water starts to come through the cup and wetting of the entire surface can be checked. Additionally, if the cup is cracked or not bonded properly to the body tube, water runs out of the tensiometer much faster than if the construction is intact. If the cup is wetted from the outside, then complete wetting must be checked by tipping the tensiometer upside down and observing water running out of the air trap. In either case, excess water must be emptied from the tensiometer body before installation as it must be filled with de-aired water.

Before placing the tensiometer into the hole, the body tube should be marked at the place where it will be level with the top of the sleeving tube (or ground surface if no sleeving tube is used) when the centre of the ceramic cup is at the correct depth. The rubber bung must also be slid onto the body tube if it has not already been done. A little silicone grease or household washing up liquid applied to the stem of the tensiometer will help to slide the bung along it. Great care must be taken to keep grease off the ceramic cup, which would block its pores.

It is important when emplacing (and removing) tensiometers to use longitudinal force only, that is, to push or pull straight along the stem. Any twisting of the tensiometer will probably break the cup at the neck. Should this happen, the remains of the ceramic can usually be broken up and most removed using an auger.

If the tensiometer cannot be pushed deep enough into the soil, it must be removed, the hole augered a little deeper and the tensiometer replaced. If it goes in too far, it should be removed, a small amount of sifted soil poured into the hole and the tensiometer reinserted. It is not acceptable simply to withdraw the tensiometer a short distance to bring the mark to the correct place and hope that it will remain at that depth indefinitely.

Sometimes, a good, tight fit of the tensiometer cup in the hole is difficult to achieve. If this occurs, a small amount of slurry made with soil or silica flour mixed with water should be poured into the hole followed immediately by pushing the tensiometer into it. After a fairly short time, the excess water will drain away, leaving the cup tightly embedded in the soil.

It is very important that, after emplacing the tensiometer in the hole, the bung sealing between the tensiometer body and access tube fits tightly to both. If there is any doubt about this, some silicone sealant should help to ensure a good seal, although it is much better to have a tight-fitting bung in the first place. If silicone sealant is used, the integrity of the seal must be checked periodically (say every 3 months) to make sure it is not peeling away. If this happens, more sealant will need to be applied.

The tensiometer is now ready for filling with water, once any work to make connections is completed. If the tensiometer will be left empty for some time before completion of other installation work, the top should be covered with a radiation shield or a cap to prevent stray materials falling into it.

12.7.3 Mercury manometer tensiometers

Before filling the tensiometer, the manometer(s) must be in place.

Installing the manometer board support

The mount for the manometer board should be vertical, so care must be taken to check with a spirit level that it goes in straight. A few degrees of error in a direction perpendicular to the manometer board will not produce a significant error in the reading, but if it leans parallel to the face of the board holding a bank of manometers, each manometer is a different distance above the ground surface and the local scale zero is a different distance above the mercury level as shown in Fig. 12.19.

For the situation shown in Fig. 12.19a, the true height of the mercury column, h is related to that read on the manometer board, h', by

$$h = h' \cos\theta, \tag{12.7.1}$$

where θ is the angle between the vertical and the board. For small angles, $\cos\theta$ is very close to one, differing by less than 1% for angles up to 8°. In Fig. 12.19, θ is 3°.

Where the tilt is parallel to the face of the board, however, the error in reading the mercury height depends on the lateral distance of the manometer from the point at which the zero was set. Assuming that this is at the centre of the bank of manometers, then the true mercury height is given by

$$h = h' \cos\theta + w \sin\theta, \tag{12.7.2}$$

where w is the distance between the manometer position and the point at which the zero was set. The term $w \sin\theta$

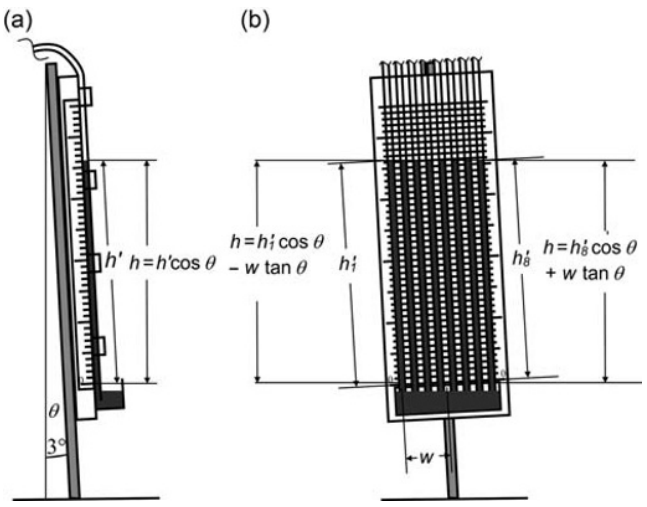

Fig. 12.19 The effect of mounting the manometer board on a non-vertical post. (a) leaning perpendicular to the face of the board; (b) leaning parallel to the board. In both cases, the board is mounted 3° from the vertical.

is not negligible. The outer manometers on a board may typically be 100 mm either side of the centre line, so for the example given with θ of 3°, the error is about 5 mm equivalent to 66 mm water. The error is of the opposite sign on the other side of the board, so there would be a difference in the apparent potential of 131 mm water between them, even if the true potential were the same for each tensiometer. This differential error is usually of much more significance than the absolute error in the readings. Figure 12.19b shows the situation where the actual mercury height is the same for all manometers (eight in this example) on the board, but it can be seen clearly that the scale indication differs from one side to the other.

Once the support post is installed securely, the manometer board can then be attached to it.

If not already done earlier, the mercury reservoir should be mounted onto the manometer board and filled with mercury. There must be enough mercury to cover the top of the wells when all of the manometer tubes contain about 700 mm of mercury. For a reservoir of cross-sectional area 2000 mm^2, and 12 manometer tubes of internal diameter 1.5 mm, this is a total volume of about 15,000 mm^3 or a depth of 7.5 mm in the reservoir. There should, therefore, be at least 10 mm of mercury in the reservoir above the top of the wells when the tubes are empty. Taking into account the volume of 12 wells of diameter 6 mm and depth 17 mm, the volume of mercury required is about 20,000 mm^3, (20 mL). Mercury is usually bought by mass. With a density of 13,600 kg m^{-3}, the amount needed is 270 g.

Great care must be taken when filling the reservoir that mercury is not spilled, as mercury is a hazardous substance. It is best done by drawing a quantity into a syringe with a short length of flexible tube attached. This can then be discharged gently into the reservoir.

Fitting the connecting and manometer tubes

The manometer tubes should now be attached to the board and, if they are not continuous with the connecting tubes, joined to them at this time. The manometer tubes must be cut at an angle and threaded through holes in the reservoir lid and then each into a separate well in the reservoir base. Any spare holes in the reservoir lid should be sealed with a small bung to prevent mercury splashing out, leaving just one hole to provide an atmospheric pressure reference.

The tensiometer end of the connecting tube should be cut at an angle as shown in Fig. 12.13. This aids threading through the neoprene bung and prevents it sealing against the bottom of the mercury trap or porous cup. The connecting tube should extend well inside the body tube (at least 100 mm but up to 500 mm or more if the tensiometer is long enough) so that its end is always below the water level in the tensiometer body. This reduces uncertainty in the reading, as it is the water pressure, not that of the airspace above it that should be measured. If the connecting tube extends inside the porous cup, any air bubbles trapped inside the cup may be dislodged during the filling or purging process (see next section and Section 12.10.1). Before passing the connecting tube through the hole in the neoprene bung, the tubing used for radiation shielding (Section 12.6.3) should be threaded onto it, taking care that it is long enough for one end to be inside the shielding over the tensiometer and the other to be inside the box over the manometer board. It may be convenient to route the manometer end of all connecting tubes through a single protective outer flexible tube. Lubrication of the tube with silicone grease or washing up liquid eases threading the tube through what can often be a tight hole. A tight fit is, however, much more desirable than a loose one, which leaks at high vacuum. Once threaded, the end of the connecting tube must be inspected to check that there are no rubber particles, grease or other debris in the tube. If so, it is a simple matter to cut a few millimetres off the end to ensure that the tube cannot become blocked or contaminate the mercury.

Zero adjustment

Before filling the tensiometers, a 'zero adjustment' must be performed. This ensures that a zero reading on the scale corresponds to a zero hydraulic potential relative to the chosen datum level. The connecting tube and manometer must first be full of water. This is most easily accomplished by injecting water from a syringe into the tensiometer end of a connecting tube though a small, bored rubber bung or a short length of flexible plastic tube. The connecting tube end is then held under the surface of a small quantity of water in a dish, such that the surface of the water is at the desired datum level. This can usually be arranged by taking advantage of a natural depression in the ground surface or creating a small hole for the dish. Care is needed to prevent air entering the end of the connecting tube, but this can happen only if the end of the tube is raised, so filling and then lowering the end into water will not draw in air.

With the connecting tube in place as described previously, the mercury level in the manometer tube relative to the zero of the scale is noted. The level can be aligned with the scale zero in four ways:

1 Add or remove mercury to or from the reservoir by using a syringe with a short length of flexible tube attached. Clearly, this method can be used to adjust the zero point by only a few millimetres. Equation 12.5.2 shows that the change in h is given by

$$\Delta h = -\frac{\left(\left(\rho_{Hg}/\rho_w\right)-2\right)}{\left(\left(\rho_{Hg}/\rho_w\right)-1\right)}\Delta s. \qquad (12.7.3)$$

The negative sign signifies that as s increases (i.e. the mercury level moves down), the height of the mercury goes down by almost the same amount – actually 92% of it because of the reduction in d.

2 Move the reservoir up or down. This has the same effect as adding or withdrawing mercury from the reservoir. However, if more than a small adjustment is needed to the reservoir position, the manometer tubes will also need to be

adjusted as the tubes will either come into contact with the bottom of the wells, preventing it from being raised further or come out of the reservoir altogether. This is not usually difficult but can be quite time consuming.

3 Move the scale(s) relative to the manometer tubes to align the zero with the mercury level in the manometer.

4 Move the complete board, reservoir, manometer, and scale assembly up or down on its supporting post. This is simple if the post is tubular and the board is mounted to it by 'U'-bolts. Otherwise, either the board or stake will need slots, through which mounting bolts pass.

This changes d in Equation 12.5.2 and h changes by

$$\Delta h = \frac{\Delta d}{\left((\rho_{Hg}/\rho_w) - 1\right)}. \qquad (12.7.4)$$

With (ρ_{Hg}/ρ_w) equal to about 13.6, the change in h is $(\Delta d/12.6)$ or about 8% of the change in d so that this is an effective way to fine tune the readings.

Provided that the board is vertical, all manometers should show the same reading of zero when the end of its connecting tube is dipped into water at ground level. It is advisable to check that this is indeed the case for manometers at each end of the board.

Filling the tensiometers

Now, the tensiometers can be filled.

When filling the tensiometers, it is essential to:

- Use de-aired water. Appendix 12.B gives instructions on preparing de-aired water.
- Avoid air bubbles.
- Minimise the opportunities for air to dissolve in the water.

To achieve these ends, the water should be poured gently into the air trap until it is completely full. Often, air bubbles are trapped inside the body tube or in the cup as they are inhibited by the narrow neck. These may rise up almost immediately, or in some cases, take up to a couple of days after the tensiometer has been commissioned before all air bubbles have collected in the air trap. Applying a modest vacuum to the tensiometer filling hole using a syringe or a small hand pump helps speed up their removal.

Once filled, a mercury trap, filled with de-aired water, should be attached to the free end of each connecting tube. This is put into its appropriate tensiometer. For a set of tensiometers installed to provide readings at different depths, it is sensible to connect the manometers in depth order so that the shallowest one is on the left-hand side and the deepest on the right. This gives an immediate visual representation of the hydraulic potential profile. A fairly smooth variation is normally expected from one depth to the next, so that if one tensiometer has a problem, this should be obvious from the pattern of mercury heights.

The sealing bung should be pushed firmly into the top of the air trap, taking care that there is no air gap beneath the bung or blades of grass or other vegetation are not trapped between the air trap and the bung.

Finally, inject de-aired water through the filling hole in the sealing bung. This is most conveniently done using a syringe into which de-aired water has been sucked. The water injected will push some of the water already in the tensiometer through the connecting and manometer tubes and out *via* the mercury into the upper part of the reservoir. The filling hole is then sealed with a small rubber bung or solid plug. Once again, care must be taken not to introduce any air into the tensiometer when injecting the water and that the purging hole is completely full of water before sealing it.

The tensiometer radiation shield and the shield for the board can now be fitted and installation is complete. A photo of a complete installation is shown in Fig. 12.20.

Once installed, the mercury level will probably rise quickly at first, as the positive pressure inside the cup provides quite a strong driving force to push water into the soil. The rate of rise will soon slow and equilibrium with the soil can take from around 1 hour to several days, depending on a number of factors, most important of which is the diffusivity of the soil. This is much smaller for dry than for wet soil and varies considerably from soil to soil, so that equilibration takes much longer in dry soil and heavy clays. Frequent monitoring of the readings allows assessment of when

Fig. 12.20 A set of mercury manometer tensiometers showing scale, radiation shielding, syringe and water supply for purging. Reproduced with permission of the Centre for Ecology & Hydrology.

equilibrium has been reached. The equilibration process involves not just waiting for water to pass through the ceramic cup but also for the water displaced to dissipate within the surrounding soil. Extra water will also inevitably pass into the soil through the cup during the filling process.

12.7.4 Bourdon gauge tensiometers and those with pressure transducers mounted at the top

For these tensiometers, the procedure depends on the fitting of the gauge. The principles are, however, the same as described for the filling of mercury manometer devices, namely, to avoid trapping air bubbles in the body tube and preventing air dissolving in the water during the filling process.

On some models, the gauge is fitted on the side of the air trap usually inclined so that air will rise out of the fitting (Fig. 12.1). In this case, the gauge should be fitted before filling the tensiometer. If it fits on top, then the tensiometer must be filled before fitting the gauge.

After filling the body tube completely, any air bubbles trapped can be encouraged to rise to the surface by applying a vacuum to the air trap as described for mercury manometer tensiometers. The body tube is then refilled and the gauge or the sealing cap fitted and sealed, taking care that no air bubbles remain. The air trap should be examined after 24 hours to check if more air has collected and to refill the tensiometer if necessary.

These tensiometers, because of their high sensitivity, are very sensitive to air temperature changes and, especially, sunlight causing large internal pressure changes. Radiation shielding and preferably insulation using expanded foam is, therefore, highly recommended to minimise spurious, thermally induced fluctuations in the readings (see Section 12.5.4).

12.7.5 Tensiometers with pressure transducer close to the ceramic cup

These tensiometers either have no hydraulic connection to the surface or small-bore tubing for refilling (Section 12.5.4).

For the first type, it is essential to fill the tensiometer with de-aired water before installation. The tensiometer is dismantled by removing either the pressure transducer or the ceramic cup, which may unscrew. Reassembly is best performed with the complete unit immersed in water. This prevents small air bubbles being accidentally left behind. Great care must be taken to keep the electrical connections at the back of the transducer dry.

For those tensiometers designed for *in situ* servicing, the tubing to the surface is too narrow to allow pouring water in. There are three alternatives:

1 Use a specially constructed reservoir feeding into flexible tubing, which can fit onto the inlet tube of the tensiometer, as shown in Fig. 12.21a. The flow of water can be turned on or off by a clamp or a small inline tap on the flexible tube. Water needs to be run into the tensiometer until the water emerging from the outlet is free of bubbles. Usually, air will appear first, then a mixture of water and air bubbles, followed by water alone. Sometimes, more air bubbles may appear a little later, so time should be taken to allow all bubbles to be eliminated.

2 Water can be injected into the tensiometer using a syringe instead of the water reservoir as shown in Fig. 12.21b. The syringe should contain enough water to fill the system. A 20-mL syringe is normally adequate. A possible problem is damage to the transducer diaphragm by applying too much pressure. Most commercial transducers will take up to about three times their rated full-scale pressure without damage (see the manufacturer's data sheet). Monitoring the pressure transducer output while filling will allow overpressurisation to be prevented. There is, in any case, no need to apply a great deal of pressure since water should flow through the tubes freely with only modest pressure. Large diameter syringes are inherently less likely to generate high pressures. This is because, for a given force, F, on the syringe piston with a cross-sectional area, A, the pressure generated is F/A.

3 The best way to fill and service this type of tensiometer is to apply a suction to the outlet and a water reservoir connected to the inlet as shown Fig. 12.21c. The advantages of this method are:

- There is no danger of straining the diaphragm of the transducer, unless it is of very low range, since a differential pressure of no more than 10 m water (1 bar) can be imposed on it.
- Any air bubbles inside the tensiometer expand and become more buoyant, making it more likely that they rise into the air trap and are sucked into the outlet pipe. Because they are larger, even if not all of the bubbles pass into the outlet, less air is likely to remain inside the device than if the operation is done under pressure. Pressurisation compresses the bubbles, which can then re-expand when the pressure is released.

There are several ways in which a suction may be applied to the tensiometer in the field. The simplest is to use a small hand-operated or battery-powered electric pump. These require a reservoir, both to avoid excessive pressure fluctuations and to keep water out of the pump, which may damage it. The arrangement is illustrated in Fig. 12.21c. The pump passes a large volume of water vapour, so it needs to be suitable for this application. Oil-based pumps are not suitable as water becomes mixed into the oil.

If a purpose-made pump is not available, one can be improvised by a syringe fitted with a three-way valve as illustrated in Fig. 12.22a. Alternatively, the syringe can be converted to a normal pump by use of two small check valves or fluidics diodes as shown in Fig. 12.22b.

Use of a pump and reservoir can simplify the procedure for several tensiometers. The reservoir, which may suitably be a 500 mL or 1 L Buchner flask, is first pumped out and

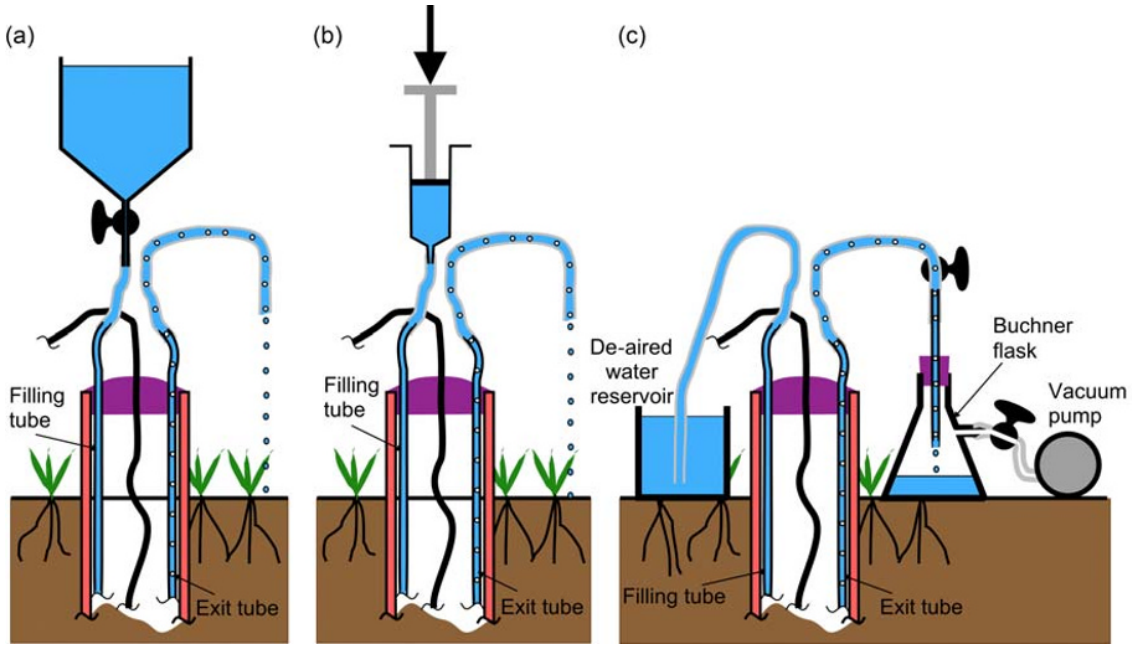

Fig. 12.21 Three ways to fill a purgeable pressure transducer tensiometer. (a) Gravity filling from a water reservoir. (b) Injection of water from a syringe. (c) The preferred method – filling by application of a suction. (*See insert for colour representation of the figure.*)

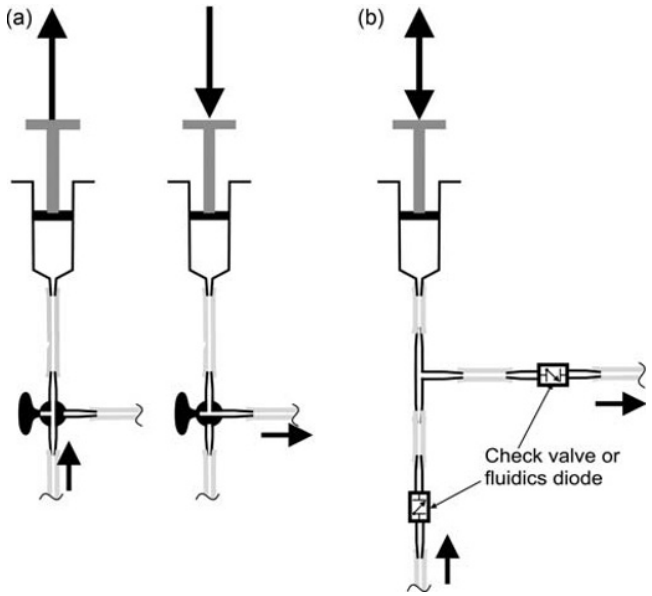

Fig. 12.22 Use of a syringe as a hand-operated pump. (a) Use of a three-way valve to move fluid alternately in each direction. (b) Use with two check valves or fluidics diodes.

sealed off then connected to the first tensiometer. After filling this, the reservoir is sealed with a clamp or tap and then used similarly on more instruments until the vacuum falls to a level where water flow becomes too slow and the reservoir should be pumped out again. The reservoir should be made of a transparent material (usually glass) to ensure that the amount of water collected can be monitored and emptied before being sucked into the pump. However, the vessel must be able to withstand the pressure differential across it when subjected to a vacuum inside. Buchner flasks and other thick-walled glass bottles are designed to be subjected to a vacuum. On no account must a thin-walled glass flask or bottle be used as it may implode and cause severe injury.

When filling a tensiometer by vacuum, a similar sequence of events as described previously for filling under pressure will occur. However, if the vacuum in the reservoir is low enough, the water in the outlet tube may cavitate, giving the appearance of air bubbles. These are usually larger than the real air bubbles seen in the last stage of de-airing the tensiometer. With experience, this phenomenon can be distinguished from a genuine leak.

Whichever filling method is used, it is essential to identify the inlet and outlet tubes correctly as reversing them will result in a large amount of air being left in the tensiometer (Fig. 12.9b).

Because the pressure transducer is below ground level and very little water in the tensiometer is above ground, radiation and temperature shielding is less important than with above-ground transducers. Some covering of the above-ground parts is, however, advisable to increase the longevity of the above-ground parts, protect against damage from animals and minimise residual thermal effects.

12.7.6 Electrical connections to pressure transducers

Strain gauge pressure transducers are very sensitive to damp, particularly if there is contamination on the contacts, which boosts the electrical conductivity of any water

bridging them (see Appendix 12.A). Keeping all electrical connections completely dry is therefore essential. In the harsh environment of most field sites, this is not easy and requires rigorous attention to all aspects of the electrical and electronic wiring. The principles to be followed include:

- All connectors should be rated as at least IP64. If there is even a small risk of immersion, this should be upgraded to IP67 or better.
- All electrical contacts should, where possible, be lacquered.
- The enclosures containing the electronics and connections should contain a drying agent to prevent condensation and an indicator, easily visible, to allow for checking the humidity.
- Venting of the enclosures should be *via* a water-repellent breather.
- If vented transducers are used, precautions should be taken to prevent condensation on the back of the diaphragm. The transducer can be vented separately through a drying agent and/or a water-repellent breather. Some transducers use the space within the cable sheath to act as the air pressure reference pathway to the back of the diaphragm. Others have a separate vent tube within the cable. Others have a separate vent port on the rear of the transducer. Whichever arrangement the transducer has, it is vital that there is an unobstructed pathway to the atmosphere. This is most easy to arrange where there is a separate vent port on the transducer. A small diameter flexible pipe can be connected to this and led to the surface, vented *via* a small transparent tube of silica gel or other drying agent with a humidity indicator so that its state can be monitored and the drying agent changed when necessary (see Fig. 12.23).
- Where the venting is within the cable itself, either through a tube or just through the cable casing, a successful arrangement is the removal of a spare pin from one half of a connector and the corresponding socket from the other part, thus enabling pressure equalisation between the interior of the connection or logger enclosure and the rear of the transducer diaphragm. The enclosure must be vented. This may be by a separate vent, similar to that used for transducers with a separate vent tube. A better solution is to place the drying agent inside the enclosure, which is ventilated *via* a hydrophobic breather. This will prevent liquid water, insects and dust from getting into the enclosure. A humidity indicator is necessary on the enclosure so that it can be monitored without opening the enclosure and letting damp air or rainwater in. A separate connector on the outside of the enclosure is recommended to connect a laptop computer or other device to download data from the logger and to make adjustments, if necessary, to the logger settings.

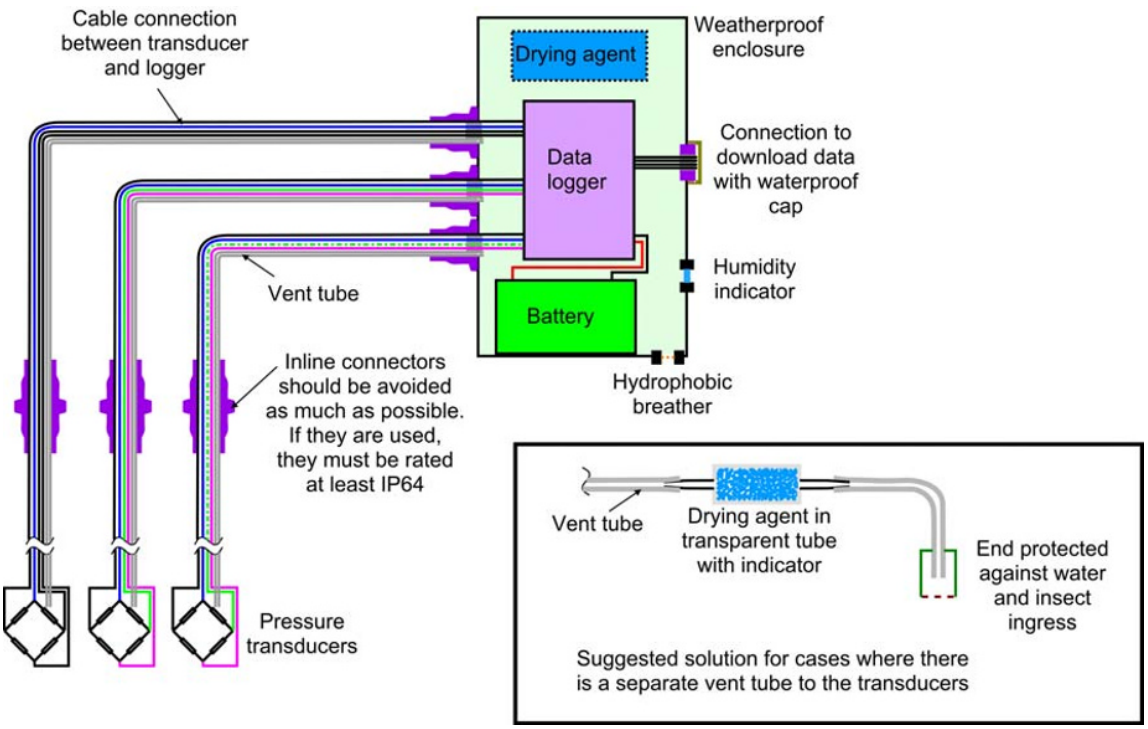

Fig. 12.23 A data logger setup for recording readings of pressure transducer tensiometers. Three transducers are shown, but usually there will be more, together with other instruments (e.g. raingauge, dielectric soil water sensors), a solar panel, etc. All should be connected using waterproof connectors rated to at least IP64. An unobstructed atmospheric pressure reference to the transducers is important while maintaining dry conditions to avoid spurious data and electronics malfunctions. An alternative arrangement for transducers with a separate vent tube is also shown. (*See insert for colour representation of the figure.*)

These precautions will ensure that the transducers are properly vented to atmosphere, while protecting both them and the other electronics from damp. Figure 12.23 shows a suggested arrangement. In most practical situations, the logger is connected to several other instruments in addition to tensiometers, for instance an automatic rain gauge, a flow meter, groundwater level piezometers, dielectric soil water sensors and porous matrix water potential monitors. These should all be connected by similar waterproof connectors.

12.7.7 Puncture tensiometers

Unlike other types of tensiometer, puncture tensiometers rely on there being a small amount of air in the system. Within certain limits, the amount is not critical, but an airspace of 20–40 mm is usually suitable. The tensiometer should be filled initially to within 20 mm of the top and then the septum fitted. If this is retained by a screw cap, a very thin smear of silicone grease should be applied to the top of the air trap and the septum before screwing the cap on moderately tightly, taking care that soil particles do not stick to the surfaces.

If, after 24 hours, the water level has dropped by more than 10 mm, more water should be added and the airspace reduced to 10 mm.

Radiation shielding and insulation of these tensiometers is essential as there is a significant volume of air in the above-ground part of the tensiometer. Diurnal pressure fluctuations of 0.35 m water were recorded by Warrick *et al.* (1998) for a soil temperature variation amplitude at 50 mm depth of 10°C in a dry soil. When the soil was irrigated, the pressure fluctuations reduced to 0.1 m water, showing the effect of soil water diffusivity.

12.8 Time before Tensiometers can be Read Reliably after Filling

Pressure transducers and, to a lesser extent, Bourdon gauges displace only a very small amount of water to register a given pressure. Because of this, they are likely to produce a reliable reading much quicker than puncture tensiometers or mercury manometers, where larger volumes of water must move through the cup and into the soil. In all cases, this time is increased by the localised wetting of the soil by water passing into it during the filling process. This can sometimes be counteracted to some extent by imposing a partial vacuum after filling using a syringe fitted to a valve on the air trap, but the extra complication is rarely justified and minimising the time that the tensiometer is open and water filled is the best strategy.

12.8.1 Sensitivity as affected by air and sensor

It is instructive to consider the relative sensitivity of different tensiometer designs. Water has a very small compressibility – about 5×10^{-6} m^{-1}. A 1 m long tensiometer contains typically about 100 mL of water and hence its volume changes by about 5×10^{-4} mL m^{-1} change in pressure. The sensitivity (Section 11.3) is the reciprocal of this, that is, 2000 m mL^{-1}. Air, on the other hand, has a compressibility of $1/P$, where P is the absolute pressure. So at atmospheric pressure (10 m water), it is 0.1 m^{-1} and at 1 m water (corresponding to a water potential of –9 m water) it is 1 m^{-1}. A 1 mL air bubble, therefore, will change its volume by 0.1 mL m^{-1} at atmospheric pressure and 1 mL m^{-1} at 1 m water; that is, by 200 and 2000 times more than 100 mL of water, with correspondingly large reductions in sensitivity. The volume of the air bubble also changes markedly. A 1 mL air bubble at atmospheric pressure becomes a 2 mL air bubble at –5 m water pressure. Its compressibility also doubles, since P halves, so that the actual change in volume is four times that at atmospheric pressure for the same small pressure change.

Other tensiometer components will change dimension to some extent as the internal pressure changes. These are more difficult to estimate given the variety of different designs and materials used. They are, however, unlikely to be comparable to the compressibility of 1 mL of air.

Pressure transducers have a very small volume change, typically 10^{-3} mL m^{-1}, corresponding to a sensitivity of 1000 m water mL^{-1}. Klute and Peters (1966) found a value of about this for their complete pressure transducer tensiometer system (see also Biesheuvel *et al.*, 1999).

The sensitivity of a mercury manometer can be calculated as follows. If the internal diameter of the manometer tube is 1 mm, its cross-sectional area is about 0.8 mm^2. A 1 m displacement corresponds to a pressure change of 12.6 m water and 0.8 mL mercury so its sensitivity is 12.6/0.8 m mL^{-1} = 16 m mL^{-1}.

For a puncture tensiometer with a 2 mL airspace at atmospheric pressure, the initial sensitivity will be 5 m mL^{-1}. If the hydraulic potential reaches 5 m water, the bubble will double in size to 4 mL and the sensitivity falls to 0.125 m mL^{-1}.

A fixed pressure transducer tensiometer with an initial 0.3 mL air bubble in the pressure port (Section 12.5.4) has a sensitivity of 2/0.3 = 7 times this, that is, 33 m mL^{-1} at atmospheric pressure and 0.83 m mL^{-1} at 5 m water because of the reduced volume of air. This may be somewhat misleading, however, as the air in the pressure port will expand as the internal pressure falls and bubble up to the top, where it will be removed at the next service.

These are summarised in Table 12.1.

Pressure transducer tensiometers often produce reliable readings within 1 hour and it is rare for any tensiometer not to reach equilibrium with its surroundings at matric potentials above – 5 m water after 24 hours. At lower matric potentials, however, response times become much longer as air that has diffused into the tensiometer comes out of solution and the diffusivity of the soil drops markedly.

Table 12.1 Volume, rate of volume change with potential and sensitivity of different tensiometer components

		Water potential (m water)			
		0	**1**	**5**	**8**
1 mL air bubble at atmospheric pressure	Volume, mL	1	1.1	2	5
	Volume change, mL m^{-1} (1/*S*)	0.1	1.2	4	25
	Sensitivity, *S*, m mL^{-1}	10	0.83	0.25	0.04
100 mL water	Volume change, mL m^{-1} (1/*S*)	5×10^{-4}	5×10^{-4}	5×10^{-4}	5×10^{-4}
	Sensitivity, *S*, m mL^{-1}	2000	2000	2000	2000
Pressure transducer	Volume change, mL m^{-1} (1/*S*)	10^{-3}	10^{-3}	10^{-3}	10^{-3}
	Sensitivity, *S*, m mL^{-1}	1000	1000	1000	1000
Mercury manometer	Volume change, mL m^{-1} (1/*S*)	63×10^{-3}	63×10^{-3}	63×10^{-3}	63×10^{-3}
	Sensitivity, *S*, m mL^{-1}	16	16	16	16
2 mL (20 mm height) airspace at atmospheric pressure in puncture tensiometer	Volume, mL	2	2.2	4	10
	Volume change, mL m^{-1} (1/*S*)	0.2	2.2	8	50
	Sensitivity, *S*, m mL^{-1}	5	0.45	0.125	0.02
Fixed pressure transducer tensiometer with an initial 0.3 mL air bubble	Volume, mL	0.3	0.33	0.6	1.5
	Volume change, mL m^{-1} (1/*S*)	0.03	0.36	1.2	7.5
	Sensitivity, *S*, m mL^{-1}	33	2.8	0.83	0.13

12.9 Reading of Tensiometers

The response time of a tensiometer depends on its sensitivity and the ease with which water can be exchanged between the bulk soil and the interior of the instrument. Tensiometers, which require only a small amount of water to be exchanged, that is, those with high sensitivity, can react much faster than those that need a large volume displacement. Therefore, fast response is associated with small volume displacement sensors (pressure transducers and Bourdon gauges), small volumes of air and wet soil. Mercury manometer and puncture tensiometers, as well as small volume displacement devices with a large volume of air inside, and dry soil lead to sluggish response. There is, therefore, little advantage in frequent reading of tensiometers, which respond slowly, as they are unable to follow rapid variations. As a rule of thumb, mercury manometer and puncture tensiometers are unsuitable for reading more frequently than once per day.

While Bourdon gauge and pressure transducer tensiometers should react quickly if there are no air bubbles, thermally induced fluctuations resulting from solar radiation or air temperature fluctuations may mean that these are unreliable.

If fast time resolution (more frequent than daily) is needed, then it is strongly recommended that pressure transducers below the ground surface are used.

12.9.1 Mercury manometer tensiometers

In principle, measurement is just a matter of reading off the height of the mercury column. However, there are a number of possible problems:

• *Parallax*. If the eye is not level with the mercury in the manometer tube, then it is possible to make an error in the reading of a few millimetres. The error arises from the separation between the mercury in the manometer tube and the scale (Fig. 12.24).

• *Broken mercury column*. The mercury column may become fragmented. This happens for several reasons, but the most common are impurities in the tube, possibly carried by the mercury from contamination of the surface, but leaching of nylon monomer from the manometer tubing (Webster, 1966) can also occur. Air diffusing through the nylon tubing and collecting in bubbles (see next paragraph) also causes breaks in the column.

When reading the tensiometer, the total length of mercury is needed. If there are several breaks, this may be done most conveniently by adding together the length of each individual segment or by noting the highest mercury level and subtracting the total length of all the breaks. Several short breaks in the column close together can often be persuaded to coalesce into one or two longer ones by gently flicking the nylon tube, leading to a more reliable estimate of total mercury length.

Sometimes, there are a sufficient number and length of breaks that some of the mercury column can pass over the top of the manometer and into the connecting tube. Under these circumstances, the system is unstable and cannot achieve equilibrium so it will continue to draw mercury along the connecting tube and into the tensiometer body. A mercury trap prevents this loss (Fig. 12.13).

• *Air bubbles*. All plastics are, to some extent, porous to gases. Nylon 66 is less so than many others, but, nevertheless, air can pass through it. Initially, fine bubbles are usually observed, which do not constitute a problem. Over time, these expand and coalesce to occupy the whole cross section of the tube. This may be in the mercury column or the water. Gross errors do not result from these bubbles in the water column, but the length of tube occupied by them has a density very close to zero and so, if the total length in the water column amounts to l, this is equivalent to an

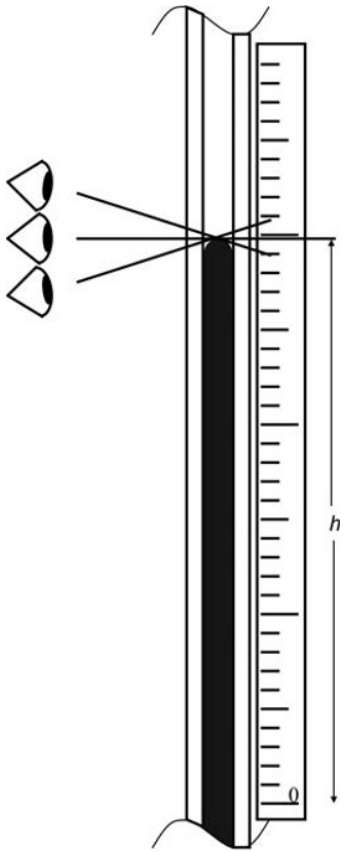

Fig. 12.24 Parallax error resulting from not reading mercury column height level with the surface. The error is minimised by making the scale and column as close to one another as possible.

error in the potential of the same length in water head units. However, an air bubble on the manometer side of the board produces an error in the opposite sense to one on the other (tensiometer) side and so they compensate one another to a significant extent.

Air bubbles in the mercury column are a different matter, since they replace mercury of density 13,600 kg m^{-3} with fluid of density very nearly zero. Subtracting the length of air bubble from the total mercury column length leads to a small error, since this assumes that the effective density is 12,600 kg m^{-3} (i.e. the difference in density of mercury and water), but in view of the uncertainties introduced in estimating the total length involved and that this normally occurs only at low potentials when the tensiometer is becoming unreliable, there is little disadvantage. In any case, it is difficult to distinguish between bubbles of air and water within the mercury column.

- *Temperature changes*. The density of the fluids (mercury and water) changes with temperature. The coefficient of expansion of water is 0.207 kg $m^{-3}{}^{\circ}C^{-1}$ and that of mercury is 2.48 kg $m^{-3}{}^{\circ}C^{-1}$. The relevant quantity is $\rho_{Hg} - \rho_w$, which has a combined temperature coefficient of 2.27 kg $m^{-3}{}^{\circ}C^{-1}$ or about 0.018%$^{\circ}C^{-1}$. Radiation shielding reduces diurnal temperature fluctuations but have negligible effect on seasonal ones. A ± 10°C change in temperature, therefore, leads to a ± 0.18% error in the readings (9 mm water at a potential of 5 m water), which is relatively small compared with some of the other likely errors.
- *Drop in reservoir mercury level*. The maximum amount of mercury extracted from the reservoir is, as described in Section 12.7.3, likely to be equivalent to a drop in the level of the mercury level by about 7.5 mm. This is equivalent to about 95 mm of water head or 9.5 hPa or slightly over 1% of the minimum achievable reading. This is a worst-case scenario and rarely will all manometers contain a column of this height. More generally, the uncertainty in reading due to a drop in the reservoir level is likely to be about 1%.

If better accuracy is desired, then a simple correction is possible. If the surface area of the reservoir is A, the internal diameter of each manometer tube is d and the mercury height in the ith tube is h_i, then the drop in the reservoir mercury level will be

$$-\Delta s = \frac{\pi d^2 \sum_i h_i}{4A}. \qquad (12.9.1)$$

Substituting for Δs from Equation 12.7.3, a correction to the column height, h, can be made as

$$h' = h + \frac{\pi d^2 \sum_i h_i \left((\rho_{Hg}/\rho_w) - 2\right)}{4A\left((\rho_{Hg}/\rho_w) - 1\right)} = h + 0.723\frac{d^2 \sum_i h_i}{A}. \qquad (12.9.2)$$

This is simple enough to implement by means of a computer program to process the data or on a spreadsheet.

- There is a tendency for the mercury to 'stick' in the manometer tube, particularly after the manometers have been in operation for some time. This is caused by impurities and leaching of plasticiser out of the tubes, which affect the surface properties of the tube. Because the tubing is flexible, it can be agitated slightly by gently flicking with a finger. This not only causes the mercury column to settle close to its equilibrium position but also often allows air bubbles to coalesce, making it easier to assess the total length of mercury.

Any visible problems with the reading should be recorded along with the readings. Many such problems are sufficiently common that a set of codes for these can be used to avoid the need to write copious notes. A suggested set of codes is:

0 No apparent problems.
1 Some air bubbles visible in the manometer tube above the mercury.
2 Some breaks in the mercury column. These have been subtracted from the overall length recorded.
3 Many breaks in the mercury column. Only an estimate of the total length of mercury can be made.
4 Reading completely unreliable or impossible.
5 Tensiometer has been purged since the last reading.
6 Reading may be unreliable because of frost.

Hydraulic potential profiles and simple field checks

If tensiometers are arranged in depth order on the manometer board, then the shape of the potential profile can be visualised easily. The hydraulic potential, when the tensiometer has been set up as described in Section 12.7.3, is given by

$$\psi_h = (\rho_{Hg} - \rho_w)h. \qquad (12.9.3)$$

A schematic of a set of manometer levels is shown in Fig. 12.25a along with the actual readings and water potentials (Fig. 12.25b). The hydraulic and component potential profiles are plotted in Fig. 12.25c along with the mercury levels. It can be seen that the shape of the profile is mirrored in the shape of the mercury levels, although there is some distortion if the tensiometers are not all installed with the same depth interval. This is of no real consequence for a rapid check in the field.

This visualisation also provides a simple means to identify possible faults with a tensiometer, as the regular pattern shown in Fig. 12.25 will not occur. Figure 12.26 shows a hypothetical set of readings, where the water potentials are the same as in Fig. 12.25, but with two faulty tensiometers. It is worth pointing out that it is very unlikely that a faulty tensiometer will indicate a lower potential than that corresponding to the prevailing matric potential at the tensiometer cup. The only circumstances in which this might occur are if potentials are rising and the faulty tensiometer reading is lagging much further behind that of the other tensiometers, perhaps because of poor soil contact or a constriction in the connecting tube, or if a rapid temperature change causes the reading to fluctuate and the tensiometer is unable to adjust sufficiently quickly.

For serious leaks, the indicated matric potential is likely to be very close to zero, as the tensiometer cup cannot

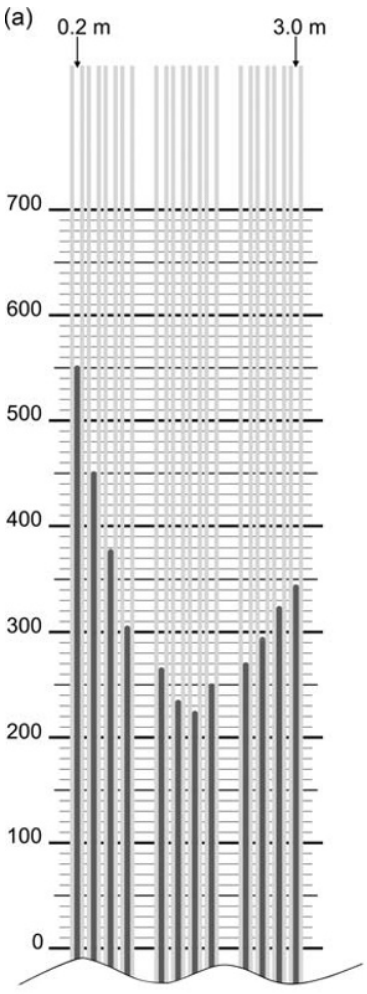

(b)

Depth (m)	Hg height (mm)	Hydraulic potential (m)	Gravitational potential (m)	Matric potential (m)
0.2	552	−6.96	−0.20	−6.76
0.4	451	−5.68	−0.40	−5.28
0.6	254	−3.20	−0.60	−2.60
0.8	305	−3.84	−0.80	−3.04
1	267	−3.36	−1.00	−2.36
1.2	236	−2.97	−1.20	−1.77
1.5	225	−2.84	−1.50	−1.34
1.8	251	−3.16	−1.80	−1.36
2.1	271	−3.41	−2.10	−1.31
2.4	193	−2.43	−2.40	−0.03
2.7	326	−4.11	−2.70	−1.41
3	346	−4.36	−3.00	−1.36

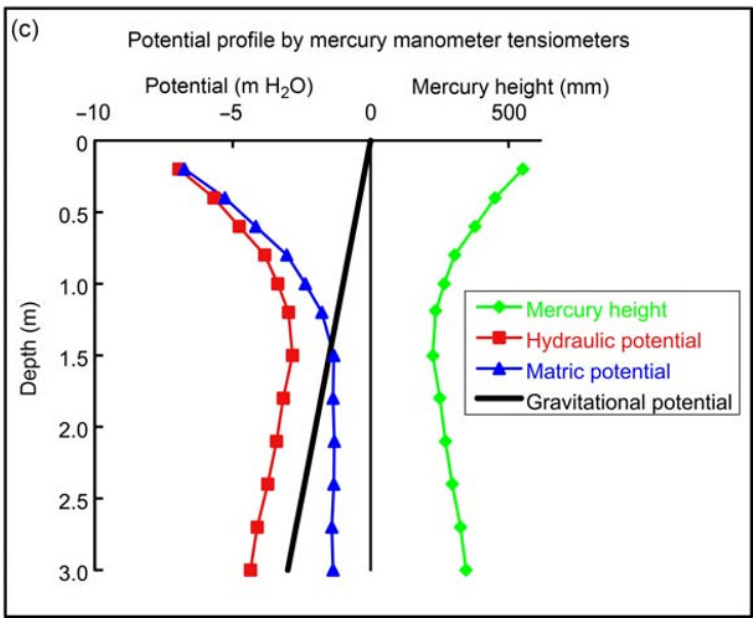

Fig. 12.25 (a) Typical appearance of a set of mercury manometers under temperate climate summer conditions. (b) Readings and water potential values. (c) Potential profile plots showing that the pattern of mercury levels in the field approximately mirrors the hydraulic potential profile.

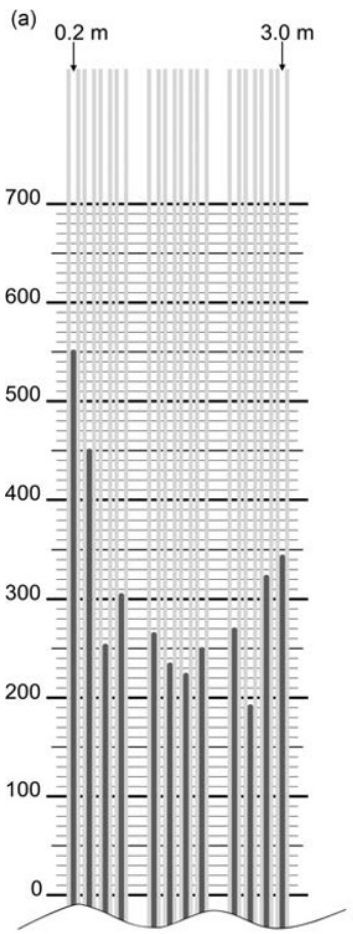

(b)

Depth (m)	Hg height (mm)	Hydraulic potential (m)	Gravitational potential (m)	Matric potential (m)
0.2	552	−6.96	−0.20	−6.76
0.4	451	−5.68	−0.40	−5.28
0.6	254	−3.20	−0.60	−2.60
0.8	305	−3.84	−0.80	−3.04
1	267	−3.36	−1.00	−2.36
1.2	236	−2.97	−1.20	−1.77
1.5	225	−2.84	−1.50	−1.34
1.8	251	−3.16	−1.80	−1.36
2.1	271	−3.41	−2.10	−1.31
2.4	193	−2.43	−2.40	−0.03
2.7	326	−4.11	−2.70	−1.41
3	346	−4.36	−3.00	−1.36

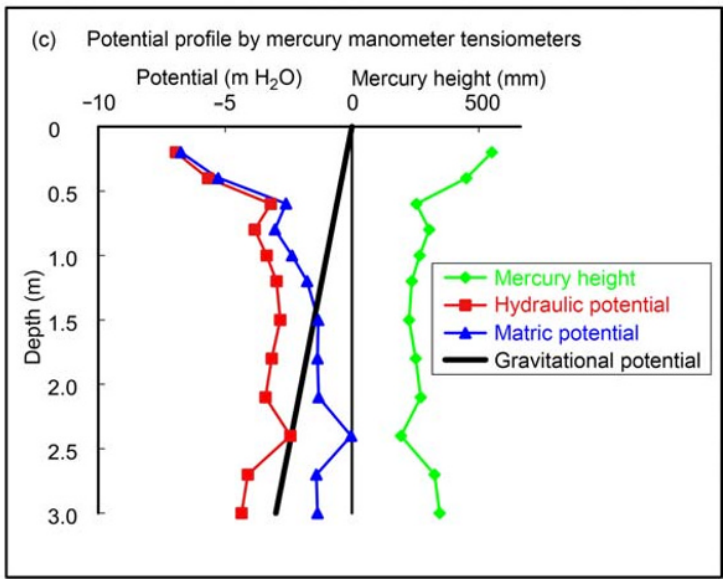

Fig. 12.26 Potential profiles as for Fig. 12.25 except for indicated potential at the 0.6 and 2.4 m depths being much higher owing to faulty tensiometers.

support a pressure differential and so the internal pressure equals that of the atmosphere. This is the case for the 2.4 m tensiometer depicted in Fig. 12.26. In other cases, a faulty seal may be able to support a certain pressure differential across it before a leak occurs and so the indicated matric potential may be accurate down to this pressure but not be capable of going any lower. The 0.6 m tensiometer in Fig. 12.26 has a leak that occurs only when the matric potential is below –2.6 m water.

A small crack or poor seal normally is able to support a small negative pressure, usually opening at a slightly lower potential from that at which it closes. The result is a reading oscillating as shown in Fig. 12.27. It is characterised by an initial rapid rise from an indicated reading of ψ_{open}, corresponding to the internal pressure at which the seal fails, to a reading of ψ_{close}, which corresponds to the pressure at which it reseals. The behaviour is characterised by a rapid rise in pressure from ψ_{open} to ψ_{close} as air enters the tensiometer followed by a slower recovery back to ψ_{open} as water leaves the tensiometer through the porous cup into the soil. As more air collects in the tensiometer, the response time

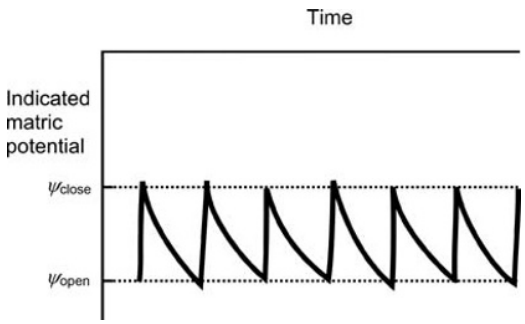

Fig. 12.27 Cycling of pressure caused by a leaking tensiometer seal. The leak opens at an internal pressure of ψ_{open} and closes at ψ_{close}. The opening and closing pressures often vary slightly from one cycle to the next as shown.

increases and so the recovery phase takes longer and the frequency of the cycling reduces. This behaviour is unlikely to be observed with infrequent readings of a mercury manometer but will show up as seemingly random variations of the reading.

Usually, faults are the result of a leak in the tensiometer. Common leak points are:

- A blade of grass or other piece of vegetation between the sealing bung and air trap. This happens easily and is sometimes surprisingly difficult to notice. It is also easily rectified.
- A loose seal between the sealing bung and the connecting tube or a leak at another joint. The sealing bung should be replaced as reducing the size of the hole for the connecting tube is not practical.
- A failed adhesive joint. If this is at the air trap-body tube junction, air bubbles may be seen leaking into the tensiometer after refilling it.
- A cracked cup. These can appear some time after installation, perhaps as a result of a small incipient crack propagating until it extends through the complete thickness of the cup, or as a result of soil movement, sometimes caused by root activity. Replacement of the cup or the entire tensiometer with one of the same length are the only solutions. It may be necessary to deepen the hole slightly if some soil has fallen in while removing the tensiometer. Alternatively, or additionally, the hole may be fractionally too large as a result of the tensiometer removal or because of variation in size between cups. The neck of a broken ceramic cup can usually be removed from a body tube by driving it out with a steel bar just small enough to fit inside the body tube. Dropping the bar into the top of the vertical tube is usually quite effective.

In all cases in which the tensiometer leaks, it loses water, so a lower than expected reading coupled with higher than expected loss of water are indicative of a leak. To save time, it is recommended that investigation of the cause of a leak be done in the order listed above.

When reading tensiometers, it is useful to make a reasonable estimate of the indicated water potential as a check on plausibility of the readings. A customised manometer scale calibrated in water potential units will obviously achieve this. However, it is usually convenient to use the more easily available scales calibrated in millimetres. In this case, the conversion factor to metres of water is 0.0126, which is close to 0.0125, and so dividing the reading in millimetres by four and adding it to the reading gives an approximate value for the magnitude of the hydraulic potential in centimetres of water or hectopascals (divide by 100 for metres of water or multiply by 10 for millimetres of water). Subtracting the depth of the tensiometer cup from this value gives the magnitude of the matric potential.

12.9.2 Bourdon gauge tensiometers

Reading of a Bourdon gauge is a straightforward matter of taking a reading from a dial. Apart from the inherent inaccuracies resulting from the very limited size of the scale and the mechanical linkage, reading of the gauge can produce similar parallax errors as for a mercury manometer. To reduce this, care must be taken that the line of sight is perpendicular to the scale.

Apart from leaks connected with cracks and poor bonding of the cup, which are much the same as for all tensiometers, Bourdon gauge instruments may leak at the filling cap, which usually screws onto the air trap and is sealed by a rubber disc. This may lose flexibility with age or become contaminated by vegetation or soil particles, leading to leaks. The other potential leakage point is the connection of the Bourdon gauge into the tensiometer body. This is usually a screw-in connection, sealed by PTFE tape on the threads or an 'O'-ring. PTFE tape works well but cannot stand many dismantlings and remakings before needing to be renewed, while an 'O'-ring is at similar risk of ageing and contamination by soil or vegetation as the rubber seal to the cap.

12.9.3 Puncture tensiometers

A puncture tensiometer is read by holding the head unit over the top of the tensiometer and pressing the needle through the septum. The tip of the needle should enter the water inside the tensiometer. If the head unit is heavy enough, it can rest on top of the tensiometer, which avoids unsteady hand movements from disturbing the readings. If the reader unit is not sufficiently heavy, an additional weight can be attached to it to overcome the force of the spring and any buffeting by wind. If this is not possible, the reader unit must be held as still as possible while the reading is taken.

Correction of puncture tensiometer readings for needle insertion

Inserting the needle disturbs the pressure inside the tensiometer somewhat. Thony *et al.* (1989) conducted a theoretical and experimental study of the effect. They found that the pressure in the airspace above the water level is disturbed when the needle is inserted. This is caused partly by the volume of the solid wall of the needle compressing the gas. But the main disturbance arises because a volume, ν, of gas in the needle and casing of the transducer beneath the diaphragm at atmospheric pressure, A, is mixed with the existing air of volume, V, at a lower pressure, P. The resulting mixture will have a volume V_1, and pressure, P_1, given by

$$V_1 = V + \nu, \tag{12.9.4}$$

$$P_1 V_1 = PV + A\nu, \tag{12.9.5}$$

$$P_1 = \frac{PV + A\nu}{V + \nu}. \tag{12.9.6}$$

The difference ΔP between the pressure before the needle was inserted and that immediately after will be

$$\Delta P = \frac{A - P}{V + \nu}\nu \approx -\frac{\psi}{V}\nu, \tag{12.9.7}$$

if ν is small compared with V. Therefore the difference between the actual water potential and that indicated immediately after insertion of the needle is very nearly

proportional to the hydraulic potential and the volume of air contained within the needle and transducer casing. This can be put another way that there is an almost proportional error in the hydraulic potential reading of ν/V.

To reduce the error, therefore, ν, the volume of air contained within the needle and the transducer casing should be as small as possible. Marthaler *et al.* (1983) measured values between 0.07 and 0.1 mL for different examples of their system, while Thony *et al.* (1989) also took a value of 0.1 mL as typical. Having an air pocket of 4 mL (a length of about 40 mm in a typical tensiometer with an internal cross-sectional area of the air trap of 1 cm^2) therefore leads to an overestimate of the hydraulic potential of about 2.5% (i.e. a smaller absolute number).

Thony *et al.* (1989) found that the initial increase in pressure was reasonably consistent with the theory outlined here.

By filling the airspace in the transducer casing and needle with water, which is almost incompressible, v can be reduced effectively to zero. However, this does not eliminate the error in the tensiometer reading as we ignored solid needle wall above. If this is full of water, then effectively the volume of the airspace is reduced by the volume of the needle case, v^*, inside the tensiometer plus the water contained within it. Applying Boyle's Law, we get

$$PV = P_1(V - v^*). \tag{12.9.8}$$

So

$$\Delta P = P_1 - P = \frac{Pv^*}{V - v^*} \approx \frac{P}{V} v^*. \tag{12.9.9}$$

In this case, the increase in pressure is greatest when water potential is high (i.e. P is close to atmospheric pressure). For a needle of outer diameter 0.5 mm and penetrated length 25 mm, the volume, v^*, is about 5 mm^3, so with V equal to 4 mL, the maximum value of ΔP when P is around atmospheric pressure, 10 m water, is about 12 mm water This is very small and comparable with the error from other sources and much less than the error resulting from gas expansion in the needle and transducer.

The tensiometer is not a closed system. An increase in pressure inside the instrument caused by introduction of air or the needle leads to water moving out through the porous cup into the soil until the water inside is once again in equilibrium with water in the soil. Depending on the characteristics of the cup, the soil and the water status of the soil, this can take from 2 minutes to more than 35 minutes (Marthaler *et al.*, 1983; Thony *et al.*, 1989; Cresswell, 1993).

Waiting for several minutes to take a reading on each tensiometer, bearing in mind that there are usually at least six and often very many more at each location, is inconsistent with one of the primary advantages of the puncture tensiometer – the ability to read a large number of tensiometers in a short time. There are two possible approaches:

1 To take a reading immediately after insertion of the needle into the tensiometer. In practice, there may be a short-term transient so that it may be necessary to wait for a few seconds to ensure that the reading is at least quasi-stable. A correction can be applied to this reading if high accuracy is important using Equation 12.9.7 or 12.9.9 as appropriate. This will require ν or ν^* to be known, or at least estimated to a good approximation, as well as V.

2 To use the method of Greenwood and Daniel (1996), which involves puncturing the tensiometer twice in rapid succession. This will produce a second reading, P_2, similar to Equation 12.9.6 given by

$$P_2 = \frac{P_1 V + Av}{V + v} \approx P_1 + A\frac{v}{V} \tag{12.9.10}$$

from which v/V may be estimated, leading to

$$P \approx 2P_1 - P_2. \tag{12.9.11}$$

The same equation is also valid in the case of a water-filled needle and transducer casing.

Leakage around the needle

A common problem with puncture tensiometers is leakage of air between the needle and septum into the tensiometer. It is characterised by an oscillatory reading as depicted in Fig. 12.27. This behaviour results from air leaking past the needle into the tensiometer, then the seal between the needle and septum being re-established, only to leak again when the vacuum has increased. Each time, more air enters the tensiometer, leading to an increase in the time taken for recovery. This behaviour is very similar to that described for other kinds of leak. Care in inserting the needle straight and avoiding any sideways movement will reduce the frequency of such problems. If one tensiometer produces such behaviour frequently, the septum should be changed as it is likely that each new hole is too close to an older one or the septum has perished. Cycling of the reading as described in Section 12.9.1 means that the reading is unreliable and should be discarded. However, the potential within the tensiometer will be lower than that corresponding to the numerically largest reading observed, so this will give an upper value for the potential.

Differences between the needle terminating in the airspace or water

The only control over the quantity of air inside the tensiometer is the amount of de-aired water used when refilling at its last service. As the internal pressure falls, the air expands and may be augmented by air diffusing into the tensiometer or exsolving from solution in the water inside the tensiometer. The size of the air bubble cannot, therefore, be predicted in advance and sometimes the needle penetrates into the water, while on other occasions it terminates in the airspace.

In the case where the end of the tensiometer needle is beneath the water level in the tensiometer, the situation is as shown in Fig. 12.28a. The pressure in the water column

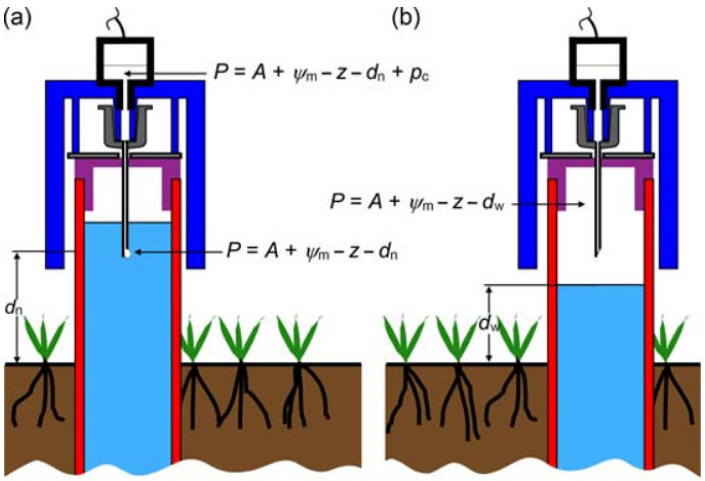

Fig. 12.28 Possible configurations for measurement of pressure inside a puncture tensiometer. (a) Needle beneath the water surface records the hydraulic potential referenced to the height of the needle end. (b) Needle end above the water surface records the pressure in the airspace, which is the hydraulic potential referenced to the height of the water surface.

decreases from $A + \psi_m$ at the position of the porous cup to $A + \psi_m - h$ at a height, h above it, where A is the atmospheric pressure. The pressure at the tip of the needle is therefore $A + \psi_m - z - d_n$, where z is the depth of the porous cup below ground level and d_n is the height of the needle tip above the ground. This is independent of the water level in the tensiometer provided that the needle tip is beneath it. The pressure recorded by the pressure transducer will be slightly greater than this by an amount p_c, owing to the capillary effect of the small internal diameter of the needle. This means that the air pressure inside the needle needs to be a little higher than that of the water for a bubble to escape from the needle. Thony *et al.* (1989) estimated that this was about 70 mm water for a needle of internal diameter 0.4 mm, which was consistent with their measurements.

If the needle tip is above the water level inside the tensiometer (Fig. 12.28b), which is most often the case, a measurement of the potential can be made but the position of the water level must be known. This is quite easy if the water level is visible, but if not, the level can be calculated from the quantity of de-aired water needed to bring the level up to a mark by dividing the water volume by the inside area of the air trap. The pressure in the airspace above the water level, which is measured by the pressure transducer, is the same as that in the water at the water level. This pressure is $A + \psi_m - z - d_w$, where d_w is the height of the water level above ground surface.

If the pressure recorded by the transducer is P_t, then the hydraulic potential, ψ, when the needle tip is under the water level is given by

$$\psi = P_t + d_n - p_c. \qquad (12.9.12)$$

And when the needle tip is in the airspace by

$$\psi = P_t + d_w. \qquad (12.9.13)$$

In both cases we assume a gauge transducer so that P_t is the difference between the absolute and atmospheric pressure.

Note that when the tensiometer contains a large volume of air, the water potential indicated may lag that of the true potential in the soil by several days.

12.9.4 Pressure transducer tensiometers

Reading of these is the most straightforward and least prone to error, requiring merely that a known voltage be applied across the strain gauge bridge and the out-of-balance voltage across the bridge in the other direction be measured. Moreover, this arrangement is very suitable for automatic recording of the tensiometer readings. Many environmental data loggers can provide an excitation voltage and also record the ratio of output to excitation voltage, thus removing the influence of excitation voltage fluctuations.

The frequency of recording tensiometer data is a matter for experience, the objectives of the monitoring and site conditions. Shallow tensiometers react rapidly to rainfall or irrigation events, while deeper ones usually do so less quickly, especially during dry periods. With a programmable data logger, the frequency of data collection can be varied by both position and environmental conditions. However, this introduces considerable extra complexity into the data analysis, and it may be better to collect frequent data for all instruments, even though much of it may be redundant. This also gives an insurance against unexpectedly rapid water potential changes. Modern data loggers can store large amounts of data and so this strategy is perfectly feasible, although it produces large data files! A recording interval of 15 minutes is suitable in many cases to capture the most rapid events.

12.10 Tensiometer Maintenance

Most soil water monitoring instruments need very little maintenance. This is not, however, the case with tensiometers, especially under dry conditions. The main

requirement is to remove air which collects by diffusion into the tensiometer and coming out of solution as the potential falls. In most tensiometer types, the presence of air is easily monitored by inspecting the air trap. The tensiometer can be topped up with de-aired water in the same way as described in Section 12.7.3.

Apart from routine refilling, faults occur occasionally leading to a leakage in the tensiometer. The fault may be a cracked porous cup or an adhesive joint or seal having failed. It is usually best to investigate the above-ground parts of the instrument first as this causes least disruption. More details of fault finding and rectification are contained in Section 12.9.1.

The other most likely problem is water leaking down the side of the tensiometer, for instance down a gap along the body tube or a poor seal between the tensiometer and sleeving tube. Regular inspection at the same time as readings are made or a logger downloaded should mean that incipient problems are detected before they affect the validity of readings.

Tensiometers become unreliable below about −8.5 m water potential. No amount of refilling will make them operate reliably when the surrounding soil is at a potential significantly below this and a great deal of effort can be expended in futile attempts to keep them operating under such conditions. An understanding of the principles of operation can help to form a judgement when to abandon their use and – more importantly – to restart readings once a dry period ends. It can take several weeks in some instances after a wet period starts for the soil at more than 1 m depth to wet up sufficiently to permit tensiometer operation.

12.10.1 Mercury manometer tensiometers

Under modest ($\gtrsim$ −5 m water) hydraulic potential conditions, mercury manometer tensiometers require little routine maintenance, provided that the water inside was thoroughly de-aired before use. As long as the mercury column is intact, there are only very small air bubbles in the manometer and connecting tubes and that there is little or no air collected in the air trap, no attention is necessary. Under such conditions, the tensiometers can often operate for several weeks without attention.

At lower hydraulic potentials, large air bubbles collect in the air trap and the manometer and connecting tubes, and it becomes increasingly difficult to maintain an intact mercury column.

To maintain reliable operation, the tensiometer must be refilled with water and air flushed out of the connecting and manometer tubes, an operation usually known as 'purging'. De-aired water must be used. The first part of the operation is to remove the sealing bung and the bung on top of the tensiometer (Fig. 12.13) and to refill the air trap to the top. The connecting tube should not be removed unless it is suspected that mercury has collected in the mercury trap, when it may be desirable to collect this mercury and to refill the mercury trap with water. The bung is carefully replaced on the air trap, taking care that no air is trapped beneath the bung and that there are no blades of grass or other extraneous objects caught between the bung and air trap. The filling hole is topped up with water and then de-aired water injected into the filling hole from a syringe, forcing water through the connecting tube, the manometer tube and the mercury reservoir. The filling hole is refilled with water and the sealing bung replaced, ensuring that the entire system is full of water and that all air has been removed.

If they are well protected from direct sunlight, rubber (particularly synthetic rubber) bungs can last a long time, but eventually they perish and need replacing. More frequently, usually after 2 or 3 years, the nylon tubing will need to replaced, as it becomes opaque and brittle. Exposure to bright sunlight accelerates this process, which is one reason why radiation shielding is so important, the other being to reduce thermal effects on the readings. The nylon will be contaminated by mercury and so must be disposed of carefully.

Also, over time, the mercury becomes contaminated with plasticizer from the nylon and other impurities. Replacement with clean mercury at the same time as the nylon tubing is replaced is recommended. Mercury can be cleaned in the laboratory, but handling it under confined conditions requires a very great deal of care. It is usually more cost-effective to send it back to a supplier who is able to deal with it safely and buy new mercury from the same source. This is not usually expensive.

Freezing of this type of tensiometer rarely causes a problem, aside from making the instrument unusable until it thaws. Ice forming in the air trap will either push water through the connecting tube or force off the rubber bung from the top of the tensiometer. On rare occasions, the air trap or connecting tube may split and need replacement.

12.10.2 Bourdon gauge tensiometers and those with pressure transducers mounted at the top

Other than routine refilling, ensuring that seals are intact and that there are no gaps to allow water to bypass the soil around the tensiometer body, this type of tensiometer requires very little maintenance.

Freezing, however, will damage the Bourdon gauge or pressure transducer through excess pressure generated and, in the case of the Bourdon gauge, freezing of the water inside the Bourdon tube. These types of tensiometer should therefore be taken out of commission during periods of cold weather.

12.10.3 Tensiometers with pressure transducer close to the ceramic cup

Apart from routine purging, as described for first filling after installation in Section 12.7.5, and checking for possible bypass paths around the body tube, the only likely maintenance required is likely to be replacement of the flexible

tube connecting the two purging tubes. This should be of the same specification as the original tube, as it has been selected to have a low permeability to air.

Those tensiometers that are not capable of being purged *in situ* must be removed, refilled and replaced if necessary.

Tensiometers with underground pressure transducers cannot be monitored easily for air collecting inside them. The purgeable type is easily flushed and so it is recommended to be done whenever the site is visited when the indicated potential is or has been lower than –4 m water. For the non-purgeable type, judgement and experience must be exercised. Keeping an eye on the evolution of water potential should provide a guide as air collecting will slow the tensiometer response and it may well reach a level, below which it appears not to fall, as air fills the entire volume. Usually, the indicated potential rises slowly beyond this point, a sure sign of attention being required.

The German manufacturer, UMS, make tensiometers containing an infrared sensor, which can detect air bubbles inside the instrument.

12.10.4 Frost protection

The only parts of a tensiometer that usually suffer frost damage are above-ground sensors such as Bourdon gauges (Section 12.5.2) or pressure transducers (Section 12.5.4). The Bourdon tube is particularly vulnerable and the pressures generated may strain a pressure transducer diaphragm. Below-ground parts are usually unaffected because the water inside the tensiometer freezes from the top downwards and so water is pushed out of the cup by expansion of the water near the surface as it freezes.

Apart from possible damage, the main problem is loss of data. With below-ground pressure transducers, this is likely to be a transient occurrence when the soil freezes around the tensiometer depth. Mercury manometer tensiometers, however, are unable to operate when the water in the above-ground parts is frozen. Ice may, additionally, push rubber bungs out of the top of a tensiometer. Even when frost occurs only ephemerally, this can cause considerable loss of data over the winter.

Three solutions have been proposed:

1 Strebel (1970) used a light immiscible organic liquid in the tensiometer, which floated above the water in the tensiometer body. This protects the parts down to the interface with the water from frost. A correction is needed for the density of the liquid, and it is important to know the location of the interface. The organic liquid expands more than water with temperature and so there is probably more disturbance to the reading from this cause in warmer weather. Some plastics may not be compatible with the organic liquid.

2 Wendt *et al.* (1978) filled tensiometers with a 30% mixture of methanol in water. This gave protection to about –18.8°C and enabled operation throughout the winter. They found differences of typically 100–200 mm and up to 300 mm water pressure between the methanol and water tensiometers. They did not detect any deleterious effects to either the tensiometer parts or a winter wheat crop. Gorden and Veneman (1995) did a more systematic investigation using several different mixtures of up to 50% methanol. They reported no problems and no differences in reading against water tensiometers but suggested that microbial growth near the tensiometer cup could be promoted by the methanol. The lower surface tension of the methanol solution may be expected to reduce the accessible range of matric potential as a result of lowering the bubbling pressure of the cup.

3 Iwata and Hirota (2005) used insulated and heated tensiometers to monitor water potential over a winter. They were able to observe water flow towards the frozen soil beneath a snow pack.

12.11 Quality Control of Tensiometer Readings

As may be deduced from the foregoing, operation of tensiometers is fraught with difficulty, particularly where the pressure sensor is above ground level and at low water potentials. Thermal effects, leaks, frost, mercury column breaks, air collection and slow response times frequently lead to there being a serious discrepancy between the indicated potential and that in the soil surrounding the porous cup. Tensiometers with a pressure transducer close to the ceramic cup, particularly those that can be purged *in situ*, present fewest problems.

The most efficient way to examine the data and to remove spurious readings is by graphical display. Three different ways to look at the data have been found to be particularly effective: examination by time series, by depth and by comparison with other readings taken at the same time, principally those from other tensiometers and water content measurements at the same depth nearby.

12.11.1 Time series

Figure 12.29 shows a series of data taken from mercury manometer tensiometers at several depths at a site in Southern England. Comparing the behaviour of tensiometers at several depths as well as with simultaneous water content values eases identification of suspicious readings.

12.11.2 Depth profiles

Figure 12.30 shows some examples of profiles of hydraulic potential recorded from the same site as in Fig. 12.29. Cross-referencing to time series readings (Fig. 12.29) aids in judgement of whether readings are reliable.

12.12 Deep Water Potential Measurements

Any pressure sensor located at or above the ground surface is, apart from its vulnerability to thermal effects, freezing,

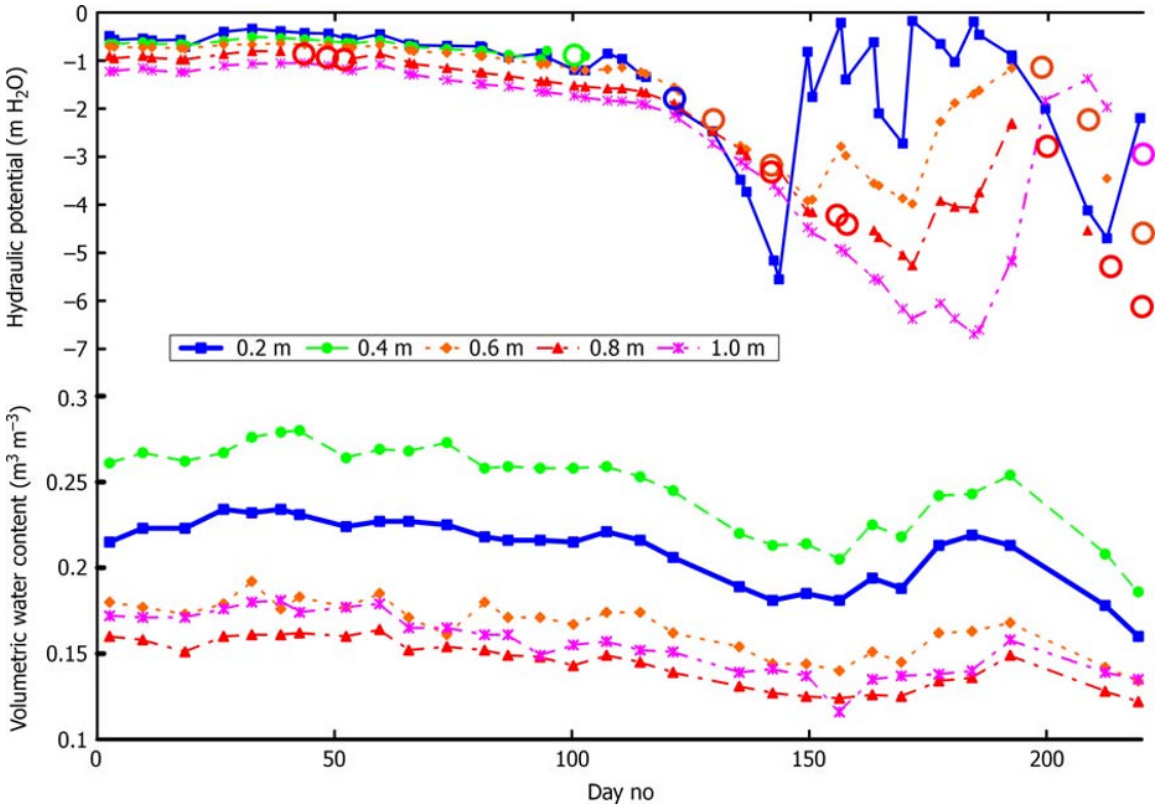

Fig. 12.29 Example of time series of twice-weekly readings of mercury manometer tensiometers at several depths at a woodland site in Southern England. Readings removed as being unreliable at the time of reading are indicated by open circles. The corresponding water content neutron probe readings are shown in the lower graph. Rising potentials after day 192 are not consistent with falling water content, suggesting that these readings are suspect and the tensiometers were failing.

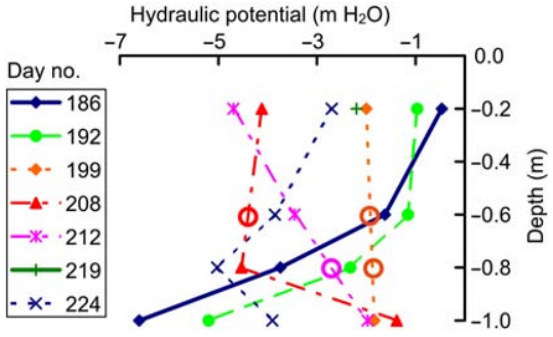

Fig. 12.30 Example of sequential potential profiles measured by mercury manometer tensiometers from the same site as in Fig. 12.29 during midsummer. The 0.4-m tensiometer was not working at this time. Readings removed as being unreliable at the time of reading are indicated by open circles.

animals and vandalism, limited in the range of matric potential that it can record by the long column of water between the porous cup and the pressure sensor. A mercury manometer tensiometer at 3 m depth will typically have 1.5 m or more of tubing above ground. This will limit the theoretical minimum matric potential that can be recorded from approximately –10 m water to –(10 – 3 – 1.5) = –5.5 m. With a pressure transducer or Bourdon gauge located close to the ground surface, this is only slightly less restrictive. A pressure transducer located close to the porous cup has less limitation, restricting the minimum observable matric potential by only the distance between the porous cup and the sensor, usually only a few centimetres.

Three approaches have been used to overcome the difficulties in obtaining water potential measurements at depth.

12.12.1 Observation from a pit

A pit (shaft or caisson) dug in the ground allows the installation of sensors through its wall into the soil and a sensor to be housed inside the pit. The tensiometer is normally installed sloping downwards at a shallow (around 5°) angle to allow air bubbles to collect at the end accessible from the pit. The installation method is suitable for tensiometers employing water and mercury manometers, Bourdon gauges and pressure transducers as well as puncture tensiometers. The arrangement is shown schematically in Fig. 12.31.

In principle, there is no limit to the depth at which tensiometers can be installed by this means. However, the

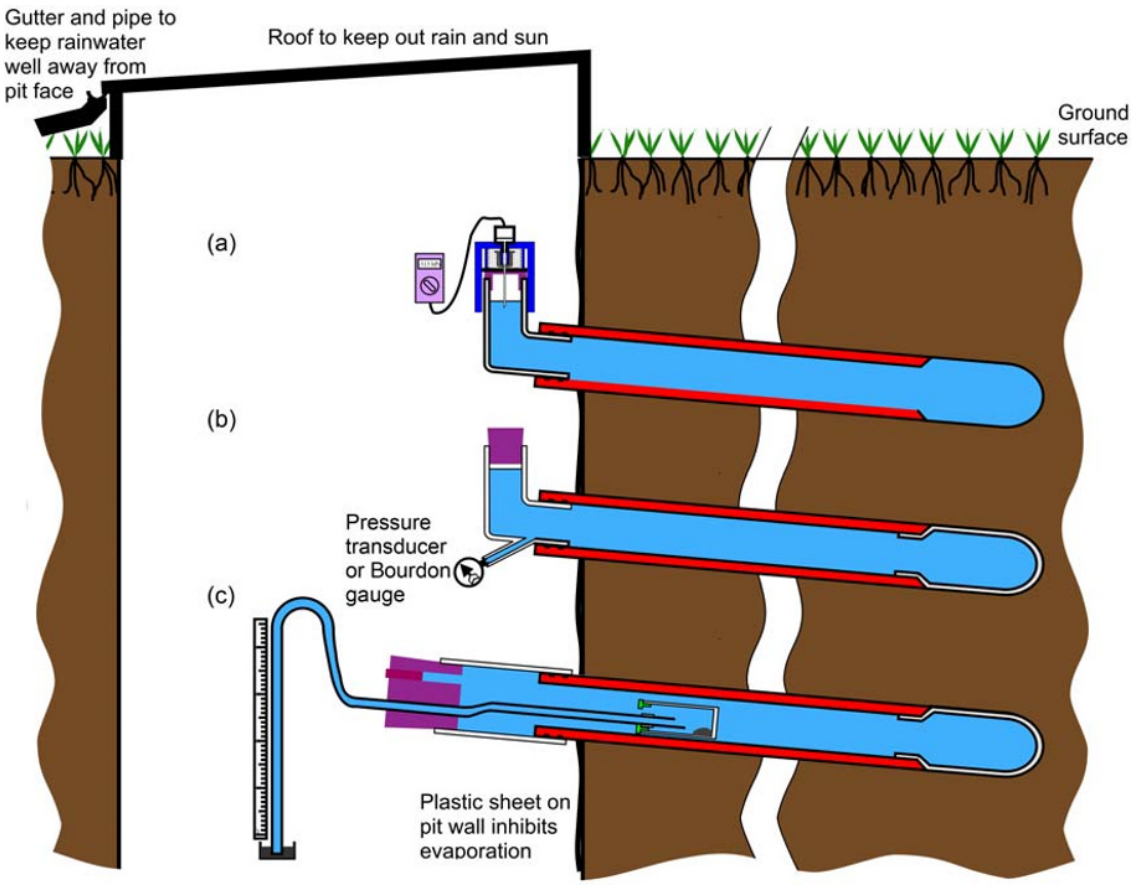

Fig. 12.31 Arrangements for installation of tensiometers from the side of a pit in the ground. (a) Suggested arrangement for puncture tensiometers similar to that used by Wierenga *et al.* (1991). (b) Bourdon gauge or pressure transducer arrangement. Note the sensor at the bottom to allow air to escape. (c) Mercury manometer arrangement similar to that described by Cooper (1979). In practice, the manometer board may conveniently be mounted on the support structure on the face of the pit.

engineering requirements are such that for depths greater than about 6 m, it is uneconomic to undertake the necessary works unless access to the profile is required for other purposes as well. It is very important that a roof be provided over the pit to keep out rainwater and the sun, which may dry the soil face. Rainwater should be led well away from the vicinity of the pit to ensure that the readings are not disturbed and the exposed soil surfaces, particularly that through which the tensiometers are inserted, covered to minimise evaporation. The pit should be sited so that rainwater does not run down this face.

Deeper installations bring with them a number of safety considerations:

- It is usually necessary to support the sides of the excavation. The deeper the pit, the more important and the more elaborate this will be. In many cases, wooden planks against the face of the soil held in place by a sturdy wooden framework are suitable, although regular inspection is needed to ensure that the wood is not weakened by rot or wood-boring insects. Covering the walls of the pit has the added advantage of suppressing evaporation from them.
- In some cases, harmful gas (e.g. methane or carbon dioxide) may collect in the bottom of the hole. Gas monitors are available to ensure operator safety.
- Precautions are needed to ensure that people or animals do not fall into the excavation and that the means of access into the hole are safe.

Even with the precautions described above, there will almost certainly be some disturbance to hydraulic conditions close to the pit wall and so tensiometers should be inserted at least 1 m into the soil. A simple jig can be constructed to ensure that the pilot holes for the tensiometers are bored at the correct angle. Even so, there will be some uncertainty about the exact depth of the porous cups, especially if making a clean hole in the soil is difficult.

12.12.2 Portable tensiometers in separate boreholes

Strebel *et al.* (1973) and Hubbell and Sisson (1996) described the use of a portable tensiometer that was put into the bottom of a series of boreholes of different depth, allowed to equilibrate with the formation and then read. These

tensiometers may take advantage of boreholes drilled for other purposes. Both sets of workers used a tensiometer with attached pressure transducer mounted close to the cup. A cable was connected to a reader on the ground surface to monitor the approach to a steady reading. Strebel *et al.* (1973) reported that this took between 15 minutes and 2 1/2 hours. Hubbell and Sisson (1996) found that 40 hours were required in some cases.

Hubbell and Sisson (1996) also described a tensiometer consisting of only a porous cup, body tube and air trap closed by a rubber septum, similar to that depicted in Fig. 12.12. This could be lowered down a borehole on a cord, left to equilibrate and then removed from the ground and a reading made immediately with a puncture tensiometer reader. Hubbell and Sisson (1996) found that retrieval over 9 minutes caused a change of less than 50 mm water head in the reading. The advantage of this device is that the parts of the tensiometer are all very cheap, which is an advantage when working on engineering sites where delicate instruments may be damaged easily.

Unless the tensiometer is located close to a water table that fluctuates rapidly, it is probable that variation of water potential at depths of more than a few metres takes place on a timescale of days or weeks, rather than minutes or hours, so that infrequent measurements and long equilibration times are not a disadvantage if other tasks can be performed while waiting for the tensiometer to reach a stable reading.

Hubbell and Sisson (1996) pointed out that the tensiometer cup is likely to have only a small surface area in contact with the formation, which slows its response.

Multiple depths could be monitored with one of these types of tensiometer from a single large-diameter borehole by using smaller diameter pipes terminating in repacked material at different depths in a similar manner to that described in the next section.

12.12.3 Semi-permanent tensiometers capable of being serviced in situ

For long-term monitoring and for those sites where water potential changes rapidly even at great depth, permanently or semi-permanently installed tensiometers may be the only answer. Where water tables fluctuate rapidly, perched water tables may form or bypass flow is important, such installations can reveal behaviour, which may be completely unsuspected if only weekly or more infrequent measurements are made. Tensiometers act as piezometers if they are below the water table, provided that the sensor and logging arrangements are set up to record positive pressures.

Arrangements for servicing of tensiometers at depths in excess of 6 m below ground, which is close to the practical limit for more conventional purgeable tensiometers, are a challenge, but two solutions have been adopted by different research groups. If matric potential is not expected to go below about –4 m water head, which is often the case in temperate and humid climates, then a sealed tensiometer, filled with carefully de-aired water, may operate without problems for several years. However, the lower the potential falls, the more often that refilling becomes necessary. Removal and replacement of tensiometers at depths in excess of 10 m is a significant undertaking and the attractiveness of a solution that does not require frequent removal of the instruments increases.

The 'advanced tensiometer'

Hubbell and Sisson (1998) devised an 'advanced tensiometer', shown in Fig. 12.9c and described briefly in Section 12.5.4, which can be refilled from a water reservoir around the transducer by raising the transducer from its seating. The solution is ingenious and appears to work well. The depth limitation is not known, but Hubbell *et al.* (2004) reported that they had been installed successfully at a depth of 145 m. The principal limitation is, presumably, the increasing weight of the support for the transducer as it gets longer. The water in the reservoir may be present for extended periods and so will have an opportunity to dissolve a significant amount of air, although a simple adaptation could probably be devised to drain it before replenishment with de-aired water, albeit that the water will be released into the matrix surrounding the tensiometer cup, which may then need a few days for the tensiometer to recover.

Installation of the advanced tensiometer should, ideally, be into a snugly fitting hole at the bottom of a borehole. This is difficult, if not impossible, to achieve at depth and so the best solution is probably to use sieved native material from the appropriate depth (or failing that, silica flour or other fine material that will ensure good hydraulic contact with the surrounding formation) tamped down around the cup after placing it resting on the bottom of the hole. In some cases, it may be more desirable to use a slurry of the material, introduced to the bottom of the borehole *via* a tremmy pipe. McElroy and Hubbell (2004) and Hubbell *et al.* (2004) found that the tensiometer equilibrated much faster with its surroundings when using a slurry than when dry material was used to embed the tensiometer.

The advanced tensiometer requires embedding in the formation at the bottom of a borehole. However, a large-diameter borehole may be used to accommodate several tensiometers as shown in Fig. 12.32 The formation must be sufficiently competent to stand up for a few hours or days between drilling the hole and installation of the tensiometers. A borehole casing should be installed to finish above the depth of the shallowest tensiometer. Each tensiometer is installed inside its own sleeving tube and embedded in sieved and repacked material from the formation (or, if this is not possible, in material no coarser than that of the formation). Most of the space between the tensiometers is filled with this same material, but there should also be a 200-mm thick layer of bentonite or bentonite-rich concrete to prevent preferential vertical movement of water through the repacked soil. McElroy and Hubbell (2004) used bentonite pellets to produce an isolating layer

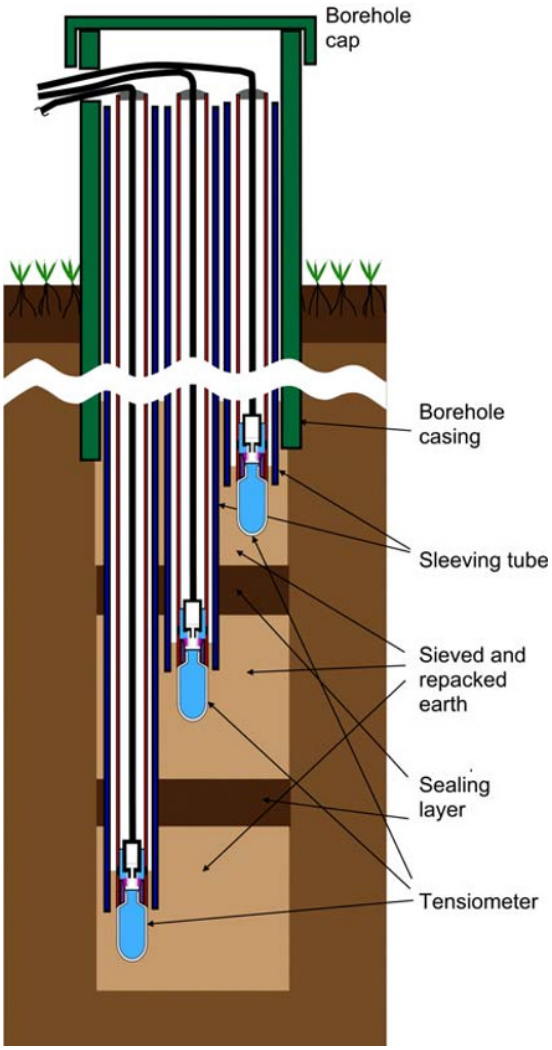

Fig. 12.32 Arrangement for installation of several embedded tensiometers in one borehole. (*See insert for colour representation of the figure.*)

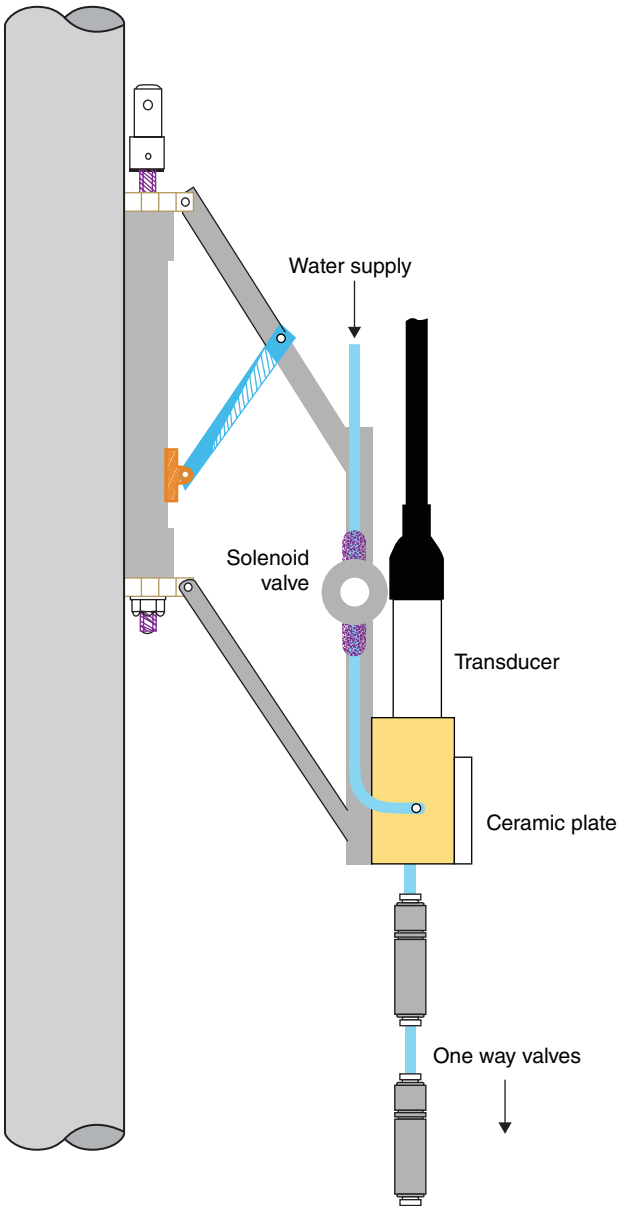

Fig. 12.33 Schematic diagram of a borehole tensiometer and jack. Drawing by A. C. Warwick. © NERC (Centre for Ecology & Hydrology). Reproduced with permission.

and, in some cases, incorporated thin layers of bentonite pellets in the intervening fill in addition.

The 'borehole tensiometer'

Cooper (1980) and Wellings (1984a) described a tensiometer that allowed multiple instruments to be installed inside an open, unlined borehole. This version was not capable of being serviced *in situ* but had to be removed, refilled and reinstalled. A modified design was used by Rutter *et al.* (2012), which could be purged without removal from the ground. The essential features of this tensiometer are shown in Fig. 12.33.

The tensiometer itself uses a conventional pressure transducer mounted onto a hollow brass block and sealed by an 'O'-ring. One face of the block is open and has a ceramic plate, with air entry value greater than 10 m of water, bonded to it to act as the porous barrier. De-aired water is admitted to the space inside the block by a flexible plastic pipe from the ground surface controlled by a solenoid-operated valve. The valve is normally closed but can be opened by applying 12 V from a small battery at the surface. A small diameter pipe runs vertically inside the block from about 1 mm below the transducer diaphragm and out through the bottom of the brass block. Two small check valves allow air and water to run out of the block from its highest point but prevent any leakage back into the tensiometer. Two check valves are used in case one fails.

Connecting a reservoir of de-aired water to the supply pipe and opening the solenoid valve purges the tensiometer. Water runs into the lower part of the chamber and out from

the top through the check valves. Closing the solenoid valve by removing the electrical supply seals the system.

The tensiometer is mounted on a sectional aluminium pole *via* a small screw jack, which is welded to the pole on one side and screwed to the tensiometer on the other. An operating rod, which extends to the surface, is fixed to the upper end of the jack's screw allowing it to be operated from the ground. Several (up to about 12) tensiometers may be mounted at different places on the support pole, limited by the space for control rods and cables.

It is possible to handle a section of mast up to about 5 m at a time. Sections are joined using a socket welded to the upper end of the mast and a pin to secure the two sections together held in place by a hose clip. Sections of operating rod are made from 12-mm diameter aluminium tube and joined by plastic ferrules secured by self-tapping screws. The cables and plastic supply pipes are in one continuous length.

A steel frame is used to suspend the mast during and after installation. It also acts as a reference level for the assembly. The frame is supported by the top of the borehole casing and has a slot, which allows the mast to fit into it, while the weight of the assembly is borne by the socket of the topmost section.

Installation of the system is by retracting all jacks, mounting the tensiometers onto them and lowering the mast into the borehole, section by section. The lowest mast section has a rope firmly attached to lower the assembly and as a precaution against losing it down the borehole. Mast and operating rod sections are joined together, keeping a careful note of which operating rod is attached to which tensiometer. When all tensiometers are at the desired location, the rope is tied off, and each tensiometer in turn is screwed out on its jack until the ceramic plate is pressed firmly against the borehole wall. Two or three jacks are usually sufficient to support the weight of the entire assembly. The number of turns of the operating rod until each tensiometer is pressed against the wall should be recorded, so that on removal, operators know when a jack is fully retracted. The operating rod should be turned sufficiently to ensure good contact with the formation, but excessive force risks breaking the ceramic plate. A cap is placed on the borehole and locked into position.

By this means, measurements of water potential have been made at a number of sites, mainly in chalk formations, to a depth of more than 60 m. By adjusting the length and arrangement of the arms of the jack, different sizes of borehole diameter can be accommodated, with 150 mm being about the smallest. The hollow pole allows for a water level monitor to be lowered to measure water table depth and/or for a neutron probe to be used to measure water content changes. Additionally, other sensors (e.g. gypsum blocks (Wellings, 1984a), temperature or electrical conductivity sensors) may be attached to the brass housing.

As described, the borehole tensiometer requires a competent formation, which does not collapse into the borehole. A steel casing is usually used to support the upper part of the borehole and tensiometers used only below this. Where there is a risk of collapse in the depth range where potential measurements are required, the tensiometers are mounted on the inside of a plastic borehole casing. Windows cut in the side of the casing opposite the tensiometers allow the porous tensiometer face to contact the borehole wall when it is jacked out.

Deep water potential measurements under arable cultivation

Ploughing, planting, spraying and harvesting operations are a challenge for any soil observation programme requiring sensors permanently or semi-permanently installed in the ground. Ireson *et al*. (2006) overcame the problem for instruments inside a borehole by using borehole casing, which terminated in a flange 300 mm below ground surface, comfortably below plough depth. A section of similar casing, 300 mm long, with a flange at each end, could be bolted to this, extending the casing to ground level. For ploughing and planting operations, this upper section was removed and a steel cap bolted to the lower flange. After planting, the borehole was located by surveying methods, although careful measurement or a metal detector may work equally well, a hole dug to the top of the casing and the upper casing section fitted onto it. With the steel cap at or just below ground level, all farming operations including harvesting could be undertaken without disturbance or damage to either borehole or machinery until ploughing was next due. If a sufficiently low-power logger is available that fits inside the borehole, no interruption to data acquisition need occur while the borehole casing is capped off below ground level, although no servicing of the tensiometers is possible. Although there is considerable local disturbance to the soil and crop around the borehole, this is of little consequence as the system is designed for measurements only at depths greater than 3 m.

Appendix 12.A Pressure Transducers

A pressure transducer is a device that converts pressure variations into electrical signals. There are many different types, all with different advantages and disadvantages. The measurement of water pressure inside a tensiometer is not a particularly challenging application, and hence cheap transducers are quite adequate. The main limitation is that good accuracy needs to be maintained over a range from close to zero (or sometimes positive) to approaching –10 m water. This requires good *linearity* (i.e. the response should be very close to a straight line relationship between pressure and output) and very low hysteresis.

The most common type of transducer has a thin diaphragm, which distorts as the pressure across it changes, as shown in Fig. 12.34. The diaphragm may be made of nickel, stainless steel, silicon or ceramic. The small movement of the diaphragm is detected by a *strain gauge*. This is a device that changes its electrical resistance according to the movement or *strain* of the diaphragm. It may be

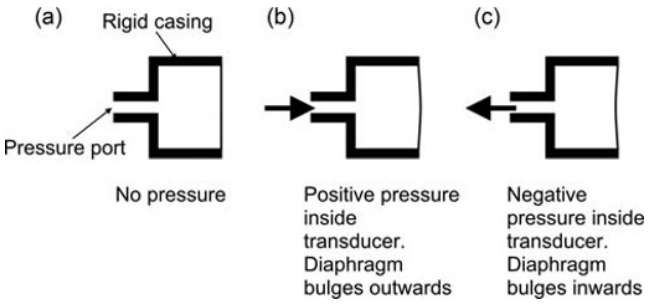

Fig. 12.34 Distortion of pressure transducer diaphragm by a pressure difference.

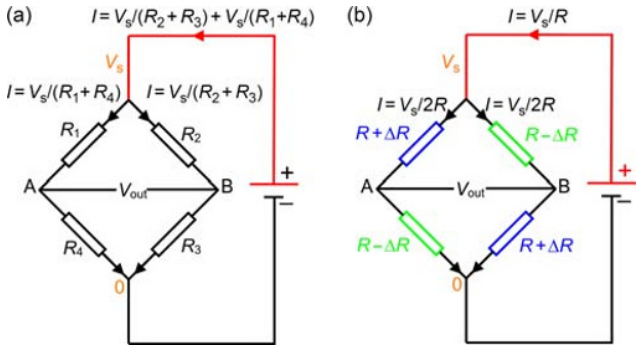

Fig. 12.35 Schematic bridge circuit. V_{out} is zero when $R_1/R_4 = R_2/R_3$ in (a). (b) Shows the arrangement in a strain gauge where opposite arms of the bridge change in the same direction.

coupled mechanically to the diaphragm, bonded to it or form part of the diaphragm itself. The most common forms in use for tensiometers have silicon diaphragms with resistors diffused into them. These change their resistance as the diaphragm distorts by the *piezoresistive effect*. Usually, there are four resistors, normally of a few kohm value, arranged such that two increase their resistance and two decrease it with movement of the diaphragm. They are wired together in a bridge arrangement, as shown in Fig. 12.35, with opposite sides of the bridge changing in the same direction. A voltage, V_s, of usually a few volts is applied across two opposite corners of the bridge, and the voltage, V_{out}, measured across the other two corners is the signal. In the ideal case, the resistors have values such that there is no output voltage when there is no distortion of the diaphragm. This is the situation in the well-known Wheatstone bridge, where the output voltage is zero when

$$\frac{R_1}{R_4} = \frac{R_2}{R_3}. \tag{12.A.1}$$

In the simplest case, all four resistors are of equal value, R. If, on application of pressure, the distortion of the diaphragm causes R_1 and R_3 to increase by an amount ΔR and R_2 and R_4 to decrease by the same amount, then the situation will be as shown in Fig. 12.35b. The current in each arm of the bridge, I, is

$$I = \frac{V_s}{2R}, \tag{12.A.2}$$

and so the voltage at point A will be

$$V_A = V_s - \frac{V_s}{2R}(R + \Delta R), \tag{12.A.3}$$

and that at point B is

$$V_B = V_s - \frac{V_s}{2R}(R - \Delta R). \tag{12.A.4}$$

So the output voltage, V_{out}, is

$$V_{out} = V_B - V_A = \frac{\Delta R}{R} V_s. \tag{12.A.5}$$

The output voltage, therefore, is proportional to the fractional change in resistance of each arm of the bridge.

So if the diaphragm distorts by an amount proportional to the pressure difference across it and the resistance of the arms of the bridge change proportional to the strain of the diaphragm, then the bridge output voltage will be proportional to the applied pressure. Provided that the strain of the diaphragm is small compared with its size and the change in resistance of the bridge resistors is small compared with their value, this will usually be the case to a very good approximation.

In the ideal case, a bridge circuit is inherently insensitive to temperature changes, as we expect the temperature coefficient of all the resistors to be the same, so that the ratios will be unaltered.

In practice, there will always be some difference in the values of the bridge resistors, and the temperature coefficients may not be quite identical. Commercially available transducers usually incorporate some additional resistors to ensure that the bridge is balanced when there is no pressure difference across the diaphragm and to compensate for any residual temperature sensitivity.

Transducers commonly found in tensiometers are available with three kinds of output:

1 Millivolt output. This is the simplest and results in the cheapest transducers. The transducer output is the output from the strain gauge bridge, possibly modified slightly by resistors incorporated to balance the bridge and provide temperature compensation. This type of transducer is typically energised by a source voltage of 10 V, and the output at the maximum design pressure is 100 mV (1% of the supply voltage).

Because the bridge circuit is simply a set of resistors, the output is directly proportional to the supply voltage. These transducers can, therefore, be operated from a wide range of supply voltages, and if the output voltage is divided by that of the supply, the same result will be obtained. For this reason, the output from this kind of transducer is often quoted as millivolt per volt (i.e. the number of millivolts output at

the full range of the transducer divided by the supply in volts. In the example given previously, the output would be 10 mV V^{-1} (100 mV divided by 10 V). It is, of course, wise not to exceed the manufacturer's recommended maximum supply voltage.

Although simple and economic, there are several drawbacks to the use of simple resistance bridges, which can, with care in design, installation and operation, be overcome.

- Fluctuations in supply voltage will reflect proportionally in the output of the transducer. A 5% change in the supply voltage will cause a 5% change in the transducer output and therefore produce a 5% error in the pressure measurement. Some data loggers can provide a standard voltage output and automatically register readings in millivolt per volt. If this is not the case, or if manual readings are being made, the supply voltage must be measured at the same time as the output.
- Long cable lengths reduce both the supply voltage as seen at the bridge terminals and the output voltage at the measuring point. This is because there is always some current flow necessary both to supply the device and in the measuring circuit. If each bridge arm is 2 kΩ, the bridge as a whole presents a resistance to the supply of 2 kΩ, and if the supply voltage is 10 V, the current drawn through the supply cables will be 5 mA. If the resistance of the cable is 5 Ω, the voltage drop in the cable is 25 mV and so the voltage at the terminals of the bridge will be 9.975 V. This is not serious but would correspond to 250-mm water pressure at the theoretical limit of the tensiometer.

In the same way that the input impedance of the transducer is equal to the value of the bridge resistors, the output impedance is also equal to the same value, that is, 2 kΩ in our example. A typical input impedance of a data logger would be 10 MΩ. An additional 5 Ω of resistance in this circuit would represent a negligible reduction in voltage at the logger terminals. The 2 kΩ output impedance would also create a very small reduction (~0.02%) in voltage measured at the logger. By making the resistors non-equal, but preserving the ratios given by Equation 12.A.1, the input and output impedance of the bridge can also be made non-equal.

- A more serious problem is likely to be caused by stray resistances across the connections in the system. The most likely source of these is damp, which can cause partial shorting of the bridge resistors. This may be across the logger terminals, at various cable connection points or inside the transducer. The source of the damp may be condensation, rainwater or from contact with the ground.

As an example, a stray 1 MΩ pathway across one of the bridge resistors, say R_1 in Fig. 12.35, will reduce its resistance by 4 Ω and reduce the output voltage by $V_s/2000$ or 0.5 mV V^{-1}. Since the full-scale output of the transducer is only in the region of 10 mV V^{-1}, this represents 5% of the full range, which is usually 10 m water. That is, the error is 0.5 m water equivalent to a pressure of 50 hPa. Damp problems usually vary considerably over time, dependent on atmospheric humidity, temperature and contamination by solutes. This illustration highlights the necessity for rigorous attention to making sure that there are a minimum number of electrical connections, that all connections that exist are completely watertight and that drying agents (e.g. silica gel) and humidity indicators are used to ensure that any residual humidity in the system is removed and monitored.

2 Voltage output. This type of transducer incorporates an amplifier to boost the output voltage. Because the amplifier is very close to the bridge resistors, the electrical connections can be sealed from the external environment. The amplifier also has a much lower output impedance than the resistor bridge, making the device even more resistant to damp and other problems. The penalty for this robustness is in additional cost and power consumption.

3 Current output. Where long cable runs and difficult environmental conditions are encountered, the answer in many industrial applications is to use transducers that give an output of electrical current in the range of 4–20 mA. These are extremely insensitive to poor connections, but there is a large penalty in cost (partly because of rugged construction) and power consumption. The housings are often large, making use in many environmental field applications impractical. For these reasons, most environmental scientists use either millivolt or voltage output transducers.

As well as a choice of the kind of output, there are three principal mechanical constructions of transducer available:

- *Gauge* transducers measure the pressure relative to local atmospheric pressure. To do this, they must have a *vent* to transmit the atmospheric pressure to the back of the transducer diaphragm. This may be a separate tube, usually strapped to the electrical connection cable, a tube incorporated into the cable sheath or may simply make use of the cable sheath itself as a pathway for air from the transducer to the outside. Because of the need to ensure that there is no potential for damp ingress into the electrical connections, there needs to be a clear, dry path for the atmosphere to communicate with the rear of the diaphragm. For this reason, it is recommended that only transducers using a separate vent tube, whether incorporated into the cable or outside it, are used. An occasional problem attending this type of transducer is blockage of the vent pipe, usually by a kink where the cable bends at a tight angle.

Gauge transducers are available with a *pressure port* (see Fig. 12.34) to connect the instrument to the fluid whose pressure is to be measured or, sometimes, with a *flush diaphragm*, which is preferred for tensiometer use, as it is possible, by careful design, to remove all air from the instrument during purging.

- *Differential* transducers are similar to gauge transducers but are made to measure the difference in pressure between two fluids. They usually incorporate an additional port to connect the second fluid on the other side of the diaphragm from the first one. Differential transducers can be used as gauge instruments by connecting a vent pipe to the second port.

• *Absolute* transducers, as the name suggests, measure the absolute pressure of the fluid on one side of the diaphragm. The other side is a small, evacuated and sealed chamber so that the instrument always measures the pressure relative to a vacuum. In almost all cases, we are interested in knowing the matric potential relative to the local atmospheric pressure. To use such transducers in a tensiometer, therefore, the local atmospheric pressure must be monitored. This requires an extra absolute transducer to be monitored and extra calculations to convert the readings to gauge referenced. This can introduce a small amount of extra uncertainty into the measurements. Fortunately, one such reference transducer can be used for many tensiometers. Spatial variations of air pressure are usually such that provided that all tensiometers are within about 1 km of the reference transducer, there is negligible difference in atmospheric pressure from place to place.
Sealing the side of the diaphragm that has the strain gauge attached means that there is no risk of moisture or contamination in this part of the system and no need to provide a vent. Precautions against moisture ingress to connections along the cable or at the logger, however, are still vital.

Absolute transducers may have a pressure port or flush diaphragm.

• A means whereby one pressure transducer could be connected sequentially to several tensiometers has been used by several groups (e.g. Rice, 1975; Blackwell & Elsworth, 1980). The setup used a multi-port valve (known commercially as a Scanivalve) arranged similarly to a rotary electrical switch. It was capable of being moved automatically from one position to the next using a stepper motor, stopping for a few minutes at each position to allow pressure equilibration. The complexity of the system and the availability of cheap pressure transducers and multichannel field data loggers mean that it is now more economical to use a separate transducer for each tensiometer.

Fig. 12.36 Collapsible plastic container for storing de-aired water. A check valve is attached to the end of the plastic tube to prevent air from being sucked into the bottle.

Appendix 12.B De-aired Water

Tensiometers require de-aired water for their operation. If a large number of them are being used, several litres may be needed, particularly when first filling them. In hard water areas, a scale of calcium carbonate is likely to form inside the tensiometer, which may affect seals and so hard water should be avoided in favour of deionised or distilled water. Most laboratories have a supply of deionised water at low cost. In most other cases, tap, stream or borehole water is quite suitable.

12.B.1 Boiling

The simplest way to produce de-aired water is to boil it for several minutes. After boiling, it must be cooled out of contact with the air until it reaches room temperature. Most laboratory glassware is unsuitable as it is not designed for vacuum use. Boiled water in a sealed container develops a considerable vacuum. Buchner flasks are suitable and have a sidearm, which can be sealed off with a flexible rubber or plastic tube and a clamp or tap. The water may be boiled in the flask, eliminating any problem of air becoming entrained during transfer. These flasks are relatively expensive and develop cracks around the bottom as a consequence of repeated heating and cooling, necessitating periodical replacement.

A convenient method for boiling and storing water is the use of collapsible plastic storage containers as shown in Fig. 12.36. Water is prepared by filling the bottle and using a small immersible electric heater to boil the water. Care is needed to prevent the heater contacting the plastic side of the bottle and melting it or even causing a small fire! After boiling for a few minutes, the bottle is sealed with a cap while collapsing the bottle slightly to squeeze out all of the air. Beware a risk of scalding during this process. Cooling can be promoted by immersing the bottle(s) in a large basin of cold water. The system can be refined by fixing a flexible plastic tube to the cap of the bottle, which has a

check valve inline. This makes squeezing the air out of the bottle safer, allows the water to be partially emptied without letting air in and can be attached directly to some tensiometers, without removal of the cap, thereby preventing any contact with the air.

12.B.2 De-airing under vacuum

If pressure is reduced sufficiently, then water boils at room temperature. It should come as no surprise, therefore, that reducing the pressure also removes air from the water. Commercial de-airing units are available from geotechnical equipment suppliers. These consist of a sealed vessel to hold the water, a vacuum pump and, usually, a spray nozzle to introduce water into the vessel as shown in Fig. 12.37. Injecting the water *via* the spray nozzle increases the surface area and rate of transfer of dissolved air to its surroundings.

12.B.3 De-airing small quantities of water

If only a small quantity of water is required, use can be made of the fact that reducing pressure will cause air to come out of solution. By pulling on the plunger of a syringe, about half full of water, with a closed tap fitted to its outlet, a vacuum can be created effectively. Doing this two or three times produces a small quantity of de-aired water suitable for purging one or two tensiometers, without requiring other special equipment.

12.B.4 Membrane contactors

Some types of plastic membrane are permeable to gases but not to liquid water. A vacuum on one side of the membrane, with water on the other side will, therefore, extract air from the water (along with water vapour). To do this, the membrane must be hydrophobic, similar to that used in waterproof garments described as 'breathable'. The efficiency of the process depends on mixing of the water, the surface area of membrane in contact with the water and the permeability of the membrane to gases. To maximise the surface area, commercial equipment uses hollow fibres of hydrophobic material such as polypropylene, with a vacuum applied inside the fibre and water flowing outside. More details are given by Wiessler (1996) and Wiessler and Sodaro (1996) and references therein. These contactors are capable of reducing the air concentration in water to a few parts per billion, well below that required for tensiometers. The principal advantage is that it is a continuous process, rather than a batch one, as is the case for the other methods described.

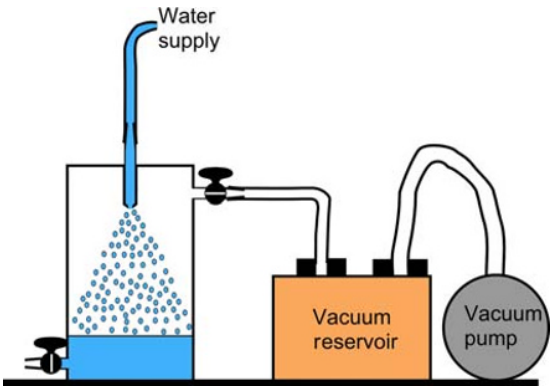

Fig. 12.37 Schematic of a vacuum de-airing unit.

13 Indirect Methods of Water Potential Measurement

13.1 Introduction

Indirect methods of measuring water potential rely on measuring the water content of a material whose water potential is in equilibrium with that of the soil. This measurement of water content is usually in itself indirect, and several different methods are used to provide the water content estimate.

The methods therefore rely on two sets of relations:

1 The relationship between matric potential and the water content of the material. The accuracy of this part of the measurement is therefore subject to three factors:

(i) The uniformity of the water content – potential relationship between different samples of the material,

(ii) The stability of this relationship over time, when buried in the soil and

(iii) Hysteresis in this relationship, which means that even if the material's water content is known accurately, the water potential is not a unique function of this quantity;

2 The relationship between the water content of the material and the property used to measure it. Three classes of method are used to make this measurement – electrical resistance, dielectric methods and heat dissipation. Electrical resistance and (to a lesser extent) dielectric methods are subject to uncertainties caused by variations in the solute concentration of the soil water. Gypsum blocks are also subject to chemical changes over time, which affects both the water release characteristic and the electrical conductivity. The filter paper method does not rely on an indirect measurement of water content.

Tensiometers are simple, capable of very good accuracy, at least above – 5 m water potential, and economical. Indirect methods, which are inherently much less accurate for the reasons just described, are therefore used mainly for the lower potential ranges and where a single sensor is required to cover the complete range of potential at a site.

13.2 Resistance Block

Resistance blocks are, historically, the best established type of indirect method for measurement of soil water potential. They were also used as an indicator of soil water content before the advent of neutron probes. Resistance blocks are very much cheaper than most water content sensors, however, and so they continue to be used in some low-budget applications. The basic principle of operation means that the primary measurement is of matric potential, and so its use for estimation of water content involves yet another indirect relationship. If the hysteresis characteristics of the block and soil, however, match approximately, then block measurements may be a reasonable surrogate for water content, provided that a suitable calibration curve is available.

13.2.1 Principles

The principle of measurement of a resistance block is quite simple. A porous block is embedded in the soil and its water content changes until it reaches equilibrium with the soil matric potential. This change in water content changes the electrical resistance of the block, and so a calibration between block resistance and water potential can be established. As mentioned earlier, this depends not only on the block's water content, but also on its solute concentration. However, if the solution inside the block is saturated with an electrolyte, the electrical conductivity of the solution is relatively insensitive to the invasion of salts from the soil. Gypsum (plaster of Paris) has been found to be very suitable for this.

Blocks may be made simply by embedding two parallel metal rods in a block of porous material, as shown in Fig. 13.1a. This arrangement may, however, be subject to influences outside the block and the reading is weighted disproportionately to the region very close to the rods. A better arrangement, therefore, is as shown in Fig. 13.1b, where a coaxial arrangement confines the electric field

Soil Water Measurement: A Practical Handbook, First Edition. J. David Cooper.

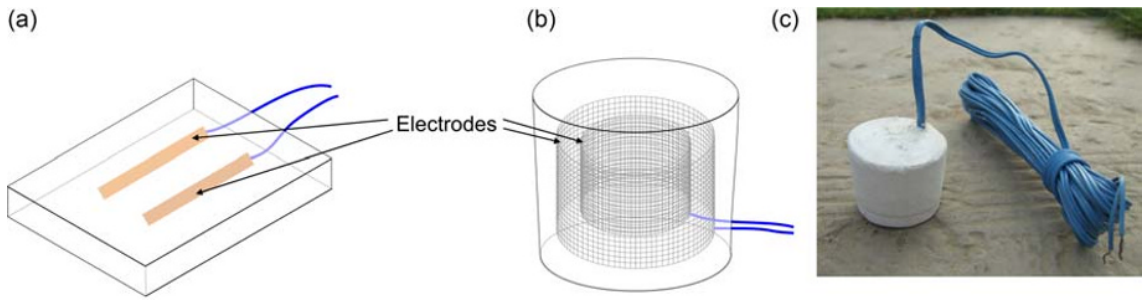

Fig. 13.1 Construction of gypsum resistance blocks. (a) Original design of Bouyoucos and Mick (1940) with parallel electrodes. (b) Coaxial electrode design. (c) Photo of coaxial block.

better within the space between the electrodes. If the diameter of the inner conductor is not too small, the distribution of the electric field and, hence, the volume contributing to the reading is reasonably uniform.

Application of a dc voltage to the resistance block electrodes causes the positive and negative ions in the solution to migrate in opposite directions, leading to a build-up of charge on the electrodes, which opposes the voltage applied to them. This process is known as *polarisation*. This results in the current gradually falling, leading to an apparent increase in resistance of the block. To counter this effect, the voltage applied to the electrodes should be reversed periodically by using an ac voltage of frequency around 1 kHz. Too high a current can cause bubbling inside the block by electrolysis, so the applied voltage should be kept below 1 V.

If several blocks are installed in the soil and they are all energised at the same time, there will be an electrical connection between them through the ground. This affects the readings, and so they should be isolated from one another during reading.

Resistance blocks are also temperature sensitive because the electrical conductivity of the electrolyte solution varies with temperature and there is a smaller temperature effect on the block's soil water characteristic.

13.2.2 Gypsum blocks

Resistance blocks are usually based on gypsum (calcium sulphate, also known as plaster of Paris). They were introduced by Bouyoucos and Mick (1940), who discovered that the saturated calcium environment buffered electrolytes in the soil solution, reducing the sensitivity of the block's electrical resistance to variations in the soil solution. Numerous improvements to the basic gypsum block have been made over the years (e.g. Bouyoucos, 1953; Perrier & Marsh, 1958; Cannell & Asbell, 1964; Fourt & Hinson, 1970).

One of the major problems is slow dissolution of the gypsum in the soil solution, leading to changes in both the soil water characteristic of the block and its electrical conductivity. This occurs much more rapidly in acid soils than alkaline ones. Attempts to improve the stability of block characteristics over time have met limited success. These include embedding a nylon or glass fibre fabric matrix in the block (Perrier & Marsh, 1958) and mixing inert material with the gypsum powder (Scholl, 1978).

The soil water characteristic of the blocks can be manipulated by using different size powder in their manufacture as well as changing the powder/water ratio. It follows that these parameters must be strictly controlled during manufacture if consistency of performance is to be maintained.

Under favourable conditions, with individually calibrated blocks, in a calcium-saturated environment and within 2 years of installation, accuracy of matric potential measurement is in the region of 10–20% in the range down to about –50 m water, becoming somewhat worse at lower water potentials (Wellings & Bell, 1980; Wellings *et al.*, 1985).

Despite problems of relatively coarse sensitivity, hysteresis and stability over time, gypsum blocks remain one of the most popular methods for monitoring water potential, particularly where the matric potential falls below –5 m water and below. This can be attributed to their low purchase cost, the ability to make them in the laboratory, ease of installation and ease of reading using simple equipment.

13.2.3 Watermark

The Watermark sensor, manufactured by the Irrometer Company in Riverside, California, is a development of the gypsum block. The gypsum porous matrix is replaced by a proprietary inert granular porous material in which two concentric electrodes are embedded. The granules are retained inside a hydrophilic fibre wrapping within a perforated stainless steel casing. A gypsum wafer inside the sensor buffers the soil solution. The quoted range of the sensor is 0 to –239 kPa (0 to –24.3 m water), although Irmak and Haman (2001) found it to be insensitive to matric potential changes in the range 0 to –1 m water. Electronics within the sensor convert a dc applied voltage to ac and the signal is converted back again to dc. Electronics within the reader unit also apply temperature compensation. Solutions are available to allow this compensation to be applied when connected to many popular environmental data loggers.

Fig. 13.2 Watermark sensor. Reproduced with permission from Irrometer Company, Inc.

Fig. 13.3 Equitensiometer. Image courtesy of Delta-T Devices Ltd.

A wide range of calibration curves has been reported for these sensors. These appear to depend, at least partly, on the type of soil in which they are embedded. For this reason, it is recommended that sensors be calibrated embedded in the soil in which they will be used. In coarse soil, contact with the sensor may be a problem, probably because of the presence of the stainless steel casing and/or fibre wrapping.

Watermark sensors are economical and available from a large number of distributors worldwide. There is also a choice between a simple resistance measurement (Model 200SS) and voltage output (Model 200SS-V), the latter incorporating temperature compensation. Their dimensions are 22 mm diameter and 83 mm long (sensing length about 75 mm). See Fig. 13.2.

13.3 Equitensiometer

The Equitensiometer, manufactured by Delta-T Devices in England, also uses a proprietary granular porous material as the porous matrix, but its water content is measured by a Theta Probe (see Section 8.8) whose electrodes are buried in the porous material. No buffering is employed, as the Theta Probe is much less sensitive to salinity effects than electrical resistance.

Each Equitensiometer comes with an individual calibration. This is provided in the form of tabulated values and a polynomial expression. Ireson *et al.* (2006) found that a form similar to that used by van Genuchten (1980) to describe the water retention curve provided a better fit to the data. Since the Theta Probe provides a reading approximately proportional to water content, this seems reasonable. The van Genuchten relation is, in any case, an empirical one, selected to have a flexible form, easily manipulated mathematically and displaying the 'S' shape usually observed in experimental data.

The Equitensiometer is 40 mm in diameter and 210 mm long, with a sensing length of 68 mm. The rest of the instrument length is accounted for by the Theta Probe body. Figure 13.3 is a photograph of an Equitensiometer. The manufacturers quote a measurement range of 0 to –1000 kPa (0 to –100 m water). Accuracy is stated as ±10 kPa (±1 m water) in the range 0 to –100 kPa (0 to –10 m water) and ±10% below –10 m water. However, the calibrations are made on a drying curve and the porous matrix is subject to hysteresis. The uncertainty resulting from this is stated as ±20 kPa (2 m water). This is consistent with data presented by Ireson *et al.* (2006).

13.4 Heat Dissipation Blocks

Heat dissipation blocks were first introduced by Phene *et al.* (1971a, b). Their device used a germanium P–N junction diode to sense the temperature, wrapped in 2 m of constantan heater wire and embedded in a ceramic block about 30 mm diameter and 40 mm length. This approximated a point heat source and detector. Later sensors, described by Reece (1996), used a line heat source and a thermocouple sensor, which allowed the ceramic block to be reduced in size to 15 mm diameter and 30 mm length, although the entire device is 60 mm long. This device is marketed by Campbell Scientific Inc. as the Model 229 (see Figs. 13.4 and 13.5).

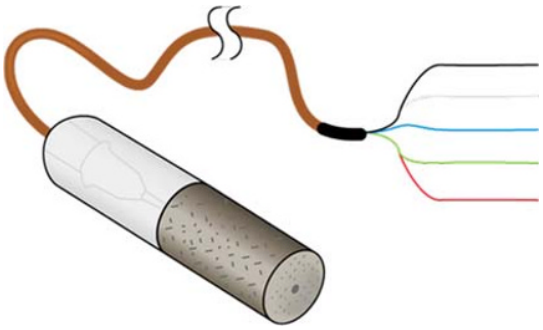

Fig. 13.4 Campbell CS229 heat dissipation matric potential sensor. The ceramic block is the grey-coloured cylinder in the foreground. Reproduced with permission from Campbell Scientific, Inc.

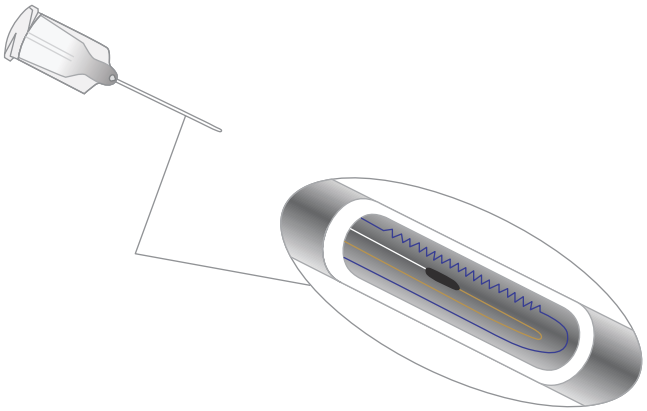

Fig. 13.5 Internal construction of the CS229 heat dissipation sensor, showing the heater wire and thermocouple mounted inside a hypodermic needle, which is placed at the centre of the ceramic block. After inserting the heater and thermistor, the needle is filled with heat-conducting epoxy. Reproduced with permission from Campbell Scientific, Inc.

For this configuration, the temperature rise at the centre of the block, ΔT, at a time, t, after switching on the heater is given by (Flint *et al.*, 2002a):

$$\Delta T = \frac{q}{4\pi k} \ln t, \qquad (13.4.1)$$

where q is the rate of heat input per unit length of the line source and

k is the thermal conductivity of the block.

The method of measurement is closely related to the methods described in Chapter 10 for dual-probe heat-pulse water content measurement. However, in this case, the heater and temperature sensor are both inside a single needle, embedded in a porous ceramic block, and the heating period is longer (about 30 s), the measurement being taken at the end. Note also that the temperature rise is related in this case to the thermal conductivity of the block material and not to the volumetric specific heat.

In use, the heater is turned on for a few seconds and the temperature rise recorded after this time. The rate of temperature rise is determined by the balance between heat supplied by the heater and the rate at which it is conducted away. The higher the water content of the block, the faster heat is conducted through the ceramic and there is a smaller temperature rise when the water content is high than when it is low. Also, as time goes on, the system begins to approach a steady state, and so the rate at which the temperature rises will slow. This is illustrated in Fig. 13.6.

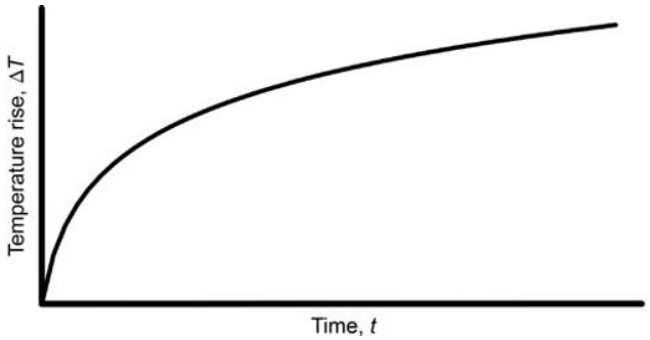

Fig. 13.6 Temperature rise of a heat dissipation block, according to Equation 13.4.1.

Heat dissipation blocks are subject to the same hysteresis problems as other porous matrix sensors. They are not, however, sensitive to solute concentration since this has a negligible effect upon the thermal properties of water. They are, however, sensitive to ambient pressure, which is important for calibration in a pressure plate apparatus (see Section 13.5), and temperature. These both arise mainly as a result of vapour flow induced by the temperature gradient produced by the heater (Flint *et al.*, 2002a). The Campbell Scientific Manual (Campbell Scientific, 2009) shows graphs implying a change in calibration slope of about 30% over a 10°C change in temperature, so that soil temperature using the thermistor in the block must be recorded.

The recommended measurement sequence is (Campbell Scientific, 2009):

1 Measure the temperature of the sensor.

2 Turn on the heater. A heater current of 50 mA is recommended, providing an input of 1.7 W to the ceramic.

3 Measure the temperature after 1 second of heating. Using this value as the starting point for measuring the temperature rise leads to more stable results (Flint *et al.*, 2002a; Campbell Scientific, 2009).

4 Measure the temperature after a further 29 seconds.Turn off the heater.

The water potential is calculated using an empirical calibration equation. Equation 13.4.2 has been found suitable:

$$\psi_m = -e^{(\alpha \Delta T + \beta)}, \qquad (13.4.2)$$

where

ΔT is the temperature rise between 1 and 30 s after turning on the heater and

α and β are empirical constants.

Flint *et al.* (2002a) proposed a normalisation procedure, which makes it unnecessary to calibrate each block individually and also allows prediction of the temperature response of the blocks. Their analysis depends on the ceramic block material being effectively identical between blocks, so that differences between blocks are caused only by differences in contact between the heater and the ceramic. Their analysis was also based on a block with a line source heater, such as the Campbell Scientific 229. Some blocks have a point source heater and it is not known if the same methodology applies.

To use this normalisation method, a value of ΔT for each sensor when saturated (ΔT_{wet}) and when dry (ΔT_{dry}) is needed. The sensor must be completely saturated for the ΔT_{wet} measurement. This can be achieved by immersing the sensor in water under a vacuum and waiting until all air bubbles have disappeared. Similarly, the sensor should be completely dry for the ΔT_{dry} measurement, by oven drying at no more than 60°C or placing it in a desiccator for several hours. Temperatures greater than 60°C may damage the sensor.

The normalised temperature rise is calculated as

$$\Delta T_{norm} = \frac{\Delta T_{dry} - \Delta T}{\Delta T_{dry} - \Delta T_{wet}}. \qquad (13.4.3)$$

This value can be used in Equation 13.4.2 in place of ΔT, with a different value for α, since the range of ΔT_{norm} is from 0 to 1.

Correction for soil temperature is less straightforward. Flint *et al.* (2002a) found a fifth-order polynomial in temperature could be fitted to predict the slope of the correction. The corrected normalised temperature rise, T^*, is found using the relation:

$$T^* = \Delta T_{norm} - s^*(T_i - T_{cal}), \qquad (13.4.4)$$

where T_i is the initial temperature of the block before the heater is turned on and

T_{cal} is the temperature at which calibration was carried out, with:

$$s^* = -0.0133T^{*5} + 0.0559T^{*4} - 0.0747T^{*3} + 0.0203T^{*2} + 0.011T^* + 0.0013. \qquad (13.4.5)$$

Unfortunately, Equation 13.4.5 requires that T^* be known to calculate s^*. An iterative procedure is used to solve this. Although this is quite lengthy, it can be implemented easily on a spreadsheet or programmable data logger.

13.5 Calibration of Sensors

Calibration can be performed in several of ways, the main ones being:

- By comparison with another sensor in soil;
- Against a hanging water column;
- By equilibration with an osmotic solution,
- In a pressure plate or membrane apparatus.

Those sensors which are in the form of a small block (e.g. resistance blocks and heat dissipation blocks) are generally easier to calibrate. Equitensiometers present more difficulties because of their relatively large size, which rules out pressure plate or membrane calibrations and makes most other methods less convenient.

13.5.1 Comparison with other sensors

In many ways, this is the simplest method, although it may take a long time to acquire enough data to cover the range of water potential needed. Calibration may be done in either the laboratory or the field. Field calibration has the advantage that all relevant aspects are present in the calibration set-up, for example, temperature fluctuations, solutes, etc. However, there are a number of disadvantages, the most serious of which is spatial variability, which means that the water potential at one sensor location may be significantly different to that at the location of another, particularly at low water potentials. To minimise any such problems, the sensors should be installed as close together as possible and in as homogeneous an environment as possible. Time can be saved by installing the sensors at a dry time of year, waiting sufficient time for them to come to equilibrium with the soil and then irrigating to obtain measurements under wet conditions. This may miss measurements at intermediate potentials, so that only measurements at the dry and wet end of the range are available, which is clearly undesirable.

Field comparisons have been reported by Phene *et al.* (1971b), Whalley *et al.* (2001) and Whalley *et al.* (2009).

A laboratory soil column is a better controlled environment than the field, although it may often be difficult to obtain conditions where the potential is lower than – a few metres water. The same considerations apply, but apparently successful calibrations have been performed by Phene *et al.* (1971b) and Agus and Schantz (2005).

The potential pitfalls with intercomparison of sensors, mean that it is usually better employed as a means of checking the performance of different designs and of separate calibrations than in producing a calibration itself.

13.5.2 Hanging water column

Long used as a means of generating soil water retention curves, a hanging water column is an effective means of applying a known matric potential to a porous body. The principles of the set-up are illustrated in Fig. 13.7.

A tray filled with a porous material – fine sand for modest matric potentials and kaolin for lower ones are popular choices – transmits the pressure from a water column hanging from the bottom of the tray to one or more porous matrix sensors in contact with the porous material. The sensors may be embedded in the material, as shown, or placed on the surface. In the latter case, they will take

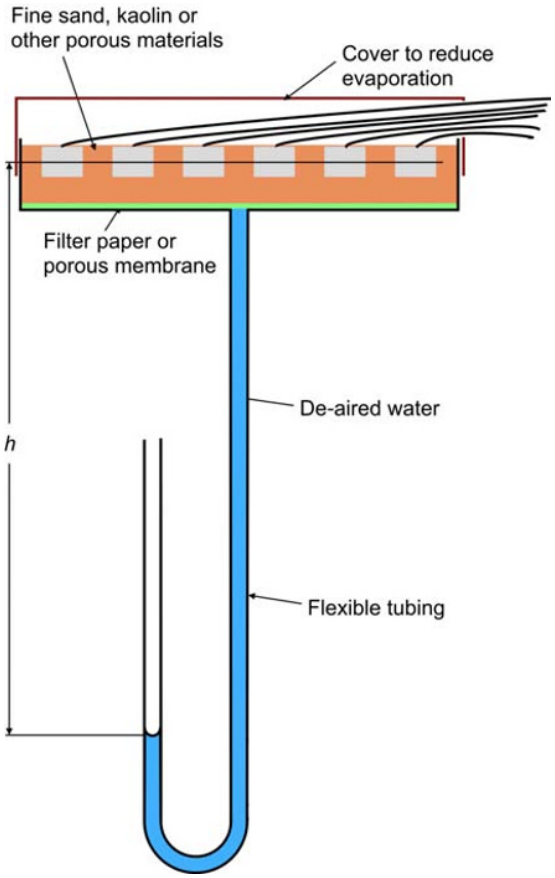

Fig. 13.7 A hanging water column to calibrate porous matrix sensors.

longer to achieve equilibrium, as the area of contact is smaller and contact may be poorer. The matric potential applied to the sensors is $-h$, and by adjusting the tube forming the U-tube, different potentials may be applied.

If the porous material used as the transmission medium has a lower air entry potential than the minimum potential required, then the system is very nearly saturated at all times. Any change in the applied potential is transmitted rapidly to the sensors and the only change in water content should be that of the sensors' porous matrix. However, if the potential falls low enough that the transmission medium starts to desaturate, more water needs to move through it. The hydraulic conductivity of the medium is also reduced, both effects increasing the time to achieve equilibrium.

A screen on the bottom of the tray is needed to retain the transmission medium. This can be any material with a small enough hole size to block the smallest particles. The tray should be covered to prevent evaporation from the surface, and in most cases, a temperature-controlled environment is needed to ensure that temperature fluctuations do not affect the process. A well-insulated container may be adequate if the laboratory environment is reasonably steady.

Air bubbles are potentially a large problem. They can be minimised by filling the system from the bottom and, once the water level reaches the base of the tray, proceeding slowly to allow entrapped air to escape from the surface. Over time, any remaining air entrapped in the medium will either migrate to the surface and escape or dissolve in the water, improving the performance of the calibration set-up.

The lowest potential achievable in theory using this method is –10 m of water. However, this requires that the length of the hanging column is 10 m, which is difficult to achieve. The method is, therefore, suitable only for modest potentials.

13.5.3 Vacuum and pressure chamber

For lower potentials, the hanging water column may be replaced with a vacuum or, alternatively, by increasing the air pressure around the upper part of the apparatus. The matric potential may be regarded as the difference in pressure between the air and the water in the medium, so that increasing the air pressure also increases the water pressure by the same amount. Even though the matric potential may be below –10 m of water (approximately atmospheric pressure), the actual pressure relative to the atmosphere outside the chamber may still be positive. If there is a water pathway to the outside, then water will flow from the porous material inside the chamber until the actual pressure of water inside the pores is equal to that of the atmosphere. Since the air pressure surrounding and within the block is much higher than atmospheric, the matric potential is equal to the difference in air pressure between the inside and outside of the chamber. This method is sometimes described as an *axis translation* technique.

A schematic diagram of a vacuum and a pressure chamber is shown Fig. 13.8.

Vacuum chamber

The vacuum applied to the lower side of the ceramic plate should be controlled by a regulator. There are two types – one switches the pump on and off to maintain the desired vacuum in the reservoir. In the other, the vacuum reservoir is maintained at a pressure well below that required in the lower part of the chamber. A valve, controlled by a diaphragm, maintains a set pressure on the chamber side of the pipe connecting it to the reservoir. The upper part of the chamber is open to the atmosphere, although it is important to prevent evaporation from the blocks and surrounding medium. If a sufficiently high accuracy vacuum gauge is not available, a mercury manometer can be used. Over time, the mercury and its tube become dirty and will, eventually, need to be replaced. There are strict controls in many countries over the use and disposal of mercury, which can lead to considerable unexpected expense. In any case, precautions are needed, by using flow constrictors and/or catching trays or pots to prevent mercury from being spilt accidentally or surging out of the manometer if the

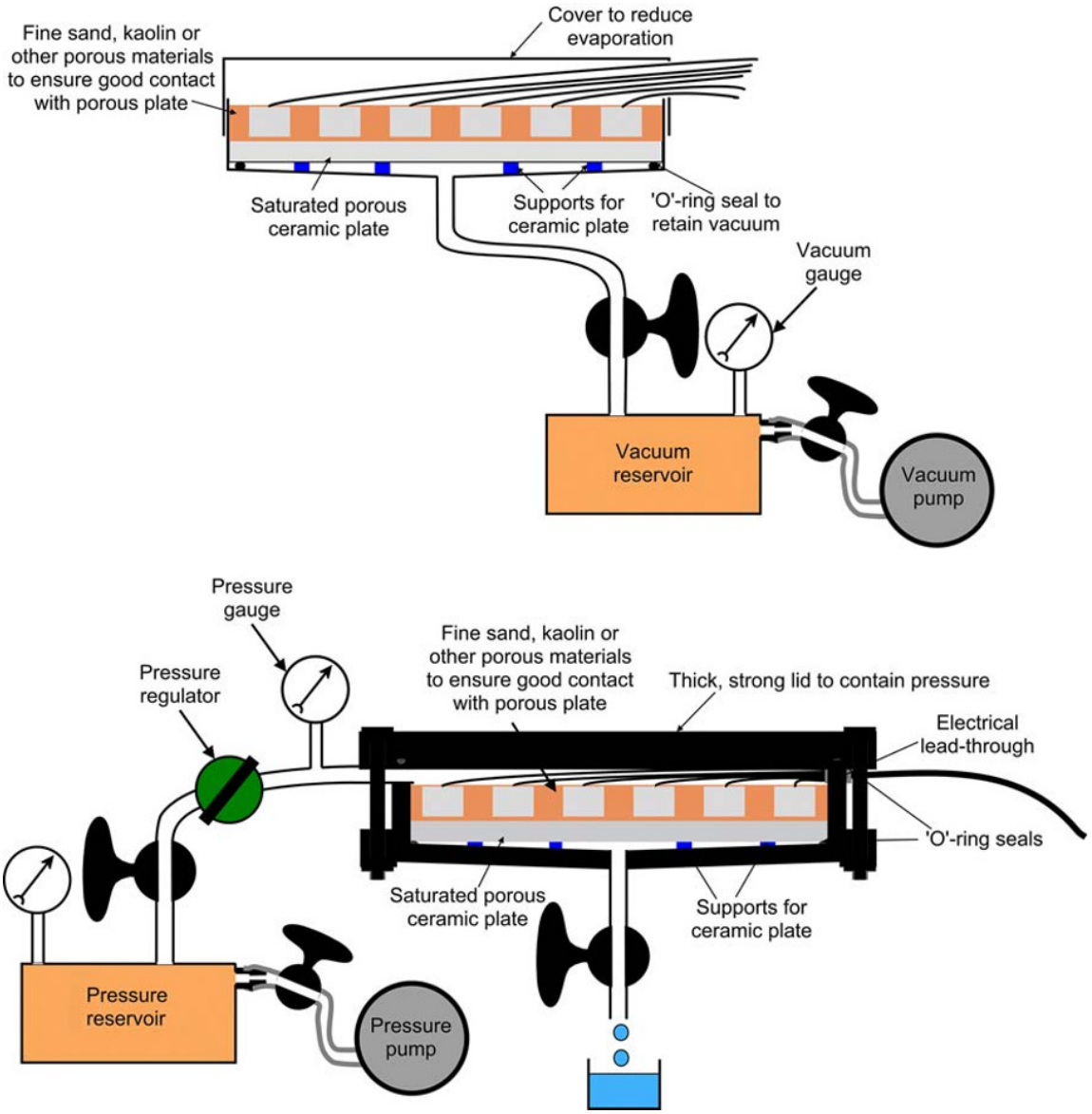

Fig. 13.8 Vacuum chamber (top) and pressure chamber (bottom) used for calibrating block-type matric potential sensors.

pressure changes suddenly. Although less hazardous than high-pressure air, precautions are needed to prevent accidents from, for instance, implosion of brittle components or a sudden loss of vacuum. A vacuum gauge requires periodic recalibration.

Pressure chamber

Pressure chambers use a source of high-pressure gas, either from a pump and reservoir, as shown in Fig. 13.8, or from a gas bottle. The choice depends on several factors – space available, financial resources and the amount of use likely to be made of the equipment. For light usage, compressed gas bottles are the most economical choice, as they avoid the considerable expense involved in purchasing pumps, reservoirs and control equipment, as well as the costs of maintenance and periodic inspection of these. For moderate usage, a self-contained and fairly compact package containing a pump and reservoir, with associated control gear, is available from Soil moisture Equipment Corporation in California and possibly other manufacturers. Regulators and pressure gauges are still required, along with the pressure chamber(s). Special high air entry value ceramic plates are available with bubbling pressures greater than 0.5 or 1.5 MPa (5 or 15 bar – 50 or 150 m water). Alternatively, some designs of chamber use a special cellulose membrane, similar to that used in dialysis machines, which performs the same function. Although the membrane material is cheaper, it degrades fairly rapidly and must be replaced frequently. In these chambers, the membrane is supported on a thick stainless steel mesh.

The potential for serious accidents when using high air pressure is very high, and in most countries, there are stringent regulations in place, which mandate roughly annual inspection and testing of all components of the system to ensure safe operation. These can make the use of such equipment expensive, particularly if it is used infrequently.

Since the upper part of the pressure chamber is well above atmospheric pressure, an electrical leadthrough, basically a set of conductors set into a plastic block that fits tightly into a hole in the wall of the chamber, is needed to allow the block to be read. Wellings *et al.* (1985) have described the pressure chamber calibration procedure in more detail.

Other considerations

In both the vacuum and pressure chambers, good contact between the blocks and the porous plate or membrane is important. In some cases, this can be achieved with a small amount of silica flour, fine clay or sand to fill any gaps between the two. In others, it might be necessary to embed the blocks in a porous matrix. While this ensures the best hydraulic contact over a large part of the surface area of the block, equilibrium can be attained only when all the water has drained out of the matrix to achieve the desired potential and so may make equilibration slower than if the contact were poorer. Some designs of pressure plate incorporate a plastic diaphragm in the lid which can be pressurised slightly above that of the chamber to press the samples into the plate or membrane.

The thermal conductivity of heat dissipation blocks varies with air pressure (Section 13.4; Flint *et al.*, 2002a) and so the blocks must be brought back to atmospheric pressure before making a measurement. The pressure plate or membrane itself will remain saturated, but there may be water in contact with its underside, which could then rewet the blocks slightly. To prevent this, the valve on the bottom of the pressure chamber should be closed before depressurising the chamber.

13.6 Block Installation

13.6.1 Installation of discrete sensors

In common with other instruments embedded in the soil, discrete sensors, such as resistance blocks (Section 13.2) and psychrometers (Section 14.2), may disturb soil water flow paths and particularly create pathways for rapid water flow from the surface. Generally speaking, it is better to have a relatively impermeable column of material above the sensors than one which bypasses much of the soil. An impermeable column, however, increases the response time of a sensor below it.

There are three basic approaches to installation of this type of sensor: multiple-hole, single-hole and side installation from a suitable access pit.

Multiple hole

In this method, each sensor is installed at or near the base of its own access hole, which may be vertical or inclined at an angle. The hole is usually most conveniently lined with an access tube. Alternatively, it may be backfilled with soil from the site or with other material.

Lining the hole with an access tube has the following advantages:

- A well-fitting access tube is impermeable, provided the tube is not open at the top.
- The sensor can be recovered fairly easily for replacement in case of failure, for recalibration or at the end of an investigation.
- Installation is often easier, as holes can be predrilled, lined and capped in advance of sensor emplacement. Little backfilling is required.

On the other hand, the disadvantages are:

- Water may run down a gap between the tube and surrounding soil. If it reaches the vicinity of the sensor, an artificially high water potential is recorded. This possibility can be minimised by drilling the access tube hole slightly undersized, by ensuring that any small gap around the top of the access tube is filled with local soil, by fitting a small skirt around the top of the access tube to direct water away from the access tube perimeter and by installing the sensor some little distance (say, 200 mm) below the bottom of the access tube. This may be either by augering a hole for the sensor through the tube and then backfilling and compacting soil above it or by drilling a hole of diameter equal to that required for the access tube to the full depth needed for the sensor and backfilling the lower 200 mm or so with soil from the appropriate depth. This is very similar to the procedure described in the section on tensiometer installation (Section 12.7).
- use of access tubing incurs additional expense, although this is normally small compared with the cost of the sensor.

Installation in an unlined, backfilled hole has the advantages of drilling the hole, emplacing the sensor and backfilling in one operation. This is simpler than performing the additional steps required to use an access tube, and if native soil is used for backfilling, little extra material is needed or disposed of. However, it is difficult to ensure that a preferential pathway for water from the surface to the sensor is not created. This can be minimised by:

- Backfilling part (usually the lower part) of the hole with material of lower permeability than that of the surrounding soil. This may be clay, clayey soil, cement, concrete or a closed-cell foam (e.g. polyurethane) mixed *in situ*. Introducing these materials into a small hole at depth, while ensuring that it forms a complete barrier, is often far from easy. The advantage of using a two-part foaming polymer, several types of which are marketed for hydrogeological applications, is that each component can be introduced individually *via* a separate small-diameter pipe. Use of swelling clay (e.g. bentonite) to form a low-permeability barrier is common in hydrogeological applications where the formation is saturated. Sometimes the bentonite is mixed with cement. This may be appropriate in unsaturated

applications. However, the sealing property of these clays depends to a large extent on their swelling on contact with water. In unsaturated situations, bentonite will also shrink. This can open up cracks, allowing water to flow through. Use of bentonite, therefore, should be reserved for situations where the formation can be guaranteed to remain wet at all times.

- Drilling an inclined hole. The intention here is that any water entering the backfilled hole drains downwards, rather than being conducted along the hole to the sensor. However, accurate positioning of the sensor is more difficult to achieve using an inclined hole. Use of a jig, anchored into the soil, reduces this problem.

For installation close to the surface (the upper ~300 mm), obtaining undisturbed measurements may be especially difficult, as any hole, skirt or impermeable material is likely to cause locally drier or wetter conditions at the sensor position than in the surrounding soil. This is because of sheltering by the impermeable material or, alternatively, water may be intercepted by the above-ground parts of the installation. Depending on the details of the surface protection, this water may be diverted away from the sensor or concentrated close to it. The possibility of water running down a gap between an access tube and soil will enhance this possibility.

Similar remarks apply to drying of the soil by evaporation, where the presence of a skirt may reduce locally surface evaporation and transpiration by shallow-rooted vegetation, again leading to unrepresentatively wet conditions.

For shallow installations, therefore, installation is best performed by horizontal insertion at least 300 mm into the soil from a shallow pit or borehole, which leaves the soil above the sensor intact. For shallow installations, the pit is best backfilled carefully after installation.

Single hole

In single-hole installation, several sensors are installed inside the same predrilled, either vertical or inclined, borehole. The hole is drilled just a little deeper than the depth of the deepest sensor, which is embedded into native soil (possibly sieved), silica flour or fine sand, as for multiple-hole installation. The connecting cable is led back to the surface. A second sensor is similarly installed some distance above it.

The most important and difficult part is in ensuring that the sensors are isolated hydraulically from one another and that there are no preferential flow paths between them. This is complicated, especially for the upper sensors, by the presence of cables from the sensors beneath. For this reason, the material between the sensors should be introduced as either a dry, fine powder, which flows freely, or as a slurry. In the latter case, precautions need to be taken to avoid the slurry intruding the area around the lower sensor, which can slow its response. The process is very similar to that described in Section 12.12.3 and Fig. 12.31.

These considerations limit the number of sensors that can be installed in a given borehole, as well as the vertical distance between successive sensors.

The choice of material into which the sensor should be embedded and the means of preventing preferential flow down the hole have been discussed previously.

Horizontal installation

Installation of sensors horizontally in the soil from a suitable access hole or pit is often an attractive option for the following reasons:

- There is minimal disturbance to the soil close to the sensors.
- Water flow in the soil between sensors is not disturbed.
- Many sensors can be installed from one access hole.

For shallow (less than about 700 mm) installation, a hole of approximately 200 mm diameter may suffice to emplace the sensors. This is sufficient to allow an operator's arm to reach the required depth and make a horizontal hole to receive the sensor, insert the sensor and backfill the hole.

The two important considerations are to ensure good contact between the sensor and soil and to ensure that backfilling the hole does not create preferential flow routes that disturb the sensor readings.

The first-named of these is a matter of ensuring that a pilot hole is sized to ensure a snug fit for the sensor. The second can be met by those described for separating sensors in a single-hole multi-sensor installation. Alternatively, the hole can be left empty, provided that it remains unsaturated at all times and is covered to exclude precipitation. The hole may need to be supported by an access tube to prevent collapse, but leaving the hole empty aids retrieval of the sensor later. If the hole is relatively large compared with the distance of the sensor from its edge, provision must be made to prevent precipitation or irrigation falling on the area occupied by the access hole from disturbing the sensor readings. In some cases, ensuring that the water is directed away from the side on which the sensors are installed may suffice; in others, the rain may need to be collected and led well away from the vicinity.

More discussion of the considerations applicable to horizontal installation is contained in Section 12.12.1.

13.7 Filter Paper Method

The principles behind this method are similar to those of other porous block methods – a porous matrix, in this case a piece of filter paper, comes into potential equilibrium with the soil with which it is in contact and the water content of the porous matrix is measured. Unlike other methods, however, the measurement is not made *in situ*, but after removal from the soil. Filter paper is very cheap and so little financial outlay is involved, the main requirement being an accurate balance to weigh the papers. These are commonly found in chemistry laboratories and, if one is available, the method involves little additional expense. The method is, however, expensive in the time required to make the measurements and, since it involves the manual insertion and removal of the papers

and their weighing in a laboratory, can be used only in situations where a time resolution of several days is acceptable. Since the method is best suited to arid conditions, this is most often not a problem, as changes in water status are usually slow in dry soil.

For field soils, measurements may be made in two ways:
1 In the most frequently used method, an undisturbed sample of soil is extracted and transported to a laboratory, where it is kept in contact with a filter paper inside a closed container for several days. Alternatively, it may be kept very close to but out of direct contact with the soil by a metal grid. In the first case, the measurement will be of matric potential, since solutes will be free to move with the water into the filter paper. In the second case, the total (matric plus osmotic) potential is measured, since equilibration is with the vapour pressure of the water, which is lowered by the presence of salts in the soil solution.
2 It is also possible to place the filter paper in contact with soil in the field. Hamblin (1981) made slits in the soil, in which the papers were inserted. It should also be possible to place the paper, suitably weighted down, at the open bottom of an access tube. In the field situation (and sometimes in a laboratory), the filter paper may be sandwiched between two other similar ones to avoid the central paper becoming contaminated by soil. Mullins (2001), however, reported that this often resulted in the paper not attaining equilibrium with the soil.

For either method, it is difficult to estimate the length of time needed until the paper attains equilibrium with the soil solution.

The basic sequence of operations is:
1 Cut a suitable size piece of filter paper a little smaller than the container or access tube.
2 Dry the filter paper in an oven at 105°C.
3 Weigh the dry filter paper.
4 Place the filter paper in the access hole, ensuring as good contact as possible with the soil. To avoid condensation wetting the paper, it must not touch the side of the container or tube.
5 Wait for several days for potential equilibrium to be established with the soil.
6 Retrieve the filter paper and immediately place it in a sealed container of as small a volume as possible to avoid loss of water by evaporation.
7 Weigh the filter paper as soon as possible in a damp atmosphere in the laboratory.

Ensuring good quality data using this method is not easy. The relevant factors are as follows.

13.7.1 Choice and calibration of filter paper

The filter paper must have a suitable water retention curve for the conditions prevailing at the site in question. The most common choice is Whatman No. 42 papers, the curve for which has been established by several workers, most notably Deka *et al.* (1995) (see Fig. 13.9). Although this has been found to be remarkably consistent from one batch to another, for highest accuracy, each batch should be calibrated individually. Calibration is not a simple process, however, as, for the lower water potentials, the papers must be calibrated in a pressure plate apparatus or equilibrated over solutions of known concentration and hence osmotic potential. This latter method of equilibration is very slow, taking perhaps several weeks at the drier end of the scale. The vapour pressure of the solution is very sensitive to temperature, and so papers can be calibrated only where suitable constant temperature facilities exist.

13.7.2 Treatment of papers

In some situations, usually where the soil is high in organic matter, fungal growth on the paper may degrade it. To avoid this, many workers have treated the papers with a fungicide (0.005% HgCl or 3% pentachlorophenol in ethanol) and allowed them to dry before use. This is reported not to affect the calibration curve (Fawcett & Collis-George, 1967; McQueen & Miller, 1968). In many situations, however, this is not necessary (Mullins, 2001), and so it may be advisable to test whether fungal growth occurs before making serious measurements.

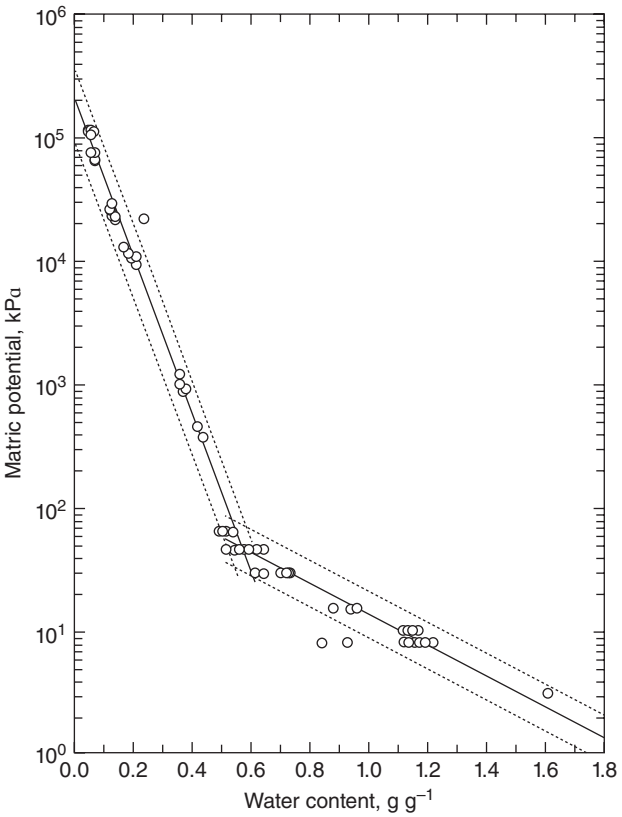

Fig. 13.9 Calibration curve for Whatman No. 42 paper determined by Deka *et al.* (1995), showing the characteristic 'broken stick' shape. It is believed that the portion at higher potentials is controlled by water held between paper fibres, while the portion at lower potentials depends on water held within fibres.

13.7.3 Handling of papers

The quantity of water held by the paper is very small, even when wet, and much less near the dry end of the range. Hence even a very small loss of water or additional water or other material, perhaps from an operator's fingers; evaporation; loss of a small amount of the paper; or soil particles adhering to the paper can change the measured amount of water seriously. To minimise this risk, handling of the papers must be planned in advance and carried out as swiftly as possible. Suggested measures include:

- Operators should wear thin rubber or PVC gloves to prevent moisture transfer between fingers and paper.
- Handling of papers should take place as far as possible in a high-humidity environment – a humidified glove box is ideal. Deka *et al*. (1995) used a wooden box lined with wet paper towels, although care is needed to prevent the paper coming into contact with the towels.
- Measures must be taken to ensure that papers are not damaged during handling and that they are shaded from direct sunlight at all times.
- Soil particles adhering to the paper should be brushed off before weighing. If this is not possible, then the mass of soil can be measured after drying, although estimation of the amount of water contained in that soil may be very difficult.

13.7.4 Weighing

Both the filter paper and the water within it have very small mass (~200 mg for a filter paper, down to ~10 mg for the water at –10,000 m water matric potential and 320 mg close to saturation) (Deka *et al.*, 1995). Weighing accuracy therefore needs to be better than 1 mg (Deka *et al.*, 1995). This level of accuracy can sensibly be achieved only in a laboratory with high-quality equipment.

13.7.5 Accuracy of the method

Assuming no contribution from temperature gradients, inadequate equilibration time, loss of water by evaporation, soil adhering to the paper, etc., Deka *et al.* (1995) estimated the accuracy of water potential as being within a factor of 1.5–1.8, depending on the range of potential. Thus the method is not useful for calculating gradients of water potential for use in estimation of water flux. However, it is competitive with other porous matrix methods at low water potentials.

14 Beyond –10 Metres Water Head

14.1 Introduction

The range of conventional tensiometers is limited by the lowering of the boiling point of water to normal ambient temperatures as the internal pressure falls towards zero. The pressure at which boiling occurs is the saturated vapour pressure of water at the appropriate temperature. This is equivalent to about 23 cm water pressure, and so tensiometer failure occurs theoretically at a water potential where the lowest pressure (i.e. at the highest point) in the system relative to atmospheric is very close to –10 m water. In practice, failure usually occurs above that because of air diffusion into the tensiometer. In any case, readings often lag well behind the true water potential through a combination of reduced diffusivity of the soil and low sensitivity of the tensiometer because of air in the system (Whalley *et al.*, 2009).

The traditional approach to this problem is through the use of porous matrix sensors, which operate over a wide range of water potential and are described in Chapter 13. Porous matrix sensors are robust but often have unacceptably large hysteresis, and their calibration may shift considerably over time.

Instruments which give a more direct reading of water potential in the range below –10 m water are described in this chapter. They comprise soil psychrometers, osmotic tensiometers and high-capacity tensiometers.

14.2 Soil Psychrometers

The name *soil psychrometer* is usually applied both to true psychrometers, which measure the temperature depression below ambient of a wetted sensor in a humid environment, and to *hygrometers*, which measure the dew point of the soil atmosphere. In either case, the measurement is of the *vapour pressure deficit* (i.e. the amount by which the water vapour pressure in the soil is lower than that at saturation at the same temperature and atmospheric pressure) or the *relative humidity* (the ratio of the actual vapour pressure of water to that of the saturated vapour pressure at the same temperature).

A good review of the design and use of soil psychrometers can be found in Andraski and Scanlon (2002), which should be consulted for more information.

All practical soil psychrometers sense temperature by a sensitive thermocouple. One type, the *wet-loop* psychrometer of Richards and Ogata (1958), requires that a droplet of water be placed manually onto a small ring at the thermocouple junction and so is unsuitable for field use. The *Peltier* type of psychrometer, also known as a *Spanner psychrometer* (Spanner, 1951), uses the *Peltier effect* to cool the junction and condense a droplet of water onto the junction.

14.2.1 Theory

Effect of water potential on water vapour pressure

The soil water potential affects the water vapour pressure of the air in the pores. This may be appreciated by considering that the soil matrix holds onto the water more tightly as water content decreases and, at the same time, restrains water molecules from evaporating from the liquid. In quantitative terms, the vapour pressure is related to the soil water potential through the *Kelvin equation*:

$$\psi = -\frac{RT}{V_w}\ln\left(\frac{p}{p_0}\right), \qquad (14.2.1)$$

where

R is the gas constant (8.314×10^{-6} MJ mol^{-1}°C^{-1});
T is the absolute temperature;
V_w is the molar volume of water (1.8×10^{-5} m^3 mol^{-1}) and
p/p_0 is the relative humidity, p being the actual vapour pressure in equilibrium with the pore water and p_0 the saturated vapour pressure, both at temperature T

Unfortunately, because of the logarithmic relationship, the actual vapour pressure, p, is very close to the saturated value for even quite low (in soil terms) water potentials. At 25°C, a water potential of –150 m water (–1.5 MPa),

Soil Water Measurement: A Practical Handbook, First Edition. J. David Cooper.

traditionally the wilting point for vegetation, is equivalent to a relative humidity of 99% (Andraski & Scanlon, 2002). Measurement of water potential using the technique, therefore, requires both very good temperature stability and accurate measurement of relative humidity. Because a thermocouple is used to measure relative humidity, the latter implies accurate temperature measurement of the thermocouple junction, which in turn demands accurate voltage measurement.

It should be noted that a psychrometer measures the total local water potential in the soil, that is, the sum of the matric and osmotic components. This contrasts with most other methods, which measure just the matric component of water potential.

Dew point The dew point is the temperature at which water vapour in air condenses. Condensation is commonly observed on a cold surface, for example, a glass window. When the humidity is high, water condenses on a warmer surface than it does when the humidity is lower. Dew point is often measured by cooling a mirror until water condenses on it, at which point the mirror no longer reflects a light beam. At any ambient temperature, the dew point depends only on the quantity of water vapour per unit volume of air, that is, on the vapour pressure, p.

For high humidity, which is the case in our situation, the dew point, T_d, is very close to

$$T_d \approx T - 16\left(1 - \frac{p}{p_0}\right). \qquad (14.2.2)$$

The slope factor varies by about 20% between 5 and 30°C. This is easily corrected for, since it is essential to know the soil temperature to measure the temperature depression.

Psychrometric method

In the psychrometric method, a water droplet on the thermocouple junction evaporates into the space around it. The latent heat of evaporation required for this comes from cooling of the water droplet. The resulting *wet-bulb temperature* is higher than the dew point but below the ambient, or *dry-bulb temperature*. The situation is very similar to that encountered in meteorological stations, which use a water-saturated wick over one of a pair of thermometers to monitor atmospheric humidity. The temperature depression of the wet bulb is about 60% of the dew point depression (Campbell, 1979) but varies a little from one instrument to the next as a result of differences in heat conduction along the thermocouple wires, radiation inside the soil cavity, etc.

The Seebeck effect

Temperature measurement by a thermocouple depends on this effect, otherwise known as the *thermocouple effect*. It was discovered in 1821 by Seebeck, who found that a voltage is generated proportional to a temperature gradient in any metal. Different materials produce a different voltage, and so, by joining wires of dissimilar metals together, a voltage is produced proportional to the temperature difference between the two junctions. The Appendix 14.A to this chapter gives more details about thermocouples and their operation.

The Peltier effect

The Peltier effect is related to the Seebeck effect in that by imposing an electric current on a thermocouple junction, heating or cooling of the junction occurs, depending on the direction of current flow.

14.2.2 Design of soil psychrometers

The essential elements of a soil psychrometer are shown in Fig. 14.1. The primary thermocouple is made of very fine wire chromel and constantan. The wires need to be as fine as possible to minimise heat conduction to the junction.

There is also an auxiliary thermocouple of copper and constantan to measure ambient temperature of the instrument. In some designs this is at the top of the PTFE plug as shown, while in others it is within the cavity containing the primary junction.

The primary thermocouple is very delicate and so must be protected well by a porous ceramic shield or a metal

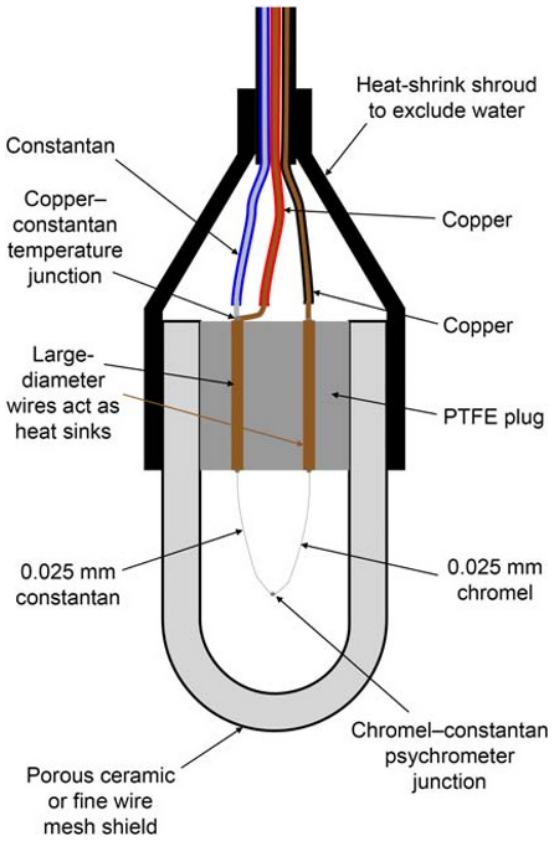

Fig. 14.1 Components of a soil psychrometer. (*See insert for colour representation of the figure.*)

mesh screen sufficiently fine to keep out soil particles. Ceramic is usually more robust, but if it is broken, it then cannot be repaired readily. A ceramic shield-equipped psychrometer is unlikely to achieve vapour equilibrium with the soil as quickly as one with a metal screen. Should the soil become saturated at any point, then the ceramic version is likely to protect the psychrometer junction from contamination rather better. However, the ceramic may also absorb salts from the soil solution, which could depress the measured water potential artificially.

The temperature difference of the junction from that of the soil is very small, even for what are normally regarded as low water potentials. Therefore to measure this reliably is quite difficult. Some of the design measures are:

- Using chromel (90% nickel, 10% chromium)–constantan (55% copper, 45% nickel) for the thermocouple junction (also known as Type E). This has a relatively large (68 $\mu V°C^{-1}$) output. For comparison, a copper–constantan thermocouple has a sensitivity of 41 $\mu V°C^{-1}$ at 25°C.
- Using fine wire for the primary thermocouple to minimise heat conduction down the wire. However, this must not be too fine since, as well as needing to be sufficiently robust, the finer the wire the higher its resistance and so the greater ohmic heating when a cooling current is passed through it (see Section 14.2.3).
- Having large cross-sectional pins, of high thermal conductivity metal, connecting to the thermocouple to ensure temperature stability of the junctions between the chromel and constantan wires with the pins. Heat extracted by Peltier cooling at the chromel–constantan junction appears as heat at the other end of the fine wire thermocouple. Having large conductors at these junctions minimises the temperature rise at this point.

14.2.3 Principles of measurement

Soil psychrometers measure the wet- and dry-bulb temperature of the soil atmosphere, or its dew point temperature, using the theory outlined in Section 14.2.1.

The basic operation is to measure the thermocouple voltage of the primary junction in its dry state. A current is then passed through the junction to induce Peltier cooling of the junction, which condenses a small droplet of water from the cavity around it onto the junction.

In the *psychrometer mode*, the droplet is allowed to evaporate and attain a stable wet-bulb temperature, from which the relative humidity of the cavity and hence the soil water potential can be calculated.

In the *dew point mode*, the reader unit is switched alternately between a reading of the temperature and application of a cooling current to the primary thermocouple. The cooling is needed to compensate for heat gained by conduction through the air in the cavity and the thermocouple wires, radiation from the cavity sides, etc. A sensor-dependent factor, 'π_v' is required which characterises the rate of heat gain from these extraneous sources.

In both cases, a correction for the temperature of the sensor is required, as the relative humidity, psychrometric constant and π_v are all temperature dependent.

14.2.4 Calibration

Although there is an apparently good theoretical basis for psychrometers, small differences in manufacture affecting heat flow to the sensor junction make it necessary to calibrate each psychrometer separately.

Calibration over osmotic solutions

This is often the most convenient method. The psychrometer is suspended over a solution of known concentration and, hence, osmotic potential. Great care is needed over preparation of the solutions and avoiding cross-contamination between them. Good temperature control is also essential. The work should be done in a temperature-controlled room, using a water bath to keep the temperature constant to better than 0.01°C. For relatively high potentials, the solutions are fairly weak, and ceramic sensors can be partially immersed in the solution, rinsing them thoroughly several times in distilled water and dried between each rinsing to avoid cross-contamination between solutions. It is recommended that sensors be calibrated in small, individual chambers to ensure that the environment around each individual sensor is not affected by gradients in a large chamber. This also mimics better the situation when the sensor is installed in the soil. Each chamber has either a small quantity of calibration solution or a filter paper just saturated with solution. Condensation inside the chamber can be prevented by cooling the chambers initially below the water bath temperature.

Calibration in a pressure plate or membrane apparatus

This technique is very similar to that described in Section 13.5.3. Because of the pressure dependence, the measurements must be made at ambient pressure, entailing precautions to prevent the matrix in which the sensors are embedded from rewetting on depressurisation.

Accuracy

The calibrations are temperature (and pressure) dependent and so must be corrected at least for the temperature effect. With some loss of accuracy, temperature corrections can be developed to apply to a batch of similar sensors.

Careful calibration may give an accuracy of about 3–5 m water (500 hPa).

14.2.5 Field installation

Measurements at some depth below the surface avoid problems caused by rapid temperature fluctuations of the environment. However, the dry zone near the surface is often of most interest. Commercial sensors are designed to minimise problems resulting from temperature gradients, but careful installation is still necessary to avoid unacceptably large

errors. The most important is to install the sensor horizontally. This means that all of the sensor will be as nearly as possible at the same temperature (Merrill & Rawlins, 1972). To avoid problems caused by heat conduction through the connecting cable, a length of at least 0.3 m immediately behind the sensor should be buried at the same depth in the soil.

As always, minimising soil disturbance is important. Horizontal installation into *in situ* soil from a shallow pit is recommended, making a small hole of the correct diameter of at least 0.2 m length to insert the sensor into and ramming soil back behind it. If the soil is not sufficiently stable, a small tube may be needed to keep the hole open temporarily to allow the sensor to be inserted to the end. The pit should be carefully refilled after installation.

For depths greater than about 1 m, vertical temperature gradients are usually small enough for vertical installation into holes drilled from the surface. If the hole is to be lined, then the liner material should have low thermal conductivity to avoid creating an artificial temperature gradient. The sensor should be embedded into native soil material taken from the same depth and a short length of connecting cable coiled at the bottom of the hole.

Fig. 14.2 The Wescor HR-33T manual psychrometer reader. Reproduced with permission of Wescor Inc., Logan Utah.

14.2.6 Data acquisition

Data may be acquired either manually or automatically. Because of the extreme sensitivity of the method to temperature changes in both space and time, great care must be taken to ensure thermal stability of the sensitive components. For this reason, rapid temperature changes of all components of the system must be avoided, as these translate readily into temperature differences between connection points. Connections to the data acquisition system are particularly vulnerable, and care should be taken with a manual reader, such as the Wescor HR-33T unit, to avoid direct sunlight. Cable connections should, where possible, be buried and/or insulated, while a data logger system should be placed in a well-insulated enclosure.

A photograph of a Wescor HR-33T unit is shown in Fig. 14.2. The newer PSYPRO unit makes and stores readings in psychrometric mode only or used to log up to eight psychrometers at predetermined intervals unattended. The sequence for making readings is very similar to that when using the HR-33T, but these are done either manually or automatically.

The sequence of operations to make a reading is taken from the manual for the HR-33T, but if other equipment is used, the procedure is likely to be similar.

Hygrometric mode

1 The measuring equipment incorporates a sensitive microvoltmeter. This is easily damaged by transient voltages produced when making connections to the instrument. To avoid this, the inputs must be shorted while making connections. The HR-33T has a 'Short' function on its selector switch for this purpose.

2 Connect the psychrometer to the measurement unit using either a proprietary connector or the post terminals. It is very important to get these the right way round. If the psychrometer is from a different manufacturer than the reader unit, there may be different colour coding of the connecting wires from those of the terminals. The chromel side of the thermocouple should be connected to the negative input terminal and the constantan side to the positive terminal. Getting these the wrong way round causes Peltier heating of the junction, rather than cooling! In Wescor psychrometers, the auxiliary thermocouple shares one of its connecting wires with the constantan side of the primary thermocouple. Some sensors may have separate wires for these, and so the copper side of the auxiliary thermocouple should be connected to the positive input, while the constantan side should be connected to the input provided (blue for the HR-33T). A switch alternates the measurement between the two thermocouples.

3 Set the appropriate π_v value for the sensor on the unit. This should have been supplied by the manufacturer, but if not it can be found as part of the calibration process. Note that π_v is temperature sensitive, and so a correction must be applied for the actual soil temperature.

4 Select the switch position to read the voltage of the primary thermocouple. In theory, the reading from the primary thermocouple should be zero, but small temperature differences within the psychrometer cavity may produce a small offset voltage. Either note this down and subtract it from subsequent readings, or offset the reading using the controls to bring the reading to zero. This should be done on the most sensitive range available.

5 Select 'Cool' on the function switch. There may be an option to change the cooling current, although the HR-33T uses a fixed cooling current of 8 mA. The junction should be cooled for a few seconds, the exact time depending on the state of dryness of the soil. The drier the soil, the more time is needed to condense a sufficient drop of water. In some situations, this may take 30 s or longer, but 5 s may be sufficient in fairly wet soil.
6 Set the function switch to 'Dew point'. The reading on the meter should fall initially quite quickly, as the thermocouple junction warms up to the dew point. It should then remain steady at the dew point temperature indefinitely. If no stable temperature is observed, then either not enough water was condensed on the junction (use a longer cooling time) or the π_v value was set wrongly. A contaminated thermocouple junction could also be a cause of failed readings.

Psychrometric mode
The procedure in this mode is very similar to that just described.

Follow steps 1 to 5 for the hygrometric mode, omitting step 3. Then, instead of selecting 'Dew point' on the function switch, select 'Read'. The reading will again fall as the junction warms to a stable value. This should be maintained for several seconds, before falling again to near zero, as the water droplet disappears.

Combined mode
The similarity of operation for the hygrometric and psychrometric modes makes it possible to combine both measurements in one operation. After making a reading in the hygrometric mode, the function switch is moved to the 'Read' position to make a measurement in psychrometric mode.

Other matters
Successful operation of soil psychrometers depends on careful calibration and installation, elimination of spurious temperature effects and selection of an appropriate cooling current and time. These come from experience, which is best acquired initially from laboratory calibration.

In some situations, the hygrometric mode of operation may be found more successful than the psychrometer mode, and in others the reverse.

Automatic data acquisition systems for soil psychrometers have been available for many years, based on portable PCs or programmable data loggers. These can handle a large number of psychrometers.

An alternative to *in situ* measurements in dry soil, where water potential is not sensitive to soil structure, is measurement of disturbed samples in the laboratory, where the environment can be controlled more easily. Great care is needed to prevent loss of water from the sample in this process. Psychrometric equipment for laboratory measurements is produced by Wescor Inc., with which the HR-33T or PSYPRO unit can be used, and by Decagon Devices in Pullman, Washington. Decagon Devices also make a slightly less accurate hygrometer, based on a cooled mirror, to detect dew point.

14.3 Osmotic Tensiometers

The osmotic tensiometer was introduced by Peck and Rabbidge (1966, 1969). The method was initially very promising but fell into disuse owing to reported problems with biodegradation of the membranes and breakdown and leakage of the osmotic solution (Bocking & Fredlund, 1979). Recently, the development of better membrane materials has renewed interest in the method.

14.3.1 Theory of osmotic tensiometers

The concept of an osmotic tensiometer is simple (Peck & Rabbidge, 1966). A solution of high osmotic potential is contained in a small chamber, having as one of its faces a semipermeable membrane that allows water but not solute molecules to pass through. If the membrane is in contact with water, water molecules are attracted into the chamber, causing the solution pressure to rise until it balances the osmotic attraction. If the water outside of the membrane is at a negative water potential, then the pressure differential across the membrane is still equal to the osmotic pressure of the solution in the chamber. The internal pressure is, therefore, expected to be the algebraic sum of the osmotic pressure of the solution when in contact with free water and the soil water potential. That is, if the osmotic pressure of the solution in the chamber is Π and the soil water potential is ψ, then the pressure inside the chamber at equilibrium will be $\Pi + \psi$. Under unsaturated conditions, ψ is negative, and so the pressure in the chamber will be lower than Π, but still positive if Π is large enough.

There is some uncertainly about this argument, as we have not specified whether ψ refers to the matric potential or the sum of matric and osmotic potential of the soil. This depends on whether the membrane is permeable to the solutes in the soil solution. We should expect it to be permeable to the smaller inorganic molecules, but not to some of the large ones, and therefore the indicated pressure is relevant to an intermediate value between the matric potential and the sum of this and the osmotic potential. In many cases, osmotic potential is small, and so the question would be of academic interest only.

14.3.2 Construction of an osmotic tensiometer

An osmotic tensiometer is similar in many ways to an ordinary pressure tensiometer. The space inside is, however, much smaller, and in most designs published, resembles that shown in Fig. 14.3 (e.g. Peck & Rabbidge, 1969; Bocking & Fredlund, 1979; Biesheuvel *et al.*, 1999; Bakker *et al.*, 2007). The main features are:
- A high air entry value (1.5–2 MPa – (150–200 m water)) porous ceramic disc interfacing with the soil. The high air entry value is needed to ensure good hydraulic contact with the interior of the tensiometer. The ceramic disc (usually called a *stone* in geotechnical literature) also protects and supports the semipermeable membrane.

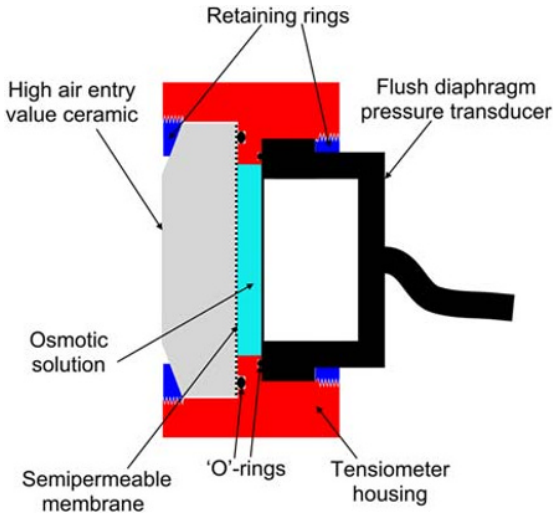

Fig. 14.3 Main components of an osmotic tensiometer.

- A semipermeable membrane. This has even finer pores than the ceramic disc and retains the osmotic polymer while allowing water to pass between the interior of the tensiometer and the soil *via* the ceramic disc.
- A chamber containing a water-soluble high molecular weight polymer. The large size of the polymer chains prevents their passing through the membrane, while the solution has a high osmotic pressure (~1.5–2 MPa).
- A rigid housing to contain the osmotic solution and ensure secure mounting of other components.
- A pressure transducer (see Section 12.13) to measure the pressure of the osmotic solution. Under normal operating conditions, the pressure in the chamber is large and positive. The transducer must be able to measure and withstand these pressures without damage.
- Means of sealing the system and assembling and disassembling it, for example, 'O'-rings and retaining rings. The details will depend on the particular components used.

The most critical components of this type of tensiometer are the membrane and the polymer solute. Early examples had cellulose-based membranes, used for dialysis and also in pressure membrane equipment for soil water retention studies (Section 13.5.3). Unfortunately, these are subject to microbial degradation, limiting their lifetime severely and causing excessive leakage of polymer and/or breakdown of the polymer itself (Bocking & Fredlund, 1979). Although only a few tens of microns thick, the hydraulic resistance of the membrane is comparable to and may exceed that of the ceramic disc. More recently, Biesheuvel *et al.* (1999) used a composite ceramic of α-alumina coated with two 2-μm thick layers of γ-alumina. The γ-alumina has pores of size of about 2.5 nm, which should retain polymer molecules effectively. Because the alumina is inorganic, it should be proof from microbial attack and therefore retain its effectiveness indefinitely. Bakker *et al.* (2007) and van der Ploeg *et al.* (2008, 2010) also used the same material.

Most osmotic tensiometers use polyethylene glycol (PEG) as the polymeric solute. Polyacrylamide (PAM) and polyvinylpyrolidone (PVP) have also been used (Biesheuvel *et al.*, 2000; Bakker *et al.*, 2007). Bakker *et al.* (2007) found PVP to be unsuitable as a result of unexplained collapse in pressure inside the tensiometers. PAM may also suffer irreversible changes in structure when exposed to divalent cations such as Ca^{++} (Biesheuvel *et al.*, 2000). PEG is, therefore, likely to remain the most popular polymer for this type of work. It is available in several different molecular weights, but the most suitable are in the range 4–20 kg mol^{-1}.

Even with very small pore size inorganic membranes and very large molecules, both Biesheuvel *et al.* (1999) and Bakker *et al.* (2007) found some reduction in tensiometer pressure over time of the order of 0.1% day^{-1} when the units were put into distilled water. It is not clear whether this represents changes to the polymer over time, leakage of smaller molecules present in the solution or some other causes. While inconvenient, the rate of reduction is sufficiently small and consistent that corrections can be made to take this into account.

Osmotic potential of the solutions is temperature sensitive. There may also be other sources of temperature sensitivity in the system, such as change in the dimensions of the osmotic cavity. A temperature sensor should therefore be attached to each tensiometer to correct for these effects.

The work of Biesheuvel *et al.* (1999), Bakker *et al.* (2007) and van der Ploeg *et al.* (2010) points to the following for successful construction and use of osmotic tensiometers:

- The membrane used should be inorganic and of as small pore size as possible. γ-Alumina on a substrate of α-alumina seems suitable.
- PEG of 4–20 kg mol^{-1} appears suitable for the purpose.
- The PEG can be packed dry into the tensiometer. It will absorb water from the soil, and because of the high pressure, any air will dissolve (Bakker *et al.*, 2007).
- The osmotic cavity should be as small as possible to reduce the response time of the tensiometer, probably through a combination of reduced fluid compressibility and stiffening the housing. Response time is likely to be of the order of hours. This is unlikely to be a problem at low potentials.
- Response time is reduced by a large area of membrane in contact with the osmotic solution.
- Osmotic tensiometers refill themselves automatically on rewetting after the soil water potential falls too low to support an internal pressure of less than –8.5 m water (van der Ploeg *et al.*, 2010). This is a very useful feature.
- Disc-shaped ceramics may not make adequate contact with the soil. Van der Ploeg *et al.* (2010) used solid cones instead and reported improved performance.

No field experiments using osmotic tensiometers appear to have been reported.

14.4 High Capacity Tensiometers

It is usually believed that boiling or cavitation limits the range of conventional tensiometers when the absolute internal pressure falls below the saturated vapour pressure of water. There are, however, a few examples of tensiometers continuing to work apparently reliably at potentials somewhat lower than –10 m water (e.g. Miller & Salehzadeh, 1993; Whalley *et al.*, 2007). The explanation for this is that, while water cannot support an absolute negative pressure indefinitely, something is needed to trigger the change of state, a process known as *nucleation*.

For water to boil, it must produce bubbles. In a very pure and clean system, the bubble must begin as a very small spherical volume of gas. However, surface tension forces make it difficult for very tiny bubbles to form initially and to grow. To see how this works, consider a small spherical bubble of radius r.

The surface tension force of the water acts tangentially to the surface of the bubble. From Equation 2.1.2, this is equivalent to a pressure, P, on the bubble of

$$P = \frac{2\gamma}{r}, \tag{14.4.1}$$

where γ is the surface tension (about 7×10^{-2} N m^{-1}) and the result is positive because in Section 2.1, we were considering the pressure in the water rather than in the gas above it. For a bubble of 1 mm radius, the excess pressure inside the bubble is therefore about 140 N m^{-2} or 140 Pa (14 mm water). The surface tension forces, therefore, resist the growth of very small bubbles and, indeed, cause their collapse.

The bubble is inside a body of water, which has an absolute pressure of P_0. The actual pressure on the bubble, P_b, therefore, is

$$P_b = P + P_0 = \frac{2\gamma}{r} + P_0. \tag{14.4.2}$$

The gas inside the bubble is mainly water vapour, which is at a pressure equal to its saturated vapour pressure, P_s (about 230 mm water or 2.3 kPa at 20°C), independent of the bubble size (except for extremely small ones corresponding to water potentials lower than about –200 m water or –2 Mpa, which does not affect the argument in a qualitative way). If the bubble is to grow, this pressure must be greater than that imposed by the surface tension forces and the external pressure of the water, P_b. That is,

$$P_s > \frac{2\gamma}{r} + P_0. \tag{14.4.3}$$

or

$$r > \frac{2\gamma}{P_s - P_0}. \tag{14.4.4}$$

For P_0 equal to atmospheric pressure (about 100 kPa), this means that the bubble will not grow for any value of r since the right-hand side of the equation is negative. For P_0 = zero (corresponding to a matric water potential of –10 m water or –100 kPa), the critical value of r is 60 μm; at P_0 = –100 kPa (ψ_m = –20 m water), it is 1.3 μm; and at P_0 = –900 kPa (ψ_m = –100 m water), it is 0.14 μm.

So, as the pressure reduces below absolute zero, the size of bubble able to grow reduces very markedly, and there is a progressively greater chance of something being present to trigger the process. This may be a small air bubble trapped in a very small crevice, a small particle, surface irregularity or slightly contaminated surface.

14.4.1 Design and maintenance of high-capacity tensiometers

The main design features of a high-capacity tensiometer are superficially very similar to those of an osmotic tensiometer: a stiff housing with a high air entry value ceramic, a small chamber containing liquid and a pressure transducer. The principal differences are that there is no semi-permeable membrane and that the liquid is water, rather than an osmotic solution.

The elements common to most devices are shown in Fig. 14.4.

The first successful attempt at a tensiometer which would work consistently at pressures below –10 m water was by Ridley and Burland (1993). Since then, several groups of workers have constructed high-capacity tensiometers (e.g. Tarantino & Mongiovi, 2001; Meilani *et al.*, 2002; Take & Bolton, 2003; Mahler & Dienne, 2007; Cui *et al.*, 2008; Lourenço *et al.*, 2008; Rojas *et al.*, 2008; Schindler *et al.*, 2010).

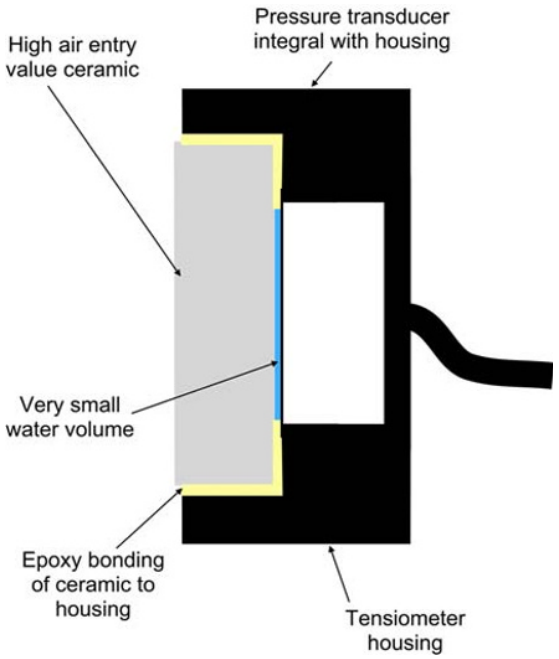

Fig. 14.4 Elements of a high-capacity tensiometer.

To keep the water from cavitating in the chamber, its volume is reduced as much as possible by reducing the space from the pressure transducer diaphragm to the ceramic (~0.1 mm). All surfaces of the interior of the tensiometer are made as smooth as possible to eliminate any crevices where air may be trapped and grow into bubbles, which can trigger cavitation. By making the pressure transducer integral with the housing, a joint is eliminated. This involves machining the diaphragm and housing as one piece. Strain gauges are affixed to the back of the diaphragm. Similarly, bonding the ceramic to the housing and ensuring a smooth join in the interior removes another possible site for bubble nucleation.

The tensiometer is filled with de-aired water at high pressure (up to 4 Mpa or 400 m water). Usually several cycles of pressurisation and depressurisation are used to dissolve all air into the water, which then allows the tensiometer to operate down to water potentials as low as –100 m water or lower in some cases.

There are few reports of field use of such devices, but it can be expected that these will become more common. Mendes *et al.* (2008) and Cui *et al.* (2008) have, however, both reported successful field tests. Cui *et al.* (2008) were able to operate a high-capacity tensiometer for a period of over 3 weeks down to a matric potential of –160 m water.

Appendix 14.A Thermocouples

A thermocouple does not detect temperature as such, but a difference in temperature between two points. It does this because there is a voltage difference (ΔT) between the two ends of a conductor held at different temperatures, T_1 and T_2. This difference is equal to

$$\Delta V = S(T_1 - T_2), \qquad (14.A.1)$$

where S is the *Seebeck coefficient* of the material.

Thermocouple measurement of temperature is possible because different conducting materials exhibit different Seebeck coefficients. Figure 14.5a shows a simple thermocouple composed of two conductors with Seebeck coefficients S_1 and S_2. The junction at the bottom is at temperature T_1, while the voltage is measured at the top, where the temperature is T_2. The measured voltage depends only on the difference in Seebeck coefficient of the two materials and the temperature difference between the junctions. Note also that if the two terminals at the top were at different temperatures, then the measured voltage would not be the same. It is important, therefore, to ensure that there is no difference in temperature between measurement terminals.

To measure absolute temperatures, there is a need for a *reference junction* at a known temperature at one of the terminals. This could be an ice–water mixture, but in modern circuitry it is usually supplied by electronic means as a virtual reference junction.

The thermocouple arrangement of a soil psychrometer in circuit diagrammatic form is shown in Fig. 14.6. Because

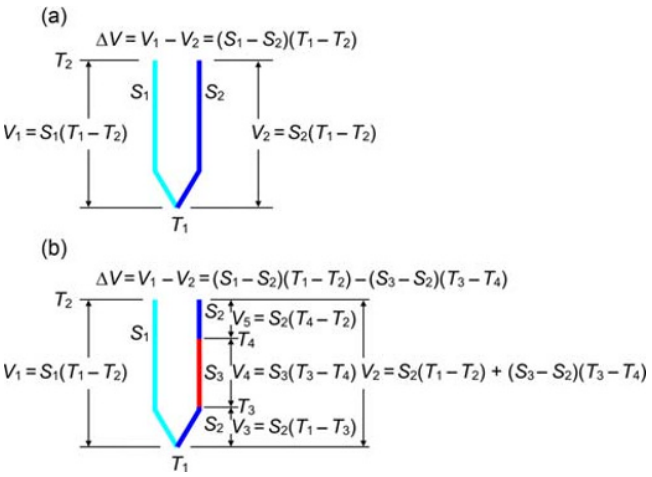

Fig. 14.5 Operation of a thermocouple. (a) A simple thermocouple composed of two conductors having Seebeck coefficients S_1 and S_2. The voltage difference is equal to the product of the difference in Seebeck coefficients and the difference in temperature between the junctions. (b) Insertion of a different type of conductor in one arm of the thermocouple changes the output even though the material at the upper junction is the same in both cases, unless $T_3 = T_4$.

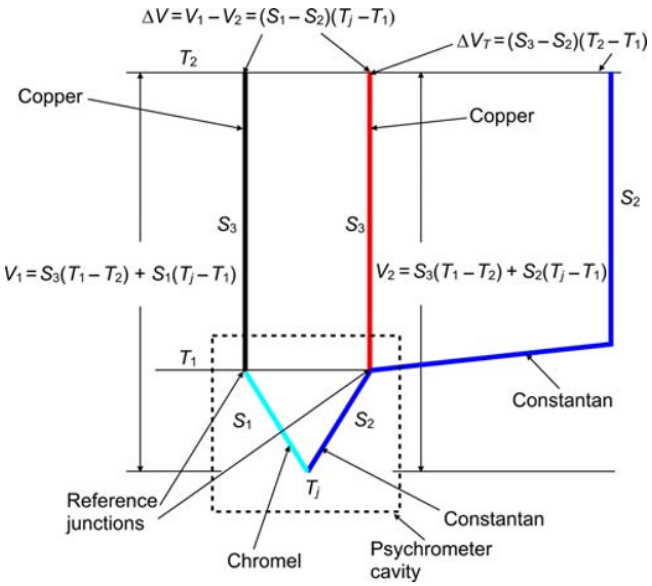

Fig. 14.6 Arrangement of thermocouples in a soil psychrometer. Copper leads from the primary thermocouple to the measuring instrument eliminate voltage differences caused by the leads. The measured voltage is proportional to the difference in temperature between the primary thermocouple junction and the reference junctions with the copper leads. The auxiliary copper–constantan thermocouple measures the difference in temperature between the measuring instrument and the thermocouple cavity. (*See insert for colour representation of the figure.*)

the copper leads from the two arms of the primary thermocouple are of identical material, the voltage difference caused by the temperature difference between the psychrometer cavity and the measuring instrument is eliminated, provided that there is no temperature difference between the two reference junctions or between the terminals of the measuring instrument. The copper–constantan auxiliary thermocouple measures the temperature of the psychrometer cavity using an internal temperature reference in the measuring instrument.

Part IV Water Content – Potential Relations

15 Soil Water Characteristic Measurement

15.1 Introduction

The relation between soil water content and potential is variously described as the 'soil water characteristic', the 'water release function' and the 'water retention curve'. The second and third of these appear to imply only the relationship where the soil starts in a wet state (possibly saturated) and measurements are made as it dries out. We shall use the term 'soil water characteristic' for this reason.

Soil water characteristic curves have traditionally been made in the laboratory with idealised materials, such as slate dust, glass beads or sand, or with soil samples taken from the field, sometimes after sieving out large particles and repacking, but also on soil cores collected as far as possible without disturbance. The most common measurement methods are tension tables, vacuum and pressure chambers and equilibration over solutions of known osmotic potential.

There are relatively few instances available of such measurements being made in the field and even fewer where the field measurements on *in situ* soil have been compared with those on 'undisturbed' cores in the laboratory. For these reasons, it is appropriate to highlight laboratory methods for measurements on field soils.

Many of the methods used to measure the unsaturated hydraulic conductivity of the soil also yield, either explicitly or implicitly, the soil water characteristic. Most of these are covered in the next chapter, but one such, mentioned in Section 15.4.9, is Wind's method.

15.2 Limitations and Hysteresis

Laboratory measurements are nearly always made on small samples of soil. Even where those samples are truly undisturbed from their field state, many structural pores (e.g. cracks or the spaces between aggregates) and macropores (old root channels, wormholes, etc.) are rarely sampled in soil cores but are usually within the measurement volume of field water content sensors. The result is a bias away from the largest pores, that is, high matric potential.

The majority of published soil water characteristic curves are for only the primary drying curve (see Section 2.1.2). This is mainly because much of the laboratory apparatus lends itself much more easily to this measurement and wetting curves usually take much longer.

Field measurement, whether by monitoring soil over the course of the seasons or by manipulation of the water regime (e.g. irrigation or covering the soil to exclude rainfall), allows observation over multiple wetting and drying cycles, with a range of different end points, thus revealing, in principle, many intermediate scanning curves. It may not (particularly if only natural changes in water status are monitored) include the primary drying and wetting curves, however.

15.3 Determination of Soil Water Characteristics

There are two approaches to measurement of soil water characteristics.

15.3.1 The monitoring approach

In this approach, water content and water potential are measured simultaneously, and a soil water characteristic for the soil built up from a series of pairs of measurements. The measurements may be made in the laboratory or *in situ* in the field.

In the laboratory, soil samples are taken from the field and stored in sealed containers to preserve the water status of the samples. A measurement is then made of the water potential by one of the methods described in Chapters 12–14. For high water potentials, this should be a tensiometer (small diameter ceramic cups are available from a number of manufacturers, as well as complete mini-tensiometers). Agus and Schanz (2005) have provided a good review and intercomparison of four methods for making measurements in the lower water potential

Soil Water Measurement: A Practical Handbook, First Edition. J. David Cooper.

range – non-contact filter paper, relative humidity meter, soil psychrometer and chilled-mirror hygrometer. The chilled-mirror hygrometer appeared to provide the most reliable measurements, followed by the soil psychrometer, although with no absolute standard to compare against, it is difficult to be categorical. These two methods are the most firmly rooted in physical theory. Agreement between the different methods improved towards the lower water potentials (–1000 m water – –10 MPa). At the higher and more hydrologically or agriculturally relevant potentials, discrepancies between the measurements of a factor of two or more were found.

Following measurement of the water potential, water content of the sample can be made by weighing and oven-drying, as described in Chapter 6.

In situ measurement in the field is made by simultaneous measurements of water content and water potential using instrumentation described in Chapters 6–14. The soil volume sampled by each type of instrument is never exactly the same, and so some uncertainty arises from this cause. To minimise this, the water content and potential sensors should be installed as close to one another as possible, consistent with their not interfering with one another, that is, the water potential sensor must be outside the volume of influence of the water content sensor.

15.3.2 The imposed status approach

The alternative approach is to manipulate the soil water status in some manner in an attempt to impose a particular value or series of values of either water content or water potential and then measure the other variable. In this way, a set of paired values of water content and potential can be collected, and the soil water characteristic relationship built up.

This approach is more suitable for laboratory determinations of the soil water characteristic than in the field, although manipulation of water content by irrigation or covering the soil to protect it from rainfall is possible.

In principle, measurements can be made for both wetting and drying sequences.

15.4 Laboratory Measurements on Field Soil Samples

15.4.1 The tension table

The principle behind the tension table is that a predetermined matric potential is imposed on a soil sample placed on the table. The matric potential is usually adjusted to the desired value by means of a hanging water column. The tension table was described briefly in Section 13.5.2. Soil samples are placed on the table and not embedded within it, as was shown in Fig. 13.7. A layer of fine sand may be used to improve contact between the soil and the porous bed of the table. Potential equilibrium is achieved between the two, although in many cases this may take several days or even weeks. The attainment of equilibrium must be checked periodically by weighing the soil sample. Once equilibrium has been achieved, the sample(s) may be replaced on the tension table, the hanging water column adjusted to a new height, and the process repeated.

An alternative to a hanging water column is use of a vacuum pump, which is set to switch on or off at the appropriate level. The lower surface of the porous bed is at a zero matric potential relative to the atmospheric pressure beneath it. So if the vacuum is set to a pressure G below atmospheric, then the matric potential at this point will be $-G$, and if the bed is of a thickness T, the matric potential at the top of the bed and hence at the base of the sample when equilibrium has been achieved is $-(G+T)$. Much more precise control of the water potential can be achieved with a hanging water column than with a vacuum pump and so is preferred for water potentials close to saturation. In most laboratories, it is difficult to achieve a hanging water column of more than about 1.5 m, however, and so a vacuum pump may be appropriate in those circumstances. The lower accuracy attainable using a vacuum pump is less likely to be a serious problem at pressures substantially below atmospheric.

Errors involved in tension table determinations

Errors in defining the precise pressure to which the sample is subjected have been discussed in the previous paragraph in relation to the vacuum pump. For the hanging water column, there is a small uncertainty involved in defining the pressure as a consequence of changes in temperature of the laboratory, thus affecting the density of water. These are, however, likely to be very small in comparison to changes in the soil water characteristic of the soil caused by temperature changes. In the simplest case, this may be envisaged as a consequence of change in the surface tension of water with temperature, through the capillary rise equation (2.1.1), but is complicated in many soils by other changes in the interfacial relationship between the water and the soil fabric (Hopmans & Dane, 1986). It is important, therefore, that the experiments be conducted in as constant a temperature environment as possible and also that the temperature be known. Ideally, this should be close to the temperature obtaining in the soil, which often varies over a substantial range, especially close to the surface.

Disturbance to the soil structure upon sampling is likely to have a significant effect on the soil water characteristic close to saturation, as it affects mostly the larger pores such as those between aggregates. Similarly, the repeated removal and replacement of the sample for weighing can disturb the structure, as well as cause loss of small amounts of soil from the sample during the procedure. Some material may also be gained if it is picked up from the bed of the tension table.

Determination of the characteristic curve on small samples means that larger-scale structural features are not sampled, and so the contribution of these to soil water content close to saturation will be ignored. Other features at a scale a little smaller than the sample are likely to vary

significantly from one sample to another nominally 'identical' one and so make interpretation of the bulk soil water characteristic difficult.

The bed of the tension table determines only the matric potential at the base of the sample, ψ_b. At equilibrium, if the height of the sample is h, the matric potential at the top of the sample is $\psi_b - h$ and the average matric potential is $\psi_b - (h/2)$. If the sample height is not too large and the soil water characteristic is reasonably linear over the height range, then the assumption that the water content of the sample relates to the average matric potential is reasonable. Where there is a sharp bend in the soil water characteristic, however, this may not be the case. The method also assumes, implicitly, that the soil water characteristic from top to bottom of the sample is homogeneous. This is very questionable, particularly close to the soil surface.

Evaporation of water from the sample during the equilibration process or while weighing will introduce errors in measurement of the water content. Therefore, it is essential that the tension table be covered, that it is not in a position where there is a large airflow and that samples be weighed quickly once removed from the table.

15.4.2 Haines apparatus

The Haines apparatus is very similar to the tension table. The main difference is that the porous bed of sand and/or kaolin is replaced by a Buchner funnel, with a porous plate. Normally only one sample can be placed into each funnel because of the size of funnels available (Fig. 15.1).

The funnel and sample ring sizes should be chosen such that it is easy to emplace and remove the sample from the porous plate. Although only one sample can be put onto each porous plate, it is quite simple to run several funnels simultaneously by including a manifold into the flexible tube.

Most of the comments mentioned in connection with the tension table apply equally to the use of the Haines apparatus.

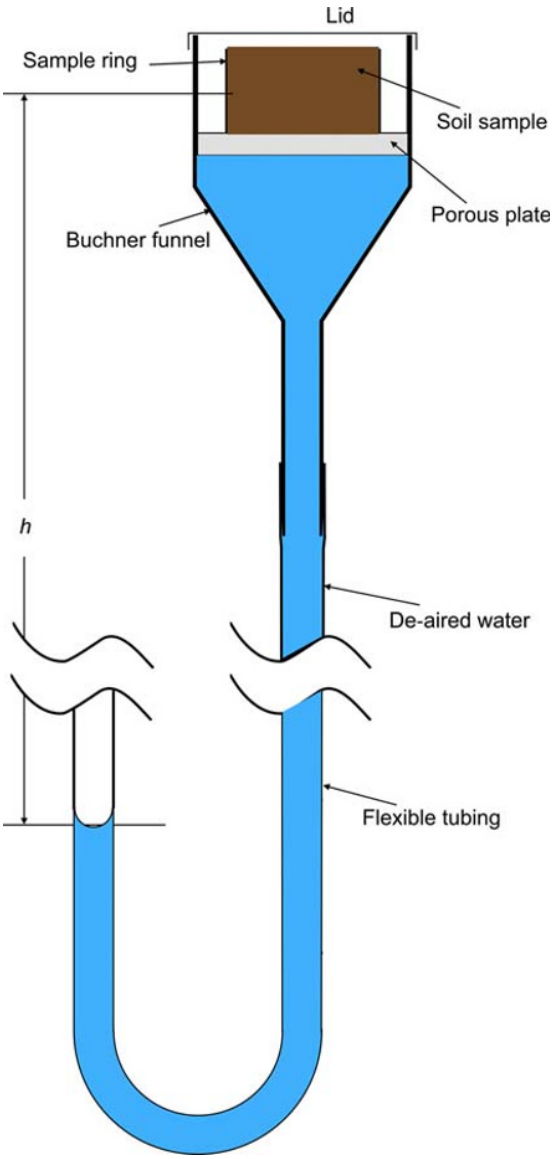

Fig. 15.1 Haines apparatus.

15.4.3 Vacuum chamber

The vacuum chamber is another variant on the tension table, in which the porous bed is replaced by a porous ceramic plate with an air entry value of about 10 m water (1 bar). It was described briefly in Section 13.5.3 and a diagram shown in Fig. 13.8. Apart from the use of a vacuum instead of a hanging water column to impose a suction on the sample(s), operation is, in essence, almost identical with that of a tension table or Haines apparatus.

15.4.4 Pressure chamber

The operation of a pressure chamber was also covered briefly in Section 13.5.3 and depicted in Fig. 13.8. Rather than impose a suction on the water-filled pores of the sample, the air pressure surrounding it is increased, with the water draining out *via* a porous ceramic disc or thin cellulose membrane into a burette or similar, with a thin layer of oil to suppress evaporation. The water collected can be measured by this means and hence the approach to equilibrium monitored.

Pressure chambers are usually used for measurement of water retention at low (<–10 m water) matric potentials. There is usually little dependence of water content on the soil structure at these potentials, and so disturbed samples are often used. Because the diffusivity of the soil becomes very small at low potentials, the approach to equilibrium is often slow, and a measurement at one pressure could take some weeks. Because of this, it is often difficult to be sure that equilibrium has been achieved and the temptation to cut short the experiment must be resisted. Plotting the water content of the sample (or the amount of

water collected in the burette) against the logarithm of time will help to avoid a false judgement of equilibrium having been reached. Also, to keep equilibration time as short as possible, the height of the sample is usually quite small (~10 mm).

An implicit assumption of the technique, as with other *axis translation* methods, is that the size and shape of the pores holding the water are unaffected by imposition of a high atmospheric pressure. This is difficult to verify.

It is difficult (though not impossible) to use a pressure chamber to investigate the wetting branches of the soil water characteristic, partly because of the time required to attain equilibrium, but also because the design does not lend itself easily to imbibing water as opposed to expelling it.

15.4.5 Mercury intrusion porosimetry

Another axis translation technique, suitable for measurement at low potentials, relies on forcing mercury, a non-wetting fluid, into the pores of an initially dry soil under vacuum. For most solid materials, the contact angle with mercury is greater than 90°, that is, the solid surface repels the mercury, in contrast with water, where wetting usually lowers the total energy of the system. Using mercury, pressure must be applied to force it into the soil pores. By monitoring the volume of mercury forced into the sample as a function of applied pressure, an estimate of the distribution of pore sizes can be made. This is similar in principle to the operation of a pressure chamber, in which a non-wetting fluid (air, rather than mercury) is forced into the pores of the soil to replace water. Therefore, intrusion of mercury into a sample corresponds with desorption of water from it.

The basic equation relating pore radius, r, to the pressure differential, P, across a fluid interface is given by Equation 2.1.1, which is

$$P = -\frac{2\gamma}{r}\cos\phi, \qquad (15.4.1)$$

where

γ is the surface tension of the fluid (0.485 N m^{-1} for mercury at 25°C; *cf.* water 0.072 N m^{-1}) and

ϕ is the contact angle.

As with water, the contact angle is not easy to predict, and, while it is most commonly assumed to be zero for water, a value of 130° is often assumed for mercury, giving a value for $\cos\phi$ of –0.643. The negative sign signifies that the soil fabric repels mercury.

Mercury intrusion porosimeters are made by several manufacturers. They are usually fully or partially automated and can measure over a wide range of pressures (*ca.* 3 kPa to 400 MPa), corresponding to pore diameters of about 0.4–3 nm. This is equivalent to water held at matric potentials of –70 mm water (–7 hPa) to –9000 m water (92 MPa). The range is much greater than can be achieved with a pressure chamber, which can usually span matric potentials down to –150 m water (–1.5 MPa) or pore diameters of 190 nm. More importantly, for most hydrological purposes, the process is much quicker, allowing the whole range to be covered in a few hours, excluding the time taken in sample preparation, which may be considerable. Unfortunately, porosimeters are also very expensive, and the maximum sample volume is only a few millilitres.

For rigid soils and rock, sample preparation is relatively straightforward, requiring that it be oven-dried and outgassed under vacuum for a few hours. Most porosimeters operate in two ranges to cover the wide span of pressures used. After pumping the sample chamber to vacuum, mercury is introduced to fill the rest of the volume and pressure increased slowly. The intruded volume is monitored by measuring the retreat of a mercury meniscus in a glass capillary using the capacitance between a metal sheath around the capillary and the mercury itself. Pressure is measured by pressure transducers with different ranges.

The instrument may be operated in a continuous mode, where the pressure is increased steadily and both pressure and intruded volume are measured continuously. Alternatively, a number of set pressures may be chosen and the pressure maintained at each for some minutes to allow both the amount of intruded mercury and the temperature to stabilise. The hydraulic resistance of small pores means that it often takes some time for mercury to intrude fully and equilibrium to be achieved (Giesche, 2006). In this mode, a measurement cycle may take a few hours. Many porosimeters are capable of measuring the pressure–volume relationship while the pressure is reducing and mercury extrudes from the sample. Hysteresis between the intrusion and extrusion cycle is observed, as for water in a porous medium, and some mercury is usually left in the sample, trapped in pores that become isolated. For rigid soils and porous rock, good agreement is often found between porosimeter measurements and those obtained by a pressure chamber (Bruand & Prost, 1987).

For soils containing a significant amount of swelling and shrinking clays, the situation is more complicated, since drying normally causes the maximum amount of shrinkage. Techniques are available to avoid significant shrinkage and alteration of the pore structure by freeze-drying, critical point drying or replacement of water by non-polar liquids (Lawrence, 1977). This would then allow mercury intrusion experiments to produce an estimated pore size distribution for the soil water status corresponding to that at which the soil was dried by one of these techniques. However, because of shrinkage, this cannot be expected to agree with the soil water characteristic. Lawrence *et al.* (1979) found considerable change in the pore size distribution resulting from freeze-drying (rapid freezing of the soil by immersion in liquid nitrogen, then drying under vacuum so that water is removed by sublimation). This was attributed to disruption caused by growth of ice crystals. Less disturbance was caused by critical point drying (replacement of water by methanol, then the methanol replaced by liquid carbon dioxide, which is evaporated).

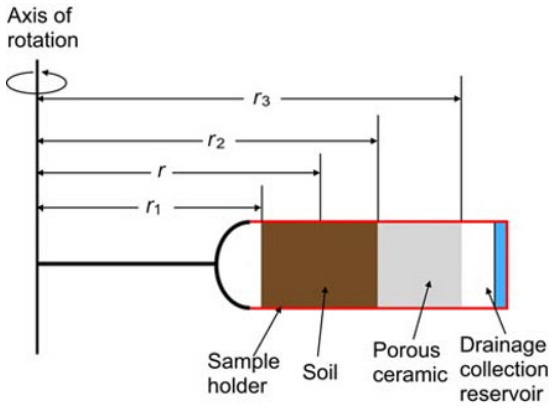

Fig. 15.2 Schematic diagram of a centrifuge to measure the soil water characteristic.

15.4.6 Centrifuge method

Rotating any body in a centrifuge is equivalent to increasing the gravitational force acting on it. The relation between the acceleration, f, speed of rotation, s, and distance from the centre of rotation, r, is given by (Fig. 15.2)

$$f = 4\pi^2 s^2 r. \tag{15.4.2}$$

This is equivalent to increasing the force of gravity at that point by a factor $4\pi^2 s^2 r/g$, where g is the acceleration due to gravity. This principle forms the basis of the centrifuge method, which effectively increases the gravitational force on the sample, and so allows more water to drain from it against capillary forces. A schematic diagram of the arrangement of a soil sample in a centrifuge is shown in Fig. 15.2.

At the distance r from the centre of rotation, the acceleration experienced by the water in the soil is given by Equation 15.4.2. This must be balanced at equilibrium by the gradient of matric water potential, which, in compatible units, is

$$\rho_w g \frac{d\psi_m}{dr} = 4\pi^2 s^2 r \rho_w, \tag{15.4.3}$$

where the density of water, ρ_w, has been introduced on the right-hand side to convert the acceleration to a force per unit quantity of water. Integrating both sides with respect to r gives

$$\psi_m(r) - \psi_m(r_3) = \frac{4\pi^2 s^2}{g}\left(r^2 - {r_3}^2\right). \tag{15.4.4}$$

But if water is to drain from the porous ceramic, the matric potential, $\psi_m(r_3)$, at this point must be zero. Hence

$$\psi_m(r) = \frac{4\pi^2 s^2}{g}\left(r^2 - {r_3}^2\right). \tag{15.4.5}$$

Because the matric potential varies quadratically, the average matric potential in the sample is not located at the midpoint nor is it the average of that at the top and bottom end of the sample ('top' and 'bottom' here referring to the ends nearest and furthest away from the axis of rotation). In some investigations, there is no ceramic plug at the base of the sample. Under these circumstances, the matric potential at the bottom of the sample is zero and that at the top is $(4\pi^2 s^2/g)({r_1}^2 - {r_3}^2)$, while the average is $(4\pi^2 s^2/3g)(r_1 - r_3)(r_1 + 2r_3)$, which is lower than the mean of the potential at the top and bottom surfaces since $(r_1 + 2r_3)/3 > (r_1 + r_3)/2$. The range of water potential is, however, large. Nevertheless, Reatto *et al.* (2008) obtained very good agreement between soil water characteristics obtained by this method and with those using a pressure chamber even though their centrifuge method imposed zero matric potential at the bottom of the sample. Khanzode *et al.* (2002) also found similar results for both methods using repacked silt and clay soils. Some significant differences between the methods were attributed to differences in dry bulk density, although compaction as a result of the large forces imposed could not be ruled out. In this case, the samples were placed on a ceramic cylinder, which would have reduced the range of potentials in the samples.

Commercially available centrifuges are obtainable in different sizes and maximum speeds. Most, however, can spin at up to several thousand revolutions per minute (divide by 60 to obtain revolutions s^{-1} for use in the above formulae), with radii up to 300 mm or more. With the larger and faster centrifuges, this can comfortably exceed the normal range of the pressure chamber of –150 m water. Centrifuges usually have temperature control which allows measurements to be made different temperatures. Non-rigid soils may compress under the high acceleration, leading to some change in pore structure and therefore the soil water characteristic.

15.4.7 Vapour equilibration over aqueous solutions

The procedure for calibration of filter papers for water potential measurement was briefly outlined in Section 13.7.1. The method is also suitable to bring a soil sample to a defined potential in the very dry range. Very good temperature control is necessary and equilibration times are often long, perhaps a few weeks, even with a sample of only a few grams. Because the practical size of a sample is so small, the soil must be disturbed, although intact small aggregates (crumbs) can be used. Apart from a very accurate balance weighing to better than 1 mg, no other special equipment is necessary, although a good desiccator is an advantage to contain the aqueous solution and the samples. The samples must be held close to, but not in contact with, the liquid. For most purposes, mercury intrusion porosimetry or the centrifuge method will give results much more quickly at the dry end of the water content range, although vapour equilibration is capable of achieving considerably lower water potentials than either of these methods.

It should also be borne in mind that, since equilibration is *via* the vapour phase, the sample's osmotic plus matric potential will come to equilibrium with the osmotic potential of the solution and so any salts in the sample will have an effect on the water content achieved.

15.4.8 Controlled osmotic pressure

In many ways, this method is the reverse of the osmotic tensiometer (see Section 14.3). The sample is allowed to come into equilibrium with a solution of high osmotic pressure, usually polyethylene glycol (PEG), through a semipermeable membrane, often made from dialysis tubing. Most soil solute ions can pass through this, but the PEG molecules, being much larger, cannot. The method therefore imposes a known matric potential on the soil.

Dialysis membranes are fragile and must be treated with great care to avoid puncturing them; they are also prone to microbiological degradation, which limits their useful life. Zur (1966) found that it was necessary to sterilise the soil before making the measurements. A schematic set-up is shown as Fig. 15.3.

Since the method is useful at low water contents, where the soil water diffusivity is very small, the approach to equilibrium may be slow. The samples need, therefore, to be thin. Zur (1966) used samples 9.5 mm thick and 16 mm diameter, with a double cellophane membrane separating it from the osmotic solution on each side. Equilibrium was attained in 72 hours, about the same time as required in a pressure chamber. The relatively small volume of solution was changed several times to counteract dilution of the solution.

Waldron and Manbeian (1970) packed samples into a 14.3-mm-diameter length of dialysis tubing and suspended this in a 7-L bath of stirred PEG 6000 solution at a range of concentrations at a constant temperature. They claimed to achieve equilibrium within 48 hours and obtained results which compared well with those derived by conventional methods for a range of soils.

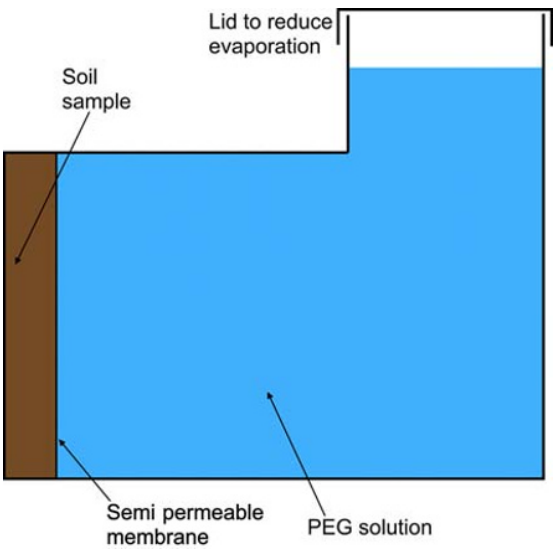

Fig. 15.3 Schematic of apparatus for controlling the water potential of a soil sample by osmosis.

15.4.9 Monitoring of the evolution of water status

All of the methods described so far aim to impose a known or series of known water potentials on the soil sample. Wind (1968) took a different approach.

In brief, Wind (1968) instrumented a soil column with matric potential sensors (in his case nylon/gypsum resistance blocks) at several depths. The column was saturated, the bottom end closed off, and the water in the column allowed to evaporate in the laboratory environment. The column was weighed periodically to determine the amount of water lost.

Since water could be lost from the column only through the top surface of the soil, the water flux at that point was known. Wind started with an assumed soil water characteristic drying curve and used this to make a first estimate of the water content as a function of time at each depth at which a sensor was installed. Wind used a similar method to estimate the change of water content in each layer between sensors as described in Section 7.9.2. The accumulated water flux at each measurement depth between reading occasions was calculated, starting with the deepest measurement depth. Since there was no water flow across the bottom of the column, the accumulated water flux across this depth was equal to the change in water storage of this layer. Similarly, the accumulated flux across the next deepest measurement depth was equal to the change in water storage of the bottom two layers. The total change of water content of the whole column could therefore be calculated and compared with the change in mass of the column. Since the former was based on an estimate of the soil water characteristic, the two would not be expected to agree. Wind therefore multiplied the water content at each potential measurement point of the estimated soil water characteristic by the ratio of the total measured water content change of the column to that calculated from the potential measurements. This was done for all of the measurement occasions, producing a fairly large number of data points, through which a corrected soil water characteristic curve could be drawn. This curve was used with the same experimental data to produce another improved estimate of the soil water characteristic. After four or five iterations, a stable curve emerged which agreed very well with the curve measured by conventional methods.

For his experiments, Wind used a 400-mm-long column of repacked soil, although he recommended ones not longer than 200 mm be used. The method depends on homogeneity of the soil, so that the soil water characteristic is the same at all depths. For field samples, much shorter (50-mm) columns can be used, together with automatic recording of the tensiometers and sample mass. Wind used

freehand graphical methods to estimate the soil water characteristic, but with digital recording and modern computers, a suitable parameterised equation, as discussed in Section 15.6, is more commonly used, with non-linear fitting of the parameters to obtain a best fit.

With more modern equipment, the water content at each depth can be measured by, for instance, TDR, and more accurate water potential measurements can be made – in the wet range by tensiometers and in the drier range by one of the methods described in Chapter 14. Schindler *et al.* (2010) used a modification of Wind's method with high-capacity tensiometers (Section 14.4) at two depths to obtain both soil water characteristics and unsaturated hydraulic conductivity functions for a wide range of soils. No water content measurements other than monitoring the column weight were made. Experiments for samples 50 mm high and 80 mm diameter took a few days each to cover the range of water potential down to –29 to –43 m water, where the tensiometers broke down.

15.4.10 Controlled liquid volume

Instead of imposing a particular water potential on a soil sample, its water content may be controlled, although the method is not commonly used, probably because excessive time is needed for undisturbed samples to achieve equilibrium.

Winfield and Nimmo (2002) describe an apparatus for making measurements on undisturbed soil samples. A sample, covered to prevent evaporation, is mounted on a porous plate with an air entry value higher than the expected absolute value of matric potential. A two-way tap allows a predetermined volume of water to be introduced into the bottom of the soil sample *via* the porousplate. The tap is then turned to connect the porous plate to a pressure transducer, which monitors the change in water potential until equilibrium is achieved. A tensiometer close to the upper surface of the sample would appear to be a useful addition to confirm whether equilibrium had actually been achieved. The method can be used equally well to monitor the soil water characteristic along a drying curve by connecting the burette to a vacuum pump, allowing water to be withdrawn from the sample.

15.5 Field Measurement of Soil Water Characteristics

The last section focussed on laboratory measurements that are suitable for making measurements of soil water characteristic curves on disturbed or 'undisturbed' field samples. Collecting such information in the field is difficult, and there are few published examples, with the result that most curves in the literature have been obtained in the laboratory with the hope that this applies to field soils. As mentioned earlier, there is a paucity of published comparisons between laboratory-measured and field-measured curves.

Reasons for a significant difference between the two approaches include the following:

- It is difficult to collect truly undisturbed samples of soil, particularly of a size suitable for most laboratory methods.
- Large structural features, particularly macropores which are spatially continuous over distances of up to several metres, are difficult if not impossible to preserve or replicate in the laboratory.
- While, in principle, it is possible to conduct laboratory experiments at almost any desired temperature, in practice they are almost always performed at an approximately constant temperature in the range 18–25°C. In the field, temperature changes on a diurnal and seasonal basis, often over a large temperature range, and, depending on geographical location, the average temperature may be well above or below that range.
- It is difficult to replicate the composition of the soil solution, which may have a significant effect on the soil's hydraulic properties and which itself changes in response to both natural and artificial (e.g. agricultural) influences.

From the foregoing, it should be clear that there may be systematic differences between laboratory- and field-measured hydraulic properties but also that there is unlikely to be a unique curve that will characterise the soil, even at a particular depth. In addition:

- Spatial variability of soil properties means that the relationship may vary dramatically from place to place.
- The range of water status observed in the field is often much more restricted than can be achieved in the laboratory. This may or may not be important, depending, for instance, on whether knowledge of the pore sizes not sampled is needed for modelling the transport behaviour of the soil or if predictions are needed for particularly wet or dry conditions.
- The sensors used for water content and water potential measurement almost always average over different soil volumes and are usually separated spatially from one another.

Field measurements, therefore, have the advantage of being carried out on soil in its natural state and in association with other aspects of its local environment. Laboratory measurements, on the other hand, are usually made on a limited number of small samples which may or may not be representative of the range of properties found in the field situation, but which can be measured individually to great precision.

The actual process of measurement is quite straightforward and can be summarised as 'install sensors to measure water content and potential at the desired depths, make measurements as often as practicable and see what emerges'. The instruments may well be installed for other monitoring purposes in any case, for instance, for agronomic monitoring or to measure water and/or solute balances, so obtaining soil hydraulic property information serves to extend the usefulness of the instrument array.

In principle, any of the water content and water potential sensors described in Chapters 7–14 may be used. Some general recommendations are:

- Place the different kinds of sensor as close to one another as is practical, consistent with their not interfering with one another either hydraulically or by affecting the measurement principle.
- If possible, install replicate sets of instrumentation, so that an estimate of spatial variability is available.
- It may be necessary to install more than one type of sensor to cover the full range of water status experienced; for example, tensiometers for high water potentials and a porous matrix sensor for lower ones, bearing in mind that the latter has much lower accuracy.

It should be clear from the discussions above that, while almost all laboratory procedures are of the imposed status type, field measurements employ almost entirely the monitoring approach. Manipulation of soil water status in the field is possible, for instance, by irrigation or excluding rainfall, and hence extending the range of conditions, achieving a target water potential or water content with any accuracy, is, in most situations, impossible.

Some practical examples of field-measured soil water characteristics will now be given.

15.5.1 Neutron probe with manual tensiometer measurements

Because of the large measurement volume of the neutron probe, a tensiometer cannot be placed safely closer than about 0.5 m away. There may, therefore, be problems caused by the two measurements being in somewhat different environments, particularly if there is significant spatial variability at this scale. Water-repellent soils and others where fingering is induced are an obvious such situation. Likewise, there can be a problem when a wetting front penetrates the soil. The large measurement volume means that the neutron probe is likely to detect the presence of the wetting front before the tensiometer at the same depth, suggesting that water content rises before a concomitant rise in potential resulting in a hysteresis loop going in the opposite direction from those depicted in Fig. 2.3. Good data can, however, be obtained using such a pairing, as illustrated in Fig. 15.4.

The two sites illustrated in Fig. 15.4 show a large contrast both with depth and between the sites. Although the absolute water content at all depths and matric potentials in (a) is much higher than in (b), the scale increment for each is identical. Site (a) exhibits a transition from a fairly wide pore size distribution in the soil at 0.2 m,

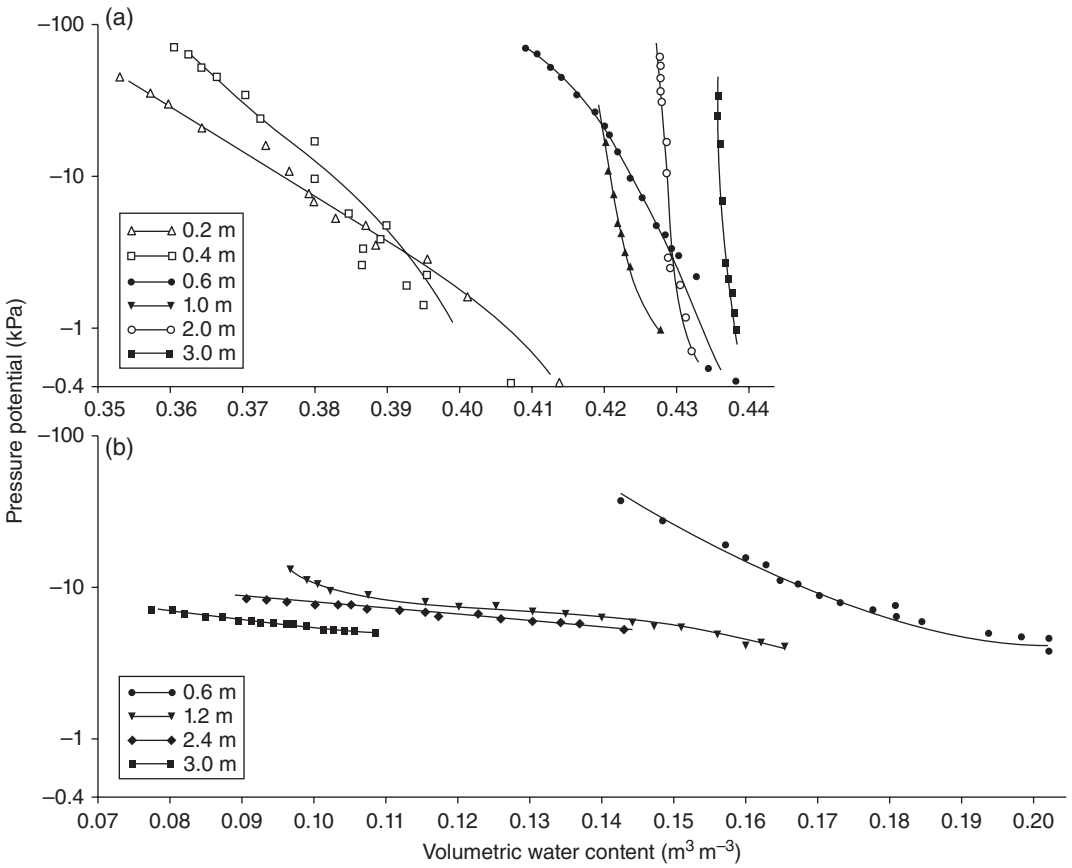

Fig. 15.4 *In situ* soil water characteristics measured at two grassland sites in southern England: (a) a thin (~0.2-m) soil over chalk and (b) a sandy loam overlying sand. From Cooper *et al.* (1990).

through weathered chalk (0.4–1.0 m) to essentially fresh chalk at 3.0 m. The last has storage in fractures only at matric potentials down to about –0.25 m water and loses no more water until matric potential falls below –10 to –30 m water. Site (b) also shows a transition from loamy soil above 1 m to unconsolidated sand beneath. At all depths, however, much more water is released for a given change in matric potential than at site (a). Site (b) also illustrates that the range of water potential observed can be very restricted.

15.5.2 Other separate combinations

In principle, any of the methods described in Chapters 7–9 for water content and Chapters 12–14 for water potential measurements at a 'point' can be paired to produce soil water characteristic relations. For instance, Mahmood-ul-Hassan and Gregory (2002) used both neutron probes with puncture tensiometers read manually and Theta Probes with pressure transducer tensiometers recording half-hourly. Some of the soil water characteristic curves they derived are shown in Fig. 15.5.

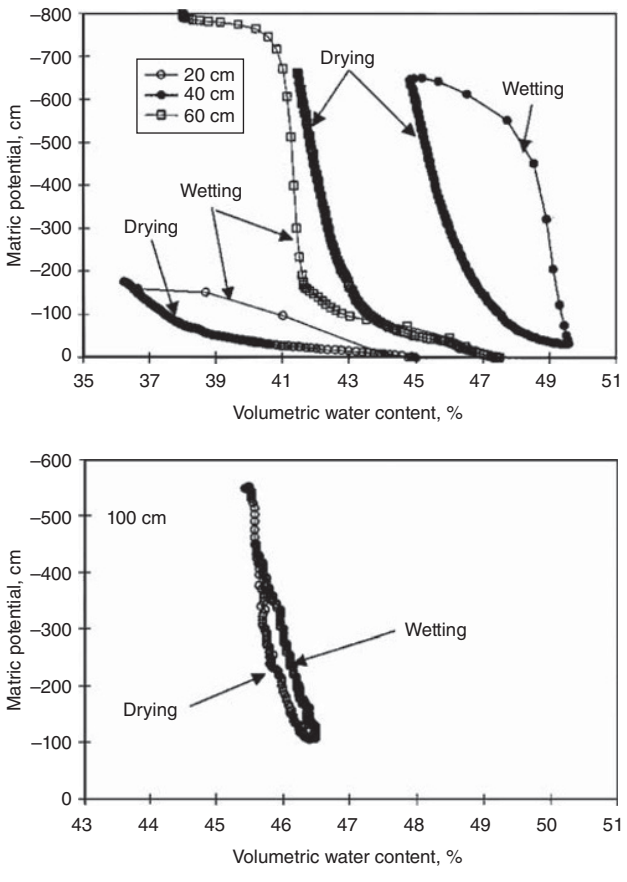

Fig. 15.5 Soil water characteristic curves published by for a grassland site on chalk in southern England (Mahmood-ul-Hassan & Gregory, 2002). From Mahmood-ul-Hassan & Gregory (2002). Reproduced with permission of Elsevier.

Note that the hysteresis loops for three of the depths are in the opposite sense to those illustrated in Fig. 2.3 which are generally accepted as being of universal applicability. Mahmood-ul-Hassan and Gregory (2002) speculated that this might be associated with the dual porosity nature of the soil. However, two other explanations seem equally likely. The 0.5-m lateral separation between the tensiometers and the Theta Probes may mean that the tensiometers were fortuitously placed in a location where the soil wetted slightly later than the location of the associated Theta Probe. Alternatively, the wetting may well have proceeded at a rate too quickly for the tensiometers to respond fully. In the case of the 60-cm tensiometer, wetting starts at a low potential, where there is a very good chance of there being a significant amount of air in the tensiometer. In addition, the tensiometers were embedded into chalk slurry during installation, which may have provided a low conductivity barrier around the cup. Either of these effects would slow down the tensiometer response.

Similar studies have been published by Arya *et al.* (1975a), who used gravimetric samples with tensiometer measurements in the field to obtain good (although rather noisy) agreement with conventional soil water characteristic measurements; by Watson *et al.* (1975), who used frequent gamma ray transmission and pressure transducer measurements collected automatically from an isolated soil monolith in the field to resolve a single hysteresis loop; and by Royer and Vachaud (1975), who were able to resolve substantial hysteresis loops from field-measured water content and potential using daily neutron probe measurements and automatically recorded pressure transducer tensiometers (Fig. 15.6).

15.5.3 Combined water content and potential sensors

Baumgartner *et al.* (1994) and Whalley *et al.* (1994) both described a combined TDR and soil matric potential sensor using metal tubes to act also as the TDR rods. In the former, the porous barrier for the tensiometer part was a short length of porous stainless steel tube and in the latter, small diameter porous ceramic cups. In both cases, the tensiometer was of the puncture type (Section 12.5.5). The major advantage of the design is that, although both the TDR and the tensiometer parts do not measure in the same volume of soil, they are very close to one another (with some overlap in the case of Baumgartner *et al.*'s (1994) design). As a result, the instruments produced much better-defined soil water characteristic curves than those using separated sensors. A diagram of Whalley *et al.* (1994)'s design is shown in Fig. 15.7, with an example of a hysteresis curve for a sandy loam soil produced by it in Fig. 15.8. Whalley *et al.* (1994) used the instrument to measure the hydraulic conductivity as a function of matric potential in the field.

A similar arrangement of a tensiometer cup fixed to the end of a TDR probe was described more recently by Karunarathna *et al.* (2010). In this case, the TDR probe was similar to that of Nissen *et al.* (1998) and shown in Fig. 8.25.

Noborio *et al*. (1999) used TDR to measure both the water content of the soil and that of a porous matrix located on different portions of the length of the rods. The rod spacing and diameter was different in the two parts to allow a clear distinction to be made of each on the TDR trace. Vaz *et al*. (2002) also used TDR in a combination probe. Their version used a coiled TDR probe wrapped around a tensiometer cup. The relationship between TDR travel time and relative permittivity of the medium is different from that of rods buried completely in the medium because of the presence of the ceramic cup. The permittivity of the ceramic cup was also found to vary with matric potential. Good agreement between soil water characteristics and those determined by conventional means was found in laboratory tests, although the region of influence of two wires 3 mm apart wrapped around a cylinder is presumably very small and likely to be subject to disturbances caused by the installation process in the field.

Sun *et al*. (2010) used a commercially available stainless steel-bodied pressure transducer tensiometer to measure both water content and water potential in a laboratory

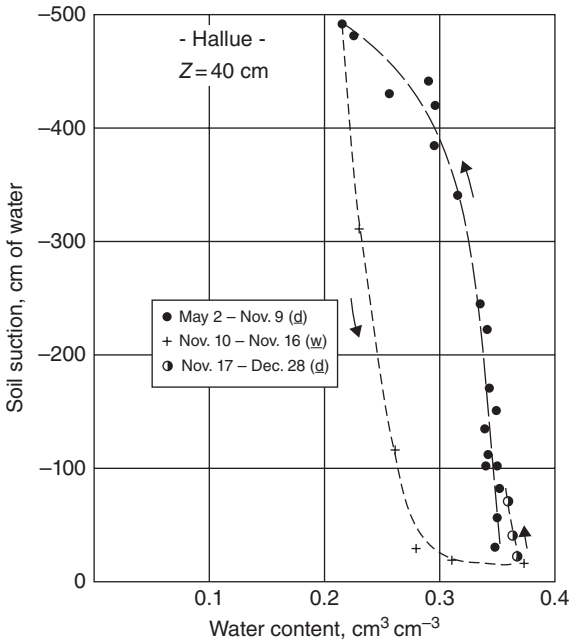

Fig. 15.6 Soil water characteristic for a clay soil measured using a neutron probe and pressure transducer tensiometers showing substantial hysteresis (Royer & Vachaud, 1975). From Royer & Vachaud (1974). Reproduced with permission of the Soil Science Society of America.

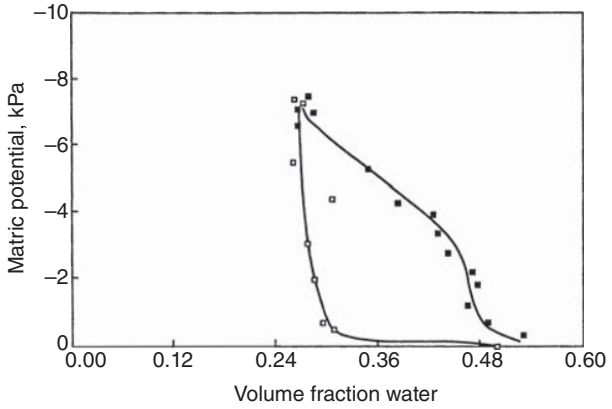

Fig. 15.8 Hysteresis curve obtained from the combined instrument of Whalley et al. (1994). From Whalley et al. (1994). Reproduced with permission from Elsevier.

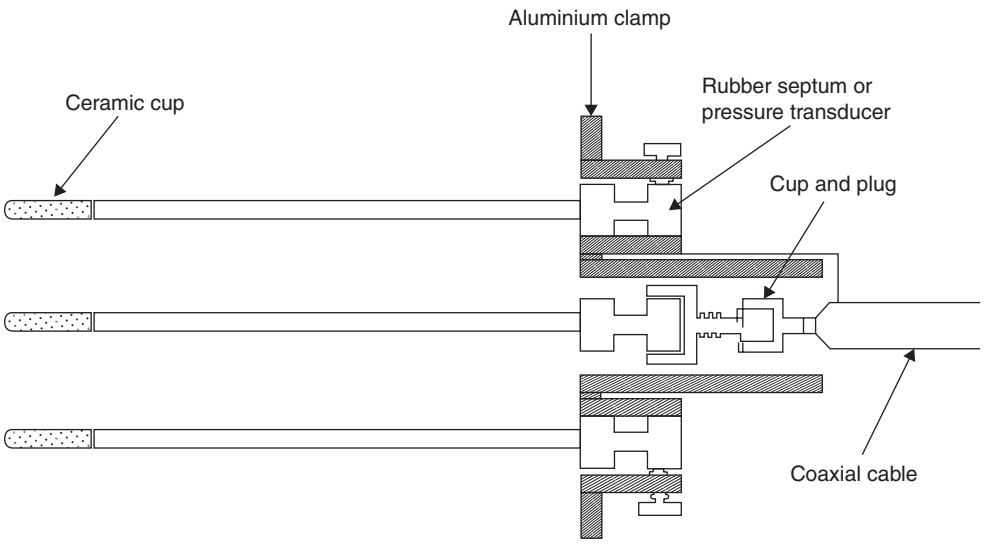

Fig. 15.7 Diagram showing the arrangement for a combined tensiometer and TDR water content sensor (Whalley *et al*., 1994). From Whalley *et al*. (1994). Reproduced with permission from Elsevier.

setting. The 37-mm-long metal body formed an aerial for a 100-MHz wave which radiated into the surrounding medium. The permittivity of the material was calculated from the impedance offered by the medium to the radiation. Laboratory tests were promising. The water content and matric potential sensing portions of this design are not coincident, but, as with the Baumgartner *et al.* (1994) and Whalley *et al.* (1994) instruments, very close to one another. For field use, the device would need to be installed horizontally (or almost so) to eliminate vertical gradients in water status.

15.6 Parameterising the Soil Water Characteristic

For many purposes, it is useful, and for some essential, to be able to express the soil water characteristic as a mathematical relationship between water content and matric potential. A large number of relationships have been suggested, but by far the most common is that attributed to van Genuchten (1980). Van Genuchten's expression is

$$\theta = \theta_r + \frac{\theta_s - \theta_r}{\left[1 + (\alpha h)^n\right]^m}, \tag{15.6.1}$$

where

θ_r is known as the *residual water content*;
θ_s is the saturated water content;
h is the matric potential expressed as a positive number, that is, $h = |\psi_m|$, and
α, m and n are parameters used in the fitting.

The residual water content, θ_r, is supposed to be the water content of the soil at some very low water potential, that is, the water that remains after all the other water which can be extracted has been removed. For this reason, it is often assumed to be zero. More commonly, recognising that the expression is usually fitted to data from a limited range of water content or potential, it is treated as an additional fitting parameter with little or no physical significance.

The equation has proved successful for fitting a very wide range of experimentally obtained soil water characteristic curves and offers considerable flexibility with a relatively small number of parameters. It is described as *closed form* because it is composed of a finite number of simple functions. It is also relatively easily manipulated mathematically, especially if it is assumed that $m - 1 + (1/n)$ is an integer (van Genuchten, 1980). Frequently, this is assumed equal to zero, that is, $m = 1 - (1/n)$, thus reducing the number of parameters by one while sacrificing relatively little flexibility.

The equation does not provide for an air entry potential for the soil, but it can be modified simply to do so. Hysteresis in the $\theta - \psi$ relationship (Kool & Parker, 1987; Luckner *et al.*, 1989) can also be described within the framework of the van Genuchten equation.

For some purposes, simpler equations are appropriate, that of Brooks and Corey (1964) being the most common. Brooks and Corey's equation is

$$\frac{\theta - \theta_r}{\theta_s - \theta_r} = \left(\frac{\psi_a}{\psi_m}\right)^{\lambda}, \tag{15.6.2}$$

where

ψ_a is the air entry potential of the soil and
λ is a 'pore size distribution index', which is usually in the range of 2–5.

Small values of λ are characteristic of soils having a wide distribution of pore sizes, while a large value characterises a soil with quite uniform pore sizes.

The other variables are the same as for Equation 15.6.1.

Parameterisation of the soil water characteristic facilitates similar parameterisation of the hydraulic conductivity relationship (Section 16.2), as well as simultaneous estimation of both the soil water characteristic and unsaturated hydraulic conductivity (Section 17.13).

15.7 Predictive Methods

Because of the time and expense involved in measuring soil water characteristics, much attention has been given to predicting the relationship from more easily measured soil attributes. This is usually the particle size distribution of the soil but may also incorporate bulk density, organic matter content or other factors. The resulting relationships relating these attributes of the soil to its hydraulic properties are known as *pedotransfer functions.*

At its simplest, these are derived from multiple regression analysis between the particle size distribution of a number of soils and their measured hydraulic properties. These can then be used to predict the hydraulic properties of another soil whose particle size distribution is known. The soil water characteristic may be expressed as the water content at a series of different matric potentials or as the parameters of a model relating the two, such as that of van Genuchten (1980). More sophisticated techniques include neural network techniques and more advanced statistical methods to predict hydraulic properties. Recent studies include those of Schaap *et al.* (2001), Pachepsky and Rawls (2003), Rubio *et al.* (2008), Al Majou *et al.* (2008a, b) and Dashtaki *et al.* (2010).

Part V Hydraulic Conductivity

16 Hydraulic Conductivity Measurement and Prediction

16.1 Introduction

The hydraulic conductivity, K, expresses in quantitative terms the ease with which water can flow through the soil from one place to another. It relates the *flux*, q, of water to the gradient of water potential, $d\psi/dz$ as

$$q = -K\frac{d\psi}{dz}. \qquad (16.1.1)$$

This was explained in Section 2.2.1 and Equation 16.1.1 repeats Equation 2.2.1. Because the flux is a volume per unit area per unit time, it has dimensions of a velocity, and the gradient of potential is dimensionless if ψ is in head (i.e. length) units, so K will also have dimensions of velocity ($m\ s^{-1}$ or $m\ d^{-1}$). Very often, the gradient of water potential and the soil water flux is in one direction only, usually vertical. It should, however, be borne in mind that the subsurface environment is actually three dimensional and that both the hydraulic gradient and water flux at any point has components in three orthogonal directions. The hydraulic conductivity may be *anisotropic*, that is, its value may be different in different directions because of layering, clay platelet orientation or a sloping surface. If the direction of measurement does not coincide with one of the *principal axes* of the hydraulic conductivity, then the water flux is not parallel to the potential gradient. In the saturated zone, anisotropy has been studied extensively, but for unsaturated conditions, there is very little information about the magnitude of anisotropy and how it might vary with water status. Equation 16.1.1 is readily extended to anisotropic conditions, but in view of the practical difficulties in making relevant measurements in the field or on field soils, it will not be considered further, and we will confine ourselves to the one-dimensional case as embodied in Equation 16.1.1.

Like the measurement of soil water characteristics, hydraulic conductivity may be measured both by a monitoring approach or by imposing conditions on the soil, in this case usually a known flux of water. However, it is more convenient to divide the available methods by measurements in which the flow paths are constrained by an external barrier, such as a sample ring or a collection cylinder for large monoliths, and those where there is no such constraint and measurements are made in the natural field environment. In the former case, the soil is usually removed from the field and measurements made in a laboratory or other indoor space, although not always. There is, however, some overlap between methods for confined and unconfined measurements. For instance, imposition of a constant flux at the surface can be done over a small area in the case of confined samples, but a large area is needed in an unconstrained field situation to achieve very similar conditions. A further subdivision is possible into methods suitable for measurement of saturated and unsaturated hydraulic conductivity.

16.2 Predictive Models of Hydraulic Conductivity

In common with measurement of soil water characteristics, measurement of hydraulic conductivity is both time consuming and expensive, especially at the drier end of the range. This is doubly the case for *in situ* measurements in the field, where for highly permeable soils, measurements at or near saturation are also difficult. As a result, predictive methods have been developed to provide input to models of soil hydraulic behaviour where experimental data is unavailable or inadequate. Such models provide not only a convenient, albeit often untested, way to obtain data on soil hydraulic properties. They are also a means for fitting measured data into easily manipulated equations to predict system behaviour, for extrapolating measurements beyond the observed range and to provide a framework to convert experimental observations into hydraulic conductivity estimates. For this last reason, these models will be discussed first.

16.2.1 Empirical models

As with soil water characteristic functions, several relationships have been proposed to relate the hydraulic

Soil Water Measurement: A Practical Handbook, First Edition. J. David Cooper.

conductivity of soil to either its water content or its matric potential. These include:

$$K = K_s \left(\frac{\psi_a}{\psi_m} \right)^{\mu} \tag{16.2.1}$$

(Brooks & Corey, 1964)
and

$$K = K_s e^{\alpha \psi_m} \tag{16.2.2}$$

(Gardner, 1958; Wooding, 1968).

Note that α in (16.2.2) is different from α in van Genuchten's Equation 15.6.1.

Comparison of the Brooks and Corey Equation with that of the same authors for the soil water characteristic, Equation 15.6.2, shows that Equation 16.2.1 can be expressed equally well in terms of water content. Many other simple and less simple empirical equations have been proposed, details of which can be found in standard soil physics texts, and some of which will be encountered later.

16.2.2 Capillary models

To predict the hydraulic conductivity relation from other soil properties, several authors have conceived the pores in the soil as short capillary tubes in which flow can be computed according to Poiseuille's Law. These are assumed to be matched randomly with one another and the flow paths, rather than being straight, become increasingly tortuous as water content reduces. Examples of these models are due to Childs and Collis-George (1950), Burdine (1953), Marshall (1958), Millington and Quirk (1959, 1961) and Mualem (1976). These models all have a similar form with relatively minor differences between them. The most commonly used versions are those of Mualem and Burdine. Mualem's equation is

$$K = K_s \Theta^{\frac{1}{2}} \left[\frac{\int_0^{\Theta} \frac{1}{h(\Theta)} d\Theta}{\int_0^{1} \frac{1}{h(\Theta)} d\Theta} \right]^2 . \tag{16.2.3}$$

And Burdine's equation is

$$K = K_s \Theta^2 \frac{\int_0^{\Theta} \frac{1}{h^2(\Theta)} d\Theta}{\int_0^{1} \frac{1}{h^2(\Theta)} d\Theta}, \tag{16.2.4}$$

where $\Theta = \dfrac{\theta - \theta_r}{\theta_s - \theta_r}$ (see Section 15.6).

The exponent of 1/2 or 2 for Θ in these equations is a tortuosity factor. It is sometimes replaced by a different number or left as a free parameter when fitting the equations to experimental data (Hopmans *et al.*, 2002b). If the theory behind the various models were entirely correct, then the equations would be expected to predict the saturated hydraulic conductivity, K_s, correctly. In practice, it is found that there are usually very large discrepancies and so a *matching factor* is used. A matching factor of K_s is very often not appropriate, particularly for field soils which exhibit aggregation and macropores. The equations are, therefore, often adjusted to incorporate a matching factor at a small negative potential or at a value of around –0.2 m water, which approximates a field capacity value (Rajkai *et al.*, 2004). Many authors, however, continue to use K_s as a matching factor, most often inappropriately.

The van Genuchten soil water characteristic model, Equation 15.6.1, can be used to solve for h as a function of Θ in either of the above two equations to give

Mualem

$$K = K_s \frac{\left\{ 1 - (\alpha h)^{n-1} \left[1 + (\alpha h)^n \right]^{-m} \right\}^2}{\left[1 + (\alpha h)^n \right]^{\frac{m}{2}}} \tag{16.2.5}$$

or

$$K = K_s \Theta^{\frac{1}{2}} \left[1 - \left(1 - \Theta^{\frac{1}{m}} \right)^m \right]^2, \quad m = 1 - \frac{1}{n} \tag{16.2.6}$$

Burdine

$$K = K_s \frac{1 - (\alpha h)^{n-2} \left[1 + (\alpha h)^n \right]^{-m}}{\left[1 + (\alpha h)^n \right]^{2m}} \tag{16.2.7}$$

or

$$K = K_s \Theta^2 \left[1 - \left(1 - \Theta^{\frac{1}{m}} \right)^m \right], \quad m = 1 - \frac{2}{n}. \tag{16.2.8}$$

Apart from requiring a matching factor, these equations involve no extra parameters than the van Genuchten (1980) soil water characteristic Equation 15.6.1, which allows both the soil water characteristic and unsaturated hydraulic conductivity functions (often described together as the *hydraulic properties*) to be described mathematically by five parameters – θ_s, θ_r, K_s (or another matching factor), α and n (or m) – six if tortuosity is also a free parameter.

They also mean that having a soil water characteristic curve and one value for the hydraulic conductivity at some point on it, the hydraulic conductivity can be predicted. This may appear too good to be true and it often is, but nevertheless, like the use of pedotransfer functions (Section 15.7), they allow at least a first approximation to the hydraulic conductivity function to be derived for areas where no other information is available. Indeed, soil water characteristics derived from pedotransfer functions are often used, together with one of the predictive equations above, to predict the complete hydraulic properties of a soil for which only rudimentary particle size data may be available. While this is no substitute for proper measurements of hydraulic properties, provided that the (very wide) limitations of the methodology are recognised, useful results can be obtained at a survey or 'ballpark figure' level for a range of environmental and agronomic purposes.

17 Hydraulic Conductivity Measurement of Confined Soil Samples

17.1 Isolation of Well-Defined Soil Volumes

Soil samples for laboratory measurements are usually taken from the field in sleeves of metal, plastic or glass fibre-reinforced plastic. Hydraulic conductivity is more sensitive to disturbance of the soil structure than is the soil water characteristic, especially close to saturation. Great care is required, therefore, to avoid such disturbance. A further danger is the creation of a fast bypass route for water between the soil and the container wall. Samples obtained are not necessarily small cores taken by one of the methods described in Chapter 6. With care, heavy lifting machinery and considerable effort, large monoliths can be excavated from the field of dimensions approaching about 2 m long and 1 m diameter. There are two basic approaches:

- The first upscales the collection of known-volume cores, as described in Section 6.2.2. A cylinder of steel, glass fibre-reinforced plastic or other suitable material of the desired size is mounted on a steel cutting edge, bevelled on the outside and with an inner diameter equal to that of the cylinder. The cylinder must have as smooth an inner surface as possible. One or more hydraulic jacks, capable of exerting a downward force of several tonnes, are used to press the cylinder into the ground. To provide a reaction for the jack, heavy-duty ground anchors or a heavy vehicle may be used. As the cylinder goes into the ground, the soil around it is excavated a little beyond the cutting edge and the soil surrounding it pared back to just outside of the cutting edge. This eliminates friction on the outside of the cylinder and that the cutting edge encounters as little resistance as possible. There will still be friction between the inside of the cylinder and the soil. Any compression of the soil will be clear from a difference in the ground level within and outside the cylinder. Once the desired depth has been reached, the bottom edge of the monolith is separated from the underlying material. In some soils, there is enough friction between the monolith and the inside of the collecting cylinder to retain the monolith inside the cylinder. If this is the case, then supporting the weight of the cylinder on a small crane or a tripod with lifting chains allows manual digging of the soil from beneath the cylinder. The monolith can then be lifted out of the ground and the bottom trimmed flush with the bottom of the cylinder. A cover should be placed on the bottom of the cylinder and fixed securely to prevent disturbance of the sample during transportation. Jacking a metal plate under the cutting edge while the soil inside the cylinder is still attached to the underlying material is safer. Fixing this plate securely to the cylinder then ensures that the monolith cannot slide out of the collecting cylinder. The procedure is clearly laborious, the equipment is expensive and there are potential hazards from the mass of the equipment and the sample as well as collapse of the necessary excavation. Belford (1979) describes a procedure for collecting monoliths of 0.8 m diameter and 1.35 m length using these principles. For this size of monolith, a 10-tonne hydraulic jack was needed to provide sufficient force to drive the cylinder into the ground, and the monoliths collected weighed about 1.45 t. Cameron *et al.* (1992) questioned whether a 'close-fitting' sleeve prevented flow down the sides of a monolith. Their procedure was similar to Belford's (1979), except that the cutting ring inside diameter was smaller than that of the collecting cylinder and the few mm gap around the edge was filled with petroleum jelly (petrolatum) heated to about 50°C to liquefy it. Once cooled and set, it provided an effective seal. Measured saturated conductivity of smaller cores was about half that for an unsealed core, and the time to breakthrough of a tracer was about twice as long, providing strong evidence for edge flow past the unsealed core. Takamatsu *et al.* (2007) described a similar procedure to collect 1.5-m long by 0.8-m diameter monoliths in a titanium cylinder. In their, case, they used a large screw auger outside the cylinder wall and adjustable cutting teeth at the bottom of the auger to ensure an exact fit of the core inside the cylinder.
- The alternative approach is suitable for cohesive soils that can remain intact without support for short periods. It is also more suitable for soils containing large stones or rocks or those which may compress as a result of friction

Soil Water Measurement: A Practical Handbook, First Edition. J. David Cooper.

between a collecting sleeve and the monolith. A pedestal or column of soil is formed by excavating soil around it to leave the pedestal free standing. The pedestal should be formed quite roughly at first and larger than the desired final size. It can then be carved carefully to the final size. Before separation from the underlying soil, the pedestal is encased in a jacket of supporting material. A resin layer (e.g. polyester or epoxy) should first be coated onto the pedestal to prevent water transfer across the vertical face. This may penetrate a little way into the monolith, and so the first coat should be done sparingly. Two or three coats should, if possible, be applied. There are two or three options at this stage. The monolith may be wrapped in glass fibre matting and polyester or epoxy resin used to bond it. Successive layers are built up until the structure is rigid enough for it to be separated from the underlying material and transported without disturbance. Alternatively, a rigid cylinder, of larger diameter than the pedestal, is slipped over it and the space between the two filled with a rigid material which can be cast *in situ*, for example, plaster of Paris, concrete or expanding polyurethane foam. The material should preferably be impermeable in case the coating around the pedestal is not complete. In some cases, the pedestal cannot be made a regular shape because of large fissures, rocks or other features. This is not a great disadvantage, although it helps subsequent data analysis if the shape of the pedestal is recorded before encasing.

In either of the methods described here, the separation of the monolith from the underlying material is not the only option. In some situations there are advantages in leaving it in contact with its natural surroundings, although that precludes collection of drainage water from the bottom of the column and other measurements may be more difficult away from laboratory facilities.

Once the sample has been collected, it may be instrumented in a variety of ways. Tensiometers, porous matrix sensors, solution samplers, TDR or capacitance-type probes, thermometers, etc., may all be inserted relatively easily through the side wall of the monolith. Irrigation, illumination or coverage of the upper surface to prevent water flux across it can all be accomplished. If it has been separated from its underlying material, the monolith can also be weighed, a hydraulic potential imposed on the bottom and the outflow collected. This opens up a myriad of experimental opportunities other than hydraulic conductivity measurement, considered further in Section 24.3.8.

17.2 Instrumentation

The amount of instrumentation installed clearly depends not only on its availability but also on the size of the soil sample. To satisfy Equation 16.1.1, the minimum requirement is a knowledge of the water flux and the potential gradient. These may not, however, be measured explicitly. For unsaturated conditions, the hydraulic conductivity must be related to the water status of the soil – water content and/or matric potential. As a general rule, the more variables that are measured, the less likely it is that erroneous or misleading hydraulic conductivity values will be obtained.

For very small samples, only conditions at the upper and lower surface can be either monitored or controlled. For slightly larger ones of greater than about 20-mm height and diameter, a single tensiometer with a cup of a few mm diameter can be inserted into the side. Longer and wider columns allow the installation of TDR probes and tensiometers or porous matrix sensors at several depths, facilitating the estimation of hydraulic conductivity as a function of depth and layering. For large-diameter monoliths, a neutron or capacitance probe access tube can be inserted down the centre (e.g. Belford, 1979; Dane & Hruska, 1983).

17.3 Water Flux Determination

Similar to the measurement of soil water characteristics, measurements can be made either by imposing conditions on the soil sample, either a flux or a specified water potential at the upper and/or lower boundary, or by observing the evolution of the water status from an initial condition. Unlike the soil water characteristic case, however, the transition from one imposed state to another, as in one-step or multi-step outflow methods, is often used to yield the desired information.

17.4 Measurement Principles

In the most straightforward approach, soil water flux and the water potential gradient are measured or estimated, and the hydraulic conductivity calculated from Equation 17.5.1. The measurements are usually made in a laboratory but can be made *in situ* in the field if a pedestal is left attached to its underlying formation. If the soil column is unsaturated throughout, then no impermeable barrier around the edge of the column is actually necessary to confine the flow, although one is usually used, both to support the soil and to prevent evaporation (or sometimes wetting) through the sides.

As mentioned in Section 17.1 samples may range in size from several millilitres to about 0.75 m^3 and in mass from a few grams to over 1000 kg. While the general principles are the same, the practicalities of making measurements on such a wide range of sizes obviously differ markedly. Apart from this, measurements on large samples differ in one sense from that of small ones. Some methods assume homogeneity of the sample properties. For small samples, this is more probable than for much larger ones, especially as a function of depth. Larger samples can be instrumented much more extensively than small ones so that the hydraulic conductivity in different depth layers can be measured. It is, however, very difficult to gain more than a qualitative

idea of lateral variations of hydraulic conductivity from horizontal variations in matric potential and/or water content.

With advances in both computer power and in efficient methods for estimation of the parameters of non-linear functions, it is now possible to identify the parameters of functions relating both hydraulic conductivity to water status and the soil water characteristic simultaneously from one set of experimental measurements. This is described in Section 17.13.

17.5 Constant Head Measurement

The experimental arrangement for a constant head measurement technique is illustrated in Fig. 17.1. With some simple modifications, this basic set-up is suitable for measurement of both saturated and unsaturated conductivity and on large and small samples. Note that for unsaturated conditions, the only route for air to enter the sample is through the wall of the supporting cylinder, which must therefore have holes to allow this. For a saturated sample, however, the holes must be blocked off.

The water flux, the matric potential and the potential gradient within the sample are all controlled by the head applied at the top of the upper porous plate *via* the Mariotte bottle (see Appendix 18.B), the hydraulic conductance of the two porous plates and the level of the outlet tube. Assuming saturation of the two porous plates, negligible resistance to flow by the connecting tube from the Mariotte bottle and the outlet tube and that the outlet pipe is of sufficiently small diameter to remain full (3 mm should be quite adequate), then the flux through the sample is given by

$$q = \frac{H_1 + H_2 + L + t_1 + t_2}{(L/\bar{K}) + AR}, \tag{17.5.1}$$

where

L is the total length of the sample

t_1 and t_2 are the thickness of the plates;

$\bar{K}$ is the average hydraulic conductivity of the sample;

A is the cross-sectional area of the flow cell;

$R = \frac{1}{C_1} + \frac{1}{C_2} + r_1 + r_2$ is the combined hydraulic resistance of the porous plates and the contact resistances;

C_1 and C_2 are the conductances of the lower and upper porous plates and

r_1 and r_2 are unknown hydraulic resistances caused by imperfect contact between the plates and the sample.

C is related to the hydraulic conductivity of the plate material, K_p, as

$$C = \frac{K_p A}{t}. \tag{17.5.2}$$

The contact resistances, r_1 and r_2, can be minimised, but usually not eliminated, by using a very thin layer of fine sand or silica flour between the porous plates and the sample to fill any small gaps between them. In the absence of r, the water potential at the top and bottom of the sample could be predicted from the water flux, the plate conductances, the cross-sectional area and the two heads, H_1 and H_2. Because of this contact resistance, tensiometers should be used to measure the actual matric potential near each end of the sample. In longer samples, tensiometers can be installed to detect changes in hydraulic conductivity along the length of the sample. Where there are different layers within the sample, these should not be positioned too close to the layer boundaries (see Section 17.8).

Under unsaturated conditions, since K is a strong function of the matric potential, variations in this along the length of the sample must be minimised. Application of Darcy's law to the upper and lower plates gives for the matric potential at the upper and lower boundaries:

$$\psi_1 = H_1 - qA\left(\frac{1}{C_1} + r_1\right), \tag{17.5.3}$$

and

$$\psi_2 = -H_2 + qA\left(\frac{1}{C_2} + r_2\right). \tag{17.5.4}$$

For the matric potential to be the same throughout the sample, ψ_1 and ψ_2 must be equal. This leads to the condition

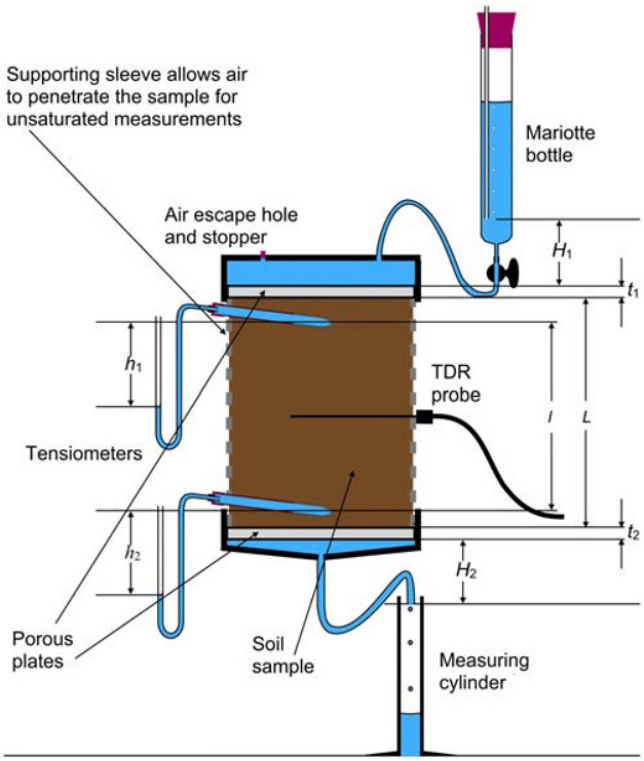

Fig. 17.1 Basic set-up of apparatus for the measurement of hydraulic conductivity under constant head conditions.

$$H_1 + H_2 = ARq. \quad (17.5.5)$$

The value of AR may be calculated by making measurements on the saturated sample when K is not expected to depend on hydraulic head. In this case, $\bar{K}_s$ can be calculated from the measured water flux, q, and the gradient between the tensiometers:

$$\bar{K}_s = \frac{q}{h_1 - h_2 + L}. \quad (17.5.6)$$

AR can then be calculated by substituting this value, together with the measured values of q, H_1, H_2, L, t_1 and t_2 into Equation 17.5.1. The accuracy of the procedure can be checked by substituting the value of AR derived into Equation 17.5.5 and setting $H_1 + H_2$ accordingly while ensuring that saturated conditions still apply. If $H_1 > H_2$ this is likely to be the case. Since the system is saturated, the water flux and potentials should adjust rapidly.

For unsaturated measurements, using the value of AR calculated using this procedure is a good starting point. However, the contact resistances, r_1 and r_2 may well be water potential dependent, and so some head adjustment may be necessary to ensure that the two tensiometers read the same. Changing H_1 has the greatest effect on h_1 and similarly for H_2 and h_2.

17.5.1 General procedures

To ensure consistent measurements, it is important that the porous plates are completely saturated before measurements start. This is most reliably done by putting the plate in a vacuum chamber, evacuating it and then filling the chamber through a tube with its end dipping into deaired water. This ensures that the pores of the plate are completely filled with water. If the necessary equipment is not available, then dipping one side of the plate into deaired water so that the air can escape from the opposite side will minimise the amount of entrapped air. This can be further reduced by running deaired water through the plate for several minutes. Some workers flood the plate with carbon dioxide before this. CO_2 is quite soluble in water and so is readily removed from the plate by dissolution. Failure to remove air adequately results in inconsistent plate conductance and the appearance of air bubbles in the water, which can be difficult to remove and may interfere with the measurements. Preparation of deaired water was described in Section 12.14.

Measurements under saturated conditions require good sealing of the plates to the outer sleeve, either by, for instance, silicone sealant, or an 'O-'ring and that all other parts of the system are well sealed. It is also essential that there be no gaps between the sample and the outer sleeve (Section 17.1).

To ensure that the water flux throughout the sample is known, the column must be at steady state. For reasonable flow rates, both the input and output flows can be measured from the rate of change of level in the Mariotte bottle and the quantity of water collected from the outlet tube. For slow flow rates, the progress of an air bubble through a fine capillary can be monitored to measure both inlet and outlet flows. Standing the collecting vessel on a sensitive balance is another way to measure output flow. An alternative or additional check on the attainment of steady state is to monitor the tensiometer readings.

Hydraulic conditions in the sample are controlled by a combination of the porous plate conductances and the input and outlet heads. In principle, both of the latter can be varied over a wide range of positive and negative values. A low conductance for the upper plate will lower the water potential below it by (Aq/C_1), while the potential above the lower plate will be (Aq/C_2) higher than at its lower side. A further consideration in selecting a porous plate is its bubbling pressure. It is wise to ensure that the plate will remain saturated over the range of matric potentials likely to be imposed. This will help to reduce the chances of unexpected behaviour from the apparatus.

17.5.2 Saturated hydraulic conductivity

If the sample is short ($\lesssim$50 mm height) and/or homogeneous, then both the upper and lower porous plates may be omitted and the sample fed under a positive head from the Mariotte bottle. The lower surface can be allowed to drip directly into a collecting vessel *via* a funnel. In this case, the lower surface is at zero matric potential. The upper surface needs to be protected from disturbance by a gauze, filter paper or similar when water is first ponded onto it. The lower surface should be stood on a similar fine porous material to avoid loss of soil particles and supported by a coarse wire mesh.

For longer or less uniform samples, saturation throughout may not be achieved if there is a less conductive layer within the sample or if hydraulic conductivity increases downwards. A porous plate beneath the sample can provide some hydraulic resistance and ensure saturation throughout. Raising the level of the outflow (i.e. ensuring that H_2 is negative) has a similar effect.

For samples with low hydraulic conductivity, precautions are needed to protect against loss of outflow water by evaporation, such as covering the surface of the water collected by a thin layer of oil. Low saturated hydraulic conductivity samples are probably better measured using the falling head technique (Section 17.6).

Entrapped air in the sample reduces the hydraulic conductivity. Over time, the air can dissolve or be entrained in the outflow water, leading to a time dependence in the measured flow rate.

17.5.3 Unsaturated hydraulic conductivity

The apparatus shown in Fig. 17.1 is suitable for measurement over a range of water potentials down to about –2 m water head. In most soils, hydraulic conductivity

becomes too low for water flow rates to be measured with sufficient accuracy to make reliable measurements. The amount of headroom required is also a limitation in many laboratories, although using a low-conductance plate at the top of the sample and/or a bubble tower (see Appendix 18.B) reduces the room needed at the top of the sample.

Hysteresis in hydraulic conductivity under unsaturated conditions must be considered. For this reason, it is best to start with saturated conditions and reduce the imposed head. Measurements along a wetting branch can then be made after the lowest potential has been achieved.

17.5.4 Long columns

Measurements on a long column can be made in the same way as for a short sample. However, natural field monoliths are almost never uniform, usually exhibit preferential flow paths caused by macropores or non-uniform soil properties and may contain active soil fauna such as earthworms.

As a result, measurements may not produce the same smooth dependence on water potential or water content as exhibited by small samples, with increases in flow rate occurring when the apparent water potential falls and flow being unsteady. This is much more likely near the wet end of the water status range. Hence it is important to collect as much information about hydraulic conditions within the sample as possible. Tensiometers and water content sensors should be installed to give a good picture of variation with depth but also across the area of the sample. Unfortunately, a simple interpretation of the resulting data may not be possible.

17.5.5 Measurements *in the field*

The same principles can be applied to measurements on undisturbed soil columns in the field. The principal advantage is that the soil is kept intact in its natural surroundings without possible disruption caused by transport to a laboratory. The method is generally referred to as the *crust method*. It was first described by Hillel and Gardner (1970) and improved by Bouma *et al*. (1971) and Bouma and Denning (1972).

Measurements are made on a pedestal or column carved *in situ* and left intact connected to the underlying formation, as described in Section 17.1. For unsaturated measurements, it is unnecessary to encase the pedestal, although it is wise to wrap the sides in plastic sheet to prevent evaporation. For both saturated conditions and if the pedestal material is not completely stable, an impermeable layer of supporting material is needed (Section 17.1).

The pedestal should be instrumented with two or more tensiometers at different depths so that the hydraulic gradient and the approach to steady state can be monitored. TDR or dual-probe heat-pulse sensors inserted through the sides of the pedestal should also, if possible, be used to monitor water content. Large-diameter pedestals may have a neutron or capacitance probe access tube installed instead. This should be installed before carving out the pedestal, as the installation process may affect the structure of the pedestal.

In the crust method, the surface of the pedestal is first smoothed, and then a close-fitting cylinder is pushed over the top of the column, and a resistive crust is cast inside the cylinder. Usually, this consists of a mixture of sand and plaster of Paris (gypsum), although very weak cement may be suitable in some circumstances. Some experimentation is necessary to arrive at suitable mixtures and thicknesses. The crust is allowed to cure for about 24 h before it is suitable for use. Water is then ponded inside the cylinder on top of the crust, the head being controlled by a Mariotte bottle, which also allows the water flux to be measured. Once steady state has been achieved, which may be judged from the flow out of the Mariotte bottle as well as the tensiometer and water content readings, the head is changed (usually increased) and measurements made with a different applied head and hence flow rate. If the cylinder is sealed with a lid, a negative head can be applied to the crust by the Mariotte bottle.

Once measurements with one crust have been completed, the crust may be replaced by another (usually less impeding) one and another series of measurements taken.

Although it may appear intuitively that measurements should be made at decreasing flow rates, with steadily thicker or more impeding crusts applied on top of those already there, in practice this is very inconvenient, as drainage is a much slower process than wetting, and so establishing a reduced steady flow rate takes much longer than an increased one. This requires replacement of the crust by a less impeding one.

In some soils, alteration of the soil's hydraulic properties by chemicals in the crust is a problem (Dirksen, 1991, 2001).

17.6 Falling Head Measurement

Measuring the saturated hydraulic conductivity under a falling head is an alternative to constant head measurements, particularly for soils of low hydraulic conductivity. The set-up is shown diagrammatically in Fig. 17.2. The small-diameter capillary tube on top of the sample effectively magnifies the flow through the sample, which must be saturated at the beginning of the test.

If the pressure head across the sample is H_1, then at any time, the flux, q, through the sample is

$$q = \frac{H_1 K_s}{L}, \tag{17.6.1}$$

where K_s is the saturated hydraulic conductivity of the sample. Note that in Fig. 17.2, the pressure head at the bottom of the sample is slightly positive to ensure saturation.

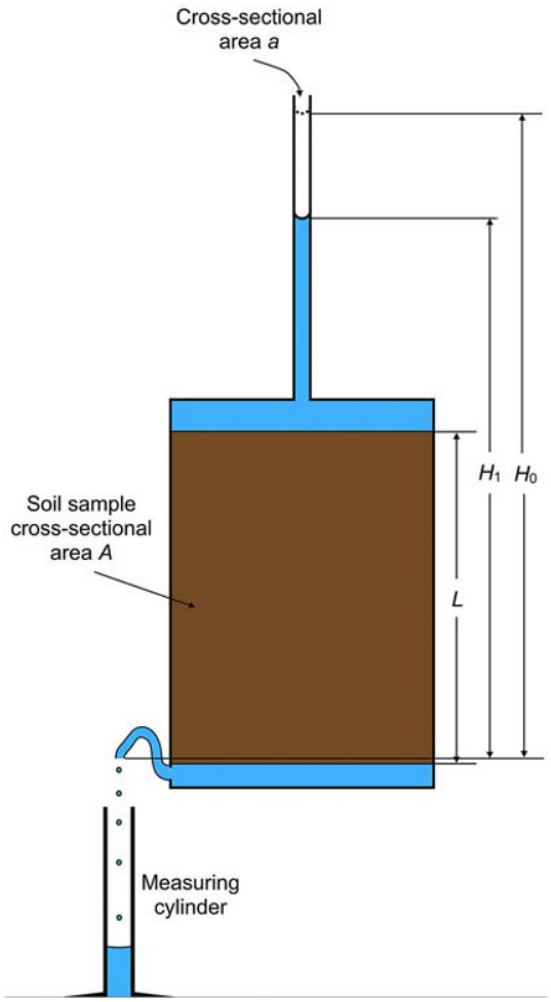

Fig. 17.2 Schematic of a falling head permeameter for saturated hydraulic conductivity measurement.

The flux through the sample can also be related to the fall in the level of water in the tube on top of the sample, so

$$q = -\frac{a}{A}\frac{\mathrm{d}H_1}{\mathrm{d}t}. \tag{17.6.2}$$

where a and A are the cross-sectional area of the tube and sample, respectively.

Combining Equations 17.6.1 and 17.6.2, we obtain

$$\frac{1}{H_1}\frac{\mathrm{d}H_1}{\mathrm{d}t} = -\frac{AK_s}{aL}. \tag{17.6.3}$$

The solution to this is

$$K_s = \frac{aL\ln\left(\frac{H_0}{H_t}\right)}{A(t-t_0)}, \tag{17.6.4}$$

where H_0 and H_t are the heights, H_1, at times t_0 and t.

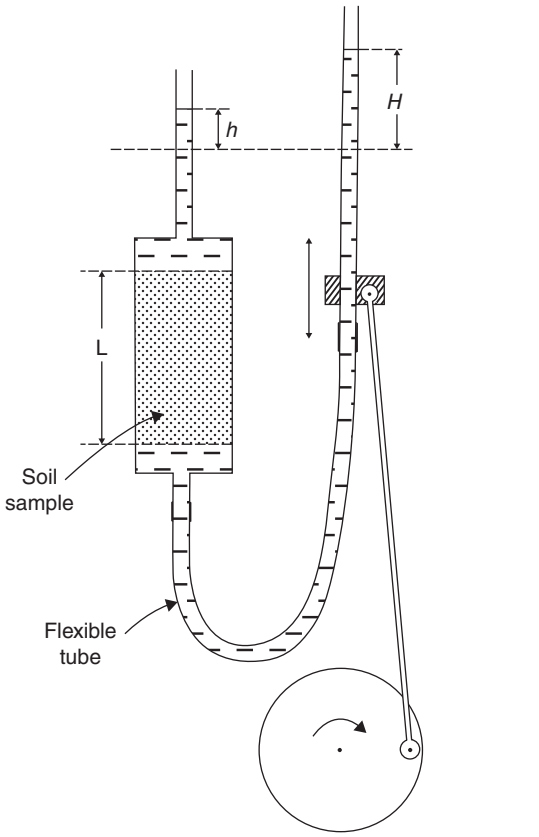

Fig. 17.3 Arrangement for oscillating permeameter. Republished with permission of Taylor & Francis Group LLC Books, from Youngs (1991); permission conveyed through Copyright Clearance Center, Inc.

17.7 Oscillating Head Measurement

Both the constant and falling head methods require significant quantities of water, which is difficult to recycle. In some clay soils, the water used may exchange cations with the clay minerals leading to changes in the soil's hydraulic properties. To avoid these problems a solution, suitable only for laboratory and saturated conditions, entails a small modification to the falling head test (Childs & Poulovassilis, 1960), as depicted in Fig. 17.3.

The motor causes the height of water in the tube on the left, H, to oscillate with a frequency, f. In response, the height of water, h, in the tube above the sample oscillates at the same frequency, but because of the resistance to water flow by the soil sample, the change in water level is smaller than that of H and also lags behind it.

The flow, Q, of water at any time through the sample of cross-sectional area, A, and hydraulic conductivity, K_s, will be given by

$$Q = \frac{A(h-H)}{L}K_s \tag{17.7.1}$$

where a positive value for Q represents a downward flow. This water flow leads to a decrease in h, determined by the cross-sectional area of the tube above the sample, a:

$$\frac{dh}{dt} = -\frac{Q}{a}. \tag{17.7.2}$$

Note the similarity between these equations and Equations 8.3.6 and 8.3.7, which described current flow through a capacitor and resistor in series. The analogue of the resistance, R, is (L/AK), that is, the hydraulic resistance of the sample, that of the capacitance, C, is a, the cross-sectional area of the tube, which is the capacity of the tube per unit length, and variations of head $(h - H)$ provide the driving force, just as the voltage, V, does in the electrical case. Substituting Q from Equation 17.7.1 into Equation 17.7.2 leads to

$$\frac{dh}{dt} = -\frac{AK(h-H)}{aL}. \tag{17.7.3}$$

Now if H varies as

$$H = H_0 \cos \omega t, \tag{17.7.4}$$

then, using similar analysis as in Section 8.3.5 or 8.3.6, we get

$$h = h_0 \cos(\omega t + \phi), \tag{17.7.5}$$

where

$$h_0 = \frac{H_0 AK}{\sqrt{a^2L^2\omega^2 + A^2K^2}}, \tag{17.7.6}$$

and

$$\tan\phi = \frac{aL\omega}{AK}. \tag{17.7.7}$$

This leads to two alternative ways to calculate K.
From Equation 17.7.6,

$$K = \frac{aL\omega}{A\sqrt{\frac{H_0^2}{h_0^2} - 1}}, \tag{17.7.8}$$

and from Equation 17.7.7,

$$K = \frac{aL\omega}{A\tan\phi}. \tag{17.7.9}$$

In other words, the sample conductivity can be calculated from the ratio of amplitudes of the head on each end of the sample or from the phase angle between them.

To get reasonable precision of the measurement, a suitable speed for the motor providing the oscillating head must be chosen. If this is too fast (large ω), then the fluctuations of h will be very small, and if it is too slow, then h will follow the changes in H with little reduction in amplitude or phase lag.

As an illustration, assume that the sample diameter is 50 mm (0.05 m), making A 0.002 m^2, its length is 100 mm (0.1 m) and the upper tube diameter is 5 mm (0.005 m), making a 0.00002 m^2. Then (aL/A) is 0.001 m. A reasonable target for (h/H) is 0.5, which would correspond to a phase shift of $(\pi/4)$ (45°). Then for a permeable soil of hydraulic conductivity 10^{-4} m s^{-1}, an appropriate value of ω would be 0.1 s^{-1} or a rotation speed of the motor of about 1 rpm. For a heavy clay, on the other hand, with a hydraulic conductivity of 10^{-9} m s^{-1}, the rotation speed should be much slower, with one rotation in approximately 73 days! This is not practical in most situations, particularly as a few cycles are needed to establish a regular pattern. Making the upper tube diameter smaller, decreasing the sample length or increasing the area of the sample would all reduce the time required.

17.8 Constant Flux Measurements

An alternative to the imposition of a constant or varying head at the soil surface is to apply a known flux on the soil column and measure the resultant water potential and its gradient, also preferably the water content. The number of such sensors will clearly depend on the size of the sample, but as with most soil measurement problems, the more information collected makes unambiguous interpretation of the data more likely, sometimes at the expense of making it difficult!

One problem with constant flux measurements is that, while it is possible to impose a flux on the top of a sample, either in the laboratory or on a pedestal in the field, the conditions at the lower boundary of the sample will usually have a strong impact on the measurements. As an example, if the experiment is designed such that drainage from the bottom of the sample occurs under free drainage conditions, then this can be achieved only when the base of the sample is saturated, that is, at zero matric potential. If the water flux is much lower than the saturated hydraulic conductivity, the potential gradient must be small, implying that the gradient of matric potential almost balances the gravitational gradient near the lower boundary. If the soil exhibits a distinct air entry value, ψ_a, it will be saturated up to a height ψ_a above the bottom of the sample when there is no flow and to a greater height when downward flow occurs. For fine-textured soils, this means that the soil has saturated hydraulic conductivity for a considerable height above the base, possibly many metres in some cases. Under static (no flow) conditions, the matric potential at the top of the sample is equal to that at the bottom minus the height of the sample. Imposing a flow raises the potential and hence the hydraulic conductivity throughout the column. There is therefore only a limited range of hydraulic conductivity achievable, especially for short

columns. A possible solution is to impose a negative water pressure at the base of the sample, through a hanging water column or a vacuum. This lowers the potential and hydraulic conductivity throughout the sample. By conducting the experiment at a number of different lower boundary pressures, the range of water status may be increased, although they will inevitably be at the wet end of possible conditions.

For these reasons, constant flux measurements are best suited to long columns (monoliths) in the laboratory or pedestals in the field, which are connected to the underlying formation. The matric potential profile of a long homogeneous column with free drainage at the base is expected to resemble that shown in Fig. 17.4. For both the sandy soil examples, the upper part of the column attains a constant hydraulic gradient of unity (matric potential gradient zero) with the hydraulic conductivity equal to the irrigation rate. However, there is a long transition zone above the top of the capillary fringe, and a constant hydraulic gradient is observed only above 0.4 m for the higher irrigation rate and above 0.5 m for the lower one. The clay soil, on the other hand, does not attain a zone of constant matric potential gradient even at 1 m height above the base. Its hydraulic conductivity is well above the irrigation rate at all depths. Field soils are rarely homogeneous, and layers of different hydraulic conductivity produce distortions similar to those shown in Fig. 17.4 near the boundaries.

The achievement of a constant flux is usually accomplished by means of one or more sprinklers, an atomising spray (Dirksen & Matula, 1994; Dirksen, 1999, 2001) or an array of closely spaced hypodermic needles fed from a syringe or peristaltic pump. If lower flux rates are needed than the equipment available is able to provide, the water input may be controlled by turning the water supply on and off automatically on a preprogrammed schedule. Since the rate of adjustment of the soil profile at low flux rates is slow (hours to days), this should not create problems if the repetition rate for water delivery is of the order of minutes.

17.9 Wind's Method

This was described briefly in Section 15.4.9. It is one of a class of *inverse methods*, which aim to fit hydraulic property relationships from experimental data on the behaviour of a system.

Wind (1968) allowed a sample of soil in a short cylinder to evaporate naturally from the top. Nylon resistance blocks were inserted into the cylinder, which was weighed periodically to allow the change of water content to be followed. By starting with an assumed soil water characteristic curve, the water loss at each measured depth could be calculated. This was compared with the recorded water loss from the weighing measurements and the soil water characteristic curve adjusted to bring the two into agreement. The water losses were again estimated from the new soil water characteristic curve and adjusted again. Within four or five iterations, a stable curve can be obtained.

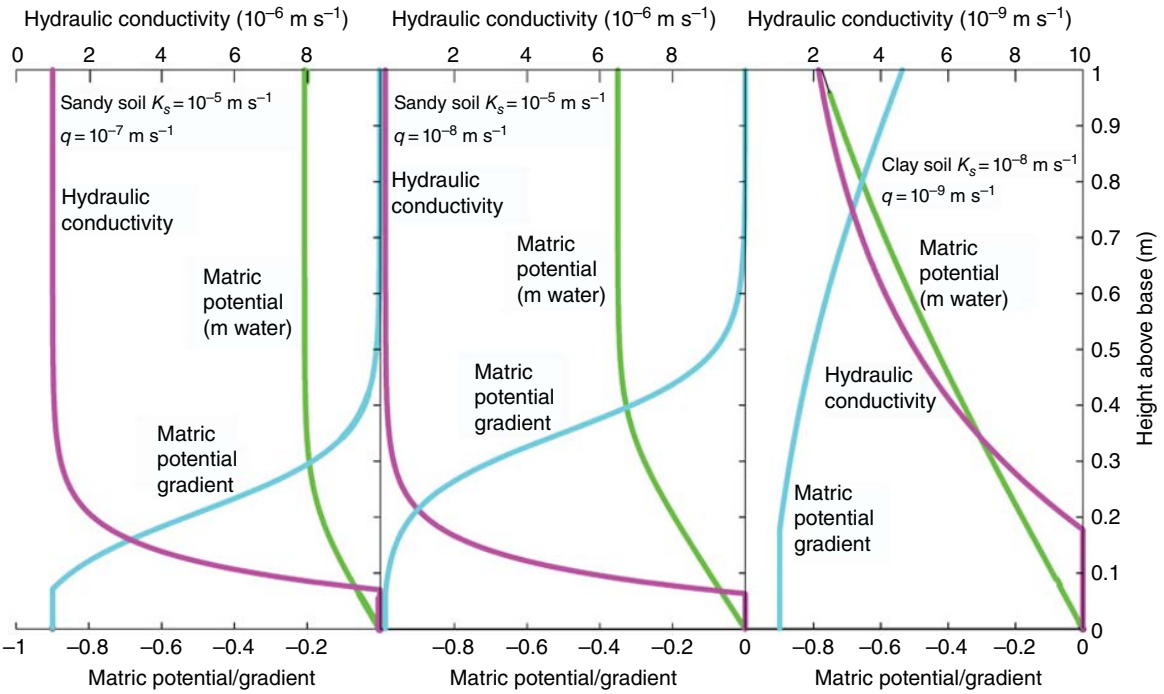

Fig. 17.4 Expected matric potential, hydraulic conductivity and matric potential gradient profiles under constant rate irrigation with free drainage at the base of a 1 m column for two sandy soils irrigated at 10^{-7} m s^1 (1% of K_s) and 10^{-8} m s^{-1} (0.1% of K_s) and one clay soil irrigated at 10^{-9} m s^{-1} (10% of K_s).

The same iterative procedure yields an estimated water flux for each layer as a function of time. These fluxes can be used together with the measured water potentials to estimate firstly the hydraulic gradient and then the hydraulic conductivity as a function of either water content or matric potential using Equation 16.1.1.

17.10 The Bruce and Klute Method

This method measures the diffusivity of the soil, rather than its hydraulic conductivity directly. Diffusivity was defined in Equation 3.1.1 as

$$D = K\frac{d\psi_m}{d\theta}. \tag{17.10.1}$$

For one-dimensional horizontal flow, the gravity term in the Richards equation 3.1.2 is zero, and it reduces to

$$\frac{\partial\theta}{\partial t} = \frac{\partial}{\partial x}\left[D(\theta)\frac{\partial\theta}{\partial x}\right], \tag{17.10.2}$$

where x has been used in place of z to indicate that flow is in the horizontal (x) direction. Solution of this equation is simplified considerably by using the *Boltzmann transformation*:

$$\lambda = xt^{-1/2}. \tag{17.10.3}$$

The partial differentials of λ with respect to x and t are

$$\frac{\partial\lambda}{\partial x} = t^{-1/2}, \tag{17.10.4}$$

and

$$\frac{\partial\lambda}{\partial t} = -\frac{xt^{-3/2}}{2} = -\frac{\lambda}{2t}. \tag{17.10.5}$$

Expressing

$$\frac{\partial\theta}{\partial t} = \frac{d\theta}{d\lambda}\frac{\partial\lambda}{\partial t}, \tag{17.10.6}$$

and similarly for $(\partial\theta/\partial x)$, Equation 17.10.2 can be written as

$$\frac{d\theta}{d\lambda}\frac{\partial\lambda}{\partial t} = \frac{\partial\lambda}{\partial x}\frac{d}{d\lambda}\left[D(\theta)\frac{d\theta}{d\lambda}\frac{\partial\lambda}{\partial x}\right], \tag{17.10.7}$$

or using (17.10.4) and (17.10.5),

$$-\frac{\lambda}{2}\frac{d\theta}{d\lambda} = \frac{d}{d\lambda}\left[D(\theta)\frac{d\theta}{d\lambda}\right]. \tag{17.10.8}$$

This allows the behaviour to be expressed in terms of the single variable, λ, which is a function only of θ. This means that for any combination of x and t, which has the same value of λ, θ will be the same. So the water content at $x = 10$ mm and $t = 1$ s will be the same as at $x = 20$ mm and $t = 4$ s or at $x = 30$ mm and $t = 9$ s.

To calculate $D(\theta)$, Equation 17.10.8 is integrated with respect to λ:

$$-\frac{1}{2}\int_{\theta_i}^{\theta_f}\lambda d\theta = \int_{\theta=\theta_i}^{\theta=\theta_f} d\left[D(\theta)\frac{d\theta}{d\lambda}\right], \tag{17.10.9}$$

where
θ_i is the initial water content of the column and
θ_f is the water content at a particular value of λ.

Bruce and Klute (1956) started with a uniform, horizontal column of dry soil and at a time $t = 0$ imposed a saturated condition at one end, $x = 0$, that is, this end was brought to and kept at a water content of θ_s and zero matric potential. After some time, t, the infiltration was stopped and the column quickly sectioned into short lengths, each of whose water content was measured gravimetrically. In this case, t is fixed and known and Equation 17.10.9 becomes

$$-\int_{\theta_i}^{\theta_f} x d\theta = 2t\int_{\theta=\theta_i}^{\theta=\theta_f} d\left[D(\theta)\frac{d\theta}{dx}\right]. \tag{17.10.10}$$

This leads to

$$D(\theta)\frac{d\theta}{dx}\Big|_{\theta_f} - D(\theta)\frac{d\theta}{dx}\Big|_{\theta_i} = -\frac{1}{2t}\int_{\theta_i}^{\theta_f} x d\theta. \tag{17.10.11}$$

To understand this, it is best to look at the distribution of water content in the column, as shown hypothetically in Fig. 17.5. The integral on the right-hand side of Equation 17.10.11 is the shaded area of the graph. If the column is initially sufficiently dry that $\frac{d\theta}{dx}\Big|_{\theta_i} = 0$, as shown, then the diffusivity is given by

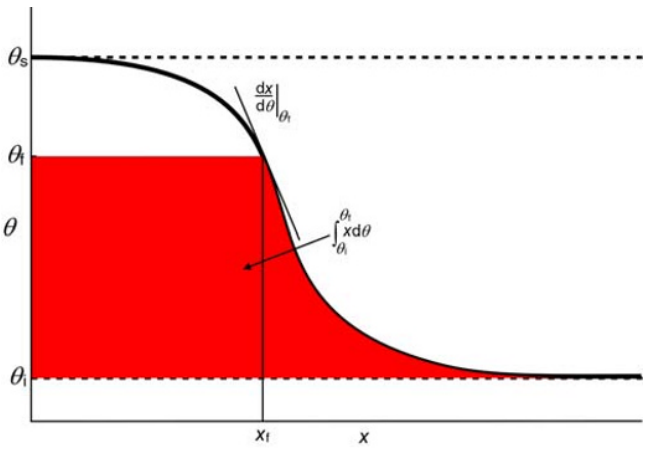

Fig. 17.5 Water content distribution in a homogeneous horizontal column after infiltration.

$$D(\theta_f) = -\frac{1}{2t}\frac{\mathrm{d}x}{\mathrm{d}\theta}\bigg|_{\theta_f}\int_{\theta_i}^{\theta_f} x\,\mathrm{d}\theta. \qquad (17.10.12)$$

Since $(\mathrm{d}x/\mathrm{d}\theta)$ is negative, D is a positive quantity.

Both $(\mathrm{d}x/\mathrm{d}\theta)$ and the integral can be obtained from a graph of θ *v* x derived from the slicing of the column.

As an alternative to stopping the infiltration at a particular time, which fixes t in Equation 17.10.9, Whisler *et al.* (1968) measured the change of water content in time at a fixed position using gamma ray absorption in a similar way to that described in Section 6.5.3. This could be done with a small TDR, other dielectric probes or a DPHP probe, none of which was available in 1968. In this case, plotting θ v $t^{-1/2}$ will give an identical curve to that depicted in Fig. 17.5, and the diffusivity will be given analogously to Equation 17.10.12 by

$$D(\theta) = -\frac{x^2}{2}\frac{\mathrm{d}\left(t^{-1/2}\right)}{\mathrm{d}\theta}\bigg|_{\theta_f}\int_{\theta_i}^{\theta_f} t^{-1/2}\mathrm{d}\theta. \qquad (17.10.13)$$

The hydraulic conductivity is calculated as

$$K(\theta) = D(\theta)\frac{\mathrm{d}\theta}{\mathrm{d}\psi_m}. \qquad (17.10.14)$$

It is necessary, therefore, to know the soil water characteristic to calculate the hydraulic conductivity from the diffusivity.

17.11 The Steady-State Centrifuge Method

Most methods for measurement of unsaturated hydraulic conductivity are suitable only for conditions close to saturation, down to a matric potential of about –0.2-m water head. A method suitable for dry soils using a centrifuge has been described by Nimmo *et al.* (1992, 1994, 2002a). The apparatus, depicted in Fig. 17.6, is designed to fit into a 1-L centrifuge bucket, which is somewhat larger than is normally used for constructing soil water characteristic curves (Section 15.4.6) or for extraction of soil solution (Section 20.1.2). The technique can be used either as a constant head method, essentially the same as described in Section 17.5, or, in later development, as a constant flux method. Figure 17.6 is of the later constant flux design. In both designs, instead of relying on gravity to supply the driving force through the soil, it is the centrifugal field.

A water supply reservoir feeds water through a porous ceramic disc to a flux-controlling reservoir. The hydraulic

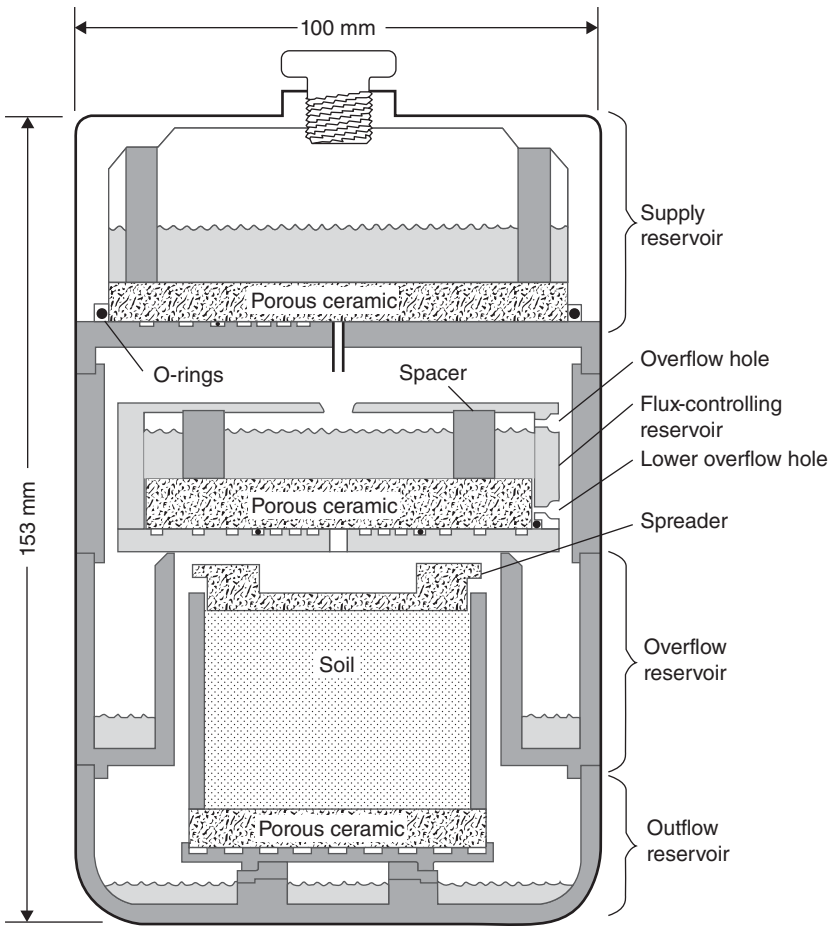

Fig. 17.6 Steady-state centrifuge. From Nimmo *et al.* (2002b). Reproduced with permission of John Wiley & Sons. © American Geophysical Union.

conductance of the ceramic disc is chosen such that it always supplies enough water to keep the flux-controlling reservoir full to its overflow level, without running out of water during an experiment.

Water flows out of the flux-controlling reservoir through a second porous ceramic disc and through a hole to a spreader on the surface of the soil sample. The rate of water delivery to the spreader is controlled by the centrifuge speed, the height of the overflow hole in the flux-controlling reservoir, the conductance of the ceramic disc and its effective area. The soil sample is supported by a third ceramic disc, through which the water flows into the outflow reservoir. It is this water that is measured at the end of the experiment to determine the amount of water flowing through the sample.

An alternative method for delivering a constant flux of water to the soil sample has been described by Conca and Wright (1998). Their design used a pump to deliver water at a metered rate directly to the spreader through a rotating seal on the centrifuge rotor.

Samples can be collected by hydraulic or percussive samplers. The outer layers of these may well be disturbed by the sampling process, and so these should be discarded by a secondary sampler which retains only the inner 50 mm or so of the core inside a liner. With care, this could be performed by hand-shaving the core, although this would probably preclude measurement of the field water content because of drying of the core during the process.

As explained in Section 15.4.6, unlike gravity, the effective force on the sample varies from one end of the sample to the other. At any distance, r, from the centre of rotation, the effective 'gravitational acceleration' is, from Equation 15.4.2, $4\pi^2 s^2 r$, where s is the rotation speed. The work done in moving a distance $(r_0 - r)$ against this force per unit weight of water is

$$\psi_g = \frac{4\pi^2 s^2}{g}\int_r^{r_0} r\,\mathrm{d}r. \qquad (17.11.1)$$

Therefore, assuming that osmotic, etc., contributions to the potential can be ignored, the water potential is given by

$$\psi = \psi_m + \frac{2\pi^2 s^2}{g}\left(r_0{}^2 - r^2\right), \qquad (17.11.2)$$

where r_0 is the radius at which the matric potential is zero (i.e. the bottom of the ceramic disc supporting the sample; r_0 is towards the outer edge of the rotor), and the potential gradient is

$$\frac{\mathrm{d}\psi}{\mathrm{d}r} = \frac{\mathrm{d}\psi_m}{\mathrm{d}r} - \frac{4\pi^2 s^2}{g}r. \qquad (17.11.3)$$

Substituting this into Darcy's law, Equation 2.2.1 or 16.1.1, the flux, q, is

$$q = -K\left(\frac{\mathrm{d}\psi_m}{\mathrm{d}r} - \frac{4\pi^2 s^2}{g}r\right), \qquad (17.11.4)$$

or

$$K = \frac{q}{\dfrac{4\pi^2 s^2}{g}r - \dfrac{\mathrm{d}\psi_m}{\mathrm{d}r}}. \qquad (17.11.5)$$

There are two criteria for obtaining good estimates of K. First, the denominator of the right-hand side of Equation 17.11.5 must be large enough that a meaningful value of K can be calculated. Secondly, since K is a sensitive function of ψ_m, it should be as uniform as possible over the height of the sample, that is, $(\mathrm{d}\psi_m/\mathrm{d}r)$ should be as small as possible. These both tend to be satisfied for higher values of the rotation speed, s. They are also easier to satisfy in coarse-textured soils than in finer ones (Nimmo *et al.*, 1994), which also suffer from potential problems of compaction under the high g-forces.

A feature of this method is that the centrifugal forces effectively exert an overburden pressure on the sample. If the 'top' of the sample is at a radius r_1 from the centre of rotation and the mass resting on top of the sample is m_a (the spreader in Fig. 17.6), the effective overburden depth, z, at a radius r from the centre of rotation is (Nimmo *et al.*, 1994)

$$z = \frac{4\pi^2 s^2}{g}\left(\frac{m_a r_a}{A\rho} + \frac{r^2 - r_1{}^2}{2}\right), \qquad (17.11.6)$$

where

r_a is the radius of the centre of the mass on top of the sample
ρ is the wet density of the sample
A is the area of the sample

Further information and examples of the application of the method can be found in Nimmo *et al.* (1994) and Nimmo *et al.* (2002a, b).

17.12 The Hot Air Method

A drawback of the Bruce and Klute method is that, since it involves the slope of the θ *v* x relation, it is difficult to get an accurate estimate of D where this curve is either very steep or very shallow. $(\mathrm{d}x/\mathrm{d}\theta)$ is very large, close to both the saturation and the dry end of the water content range. It may be very small in coarse-textured materials such as sands. The definition of the differential is improved if infiltration is allowed to proceed for some time, which effectively stretches out the θ *v* x curve (remember that quadrupling the time of infiltration doubles the distance to an equivalent water content value). This also means that the total quantity of water infiltrated is proportional to $\sqrt{t}$. To circumvent some of this disadvantage and also to allow shorter (76.5 mm) columns to be used, which then allows the diffusivity of cores from field soils to be measured, Arya

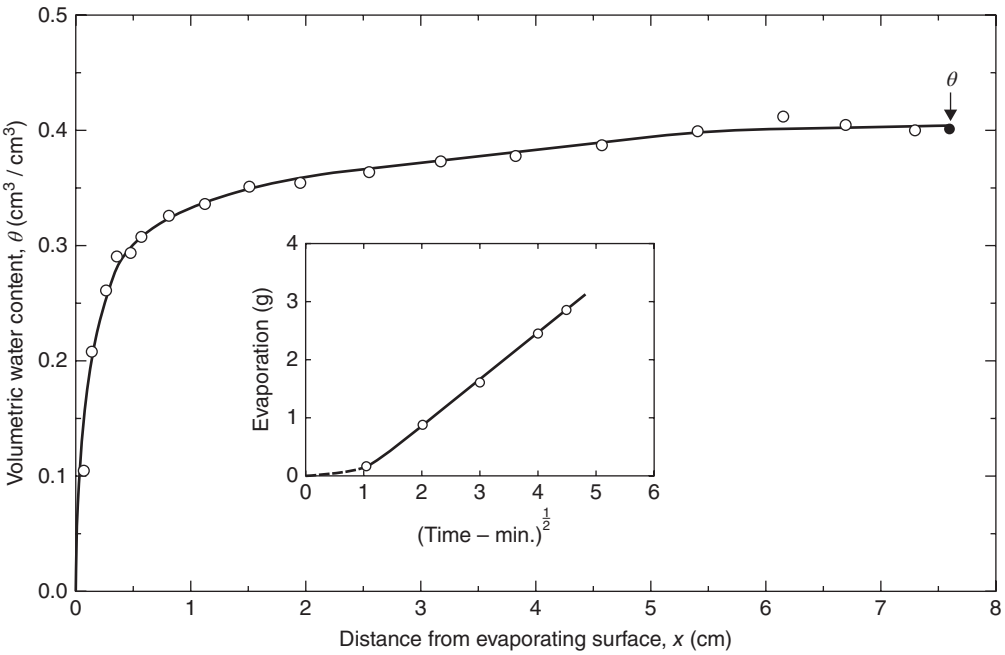

Fig. 17.7 Example of water content profile for a soil core evaporated by the hot air method with (inset) relation between evaporation and $t^{1/2}$, showing the attainment of $\sqrt{t}$ proportionality. From Arya *et al.* (1975a). Reproduced by permission of ASA, CSSA, SSSA.

et al. (1975a) effectively ran the experimental procedure in reverse and introduced what has come to be known as the hot air method. A major advantage of the hot air method is that it allows measurements to be made at the drier end of the scale of water content to be experienced, like the steady-state centrifuge method (Section 17.11).

In the hot air method, the cores are initially saturated carefully from the bottom up to avoid significant air entrapment. The bottom is sealed and the core mounted horizontally after weighing. A jet of hot air at a temperature of 90°–100°C (some workers have used temperatures up to about 200°C) is directed at the open end of the core. The open surface rapidly attains a constant water content, at which point the total water content of the core falls at a rate proportional to the square of time. This can be verified by periodic weighing. It is important to ensure that the drying front does not reach the closed end of the core, as this would then violate the implicit assumption that the core is of infinite length and the square root of time proportionality would no longer hold. Following evaporation for some time, usually less than about 30 min., the core is sectioned as described for the Bruce and Klute method and water content measured as a function of length. The calculation procedure is exactly the same as described earlier, the only difference being that the water content rises with distance from the open end. The variation of water content with distance was found by Arya *et al.* (1975a) to yield much more reliable gradients than the Bruce and Klute method (see Fig. 17.7). Good agreement was obtained for depths >0.1 m with field-measured hydraulic conductivity using the zero flux plane method (see Section 18.3.2).

Slicing of the soil core to determine the increase in water content at a series of distances from the evaporating end requires both speed to avoid redistribution of water and accuracy to ensure good data quality. With natural field soil cores particularly, some heterogeneity of the soil profile is to be expected, which is likely to make the job of determining a smooth profile more difficult. Van den Berg and Louters (1986) found that the empirical equation

$$\theta_f(x) = \theta_i - (\theta_i - \theta_0)\left(\frac{b}{x+b}\right)^n, \qquad (17.12.1)$$

Where
b and n are empirical constants and
θ_0 is the value of θ_f at $x = 0$,

fitted experimental data well. Gieske and de Vries (1990) found that, under some circumstances, a single-parameter equation of the form

$$\theta_f(x) = \theta_i - (\theta_i - \theta_0)e^{-\alpha x}, \qquad (17.12.2)$$

where a is another empirical parameter, fitted the data equally well.

Following on from this work, Tyner *et al.* (2006) modified the method to avoid having to section the core altogether and determine each individual section water content gravimetrically. They suspended the core horizontally from a load cell at each end and recorded the output from each load cell continuously during evaporation. By assuming a water content distribution of the form of Equation 17.12.1 or 17.12.2, the distribution of water

content at each point in the core could be calculated as the experiment progressed. The diffusivity of the soil can then be calculated for many different times during the experiment, as well as detecting the point at which evaporation departs from linearity with the square root of time.

17.13 Inverse Methods: Single- and Multi-step Outflow

All of the methods discussed so far have taken a fairly straightforward approach by performing calculations on the experimental data to yield directly hydraulic conductivity or, in the case of the Bruce and Klute and hot air methods, diffusivity. Inverse methods take a different approach. They use all of the data on the behaviour of a system to optimise the value of parameters which characterise the mathematical functions describing properties that are assumed to control that behaviour.

Inverse methods have been encountered previously in this book in connection with the estimation of water content using ground-penetrating radar (Section 8.15) and electrical resistivity imaging (Chapter 10) and in Wind's method (Sections 15.4.9 and 17.9). In principle, inverse methods can quantify the parameters of equations describing the properties which control any system. There are, however, a number of constraints which, if ignored, can lead to highly ambiguous parameter estimates and/or to results which produce seriously erroneous predictions of the system behaviour under conditions different from those used to collect the original data.

In some ways, inverse methods may be regarded as an extension of the more familiar processes of regression. In regression, a function is fitted to a set of data. The best fit is usually identified by finding a set of parameters which minimise the sum of squares of the differences (SSD) between the value of data points and that of the function evaluated using those parameters. If the function can be expressed as a *linear* combination of the parameters, that is, it is of the form

$$F = a_0 + a_1 f_1 + a_2 f_2 + \cdots, \qquad (17.13.1)$$

where f_ns are the known functions and contain no unknown parameters, then the parameters a_n can be calculated analytically. In most cases where the function F is a non-linear function of the a_ns (e.g. powers of a_n, trigonometric, elliptical or logarithmic functions), then no analytical solution is usually possible, and the parameters must be identified by a process of iteration. Usually a set of initial values for the parameters is assumed, and their values are adjusted until the smallest SSD (often called the *objective function*) is obtained. The *Marquardt (1963) algorithm* is often used to make this process as efficient as possible.

The SSD as a function of the parameters is called a *response surface*. This exists in a multidimensional space, which is difficult to envisage. In the case of only two parameters, however, it can be imagined as a real surface in a three-dimensional space defined by x, y and z axes, with x and y being the two parameters and z the value of the SSD. The optimum value for x and y is the lowest point (value of z) on this surface.

In the inverse method, the process is taken a step further and, rather than simply finding a function with several parameters to fit the data, the functions with their associated parameters are incorporated into a numerical model of the system's behaviour. The model is run multiple times with different parameter sets and model output(s) compared with the experimental data in a similar way as for non-linear regression to find the 'best' parameters. In the case of soils, the functions are principally the soil water characteristic and the unsaturated hydraulic conductivity function. The functions may be based on a physical theory, such as the Mualem (1976) equation for hydraulic conductivity or an empirical model, such as the van Genuchten (1980) model for the soil water characteristic. These functions are combined into the parameters of a flow model, usually the Richards equation (see Section 2.2.3) to give an overall description of the system behaviour.

Inverse methods are a powerful way to obtain the characteristics of a system, since they use all of the available data in an efficient way to minimise the errors in prediction. However, a number of points should be borne in mind before embarking on using inverse procedures:

- Inverse procedures are computationally intensive and rely on the availability of significant computer power.
- Inverse procedures optimise the value of the parameters which are assumed to describe the properties of the system. Any of these elements (the main model – the Richards equation – or the sub-models – the Mualem and van Genuchten models in our case) may not be appropriate for the particular system under study. For instance, the Richards equation breaks down when preferential flow is an important process. This does not necessarily mean that the procedure fails to identify a suitable set of parameters which provide a good fit to the available data. Within the range of conditions under which the data were obtained, the model and parameters are expected to provide a reliable prediction of the system behaviour. On the other hand, extrapolation to conditions outside that range may be highly misleading, and a good fit to available data does not necessarily mean that either the model or the parameters are correct.
- Models of the system, constructed in the way just described, rapidly acquire a large number of parameters, which makes for high demands on computer resources to run a large number of simulations using different parameter combinations. A large number of parameters also often introduce difficulties of *identifiability* and *uniqueness*. In essence, it is often found that different combinations of the value of some parameters lead to almost equally good fits to the data. Additionally, identification of the parameters is made more difficult by *local minima* of the response surface. Reverting to the two-parameter example,

the response surface can be envisaged as having a number of wells, from the bottom of each of which it is necessary to climb upwards to higher values of the SSD. Once having done so, it may be possible to fall into an even deeper well, and there may well be an even deeper one somewhere in the parameter space – this is known as the *global minimum*. Techniques are available to make the discovery of the global minimum more likely, but the more parameters that are involved, the more difficult the search generally becomes.

Success in achieving a good set of parameters is enhanced by taking some common-sense measures. These include:

- Splitting the available data into two sets. One of these is used for optimising the parameters of the system. The other acts as a check on those parameters. The parameters from the first set are fed into the model and used to simulate the second data set. If the model is a good one and the parameters are close to the correct ones, then it is expected that the average SSD for the second set will be only a little larger than that for the set on which the parameters have been fitted.
- Examining the data fits critically in a graphical format to see where the fit is poorest. Although the overall SSD may be small, a consistently poorer fit in one part of the water content range is often found. This indicates that the model may need some modification. A poor fit at the wet end of the range may mean that the model fails to deal adequately with macropore flow, for instance.
- Acquiring data over as wide a range of conditions as possible, preferably with different data types (e.g. water content, water potential, input and/or output flow).

There is a conceptual problem involved in mixing data types, since the units are not compatible. This is usually dealt with by weighting the different kinds of data according to the variance or the range of each type of data in the total data set. So if the volumetric water content varies over a range of 0.3 $m^3\,m^{-3}$ and matric potential varies from zero to –5 m water, then when calculating the SSD, water content deviations squared would be weighted $(25/0.09) = 278$ times each water potential deviation squared. Additional weighting factors might be introduced to account for the perceived precision of different measurements.

17.13.1 One-step outflow

The one-step outflow method consists of placing a soil sample, usually housed in a supporting sleeve, often used to collect the sample from the field, on a porous ceramic plate and changing the water potential at the bottom boundary rapidly by a substantial amount. A fine-textured soil should have a larger step-change in potential applied than a coarse-textured one to reflect the wider range of matric potential over which most of the water is held. Ideally, the size of the step should approximate this range. Hence the name 'one-step'. The change may be effected by applying a suction to the lower side of the plate with a hanging water column or vacuum pump or by placing the sample inside a pressure chamber and increasing the imposed pressure. As a minimum, the outflow from the sample *via* the plate is recorded, but one or more tensiometers within the sample increase both the amount of and the types of data and therefore help to ensure that a solution close to the true hydraulic properties is obtained.

The method was first proposed by Doering (1965) before computers were commonly available. Early users of the technique, therefore, used approximate analytical solutions to the water flow equations and neglected gravity. Neglecting gravity and the hydraulic resistance of the plate, an approximate solution for the diffusivity is

$$D = -\frac{4L^2}{\pi^2(\theta_t - \theta_f)}\frac{d\theta_t}{dt}, \qquad (17.13.2)$$

where

L is the sample length;
θ_t is the average sample water content at time t, and
θ_f is the final average sample water content.

Knowing the initial water content of the sample, θ_t and θ_f can be calculated from the outflow volume.

Several authors have proposed improvements to both the procedure and the analysis, but reliable use of the method has come from the development of inverse procedures.

17.13.2 Multi-step outflow

The multi-step outflow method splits the single step into a number of smaller ones, with the aim to obtain approximately equal quantities of outflow from each step. If some information on the soil water characteristic is available, then this can be used to guide the size of step (Hopmans *et al.*, 2002b). Four to six steps is a reasonable number. Analysis of the data for both single- and multi-step outflow experiments is aided by using a thin, conductive membrane instead of a thicker ceramic plate to support the sample. If a ceramic plate is used, its hydraulic resistance must be measured to incorporate it into the flow equation. There is also a danger that this resistance may change over the course of the experiment as a result of exsolution of air or microbial growth.

When combined with inverse procedures, multi-step outflow experiments have proven to be more successful at providing stable and reliable parameters describing the hydraulic properties than the single-step method, probably because of the extra information acquired (Hopmans *et al.*, 2002b). Multi-step experiments also appear to be less prone to local minima of the objective function.

17.13.3 The inverse modelling procedure

It may be obvious, but the closer the initial parameters fed into the model are to the true values, the quicker it is likely to converge to the best description of the hydraulic

properties and the smaller the likelihood that the model will be trapped in a local minimum. Nevertheless, identification of all of the parameters is not guaranteed, and the response surface may exhibit long, shallow valleys which make finding the lowest point difficult and (computer) time consuming. The model may well exhibit strong correlation between different parameters, which mean that a range of pairs of values of these parameters will produce almost equally good fits to the data. It may be possible to adjust the experimental design to avoid some of these problems or to formulate the model differently. Some initial investigation with simulations using the model and expected parameters will help guide these choices.

After producing a set of apparently 'good' parameters, it is important to look critically at the outputs to judge visually whether, in fact, the data has been reproduced satisfactorily or whether it fits badly in any particular part(s). It is usually revealing to plot out the residuals (i.e. the differences between the modelled data and the observations). Ideally, they will be randomly distributed about a zero line. This almost never happens and there will be some correlation between groups of adjacent data points. Most likely, this will reveal that the model is not a perfect description of the system, but it is up to the judgement of the experimenter whether this is sufficiently serious to revise the model.

It is usually wise to limit the number of parameters in the model to avoid problems of local minima, slow convergence and strong correlations between parameter values. It may be possible to fix some parameters by using information obtained separately from the main experiment (e.g. the saturated hydraulic conductivity or saturated water content).

Despite the number of reservations, inverse modelling is a powerful tool for determining hydraulic properties of the soil but does require appropriate computing resources and a high level of skill in formulating the models and in evaluating the results. An excellent description of the methods available and guidelines for both running the experiments and using the inverse method to analyse them is given by Hopmans *et al.* (2002b).

17.14 Sorptivity

Sorptivity is related to hydraulic conductivity *via* the diffusivity function (Section 3.3), although the relationship is not a simple one. In most cases, sorptivity is best measured *in situ* in the field (see Section 18.2). However, it is often useful to measure the sorptivity of individual aggregates so that infiltration can be partitioned unequivocally between aggregates and the surrounding macropores. Leeds-Harrison *et al.* (1994) devised a method for measuring the sorptivity of a single isolated aggregate. The method is, in essence, a miniaturisation of the single-ring infiltrometer (Section 18.2.2) and illustrated in Fig. 17.8.

The sponge in the vertical, tapered tube allows good contact with the aggregate over a well-defined area of a few mm diameter. In use, the system is first filled with water from the reservoir until the capillary tube is almost full and water is just dripping from the vertical tube. The supply is turned off and the vertical tube raised until water just stops dripping from the sponge. This ensures zero matric potential at the tube tip. The aggregate is then placed on the scissor jack and raised to make contact with the tip of the tube. The infiltration rate is measured by recording the movement of the meniscus in the capillary tube, whose cross section is known.

The infiltration rate, Q, quickly reaches a steady state, given by (Leeds-Harrison *et al.*, 1994):

$$\frac{Q}{\pi R^2} = K_s + \frac{4bS^2}{\pi R(\theta_f - \theta_i)}, \qquad (17.14.1)$$

where
R is the radius of the vertical tube tip;

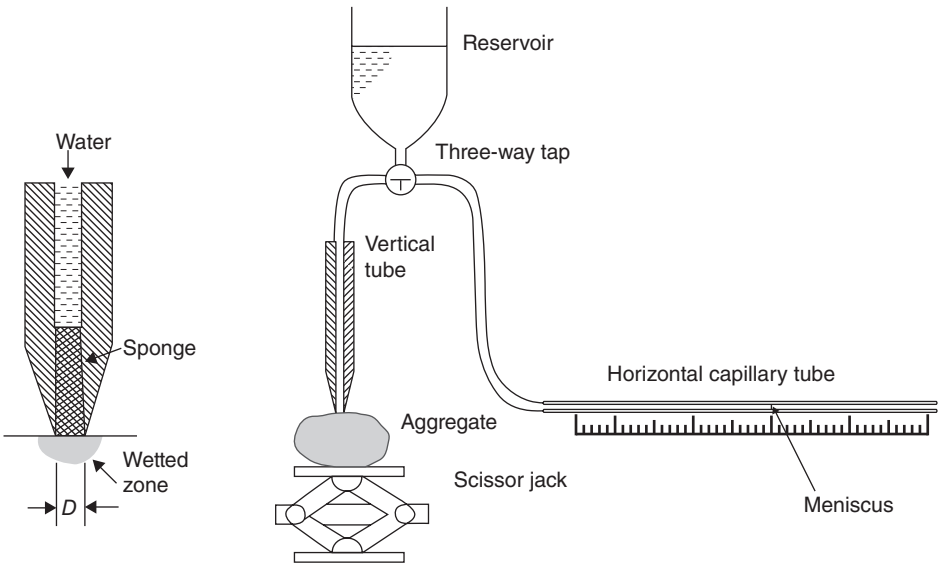

Fig. 17.8 Sorptivity measurement of a single aggregate. From Leeds-Harrison *et al.* (1994). Reproduced with permission of John Wiley & Sons.

K_s is the saturated hydraulic conductivity of the aggregate;
b is a "shape parameter", which can often be taken to be about 0.55 (White & Sully, 1987);
S is the sorptivity, and
θ_i and θ_f are the initial and final volumetric water content of the wetted zone.

For small values of R, K_s is much smaller than the second term on the right-hand side of this equation and so can be neglected (Leeds-Harrison *et al.*, 1994), leading to

$$S = \sqrt{\frac{Q(\theta_f - \theta_i)}{4bR}}. \qquad (17.14.2)$$

The quantity $(\theta_f - \theta_i)$, called the *fillable porosity*, can be calculated by weighing the aggregate before the experiment and afterwards to determine the amount of water imbibed and then measuring its volume, V, by the method described in Section 6.3.3.

Other workers (e.g. Hallett & Young, 1999) have used the technique to investigate the wettability of soil by comparing sorptivity values with both water and an ethanol solution as the infiltrating fluid. These workers also used a small (–20 mm water) negative fluid pressure at the vertical tube tip as well as estimating hydraulic conductivity directly, following Leeds-Harrison and Youngs (1997).

18 Unconfined Measurements in the Field

18.1 Introduction

Measurement of the dynamic properties of soil water in the field usually involves a lot of labour, equipment and water, as well as overcoming problems of accessibility to sites. This makes measurements on small samples, usually in a laboratory environment, an attractive alternative. Several methods applicable to field soil samples were described in the previous chapter. However, these do not generally take account of large-scale features often found in the field, such as macropores induced by soil structural organisation or root and animal activity, the interplay of different soil horizons, microtopography or mesoscale spatial variability. Even without such problems, field measurements are needed to check that laboratory measurements are representative of the field situation. This chapter explores the more common field measurement techniques, starting with those applicable mainly to saturated soils and then those for unsaturated soil.

18.2 Saturated Measurements

Measurements in the saturated zone, that is, beneath the water table, were developed earlier than those for the unsaturated zone, partly because this is a more stable environment. The measurements were also of practical importance in the design of land drainage schemes and for developing water supplies from pumped boreholes. Measurements of saturated hydraulic conductivity can also be made in the normally unsaturated zone, and these methods often also yield information about unsaturated soil properties close to saturation.

18.2.1 Borehole methods

Use of a borehole drilled into the saturated zone provides a relatively simple way to make measurements at almost all depths. As a consequence, methods have been developed to estimate hydraulic conductivity measurements made in boreholes.

Drilling of a borehole appears at first sight to be relatively simple, but there are a number of pitfalls. The theory usually assumes a perfectly cylindrical hole, which may be difficult to achieve in practice, particularly where there are large stones in the profile. Some soils, for example, running sands, may slump into the hole, making it both difficult to clear the hole and leaving a large cavity behind. Using a slotted casing in the hole to support the profile while allowing free passage of water can prevent this. Selection of a suitable size and density of slots requires some consideration to ensure that the borehole does not silt up, while the casing offers negligible resistance to flow. Use of a geotextile in association with a slotted casing may offer a good solution, combining a fine filter with good hydraulic transmission. In clay soils, the drilling of the borehole or insertion of a casing may produce smearing of the sides of the hole by orienting the clay platelets along its surface. This can prevent the free exchange of water between the formation and the hole. In this case the borehole may be *developed* by pumping water out, inducing an inflow of water, the force of which disrupts the thin skin of oriented clay. This may need to be repeated a few times. Alternatively or additionally, the sides of the hole can be abraded by a stiff brush or by using a spiked wheel (Reynolds & Elrick, 1986) to disrupt or remove a lot of the skin.

The auger hole method or slug test

This is perhaps the simplest method, requiring only an open or slotted cased borehole drilled some distance below the water table, as shown in Fig. 18.1a. With the water level in the hole in equilibrium with the water table, the water level is changed, either by pumping water out of or into the hole and monitoring the subsequent recovery. A simple method to alter the water level without the use of pumps is to drop a solid object of known volume into the hole. Removal of the object after re-equilibration of the water level allows the test to be performed with a lowered water level.

The water level is most accurately monitored by a pressure transducer in the hole connected to a data logger.

Soil Water Measurement: A Practical Handbook, First Edition. J. David Cooper.

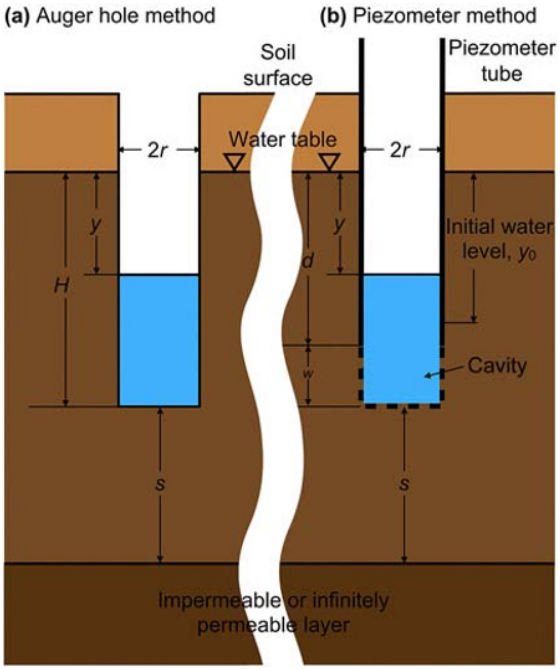

Fig. 18.1 Experimental arrangement for (a) the auger hole method and (b) the piezometer method of measuring saturated hydraulic conductivity below the water table. Adapted from Youngs (2001).

Manual recording of the level is, however, possible. The simplest method uses a float attached to a measuring tape, which is read against a fixed point at the top of the borehole.

Analysis of the data depends on assuming that the water table level outside the hole is unaffected by disturbance to the water level inside. For a substantial change in water level, this implies that only measurements taken during the early part of the borehole level recovery are used.

With these assumptions, the rate of decrease of the water level drawdown, y, is proportional to the hydraulic conductivity (Kutilek & Nielsen, 1994; Youngs, 2001):

$$K_s = C\frac{dy}{dt}, \qquad (18.2.1)$$

where
C is a *shape factor*, dependent on the radius of the hole;
y is the drawdown of water in the hole, and
H is the depth of the bottom of the hole beneath the rest water table level, and
s is the height of the bottom of the hole above an impermeable boundary.

Youngs (2001) quoting Ernst (1950) gives approximate solutions for Equation 16.1.1 as

$$K_s = \frac{4.63}{\left(20+\frac{H}{r}\right)\left(2-\frac{y}{H}\right)}\frac{r}{y}\frac{dy}{dt} \quad \text{for } s > 0.5H; \qquad (18.2.2)$$

$$K_s = \frac{4.17}{\left(10+\frac{H}{r}\right)\left(2-\frac{y}{H}\right)}\frac{r}{y}\frac{dy}{dt} \quad \text{for } s = 0. \qquad (18.2.3)$$

Equation 18.2.2 applies to a soil that is effectively infinitely deep, while Equation 18.2.3 applies to a hole that penetrates to the impermeable layer. Boast and Kirkham (1971) derived values of the shape factor, C, for combinations of a wide variety of parameter values. These are also quoted by Youngs (1991, 2001).

Flow into the borehole is almost exclusively horizontal in this method and so it produces estimates of the horizontal saturated hydraulic conductivity.

The piezometer method

Like tensiometers, piezometers measure the pressure of water in the ground, but unlike tensiometers, they will do so only in the saturated zone. A piezometer consists, at its simplest, of an open-ended tube sealed into a borehole. There is usually a section of unscreened borehole of height w at the bottom to allow water to pass between the formation and the piezometer. In an unstable formation, a perforated or slotted screen is needed. The pressure may be measured by one of the pressure measuring devices described in Chapter 12 on tensiometers, but most often the tube is open and the level in the open hole is measured by a float and measuring tape or an electronic level sensor. A piezometer for groundwater monitoring is usually a relatively narrow tube, typically 25–50 mm diameter. For measurement of hydraulic conductivity, it is normally at least 100 mm diameter, although narrow piezometers installed for water head monitoring can be used (Goss & Youngs, 1983). The arrangement is shown in Fig. 18.1b. The experimental method is almost exactly the same as for the auger hole method – a sudden change in water level inside the hole is induced and the subsequent recovery monitored.

The hydraulic conductivity in this case is given by (Youngs, 2001)

$$K_s = \frac{\pi r^2 \ln\left(\frac{y_0}{y}\right)}{A(t-t_0)}, \qquad (18.2.4)$$

where
y_0 is the water drawdown at an early time, t_0;
y is the drawdown at a later time, t, and
A is a shape factor dependent on the ratio of the depth from the surface to the top of the cavity, d; the height of the cavity, w, and the distance to an impermeable layer, s, to the radius of the well, r.

A table of shape factors can be found in Youngs (1968, 1991, 2001).

When the height of the cavity, w, is small or even zero, water flow is predominantly in the vertical direction, and so this method is biased towards an estimate of the vertical saturated hydraulic conductivity.

Two-well method

In this method, two wells of the same depth are sunk below the water table and water is pumped from one to the other, depressing the water level in one and raising it, in principle by the same amount, in the other. At steady state, the hydraulic conductivity is given by (Smiles & Youngs, 1965; Youngs, 1991, 2001)

$$K_s = \frac{Q}{\pi \Delta H (L + L_f)} \cosh^{-1}\left(\frac{b}{2r}\right), \qquad (18.2.5)$$

where

Q is the pumping rate;

ΔH is the difference in water level height between the two wells;

L is the length of each well below the rest water table depth;

L_f is a correction for flow within the capillary fringe and water flow beneath the bottom of the wells;

b is the distance between the wells, and

r is the well radius.

Variants of the method use several wells arranged in a circle with water being pumped between alternate ones (Smiles & Youngs, 1963) and using the water level observed in inspection wells located between the pumped wells to eliminate the effect of clogging.

Single pumped wells

Groundwater hydrologists have, for many years, used measurements of the water table drawdown close to a well pumped at constant rate to estimate aquifer characteristics. The drawdown, y, at time t after pumping starts is given by the *Theis formula* (Theis, 1935):

$$y = -\frac{Q}{4\pi T} Ei\left(-\frac{R^2 S}{4Tt}\right), \qquad (18.2.6)$$

where

Q is the steady pumping rate;

T is the aquifer *transmissivity* (the product of saturated hydraulic conductivity and aquifer thickness);

R is the distance of the observation well from the pumped well and

S is the storage coefficient of the aquifer (the specific yield for a free water table aquifer – the amount of water released by a unit reduction in the groundwater level).

$Ei(x)$ is the *exponential integral* $-\int_{-x}^{\infty} (e^{-v}/v)\mathrm{d}v$. Although this looks like a fairly straightforward function, it is not, owing to a singularity at $v = 0$.

Both S and T can be estimated by matching a log–log plot of y against R^2/t to the function $Ei(x)$.

Inverse auger hole method

Saturated hydraulic conductivity may also be measured above the water table, provided that there is enough water available to saturate a substantial volume of soil. In the inverse auger hole method (so called because water flows out of the hole, rather than into it, as in the auger hole method), water is added to an auger hole of radius, r, to some depth and the depth, h, is monitored over time, t (Kessler & Oosterbaan, 1974). The field-saturated hydraulic conductivity, K_{fs}, to distinguish it from the true saturated conductivity, is given approximately by

$$K_{fs} = \frac{r}{2(t - t_0)} \ln\left(\frac{1 + 2\frac{h_0}{r}}{1 + 2\frac{h}{r}}\right), \qquad (18.2.7)$$

where h_0 is the depth at time t_0 at the beginning of monitoring.

K_{fs} is often found to be only about half of the true saturated conductivity, mainly because of the presence of air trapped in soil pores (Stephens *et al.*, 1987). However, over time, the air is dissolved or able to escape. A short test may therefore lead to a value of hydraulic conductivity which is unrealistically low when the measurement is used to predict behaviour when the soil is saturated for extended periods.

The analysis assumes that there is a unit hydraulic gradient in the soil, and so the results may be regarded as approximate at best.

Borehole permeameter or Guelph Permeameter

The borehole permeameter maintains a fixed water level in an open borehole by means of a Mariotte device (see Appendix 18.B), a float valve or other means. Theoretically, the rate at which water infiltrates into the soil surrounding the hole falls initially and then levels off to a steady rate. Solving the Richards equation in three dimensions is a complex task, but approximate analytical solutions have been derived by Reynolds *et al.* (1985) and Philip (1985), assuming that the Gardner (1958) form of the hydraulic conductivity relation, Equation 16.2.2, applies.

The basic theoretical foundation for this is outlined in an appendix to this chapter (Section 18.A.3).

A schematic representation of a borehole permeameter is shown in Fig. 18.2. The water level in the hole is controlled by the elevation of the bottom end of the air tube, which can be adjusted by sliding it up and down. The rate of infiltration out of the hole is measured by monitoring the fall of the water level in the transparent reservoir against a scale. Automatic recording and better precision can be obtained by using a pressure transducer as shown in Fig. 18.2 (Constantz & Murphy, 1987) or better a differential transducer (Casey & Derby, 2002), see the appendix, Section 18.B.2. The size of the reservoir is a compromise between sensitivity of level (i.e. volume) measurement and its holding sufficient water to complete a test. In low permeability soil, the volume of water needed is fairly small (usually less than 0.5 L), so that a small cross-sectional reservoir of about 20 mm inside diameter should suffice, giving a resolution of just over 2 mL per mm of water level change when the volume of the air tube is taken into account. For soil with high hydraulic conductivity, more water storage is obtained by increasing the cross-sectional area of the reservoir.

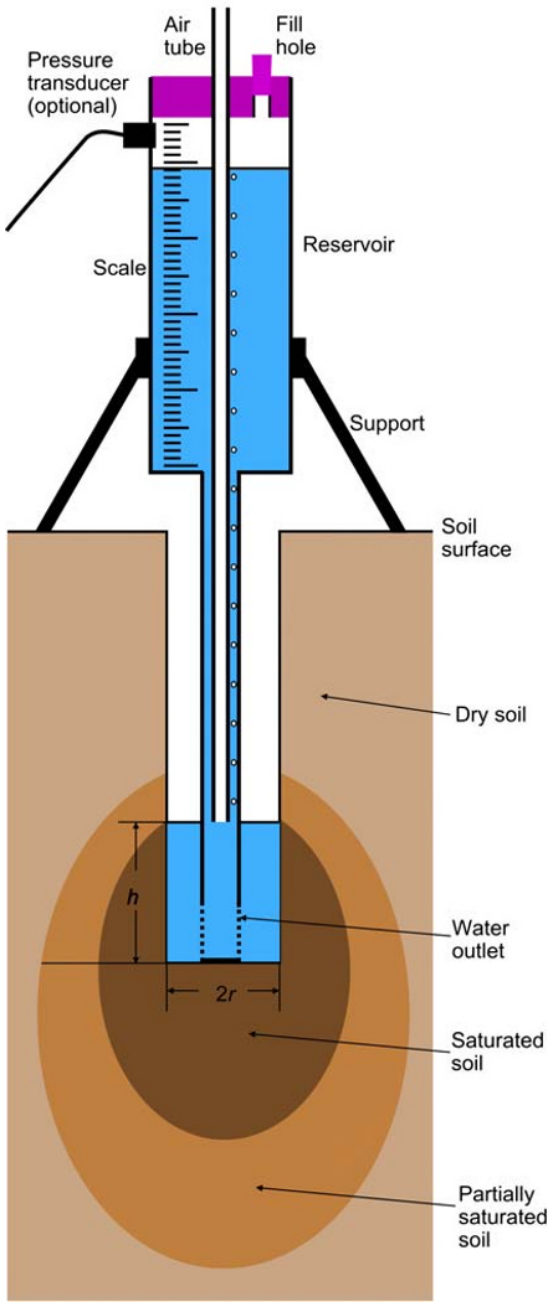

Fig. 18.2 Schematic of a borehole permeameter.

The basic design and operation of a user-friendly version of the borehole permeameter, the 'Guelph Permeameter', was described by Reynolds and Elrick (1986). It incorporates features to allow control of water inlet to the hole, adjustment of the water level in the hole and prevention of water swirling too quickly into the hole, causing possible erosion of the sides. For the last function, Reynolds and Elrick (1986) used fine gravel inside the bottom of the supply pipe.

Other designs of borehole permeameter have been published by Amoozegar (1992) and Bell and Schofield (1990). The latter authors describe an instrument for measuring soils of high hydraulic conductivity using a 40 L reservoir and separate water delivery and air tubes, controlled by taps. The basic control of the water level by shutting off the air into the upper part of a sealed reservoir is, however, the same as in the Guelph Permeameter.

Problems with borehole permeameter measurements arise because the progress of infiltration sometimes fails to follow the theoretically expected course. Stephens *et al.* (1987) discovered that, in some of their measurements, the rate of infiltration dropped initially, as expected, and then rose again after some time, to reach a new (and higher) steady rate. Bell and Schofield (1990) also reported increasing infiltration rates with time, not necessarily reaching a steady state.

Operation The first requirement is to prepare a suitable auger hole for the test. It is important that the lower part of this, which will be used for the test, is of as uniform diameter as possible and that the bottom of the hole is flat. Special augers are available from several manufacturers to achieve this, but if a spiral auger is used, it should have the small lead tip ground off. If the soil contains a significant quantity of clay, it may be necessary to remove the smeared layer (see Section 18.2.1). If the hole is sufficiently shallow, smearing can be identified by shining a light onto the exposed surface. Smeared soil appears smooth and may look a little shiny. Suitable diameters range from 20 to 100 mm, although the larger the diameter, the more water is required and the greater depth of water in the hole needed to ensure a reliable result (Bell & Schofield, 1990). This reduces the depth resolution, uses more water and takes a longer time to achieve steady state.

Assemble the permeameter and place it in the hole. The base of the water delivery tube usually most conveniently sits on the bottom of the hole. In shallow holes, lateral support for the reservoir is needed, using a tripod or other stand. The permeameter can now be filled with water. Note that in Fig. 18.2, there is no provision to prevent water filling the hole during this operation. Several ways are possible for this, including taps (Bell & Schofield, 1990), screwing the air tube into the water delivery tube (Reynolds & Elrick, 1986) or pushing a soft plastic seal against the bottom of the water delivery tube (Soilmoisture Equipment Corp., 2012). The reservoir should be full. This is because control of water supply into the hole depends on developing a partial vacuum in the top of the reservoir. If there is too much air initially in the reservoir, then a considerable quantity of water must flow into the hole before a vacuum is established in the reservoir to oppose water flowing into the hole.

Seal the reservoir and raise the air inlet tube to set the desired depth of water in the well. Air will enter the air inlet tube, allowing water to flow out into the well until water covers the bottom of the air inlet tube and cuts off the air. The Mariotte principle will now control the water level in the hole, with only minor fluctuations of the level.

Selection of suitable water head(s) in the well is a compromise between accuracy, depth resolution and water economy. Bell and Schofield (1990) recommended that the ratio of the water depth to the borehole radius, h/r, be at least 10 to ensure reasonable accuracy of calculated saturated hydraulic conductivity at any given flow rate. However, this usually results in large depths of water in the well, which increases water use, takes longer to achieve a steady flow rate and increases the chance of spurious measurements resulting from heterogeneities in the well. Most workers appear to use ratios between 2 and 5.

Monitor the water level in the reservoir at set time intervals, which is a measure of the flow rate into the hole. A 1- or 2-min interval is suggested as an initial try, but in slowly permeable soils, much longer intervals may be appropriate.

If the soil is very permeable, water may drain out of the hole so rapidly that there is an almost continuous flow of air up the air tube, resulting in large bubbles and consequent large fluctuations in the water level in the reservoir.

Continue the test until a steady rate of fall of the water level in the reservoir is achieved. This is the desired measurement.

There are two basic modes of operation. One is a test at a single level of water in the hole, while the other uses two or more levels sequentially (see the following text). If more than one level is used, the shallowest water level should be used first, followed by successively deeper ones. To change the water level, raise the air tube to the next desired height and repeat the test.

After testing the hole as described in the previous text, the hole may be deepened and measurements made at a new depth.

Calculations Much of the complication in making the calculations can be avoided by setting up the relevant equations in a spreadsheet, so that only a few numbers need be entered to perform what may otherwise be a complex calculation. Provided that the formulae have been well tested beforehand, it also makes errors in the calculations much less likely. A suitable spreadsheet is available on the website of Soilmoisture Equipment Corporation (www.soilmoisture.com) in the Operating Instructions (Guelph Permeameter) section.

First, changes of water level in the reservoir must be converted to volumes of water. The effective cross-sectional area of the reservoir can be calculated, knowing the inner diameter, D, of the reservoir tube and the *outer* diameter, d, of the air tube. The effective cross-sectional area, A, is then given by

$$A = \frac{\pi(D+d)(D-d)}{4}. \qquad (18.2.8)$$

Multiplying A by the level change yields the volume of water flowing out of the hole. Alternatively, the effective cross-sectional area can be measured directly by filling the reservoir (containing the air tube) with water, collecting and measuring the water flowing out of it from a measured fall in the water level.

The shape factor(s), C, must also be calculated according to Equation 18.A.30. These are incorporated into the spreadsheet on the Soilmoisture Equipment Corporation website.

CALCULATION WITH MULTIPLE HEADS Where the test is run with two different heads of water in the borehole, Equation 18.A.29 may be solved for each value of h, to derive both K_{fs} and α.

The solutions for steady flow rates Q_1 and Q_2 at heads h_1 and h_2 are given by Reynolds and Elrick (1986) and can be rearranged to give

$$K_{fs} = \frac{h_1 C_2 Q_2 - h_2 C_1 Q_1}{\pi[2h_1 h_2(h_2 - h_1) + r^2(h_1 C_2 - h_2 C_1)]}; \qquad (18.2.9)$$

$$\alpha = \frac{2(h_1 C_2 Q_2 - h_2 C_1 Q_1)}{\left(2h_2^{\,2} + r^2 C_2\right) C_1 Q_1 - \left(2h_1^{\,2} + r^2 C_1\right) C_2 Q_2}, \qquad (18.2.10)$$

where C_1 and C_2 are the values of C corresponding to h_1/r and h_2/r.

If tests have been run at more than two depths, then a least squares approach is possible, as described by Reynolds and Elrick (1986). Unfortunately, the equations are *ill conditioned*, which means that a small error in measuring Q or h is likely to produce a large error in K_{fs} or α or both. The theory also assumes that the soil is homogeneous over the largest depth range measured. Changes in soil hydraulic properties over the depth range of heads employed, macropores or other preferential flow paths or changes in borehole conditions between measurement runs (e.g. partial collapse of the borehole) will affect the results and lead to poor estimates of K_{fs} or (especially) α, often producing a negative value for one or both parameters. Ragab and Cooper (1993) reported negative values of α being recorded in 34–55% of measurements in a small catchment in South West England.

CALCULATION WITH A SINGLE HEAD K_{fs} is relatively insensitive to α. Bell and Schofield (1990) estimated a maximum error of 20% in K_{fs} when α was varied from 10 to 100 m^{-1}, appropriate for coarse soils. For these reasons, several workers prefer to use a single head measurement, with either an independently measured or estimated value of α. Appropriate values of α according to Elrick *et al.* (1989) are:

Compacted, heavy, structureless clays and silts	1 m^{-1}
Unstructured clays, silts and very fine sands	4 m^{-1}
Most structured clays, loams and medium and fine sands	12 m^{-1}
Coarse and gravelly sands; highly structured macroporous soils	36 m^{-1}

Bell and Schofield (1990) recommended a single value of 20 m^{-1} for high permeability soils where no other estimated value of α was available, being in the middle of the range and close to where a minimum error resulting from an incorrect value of α may be found.

In any event, if the calculation for a two-head experiment returns an unrealistic value for α, it is still possible to derive an estimate for K_{fs} from the measurements with each of the two heads and an assumed value for α.

For a single head, K_{fs} is estimated directly from Equation 18.A.29 as

$$K_{fs} = \frac{Q}{\pi\left[r^2 + \frac{2h}{C}\left(h + \frac{1}{\alpha}\right)\right]}. \qquad (18.2.11)$$

Commercially available equipment A fully engineered version of the Guelph Permeameter is sold by Soilmoisture Equipment Corporation, Santa Barbara, California. A photograph is shown in Fig. 18.3. This makes setting up the equipment quite simple. It has dual concentric reservoirs to cover both high and low hydraulic conductivity soils, which can be selected by means of a knob on the body of the device. The standard instrument is suitable for operation at depths to 0.8 m, but deeper measurements can be made using an extension kit(s), with a limit of about 6 m depth. The theoretical limit is set by the maximum length of a column of water that can hang from the partial vacuum in the head space of the reservoir.

Fig. 18.3 Guelph Permeameter. Photograph reproduced with permission from Soilmoisture Equipment Corporation. (*See insert for colour representation of the figure.*)

The various parts fit together with plastic push-on connectors, which in many cases also seal the tubes. These can wear, sometimes surprisingly quickly, with the result that components may come apart and/or leaks develop. It is recommended, therefore, to purchase spares of those parts that are used frequently.

The device is simple to set up and, provided that precautions are taken to avoid scouring of the hole by limiting the rate at which water enters the hole initially, it is the most convenient way to perform constant head borehole tests.

18.2.2 Infiltration from rings at the surface

Single-ring infiltrometer

Perhaps the best-established technique for measurement of near-surface hydraulic conductivity is the ring infiltrometer. This is partly a result of its simplicity, requiring just a circular ring pressed a little way into the surface to avoid leaks, a means of maintaining an approximately constant head of water above the soil surface and measurement of the infiltration rate from the amount of water used to replenish the ring. Early applications assumed that the flow out of the ring divided by its surface area could be equated with the saturated hydraulic conductivity of the soil. Youngs (1987, 2001) showed from experiments with rings of different sizes that the infiltration rate depended very heavily on the ring diameter and inferred that the effect of capillarity (i.e. the additional force associated with matric potential) could not be ignored. This effect had previously been explored by Wooding (1968) for a soil whose hydraulic conductivity corresponds to the Gardner (1958) form, Equation 16.2.2.

Some authors (e.g. Lassabatère *et al.*, 2006) have used a simplified experimental technique. Rather than try to maintain a constant head in the ring, they noted that if a known volume of water sufficient to make only a shallow pool of water is put into it, then the fluctuation in head at the soil surface to when the water disappears is very small. The water is then replenished and the procedure repeated several times until a constant infiltration rate is achieved. An infiltration rate v time curve can be constructed from the replenishment times. Lassabatère *et al.* (2006) labelled this procedure the Beerkan method. They also extended the analysis method using the van Genuchten (1980) and Brooks and Corey (1964) models with particle size distribution of the soil, initial and saturated water content. By applying the theoretical model of Haverkamp *et al.* (1994), they were able to estimate the parameters describing both the soil water characteristic and unsaturated

hydraulic conductivity, as well as the field-saturated hydraulic conductivity.

Double-ring infiltrometer

The effects of capillarity had been recognised long before this, and attempts made to combat it by use of double rings, in which a small diameter ring sits inside a much larger one. The water level is maintained equally inside both rings, but only measurements from the inner one are used. The area inside the large ring provides a 'buffer zone', where the vast majority of the lateral flow should occur. Double-ring infiltrometers are still used extensively but require an outer ring diameter of at least 300–500 mm and so usually consume large quantities of water, as well as operator attention, to keep the water level in both inner and outer rings sensibly constant and equal to one another. The infiltration rate from the inner ring is assumed equal to the saturated hydraulic conductivity of the soil.

Talsma's method

Another solution to the lateral flow problem is to bury the ring some distance into the soil, so that flow is confined to be one-dimensional. In the early stages of infiltration, capillary effects usually dominate over those due to gravity and infiltration proceeds proportional to the square root of time, as described in Section 3.3. This can be used to estimate the sorptivity, while a more reliable means of measuring the saturated hydraulic conductivity is obtained by carefully removing the ring and contained soil and infiltrating water through it at a constant head until water drips out of the bottom. See Talsma (1969) or Clothier (2001) for more detail. This method is clearly only applicable for soil in which it is possible to insert a ring to some depth (Talsma used 250 mm) without unacceptable soil disturbance.

Twin rings

The analysis of Wooding (1968), Equation 18.A.21, showed that the infiltration from a single ring has two components, which can be easily separated. The component relating to the saturated hydraulic conductivity of the soil is equal to that which would occur under gravity alone through the area of the ring; that is, proportional to r^2. The part due to capillarity is proportional to the length of the perimeter of the ring or to r. Therefore, using two rings of different diameter, the two components can be distinguished. However, spatial variability means that there will usually be appreciable scatter between measurements at different locations with the same diameter ring. It is necessary, therefore, to make several (10–20) replicate measurements with each ring. Using Equation 18.A.21, for two rings of radius r_1 and r_2, we obtain

$$Q_1 = \pi {r_1}^2 K_{\mathrm{fs}} + 4 r_1 \phi_{\mathrm{s}} \tag{18.2.12}$$

and

$$Q_2 = \pi_2 {r_2}^2 K_{\mathrm{fs}} + 4 r_2 \phi_{\mathrm{s}}. \tag{18.2.13}$$

Then

$$K_{\mathrm{fs}} = \frac{Q_1 r_2 - Q_2 r_1}{\pi r_1 r_2 (r_1 - r_2)} \tag{18.2.14}$$

and

$$\phi_{\mathrm{s}} = \frac{Q_1 {r_2}^2 - Q_2 {r_1}^2}{4 r_1 r_2 (r_2 - r_1)}. \tag{18.2.15}$$

Choosing the diameter of the rings is important. Large rings have only a relatively small capillarity effect, while infiltration from small rings is dominated by capillarity. Scotter *et al.* (1982) found that adequate separation of K_{fs} and ϕ would be achieved if the larger ring was at least twice the size of the smaller one and suggested that rings of 250 and 500 mm would be suitable for a wide range of soils (Clothier, 2001). Youngs (1983) suggested that rings smaller than 150 mm do not usually provide sufficient sampling area to allow for a representative elementary volume. Data presented by him showed a rapid reduction in scatter between replicate measurements over a field as the size of the ring increased.

The pressure infiltrometer

A variant on the simple ring infiltrometer, the pressure infiltrometer, was introduced by Reynolds and Elrick (1990). The ring is inserted some depth into the soil, typically 50 mm, and a positive head of the order of 250 mm water maintained above it, usually by a Mariotte device. Reynolds and Elrick (1990) found that an equation of very similar form to that for the borehole permeameter (18.2.11) could be used to analyse the steady flow obtained for a single depth of ponding:

$$K_{\mathrm{fs}} = \frac{QG}{\pi r^2 G + r\left(h + \frac{1}{\alpha}\right)}, \tag{18.2.16}$$

with

$$G = 0.316\frac{r}{a} + 0.184, \tag{18.2.17}$$

where

d is the depth to which the infiltrometer ring has been inserted and

G is a shape parameter.

Reynolds and Elrick (1990) found that by assuming a value for α, substantial errors in estimation of K_{fs} would occur. They therefore recommended that measurements be taken sequentially at two widely different pressure heads, h, when both K_{fs} and ϕ_{s} can be calculated separately. This improves the robustness of the solutions to small measurement uncertainties. In this case, for steady flow rates of Q_1 and Q_2, corresponding to heads of h_1 and h_2:

$$K_{fs} = \frac{G}{r}\left(\frac{Q_2 - Q_1}{h_2 - h_1}\right); \qquad (18.2.18)$$

$$\phi_s = \frac{G}{r}\left(\frac{h_2 Q_1 - h_1 Q_2}{h_2 - h_1} - \pi r G \frac{Q_2 - Q_1}{h_2 - h_1}\right), \qquad (18.2.19)$$

and from (18.A.12)

$$\alpha \approx \frac{K_{fs}}{\phi_s}. \qquad (18.2.20)$$

The use of large pressure heads also makes measurement more rapid, which is a big advantage in slowly permeable soil.

The device is available as an attachment to the Guelph Permeameter or as a stand-alone instrument produced by Soilmoisture Equipment Corporation. Extreme care is needed when inserting the ring to prevent rapid flow paths from being created. This can be difficult in dry soils, for which it is recommended that they be wetted beforehand. The pressure infiltrometer is particularly useful for measurements of very slowly permeable soils, for example, heavy clays and clay liners.

The tension infiltrometer

This device is also commonly known as the disc permeameter. It is a variant on the single-ring infiltrometer, but instead of applying a small positive head of water on the soil surface, there is a small negative head. Clothier (2001) describes the evolution of the device.

The essential elements of a tension infiltrometer are depicted in Fig. 18.4. A water reservoir, controlled by a bubble tower (see the appendix, Section 18.B.2), delivers water through a porous membrane to the soil surface. The water potential just above the membrane is equal to the depth of the lower end of the air tube below the water surface in the bubble tower and can be adjusted by raising or lowering the air tube. A thin layer of fine sand or silica flour is used to ensure good contact with the soil surface. This needs to remain saturated at the lowest potential employed and be as thin as possible while filling all gaps between the membrane and soil surface. The porous membrane may be of sintered glass (Clothier & White, 1981), high conductivity porous ceramic or fine nylon mesh (Perroux & White, 1988), with an air entry value greater than the lowest potential to be used. Some designs (e.g. Chong & Green, 1983; Jarvis *et al.*, 1987) dispense with the porous membrane in favour of a mesh screen and rely on the contact sand to provide the porous barrier to air entry. This is simpler to construct and more robust but less convenient in use. Both Chong and Green (1983) and Jarvis *et al.* (1987) inserted a ring into the soil to confine flow in the early stages to the vertical direction and to support the infiltrometer. Some designs (e.g. Chong & Green, 1983; Jarvis *et al.*, 1987) use hypodermic needles inserted through ports in the side of the reservoir instead of a bubble tower. The needle size and its height

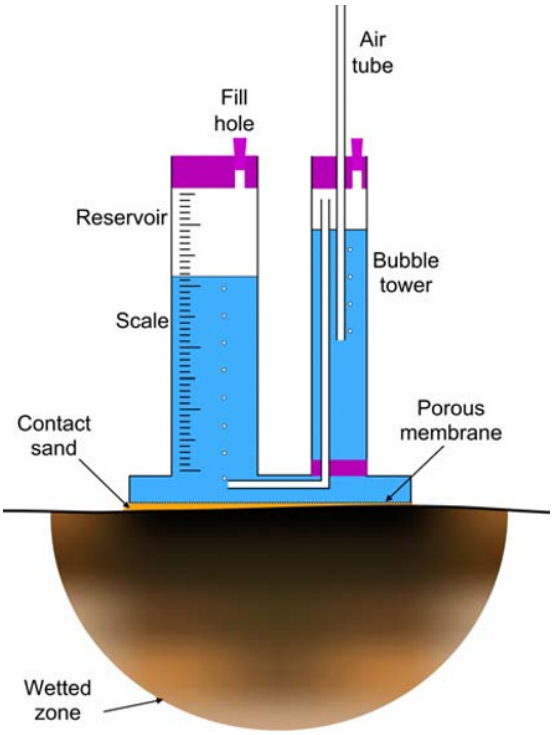

Fig. 18.4 Schematic of a tension infiltrometer.

in the reservoir control the applied potential, but it is difficult to predict it precisely in advance without calibration. Jarvis *et al.* (1987) used a pressure transducer in the base of the infiltrometer to measure the pressure. A bubble tower is a more flexible, but expensive, arrangement.

Operation of the infiltrometer is simple, the most difficult part being to ensure good contact between the porous membrane and the soil surface *via* the contact sand. With a smooth surface prepared using the sand, the infiltrometer is filled with water and the air tube set at the desired height. Blocking off the air tube prevents water from running out of the base while positioning the infiltrometer. Once this has been done, the air tube can be unblocked and measurements of infiltration at fixed time intervals made by reading the level from the scale. Measurements need to be made until a steady infiltration rate has been achieved. This may take anything from several minutes to several hours and there may be a temptation to finish the experiment prematurely as a result. This should be resisted.

The analysis of Wooding (1968), Equation 18.A.23, can be used to estimate K_t and ϕ_t from the steady infiltration rate. These are the hydraulic conductivity and matric flux potential of the near-surface soil at the applied matric potential. This equation involves two unknowns. To separate them, there are a number of possible strategies.

The early-time infiltration is dominated by vertical flow under capillary conditions, that is, it should conform to infiltration proceeding according to the square root of time, as described for Talsma's method in Section 18.2.2, which yields the sorptivity from Equation 3.3.2. By measuring the

change of water content, $(\theta_f - \theta_i)$, from before (usually by taking a sample of soil close to the infiltrometer position), and after the experiment (from beneath the infiltrometer), the sorptivity can be used to calculate an approximate value for ϕ_t and α from (White & Sully, 1987; Clothier, 2001)

$$\phi_t \approx \frac{0.55S^2}{\theta_f - \theta_i}, \tag{18.2.21}$$

and

$$\alpha \approx \frac{K_t(\theta_f - \theta_i)}{0.55S^2}. \tag{18.2.22}$$

Where the approach to constant rate infiltration is rapid or where a fairly thick layer of contact sand has been used, the square root of time phase may be difficult to identify.

The same strategy as for ordinary twin ring infiltrometers, described in Section 18.2.2, can be used to circumvent this problem (Smettem & Clothier, 1989). This gives two sets of equations which can be solved to yield K_t and ϕ_t. The same limitations apply as described in that discussion. Thony *et al.* (1991) proposed using three (or more) different radius rings, each used at several different pressure heads, with a regression of infiltration rate against ring radius. This was labelled Triple Ring Infiltrometers at Multiple Suctions (TRIMS) and claimed to overcome some of the problems associated with the spatial separation of rings.

A further possibility, due to Ankeny *et al.* (1991), is to run the experiment with the infiltrometer in one position but at two (or more) different heads. With two heads, the steady infiltration rate is described by

$$Q_1 = \pi r_0^2 K_{fs} e^{\alpha\psi_1} + 4r_0 \frac{K_{fs} e^{\alpha\psi_1}}{\alpha}, \tag{18.2.23}$$

and

$$Q_2 = \pi r_0^2 K_{fs} e^{\alpha\psi_2} + 4r_0 \frac{K_{fs} e^{\alpha\psi_2}}{\alpha}, \tag{18.2.24}$$

where Equations 18.A.10 and 18.A.12 have been used to substitute for $K(\psi_t)$ and ϕ_t in Equation 18.A.23. These can be solved for K_{fs} and α by an iterative technique.

Performing the experiment at several different values of h allows the unsaturated hydraulic conductivity function to be built up over a range of near-saturated water potentials. Although there is an assumption that the exponential form of the hydraulic conductivity function applies, this needs to be approximately true only over the limited range between two measurement potentials.

The tension infiltrometer method's main strength is that it allows the hydraulic conductivity of the soil at high, but not saturated, matric potential to be measured. This takes out some or all of the macropores from the flow field, allowing their influence to be partially or wholly excluded, depending on the selected head and hence the macropore size distribution as well as the soil's intrinsic hydraulic conductivity to be investigated (e.g. Jarvis *et al.*, 1987).

Sorptivity measurement from horizontal boreholes

An interesting application of unsaturated infiltration theory was demonstrated by Flint *et al.* (1994) to measure sorptivity of volcanic tuff at depths of several tens of metres, accessed by a large shaft. Horizontal boreholes 9 m long and 0.11 m diameter were drilled from the shaft, and a packer was inserted to seal off the open end. A pipe, passing through the packer, injected water into the hole from a 160 L Mariotte device to maintain a zero constant pressure at the top of the borehole. Flint *et al.* (1994) argued that at early times, the effect of gravity and the non-planar wall could be ignored and that infiltration would proceed according to the square root of time. The sorptivity of the formation surrounding the borehole could thus be estimated from the infiltration rate. After infiltration for some time, the increase in water content of the formation was measured using a neutron probe. This showed fair agreement in most cases with the amount of water that had infiltrated, as measured by the Mariotte device. In other cases, it seemed likely that water had infiltrated cracks in the tuff, enhancing infiltration and reducing the water detected by the neutron probe. Fair agreement was also obtained between sorptivity estimated from the boreholes in the field and from laboratory measurements on soil cores taken from them.

18.3 Unsaturated Measurements

As well as saturated hydraulic conductivity, some of the methods described in Section 18.2 estimate unsaturated hydraulic conductivity very close to saturation, relying on an assumed exponential form of the unsaturated hydraulic conductivity function, Equation 18.A.10. They also apply only to small volumes of soil.

The methods described here measure hydraulic conductivity on large volumes of soil over a wider range of water status, although to only a little drier than 'field capacity'. Reliable field measurement techniques at the dry end of the water range remain elusive. The methods are also amenable to measuring variations of the hydraulic conductivity function with depth.

18.3.1 Instantaneous profile method

The instantaneous profile method is a popular field technique, simple in concept and fairly easy to implement experimentally. The term appears to have been originated by Watson (1966), although the method was in use before this.

The essential requirements are a reasonably flat, bare site that can be flooded over an area of at least 5 m diameter (larger if measurements are needed to depths greater than 2 m),

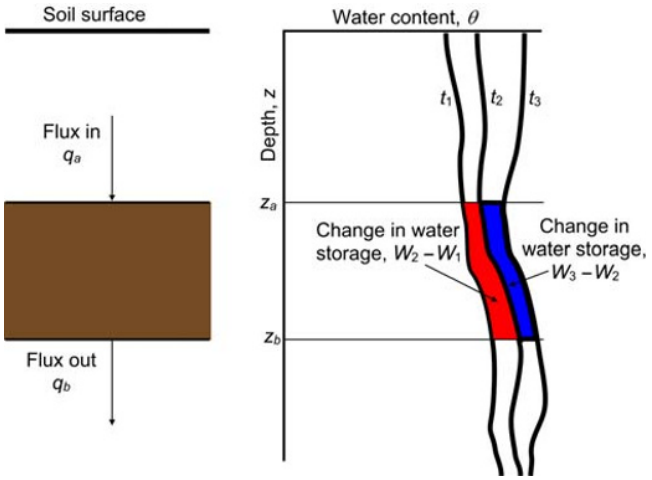

Fig. 18.5 Relationship between one-dimensional water flux across two depths and change in water storage between them.

a means of measuring the water content and water potential of the soil as a function of depth and time, a means of covering the soil surface over the area to prevent evaporation and rainfall input for a period of a few weeks and a supply of water sufficient to saturate the profile over the experimental area to the maximum depth of measurement.

Theory

The hydraulic conductivity is defined as the ratio of the water flux to the hydraulic potential gradient. In one dimension (vertical), this can be written as

$$K = -\frac{q}{\left(\frac{\partial \psi}{\partial z}\right)}. \qquad (18.3.1)$$

The hydraulic potential gradient can be measured fairly readily by tensiometers placed at different depths. The soil water flux, q, however, is more difficult, and reliable field instruments are not available for the range required. It can, however, be calculated from the change in water content of a volume of soil. In the one-dimensional case, this can be regarded as a slab of soil with no flow across the vertical faces, since all water is assumed to flow vertically. This is illustrated in Fig. 18.5 for two depths, z_a and z_b, at three times, t_1, t_2 and t_3. In the absence of any flow out of the sides of the slab or any other sources or sinks of water (e.g. root extraction), the rate of change of water stored in the slab, W, is equal to the difference between the flux of water into it, q_a, and that flowing out, q_b, that is,

$$\frac{dW}{dt} = q_a - q_b. \qquad (18.3.2)$$

Over a period of time, say, between t_1 and t_2, this results in a change of water storage in the slab of $W_2 - W_1$. This can be related to the average flux $\overline{q_a}$ and $\overline{q_b}$ across z_a and z_b over the time interval $(t_2 - t_1)$ as

$$W_2 - W_1 = \int_{z_a}^{z_b} [\theta(t_2) - \theta(t_1)]dz = (\overline{q_a} - \overline{q_b})(t_2 - t_1). \qquad (18.3.3)$$

This can be rearranged to

$$\overline{q_b} = \overline{q_a} - \frac{W_2 - W_1}{t_2 - t_1} = \overline{q_a} - \frac{\int_{z_a}^{z_b} [\theta(t_2) - \theta(t_1)]dz}{t_2 - t_1}, \qquad (18.3.4)$$

that is, if we know the average flux over a period of time across one depth, together with the change of water storage between that depth and another one over that time, then we can calculate the average flux across the second depth.

In the instantaneous profile method, the depth at which we know the water flux is the soil surface and the known flux is zero, that is, $z_a = 0$ and $q_a = 0$ at all times. So by measuring the water content at a series of times and at several depths, the average water flux across any chosen depth can be calculated from the integrated change in water content from the surface to that depth.

Experimental methods

The first requirement is for a reasonably level site, which can be kept flooded, usually for several days, to saturate the profile uniformly. Unless the site is reasonably level, it is not possible to pond water over the whole surface. The amount of water needed to do this is quite large. For a plot of 5 m square, at initial and field-saturated water content of 0.2 $m^3\,m^{-3}$ and 0.5 $m^3\,m^{-3}$, this theoretically requires 15 m^3 water to wet it to a depth of 2 m, although some will flow out of the bottom and there will inevitably be some other water losses, so that planning on 25 m^3 would be wise. The plot will need to be confined by a bund or plastic-covered boards to keep a small head of water over the area.

Clearly, the more frequently and the more depths at which water content is measured, the better can the changing flux over both time and depth be determined. TDR with rods inserted vertically from the surface is very well suited for this, as it inherently measures water content down to the depth of the length of the rods and frequent automatic logging is possible, although the maximum depth of measurement may be limited. Capacitance probes (e.g. Sentek EnviroScan) are able to measure frequently at a limited number of discrete depths, and so some degradation of data quality will be experienced from this cause. Manual methods of water content measurement (e.g. neutron probe or Sentek Diviner) limit both the depth and time resolution. Nevertheless, many investigations have used neutron probes for measuring the water flux using the instantaneous profile method (e.g. Flühler *et al.*, 1976; Dane, 1980; Dane & Hruska, 1983; Hodnett & Bell, 1986; Moutonnet *et al.*, 1988; Sisson *et al.*, 1988). Others have relied, apparently successfully, on laboratory-measured soil water characteristic curves, together with tensiometer measurements, to estimate water content changes (e.g. Arya *et al.*, 1975a;

Matzdorf *et al.*, 1975; Rice, 1975; Reicosky *et al.*, 1977). With measurements of water content made at discrete depths, interpolation and integration of this variable over a depth range are needed using methods discussed in Section 7.9.2.

Potential gradient is measured almost exclusively by tensiometers (Chapter 12), although gypsum blocks have been used where low water potentials are experienced (Wellings, 1984a). This is not usually necessary, as it is very unusual for matric potential to fall below about –5 m water in this type of experiment. The use of pressure transducer tensiometers connected to a data logger is useful to aid collection and processing of a large amount of data and to follow the early stages of drainage, which happen very quickly in most soils. TDR or capacitance probes can be connected to the same data logger to ensure that data are collected on a common time base.

Selection of appropriate monitoring depths should be guided by a survey of the profile before the experiment. This should identify depths at which there are likely to be sharp changes in hydraulic properties. As far as possible, the immediate vicinity of layer boundaries should be avoided, so that potential profiles, in particular, are not affected by them. Some workers like to install tensiometers at depths halfway between water content monitoring depths, arguing that this will make definition of the potential gradient better. The disadvantage of this is that it makes the relation of water content and matric potential more uncertain. Except for the problem of layer boundaries described in the previous text, potential profiles are usually quite uniform and so there is little disadvantage in practice if potential and water content data are collected at the same depths. Depending on the equipment and other resources available, there is no reason why the same number of depths should be monitored by each type of instrument.

To reduce the problems caused by spatial variability, water potential and water content should be measured as close together horizontally as possible, consistent with no disturbance to the reading of one instrument by the other. For a neutron probe and tensiometer combination, for instance, a separation of 0.5 m should be adequate. With an access tube-mounted dielectric probe, a closer separation is possible. Where resources permit, replication of instrument arrays is advisable.

Once the monitoring equipment has been installed, the plot may be flooded, and the progress of wetting monitored by following the evolution of water content and/or water potential. Complete saturation may not be achieved throughout the profile. For instance, beneath a less permeable layer, the water flux will not be sufficient to bring the soil to saturation. Provided that a stable water content and potential profile has been achieved, this will not cause a problem, other than restricting the range of water status achieved. One problem that can be caused by a less permeable horizon, however, is ponding of water on top of it, which can run off laterally, especially if there is a significant slope to the layer. This may mean that more water (and time) are needed to achieve steady conditions. Investigation of the profile before the experiment should help to identify the presence of such horizons. Because rapid wetting may trap significant quantities of entrapped air, it is wise to maintain a flooded surface for 1 or 2 days after the wetting front has reached the bottom of the profile. This should show a small and slow increase in water content, while water potential stays effectively constant.

As soon as the profile has been wetted and surface water has disappeared, it should be covered by a plastic sheet to prevent evaporation and exclude rain. Access will be required for reading the instruments if they are not all automatic. In most cases, tensiometers should not need to be refilled over the relatively short period of an experiment with fairly modest matric potentials generated, unless there is a fault. Where access is needed and/or instruments need to protrude through the plastic sheet, it should be raised up and taped securely around them to prevent rain ingress at these points. Rainfall during the period of the experiment, which can take typically 90 days, can cause particular problems apart from possible entry *via* the plastic sheet. A small slope on the experimental site may cause water to run over the surface and into the experimental area. During the later part of the experiment, lateral subsurface flow may cause unexpected wetting at depth when the surrounding soil is much wetter (C.M.K. Gardner, personal communication). In sunny weather, the surface beneath the plastic sheet gets quite hot. A surface mulch beneath the cover helps to maintain temperature closer to that outside while suppressing evaporation.

Once irrigation has ceased, the initial stages of drainage are usually rapid, requiring frequent measurement, ideally every few minutes, especially near the surface. With automatic instrumentation, this is not a problem, but with manual recording of water content and/or potential, the first few hours after beginning observations are likely to be hectic. After 24 h, the rapid phase of drainage is usually over and measurements of the instruments four times a day will usually suffice, reducing to once or twice daily after 3 or 4 days.

Data analysis

Analysis of the data is straightforward, requiring only estimation of the water flux by difference of the integrated water content profiles and of hydraulic gradient by difference of water potential at adjacent depths divided by the depth interval. If tensiometer readings are made at the same depths as those of water content, the relevant potential gradient is obtained from the difference between the water potential at the depth above and that below. If the profile is fairly uniform, this should cause no particular problem. Where there is a sharp change in soil properties, there should also be no problem, provided it was recognised during the experimental design and depths were selected accordingly. It is not wise to interpolate water potential readings across a sharp boundary, although if its position is sufficiently well known, a good estimate of the potential

profile can be made by extrapolation of readings from tensiometers above and below the boundary.

Data from automatically recording instruments are usually considerably less noisy than from manually collected ones (although not necessarily more accurate – see the discussion on accuracy and precision in Section 7.5). This is particularly true for a neutron probe *versus* electromagnetic water content measurement but applies also to mercury manometer or puncture tensiometers and ones with pressure transducers close to the cup. With neutron probe measurements and frequent monitoring, the noise in the measurements may well be comparable with, or even much greater than, the change from one reading occasion to the next. Even though the water content of the profile may be reducing steadily, the measured value can well increase from one occasion to the next. This is clearly unrealistic. Tensiometers with parts above ground can exhibit diurnal fluctuations caused by air temperature variations or solar heating. With strictly random noise, as for the neutron probe, three approaches are possible:

1 A *moving average* of the readings can be used. This will assign a reading at one time to the average of the same number of readings taken both before and after that occasion. This can be done for a single depth or for the integrated water content from the surface to each depth in the profile. Since the integrated water content combines readings for several depths, this is expected to be inherently less noisy than that for a single depth, and so fewer readings will need to be averaged. This is preferable because the averaging process reduces the time resolution of the data. Also, a smaller number of readings may be averaged when the water content is changing rapidly than when it slows down. The advantage of using a moving average is that it makes no assumption about the actual form of the water content–time relationship.

2 Fitting the water content variations with time to an assumed functional form, usually by minimising the sum of squares of differences between the assumed curve and the actual readings. Once again, there is a choice between fitting data for individual depths and that integrated over some depth of profile. Suitable functional forms may be a polynomial, an exponential relationship with time (or a sum of these) or something like $A/(1+Bt^x)$. Polynomials are generally quite simple but suffer in some cases from unexpected 'bumps' and often fit poorly near the ends of a data set. Exponentials or reciprocal relationships have the merit of reducing with time, which mirrors the expected qualitative behaviour. In the end, it is a matter of judgement which relationship gives the most appropriate behaviour.

3 To use the data 'raw' and postpone any smoothing to the point at which the hydraulic conductivity curves are calculated, when noise from other data sources will also be incorporated.

All of these strategies have their merits and no particular recommendations are made here, although my own preference has been to use the second of those described.

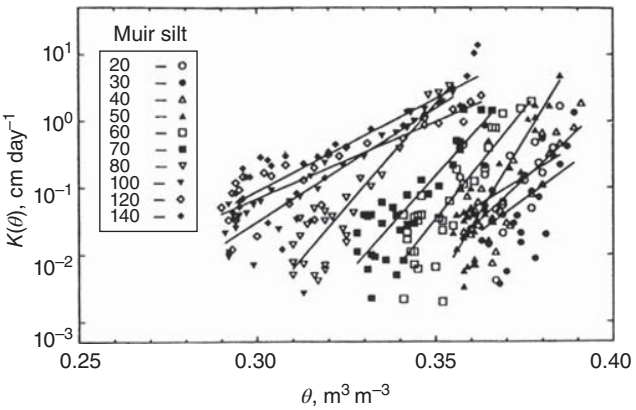

Fig. 18.6 Example of instantaneous profile measurements of unsaturated hydraulic conductivity for a silty soil. Sisson *et al.* (1988). Reproduced with permission from John Wiley & Sons.

Whichever strategy is adopted, it is important to examine critically the fitted data against the raw readings to make sure that no essential features have been smoothed away or that no one part of the data set fits significantly less well than any other.

The end result of the process is a set of relationships between water content, matric potential and hydraulic conductivity. Although the general shape of the relations should be quite clear, experience suggests that there is still a lot of uncertainty in the data, even after smoothing. This is illustrated in Fig. 18.6. In this example, water potential was measured using mercury manometer tensiometers to 1.6 m depth arranged around a neutron probe access tube in a circle of 0.8 m diameter. Water was ponded over a 3 m by 4 m area at a depth of 50–60 mm for 16 days. After covering the plot, measurements were made initially every 2–4 h and then with decreasing frequency for at least 28 days.

Limitations and problems with the technique

Baker *et al.* (1974) reviewed the instantaneous profile method critically. They pointed out:

- That wetting of the profile to achieve ponded conditions at the surface carries a danger that water may infiltrate down the side of poorly fitting tensiometers to produce wetting of the profile around a tensiometer in or beneath poorly conducting soil. This may take a long time to disperse and produce misleading results. Following the advice in Section 12.7 should minimise this hazard.
- That neutron probe measurement of water content is preferable to using water content estimated from soil water characteristic curves.
- An impeding horizon in the soil may cause lateral runoff (or run-in from the surroundings if they become wetter).
- The soil below an impeding layer will not reach as high water potentials as soil above it.
- The method is not suitable for sites with more than a very shallow slope.

• The method cannot be used in forested areas or where lateral roots from surrounding vegetation intrude beneath the experimental plot. In such cases, isolating the plot by trenching is possible but expensive in labour.

Flühler *et al.* (1976) examined the likely errors in the method arising from measurements and manipulation of the data. They found that in the early stages of drainage, errors in water content measurement by neutron probe contribute most to the error in K and, in the latter stages, the hydraulic gradient becomes small, and so tensiometer errors are more important. In their example, the latter were much larger than the relative errors caused by uncertain water content readings at the beginning of the experiment. In practice, errors near the beginning of the experiment resulting from water content measurements may be larger than assumed by Flühler *et al.* (1976) because of the finite time taken to collect the water content data and the rate at which the profile drains. This is especially true in permeable soils.

18.3.2 Zero flux plane method

It is possible under some conditions to extend the range of values measured using the instantaneous profile method. Arya *et al.* (1975a) used the zero flux plane (ZFP) technique in preference to the instantaneous profile method to measure unsaturated hydraulic conductivity. The ZFP method is more commonly employed to measure the soil water balance of a soil profile, and its detailed description will be deferred to Section 24.3.5. The experimental procedure is much the same as for the instantaneous profile method, except that the soil surface is left uncovered, so that water evaporates from the surface as well as draining through the bottom of the profile.

Arya *et al.* (1975a) left their soil uncovered throughout the experiment, but there is no reason why it should not be covered initially and then uncovered to extend the range to drier conditions after some time. This does, however, depend on the soil at the surface drying steadily and not being periodically wetted by rain, which would make the method unsuitable in many areas. In principle, a shelter with open sides could be placed over the plot to allow evaporation, but non-uniform evaporation beneath the shelter would potentially cause problems.

18.3.3 Simplified versions of the instantaneous profile method

Several methods have been proposed to simplify the instantaneous profile procedure, to reduce either the computational or the experimental burden.

The θ method (Libardi *et al.*, 1980)

Libardi et al. (1980) noted that during drainage, the hydraulic potential profile for many soils is very close to unity (i.e. the matric potential is the same at all depths). It can be shown that this will be approached for any uniform soil profile over a sufficiently deep water table. Libardi *et al.* (1980) also assumed that the hydraulic conductivity could be represented as a function of water content as

$$K = K_0 e^{\beta(\theta-\theta_0)} \tag{18.3.5}$$

where K_0 and θ_0 are the hydraulic conductivity and water content at the beginning of the drainage phase, that is, close to K_{fs} and θ_{fs}.

They further assumed that the average water content of the profile, θ^*, above any depth, L, was linearly related to the water content at that depth:

$$\theta^*(L,t) = \frac{1}{L}\int_0^L \theta(z,t)\mathrm{d}z = a\theta(z,t) + b, \tag{18.3.6}$$

where a and b depend only on depth.

The one-dimensional form of the Richards Equation 2.2.6 is

$$\frac{\partial\theta}{\partial t} = \frac{\partial}{\partial z}\left(K\left[\frac{\partial\psi_m}{\partial z} - 1\right]\right). \tag{18.3.7}$$

With the unit gradient assumption, $(\partial\psi_m/\partial z) = 0$, this simplifies to

$$\frac{\partial\theta}{\partial t} = -\frac{\partial K}{\partial z}. \tag{18.3.8}$$

Using (18.3.5) and (18.3.6) and integrating, (18.3.8) reduces for large times (>a few hours) to

$$\theta_0 - \theta = \frac{1}{\beta}\ln t + \frac{1}{\beta}\ln\left(\frac{\beta K_0}{aL}\right). \tag{18.3.9}$$

β and K_0 are obtained from the slope and intercept of a plot of θ *v* ln t. Equation 18.3.9 is also valid when θ^* and $\theta_0{}^*$ are substituted for θ and θ_0, which allows the value of a to be derived.

The flux method (Libardi *et al.*, 1980)

This method derives from the same assumptions as for the θ method, but they are inserted directly into Equation 18.3.8:

$$-aL\frac{\partial\theta^*}{\partial t} = K_0 e^{\beta(\theta-\theta_0)}. \tag{18.3.10}$$

Taking logarithms, we obtain

$$\ln\left(-aL\frac{\partial\theta^*}{\partial t}\right) = \ln K_0 - \beta(\theta_0 - \theta), \tag{18.3.11}$$

allowing β and K_0 to be estimated from a plot of $\ln\left(-aL\frac{\partial\theta^*}{\partial t}\right)$ *v* ln K_0. This method does not have the same time restriction as the θ method.

Lax's (1972) method
Equation 18.3.8 can be written as

$$\frac{\partial\theta}{\partial t} = -\frac{\mathrm{d}K}{\mathrm{d}\theta}\frac{\partial\theta}{\partial z}. \qquad (18.3.12)$$

By assuming a functional form for the relation between K and θ, the parameters can be estimated from the measured θ *v* t curve. Taking the form of Equation 18.3.5, for instance, an equation similar to (18.3.9) is obtained:

$$\theta_0 - \theta = \frac{1}{\beta}\ln t + \frac{1}{\beta}\ln\left(\frac{\beta K_0}{L}\right). \qquad (18.3.13)$$

This differs from (18.3.9) by the omission of the factor a, as this method does not involve the assumption of Equation 18.3.6. The parameters K_0 and β can be obtained by plotting θ against ln t (Lax, 1972; Sisson *et al.*, 1980).

The CGA method (Chong *et al.*, 1981)
Like the preceding simplified methods, the CGA method relies on the assumptions of a unit hydraulic gradient and that we can define θ^* as in Equation 18.3.6, but in this case the water content is assumed to vary with time as

$$\theta = At^B. \qquad (18.3.14)$$

Substitution into Equation 18.3.8 yields with some manipulation

$$K(\theta^*)|_L = -LA^{\frac{1}{B}}B\theta^{*\frac{B-1}{B}}. \qquad (18.3.15)$$

A and B can be estimated from fitting observed θ *v* t curves.

Comparison with the full instantaneous profile method
All of the aforementioned methods require only water content data, which is the more common measurement of water status, but assume that the profile is sufficiently homogeneous that the unit gradient approximation holds.

Dane (1980) compared the Libardi *et al.* (1980) θ method with the full instantaneous profile method. He found that the $(\theta_0 - \theta)$ *v* ln t plot fitted a different straight line in different time intervals. With this modification, moderately good agreement was obtained with results from the full analysis.

Tseng and Jury (1993) compared the simplified methods with the full instantaneous profile method in a numerical experiment. They generated two profiles with hydraulic properties obeying the van Genuchten–Mualem relations (van Genuchten, 1980), whose parameters varied in a random manner. In other respects, however, the profiles were homogeneous on a macroscopic scale, that is, there was no systematic dependence on depth.

Comegna *et al.* (2012) conducted a field experiment on a volcanic soil and analysed the results using both the full instantaneous profile technique and the simplified methods.

In both cases, the results of the simplified methods compared poorly with the full analysis. The additional effort required to install and read tensiometers as well as analyse the resulting data, when compared with the overall resource requirements of conducting the experiment, makes it difficult to justify the reduction in accuracy from leaving out vital information.

18.3.4 Constant rate flux methods

Imposing a constant and positive flux at the soil surface, rather than zero, allows the hydraulic conductivity to be measured at a steady state, similar to the crust test and constant rate irrigation methods for confined samples described in Section 17.8. In the case of unconfined soil, only constant rate irrigation is a realistic option and the lower boundary condition cannot be controlled. Provided that there is a good depth to a water table or confining layer, however, this should not pose a problem.

The most common way to impose a constant flux over a large area is by a rainfall simulator, sometimes called a sprinkling infiltrometer. Rainfall simulators are used extensively for research on soil erosion and usually have high water and power demands, which limits their use to sites where these can be supplied readily. The most common arrangement is for a nozzle or square array of nozzles to be fed from a pump at constant pressure. Different nozzles can give coarse control of the rate of delivery of water to the soil surface. Finer control is usually by means of a rotating disc with an adjustable size sector cut out of it. The solid portion of the disc intercepts the water from the nozzle and allows it through only when the open sector is in front of the nozzle. This has been found to be a more reliable method than changing the pressure of water feeding the nozzle. Further control can be exerted by changing the duty cycle of an intermittently operating feed pump, as discussed in Section 17.8.

A number of different nozzles in an array is preferred to a single nozzle with a wide coverage, as it is difficult to achieve uniform coverage of the area with one nozzle.

In reviewing different simulators, Green *et al.* (1986) concluded that the lowest achievable constant rate of input to the soil surface by such means was about 1 mm h^{-1}, which is high compared with the soil water flux in many soils during and following rainfall.

Prevention of evaporation, especially at the lower input rates, and interference by rainfall means that the soil surface must be protected. This normally requires a shelter with sufficient headroom to accommodate the sprinklers and for reading the instrumentation. The soil surface should be protected by a mulch to reduce the effect of raindrop impact, control temperature and further suppress surface evaporation.

18.3.5 The Poulovassilis combination method

In permeable and macroporous soils, the initial stage of drainage from a near-saturated condition occurs very

rapidly, making it difficult to capture the changes adequately, especially with manual measurements of water content and/or potential. On the other hand, it is difficult to apply constant rate irrigation at a rate lower than several mm d^{-1}.

To overcome these limitations, Poulovassilis *et al.* (1974) combined the two methods, using constant rate irrigation to measure the higher values of hydraulic conductivity and the instantaneous profile method for the lower values. They used a series of drippers over an area of a layered soil in Cyprus to measure high hydraulic conductivities with a decreasing series of constant irrigation rates, followed by the instantaneous profile method when it became impractical to impose a smaller constant flux. Hillel and Benyamini (1974) also used both steady rate irrigation, in this case using sprinklers, to impose irrigation rates increasing from 24 to 2400 mm d^{-1}, and the instantaneous profile method, but on a separate plot in the same field. There was a large overlap between the water flux range for each method. Good agreement was obtained between hydraulic conductivity as a function of water content calculated using the two methods (one steady state, the other dynamic).

Subsequently Cooper (1979) used a similar method to measure hydraulic conductivity down to 6 m depth in a volcanic soil in western Kenya. A 10 m square plot was covered by a fully enclosed shelter to exclude rainfall and suppress evaporation, which was reduced further by a grass mulch over the soil surface. The plot was divided into 25 2 m squares, each of which was supplied by water from an adjustable trickle source fed from a constant head supply. The supply to the central nine squares was subdivided by a manifold into four, each feeding a 1 m square, while the central 1 m square was further subdivided into 0.5 m squares.

Five neutron probe access tubes were used to monitor water content at the centre and towards the edges of the plot, while mercury manometer tensiometers, installed sub-horizontally from an access pit, measured water potential.

Irrigation at an initial rate of 23.4 mm d^{-1} took 21 days to achieve a steady state. This was followed by irrigation at a rate of 5.8 mm d^{-1} for a further 10 days, when steady state was again achieved. After this, irrigation ceased and measurements were made twice daily for 7 days, daily for a further 14 days, followed by daily readings of the tensiometers and twice-weekly neutron probe readings for 24 weeks.

Figure 18.7 shows cumulative drainage at three depths calculated from neutron probe readings during the free drainage (instantaneous profile) phase of this experiment, illustrating the amount of scatter to be expected in measurements of water content change. The lines have been drawn by eye to provide a smooth value for estimation of drainage flux. It is notable that measurable drainage was occurring even after more than 120 days.

The resulting K v θ curves for five depths are shown in Fig. 18.8. A further level of data smoothing was necessary to produce realistic curves. Note the clear similarity between the curves from 2.7 m and lower and also that

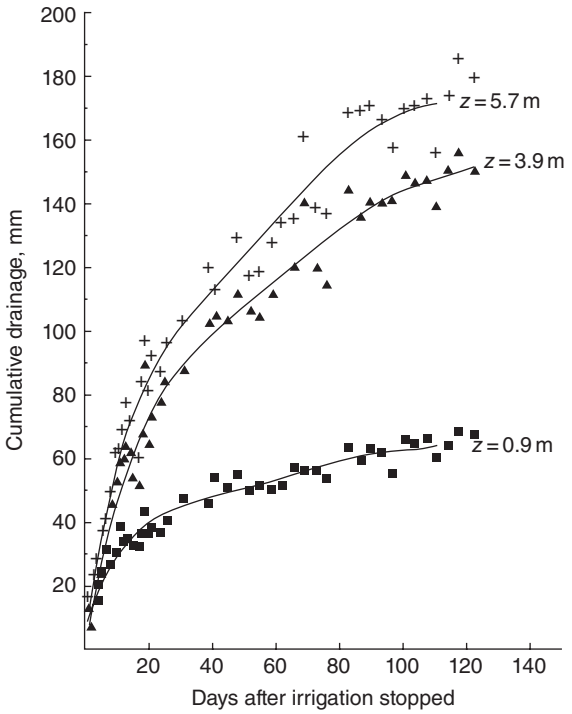

Fig. 18.7 Cumulative drainage across various depths during the instantaneous profile phase of a hydraulic conductivity measurement experiment in a deep volcanic soil in western Kenya (Cooper, 1979). Reproduced with permission from the *East African Agricultural and Forestry Journal*.

there is a progressive displacement towards higher water content at the deeper depths. The curve for the 5.7 m depth was used to predict drainage at a plot located about 30 m away, where the ZFP method had been used to make independent measurements of this quantity. The shape of the two curves corresponded very well, but use of the measured curve from the hydraulic conductivity plot underpredicted drainage by a factor of four. This was ascribed to the large sensitivity of the drainage curves to depth.

The combination method lends itself very well to measurements in fractured porous rock and, indeed, in many dual porosity media, where the fracture or macropore system requires high flow rates to characterise it and drains very rapidly once water input ceases. The matrix conductivity is often too small to be within the range accessible to steady infiltration rates.

Wellings and Cooper (1983), Wellings (1984a), Gardner *et al.* (1990) and Cooper *et al.* (1990) used the combination method to characterise the hydraulic properties of unsaturated chalk, a soft limestone containing numerous fine fractures, at several sites in southern England. They used a portable polythene tunnel-type greenhouse to provide a shelter over the plot of either 5 or 10 m square. A hundred drippers fed from a constant head tank, controlled by a float valve, provided irrigation evenly over the experimental area. Hypodermic needles were used for the drippers, which

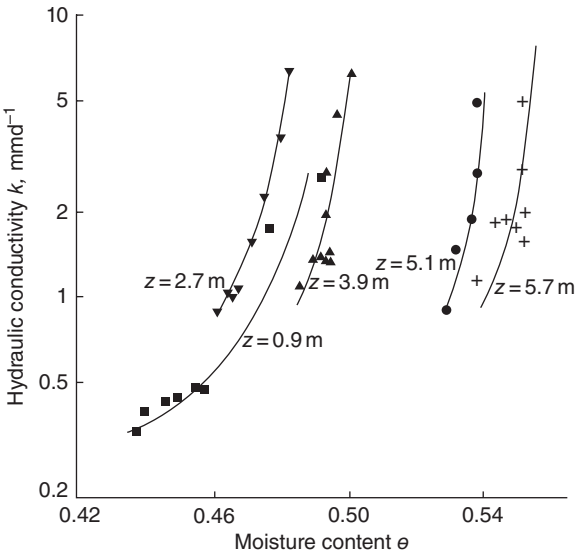

Fig. 18.8 Unsaturated hydraulic conductivity estimated using the Poulovassilis combination method from the same experiment as depicted in Fig. 18.7 (Cooper, 1979). Reproduced with permission from the *East African Agricultural and Forestry Journal*.

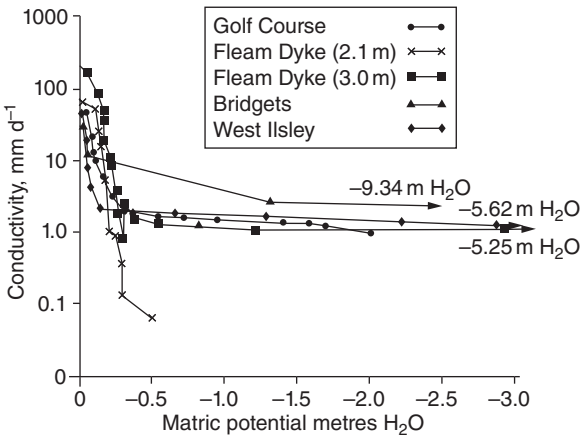

Fig. 18.9 Unsaturated hydraulic conductivity of chalk at 2.1 m depth at four sites in southern England, measured by the Poulovassilis combination method (instantaneous profile method only at West Ilsley) (Wellings & Cooper, 1983). Reproduced with permission from Elsevier.

were a push fit onto plastic Luer connectors connected to black polythene tubes and mounted on wire stands. Fine control of the flow rate was achieved by moving the drippers up or down on the wire stands, while several different overall irrigation rates between 500 and 2 mm d^{-1} were achieved by using different gauge needles. Monitoring of flow rate was by a tipping bucket rain gauge beneath one nozzle, which revealed a large diurnal change of flow, and periodic checks on individual nozzles by collecting water in a measuring cylinder for a short time. Any transparent or translucent parts of the water distribution system rapidly grew algae if the water source was not a public supply. This was combated successfully by adding small quantities of household bleach to the supply tank to maintain a level of 1 or 2 ppm of chlorine.

At these sites, the chalk has very uniform pore sizes of a few μm diameter. This equates to an air entry value of –10 m water or lower. As a result, once irrigation ceased, water potential fell very rapidly, but water content (measured four times daily by neutron probe) changed very little. At depths greater than about 2 m, where there is little evidence of weathering, this resulted in an apparently constant hydraulic conductivity between matric potentials of –0.5 and less than –3 m water in the range of 1 and 10 m d^{-1}, depending on depth and site. During the irrigation period, a rapid fall in conductivity was observed from several hundred mm d^{-1} close to saturation to the near-constant matric conductivity. These results are consistent with published values for the saturated hydraulic conductivity of the chalk matrix (Edmunds *et al.*, 1973) and with a fairly narrow range of fracture widths peaking at about 100 μm and with a spacing of about 0.1 m, consistent with the observed block sizes of chalk (unpublished data).

The calculated hydraulic conductivity at 2.1 m depth at four sites on chalk is shown in Fig. 18.9 (Fleam Dyke also at 3.0 m, as a low permeability band occurred at around 2.1 m at that site). At West Ilsley the instantaneous profile method alone was used, utilising automatically recording pressure transducer tensiometers and very frequent neutron probe measurements in the early stages. These measurements should be compared with the *in situ* measured soil water characteristics at the West Ilsley site (Fig. 15.4a).

Transition from one steady irrigation rate to another involves some drainage of water from the soil and therefore does not occur instantaneously, especially at the lower rates. Application of a time-dependent function to the neutron probe measurements during this period improved the estimation of water flux at the lower irrigation rates, although statistically there was no justification for any more sophisticated relation than a linear reduction with time. Comparison of the Fleam Dyke 3.0 m curve in Fig. 18.9, where this correction has not been applied, with the Golf Course one, where it has, illustrates how an apparent anomaly has been eliminated.

18.3.6 Hydraulic conductivity measurements from routine water balance measurements

Measurement of the water balance of a soil profile from storage changes (e.g. the ZFP method – see Section 24.3.7) yields integrated water flux over the time between reading occasions at a series of depths. Where the water flux can confidently be ascribed to flow of water in the soil matrix and not partially *via* roots, these

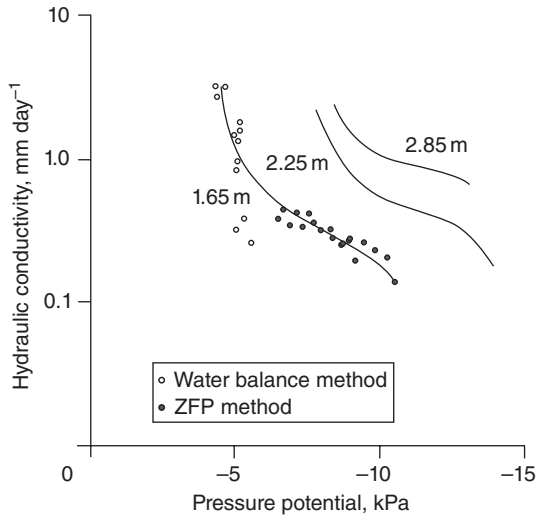

Fig. 18.10 Hydraulic conductivity of sandy soil estimated from water balance monitoring using the same instruments as for Fig. 15.4b (Cooper *et al.*, 1990). Reproduced with permission from John Wiley & Sons.

can be used to estimate the instantaneous water flux, in the same way as for the instantaneous profile technique. The estimated water flux can then be combined with the measured hydraulic potential profile to produce a measurement of unsaturated hydraulic conductivity in the same way as for the more artificial methods previously discussed.

Figure 18.10 shows an example for the same site and instruments as used for the *in situ* soil water characteristic data shown in Fig. 15.4b. Unless the data are collected automatically, the interval between measurements may be several days, and so caution needs to be exercised in interpreting the data to ensure that interpolation between reading occasions is valid, for example, was the water flux likely to have been sufficiently steady between those occasions to ascribe it to the average conditions between measurements?

Appendix 18.A Three-Dimensional Infiltration with Cylindrical Symmetry

The three-dimensional form of the Richards Equation 2.2.6 is

$$\frac{\partial\theta}{\partial t} = \nabla.(K\nabla\psi_{\mathrm{m}}) - \frac{\partial K}{\partial z}. \qquad (18.A.1)$$

This can be written, similar to Equation 3.1.2, as

$$\frac{\partial\theta}{\partial t} = \nabla.(D(\theta)\nabla\theta) - \frac{\partial K}{\partial z}, \qquad (18.A.2)$$

where $D = K(\mathrm{d}\psi_{\mathrm{m}}/\mathrm{d}\theta)$ is the diffusivity, defined in Equation 3.1.1.

Analytical solutions to the Richards equation are difficult to find, but use of the concept of the matric flux potential, ϕ (Section 3.2), makes it more tractable. For convenience, the definition of matric flux potential, Equation 3.2.1, is repeated here:

$$\phi(\theta) = \int_{\theta_{\mathrm{i}}}^{\theta} D(\theta)\mathrm{d}\theta = \int_{\psi_{\mathrm{i}}}^{\psi_{\mathrm{m}}(\theta)} K(\psi_{\mathrm{m}})\mathrm{d}\psi_{\mathrm{m}}. \qquad (18.A.3)$$

So

$$\frac{\mathrm{d}\phi(\theta)}{\mathrm{d}\theta} = D(\theta), \qquad (18.A.4)$$

and

$$\nabla\phi(\theta) = \frac{\mathrm{d}\phi(\theta)}{\mathrm{d}\theta}\nabla\theta = D(\theta)\nabla\theta. \qquad (18.A.5)$$

Similarly

$$\frac{\mathrm{d}\phi}{\mathrm{d}\psi_{\mathrm{m}}} = K(\psi_{\mathrm{m}}), \qquad (18.A.6)$$

and

$$\frac{\partial\phi}{\partial z} = \frac{\mathrm{d}\phi}{\mathrm{d}\psi_{\mathrm{m}}}\frac{\mathrm{d}\psi_{\mathrm{m}}}{\mathrm{d}K}\frac{\partial K}{\partial z} = K\frac{\mathrm{d}\psi_{\mathrm{m}}}{\mathrm{d}K}\frac{\partial K}{\partial z}, \qquad (18.A.7)$$

which allows (18.A.2) to be written as

$$\frac{\partial\theta}{\partial t} = \nabla^2\phi(\theta) - \frac{\partial K}{\partial z}, \qquad (18.A.8)$$

or

$$\frac{\partial\theta}{\partial t} = \nabla^2\phi(\theta) - \frac{1}{K}\frac{\mathrm{d}K}{\mathrm{d}\psi_{\mathrm{m}}}\frac{\partial\phi}{\partial z}. \qquad (18.A.9)$$

To make further progress, several authors have assumed a relation between the hydraulic conductivity and matric potential of the form

$$K = K_{\mathrm{s}}e^{\alpha\psi_{\mathrm{m}}} \qquad (18.A.10)$$

as a good approximation to the actual relationship (Gardner, 1958). The matric flux potential is then, from Equation 18.A.3

$$\phi = \frac{K_{\mathrm{s}}}{\alpha}(e^{\alpha\psi_{\mathrm{m}}} - e^{\alpha\psi_{\mathrm{i}}}), \qquad (18.A.11)$$

and if there is sufficient difference between ψ_{i} and ψ_{m}, the second term in the brackets is negligible compared with the first, leading to

$$\phi \approx \frac{K}{\alpha}. \tag{18.A.12}$$

Equation 18.A.9 now becomes

$$\frac{\partial \theta}{\partial t} = \nabla^2 \phi(\theta) - \alpha \frac{\partial \phi}{\partial z}. \tag{18.A.13}$$

In borehole permeameter, ring and tension infiltrometer applications, it is usually found that a steady state is achieved quite quickly, so that within the wetted volume, $\partial\theta/\partial t = 0$. So for a steady state, the matric flux potential, ϕ, is the solution of

$$\nabla^2 \phi(\theta) = \alpha \frac{\partial \phi}{\partial z}. \tag{18.A.14}$$

Several methods for measurement of hydraulic properties in the field rely on monitoring infiltration either from a circular cross-sectional borehole or from a circular area of the surface. In both cases, the problem has *cylindrical symmetry*, that is, it looks the same at all points around a circle drawn with its centre at the borehole axis or a vertical line drawn through the middle of the infiltrating area. To characterise such a system, just two length scales are needed, the radius of a point, r, from the axis and the depth, z. For such a system (18.A.14) can be written as

$$\frac{1}{r}\frac{\partial}{\partial r}\left(r\frac{\partial \phi}{\partial r}\right) + \frac{\partial^2 \phi}{\partial z^2} = \alpha \frac{\partial \phi}{\partial z}. \tag{18.A.15}$$

18.A.1 Relation between matric flux potential and sorptivity

Equations 18.A.13 and 18.A.14 show that infiltration is controlled by matric flux potential, but we also know that infiltration is controlled by the sorptivity (Section 3.3). White and Sully (1987) showed that an approximate relation

$$S = \sqrt{\frac{\phi_s(\theta_s - \theta_i)}{b}}, \tag{18.A.16}$$

should hold. Values of b must theoretically lie in the fairly narrow range of 0.5 to $\pi/4$ (0.785), with values likely to be closer to the lower end of the range. A value of 0.55 is often assumed.

18.A.2 Ring and tension infiltrometers

For a shallow circular pond of radius r_0, such as is produced by a point source dripping onto the soil surface, a ring infiltrometer or (with a small modification) a tension infiltrometer, the boundary conditions are

$$\phi = \frac{K_{fs}}{\alpha}, \quad z = 0;\ 0 < r < r_0;\ t > 0; \tag{18.A.17}$$

$$\frac{\partial \phi}{\partial z} = \alpha\phi, \quad z = 0;\ r > r_0; \tag{18.A.18}$$

$$\phi = 0, \quad r, z \to \infty. \tag{18.A.19}$$

K_{fs} has been used here in place of K_s as this is more appropriate for a short-term test.

Equation 18.A.18 arises because the flux outside the ring, $-K(\partial\psi_m/\partial z) + K$, must be zero across this boundary, assuming no evaporation. Utilising (18.A.6) to substitute for the first appearance of K in this expression and (18.A.12) for the second one:

$$-\frac{d\phi}{d\psi_m}\frac{\partial \psi_m}{\partial z} + \alpha\phi = 0, \tag{18.A.20}$$

we obtain $(\partial\phi/\partial z) = \alpha\phi$.

Wooding (1968) used (18.A.15) with these boundary conditions in a very involved procedure to develop a series solution for the steady infiltration rate from the wetted area. He showed that this approximated very closely to

$$Q = \pi r_0^2 K_{fs} + 4 r_0 \phi_s, \tag{18.A.21}$$

where ϕ_s is the saturation matric flux potential, defined as

$$\phi_s = \int_{\theta_i}^{\theta_s} D(\theta)\,d\theta = \int_{\psi_i}^{0} K(\psi_m)\,d\psi_m. \tag{18.A.22}$$

The first term on the right-hand side of (18.A.21) is the steady one-dimensional infiltration expected for a material of saturated hydraulic conductivity, K_{fs}, which is driven only by gravity. The second term may be regarded as the additional flow out of the ponded area resulting from capillary forces.

For a tension infiltrometer, where the matric potential within the radius r_0 is maintained at a particular value, ψ_t, then (18.A.21) and (18.A.22) become

$$Q = \pi r_0^2 K(\psi_t) + 4 r_0 \phi_t, \tag{18.A.23}$$

and

$$\phi_t = \int_{\theta_i}^{\theta_t} D(\theta)\,d\theta = \int_{\psi_i}^{\psi_t} K(\psi_m)\,d\psi_m. \tag{18.A.24}$$

18.A.3 Auger holes in the unsaturated zone

For an auger hole, whether with a falling head, as in the inverse auger hole method, or a constant head, as for the borehole permeameter, the matric potential at the bottom of the hole, at depth, Z, is equal to the height of water in the hole, h. Along the side walls below the water level, it is equal to the distance below the water surface. And above the water level, there is no flow across the interface. This translates to

$$\psi_m = h, \quad 0 < r < r_0;\ z = Z;\ t > 0; \tag{18.A.25}$$

$$\psi_m = h - Z + z, \quad r = r_0;\ Z > z > Z - h;\ t > 0; \tag{18.A.26}$$

$$\frac{\partial \psi_m}{\partial r} = 0, \quad r = 0;\ z < Z - h; \tag{18.A.27}$$

and

$$\psi_m \to -\infty, \quad r, z \to \infty. \tag{18.A.28}$$

Note that matric flux potential is not used here, since hydraulic conductivity does not vary at positive values of matric potential.

For the borehole permeameter, Reynolds *et al.* (1985) derived an equation for the flow out of a well with a constant height of water, h, and radius, r, as depicted in Fig. 18.2. Their solution was

$$Q = K_{fs}\left[\pi r^2 + \frac{2\pi h}{C}\left(h + \frac{1}{\alpha}\right)\right], \tag{18.A.29}$$

where C is a dimensionless shape factor, derived by numerical modelling of flow around the borehole and is dependent mainly upon the ratio h/a and weakly upon soil texture (embodied in α). Zhang *et al.* (1998) derived the following empirical expression for C, based on numerical solutions developed by Reynolds (1986) and which are embodied in the spreadsheet available from Soilmoisture Equipment Corp. The equation is

$$C = \left(\frac{(h/r)}{a + b(h/r)}\right)^c, \tag{18.A.30}$$

where
$a = 2.081$, $b = 0.121$ and $c = 0.672$ for $\alpha = 1\ \text{m}^{-1}$;
$a = 1.992$, $b = 0.091$ and $c = 0.683$ for $\alpha = 4\ \text{m}^{-1}$, and
$a = 2.074$, $b = 0.093$ and $c = 0.754$ for $\alpha = 12$ and $36\ \text{m}^{-1}$.

Philip (1985) also produced an approximate analysis of the problem using much the same approach and came up with a similar equation to (18.A.29). Equation 18.A.29 contains two unknown soil variables, K_{fs} and α.

Stephens *et al.* (1987) also examined the borehole permeameter from a theoretical point of view. Using numerical simulations and regression techniques, they developed an alternative formulation for the parameter C, based on different models of the θ–ψ_m relationship. Stephens *et al.*'s (1987) formulation gives generally lower estimates of K_{fs} than either the Reynolds *et al.* (1985) or the Philip (1985) versions.

Appendix 18.B Mariotte Bottles and Bubble Towers

18.B.1 Mariotte bottle

Mariotte bottles are a popular choice for maintaining a constant water pressure at a point while delivering a variable flow rate for relatively small (0.5–50 L) volumes of liquid. They combine the function of reservoir, water delivery system and pressure control. For larger volumes, a float or solenoid operated valve may be more appropriate.

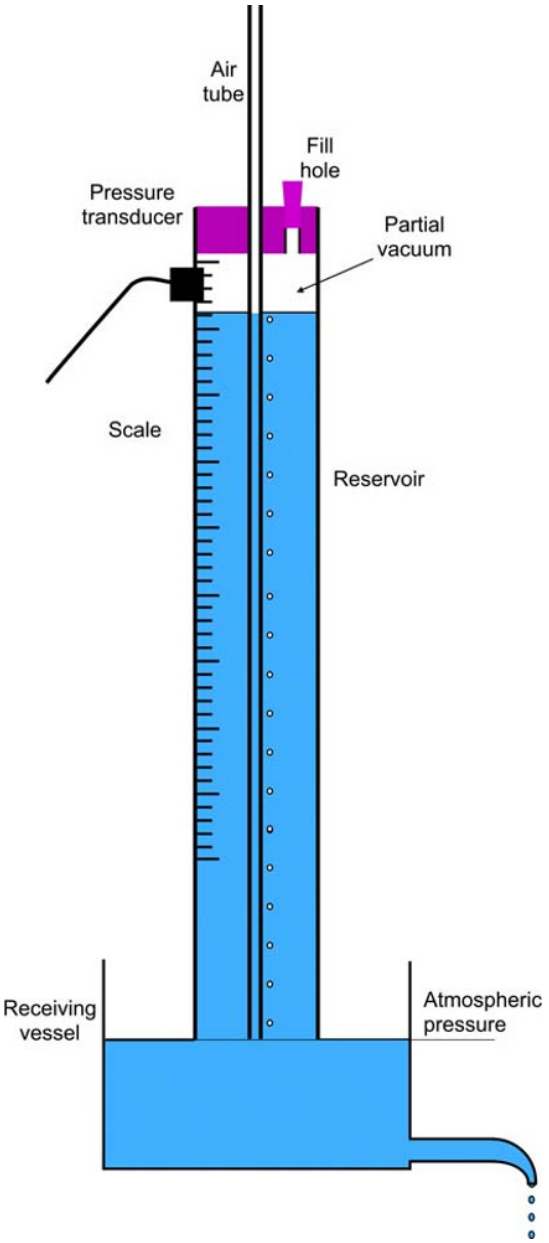

Fig. 18.11 Mariotte device for maintaining a fixed level of water below the reservoir.

For the applications in which we are likely to be most interested (maintaining a fixed water level below the reservoir, as in an infiltration ring or borehole permeameter), an arrangement of the form shown in Fig. 18.11 is most appropriate.

The weight of water in the reservoir causes water to flow initially out of the reservoir bottom into the receiving vessel. This creates a partial vacuum above the water level in the reservoir and, once the level in the receiving vessel is above the mouth of the reservoir, air is drawn through

the air tube. Once the water level in the receiving vessel is above the bottom of the air tube, the water pressure here is greater than atmospheric and air cannot flow into the reservoir any more. The water column in the reservoir is then balanced by the partial vacuum, and so no more water flows out of the reservoir until the water level outside drops below the level of the bottom of the air tube. Air can then once again enter, reducing the partial vacuum and allowing more water out. The water level in the receiving vessel is thus held at the level of the bottom of the air tube (with a small correction for surface tension effects).

The amount of water in the reservoir can be monitored by noting its level against a scale. Alternatively, the vacuum in the space at the top of the reservoir is equal to the height of water above the bottom of the air tube. A pressure transducer in this space, therefore, will record the water level change. This volume is equal to that dripping out of the receiving vessel.

Small fluctuations in the level of water in the reservoir are caused by individual bubbles reaching the water surface. These are related to the diameter of the air tube and so this should be kept fairly small. If it is too small, however, and the outflow from the receiving vessel is fast, such as in a borehole in permeable soil, then air may not be able to bubble quickly enough from the air tube into the reservoir.

At the beginning of an experiment, the reservoir should be very nearly, if not completely, full. If there is a significant amount of air in the top of the reservoir, then a relatively large volume of water needs to flow into the receiving vessel before a sufficient vacuum develops to stop the flow. The level in the receiving vessel then becomes too high until enough flows out of the outlet to bring the level down to the target depth.

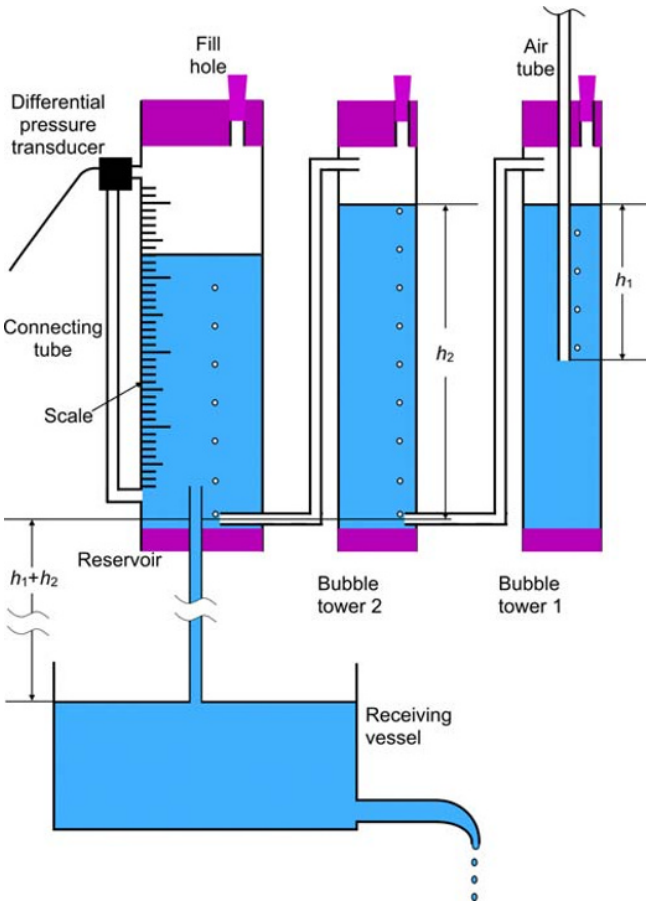

Fig. 18.12 Two bubble towers used to control a water level below a reservoir or to impose a suction at the base of the reservoir.

18.B.2 Bubble tower

An alternative to the Mariotte bottle is a bubble tower. The principle of control is similar and shown in Fig. 18.12. This allows a negative pressure to be exerted at the outlet of the reservoir. This is done by using the vacuum in the air space of the bubble tower to define the pressure near the base of the reservoir. The pressure in the air space of bubble tower 1 in Fig. 18.12 is $-h_1$ as long as some air passes through the air tube to keep bubbles going. This pressure is fed to the base of bubble tower 2, where the pressure in its air space is $-(h_1 + h_2)$. This in turn is fed to the base of the reservoir, which can be used to control the level of water in a receiving vessel or borehole in a permeameter. Measuring the change in the water level of the reservoir monitors flow from the borehole in the same way as for a Mariotte bottle. Note that there is no water transfer from either bubble tower. These water heads merely control the vacuum generated. Any number of bubble towers may be connected together as shown. Most applications use just one, but with more than one, a considerable negative head can be generated without needing a tall structure.

As with the Mariotte design for the borehole permeameter, a pressure transducer in the air space of the reservoir can be used to monitor the water level. Ankeny *et al.* (1988) improved on this by using two transducers, one at the base and one at the top of the reservoir, which reduced the effect of individual bubbles very considerably. Casey and Derby (2002) further improved the design by using a single differential pressure transducer, which inherently measures the difference in pressure between the top and bottom of the reservoir. More detail on pressure transducers can be found in Section 12.13.

Perroux and White (1988) introduced the use of a bubble tower for tension infiltrometers and many designs in current use employ a single bubble tower to control the tension applied to the disc. The tension is easily changed by sliding the air tube up to increase the pressure at the reservoir base or down to reduce it.

Part VI Solute Measurement

19 Principles and Pitfalls

One of the major motivations for understanding and measuring water in soil is to monitor and predict the behaviour of solutes in the unsaturated zone. The solutes in question may be:

- agricultural chemicals, principally fertilisers and pesticides;
- pollutants of various kinds – including the same agricultural chemicals which travel beyond the root zone and threaten to pollute groundwater, but also radioactive or other elements carried in precipitation, or chemical species spilt accidentally onto the land;
- *tracers*, either occurring in precipitation or applied artificially to the soil, usually at the surface (tracers are used to identify water pathways, to aid in the measurement of water balances and soil water flux or to act as surrogates for other less benign chemicals to help predict the fate of those chemicals if introduced into the soil);

Substances of concern are not always dissolved in the water. These include bacteria, viruses, nanoparticles and non-soluble or only slightly soluble liquids, usually called nonaqueous phase liquids (NAPLs). The last-named are usually grouped into light and dense varieties (LNAPLs and DNAPLs), depending on whether they are less or more dense than water. We will not, however, consider non-dissolved substances here.

19.1 Principles of Solute Transport

If measurement of the movement of water in soil is difficult, then extending this to the transport of dissolved substances is even more so. In general, we need to know not only the water content, potential, hydraulic conductivity, etc., but also the concentration of the solute in the water, together with its propensity to interact with the soil matrix and the factors controlling the spreading of the solute through the water – diffusion and dispersion.

19.1.1 Simple theory

The simplest representation of solute flow in soil is to assume that the amount of solute in solution remains constant and moves with the water. This implies that its *concentration*, C, which is the mass of solute in a unit volume of water is constant. Thus C is given by

$$C = \frac{m}{v}, \tag{19.1.1}$$

where m is the mass of solute dissolved in a volume, v, of water. Quite often, the mass of solute is expressed in terms of *moles*, that is, the actual mass divided by the molecular mass. However, we shall stick to ordinary mass in expressing concentrations.

It is often useful to know the amount of solute in a given volume of soil. This is easily converted from Equation 19.1.1 since the volume of water in a given volume of soil, V, is θV. Hence the mass, M, of solute in the volume, V, is given by

$$M = C\theta V. \tag{19.1.2}$$

If the soil water flux is q, containing a concentration of solute, C, then the flux of solute, F, is

$$F = Cq, \tag{19.1.3}$$

and its velocity, u, in the direction of movement is

$$u = \frac{q}{\theta}, \tag{19.1.4}$$

which is the same as the water velocity, v. This form of movement is often termed *piston flow*, as the water containing a particular amount of solute is envisaged as being pushed from behind by water infiltrating the soil above it and, in turn, pushing other water in front of it. A consequence of this sort of transport is that the actual

Soil Water Measurement: A Practical Handbook, First Edition. J. David Cooper.

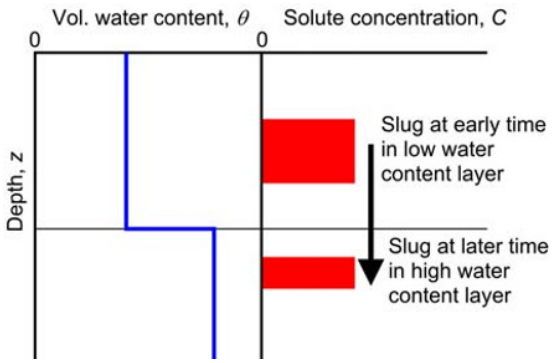

Fig. 19.1 Transformation of a slug of solute as it traverses the boundary between soil layers of different water content.

depth of soil occupied by a slug of solute will vary according to the water content. This is illustrated for an idealised soil profile in Fig. 19.1, where the slug travels from a layer of low to high water content and, in consequence, is compressed in space. The solute concentration remains the same, but to preserve its total mass, the depth occupied by the slug is reduced in inverse proportion to the water content. In Fig. 19.1, the water content of the lower layer is twice that of the upper one and, consequently, the depth occupied by the slug is half of what it was in the upper layer.

19.1.2 Complicating factors

In some cases, piston flow gives a good approximation to actual observed solute concentrations over time, but in others, it fails completely. Some of the reasons for behaviour departing from this idealised picture are:

- **Diffusion**. When there is a difference in solute concentration from one place to another, there is a tendency for solute ions to travel from the higher to the lower concentration region and so to equalise out the concentration. Diffusion occurs according to *Fick's Law* and can be characterised by a *diffusion coefficient*, D, which relates the net flux of solute, F, to the concentration gradient, $\partial C/\partial x$, as

$$F = -D\frac{\partial C}{\partial x}. \qquad (19.1.5)$$

- **Dispersion**. Water velocities, both within and between soil pores, vary widely depending on distance from pore wall and size of pore. Solute dissolved in slower-moving water obviously travels less far than that in faster-moving water (further from the pore wall or in larger occupied pores). This spreads the solute out in the direction of travel, often in a similar manner to diffusion but to a greater degree. It also spreads the solute out in a direction transverse to the direction of travel, but usually to a much smaller extent. A *dispersion coefficient* can often be defined, in a similar way to the diffusion coefficient, dependent on the pore water velocity.
- **Preferential flow**. Water in macropores, interaggregate pores or fingers in unstable flow, bypasses the majority of the soil matrix. Solutes contained in this water also travel much faster than the water in the matrix, usually leading to *forward tailing* of solute profiles, where solute is found ahead of the main body of solute. In some cases, this leads a single slug of solute to break up into a double peak.
- **Immobile water**. Water in blind pores, that is, those with no exit, may account for a significant proportion of the water in some soils and act as a buffer for solute. It absorbs solute by diffusion when more concentrated solution flows past it and releases it again when the surrounding mobile solution becomes less concentrated. This has the effect of retarding, reducing the height of and increasing the width of the peak.
- **Adsorption**. Many solutes, usually positively charged ions (*cations*, e.g. Na^+, Ca^{++}), have an affinity for soil particle surfaces and so tend to stick to them, thereby slowing down their transport relative to that of the water. For more information, see Section 20.1.2.
- **Anion exclusion**. The surface of clay particles is usually negatively charged. This repels negatively charged ions (*anions*, e.g. Cl^-, Br^-, NO_3^-), forcing them into the centre of the pore, where the water velocity is faster than the average and so the anions actually travel faster than would be expected from straightforward piston flow.
- **Reactive solutes**. Some solutes undergo chemical or biochemical transformations while in transit through the soil, for example, degradation of pesticides, uptake by plant roots or radioactive decay. This complicates the interpretation, not only because the rate at which such transformations occur may be difficult to measure but also because the products of the reactions can have very different transport properties than those of the parents. These are often referred to as *nonconservative* ions, in contrast to *conservative* ions.

There is clearly an overlap between some of these mechanisms. For instance, preferential flow can be regarded as an extension of the dispersion mechanism, as exchange of solute between highly mobile water in faster pathways with more slow-moving water blurs the distinction between mobile and immobile water.

The earlier discussion should indicate that there is an order of magnitude more complexity involved when dealing with transport of solutes than if only water flow is involved. Some sophisticated modelling methods are being developed to cope with this degree of complexity. In this book, however, we confine ourselves to the rather simpler (though not necessarily easier!) task of measurement of solute in and movement through field soils.

19.2 Tracers

The use of tracers to elucidate details of both water and solute transport in the subsurface has received a great deal of attention over a period of 50 or more years. The variety of substances and their methods of use are quite bewildering and it is not possible to do much more here than scratch the surface.

Classification of tracers can be done in a number of ways:

- Particulate, dissolved solids, liquids or gases.
- Dyes, stable isotopes, radioactive isotopes, biological agents, nanoparticles or chemicals.
- Naturally or semi-naturally (e.g. as part of an agricultural operation) introduced or artificially applied.

We will use the second of these schemes.

19.2.1 Dye tracers

Dyes can be used in one of two ways: to indicate pathways through the soil or to label the water to track its progress through the soil.

When used as a pathway indicator, the information is essentially qualitative, as it relies on the ability of the dye to be absorbed onto soil surfaces and on a proportion of it to remain on the surfaces, while most of the dye carries on in the water stream to stain areas further along the flow path. The selected dye needs, therefore, to adsorb to soil materials, usually clays and organic matter, but not too strongly so that it is not all lost in the first few centimetres of travel. Popular dyes for the purpose are Brilliant Blue FCF, Methylene Blue, Rhodamine WT and Fluorescein. The latter two are fluorescent and so may be detected at very low concentration by shining an ultraviolet lamp on the soil when there is no other illumination. Usually a dye-rich solution is irrigated onto the soil. After some time, sections of soil are exposed and the areas stained by dye are recorded. This may be done photographically or by manual recording. It is important to be aware that areas with the heaviest staining are not necessarily where most dye-rich water has visited, but may instead be a consequence of the soil fabric having greater affinity for the dye. The methodology is suitable for use on undisturbed field plots or on monoliths recovered from the field (see Section 17.1).

When used for tracking either water or solute flux through the soil, fluorescent dyes are often employed, as the ability to detect very low concentrations is valuable. Quantitative analysis is possible by using a *fluorometer* and, in some cases, can be done in real time, for instance on the outflow from a soil monolith in the laboratory or a lysimeter in the field. Great care should be exercised in interpreting the results, as there will almost always be considerable retardation as a result of selective adsorption on soil constituents. Progress is being made in quantifying nonfluorescent dye concentrations by image analysis of photographic images (e.g. Germán-Heins & Flury, 2000).

Many dyes, particularly fluorescent ones, are carcinogenic and so must be selected and handled with great care. When used in the field, regulatory requirements may have to be followed, which can limit the choice of dyes.

19.2.2 Inorganic compounds

Apart from dyes, which are at best semi-quantitative indicators, simple inorganic compounds are effective tracers, usually being cheap and easy to measure quantitatively. Common salt (NaCl) can be used, but is toxic to most plants, and in many areas a high background level already exists. This complicates interpretation and requires that a high concentration is applied. The Cl^- ion is, however, highly mobile and therefore makes a very good tracer. Sodium may cause flocculation of clay minerals. Alternative cations are potassium, which is a plant nutrient, or calcium, particularly in calcareous soils. Bromide (usually in the form of potassium bromide – KBr) is a more common choice of anion than chloride, as it is commonly found in only low concentration in field soils, is not absorbed to a significant extent by plant roots and is similarly mobile as Cl^-.

Long-term recharge has been measured by several workers using a naturally occurring chloride mass balance approach (see Section 24.4).

19.2.3 Stable isotopes

Isotopes of common elements applied to soil, or entering soil naturally, are common tracers. Popular examples are deuterium (^2H), oxygen-18 (^{18}O), nitrogen-15 (^{15}N) and carbon-13 (^{13}C). Being stable, they do not pose a health hazard at modest concentrations and are conservative. Both deuterium and oxygen-18 can be incorporated as part of the water molecule and nitrogen-15 can be used as part of the molecule of nitrogen fertilisers. Stable isotopes are detectable at very low levels, which means that very little is required to conduct an experiment, although the analysis requires access to an expensive and sophisticated mass spectrometer and associated laboratory facilities.

Deuterium

Otherwise known as heavy water, deuterium oxide (^2H_2O or D_2O) is readily available from laboratory chemical suppliers. While quite expensive, a 100 mL bottle can be diluted in a fairly large quantity of ordinary water. When mixed with ordinary water, the ^2H_2O rapidly dissociates and reassociates so that by far the most abundant molecules are $^2H^1HO$, that is, composed of one deuterium, one ordinary hydrogen and one oxygen atom. Deuterium forms part of the water molecule and can be assumed to flow in the same way as ordinary water. Because they are about 5.5% heavier than ^1H_2O molecules, $^2H^1HO$ molecules have a lower vapour pressure than ordinary water, which reduces the fraction of deuterated water evaporated from the soil surface. It is normally assumed that root uptake of heavy water is the same as for normal water, and so the composition of transpired water is not affected. Where soil surface evaporation is not significant, therefore, it can be assumed that the total loss of deuterated water by evaporation is the same proportionally as its concentration in soil water. This can be used to estimate the distribution by depth of water uptake by roots.

The concentration of deuterium and other isotopes found in water (^3H, ^{17}O and ^{18}O) are usually expressed as a difference (δ) in parts per thousand or per mil – ‰ from that found in *Vienna Standard Mean Ocean Water*

(VSMOW), which is an international standard. The VSMOW standard contains one atom of ^{2}H to every 6420 atoms of ^{1}H. Modern mass spectrometers can measure $\delta^{2}H$ to about 1‰ (Leibundgut *et al.*, 2009).

The lower vapour pressure of deuterated water affects its rate of both evaporation and condensation. The fraction of ^{2}H atoms in precipitation depends on the temperature at which it was evaporated and recondensed and, thus, varies both regionally and seasonally. This natural seasonal variation allows deuterium in precipitation to be used as a tracer (Bath *et al.*, 1982).

Oxygen-18

The most abundant isotope of oxygen is oxygen-16. Oxygen-18 is, however, found in reasonable abundance in rainwater and is commonly used as a tracer for a variety of environmental applications. Unlike deuterium, the most common application relies on naturally occurring ^{18}O. The abundance of ^{18}O in VSMOW is 1 atom per 498.7 atoms of ^{16}O, which is considerably higher than the equivalent for ^{2}H, and the measurement precision of $\delta^{18}O$ is better than for $\delta^{2}H$, about 0.1‰ (Leibundgut *et al.*, 2009). Measurement of $\delta^{18}O$ is therefore more sensitive than that of $\delta^{2}H$. For very similar reasons as for deuterium, discussed earlier, interpretation of data on ^{18}O in soil is complicated by estimation of the loss from soil by evaporation. The range of $\delta^{18}O$ in precipitation and natural waters has been reported between –50 and +20‰, with more common values between –20 and +5‰ (Leibundgut *et al.*, 2009).

Nitrogen-15

The main use of nitrogen-15 in soil water studies is to "label" agricultural fertiliser. Nitrogenous fertiliser is usually in the form of ammonium nitrate (NH_4NH_3), urea ($CO(NH_2)_2$), or sodium or potassium nitrate ($NaNO_3$ or KNO_3). By incorporating a proportion of ^{15}N in the fertiliser, the fate of a particular application can be tracked, both in the soil and in the crop or roots. Ammonium nitrate has nitrogen in both the ammonium and nitrate ions. By labelling only one of these, the relative mobility of the two ions or metabolic pathways of fertiliser use can be studied.

Nitrogen compounds are important nutrients and are readily taken up by roots. To ensure a full ^{15}N balance, therefore, the ^{15}N content of plant material must be added to that in the soil profile. Unlike ^{2}H and ^{18}O, however, negligible amounts are lost to the atmosphere, making it possible, in principle at least, to close the nitrogen balance (Barraclough *et al.*, 1994).

Apart from the problem of accounting for plant uptake *via* the roots, nitrate is very mobile in the soil and therefore a good tracer of water flow.

19.2.4 Radioactive tracers

Licensing requirements for use of radioactive tracers in open field situations are even more onerous than for sealed sources in most countries because of their unconfined nature. Therefore, the use of artificially applied radioactive tracers is now limited almost entirely to laboratory situations.

The most commonly used radioactive tracers are tritium (^{3}H) and chlorine-36 (^{36}Cl). Both were produced in large quantities by nuclear bomb testing in the 1950s and 1960s and injected into the upper atmosphere, which meant worldwide distribution in rainfall.

^{3}H has a half-life of 12.32 years, which means that much of that contained in rainwater from the years when it was most concentrated (1962/1963) has now decayed. Tritium concentrations are usually reported in *Tritium Units* (TU). One TU is 1 tritium atom to 10^{18} hydrogen atoms. As for deuterium, tritium's major advantage as a tracer is that it forms part of the water molecule and so, under most circumstances, can be assumed to be a near-perfect indicator of water flow. Detection of tritium is by measurement of weak β particles (electrons) from its decay. Measurement of environmental samples requires very specialised equipment, involving enrichment and long counting times in specialised counters at dedicated laboratories. In laboratory studies, much higher concentrations can be used, which require a liquid scintillation counter. These are affordable by many laboratories, although arrangements for both the use and disposal of the liquids usually require licensing. More information on radioactivity and radiation safety can be found in Section 7.11.

^{36}Cl was produced by irradiation of seawater in nuclear bomb tests between 1952 and 1958. Its half-life is about 301,000 years and so persists much longer than tritium. However, it is useful as an environmental tracer only for very deep and/or slow-moving arid region water movement. Detection is, like tritium, by measurement of β particles.

19.3 Solute Concentration Measurement

Two approaches to measurement of solute concentration in field soils are in common use.

One collects samples of soil solution for subsequent laboratory analysis, whereas the other aims to measure the solute concentration *in situ*, either directly or indirectly. Both approaches have strengths and weaknesses. Modern laboratory techniques can analyse a wide range of chemical species, usually with high accuracy, and are capable of measuring very low concentrations – important where toxic chemicals in trace quantities are a concern. The samples may be soil solution extracted from field-collected soil samples transported to the laboratory or come from direct sampling of soil solution in the field.

Detection of the concentration of soil solution directly *in situ* is clearly more limited in scope and sensitivity, but allows for continuous measurements to be made, with good time and spatial resolution.

Chapters 20 and 21 detail these two approaches.

20 Solution Sampling

Sampling of soil solution for later chemical or other analysis can be done either by taking samples of soil and then extracting the soil solution or by sampling the soil solution *in situ*. Both approaches are in common use.

20.1 Soil Sampling and Extraction of Solution

20.1.1 Collection of soil samples

Collection of soil samples for measurement of the soil solution is a reasonably straightforward activity, employing much the same methods as described in Chapter 6. Some additional considerations are:

- Is it important to know the exact volume occupied by the soil sampled? If so, then either a known volume sample must be taken or the dry bulk density of the soil must be measured separately. Details are given in Chapter 6.
- How big a sample is needed? The total amount of solute is given by the volume of soil × the volumetric water content × the concentration of solute × the extraction efficiency. The last three quantities may need to be estimated. By comparing them with the amount required for analysis, the volume of soil needed can be estimated. Since the object is usually to measure the solute concentration, it is prudent to collect a generous quantity of soil.
- What precautions are needed to ensure that the samples are not contaminated by extraneous sources of the solute(s) of interest? This varies from one type of solute to another and so it is difficult to generalise. Cleaning and possibly disinfection of the equipment between samples are obvious measures, but operators may also need to clean themselves.
- Are the samples to be collected likely to be hazardous? This covers poisons, carcinogens, gases, radioactive and biological agents. Protective clothing or other equipment may be necessary.
- What precautions are needed to prevent contamination or degradation of the sample once it is extracted? Cross-contamination of samples occurs very easily, particularly where concentrations are very low. Sunlight, high (or sometimes very low) temperatures, can cause samples to dry out or chemical or biological reactions to occur before or during transport and storage.

In most cases, the measures needed are similar to, but more stringent than, collection of samples for bulk density or water content measurement.

20.1.2 Extraction of soil solution from soil samples

Solutes in soil may exist simply as a normal solute in the soil water or be held more or less tightly bound to the surface of clay minerals, colloids or organic matter. The geochemistry of many of the more readily adsorbed species is well beyond the scope of this book and the subject of active research. Nevertheless, some consideration needs to be given to the meaning of 'soil solution' when many of the chemicals may have only limited freedom to move with the water in which it is contained. This affects the difficulty in obtaining a 'representative' sample of the soil solution.

The most common and simplest way to represent the relationship between the concentration of solutes in the bulk soil solution and that adsorbed onto surfaces is by means of a *distribution coefficient*, usually designated by the symbol K_d:

$$C_s = K_d C, \tag{20.1.1}$$

where

C_s is the amount of solute adsorbed onto particle surfaces per unit mass of dry soil and

C is the concentration of solute in the bulk soil solution.

This assumes equilibrium between the solute in solution and that adsorbed, that there is plenty of spare capacity on the surfaces to accept more solute if C increases and that a single proportionality constant is appropriate. For static samples collected from the field, equilibrium is a reasonable assumption, but proportionality between C_s and C may not be realistic if, for instance, the available sites for solutes to bind to start to run out, in which case they are said to be

Soil Water Measurement: A Practical Handbook, First Edition. J. David Cooper.

saturated. The relationship defined by Equation 20.1.1 is known as a *linear* isotherm. More complex isotherms (e.g. Langmuir, Freundlich), which take account of saturation and other effects, are often used.

The Langmuir isotherm is given by

$$C_s = \frac{\alpha C}{1 + \alpha C}, \tag{20.1.2}$$

where α is a constant and the Freundlich isotherm is of the form

$$C_s = \beta C^{\frac{1}{n}}, \tag{20.1.3}$$

where β and n are constants.

In a dynamic situation where solution of one concentration invades soil at a different concentration, equilibrium between the two may take a considerable time to establish. The total mass of solute, M_t, in a unit volume of soil is given by

$$M_t = C\theta + C_s\rho_d. \tag{20.1.4}$$

Appropriate methods for measurement of solute concentration depend, therefore, on whether it is desired to measure C or M_t. C_s can be derived from Equation 20.1.4. Even then, things are less simple than they may at first appear, since there can be a range of energies binding a particular solute to sorption sites on the solid particles, with some ions being easily removed, while others are very difficult. This implies a range of different values of the constants in Equations 20.1.1–20.1.3. Different extraction methods therefore often produce different concentration estimates.

A further complication in defining concentration arises as a result of diffusion and dispersion. If we take D to represent a combined diffusion and dispersion coefficient (see Section 19.1.2), then Fick's Law, Equation 19.1.5, gives the rate of mass movement resulting from these processes. In one (vertical) dimension the combined flux of solute, F, is given by

$$F = C_f q = Cq - D\frac{\partial C}{\partial z}, \tag{20.1.5}$$

where C_f is the *flow concentration*, that is, the apparent concentration actually flowing across a plane. The difference arises because as well as the *convective flow* arising from the solute concentration, C, being carried along with the water, there is an additional flux caused by diffusion and dispersion in the concentration gradient. Depending on the direction of this gradient, C_f may reduce or increase compared with C. From Equation 20.1.5, the relation between C_f and C is

$$C_f = C - \frac{D}{q}\frac{\partial C}{\partial z}. \tag{20.1.6}$$

There is therefore likely to be a significant difference between the two where the diffusion–dispersion coefficient and/or the concentration gradient are large and/or the water flux is low. Conversely, at high flux rates or small concentration gradients, there will be only a small difference between the concentration in the soil solution and the apparent concentration of flowing water. This is clearly relevant only where the water and solute flux across a plane is sufficiently homogeneous. Where preferential flow is important, the description breaks down or is valid only for the non-preferential portion of the flow.

For soils low in organic matter and clay content, most of the above is not relevant, but where adsorption processes are important, the simple-minded approach does not necessarily yield the appropriate result.

Centrifuge extraction

A substantial quantity of solution can drain out of a saturated soil sample, but in general, this is not the case when the soil is more than slightly unsaturated. To collect a reasonable quantity of solution, the effective force of gravity can be increased by using a centrifuge. The operation of a centrifuge was described in Section 15.4.6, where a relation between the speed of rotation, radius of the rotor and effective matric potential was presented. A centrifuge is therefore useful for extracting solution from soil samples for analysis. The centrifuge is expected to extract predominantly the bulk soil solution, although because of the effect on matric potential and the physical deformation of the soil, the equilibrium relation between concentration of the bulk solution and the adsorbed phase may change.

In many soils, centrifugation yields disappointing quantities of solution. Kinniburgh and Miles (1983) developed a method using a heavy liquid, immiscible with water, to enhance the amount of soil solution extracted. The liquid is usually an organic solvent poured on top of the soil sample in the centrifuge sample holder, see Fig. 20.1. The liquid (displacent) is forced to infiltrate through the soil by the

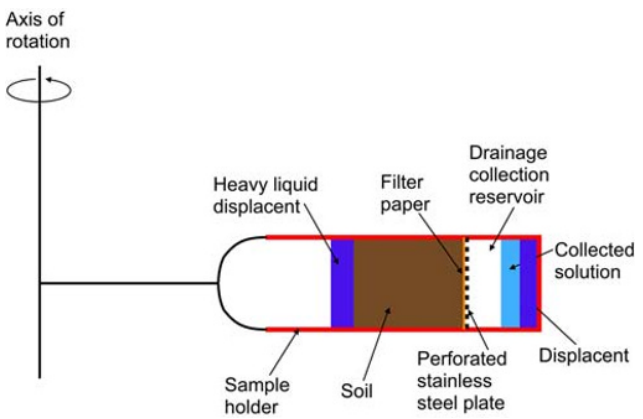

Fig. 20.1 Arrangement for enhanced recovery of soil solution with a centrifuge by displacement using a heavy immiscible liquid.

large artificial gravity and pushes the water in front of it. The displacent collects in the bottom of the sample holder, beneath a filter paper and stainless steel screen supporting the sample, with the displaced solution floating on top of it. The method can enhance recovery of solution by several times over centrifuging at the same speed (Kinniburgh & Miles, 1983), although the liquid must be lighter than the soil particles, which can be a problem with organic soils (Absolom *et al.*, 1995).

Saturated paste and dilution extracts

The oldest, and still most common, way to obtain samples of soil solution systematically for analysis is to mix the soil sample with a quantity of distilled water and then to filter off the liquid. This clearly dilutes the bulk soil solution and changes the partitioning between C_s and C, depending on the degree of dilution and the speed at which equilibrium is attained. In many soils this has only a minor, if any, effect, but for soil high in organic matter or clay, it may be very important. Because the soil solution is necessarily diluted, analysis for species present in only low concentration becomes more difficult. The method is generally used to obtain either a *saturated paste* extract or one of a given dilution, usually either 1 : 1 or 1 : 5.

In the former case, air-dry soil is mixed carefully with distilled or deionised water until it is just saturated. This often requires that the mixture be left covered for a few hours to attain full saturation, remove air, etc., then topped up with either more water or, if too much water had been added, more soil. The solution is then extracted by placing the sample on a filter paper on a Büchner funnel and applying a vacuum.

For 1 : 1 or 1 : 5 extracts, the soil is mixed with either an equal mass of water or five times this, shaken for an hour, and then the suspension filtered.

In both cases, an adjustment to the amount of water added is necessary to account for the water in the air-dry soil, and a drop of 0.1% sodium hexametaphosphate should be added to prevent precipitation of $CaCO_3$. Further details are given by Bower and Wilcox (1965) or Rhoades (1996).

Extraction with ionic solutions

Where the species of interest are tightly bound to soil particle surfaces, preventing efficient extraction by mixing with distilled water, the process can be enhanced and/or accelerated by using a solution containing ions, which have greater attraction to the surfaces than those already adsorbed. The particle surface exchanges the ion from the solution with that adsorbed, thereby freeing it into the bulk solution. Examples (with increasing ability to dislodge stubborn species) are $CaCl_2$, $Ba(NO_3)_2$ and HNO_3 (Gooddy *et al.*, 1995).

20.2 *In situ* Collection of Soil Solution

For much the same reasons that methods for *in situ* measurements of soil water content and potential have been developed, so sampling of soil solution from equipment embedded in the soil is desirable. Most such devices, however, suffer from uncertainty in:

- The volume from which the sample is taken
- The proportions of water collected from preferential routes or slower moving water
- The effect of the equipment itself on modifying the chemical composition of the water
- Chemical transformations occurring between sampling and collection

In short, the same sort of problems that attend all methods for monitoring water content and potential *in situ* but more complex. In the same way as for water measurements, this should not be a deterrent to making the effort, but a recognition of the limitations allows precautions to be taken against the most obvious defects and engenders a healthy scepticism when interpreting the results.

20.2.1 Suction samplers

Otherwise known as vacuum or tension samplers, suction (or vacuum) lysimeters, ceramic cup samplers and several other variants, these are the workhorses of the solution sampling world. Wagner (1962) is credited with introducing this particular form of sampler, which need not produce a great deal of disturbance to the natural soil environment. The suction sampler resembles a tensiometer very closely, and some workers use slightly modified tensiometers for the purpose. Usually, however, the suction sampler is constructed from a larger porous cup cemented to a tube of about 50–75 mm diameter. This increases both the area of contact with the soil and the volume of vacuum reservoir available within the device over that of a normal tensiometer. The essential elements of a suction sampler are shown in Fig. 20.2. The sampler and collecting vessel can be evacuated by use of a small hand- or battery-operated pump, and then sealed off by closing the tap. Soil solution is attracted into the sampler body if the vacuum pressure inside it is lower than the matric potential of the soil water. The amount collected depends on the conductivity of the porous cup, its size, the goodness of contact between it and the soil, the hydraulic properties and the water status of the soil. In wet conditions, therefore, large quantities of water may be collected in a few hours, whereas in drier conditions, no sample or only a few millilitres may be collected. If the soil is too dry, the porous cup may fail to preserve the vacuum. A vacuum gauge is a useful optional extra to allow monitoring of the collection progress. As soil solution collects in the sampler, the vacuum will fall. In the absence of leaks, the vacuum, ψ_v, below atmospheric pressure, A, in the sampler when a volume v of sample has been collected will be

$$\psi_v = \frac{\psi_0 V_0 - Av}{V_0 - v} \qquad (20.2.1)$$

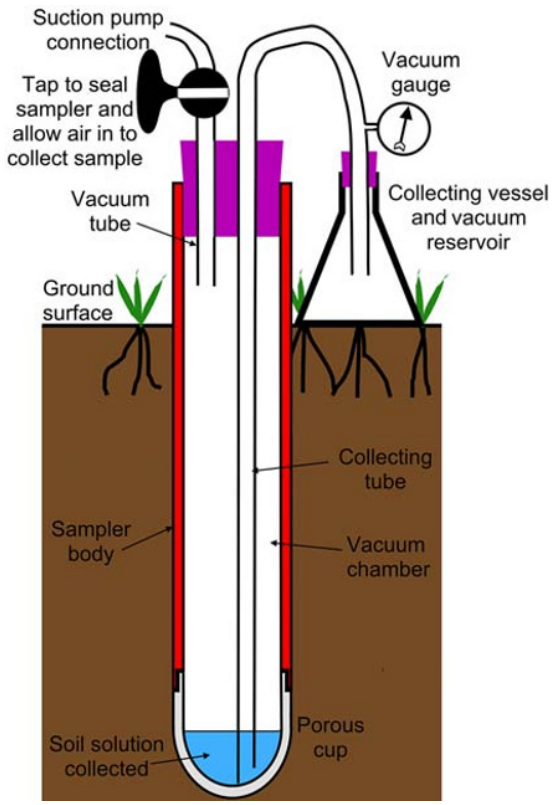

Fig. 20.2 Suction sampler for shallow sample collection.

or

$$v = \frac{\psi_0 - \psi_v}{A - \psi_v} V_0. \qquad (20.2.2)$$

where
ψ_0 is the initial vacuum in the sampler and
V_0 is the total volume of the sampler plus collecting vessel.

Temperature and atmospheric pressure changes will have a slight effect on this.

The gauge will also warn of failure of the sampler.

Once a predetermined time of collection has passed or it is judged that sufficient sample has been collected from the rise in internal pressure, the sample may be collected simply by opening the tap. This allows air into the sampler and pushes the collected solution up the collecting tube into the collecting vessel. This is only possible if there is enough vacuum in the collecting vessel to lift the water up the length of the collecting tube. For deep installations, or where there is insufficient vacuum at the end of the collection period, pressure must be applied to the suction pump connection and a vent supplied to the collecting vessel. For sample collection under pressure, the sealing bung on top of the sampler body and some of the other joints may need to be made with engineered connectors to avoid them coming apart.

Precautions should be taken to avoid the danger of any part of the system causing injury from implosion (under vacuum) or explosion (under pressure). Wrapping a glass vessel in adhesive tape may be sufficient. Commercially available Buchner flasks are designed for evacuation and are convenient. The sidearm can be used for a pressure gauge, a vent when collecting solution under pressure or, with a vacuum pump, to suck the sample from a shallow installation when the system vacuum has declined too far.

It is important that the collecting tube terminates as close as possible to the lowest point in the sampler to collect as much solution as possible and leave as little behind to mix with the next sample.

Porous cups

Tensiometer cups are usually made from sintered glass, aluminium oxide or ceramic. For many ionic species that are not strongly adsorbed to soil materials (e.g. Cl^-, Br^-, NO_3^-, K^+, Na^+, Ca^{++}), these are perfectly suitable. Most references in the literature recommend that they be washed before use by flushing two or three times with dilute hydrochloric acid (Grossmann & Udluft, 1991), followed by flushing well with distilled or deionised water. This should remove most soluble impurities in the cup material. Most materials have some cation exchange capacity and flushing with HCl will saturate the exchange sites with Cl^- ions, which can be displaced into the solution collected while removing some other anions from the solution. It is likely, therefore, that the first few samples collected will not be representative of the soil solution because of the cup's exchange capacity. More specialised cups are available made of sintered or porous stainless steel, PTFE or other materials. These are much less likely to alter the chemical makeup of the soil solution and are necessary for sampling species such as phosphate, some heavy metals and many pesticides. Most alternative cup materials, however, do not have an air entry value as low as ceramic and so cannot be used to collect samples from drier soil.

Vacuum pumps

Handheld vacuum pumps, whether of the Nalgene 'trigger' type or similar to a traditional bicycle pump, are fine for evacuating one or two small samplers but are very tiring if a large number of samplers need to be evacuated. A better solution is a pump similar to a bicycle floor or 'track' pump, which can be held down with one foot, while two hands can be used to pump with a long stroke. Small, battery-operated vacuum/pressure pumps are also available at reasonable cost. These run from a small sealed lead–acid battery and have proved very convenient. They are also useful for a variety of other tasks in the field, such as flushing pressure transducer tensiometers (see Section 12.7.5). Care needs to be taken that water does not get into the pump, which can damage it.

Installation

Precautions to avoid rapid bypass of the soil matrix by water from above are even more important than for installation of soil water observation equipment. Even small quantities of solute reaching a depth, where otherwise there would be none, can lead to seriously erroneous

conclusions. Small 'skirt'-type deflectors fitting well around the top of the sampler body, installation inside a sleeve terminating some 200 mm above the cup (see Fig. 12.18) and/or a bentonite seal pressed around the top of the sampler body should be employed. The hole, whether for the sampler body or a sleeving tube, should be tight fitting. Good contact of the porous cup with the surrounding formation is even more critical than for tensiometers. Installation into a slurry of native soil from the appropriate depth should ensure this, but great care must be taken that exotic solutes are not introduced in the process. Some clay-rich soils may produce a slurry that, when dried, becomes effectively impermeable. Use of silica flour in such a circumstance may be a better option.

In many cases, a few months will be needed before samples from suction samplers become representative of the ambient soil solution. During this time, samples should be taken on a regular basis to keep solution flushing through the cup and decreasing the time taken for equilibrium with the soil solution. This process may be accelerated by preconditioning the sampler cup by soaking in a solution similar to that expected in the soil (Grossmann & Udluft, 1991).

Sampling regime

Frequency and elapsed time of sample collection The frequency of sample collection depends on the reasons for collection, the amount of solute needed, the water status of the profile and available manpower. In all cases, some time is needed between evacuation of the sampler and sample collection. In a profile close to or above field capacity, it may take only a few minutes to collect sufficient sample, whereas in other soils or at other times, very little or no sample may be obtainable over a period of a week. The sampler is unable to collect solution unless its internal pressure is lower than the matric potential outside the porous cup. Even then, the hydraulic conductivity of the soil may be too low to conduct sufficient water, or the specific water content (see Section 3.1) may be too small to yield enough solute. The two factors are combined in the diffusivity (see Section 3.1).

Collection over a short time period causes least disturbance to the water and flow distribution in the surrounding soil. Nevertheless, the solute collected may not be representative of the soil matrix. For instance, if the porous cup is close to a macropore, which is active when the sample is being taken, then the solute collected is probably more representative of the solution flowing in the macropore than of the soil matrix. On the other hand, if the sample is taken at another time, when there is no flow down the macropore, the sample is likely to be representative of the matrix solution. If the sampler is evacuated and left for an extended period (say a week), over which time there is wetting and drying of the soil, then the composition of the sample collected is even more difficult to interpret. However, that may be the only way to collect sufficient sample. Changes in the soil water regime over the time that the sampler is left evacuated also bring a danger that if the soil dries over that period, coupled with the internal pressure rising as sample is collected or there is a little air leakage, solution may be reabsorbed into the soil from the sampler.

Choice of vacuum Least disturbance to the flow regime outside the sampler will result if the internal pressure in the sampler is only slightly below that of the surrounding soil water. However, the rate of solution flow into the sampler increases as the difference between the two pressures increases (not necessarily proportionally so). Less disturbance, as well as better time resolution of the sampling, results from keeping the sampling time short. A compromise must, therefore, be made between a short sampling time with large differential pressure and a long sampling time with a smaller pressure difference. It is difficult, if not impossible, to generalise on these choices. Dynamic matching of the vacuum to just below the prevailing matric potential is possible (see the discussion of porous plates in Section 20.2.4), but requires sophisticated control gear and, for most uses, destroys the simplicity of suction samplers.

Sample collection

For shallow installations, if there is still a reasonable vacuum left in the sampler, opening the tap on the vacuum tube in Fig. 20.2 will force the collected solution into the collecting vessel. If this is not the case, or for deeper installations, external pressure will be needed and the collecting vessel should be vented to atmosphere.

20.2.2 Lysimeters

A lysimeter is a rigid container containing soil. The soil may be an undisturbed monolith, as described in Section 17.1, or repacked to mimic the natural profile. Usually, the drainage water is collected from the base of the lysimeter under gravity (often termed a *drainage lysimeter*). This requires that the bottom of the lysimeter is at zero matric potential, that is, saturated. When the soil at the bottom becomes unsaturated, flow ceases. This introduces some uncertainty into the representivity of solute concentrations and totals. It is possible to apply a suction to the bottom of the lysimeter, either by means of a hanging water column or a vacuum pump. This may be a fixed suction or controlled to match the ambient water potential of the surroundings, as described for porous plates below (Section 20.2.4). More discussion of lysimeters is contained in Section 24.3.6.

20.2.3 Pan samplers

Sometimes called *zero tension lysimeters*, these are probably the simplest samplers of all for *in situ* applications. They do, however, require a vertical face on the soil (usually a pit) to install the sampler. The general arrangement is depicted in Fig. 20.3. The floor of the pan slopes towards the outlet end, while the upper edge of the sides is in contact with the soil. The pan sampler may be regarded as a drainage lysimeter without the confining walls.

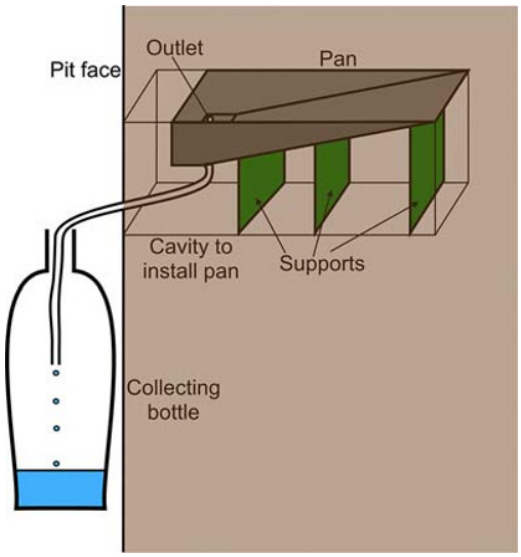

Fig. 20.3 Pan sampler.

Disturbance to the water flow is quite serious, since water can flow out of the soil only if it is at zero matric potential. Unless the pan is installed in a position where this is the case, water flow will tend to be mainly around the pan, rather than into it, so that the amount collected is less than would be expected from the average water flux. The composition of the solution collected is also likely to be biased towards that flowing in macropores.

Installation

The pan sampler collects water from above it and so should be installed into a small tunnel more or less horizontally excavated from the face of a pit (see Fig. 20.3). There may need to be a perforated plate between the soil and the pan to prevent soil falling into the pan and possibly blocking the outlet. The arrangement for installation is shown in Fig. 20.7. Sampled soil solution flows directly from the outlet into a collecting vessel.

20.2.4 Porous plates

Porous plates are similar in principle to suction samplers but usually have a larger collecting area, which can be orientated perpendicular to the water flow direction, usually horizontally. A diagram of a porous plate sampler is shown in Fig. 20.4.

The porous plate, selected to have an air entry value lower than the lowest soil water matric potential likely to be experienced, is cemented into a chamber as shown. The chamber is evacuated and soil solution collects below the porous plate. Porous plates are usually made of ceramic but may be of sintered glass, porous stainless steel or plastic (e.g. PTFE), where higher flow rates and/or avoidance of adsorption by the plate material are important.

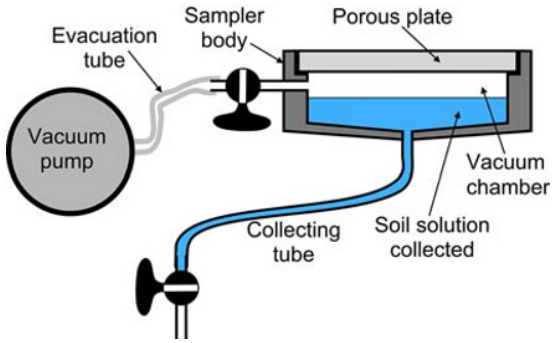

Fig. 20.4 Schematic diagram of a porous plate sampler.

Installation

Good contact between the plate and the soil are important. Installation is usually in a small tunnel similar to that for pan samplers. The top of the tunnel needs, however, to be flat to maximise the contact area and the plate pressed upwards with moderate force. Hydraulic jacks, turnbuckles and wedges have been used for this purpose. Periodic checking that contact is tight will be necessary. A little loose native soil or silica flour helps to maximise contact.

Operation

Porous plate samplers may be operated in the same ways as described for suction samplers above. Because the collecting area is designed to intercept flow, the volume collected is expected to be closer to the integrated flux over the area of the plate and the time of collection. However, if the matric potential at the upper surface of the plate is not very close to that in the surrounding soil at the same depth, then water will be either diverted into or away from the sampler.

Recognising this, various workers have attempted:

- To confine flow by a vertical tube above the sampler, installation of which causes soil disturbance.
- To evacuate the sampler initially to a pressure approximating the matric potential as measured by a tensiometer at the same depth.
- To control the vacuum inside the sampler to equal that indicated by an external tensiometer (sometimes with a correction for the expected pressure difference across the plate) (Booltink *et al.*, 1988; Brye *et al.*, 1999; Lentz & Kincaid, 2003; Barzegar *et al.*, 2004; Siemens & Kaupenjohann, 2004; Ciglash *et al.*, 2005). This uses a pressure transducer tensiometer, electronic control circuitry, electrically controlled valves and an electrical vacuum pump. A problem with this arrangement is that the pressure drop across the porous plate depends on the flow rate, and so it is not possible to match the conditions at the upper surface of the porous plate exactly to those in the ambient soil at all rates of flow.
- To control the vacuum in a similar manner to bring the reading of a tensiometer just above the plate equal to that of a tensiometer at the same depth some way to the side. The most successful method to date, however, appears to be to

control the external water potential by rapid cycling of the internal pressure of the sampler. When the matric potential at the plate surface, ψ_p, is higher than that in the natural soil, ψ_n, a vacuum pump reduces the internal pressure well below that of the ambient matric potential. This will cause ψ_p to fall below ψ_n. A valve is then opened to release the vacuum in the chamber, allowing ψ_p to recover. Van Grinsven *et al.* (1988) used a monitoring interval of 3–6 min for the control of the vacuum. Kosugi and Katsuyama (2004) found that under high flow conditions, this gave inadequate control and used an interval of 3 s.

The last two configurations are sometimes referred to (not very appropriately) as *passive pan samplers*. As well as providing a representative sample of the soil solute flux, these control mechanisms give a very good measurement of the water flux, since there is only minimal difference maintained between the ambient matric potential and that at the plate surface. Soil water flux arriving at the plate surface is, therefore, expected to be close to that in the undisturbed soil. Hydraulic properties variability, fingering and macropore flow, however, may result in considerable spatial variability in water flux and, possibly, in solute concentration. It is wise, therefore, to use either a substantial number of small samplers or a smaller number with a large collecting area. For instance, based on the work of de Rooij and Stagnitti (2000), Ciglash *et al.* (2005) used 16 approximately 75-mm diameter glass sintered plate collectors. One obvious difficulty with either type of passive pan sampler is the high capital cost and power requirement for the pump, especially with the Kosugi and Katsuyama variant.

20.2.5 Wick samplers

A hanging water column is an effective and passive way to exert a suction on soil. A wick, made of a bundle of fibres, can emulate this. A wick sampler is made of a chemically inert material, hanging more or less vertically, with its upper end in contact with the soil. The matric potential at its interface with the soil will be approximately equal to the negative height above the lower end of the wick. This varies slightly according to the amount of flow in the wick. A schematic diagram of the arrangement is shown in Fig. 20.5.

Unlike the pan sampler, the wick sampler does not depend on saturation at the point of contact with the soil, but the minimum matric potential at which it can operate is set by the length of the wick (typically 500 mm). In most soils, this is not a significant limitation. Drainage volume collected is reported to be close to that expected from estimates made by other means (Boll *et al.* (1992), 103%; Brandi-Dohrn *et al.* (1996), 66–80%; Zhu *et al.* (2002), 106%). This lends confidence that the solute concentrations will also be similar. Zhu *et al.* (2002)'s figure of 106% included a range from year to year from 99 to 129% and excluded one very wet year, when the volume was 206% of that expected. Under very wet conditions, therefore, wick samplers are likely to cause some flow convergence towards the sampler (Holder *et al.*, 1991; Zhu *et al.*, 2002).

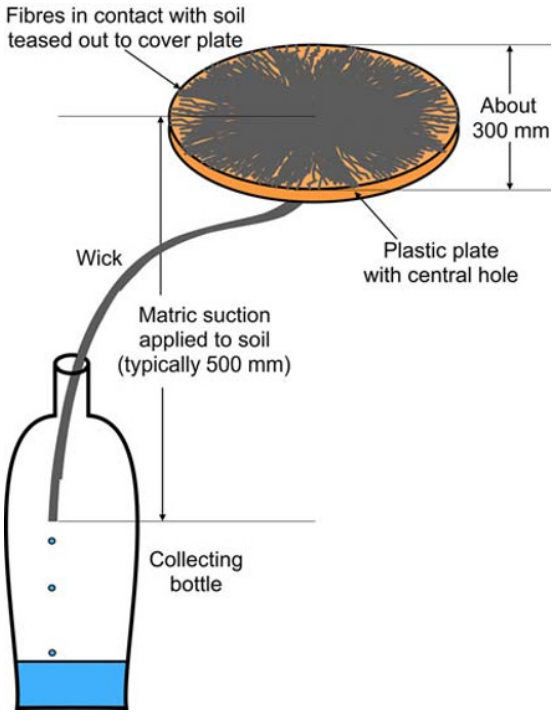

Fig. 20.5 Wick sampler schematic.

The most popular wick material is glass fibre, as it is almost inert. Some sodium from the glass may, however, leach into the collected sample so that caution should be exercised in interpreting concentrations of this element. Problems of chemical interpretation have not been reported for any other species. The wick material, in the form of glass fibre ropes, is widely available in a variety of different sizes mainly for industrial insulation applications (Selker, 2002). There is therefore a wide choice available that can match the pore size distribution of many soils. The manufacturing process leaves a number of residues on the fibres, which may contaminate the solution collected and/or be hydrophobic (Selker, 2002). This can be eliminated by heating at 400°C for about 3 h (Knutson *et al.*, 1993).

20.2.6 Resin box samplers

Ion exchange resins offer an alternative way to collect ions in soil solution. In this case, the liquid carrying the ions is not preserved, and so there is no information on either the amount or concentration of the liquid passing through the sampler. A schematic diagram of a resin box sampler is shown in Fig. 20.6.

The most common materials for the resin, which is usually in the form of 0.5–1 mm beads, are based on polystyrene, which has an open molecular structure, allowing solutes to penetrate into the polymer. Incorporation of

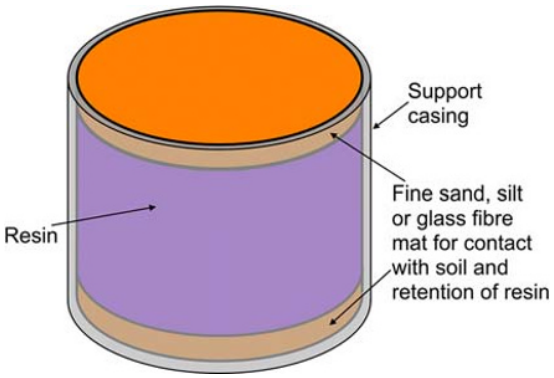

Fig. 20.6 Schematic of a resin box sampler. The resin may be of a single type, mixed anionic and cationic or in layers of different kinds. (*See insert for colour representation of the figure.*)

sulphonic acid groups into the structure produces a strongly anion adsorbing resin, while quaternary amino groups lead to strongly cation adsorbing properties. A mixture of the two types traps both anions and cations or they may be placed in separate layers. The resin is usually saturated with a weakly sorbing ion (e.g. H^+, Na^+, OH^-, HCO_3^- or Cl^-), which is displaced by more strongly adsorbing ions in the soil solution passing through. After installation in the soil for some time, often weeks, the resin box is removed. If there is a mixture of both anionic and cationic adsorbing resins, these can be separated by their different density. The solutes sorbed onto the resin can be recovered after removal from the soil by flushing with a concentrated solution containing ions not under investigation. The solutes are detected by chemical analysis of the solution leached out of the resin.

Because the resin box method depends on solute flowing through the resin, if the hydraulic properties of the resin do not match those of the surrounding soil, water flow may be diverted either away from or towards the resin box. The accumulated quantity of solute may therefore be less than or greater than that passing through an equal area of soil at the same depth.

Installation

Resin boxes are most conveniently installed from the side of a pit in a very similar manner to that of pan samplers or porous plates, although both upper and lower surfaces of the box must be in good contact with the soil. The upper and lower surfaces of the resin should be protected by a layer of fine sand, mesh (Weihermüller *et al.*, 2007) or glass fibre mat (Siemens & Kaupenjohann, 2004) to avoid loss of resin. Soil should also be backfilled around the box to minimise disturbance to the water flow field.

20.2.7 In situ *collection of soil solution: Conclusion*

All systems described in the foregoing for collection of soil solution *in situ* have several drawbacks, which lead to considerable uncertainty of whether the solute concentrations are representative of the resident soil solution, the flow concentration or neither; what soil volume the sample is taken from; the amount of disturbance to the natural flow regime and what chemical changes to the solution may have taken place over the time between sampling and collection (which in some cases may be quite long). Nevertheless, valuable information on solute concentrations has been collected by many investigators and, provided that the possible limitations are taken into account, the results can often be interpreted to give useful estimates of solute flux.

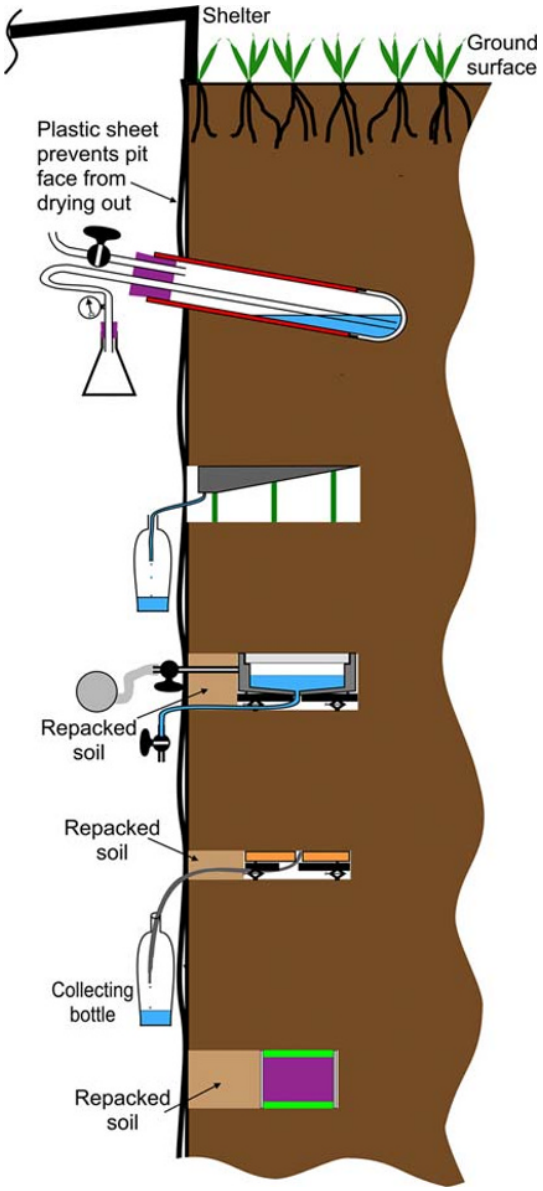

Fig. 20.7 Installation arrangements for different solute samplers from an access pit. From top, suction sampler, pan sampler, porous plate, wick sampler and resin box. (*See insert for colour representation of the figure.*)

Many of the samplers described require installation from a vertical surface, which usually requires an access pit to be dug and all the precautions described in Section 12.12.1 taken to ensure minimum interference from the presence of the pit and for personal safety. In addition, a tunnel or gallery needs to be excavated to emplace a sampler, which is usually somewhat larger than instruments for water content or potential measurement. To reduce disturbance to the flow regime as much as possible, soil should be repacked around the samplers as nearly as practical to its condition in the undisturbed soil (soil from the same depth, the same bulk density, etc.). A suggested arrangement is shown in Fig. 20.7 for each type of sampler.

The different sampler designs are likely to produce different estimates of soil solution concentration. This arises partly from the time over which the sampler collects solution, with some samplers left in the soil for several weeks, while others can collect a sample in a few minutes. The soil matric potential at the time of sampling is also important. Pan samplers can collect a sample only when the soil immediately above it is saturated. The water collected is, therefore, likely to be biased towards that flowing in macropores and during wetter periods of weather. Suction samplers, on the other hand, collect water from a volume around the cup. Therefore the sample is likely to be fairly representative of the resident soil solution in its immediate vicinity over the period that the sampler collects water. If it intercepts a macropore or is close to one which is active during the time that it is collecting, then this is expected to have a major influence. Wick samplers are claimed to collect representative volumes of flowing soil solution (Selker, 2002; Zhu *et al.*, 2002). This is not likely to be the case where significant amounts of drainage occur when the prevailing matric potential is numerically greater than the length of the wick. This will be true for many fine textured soils. Porous plates with vacuum control to match the ambient matric potential should cause least disturbance to the flow, so that they should intercept all water from vertically above them, giving both an accurate measure of the integrated water flux and the flow-weighted solute concentration over the time that they are collecting, but are expensive and power hungry.

21 Solute Concentration Estimation by Electrical Conductivity

Ions in the soil solution make it electrically conductive. From the point of view of the soil scientist, the electrical conductivity of distilled or deionised water is effectively zero. Any increase in conductivity is therefore a result of solutes dissolved in the water. This conductivity results only from ionic solutes. Many pesticides, for instance, are covalently dissolved and confer negligible conductivity to the solution. In any case, these are normally of such low concentration by comparison with ionic solutes that the method could not detect them against the large ionic background.

The principal limitations for using electrical conductivity to measure solute concentration are:

- It measures only one quantity, the aggregate effect of all the ions in the soil solution.
- Converting the measurement of bulk soil electrical conductivity into an estimate of the intrinsic conductivity of the soil solution is, in many cases, not straightforward.

21.1 Electrical Conductivity of Soil Solution

The concept of electrical conductivity was introduced briefly in Section 8.3.7. It is defined as the conductance between two metallic plates of unit area separated by a unit distance. In SI units, the length scale is a metre and conductance is the siemen (S), and so conductivity has units of $\mathrm{S\,m^{-1}}$. Much of the literature about soil conductivity uses units of $\mathrm{dS\,m^{-1}}$ (i.e. 1/10th of a $\mathrm{S\,m^{-1}}$), which corresponds to the earlier common usage of $\mathrm{mS\,cm^{-1}}$. Some branches of environmental science work with resistivity in preference to conductivity (e.g. electrical resistivity imaging, see Chapter 10). Resistivity in Ω m is merely the reciprocal of conductivity in $\mathrm{S\,m^{-1}}$, and so the two are easily converted.

The electrical conductivity of an ionic solution is proportional to the concentration of those ions. For one ionic species, the solution conductivity, σ_s, is given by

$$\sigma_s = KC_m\mu|z|, \tag{21.1.1}$$

where

K is a proportionality constant;

C_m is the *molar concentration* (i.e. the number of moles of the ion in unit quantity of solution, essentially a measure of the number of ions of the particular species);

μ is the *mobility* of the ion in the solution (the mobility depends on the size of the ion, collisions with other molecules and ions as well as temperature), and

z is the valence (i.e. the electrical charge) of the ion.

Real solutions contain both positively and negatively charged ions (cations and anions) and usually have a mixture of different ions of each type. These will each add their own conductivity to the solution

$$\sigma_s = K\sum_i C_{mi}\mu_i|z_i|, \tag{21.1.2}$$

where the subscript i refers to a particular ionic species. The solution conductivity is therefore dependent on the concentration of the various ions, their valence, both of which are well-defined quantities, and their mobility, which is a more variable quantity.

Conductivity is usually quoted for a standard temperature of 25°C. For other temperatures, T, in the normal range experienced in soil, a suitable correction is

$$\sigma_s(T) = \sigma_s(T)[1 + \alpha(T - 25)]. \tag{21.1.3}$$

The value of α depends only slightly on the particular ions in the solution. For a 0.01 M potassium chloride (KCl) solution, it is $0.019^{\circ}\mathrm{C^{-1}}$ (De Neve *et al.*, 2000). Note that this correction factor also applies to the mobility.

Other ions in the solution also affect the mobility. This arises from two sources – a shielding of the ion from the electrical field by the other ions in its vicinity and a drag on movement of the ion by ions of opposite charge moving in the other direction (*electrophoresis*). These are combined in *Kohlrausch's law*:

Soil Water Measurement: A Practical Handbook, First Edition. J. David Cooper.

$$\mu = \mu_0 - b\sqrt{I}, \tag{21.1.4}$$

where
μ_0 is the mobility at infinite dilution;
b is an empirical constant, and
I is the *ionic strength* of the solution

$$I = 0.5\sum_i C_{\mathrm{m}i} z_i^2. \tag{21.1.5}$$

The situation is actually more complicated than this, as there are other interactive effects, such as oppositely charged ions combining loosely to form short-lived uncharged *ion pairs* (see, for instance, Visconti *et al.*, 2010). However, the previous discussion should give a flavour of the situation.

21.2 Conductivity of Soil

To use measurements of soil conductivity to estimate solute concentration, we need to know not only the relation between solute concentration of the solution and its electrical conductivity but also the relation between the electrical conductivity of soil solution and that of the bulk soil. In unsaturated soil, this depends on both the solution conductivity and the soil water content. This was discussed in Section 10.2.1, where Archie's (1942) law, which is relevant for clay-free formations, and its extension by Waxman and Smits (1968) were described. Other descriptions of the relationship have been attempted over the years by, among others, Rhoades *et al.* (1976), Nadler and Frenkel (1980), Rhoades *et al.* (1989), Mualem and Friedman (1991) and Mojid *et al.* (2007). The models all attempt to account for conduction through the 'free' solution in the soil outside the immediate vicinity of clay surfaces and that *via* the ion-rich double layer in contact with the clay. Some also introduce a third pathway through the solid particles, which is often negligible. With the exception of the Rhoades *et al.* (1989) model, which introduces a serial pathway, the different models treat the different pathways as acting in parallel, so that there is a general form of

$$\sigma_{\mathrm{b}} = \sigma_{\mathrm{w}}\theta T(\theta) + T(\theta) f(\sigma_{\mathrm{w}}, f_{\mathrm{c}}, \theta) + \sigma_{\mathrm{s}}, \tag{21.2.1}$$

where
T is a *transmission* factor to account for tortuous actual current paths (T is expected to increase as θ decreases);
f_{c} is the fraction of clay (note that different clay minerals affect current flow through the double layer by different amounts) and
σ_{s} is the conductivity of the soil solids.

The various variables are usually simple functions (linear or quadratic) of the soil constituents. In view of the number of variables, the wide range of different soil types and the difficulty in characterising their response to different levels of solute, it is no surprise that there is no consensus on an appropriate formula nor that it is unlikely that one formula will fit all soils.

21.3 Measurement of Soil Electrical Conductivity

Several approaches can be taken to measure the electrical conductivity of soil, both in the laboratory and in the field. In line with the general difficulty of characterising the concentration of soil solution, none of them has the same standard of precision that characterises measurement of water content. Nevertheless, major advances have been and continue to be made in the ability to monitor solutes in soil *in situ*.

21.3.1 Laboratory methods

Laboratory measurements can be made of the electrical conductivity of soil solution samples obtained either from soil samples extracted from the field, as described in Section 20.1, or from *in situ* samplers (Section 20.2). The conductivity is most conveniently measured by a simple ac bridge with the solution in a conductivity cell. These are widely available at modest cost.

Translation into solute concentration may be difficult. Equation 21.1.2 shows that the ions in solution each have a different mobility as well as there being possible valence differences. If the composition of the solution is known, at least approximately, then the appropriate values for valence and mobility can be used to calculate the total concentration in the solution.

It is important to stress that the conductivity of ionic solutions is very sensitive to temperature. The standard temperature for measurement is usually 25°C. If it is not possible to make measurements at this temperature, then it should be corrected to 25°C by use of an equation similar to (21.1.3). Good temperature control is also important, and measurements must be made in an environment where temperature does not vary by more than about 0.5°C. This ensures an imprecision from this source of about 1%. ac measurements are also important. The imposition of a dc voltage to a solution causes migration of positive ions in one direction and negatively charged ones in the other, with a consequent build-up of charge (*polarisation*) on each current electrode, which acts to reduce the voltage (and therefore the current) within the bulk of the solution. A frequency of around 1 kHz is frequently used.

21.3.2 Field methods

In the same way that electrical methods can be used to measure water content of soil, they are also sensitive to solute concentration. As explained in Section 21.2, using electrical conductivity of soil to estimate solute concentration involves knowing not only the relationship between solute concentration and solution conductivity but also that between solution and soil conductivity. The latter relation

also requires knowledge of soil water content. Electrical conductivity of the soil, therefore, is sensitive to both water content and solute concentration. In Chapter 10, we described electrical resistivity imaging (ERI) as a means of measuring water content, but it could equally well have fitted into this chapter as a method for solute concentration estimation. In many situations, soil solution electrical conductivity is relatively stable, particularly where no agricultural chemicals are applied and there is sufficient buffering by clay minerals in the soil. In such situations, the main change in soil electrical conductivity results from water content change. On the other hand, tracking the movement of ionic substances applied artificially to the soil can be accomplished, at least in principle, if both soil electrical conductivity and water content are measured or if water content can be assumed constant.

Ceramic disc salinity sensors

Another porous body in the soil not only achieves matric potential equilibrium with the soil but also solute concentration equilibrium with the soil solution by diffusive exchange with the porous body. The ceramic disc salinity sensor is a disc of porous ceramic with a high air entry value. This is brought into contact with the soil at the depth of interest. Once equilibrium has been attained between the soil solution and that in the disc, the electrical resistance of the latter is measured using platinum electrodes embedded in the disc. A spring, situated behind the disc mounting and retained before installation by a pin, is used to ensure good contact between the disc and soil. Once in position, the pin is removed by pulling on a string or wire attached to it. A thermistor is also incorporated to allow temperature correction of the readings. A schematic diagram of a salinity sensor appears as Fig. 21.1.

The ceramic is of a high air entry value (about 150 m water — 1.5 MPa), which should ensure that it remains saturated under most field conditions. However, it has been reported that the resistance between the platinum electrodes is reduced by about 10% at a matric potential of –10 m water (Rhoades, 1996).

Preparation for installation The sensor must be prepared before installation by soaking in water for at least 24 h (preferably for several days) to ensure that the ceramic is field saturated. Saturation under vacuum is not recommended, as this would create artificially high saturation (Rhoades, 1996). The manufacturers recommend that a weak (~2 dS m^{-1}) solution rather than pure water be used for this process. The sensor should be kept saturated until installation.

Installation The sensor is usually installed from a small (~32 mm diameter) access hole with the long axis of the sensor at right angles to the axis of the hole using a suitable rod to place it in position at the correct orientation. The release pin is then pulled out, allowing the spring to force the ceramic disc against the side of the hole. The hole is then backfilled with soil, preferably with some bentonite to prevent water preferentially infiltrating down the hole. Because the spring pushes the ceramic disc hard against the side of the hole, recovery of the sensor may be difficult except for shallow installation. A version of the sensor is available without the spring, designed for installation at the end of the access hole and aligned along it. Greater care will be needed to ensure good contact with the formation, although recovery from a lined hole should be straightforward.

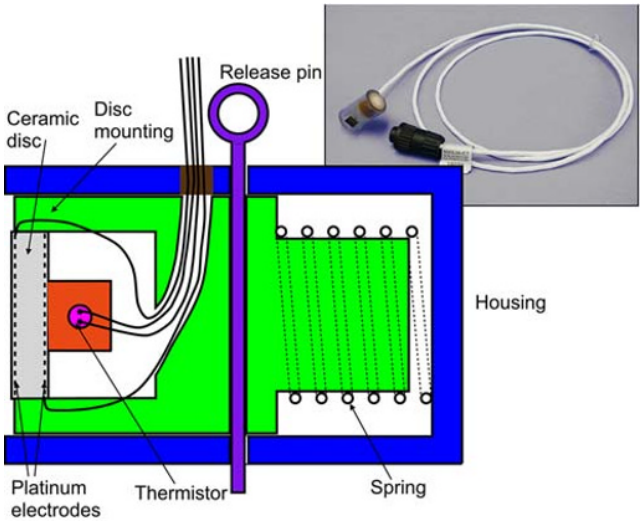

Fig. 21.1 Salinity sensor with release pin in position ready for installation. Reproduced with permission of Soilmoisture Equipment Corp.

Reading the sensor Soilmoisture Equipment Corp. recommends the use of its dedicated reader unit for the sensors, as they are optimised for this sensor. This can also be used for reading the thermistor and is suitable for gypsum resistance blocks as well as other resistive devices. Other reader units can be used but should be calibrated with the sensor. The platinum electrodes are only 1 mm apart and this introduces a significant capacitance into the circuit.

Several days are needed for the sensor to come to equilibrium with the soil conditions in which it is installed. After that, the response time to changes in salinity is of the order of a few hours (Rhoades, 1996).

Electrical resistivity imaging

ERI was described in some detail in Chapter 10 and will not be repeated here. As pointed out previously, the electrical resistivity of the soil is dependent on both water content and soil solution conductivity. Where independent measurements of water content are available, the measurements can be used to infer soil solution conductivity. An example is the study by Slater *et al.* (1997) to track chloride migration through a Chalk profile using cross-borehole imaging.

Four-point measurement

A simplified version of ERI, a system uses four electrodes, often mounted rigidly on a wooden frame for convenience in insertion and keeping the correct spacing. Two outer electrodes are used to inject electric current into the soil and voltage read from two inner ones. The resistivity of the soil in the vicinity of the electrodes can be calculated from Equation 10.3.8, and discussion of other relevant points can be found in Chapter 10.

The size of the array can be varied to suit the objectives of the investigation. One hundred millimetres between the outer electrodes is probably the smallest sensible array size, and up to about 1.2 m is the maximum that can be handled in one piece. Larger arrays need to have separate electrodes, which is more inconvenient. The theory assumes that all electrical contact occurs at the surface. This is not possible to achieve in most instances, but the electrodes should be pushed into the soil as small a distance as possible while remaining in a stable position. Arrays can be left in place for repeated measurements if non-corroding electrodes are used.

Time domain reflectometry

The theory of time domain reflectometry (TDR) for determination of the real part of soil permittivity and hence water content measurement was described in Chapter 8. The imaginary part of the permittivity is, in many cases, dominated by the soil solution electrical conductivity. Therefore, if this part can be measured, the soil's electrical conductivity may be estimated. The measurement may, however, be influenced by relaxation effects, which have nothing to do with the dc conductivity.

Although the imaginary part of the permittivity has only a small effect on travel time (Section 8.5.4), it does have a significant effect on the reflection amplitude, in many cases making identification of the reflected pulse difficult or even impossible (Section 8.6). To see how the attenuation might be used to estimate electrical conductivity, it is useful first of all to see how the TDR trace is displayed and the way in which attenuation can be measured.

TDR traces in the literature are presented as voltage measured at the TDR unit, reflection coefficient or occasionally impedance or resistance. The differences between these may cause some confusion.

Voltage This is the most straightforward method of presentation and merely presents the voltage detected by the unit as a function of time. Time is often expressed in terms of a hypothetical distance. This reflects the primary use of TDR instruments for detecting faults and other discontinuities in cables, so that the distance along the cable to the point detected can be read directly from the display.

Reflection coefficient This is usually related to a 50 Ω line. Referring to Equation 8.5.29, the reflection coefficient for a 30 Ω load is –0.25. Reflection coefficients for other termination resistances are shown in Table 21.1. The reflection coefficient is linearly related to the voltage according to $\rho = (V/V_0) - 1$.

Table 21.1 Equivalent values of voltage, reflection coefficient and impedance for a TDR unit with 50 Ω output impedance

Voltage (fraction of V_0)	Reflection coefficient	Impedance (Ω)
0	–1	0
0.25	–0.75	7.14
0.5	–0.5	16.7
0.75	–0.25	30
1	0	50
1.25	0.25	83.3
1.5	0.5	150
1.75	0.75	350
2	1	∞

The reflection coefficient just after the voltage step, where $V = V_0$, should, therefore, be zero and just before this, it will be –1. Small departures of the components of the TDR unit from their nominal value may mean that there is a small difference in the display. Both the Tektronix 1502 series and the Campbell TDR100 instruments display the output as reflection coefficient by default.

Resistance or impedance This is related to the voltage detected by the unit. There is some inconsistency between papers in what is meant. The output impedance of the unit is commonly 50 Ω, so that the voltage at the top of the step output pulse would be displayed as 50 Ω.

In some papers (e.g. Mojid *et al.*, 1997; Evett *et al.*, 2005, 2006b), the voltage output seems to be scaled to this value, so that 'impedance' is actually a measure of voltage.

Alternatively, the Tektronix 1502 series cable testers have a facility to display 'ohms at cursor', which will show the impedance apparently 'seen' from any point on the line according to Equation 8.5.29 on the screen. This can be used to estimate the impedance of the waveguide at large time, and hence the bulk soil electrical conductivity according to Equation 8.5.29. Caution is needed, however, because it fails to take into account attenuation of the voltage along a long coaxial cable, losses in connectors, multiplexers, etc. (Castiglione & Shouse, 2003). For instance, if a 50 Ω coaxial cable connected to the unit were terminated by a 30 Ω resistor, this would cause a reflected pulse to propagate back along the line, according to Equation 8.5.29, of $(30-50)/(30+50) = -0.25$ of the output voltage, so that the voltage detected by the unit would be $0.75V_0$. $0.75V_0$ would be displayed by the unit as 30 Ω. Other equivalents are shown in Table 21.1.

Measurement of electrical conductivity from TDR reflections Giese and Tiemann (1975) proposed a method which provides a close approximation to the true dc conductivity and is the most commonly used method. It relies on waiting until all reflections between discontinuities in the electrical conductors have died away and the TDR

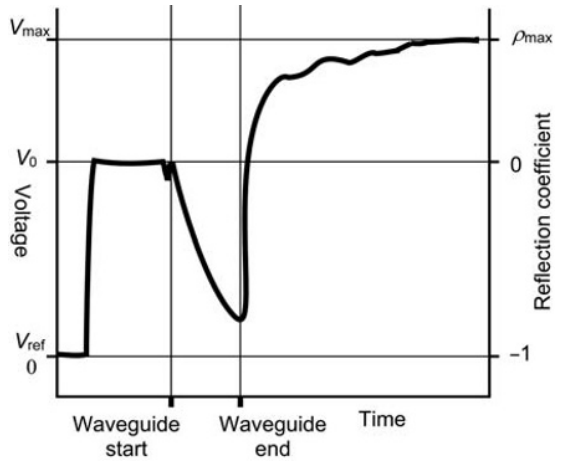

Fig. 21.2 Time domain reflectometer trace for waveguide in conductive medium.

signal is steady. This corresponds to a very low-frequency signal. The TDR trace will look something like that shown in Fig. 21.2.

The analysis of Section 8.5.2 can be applied to this problem by regarding the waveguide as a load, Z_L, on the end of a transmission line formed by the coaxial cable, as in Fig. 8.17. This is valid when the frequency is very low, that is, at large times when all internal reflections have died out and the reflected voltage has stabilised at V_{max}, as shown in Fig. 21.2. By designating the characteristic impedance of the coaxial cable by Z_c (in place of Z_0), $(V_{max} - V_0)$ the reflected voltage (in place of V_2) and $(V_0 - V_{ref})$ the incident voltage (in place of V_1), we find

$$\frac{V_{max} - V_0}{V_0 - V_{ref}} = \frac{Z_L - Z_c}{Z_L + Z_c}, \tag{21.3.1}$$

so

$$Z_L = Z_c \frac{V_{max} - V_{ref}}{2V_0 - V_{max} - V_{ref}}. \tag{21.3.2}$$

or alternatively

$$Z_L = Z_c \frac{1 + \rho_{max}}{1 - \rho_{max}}. \tag{21.3.3}$$

The minimum value of reflection coefficient is –1, since ρ is referenced to the voltage provided by the TDR unit, $(V_0 - V_{ref})$. The maximum theoretical value of ρ is +1, corresponding to a perfect open circuit. In the absence of any leakage across the waveguide rods or other losses, this is what would be recorded.

The load, Z_L is given according to Equation 8.5.36, which is valid for lines at low frequency, by

$$Z(l) \approx \frac{1}{j\omega C l}, \tag{21.3.4}$$

with

$$C = g\varepsilon. \tag{21.3.5}$$

For a two-rod line, g is given by Equation 8.5.1 and ε is given by Equations 8.3.57 and 8.3.58. For small values of ω, therefore, the imaginary part dominates and permittivity approximates to

$$\varepsilon = -j\frac{\sigma}{\omega}, \tag{21.3.6}$$

and hence

$$Z_L \approx \frac{1}{g\sigma l}, \tag{21.3.7}$$

which is purely resistive and the contribution from both the real part of the permittivity and relaxation effects is negligible compared with that from ohmic conduction.

So the electrical conductivity of the soil is

$$\sigma = \frac{1}{glZ_c} \frac{2V_0 - V_{max} - V_{ref}}{V_{max} - V_{ref}}, \tag{21.3.8}$$

or

$$\sigma = \frac{1}{glZ_c} \frac{1 - \rho_{max}}{1 + \rho_{max}}. \tag{21.3.9}$$

This analysis assumes that the cable is made of perfect conductors separated by a perfect dielectric and has ignored the effect of any connectors and multiplexers, which will reduce the energy going into the waveguide, as will attenuation by resistive losses in the cables. This was investigated by Castiglione and Shouse (2003), who showed that these effects could be taken into account by measuring the reflection coefficient of the waveguide in air with the end both open- (ρ_{air}) and short-circuited (ρ_{sc}). This leads to an effective value for ρ_{max} (ρ_{eff}), given by (Castiglione & Shouse, 2003)

$$\rho_{eff} = 2\frac{\rho_{meas} - \rho_{air}}{\rho_{air} - \rho_{sc}}, \tag{21.3.10}$$

where ρ_{meas} is the measured value of ρ_{max}.

Electromagnetic induction

Similarly to ERI, electromagnetic induction (EMI) measures the electrical resistivity of the near surface and is affected by both water content and solute concentration. ERI was described in Part II (Water Content) of this book but could equally well have been in this Part. Similarly, EMI could have been placed in the Part II.

The method is rapid, capable of making measurements sensitive to different depth distributions and does not

require any fixed equipment, being non-invasive and portable. This gives, similarly to GPR with a fixed antenna separation (Section 8.15.3), the ability to collect data over a large area in a short time by moving the instrument along a series of transects. Also similarly to both ERI and GPR, measurements are integrated over a substantial volume of soil with a depth weighting which depends on transmitter–receiver separation, but in the case of EMI also on the relative orientation of the transmitter and receiver coil.

Principles Current flowing through a multi-turn wire coil generates a magnetic field, as shown diagrammatically in Fig. 21.3. At a distance of a few coil diameters, the field is indistinguishable from that of a *magnetic dipole*. Note that the dipole orientation is at right angles to the plane of the coil. If the coil is horizontal, as shown, and close to the ground surface, then a steady current induces a vertical magnetic dipole almost exactly the same as a permanent magnet, with the field penetrating into the ground. There is some confusion in the literature caused by the different orientation of the coil and dipole. Some authors refer to the dipole orientation, while others use that of the coil. In this book, we will use the dipole orientation when referring to the direction of the instrument relative to the ground surface (i.e. if the dipole orientation is parallel to the ground surface, the plane of the coil is vertical). If the current through the coil varies in a sinusoidal manner, that is, it is ac, then the field in the soil, which is predominantly vertical close to the axis of the coil, will experience the same variation in intensity, with reversals in phase with the coil current.

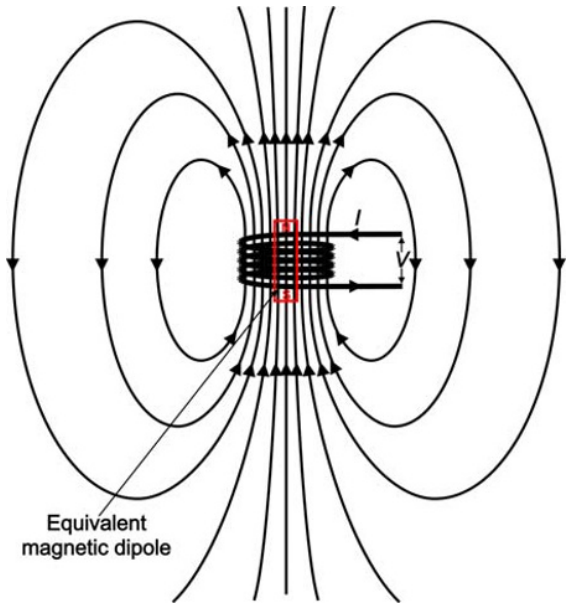

Fig. 21.3 Magnetic field created by current flowing through a wire coil. An approximately equivalent magnetic dipole (represented as a bar magnet) is shown. Note that the dipole is oriented at right angles to the plane of the coil.

A time-varying magnetic field induces an electric field at right angles to the magnetic field, according to *Faraday's law*. This is circular around the magnetic field lines, since if it were radial outward or inward, charge would be depleted or accumulate. The electric field is given by

$$\frac{1}{r}\frac{\partial}{\partial r}\left(rE_\phi\right) = -\frac{\partial B_z}{\partial r}, \tag{21.3.11}$$

where

r is radial distance from the magnetic field line;
E_ϕ is the tangential component of the electric field (the radial and vertical components being zero), and
B_z is the vertical component of the magnetic field (the horizontal components being assumed zero).

If the magnetic field were spatially uniform, the electric field from adjacent field lines would cancel one another out. As it spreads out away from the axis of the coil, however, there is a net circular component, and so a current is induced in a circular direction around the axis of the coil. The magnitude of this current is proportional to the amplitude of the magnetic field variations, B_0, and to the electrical conductivity, σ, of the ground at that depth. The details are very complicated and will not be shown here.

Because the induced currents are proportional to the rate of change of the magnetic field, they are $\pi/2$ (90°) out of phase with the magnetic field variations, that is, if we characterise the magnetic field as $B_0\cos(\omega t)$, the current is proportional to $B_0\omega\sigma\sin(\omega t)$. This is sometimes referred to as being in *quadrature*.

The circular current induced in the ground varies in a complex manner with both depth and radial distance from the coil axis. It will itself induce a magnetic field, varying at the same rate as the primary magnetic field and proportional to, but $\pi/2$ out of phase with it. Provided that the ground is non-magnetic (i.e. the magnetic permeability, $\mu = \mu_0$) the primary magnetic field at low frequency is not affected by the electrical properties of the ground. In principle, the secondary magnetic field produced by the induced current will itself induce other currents and hence tertiary, etc. fields. In practice, provided that the *induction number* $s\sqrt{\omega\mu_0\sigma/2}$ is small compared with one, these can be ignored (McNeill, 1980). Here s is the horizontal separation between the primary field coil and a coil detecting the secondary magnetic field (see Fig. 21.4), and ω is the angular frequency of the field fluctuations.

Although the secondary magnetic field is very small, it can be detected against the background of the primary one because it is out of phase, so the secondary field is maximum when the primary field goes through zero.

Similar but more complex arguments apply where the dipole is horizontal, that is, the coil is edge on to the ground surface. In this configuration, the induced currents in the ground are still circular loops in a horizontal plane (McNeill, 1980). The depth distribution of the measurement is, however, quite different for the three orientations. These are illustrated in Fig. 21.5 and show that the orientation with vertical dipoles (i.e. with the coils horizontal)

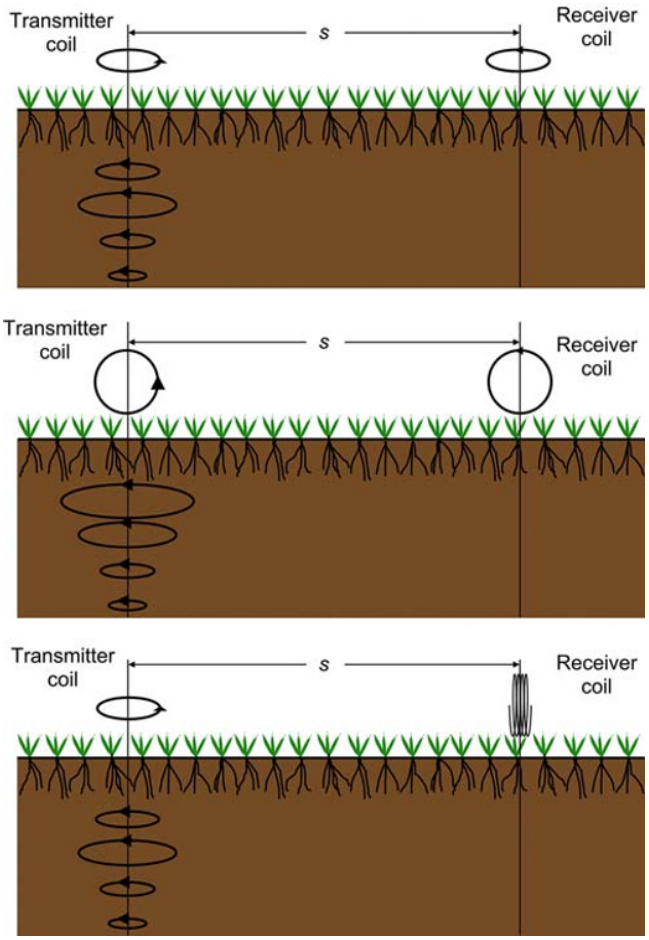

Fig. 21.4 Arrangement of transmitter and receiver coils for EMI measurement. Top, vertical dipole orientation. Middle, horizontal dipole orientation. Bottom, perpendicular dipole orientation.

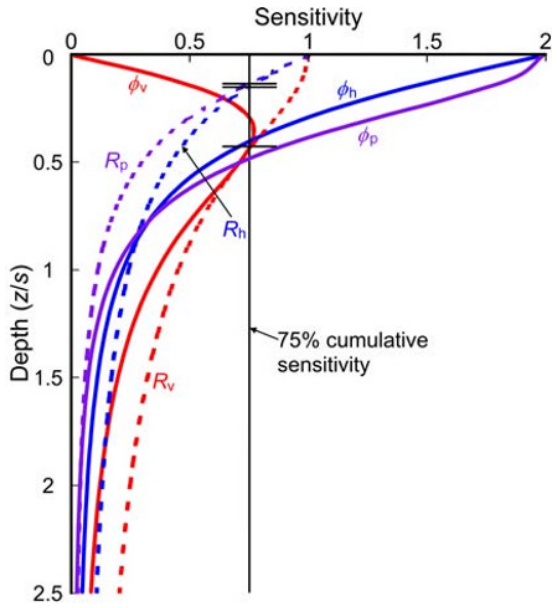

Fig. 21.5 Sensitivity of measurement with depth for EMI dipole orientations vertical (ϕ_v – horizontal coils), horizontal (ϕ_h – vertical coils) and perpendicular (ϕ_p – horizontal transmitter and vertical receiver coil), with cumulative upward values, R_v, R_h and R_p. Note that depth is expressed as the ratio of depth below the coil plane to the spacing between the coils.
(*See insert for colour representation of the figure.*)

detects electrically conductive layers deeper in the profile than either horizontal dipoles or perpendicular dipoles. Most instruments have the coils mounted on a single beam, so that turning the instrument on its side changes the orientation of the coils.

Provided that the low induction number criterion is satisfied, the sensitivity of the reading with depth scales with the distance between the transmitter and receiver coils. Also, unlike most other methods for measurement of either water content or electrical conductivity, the contribution of different volumes or depths is independent of the value at that depth. There are, therefore, at least in principle, three ways in which the variation of electrical conductivity with depth can be investigated:

1 By changing the spacing between coils. Some instruments offer up to three different inter-coil spacings, although it is difficult to manufacture an instrument which provides many more different spacings.

2 By making measurements with different coil orientations. In the vertical dipole orientation, the instrument is insensitive to material immediately below the coils, but it increases to a maximum at about 0.4s below the coil plane. By contrast, the horizontal dipole orientation has a maximum sensitivity immediately below the coil plane, and this falls off steadily with depth. The sensitivity of the perpendicular orientation falls off even faster. The vertical dipole orientation therefore provides information weighted more towards deeper depths than either the horizontal or perpendicular orientation. Figure 21.5 shows that 75% of the sensitivity comes from the ground below 0.44s for the vertical dipole orientation and from that only 0.15s for the horizontal dipoles and 0.13s for perpendicular dipoles.

3 By making measurements with the instrument at different heights above the ground surface. This exploits the fact that, provided that the soil is non-magnetic, the contribution of different depths below the plane of the coils is constant. For instance, if a reading is made with the instrument directly on the ground, the maximum contribution to the reading in the vertical dipole orientation occurs at a depth of 0.4s. If it is raised by a distance 0.2s, then the maximum contribution will come from around a depth of 0.2s.

The weighting of measurements with depth below the coil plane is (Wait, 1962; McNeill, 1980):

Vertical dipoles

$$\phi_v = \frac{4b}{(4b^2+1)^{\frac{3}{2}}}; \qquad (21.3.12)$$

Horizontal dipoles

$$\phi_h = 2 - \frac{4b}{(4b^2+1)^{\frac{1}{2}}}; \quad (21.3.13)$$

Vertical–horizontal dipoles

$$\phi_v = \frac{2}{(4b^2+1)^{\frac{3}{2}}}, \quad (21.3.14)$$

and the cumulative weighting from below a normalised depth, $b = z/s$, is:

Vertical dipoles

$$R_v = \frac{1}{(4b^2+1)^{\frac{1}{2}}}; \quad (21.3.15)$$

Horizontal dipoles

$$R_h = (4b^2+1)^{\frac{1}{2}} - 2b; \quad (21.3.16)$$

Vertical–horizontal dipoles

$$R_p = 1 - \frac{2b}{(4b^2+1)^{\frac{1}{2}}}. \quad (21.3.17)$$

These functions are plotted in Fig. 21.5.

Equations 21.3.15 and 21.3.16 may be misleading if they are interpreted as meaning that 25% of the reading for horizontal dipoles comes from above $0.15s$. If the instrument is suspended a distance $0.15s$ above the ground surface, then the air will contribute nothing to the reading and all of the reading will come from the ground below this. The correct way to view these equations is that the ϕ values are weighting functions and so

$$\bar{\sigma} = \int_0^\infty \phi(b)\sigma(b)\mathrm{d}b \quad (21.3.18)$$

where $\bar{\sigma}$ is the electrical conductivity displayed by the instrument. Alternatively, if there are two layers of conductivity, σ_1 to a depth $0.15s$ and σ_2 below this, with the instrument on the ground surface, then the reading, $\bar{\sigma}$, will be $0.25\sigma_1 + 0.75\sigma_2$.

Practical instruments for EMI measurement EMI instruments have been manufactured for many years by Geonics Ltd. of Mississauga, Ontario, Canada. For soil water applications, the most useful models are the EM38-MK2 and the EM31. The former is a convenient size for carrying over the ground, being just over 1 m long. Three versions are available, one with a 1-m coil separation, one with an additional receiver coil at 0.5 m from the transmitter and one (EM38-DD) which is effectively two EM-38s joined one above the other. The version with two receiver coils has the ability to measure with four different sensitivity profiles (two separations and two orientations), while the EM38-DD can make both horizontal and vertical orientation measurements simultaneously. Frequency of operation is 14.5 kHz. A larger (2 m coil separation operating at 9.8 kHz) instrument, the EM31-SH, giving a deeper depth of sounding can still be easily carried by one person, while the EM31-MK2 is 4 m long. Geonics also manufactures a 36 mm diameter EMI instrument for use in plastic or unlined boreholes, with coaxial transmitter and receiver coils separated by 0.5 m and operating at 36.2 kHz.

Dualem Inc. of Milton, also in Ontario, Canada, also manufactures EMI instruments but incorporates up to three pairs of receiver coils. In each pair one receiver coil is set parallel to the transmitter coil and can be used with the dipoles horizontal or vertical. The other receiver coil is at right angles to the transmitter coil to form the perpendicular orientation. This allows data from both orientations to be collected simultaneously. Similarly to the Geonics instruments, Dualem offers a 1 m separation instrument, operating at 9 kHz (Dualem-1), a 2 m version (Dualem-2), a dual 1 and 2 m (Dualem-21), a 4 m variant (Dualem-4) and a dual 2 and 4 m device (Dualem-42). In addition, there is the Dualem-421, which has receiving coils at 1, 2 and 4 m from the transmitter. Dualem instruments have an internal calibration facility, which has been found to work well (Abdu *et al.*, 2007).

Use of EMI sensors Most EMI sensor applications use it in a survey mode, operating it over a traverse to map ground

Fig. 21.6 Geonics EM38-MK2 in use in the field. The instrument is carried close to the ground surface and the operator has a portable GPS system on his back. Both instruments are connected to a handheld field data logger. Photograph reproduced with permission from Geonics Ltd.

conductivity. The devices come equipped with data loggers or appropriate interfaces to connect to a variety of field data loggers and GPS systems to enable rapid data acquisition over a large area. With appropriate backup systems, readings can be acquired every few seconds and geo-referenced to about 1 m accuracy.

The effective depth to which the field-portable sensors measure is relatively shallow, and so it is usually wise to keep them as close to the ground surface as practical. When carried, a height of about 100 mm above ground is usually reasonable. Alternative methods of survey are dragging the device on a small sled behind a vehicle or on a small cart. Figure 21.6 shows one of the smaller instruments being used to conduct a survey in remote terrain.

Because of the susceptibility to electrically conducting material, operators should not have any metal objects attached to them close to (about the inter-coil separation) the instrument. Equally, any sled or cart must be made entirely of non-conductive and non-magnetic material. This includes, for instance, axles and tyre beads.

Although temperature compensated, Robinson *et al.* (2004) and Abdu *et al.* (2007) found that temperature variation could be a problem if all of the instrument was not at the same temperature. They recommended shading the instrument from direct sunlight and switching on and allowing it to warm up for at least an hour at the ambient temperature of operation.

The methodology has been used for a large number of geophysical applications. Of relevance for soil water, are depth of soil (Jung *et al.*, 2005; Abdu *et al.*, 2008), soil water holding capacity (Abdu *et al.*, 2008), mapping of saline and sodic soils (Corwin & Lesch, 2003; Lesch *et al.*, 2005; Amezketa, 2007; Herrero *et al.*, 2007; Moffett *et al.*, 2010), precision agriculture (Corwin & Lesch, 2003; Corwin & Plant, 2005; Jung *et al.*, 2005), linking soil hydraulic properties and depth with ecology (Robinson *et al.*, 2008; Franz *et al.*, 2011), soil water content monitoring (Reedy & Scanlon, 2003; Sherlock & McDonnell, 2003; Robinson *et al.*, 2009, 2012), groundwater level estimation (Sherlock & McDonnell, 2003) and groundwater pollution monitoring (Triantafilis *et al.*, 2011).

Part VII Water and Solute Movement

22 Water and Solute Transport Applications

22.1 Introduction

So far, this book has looked at ways of measuring quantities of water and solutes in a soil profile, the forces that retain them and cause them to move from one place to another and the measurement of the soil properties that control the storage and movement of water and solutes. Scant attention has, however, been paid to the reasons for making the measurements and what uses they might be put to.

The dynamics of water and solute transport affect many human activities, principally water supply, disposal of waste water, agriculture, forestry, waste management, military activities, recreation and reclamation of polluted land. Monitoring the movement of both water and solutes has the potential for improvements in all of these activities, whether the measurements are used directly to provide a picture of the present situation or as an adjunct to modelling activities by providing system parameters or driving data or for validation of model outputs.

This last part of the book therefore describes ways in which the methods described earlier can be combined to provide estimates of the transport of both water and chemical species in the subsurface environment.

22.2 Uses of Water and Solute Flux Measurements

Knowledge of water and solute flow in the shallow subsurface is important for many reasons. These include:

- The water used by different crop–soil combinations, useful for farmers in assessing irrigation requirements or planning the next season's crop and for water managers in planning water resources development.
- Monitoring and predicting the fate of naturally and artificially applied chemicals to the soil – useful for farmers to assess fertiliser and pesticide needs and to plan the most efficient strategy for application and for water and environmental managers to plan mitigation measures to combat pollution.
- Knowledge of infiltration into the soil allows surface run-off to be calculated from the difference between it and the rainfall input. This is important to help predict fast run-off to streams, flooding of land, surface transport of potential pollutants, such as pesticides and fertilisers, and water erosion of the soil. Local run-off of water may become run-on to nearby, more permeable areas, feeding preferential recharge to groundwater as well as pollutant transport.
- Water flux affects many agricultural activities. For instance:
  - The rate of infiltration into the soil controls the rate at which overhead irrigation can be applied without inducing surface run-off.
  - It also controls the efficiency and areal distribution of flood, furrow or border irrigation.
  - The amount of water consumed by a growing crop is controlled by the rate at which water can be conducted from the bulk soil to plant roots.
  - Water flux out of the root zone determines the need for artificial drainage if the water table is too near the ground surface.
  - Water flow within the profile controls the rate at which the surface layers of soil dry after a wet season and therefore when it is suitable for farming operations using heavy machinery.
- Groundwater recharge in permeable areas is usually almost entirely *via* water flow through the unsaturated zone so that knowledge of water flux allows the replenishment of groundwater resources to be assessed.
- Artificial recharge of subsurface aquifers is usually *via* the unsaturated zone, and so knowledge of the hydraulic properties of the intervening formation is important for planning such schemes and ongoing monitoring. Clogging of recharge basins is an issue and water flux monitoring is an important aid in managing this.
- Pollution of groundwater *via* the unsaturated zone relies on a knowledge of the flux of the relevant solutes and the factors which control it.
- Pollutants are not necessarily dissolved in water but carried along with it. They may be biological agents (e.g. bacteria or viruses) or perhaps even inanimate particulates.

Soil Water Measurement: A Practical Handbook, First Edition. J. David Cooper.

• The world's weather and climate systems depend partly on complex feedbacks involving rainfall, evaporation, run-off, the radiation balance of vegetation and soil, recharge to groundwater and streamflow. Understanding these is needed to improve weather forecasts and climate change predictions.

22.3 Approaches to the Estimation of Water and Solute Flux

There are several ways in which estimates of water and/or solute movement in soil can be made. No method is perfect, and indeed, there is usually a significant amount of uncertainty surrounding any method. For this reason, it is wise, if possible, to use more than one method. Some of the factors affecting a suitable choice of method are as follows.

22.3.1 Objectives

A methodology must be chosen with the objectives clearly understood. For instance, is irrigation scheduling most important? Or is pollution of groundwater a significant factor? Many studies have multiple objectives, which are not necessarily mutually exclusive. These often change over time as priorities and people change; other possibilities become apparent; funding reduces (or sometimes even increases!), and unexpected problems occur. Retaining a significant level of flexibility in the initial concept and its application makes the necessary adjustments more easily achievable.

22.3.2 Timescale

Few applications require knowledge of 'instantaneous' water or solute flux, although such measurements can be integrated over time to produce an accumulated value over longer periods. For understanding soil processes, however, short-period flux measurements are useful to assess the relative contribution of matric or preferential flow to the overall soil water or solute balance.

Very often, a seasonal or even annual water balance, that is, the accumulated quantities of rainfall, irrigation, surface run-off, evaporation and drainage from the profile (or net contribution from the groundwater table), is of most interest. Similarly for solutes, a net balance of chemical applied, dry deposition, deposition with rainfall and irrigation, surface run-off, chemical degradation and output from the profile are of interest.

For other purposes, a much shorter timescale is needed. Examples include irrigation scheduling, flood warning and both surface and groundwater pollution, especially for low water-holding capacity, macroporous and low infiltration capacity soils and/or in climates where rainfall occurs sporadically but at high intensity.

The timescale of interest has a strong bearing on the choice of methodology. For instance, tracer methods are usually suitable for relatively long periods, in some cases extending over decades, whereas more active data collection can operate with a time resolution of minutes, but costs of equipment, instrument installation, monitoring and maintenance are high.

22.3.3 Area of interest

The size of the area of interest is often linked to the timescale, as the response time for a large catchment area is almost always much slower than that for a small one. Areas of interest may range from a small plot of a few square metres in area, through a field, to a farm or over a large surface or groundwater catchment area, often aggregating many smaller subcatchments.

The degree of homogeneity of soils, crops, land use, groundwater depth, meteorological conditions, etc., reduces markedly as the scale of interest increases, making it difficult to sample adequately all of the variation contributing to the combined response. Grassland, fallow areas, rangeland and woodland make installation of semi-permanent monitoring instrumentation relatively simple but are often representative of only a small proportion of an area, particularly if it is intensively farmed for arable crops. In such a situation, farming operations must be accommodated either by temporarily removing part of the instrumentation, followed by its reinstatement, as described in Section 7.4, or by hand cultivating the area immediately surrounding the instruments to mimic as nearly as possible that done by the farmer. The former strategy involves an interruption of the monitoring programme for a period, possible discontinuities in data series if the instruments cannot be replaced in exactly the same position or state and considerable extra work. The latter strategy risks the data being unrepresentative of the rest of the field if the hand cultivation does not replicate those conditions closely.

Over a large area, a balance must be struck between detailed information at a few 'points' and obtaining more areally extensive information, either by collecting data less intensively from a larger network of monitoring stations or by linking measurements made by different methods, some of which are more suited to areally extensive measurements. Examples are GPR (Section 8.15), ERI (Chapter 10), remote sensing, EMI (Section 21.3.2), COSMOS (Section 7.10), micrometeorological measurements and groundwater observations. Most of these methods are sensitive only to near-surface conditions, and none of them provide a measure of soil water potential. Linking disparate data sources with widely different footprints, precisions and sensitive volumes is usually accomplished *via* models which attempt to reconcile their varied characteristics.

22.3.4 Study area characteristics

Many factors are involved in choosing a suitable methodology to measure water or solute flux in a particular area. These include, in addition to the factors mentioned earlier

in this chapter, the climate, topography, soil characteristics, resources available and accessibility. Quite clearly an appropriate method for making measurements with high precision on a small plot in a temperate climate located close to a laboratory with good technical backup is not likely to be suitable for a remote location in an arid area of mixed land use where results are required over an extensive region.

22.4 Dealing with Uncertainty

As stated, no method is perfect or suitable for all situations. If at all possible, more than one approach should be employed so that a measure of the uncertainty is obtained. These may, for instance, be methods operating at different time- or areal scales. Detailed monitoring at high frequency on one or a few small field plots may be integrated over time to compare with a long timescale method, or with more difficulty, areally extensive measurements from remote sensing, ERI or EMI may be downscaled to the size of a small plot.

As with all experimental approaches, the more replications in time and space available, the better will be both the precision of the results and assessment of the uncertainty. It is therefore well worth spending time at the design stage to investigate ways to maximise the efficiency of a data collection strategy through examining:

- The costs of installation, maintenance, data collection and external data purchase
- The relative resources required for manual data collection (which can often be combined with maintenance and where there is a less tangible benefit of observing many things that automatic or remote data collection cannot see) versus automatic recording or telemetry.

23 Water and Solute Flux Measurement

Areally extensive measurements, whether over a field or a wider catchment area, are most often required for operational needs, as opposed to investigation of the controlling factors. Where an area is reasonably homogeneous, 'point' or plot-scale measurements of water flux at a few points over the area may well be appropriate and sufficiently representative. These methods are the best developed and often provide the reference against which other methodologies are assessed. Moreover, soil-based measurements are almost universally employed at the plot level. In this chapter, we will consider methods that aim to measure the flux of water and solute, that is, the effectively instantaneous *rate* of movement of these quantities. In the following chapter, we will look at how the accumulated amount transferred over a period of time can be assessed. The distinction is, to some extent, artificial, since one can rarely measure a truly instantaneous flux and assessment of the success of such measurements almost always involves a comparison with an accumulated value.

23.1 Solute Flux Related to Water Flux

The simplest assumption when estimating the flux of solute is that the flux of solute is equal to the water flux multiplied by the solute concentration. Section 20.1.2 described how in some soils, particularly those that are clay rich, some of the solute is bound weakly to particle surfaces. It was necessary to define two concentrations – that in the soil solution and that of solute bound to soil surfaces. To illustrate the effect on solute movement, we will take the simplest description and assume that the relation between concentration of the solution and that adsorbed is given by Equation 20.1.1 and that there is always equilibrium between the two, that is, there is no significant delay between the change in concentration of the soil solution and that on the solids. We will also assume that the water flux, q, is constant in both time and space, which implies that θ is constant in time, and that we can assume one-dimensional flow. The situation can be regarded as similar to that discussed in Section 2.2.2.

Since only the solute in the soil solution moves, the rate of increase of solute mass, $AM_t\delta z$, in a length, δz, and area, A, of soil is given by

$$A\frac{\partial M_t}{\partial t}\delta z = AC(z)q(z) - AC(z+\delta z)q, \tag{23.1.1}$$

giving

$$\frac{\partial M_t}{\partial t} = -q\frac{\partial C}{\partial z}, \tag{23.1.2}$$

and from Equation 20.1.4

$$\frac{\partial M_t}{\partial t} = \theta\frac{\partial C}{\partial t} + \rho_d\frac{\partial C_s}{\partial t}. \tag{23.1.3}$$

But from Equation 20.1.1

$$\frac{\partial C_s}{\partial t} = K_d\frac{\partial C}{\partial t}. \tag{23.1.4}$$

So Equation 23.1.3 can be written as

$$\frac{\partial M_t}{\partial t} = \theta\left(1 + \frac{\rho_d K_d}{\theta}\right)\frac{\partial C}{\partial t}, \tag{23.1.5}$$

and combining with 23.1.2 gives

$$\frac{q}{\theta}\frac{\partial C}{\partial z} = -\left(1 + \frac{\rho_d K_d}{\theta}\right)\frac{\partial C}{\partial t}. \tag{23.1.6}$$

Now the term q/θ is the average water velocity in the medium, Equation 19.1.4, which is equal to the solute particle velocity when K_d is zero. Adsorption, therefore, reduces the average solute velocity relative to that of the water by a factor $(1 + (\rho_d K_d/\theta))$, which is called the *retardation factor*.

Soil Water Measurement: A Practical Handbook, First Edition. J. David Cooper.

The same analysis applies not only to linear adsorption but also to solute movement in aggregated and other porous media as well as heat flow.

Water in aggregated and fractured porous media is often regarded as composed of mobile water in the interaggregate pores or fractures and immobile water in the intra-aggregate pores and blocks between fractures. Granular soils also often contain pores where water flow is, effectively, stationary as well as in blind pores. The immobile water is regarded as able to exchange solutes by diffusion with the mobile water, so that, conceptually, there is no difference between the solute in the immobile water and that adsorbed on clay particle surfaces. If diffusive interchange is fast enough that the immobile and mobile water are in equilibrium, then the amount of solute in the mobile water is $C\theta_m$ and that in the immobile water is $C\theta_I$, where θ_m and θ_I are the volumetric water content of mobile and immobile water. A retardation factor of $(1 + (\theta_I/\theta_m))$ would therefore be expected.

23.2 Darcy's Law Solutions

Methods for measurement of the hydraulic conductivity of soil as a function of either water content or potential were described in Part V, Chapters 16–18. It is an obvious step to use such measurements to compute the soil water flux by measuring the hydraulic gradient with tensiometers. The appropriate hydraulic conductivity value can be identified from either tensiometer or water content measurements to yield the soil water flux from Darcy's law:

$$q = -K\frac{d\psi}{dz}. \qquad (23.2.1)$$

A number of investigators have attempted to use this method to measure soil water flux. These are summarised in Table 23.1.

Most of these had no independent check on the flux calculations, although the results were mostly plausible. Where comparison was available, the results were generally poor (van Bavel *et al.*, 1968; Cooper 1979, 1985; Steenhuis *et al.*, 1985), often predicting the flux with a factor incorrect by several times. The checks could be made only against the accumulated flux over a considerable period of time.

Several authors (van Bavel *et al.*, 1968; Stone *et al.*, 1973a, b; Allmaras *et al.* 1975a, b; Arya *et al.*, 1975b, c; Rice, 1975; Reicosky *et al.*, 1977; Kengni *et al.*, 1994; Normand *et al.*, 1997) have used the measurement of water flux at different depths, together with water content changes, to estimate uptake of water by roots. This can be computed by an extension of the equation of continuity (Section 2.2.2). Assuming one-dimensional vertical flow, the water balance of a depth of soil from z to $z + \delta z$ can be written as

$$\int_z^{z+\delta z}\frac{\partial\theta}{\partial t}dz = q(z) - q(z+\delta z) - \int_z^{z+\delta x} r(z)dz, \qquad (23.2.2)$$

where $q(z)$ and $r(z)$ are the water flux (mm d^{-1}) and the rate of removal of water by roots at depth z (mm m^{-1} d^{-1}). Water uptake measurements using this procedure have been plausible.

Most investigations have been made in the upper 2 or 3 m of the soil profile, but Enfield *et al.* (1973) made measurements to 94 m over a deep water table at an arid site, Scholl (1976) to 4.5 m, Cooper (1979) to 5.7 m, Jewell (1990) to 5 m, Healy and Mills (1991) at 13 m, Nimmo *et al.* (1994, 2002b) at 3–30 m and Hubbell *et al.* (2004) to 70 m.

Only one or two investigations have been made under arid conditions. Enfield *et al.* (1973) used psychrometers to measure water potential and also estimated water flux driven by both hydraulic and thermal gradients according to the theory of Philip and de Vries (1957). The hydraulic and thermal gradients were about 0.4 and 0.046°C m^{-1}, leading to estimates of about 0.3 mm $year^{-1}$ downward flux from the hydraulic gradient and 0.04 mm $year^{-1}$ upward flux resulting from the temperature gradient. Nimmo *et al.* (1994, 2002b) used centrifuge measurements (Section 17.11) to measure low hydraulic conductivities associated with dry conditions in the Palouse Hills, Washington State, United States, and the Mojave Desert, California, with the assumptions of a unit hydraulic gradient and that at depths below about 3 m the water flux in an arid area would be steady.

23.3 Direct Water Flux Detection

A number of devices have been introduced which can detect water flux in soil directly. In general, their main drawbacks include poor sensitivity, limiting their use to high soil water fluxes (often larger than experienced under most natural conditions) and the need for major disturbance of the soil to install them.

23.3.1 The fluxmeter

Heat flux in soil is measured routinely using heat flux plates (Sauer *et al.*, 2002). These consist of a thin layer of poorly heat-conducting material with a thermopile (series of thermocouples) on either side, so that the temperature difference between each side can be measured. Knowing the thermal conductivity of the material, the temperature difference can be converted to heat flux through the insulating material. The plates are quite thin compared with their area, so that little heat bypasses the plates and so the electrical output from the plates is proportional to the heat flux.

The fluxmeter (Cary, 1968, 1970, 1971) operates on a similar principle. It uses a ceramic material of known hydraulic conductivity and sufficiently small pore size so that it will remain saturated over the expected range of water potential. The difference in water pressure at each side of the ceramic can then be related to the flux passing through the ceramic by application of Darcy's law. There is no need for tensiometer cups, since the ceramic remains

Table 23.1 Published studies using Darcy's law solutions to estimate unsaturated zone water flux

Authors	Source of water content	Source of water potential	Hydraulic conductivity method	Hydraulic conductivity location	Independent check
Rose and Stern (1967)	Neutron probe	Neutron probe/Lab SWC	IP	Same plot	N
Van Bavel *et al*. (1968)	Neutron probe	Tensiometers	IP	Same plot	Lysimeter
Stone *et al*. (1973a)	Tensiometers/Lab SWC	Tensiometers	IP	Adjacent plot	N
Enfield *et al*. (1973)	None	Psychrometers	Lab K_s and MQ	Drill cores	N
Rice (1975)	Neutron probe	Scanivalve tensiometers	IP and Laliberte procedure	Same plot	Lysimeter evaporation in previous years
Allmaras *et al*. (1975a)	Neutron probe	Tensiometers	IP/MQ	Adjacent plot	Neutron probe
Arya *et al*. (1975b, c)	Tensiometers/Lab SWC	Tensiometers	ZFP/hot air	Nearby plot	N
Scholl (1976)	Neutron probe	Neutron probe/Lab SWC	Lab K_s and Laliberte procedure	Nearby pit	Streamflow nearby catchment
Reicosky *et al*. (1977)	Tensiometers/Lab SWC	Tensiometers	IP	Nearby plot	N
Ahuja and El-Swaify (1979)	None	Scanivalve tensiometers	Heavy rain	Same plot	N
Cooper (1979)	Neutron probe	Tensiometers	Poulovassilis	Nearby plot	ZFP method
Steenhuis *et al*. (1985)	Neutron probe	Tensiometers	IP + Lab	Same plots	Water balance
Cooper (1985)	Neutron probe	Tensiometers	Poulovassilis	Same plot	ZFP method
Stephens and Knowlton (1986)	Neutron probe	Tensiometers	IP	Nearby plot	N
Healy (1989)	Moisture probe	Tensiometers	Green and Cory (1971) relation	Field	ZFP method, surface water balance, groundwater budget
Healy and Mills (1991)	Tensiometers/Lab SWC	Tensiometers	Lab SWC with VG-Mualem	Same plot	N
Klaij and Vachaud (1992)	Neutron probe	None	Unit gradient	Same plot	Numerical model
Nimmo *et al*. (1994)	Core samples	Core samples	Centrifuge	Core samples	N
Kengni *et al*. (1994)	Neutron probe	Tensiometers	ZFP method	Same plot	ZFP method; ^{15}N balance
Normand *et al*. (1997)	Neutron probe	Tensiometers	ZFP method	Same plot	ZFP method; ^{15}N balance
Nimmo *et al*. (2002b)	Core samples	Core samples	Centrifuge	Core samples	N
Hubbell *et al*. (2004)	Tensiometers/Lab SWC	PTTs	VG-Mualem	Lab	N

IP, instantaneous profile method; MQ, Millington and Quirk (1959, 1961) method (see Section 16.2.2); PTT, pressure transducer tensiometer; SWC, soil water characteristic; VG-Mualem, van Genuchten method (Van Genuchten, 1980) with Mualem (1976) formula.

saturated and so acts as its own cups. The arrangement is shown in Fig. 23.1.

To obtain a reasonable potential difference across the block and to ensure that the overall size of the sensor is not too large to fabricate and to install, the thickness/diameter ratio must be much larger than for heat flux plates. In addition, the hydraulic conductivity of soil varies over many more orders of magnitude than does its thermal conductivity. It is impossible, therefore, to match the hydraulic conductivity of the block to that of the soil over most of its range and because its dimensions are necessarily such that it effectively presents a large obstacle or, alternatively, short cut for water flow, it causes a significant distortion of flow either around or through it. The flux recorded is, therefore, likely to be significantly lower or higher than that in the surrounding soil.

To overcome this limitation, Cary (1971) installed the ceramic block inside a tube filled with soil from the surrounding area, whose hydraulic properties are similar to the natural environment. The whole assembly should, therefore, appear to have a hydraulic conductivity much closer to that of its surroundings. This soil is inevitably disturbed, which means that it is unlikely to match the surroundings perfectly and the total length of the assembly makes it almost impossible to install in the field without considerable disturbance to the surrounding soil.

23.3.2 Heat transport sensors

A small heater can inject thermal energy into the soil water, raising its temperature above that of its surroundings. The heat is carried along with the moving water, eventually dissipating as heat is conducted away into the bulk soil. Measurement of temperature change close to the heater, however, allows the water flux to be estimated using the excess heat as a tracer of water flow.

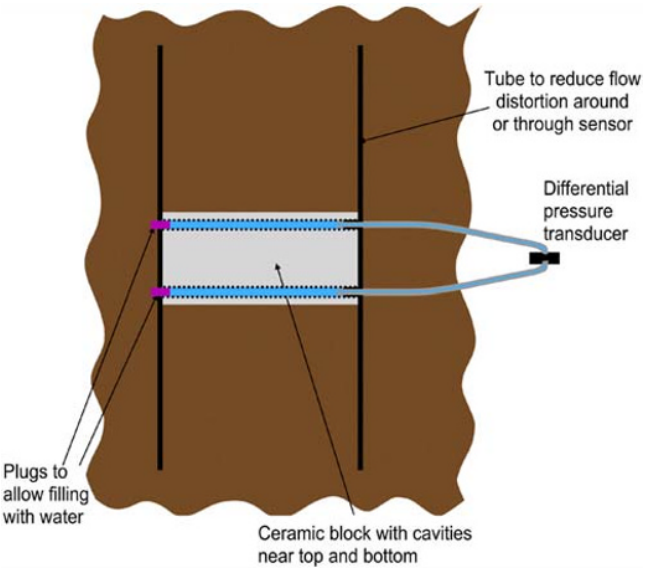

Fig. 23.1 Diagrammatic representation of a flux meter.

This kind of sensor has much in common with the thermal water content and water potential sensors described in Chapter 9 and Section 13.4. The same principle has been used for a considerable time to estimate sap flow in plant stems (Granier, 1987).

There are two approaches to the design of thermal water flux sensors:

1 A steady source of heat will, in the absence of water flow and in a homogeneous environment, heat its surroundings evenly, with temperature falling radially away from the heat source to ambient level at some considerable distance. Flowing water distorts this pattern, with a sensor downstream in the flow direction recording a higher temperature than one upstream.

2 Alternatively, a pulse of heat may be injected into the soil and its transport away from the heat source monitored to estimate flow velocity.

In either case, the arrangement is very similar and illustrated in Fig. 23.2. With the addition of an extra temperature probe, it is virtually identical to the dual-probe heat-pulse (DPHP) water content sensor (Chapter 9).

Steady heat source

Kawanishi (1983) proposed a sensor based on heating from a steady heat source. This built on earlier work by Byrne *et al.* (1967, 1968), having thermocouples placed a short distance above and below the heater. If water flow is downwards, the lower thermocouple is expected to be warmer than the upper one. The theory of the method ignores liquid and vapour flow driven by the thermal gradient set up by the heater. The water flux is estimated by solving the steady-state heat flow equations, modified by a moving water phase. An additional complication is that a correction must be made for the natural thermal gradient in the soil.

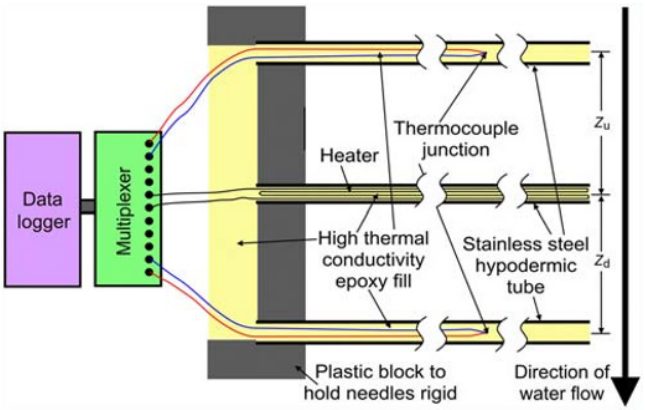

Fig. 23.2 Arrangement of a heat transport sensor.

Soil water content, heat capacity and thermal conductivity of the soil are needed to use the method. Kawanishi (1983) was able to calibrate his sensor for soil water fluxes down to 0.01 mm h^{-1}, which is a very useful range in many applications. Despite this, the method has not received general acceptance. The general principles are, however, used more widely in measurements of sap flow in woody stems (Granier, 1987).

Heat-pulse sensors

More work has been put into development of the heat-pulse method for measurement of soil water flux. The method has been in use for groundwater flow monitoring in boreholes for some considerable time. Melville *et al.* (1985) and Sisodia and Helweg (1998) conducted theoretical analyses of a commercial probe designed for groundwater flow monitoring in a backfilled borehole.

Theory The heat-pulse probe for measuring water flux is similar to the DPHP sensor for measurement of water content (Chapter 9). There it was shown in Equation 9.2.1 that if an amount of heat, E, per unit length, is released instantaneously from an infinite line source, then the temperature rise, ΔT, after a time t at a distance r from the line source is given by

$$\Delta T = \frac{E}{4\pi kt} e^{-\frac{r^2}{4\alpha t}}, \qquad (23.3.1)$$

where

k is the thermal conductivity of the soil and

α is its thermal diffusivity ($k/\rho c$).

If the line source is horizontal and parallel with the y-axis, then $r^2 = x^2 + z^2$, and so Equation 23.3.1 can be written as

$$\Delta T = \frac{E}{4\pi kt} e^{-\frac{x^2+z^2}{4\alpha t}}. \qquad (23.3.2)$$

This equation is valid for a stationary medium. If there is flow in the z direction at a velocity u, then the temperature will be modified in that direction by the heat transported by the water (*convective transport*) in addition to that by

conduction. The convective heat will not, however, be conducted at the same velocity as the fluid, since that transported by the water will also heat the soil matrix. The situation is similar to that described in Section 23.1 and leads to the velocity of heat transport being slower than the water flux in the same way as for solute.

In the case of heat transport by convection, the heat flux, H, is $q\rho_w c_w T$, where q is the water flux, $\rho_w c_w$ is the volumetric heat capacity of water and T is the excess temperature over ambient. Assuming instantaneous thermal equilibrium with the matrix, the heat velocity, s, is given by the flux divided by the volumetric heat capacity of the soil, that is,

$$s = \frac{q\rho_w c_w T}{(\rho_w c_w + \rho_b c_s)T} = \frac{q\rho_w c_w}{(\rho_w c_w + \rho_b c_s)} = \frac{\rho_w c_w \theta}{(\rho_w c_w + \rho_b c_s)}u, \tag{23.3.3}$$

where $\rho_b c_s$ is the volumetric heat capacity of the soil matrix. Note that in this case the heat velocity is smaller than the heat flux, whereas for water flow, the speed is greater than the water flux.

Now where the water is moving towards the sensor, the heat pulse will travel faster in the z direction than in the x direction. In a time t, it will have travelled a distance st further than if there had been no flow.

So to take this into account, we can substitute $z'_u = z_u + st$ for z in Equation 23.3.2 for the upstream sensor and $z'_d = z_d - st$ for the downstream sensor. Also, $x = 0$ since the sensors are both along the z-axis. Equation 23.3.2 thus becomes for each sensor

$$\Delta T_u = \frac{E}{4\pi k t} e^{-\frac{(z_u + st)^2}{4\alpha t}}; \tag{23.3.4}$$

$$\Delta T_d = \frac{E}{4\pi k t} e^{-\frac{(z_d - st)^2}{4\alpha t}}. \tag{23.3.5}$$

The ratio of the temperature rise at each sensor at any given time is

$$\frac{\Delta T_d}{\Delta T_u} = e^{\frac{(z_u + st)^2 - (z_d - st)^2}{4\alpha t}}, \tag{23.3.6}$$

leading to

$$\ln\left(\frac{\Delta T_d}{\Delta T_u}\right) = \frac{(z_u + z_d)(z_u - z_d + 2st)}{4\alpha t}, \tag{23.3.7}$$

and

$$s = \frac{2\alpha}{(z_u + z_d)} \ln\left(\frac{\Delta T_d}{\Delta T_u}\right) + \frac{z_d - z_u}{2t}, \tag{23.3.8}$$

or

$$q = \frac{2k}{\rho_w c_w (z_u + z_d)} \ln\left(\frac{\Delta T_d}{\Delta T_u}\right) + \frac{k(z_d - z_u)}{2\alpha\rho_w c_w t}. \tag{23.3.9}$$

If $z_u = z_d = z_0$, this reduces to (Wang *et al.*, 2002a, b)

$$q = \frac{k}{\rho_w c_w z_0} \ln\left(\frac{\Delta T_d}{\Delta T_u}\right). \tag{23.3.10}$$

It is difficult to make the needle spacings exactly equal, but if $z_d - z_u$ is small, at reasonably long times, the last term in Equation 23.3.9 is negligible, and so this equation reduces to

$$q = \frac{2k}{\rho_w c_w (z_u + z_d)} \ln\left(\frac{\Delta T_d}{\Delta T_u}\right). \tag{23.3.11}$$

Oschner *et al.* (2005) found that this method of analysis was quite simple and gave precise results, although they found systematic overestimation of water flux by between 26 and 78% in laboratory experiments with saturated soil of various types and at a range of different water fluxes between 1 and 372 mm h^{-1}.

While the calibration appears to be reasonably insensitive to α, it still requires a knowledge of the soil thermal conductivity, k. In the laboratory, this may not be too difficult, but it presents some problems in the field and may need to be estimated from knowledge of the soil's thermal properties and water content measurement. The latter can be measured using the DPHP method (Chapter 9) with another pair of temperature sensors perpendicular to the direction of fluid flow (Mori *et al.*, 2003, 2005) or by using the needles as TDR probes (Baker & Goodrich, 1987; Ren *et al.*, 1999, 2003a, 2005).

Use of inverse techniques (Section 17.12) (Mori *et al.*, 2003, 2005; Mortensen *et al.*, 2006; Yang *et al.*, 2013) has improved estimation of water flux. Yang *et al.* (2013), using a probe with four sensing needles arranged in a cross shape around a central heater, were able to measure soil thermal properties as well as water flux components in two perpendicular directions down to flux rates as low as 12 mm d^{-1}. This is still quite high compared with drainage flux out of many unsaturated soil profiles except under very wet conditions but is encouraging for practical field use. Mortensen *et al.* (2006) also added two extra electrodes to a similar probe to that used by Yang *et al.* (2013). With two of the existing electrodes, these formed a Wenner array (Section 10.3) and allowed measurement of the electrical conductivity of the soil, from which solute concentration could be estimated. Thus with one instrument, water content, water flux, solute concentration, solute flux and soil thermal properties may be measured within approximately the same, albeit small, volume. The principal limitation to the accuracy of these methods appears to be obtaining sufficiently accurate temperature measurements when the differences are very small.

To date, no field applications of the instrument appear to have been reported, but there seem to be no reasons why it should not be as suitable for field use as the DPHP probe, which is used in field applications, especially if the lowest flux rate that can be resolved is reduced. The sensing volume is small, so that a large number would be needed to obtain a representative area average value. This may,

however, provide an opportunity to understand the spatial variability in flow fields that other methods do not. The sensors are quite cheap to construct, so that deploying a large number should not present many problems.

23.3.3 Porous plates

The use of porous plates for solute sampling was covered in some detail in Section 20.2.4 and will not be repeated here. In Section 20.2.4, the likely representivity of solute concentration collected was judged on whether the sampler distorted the flow paths of water reaching it. The same criterion is expected to control whether the water quantity collected by the sampler is representative of the water flux over the collecting area, so that a 'good' sampler for one purpose should be equally good for the other.

Porous plates are clearly not suitable where matric potential is close to or below –10 m water, since this would imply a pressure inside the collection vessel of less than absolute zero.

Spatial variability is another problem to be confronted in any attempt to monitor water flux rates. If an aggregate water flux over an area is required, then as large a collecting area as is practical should be employed. This is more likely to be the case where water flow to field drains or recharge to an underlying groundwater body is the objective. For solute movement, it is more likely that an understanding of the areal distribution of solution flux is important and a relatively large number of individual collectors should be employed. This is particularly the case where preferential flow is likely to be important, as fast movement of dissolved substances to deep depths is likely to be of concern, both from the point of view of potential pollution and loss of agrochemical.

23.3.4 Wick samplers

These were covered in some detail in Section 20.2.5. Van der Velde *et al*. (2005) compared three designs of flux meter, one a simple zero tension device, similar to a pan sampler with a 315-mm-diameter funnel as the collecting pan; the other two were wick samplers with the upper part of the wick teased out on the inner surface of a 200-mm-diameter funnel and with 500 mm of wick draining vertically into a collector. One wick sampler drained into a collection tube, which automatically siphoned to a drain once it was full. Detection of the level in the collector was by an ECH2O water sensor (Section 8.9). The other wick sampler drained into a small tipping bucket. Tips were recorded. All samplers had a thin-walled tube of the same diameter as the funnel above them to limit flow divergence. This was packed with native soil. The smaller-diameter wick samplers had a 500-mm-long divergence control tube and the zero tension sampler had one of 200 mm.

The samplers were installed at a depth of 1 m below ground surface in a heavy clay soil in Tonga. Although the zero tension samplers did not record any drainage once the soil water content fell slightly below saturation, the total recorded was close to that estimated by a simple water balance model and a more sophisticated numerical model (HYDRUS1-D). The wick samplers, however, recorded considerably more drainage flux than the rainfall, which was attributed to probable convergence of water flow at the top of the flow divergence tube, possibly caused by the wick length being too long and therefore exerting too high a suction compared with that of the surrounding soil. In other situations, wick samplers have shown reasonably good agreement with water volumes measured independently (see Section 20.2.5), but under very wet conditions, as in this instance, the high collection efficiency appears to be similar to that reported from other studies under similar climatic regimes (Holder *et al.*, 1991; Zhu *et al.*, 2002).

Considerable caution is required, therefore, before taking the results from wick, or indeed, any fixed-potential sampler as representative of water or solute flux in its surroundings.

24 Soil Water and Solute Balance Measurement and Estimation

24.1 Introduction

There is a fine distinction between the flux and soil water or solute balance. The term 'flux' implies an instantaneous measurement of the flow, while 'balance' is usually taken to mean the accumulated quantity of water or solute flow over some time period. In reality, as explained in the introduction to the previous chapter, the two grade into one another. This chapter concentrates on methods which yield accumulated quantities of soil water or solute flow across a depth in the soil and account for the fate of all water or solute falling on or applied to the surface. The reasons for dealing with a water or solute balance rather than short-period fluxes may be because the latter are of little interest, the detail of short-period fluctuations is too confusing, constraints on observation mean that data can be collected only infrequently or the measurement methods are not sufficiently accurate to allow reliable estimates of 'instantaneous' flux with better time resolution.

Measurement of soil water and solute balances is usually connected with agricultural, ecological, forestry or hydrological objectives. These include:

- Assessing the amount of water consumed by different crops to assess, for instance, irrigation requirements or their suitability for growth in a particular location.
- Determining the water use efficiency of a crop or irrigation regime.
- Estimating losses of fertiliser by deep drainage.
- Computing pollution of groundwater by agricultural chemicals or other substances.
- Measuring the efficiency of a drainage scheme.
- Determining the factors controlling competition for water between different plant communities.
- Estimating volumes of direct runoff compared with infiltration into and drainage from the soil.
- Estimating recharge to groundwater for water resources development.

The methods employed depend on:

- The particular objectives.
- The timescale over which the water or solute balance should be measured.
- The soil hydraulic properties.
- The interactions between solutes, microbes and the soil matrix, leading to anion exclusion, retardation and chemical transformations.
- The depth at which measurements are needed.
- The climate.

Solute transport and soil water flow are inextricably linked, so that both aspects will be dealt with together.

24.2 General Principles

Although much of the earth's surface is covered with hills and mountains, which slope quite significantly, most of the land used for growing crops occurs in lowland locations, which are fairly flat. There is, therefore, less motivation for studying steeply sloping situations, which are, in any case, much more difficult experimentally. In areas of modest slope, it is often assumed, without necessarily a great deal of justification, that unsaturated water flow is very nearly vertical, and so an assumption of a one-dimensional system is justified. We will, for the most part, follow this approach.

The main components of the water balance of a typical area of land are shown schematically in Fig. 24.1. Input is mainly by precipitation or irrigation from above, while the main outputs are evaporation and drainage to the water table. There may be runoff from the area or, possibly, runon from slightly higher areas. In some cases, drainage to the water table may be reversed and upward flow, or *discharge*, may feed water into the unsaturated zone from below. Solutes may be introduced dissolved in rain or irrigation water or by dry deposition or as granular fertiliser, for instance.

A proportion (often a large one) of overhead input, whether from rainfall, irrigation or snowfall, can be intercepted by vegetation. This may be evaporated more efficiently than transpiration, especially from tall crops, which are aerodynamically rough (e.g. Calder, 1976, 1977, 1990; Dolman *et al.*, 1988). Intercepted water represents a

Soil Water Measurement: A Practical Handbook, First Edition. J. David Cooper.

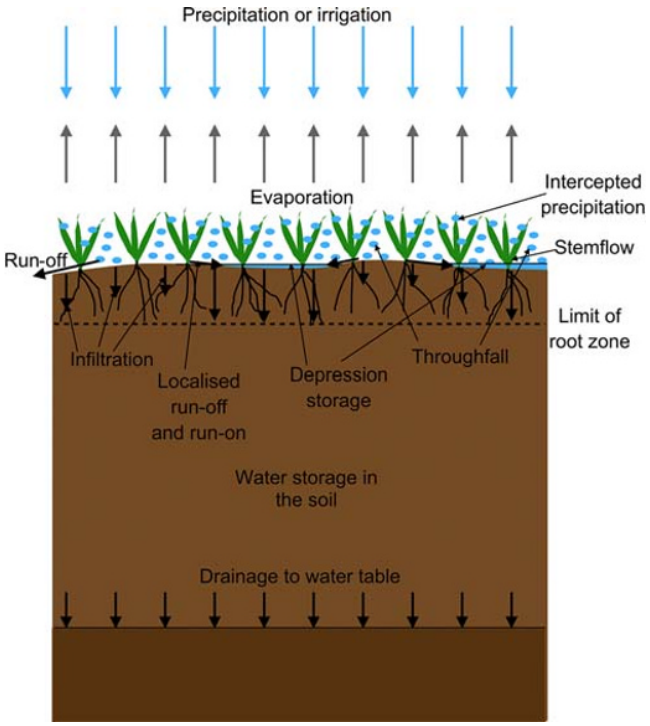

Fig. 24.1 Water balance of soil profile on fairly level land.

significant loss of water not available to plants. Water intercepted by the vegetation that is not re-evaporated immediately may be redistributed unevenly over the ground surface by leaf drips and stemflow.

The water that does reach the surface may not be able to infiltrate into the soil immediately, collecting in small pools in localised depressions through local runoff. If there is a significant slope to the area, then surface runoff may be exported (or sometimes the areas will receive a net input by runon from slightly higher land). Bare soil surfaces often seal under the impact of raindrops, enhancing the runoff/runon process. Areas where water collects as depression storage are expected to provide enhanced infiltration into the soil, with less where there is a local topographical high point. These small inhomogeneities are very difficult to quantify, although Schuh *et al.* (1993a) showed that surface relief of only 30 mm caused significant surface redistribution on a glacial till soil. However, Schuh *et al.* (1993b) showed that it had little influence on the overall soil water budget.

Assuming that vertical flow is a sufficiently good approximation to the actual situation in the unsaturated zone, then the water balance of the profile from the surface to a depth, z_d (above the water table), over some time period can be calculated from the difference between the water inputs and outputs. These must equal the increase in water storage over the depth, z_d:

$$\Delta W(0,z_d) = \int_0^{z_d} \Delta\theta(z)\mathrm{d}z = P - E - \Delta S - R - D(z_d), \qquad (24.2.1)$$

where

$\Delta W(0, z_d)$ is the change in water storage between the surface and depth z_d;

$\Delta\theta(z)$ is the change in volumetric soil water content at a depth z;

P is the precipitation (including snowmelt) and irrigation input over the same time period;

E is the total evaporation (evaporation from the soil surface, evaporation of intercepted water and transpiration);

ΔS is the increase in water stored as interception or depression storage;

R is the net amount of surface runoff from the area (runoff less runon) and

$D(z_d)$ is the amount of drainage through the depth z_d over the period.

Depending on the depth, hydraulic characteristics of the subsurface, rooting characteristics of the vegetation, depth to groundwater and climate, this component may be positive or negative, that is, the water flux may be downwards or upwards. Where it is upwards, flow may be partially or predominantly *via* plant roots.

24.3 Water Balance of a Plot

A fairly large number of studies have been conducted on small plots, which are assumed to be representative of a wider area. Where the underlying material is reasonably homogeneous, this is probably a good assumption, but it should always be borne in mind that spatial variability operates at many scales and that there will be differences from one place to another. Farmers are aware of such differences and the growing importance of precision agriculture reflects this, with micro-surveys of soil fertility, GPS-linked machinery allowing metre-scale yield recording and adjustment of fertiliser and pesticide applications to match. This would be expected to be reflected in crop water use and hence soil water balances.

24.3.1 Precipitation and irrigation input

Accurate measurement of rainfall is not as easy as it may at first appear, particularly in areas of significant relief or at high wind speeds. In most areas of the world, the standard method for rainfall measurement usually involves a rain gauge mounted such that its mouth is some distance (about 0.3–1.5 m) above the ground surface. It is generally accepted (Rodda, 1967) that this leads to an under-recording of rainfall because of acceleration of the airflow as it passes over the mouth of the gauge, as illustrated in Fig. 24.2. In very exposed locations, this can lead to an underestimate of rainfall by up to 50% (Rodda, 1967).

A rain gauge mounted on a post above the ground suffers from the same problem, owing to the solid body of the gauge. Several solutions have been proposed, including wind shields, but the simplest, and probably most effective,

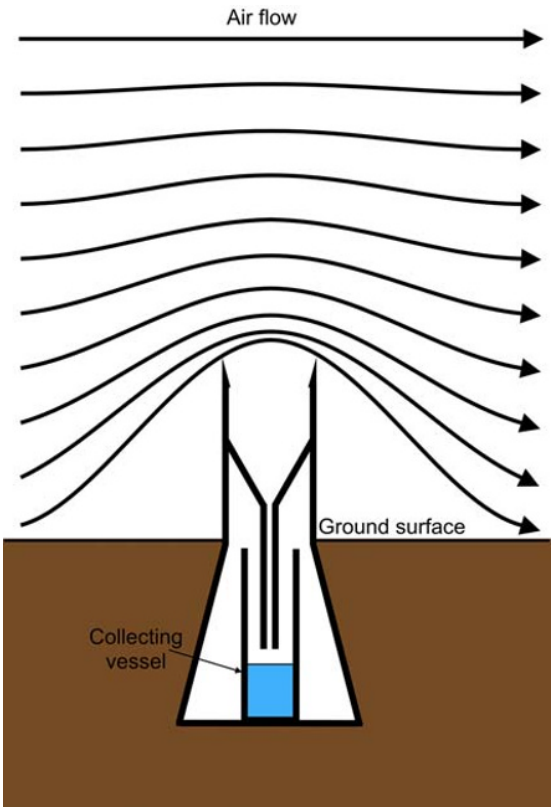

Fig. 24.2 Acceleration of airflow over a rain gauge, whose mouth is above the ground surface. The closer the flow lines are, the faster the wind speed (exaggerated).

is to mount the gauge so that its mouth is at ground level. To prevent water splashing into the gauge, it must be surrounded by a shallow pit. To eliminate disturbance to the airflow caused by the cavity formed around the gauge, the pit is covered by an open metal or plastic grid, as shown in Fig. 24.3.

Input from overhead irrigation can be measured by using small rain gauges placed around the field. A correction for aerodynamic effects may be necessary, but usually this type of irrigation is not used when it is very windy to avoid loss of water. Metering of the water input to the nozzles will also provide a check. Surface or subsurface irrigation is more difficult to measure. With flooding or border irrigation, the total water input to the irrigated area may be metered. However, there is usually considerably more infiltration close to the water source than at the other end of the field. Measurement of water storage in the profile at a number of points over the area immediately before application and after the water has infiltrated should allow the input to be estimated satisfactorily.

Drip irrigation may present more problems, as it is not only difficult to measure on a dripper by dripper basis, particularly if the drippers are buried, but is also highly spatially variable over very short distances. Average rates, based either on measurement on a number of drippers

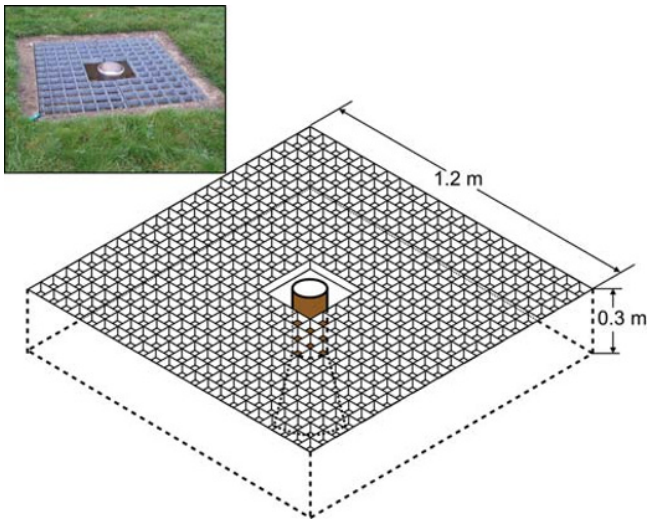

Fig. 24.3 Rain gauge in a pit covered with an open grid to allow rain to fall through while not disturbing airflow across the ground surface.

separately or by measuring the total water input, may have to be used. Measurement at a large number of points around drippers to sample the infiltration pattern adequately is also needed.

Input from snowfall poses several challenges. While the snowfall may well be evenly spread over a large area, its subsequent drifting means that once it melts the actual soil infiltration can be very uneven. With large snowpacks in temperate continental climates, there are often complex hydrological processes during the melting season, which redistribute meltwater around the pack and lead to inhomogeneous water input to the soil. Additionally, ablation (direct evaporation from the solid) of the snowpack means that even if the amount of snowfall is measured correctly, not all of the water that fell as snow appears later at the soil surface.

Heated rain gauges are available from a number of manufacturers that do, at least, allow the snowfall to be measured.

24.3.2 Evaporation estimation

Estimation of evaporation has been studied for many years, and a large number of equations, varying greatly in complexity, have been proposed.

Evaporation pans

The simplest method is probably the evaporation pan, a metal tank of several square metre area and several centimetres deep. The actual dimensions vary considerably from one country to another, some are raised above the ground and others are buried such that the upper level is flush with the ground surface. They are intended to give an estimate of *open water evaporation*, that is, the amount of evaporation

which would occur from an extensive area of open, fresh water in that location. In practice, measurements from pans are subject to many errors as a result of aerodynamic disturbance and interception of solar radiation by their metal parts. Nevertheless, they do respond to weather conditions that control evaporation from the ground surface and vegetation growing on it. In the absence of more sophisticated estimates, an empirical relation between evaporation from a pan and that from a well-watered crop at the same location (usually called *reference crop evaporation*) may be obtained. If high accuracy is not necessary, then this may be adequate. Where the crop starts to suffer from water stress or dies off, actual evaporation falls below the reference evaporation, sometimes well below.

Evaporation equations

The wide availability of meteorological data may enable an alternative method for estimation of evaporation using this source. Thornthwaite (1948) and Blaney and Criddle (1950) both used temperature data alone to give an estimate of monthly evaporation.Thornthwaite's equation is

$$ET = 16\left(\frac{L}{360}\right)\left(\frac{10T_a}{I}\right)^{\alpha}, \qquad (24.3.1)$$

where

ET is the average potential evaporation for a month in mm d^{-1};

T_a is the average daily temperature in °C for the month (0 if T_a is negative);

L is the average day length in hours for the month;

$\alpha = 6.75 \times 10^{-7} I^3 - 7.71 \times 10^{-5} I^2 + 1.792 \times 10^{-2}\ I + 0.49239$, and

$I = \sum_{i=1}^{i=12} (T_{ai}/5)^{1.514}$ is a *heat index* calculated from the 12 monthly mean temperatures, T_{ai}.

Blaney and Criddle's formula is

$$ET = C_u\left(\frac{L}{24}\right)(0.46T + 8), \qquad (24.3.2)$$

where

C_u is called a *consumptive use* factor and

T is mean daily temperature.

The main driver of evaporation, however, is solar radiation and temperature data is clearly linked to that. Penman (1948) developed a widely used equation based on a physical understanding of the evaporation process with some empirical constants. His equation is

$$ET = \frac{\Delta R_n + \gamma f(u)(e_s - e)}{\lambda_v(\Delta + \gamma)}, \qquad (24.3.3)$$

where

R_n is net radiation (i.e. the difference between incoming radiation – direct sunlight, diffuse radiation from the sky and reflected radiation from clouds – and outgoing radiation, that reflected and radiated from the surface);

$f(u)$ is a function of wind speed (there are several different versions of this in use);

e_s is the saturated vapour pressure at the ambient air temperature;

e is the actual water vapour pressure;

Δ is the slope of the saturation vapour pressure curve at the ambient air temperature;

γ is the *psychrometric constant* (~66 Pa°C^{-1}), and

λ_v is the latent heat of vaporisation of water.

The *Penman equation* shows that the potential evaporation is composed of two parts. The first is dependent on radiant energy; the second is a consequence of airflow and the difference in vapour pressure between the water on the evaporating surface (e_s) and that in the air (e). Penman recognised that net radiation is difficult to measure and so proposed a means of estimating it based on the actual compared with the theoretical maximum number of sunshine hours on a particular day. Sunshine hours is a much more commonly available measurement. This produced both an estimate of direct radiation and cloudiness, from which radiation reflected off clouds could be estimated. Using sunshine hours, the formula is usually reckoned to give a reasonably accurate measure when averaged over about 10 days, whereas Equation 24.3.3 should be accurate on a daily basis.

The Penman equation assumes that the crop is short (strictly speaking a well-mown lawn) and well supplied with water. It therefore estimates the maximum rate at which such a crop can transpire. Taller crops are usually aerodynamically rougher and so present less resistance to water vapour transfer from the leaves to the atmosphere. On the other hand, water vapour must find its way out of the leaf stomata before it can be transported into the bulk atmosphere. When the crop is under water or other stress, the stomata close and make this transfer more difficult. Monteith (1965) modified the original Penman equation to produce what is now usually called the *Penman–Monteith equation*. Monteith introduced a soil heat flux term, G, to take into account heat conducted into the ground and two conductance terms. An *atmospheric conductance*, g_a, represents the ease with which water vapour is transported away from the crop into the atmosphere. A *surface conductance*, g_s, is an integration of all the individual stomatal conductances. These two conductances were implicitly embedded into the empirical $f(u)$ term of the Penman equation. The Penman–Monteith equation is

$$E = \frac{\Delta(R_n - G) + \rho_a c_p (e_s - e) g_a}{\lambda_v\left(\Delta + \gamma\left(1 + \frac{g_a}{g_s}\right)\right)}, \qquad (24.3.4)$$

Where

E is the actual evaporation;

ρ_a is the density of dry air, and

c_p is the specific heat of dry air at constant pressure.

Given estimates of g_a and g_s, the Penman–Monteith equation allows actual, as opposed to potential,

evaporation to be calculated. This is much less easy than it sounds, and in practice, empirical *crop coefficients* are used quite commonly.

A common simplification of the Penman/Penman–Monteith formulae was devised by Priestley and Taylor (1972). They observed that the second (aerodynamic) term in the numerator of these equations was often close to 0.26 of the first (radiation) term for a short crop not under stress. They therefore proposed simplifying Equation 24.3.3 to

$$ET = \alpha \frac{\Delta}{\Delta + \gamma} R_n, \qquad (24.3.5)$$

with $\alpha = 1.26$. Where water is limiting, an estimate of actual evaporation, E, can be made by using a smaller value for α.

Bare soil evaporation can be treated within the same framework as described for cropped soil above, with appropriate adjustments to parameters to take into account the different reflection coefficient (*albedo*) of soil and its more rapid reduction in evaporation rate as it dries out. Some authors refer to bare soil evaporation as simply 'evaporation', distinguishing it from that from vegetation as transpiration. The composite term 'evapotranspiration' can be used to combine the two. Terminology is sometimes confusing and it is best to be explicit about what is referred to. A further complication is water intercepted by the vegetation canopy. Because its evaporation does not require the intervention of stomata, this is usually evaporated more efficiently than transpiration, particularly in tall crops in which g_a is small. For short crops, it is rare to distinguish between the two, which probably reflects more the difficulty in measuring interception for such crops than the difference in rate of evaporation.

This section can only scratch the surface of what is an inherently complex subject. For more detail on making and using evaporation estimates, the publication by Allen *et al.* (1998) is highly recommended. There are also several good texts explaining the basics of evaporation.

Micrometeorological evaporation measurement

Atmospheric measurements above the surface can give reliable measurements of evaporation from a fairly large area upwind of the instrumentation location. The size of the area depends on the height of the instruments above the canopy surface but is typically a few times this height. Two methods are in common use – the eddy correlation method and the Bowen ratio. In both methods, it is assumed implicitly that transport of water vapour is in a vertical direction, although in reality it is being carried horizontally by the wind. This is valid so long as there is no significant inhomogeneity in the area contributing to the measurements, or *fetch*.

Eddy correlation This method, sometimes called *eddy covariance*, depends on an assumption that all water vapour transport is through turbulence. When fluid flow is above a critical speed, laminar flow no longer occurs and the airflow breaks up mainly into rotating 'eddies', such as occurs when water is let out of a bath. In the atmosphere, these have a large variety of sizes and hence rotation periods. Entities, such as heat and water vapour, are exchanged between eddies, such that if there is a source of either at the surface, it is transported away from it more or less in an upward direction, ignoring the horizontal average movement of the air. The situation is shown diagrammatically in Fig. 24.4.

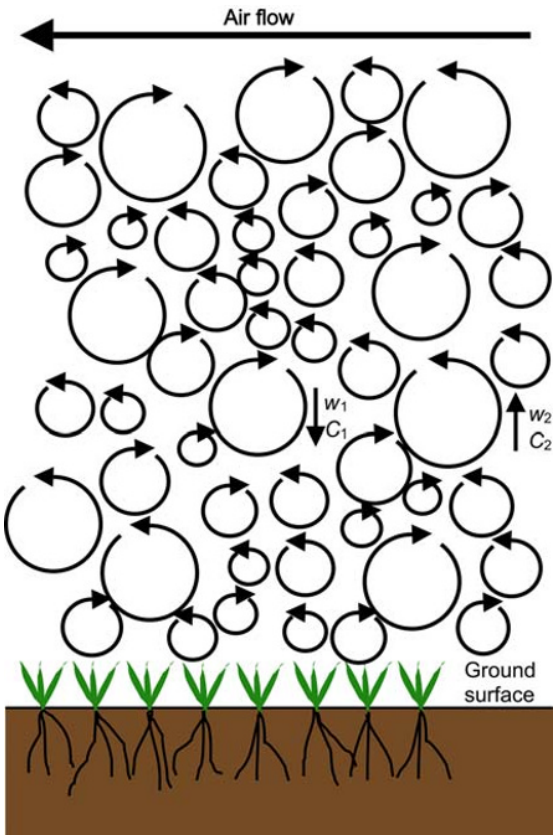

Fig. 24.4 Turbulent flow above an evaporating crop.

The air is shown rotating over the surface. At a point above the surface, the instantaneous vertical component of airflow at a time t_1 is w_1 and the concentration of water vapour is C_1. A short time later, t_2, the flow at that point may have reversed and the vertical component of airflow and water vapour concentration are w_2 and C_2. The vertical transport of water vapour at t_1 is, therefore, w_1C_1 and at t_2 it is w_2C_2. More generally, the instantaneous vertical flux, F, is given by

$$F(t) = w(t)C(t). \qquad (24.3.6)$$

The instantaneous flux alternates between upward and downward movements at a wide range of frequencies up to about 40 Hz. Sampling of this requires fast-response anemometers and humidity sensors. Air velocity is usually measured by the difference in time taken for a pulse of

ultrasound to travel from one transducer to another and in the reverse direction. The time, τ_+, taken to travel a distance, d, from one transducer to another in the direction of the airflow will be

$$\tau_+ = \frac{d}{c+w}, \tag{24.3.7}$$

where c is the velocity of sound. The time, τ_-, to travel in the opposite direction is

$$\tau_- = \frac{d}{c-w}. \tag{24.3.8}$$

So the air speed is

$$w = \frac{d}{2}\left(\frac{1}{\tau_+} - \frac{1}{\tau_-}\right). \tag{24.3.9}$$

Measurement of water vapour concentration is usually by means of an infrared hygrometer, which measures the absorption of infrared light in a particular waveband by water vapour.

Knowing $w(t)$ and $C(t)$, the average flux of water vapour, $\bar{F}$ (usually made over several minutes), is given by

$$\bar{F} = \frac{\int_{t_1}^{t_2} w(t)c(t)\mathrm{d}t}{t_2 - t_1}. \tag{24.3.10}$$

This is a very simplified description of the eddy correlation method. The equipment is expensive, but the method is also applicable to measurement of fluxes of heat, carbon dioxide, methane and other gases.

The Bowen ratio method Like the equations used to calculate evaporation described earlier, the Bowen ratio method calculates the energy used to evaporate water from the energy balance of the evaporating surface.

The net radiant energy, R_n, is converted into the energy needed to evaporate water, $\lambda_v E$, that convected into the atmosphere as *sensible heat*, H, and that conducted into the ground, G:

$$R_n = \lambda_v E + H + G. \tag{24.3.11}$$

Here
λ_v is the latent heat of evaporation of water and
E is the evaporation rate.

In Equation 24.3.11, all terms on the right-hand side are positive directed away from the soil surface, so the equation merely states that the net amount of radiant energy received by the soil and vegetation is balanced by evaporation, heating of the atmosphere and the soil. Measurement of R_n can be accomplished by radiometers and G by heat flux plates, so that the sum of $\lambda_v E$ and H can be calculated.

The Bowen ratio, B, is the ratio between these two, that is,

$$B = \frac{H}{\lambda_v E}. \tag{24.3.12}$$

So if we knew the Bowen ratio and measured R_n and G, E and H could be calculated separately.

Calculating B relies on assuming that transport of both heat and water vapour into the atmosphere is by an identical process, turbulent exchange. One is dependent on a gradient of temperature, T, and the other on a gradient of vapour pressure, e. The parameter controlling the transport of each one to the appropriate gradient should be the same. To ensure that the units are compatible, we can write

$$\lambda_v E = -\frac{\rho c_p}{\gamma} K_v \frac{\partial e}{\partial z}, \tag{24.3.13}$$

and

$$H = -\rho c_p K_H \frac{\partial T}{\partial z}, \tag{24.3.14}$$

where K_v and K_H are the transport coefficients for vapour and sensible heat, which are assumed to be equal. Then

$$B = \gamma\left(\frac{\partial T/\partial z}{\partial e/\partial z}\right). \tag{24.3.15}$$

The gradients can either be estimated from measurements of T and e at a number of heights or, more conveniently, by measurement of each at two different heights, so that B can be calculated from the differences

$$B = \gamma\frac{\Delta T}{\Delta e}. \tag{24.3.16}$$

Combining Equations 24.3.11, 24.3.12 and 24.3.16, we get

$$E = \frac{R_n - G}{\lambda_v\left(1 + \gamma\frac{\Delta T}{\Delta e}\right)}. \tag{24.3.17}$$

Once again, this has been simplified to emphasise the principles. Further information on micrometeorological methods is available in a number of books on the subject.

24.3.3 Runoff/runon estimation

Localised (i.e. within a plot) runoff and runon is very difficult to measure, being very short range, perhaps only a metre or two, and of small quantities. Observation on the ground during and immediately after a rainfall may allow storage in small depressions to be estimated, which will give some indication of the importance of the mechanism, although, since infiltration occurs simultaneously, it is likely to be an underestimate.

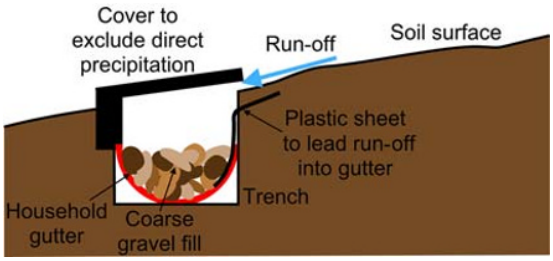

Fig. 24.5 Runoff collector.

Where there is a more general slope, runoff can be measured rather better, although high accuracy is not easy to attain. A small trench running at right angles to the slope will intercept water running down it. This can be collected and measured as shown in Fig. 24.5.

The water is directed into a length of guttering, of the kind used on house roofs, lying in the bottom of the trench, by a plastic sheet, dug about 50–100 mm into the soil on the upslope side of the trench and extending well into the gutter. The gutter should slope slightly, so that water runs to one end. This allows it to be collected in a small tank or measured by a tipping bucket flowmeter. A small shelter set just above the trench prevents direct input of precipitation. Gravel in the gutter keeps the plastic sheet in place and helps to prevent blocking by debris. The length of trench is determined by local conditions, but as a guide, 1 L of water from a 1-m-long trench represents 1 mm m^{-1} of upslope length. For instance, if there is 10 m of slope above the trench, then 1 mm of average runoff would yield 10 L of water. Collection may, therefore, be infrequent, but under conditions of heavy rainfall, a large amount of water may need to be accommodated in a short space of time.

To avoid biasing the results, runoff should not be collected from the upslope side of an experimental plot, but towards the side. An arrangement as shown in Fig. 24.6 is suggested. The two upslope trenches collect water running from the upslope side, placed a little way on either side of the plot, to avoid water that might have run onto the plot being intercepted. There is no problem with collecting water running off the plot from directly below it, as this does not affect measurements upslope of the collection point. Then the net runoff can be estimated as

$$R_{\text{off}}(\text{net}) = R_{\text{off}} - R_{\text{on}}, \qquad (24.3.18)$$

where

R_{on} is the water running onto the plot, estimated from the upslope trenches, and

R_{off} is the water running off the plot, estimated from the downslope trench directly below the plot.

Topographic effects are likely to focus flow in different ways, and so every effort should be made to estimate the collection area of the trenches. This is difficult to do accurately, and so the net runoff figure is likely to have considerable uncertainty.

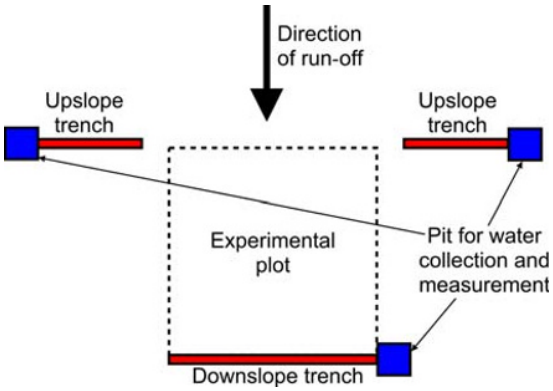

Fig. 24.6 Arrangement of collection trenches to estimate runon and runoff from an experimental plot.

24.3.4 Water balance calculations

Having estimates of all but one of the terms in Equation 24.2.1 enables the other one to be calculated by difference. Usually, we know or have a reasonable estimate of P, ΔS, R and ΔW. A good estimate of D, therefore, allows E to be calculated. Alternatively, knowing E allows D to be determined. In a flat area, runoff, R, may be assumed zero on a permeable soil, and if the period of calculation runs from one dry period to another, the depression storage, ΔS, may also be assumed zero. In many cases, particularly on smooth and/or permeable surfaces, it is probably negligible.

On more impermeable, sloping or rough soil surfaces, these assumptions may not be warranted and observation of what actually happens during rainstorms is required. In forests and other tall vegetated areas, redistribution of precipitation by leaf canopies and stemflow may be important, which will require considerable replication of instruments to ensure that the water balance of the plot is properly sampled.

The limitations of the crude water balance method, as described here, mean that if there is a small difference between precipitation and evaporation or there is significant uncertainty due to runoff or redistribution of precipitation, then the balance term, drainage, will be very poorly estimated (e.g. Gee & Hillel, 1988; Scanlon *et al.*, 2002a, b, 2006).

24.3.5 Seasonal changes to soil profile water balance

Figure 24.7 shows the changes occurring in a typical soil profile as the seasons progress:

- In the late wet season or late winter to early spring in a temperate climate, there is likely to be downward flow throughout the profile, as evaporation rates are usually lower than rainfall, or there may be a large contribution from snowmelt. There is a steady and positive water flux throughout the profile, as shown by the curve $q(t_a)$, which is associated with high water potentials, $\psi_h(t_a)$, and a

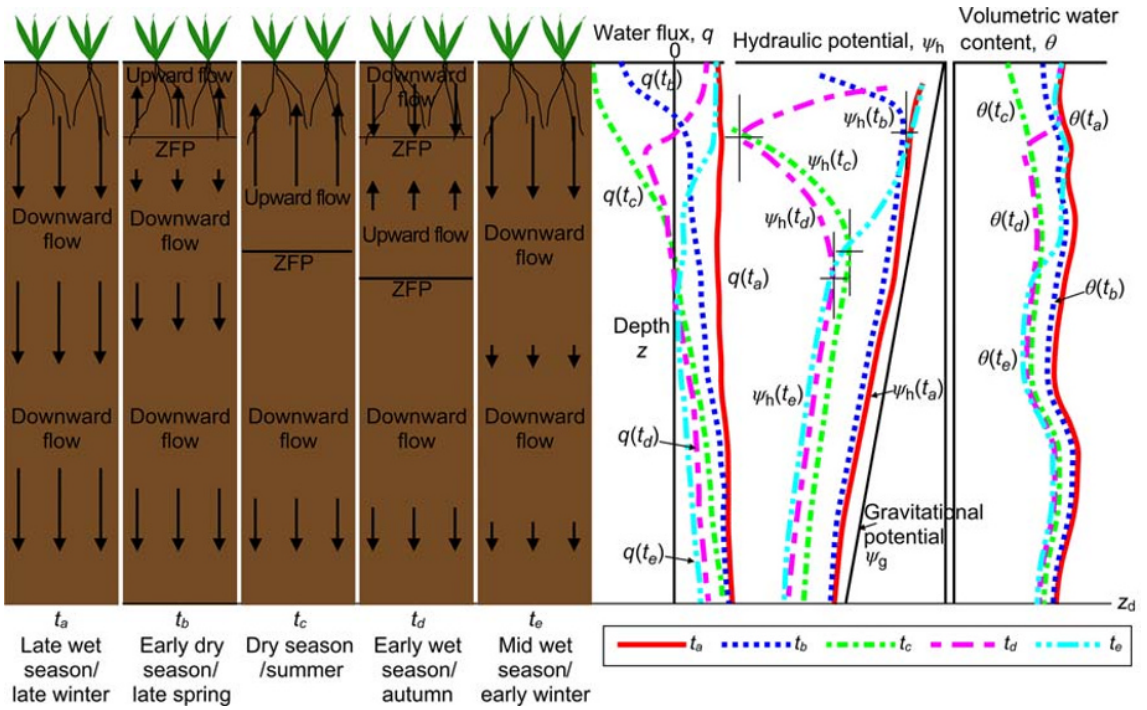

Fig. 24.7 Evolution of the water balance of a soil profile over the course of a year. ZFP positions, where the gradient with depth is zero, are indicated on the hydraulic potential graphs by horizontal lines. (*See insert for colour representation of the figure.*)

hydraulic potential gradient close to unity (i.e. almost entirely due to gravity). Water content, $\theta(t_a)$, is also high throughout.

- Later on, as crops grow and evaporation rates begin to exceed rainfall, upward flow in the upper part of the profile starts to occur, while further below, downward flow continues at a slightly reduced rate. This is shown by curve $q(t_b)$ and the associated water potential profile, $\psi_h(t_b)$. Note that the hydraulic gradient near the top of the profile is now reversed, in keeping with the reversed water flux. At the depth where the flux changes from upwards to downwards, the flux, and therefore the potential gradient, is zero. This depth is termed a zero flux plane (ZFP). Water content starts to reduce from the top down $\theta(t_b)$.
- Later still, as the growing season progresses, often a dry season or summer, the zone of upward flux expands downwards and the ZFP becomes deeper. Drainage flux, $q(t_c)$, from below the ZFP reduces as there is less supply from above and both hydraulic potential, $\psi_h(t_c)$, and water content, $\theta(t_c)$, falls throughout. Some drainage continues if the water table is sufficiently deep. If the water table is shallow, however, the ZFP may reach it and upward flow from groundwater may occur throughout the profile. In some situations, this is an important source of water for vegetation.
- At the end of the growing season or onset of wet weather, when rainfall exceeds evaporation, the profile starts to wet up, normally from the top down. In the early part of this period, this does not affect the ZFP and upward movement of water continues from above it, with slow drainage continuing beneath. The upward-moving water meets the water moving downwards, so that there is, in fact, another ZFP where the fluxes converge. The water flux in this situation is shown by $q(t_d)$ and the associated potential and water content profiles by $\psi_h(t_d)$ and $\theta(t_d)$.
- Eventually, the downward-moving convergent ZFP meets the deeper divergent ZFP to establish through drainage again. Initially, drainage at the base of the profile remains small, as depicted by $q(t_e)$, $\psi_h(t_e)$ and $\theta(t_e)$, but eventually, the wetting front reaches this depth and conditions return to those at the start of the cycle.

Some of the methods described in the following exploit these variations over the year, for instance, when either drainage or evaporation is low, even a relatively large proportional error has only a small effect on the overall annual water balance.

The course of events described has applicability in a wide range of climates, but not all. For instance, where the main growing season (and so that of highest evaporation) coincides with the wettest part of the year, there may be through drainage through most of the year and methodology needs to be adapted to this. Equally, in some areas, preferential flow caused, for instance, by water-repellent soil or deep cracks in vertisols can allow a large proportion of rainwater to bypass the upper part of the soil (e.g. Hodnett & Bell, 1986), which wets up from both the bottom of the cracks and the surface. If, as is often the case, preferential flow is confined to the upper part (perhaps 1 m)

of the soil profile, then the course of events as described previously will still be a correct description, except for the early part of the wetting-up period (t_d).

24.3.6 *Darcy's law solutions*

Much of the work done on using Darcy's law to calculate soil water fluxes was described in Section 23.2. To convert the flux so measured into a soil water balance, the flux must be integrated over time to give a total quantity of water.

The difficulties with such measurements are:

- Spatial variability. Water content and water potential are well known to vary over short distances. This is expected to apply also to hydraulic conductivity, which is highly sensitive to soil texture, structure, water content and potential.
- Large range of hydraulic conductivity. The hydraulic conductivity of most soils varies over several orders of magnitude within the range of water status experienced over a year. A small change in either water content or matric potential, therefore, can mean a large change in hydraulic conductivity. Typical accuracies of measurement are 0.01 for water content and 20 mm water for water potential. For a 'typical' loam soil, this corresponds to a change of 10 times(!) and 6%, respectively. For coarse-textured soils, the changes would be greater and less for finer-textured soils.
- Hysteresis. Normally, hydraulic conductivity is measured only on one branch of the soil water characteristic and not always on a primary draining or wetting curve. Soil under normal field conditions undergoes many reversals between wetting and drying, and so tracking the appropriate point on the hysteresis curves is very difficult, even if the appropriate functions were known.
- Difference in conditions between measurement and use. Hydraulic conductivity may be measured on small cores in the laboratory or in the field, either on the same plot with the same instruments or on an adjacent one. The technique involves infiltrating water into the soil under rather artificial conditions, which may well introduce artefacts into the data obtained, caused by temperature differences, air entrapment, chemical differences between the water used and the natural soil solution, etc.

Several attempts to use Darcy's law to estimate water flux in the field were described in Section 23.2. Few of them had an independent check on the accuracy of the results. Generally speaking, the results were plausible, and where there was an independent check, the agreement was better than might be expected from the discussion earlier.

Cooper (1979) measured hydraulic conductivity on a deep volcanic soil in western Kenya. He used the results to calculate accumulated water flux by Darcy's law and compared this with accumulated drainage on a nearby plot

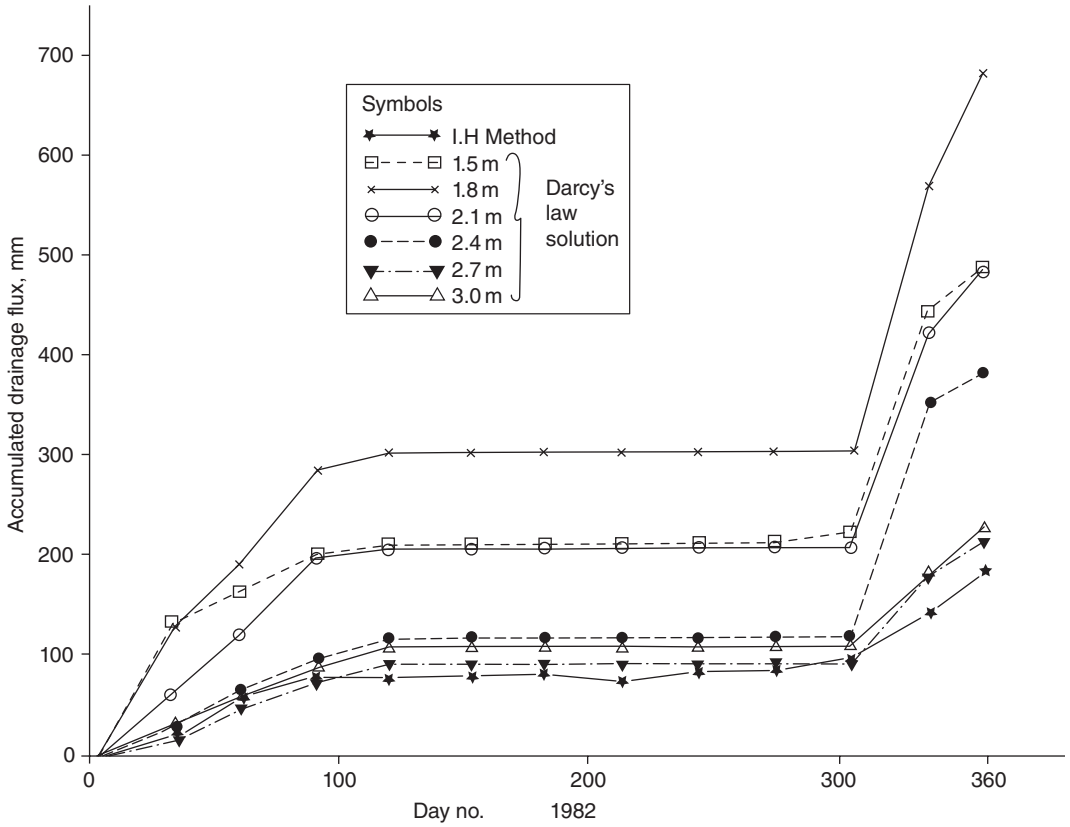

Fig. 24.8 Comparison between accumulated water flux calculated by solution of Darcy's law for several depths with that at 3 m depth measured using a combination zero flux plane–water balance method. © NERC (CEH). Reproduced with permission.

obtained using the ZFP method (see Section 24.3.7). The results differed by a factor of four (see Section 18.3.5). In another experiment on a chalk site in southern England, Cooper (1985) compared the Darcy's law solution, obtained using the measured hydraulic conductivity at several depths, with the accumulated flux over a year estimated by the ZFP method, on the same plot with the same instruments. In both cases, the hydraulic conductivity was measured using the method of Poulovassilis *et al.* (1974) (Section 18.3.5), water content was measured by neutron probe and water potential by mercury manometer tensiometers. The latter results (Fig. 24.8) show a highly variable set of estimates depending on which particular depth the Darcy's law calculations were made at. For all depths, the Darcy's law estimates overestimated measured drainage over a year, ranging from 15 to 266%, and in the latter case exceeding the annual rainfall.

Calculated accumulated drainage flux, using Darcy's law estimates at the deeper depths, agrees reasonably with the measured drainage, while that from curves measured nearer the surface, but still well below the root zone, seriously overestimates it. Most flow occurred during times when the matric potential was above –0.3 m water (Jones & Cooper, 1998). Typical hydraulic conductivity relationships with matric potential are shown in Fig. 18.9 (Section 18.3.5), from which it can be seen that the relationship is extremely steep in this region. Note the logarithmic scale of hydraulic conductivity. This means that an overestimate of matric potential (i.e. less negative) is likely to lead to a much larger increase in calculated hydraulic conductivity than an underestimate would yield a decrease. There is, therefore, an inherent bias towards overestimation. Soil water storage capacity at this site below 1.5 m depth was very small, and so annual totals of drainage would vary only insignificantly with depth. The fairly consistent relationship of overestimation with depth has not been explained.

24.3.7 The ZFP method

The difficulty in measuring hydraulic conductivity reliably, the generally poor accuracy of Darcy's law solutions for measuring soil water flux and the difficulties in estimating or measuring evaporation make a method to estimate drainage that does not depend on detailed knowledge of soil hydraulic properties or on meteorological estimates attractive. This is important in areas where annual rainfall and evaporation differ by a small amount, and so recharge to water supply aquifers is very sensitive to both of these quantities. The ZFP method can supply this information, at least for part of the year. It was first used by Richards *et al.* (1956) to measure hydraulic conductivity of a bare plot. De Boodt *et al.* (1967), Arya *et al.* (1975a) and others subsequently employed the method for measurement of hydraulic conductivity to extend the range of water status that can be achieved by free drainage (instantaneous profile method, Section 18.3.1) alone.

Giesel *et al.* (1970) and Renger *et al.* (1970) adopted the method to calculate drainage from beneath a growing crop. Since then, there have been many uses of the method, mainly for water balance measurement but also for measurement of unsaturated hydraulic conductivity. An attractive feature is that both the water balance of the soil profile and the unsaturated hydraulic conductivity can be measured simultaneously (e.g. Cooper *et al.*, 1990; Hodnett & Bell, 1986).

Theory of the method

For periods when total evaporation exceeds rainfall, the water balance of the profile over a deep water table is expected to be as shown in Fig. 24.9. This corresponds to times t_b to t_d in the discussion of Section 24.3.4 and Fig. 24.7. Water moves upwards from some distance below and within the root zone towards the soil surface. In the root zone, the proportion of upward flow in plant roots increases towards the soil surface and becomes transpiration. The remainder of the upward moving water evaporates directly from the surface. Where the surface is well covered by vegetation, virtually all evaporation is expected to be in the form of transpiration *via* plant roots. Deeper in the profile, water flow is downwards as drainage towards the water table. At the depth where water flow changes from moving upwards to downwards, the water flux is zero, giving this the name of the ZFP. There may be some periods during this time, after heavy rainfall, when through drainage from the surface to the water table occurs and overcomes the ZFP for a short time. This is more likely to happen during the early dry season or spring, when there is only a small deficit to overcome.

If we know the depth of the ZFP, then it is easy to partition the change in total water storage in the profile. Water above the ZFP is moving upwards and therefore any loss becomes evaporation, either as transpiration or soil surface evaporation. Water stored below the ZFP is all moving downwards and any loss drains out through the lowest observation depth. The ZFP depth is quite easy to identify, since from Darcy's law

$$q = -K\frac{\partial\psi}{\partial z}. \qquad (24.3.19)$$

So, when $\partial\psi/\partial z$ is zero, the water flux must also be zero. If we identify ψ with the hydraulic potential, ψ_h, then the potential profile can be measured with tensiometers and the point at which the hydraulic gradient becomes zero can be found. This is illustrated in Fig. 24.9, together with the variation of water flux with depth as well as the change in water storage partitioned between evaporation and drainage.

The ZFP technique, therefore, allows Equation 24.2.1 to be split into two equations, representing the profile above and below the ZFP:

$$\Delta W(0,z_0) = \int_0^{z_0} \Delta\theta(z)\mathrm{d}z = P - E - \Delta S - R, \qquad (24.3.20)$$

and

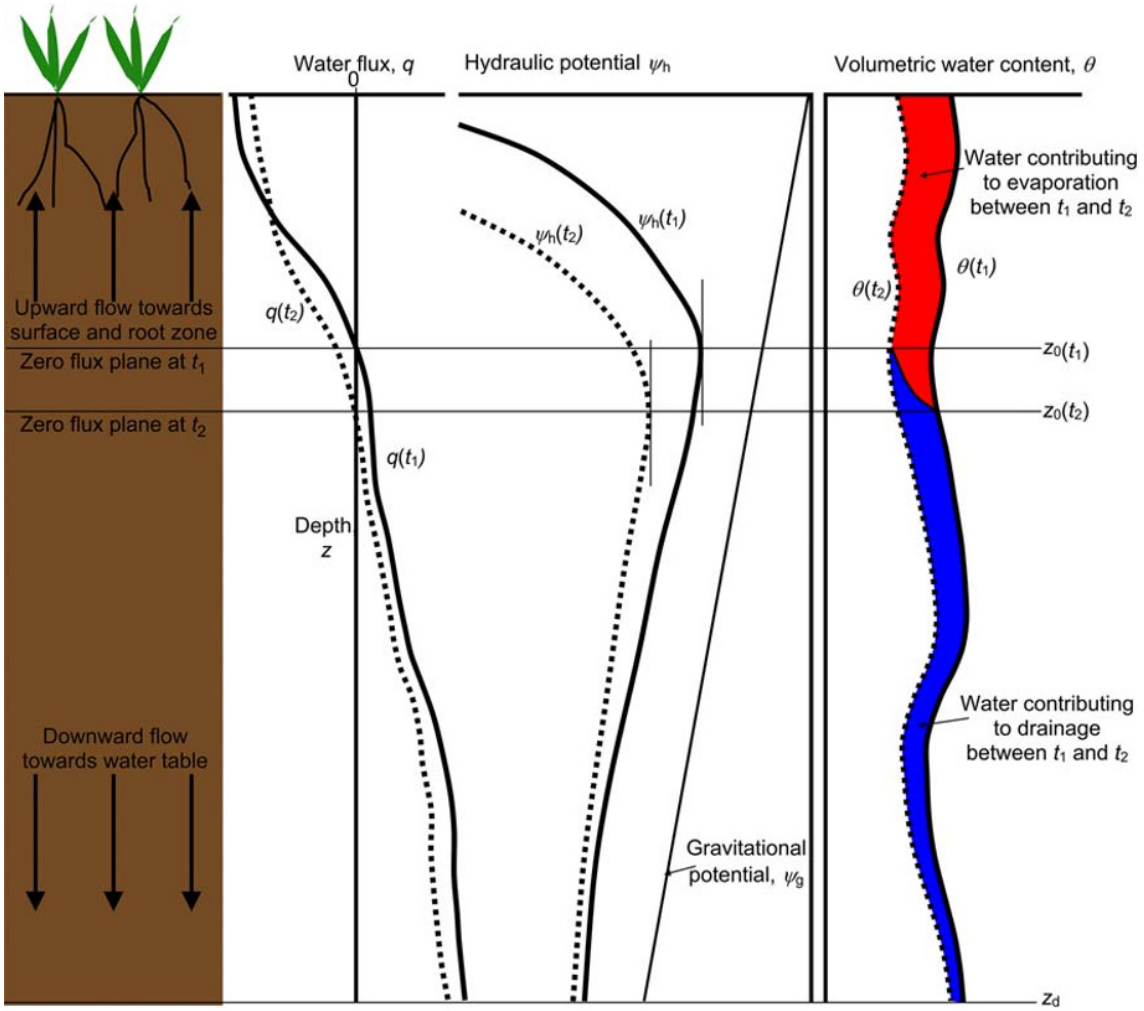

Fig. 24.9 Principle of the ZFP method. Cooper *et al.* (2015). Reproduced with permission of John Wiley & Sons.

$$\Delta W(z_0, z_d) = \int_{z_0}^{z_d} \Delta\theta(z)\mathrm{d}z = -D(z_d). \tag{24.3.21}$$

We expect $\Delta W(z_0, z_d)$ to be negative, that is, a decrease in storage, leading to a positive value for drainage. $\Delta W(0, z_0)$, however, may increase if precipitation, irrigation input and net runon in any period exceed the evaporation. Provided that these are not large enough to destroy the ZFP and establish drainage throughout the profile, this does not affect the estimate of drainage.

A complication arises because, as shown in Fig. 24.9, the ZFP usually gets deeper in the profile over time, as water in the upper part of the profile is depleted. To ensure comparability of the depth of profile measured, a correction must be applied for the change in depth of the ZFP and hence the amount of soil water taken into account. Stammers *et al.* (1973) showed that this modifies Equation 24.3.21 to

$$D(z_d) = \int_{z_0(t_1)}^{z_d} \theta(t_1)\mathrm{d}z - \int_{z_0(t_2)}^{z_d} \theta(t_2)\mathrm{d}z - \int_{z_0(t_1)}^{z_0(t_2)} \theta(z_0)\mathrm{d}z, \tag{24.3.22}$$

where $\int_{z_0(t_1)}^{z_0(t_2)} \theta(z_0)\mathrm{d}z$ is the water content at the depth of the ZFP at the time when the ZFP passes that depth. In practice, the equation is usually applied to compute drainage between observation occasions, and so the actual values of $\theta(z_0)$ between those occasions are not known. This term is usually approximated, therefore, as the average value of θ at times t_1 and t_2, $\bar{\theta}(z)$. This gives for $D(z_d)$

$$D(z_d) \approx \int_{z_0(t_1)}^{z_d} \theta(t_1)\mathrm{d}z - \int_{z_0(t_2)}^{z_d} \theta(t_2)\mathrm{d}z - \int_{z_0(t_1)}^{z_0(t_2)} \bar{\theta}(z)\mathrm{d}z, \tag{24.3.23}$$

and similarly

$$E \approx \int_{0}^{z_0(t_1)} \theta(t_1)\mathrm{d}z - \int_{0}^{z_0(t_2)} \theta(t_2)\mathrm{d}z + \int_{z_0(t_1)}^{z_0(t_2)} \bar{\theta}(z)\mathrm{d}z + P - \Delta S - R. \tag{24.3.24}$$

The third term on the right-hand side of Equations 24.3.22–24.3.24 provides the correction to

ensure that water content change is integrated over the same depth of profile. It is illustrated by the line separating the change in the water storage contributing to evaporation and that to drainage in the right-hand portion of Fig. 24.9.

There are several assumptions involved in the ZFP method. The principal ones are:

- Vertical flow predominates and there is no significant horizontal flow, for example, throughflow or interflow.
- Infiltrating water does not bypass the ZFP by preferential flow, leading to an increase in water content beneath the ZFP. Preferential flow above the ZFP does not affect the estimates, however.
- There are no water sinks, that is, root extraction, below the ZFP. All water movement beneath the ZFP is downwards.

In the case of deep-rooted perennial crops (e.g. forests, tea or coffee plantations), the last assumption may not be strictly fulfilled. However, root density usually declines rapidly with depth, so that the majority of roots is usually well above the ZFP. Also, by definition, the ZFP is at the position of lowest hydraulic potential, so that it becomes increasingly difficult for plants to extract water from below the ZFP. The combination of these two makes it unlikely that a significant amount of water is extracted by roots from beneath the ZFP, compared with that from above it, particularly since water extraction above the ZFP drives the ZFP downwards. Good agreement between evaporation estimated by this method and other estimates of evaporation supports this (see the following text). This is not conclusive evidence, since drainage from the profile is usually much smaller than evaporation under these conditions and a small error in evaporation may not be apparent.

Practical implementation of the method

Reported uses of the ZFP method have mostly employed neutron probes for water content measurement and conventional tensiometers for water potential (Table 24.1), although others have relied on water content measurements and a laboratory-measured soil water characteristic curve to infer water potential, gypsum resistance blocks or pressure transducer tensiometers. Water content has, alternatively, been measured by gamma ray transmission, gravimetric sampling or dielectric devices. Water content has also been inferred from water potential measurements.

In most cases, it is difficult to assess the success of using indirect measurement of water potential or water content *via* a laboratory-measured soil water characteristic curve, either because there is no adequate water balance comparison or because drainage from the soil profile turns out to be very small and so makes little difference to the overall soil water balance. It is strongly recommended to measure both water content and water potential independently.

Because of the large number of studies using water content measurements by neutron probe, there are almost no instances where the ZFP method has been employed to produce water balance measurements over time periods of less than several days. This is partly a consequence of the need to make manual measurements with a neutron probe, and hence the logistics of collecting more frequent data are difficult, and partly because of the inherent inaccuracy of the neutron probe (see Sections 7.5 and 7.9.2), which makes the resolution of small water content changes difficult.

Alternative means of identifying the ZFP depth

The development of a ZFP is associated with drying of the soil from the surface downwards, either from surface evaporation or root extraction of water. It might, therefore, be expected to be associated with a drying front penetrating the soil progressively from the surface. Cooper (1974) suggested that it might be possible to identify a critical water content level, akin to field capacity, at which water content started to be reduced by evaporative processes rather than drainage. He found, however, by studying water content v time curves, that there was considerable uncertainty in the critical water content and hence in the water balance. McGowan and Williams (1980) tried to identify the ZFP position with the time that depletion of water content accelerated at any particular depth. The ZFP as determined by tensiometers was slightly deeper. This method was used by Gardner (1990) to identify ZFPs in the absence of reliable tensiometer data. Also, McGowan (1974) showed that the ZFP depth for a wheat crop was closely correlated with the time at which the advancing root front reached that depth, although this is applicable only for an annual crop with an extending root system.

Water balance when no ZFP can be identified

In almost any situation, a ZFP is an ephemeral phenomenon, although in climates where there is a short wet season or where annual potential evaporation is close to or exceeds annual rainfall, it may be persistent throughout most of the growing season or even a large part of the year. Under these circumstances, the ZFP method is applicable during the time when most of the annual evaporation occurs. To complete an annual water balance, however, a reliable means to estimate the water balance components during the whole year is necessary. For those times when no ZFP can be identified and water flow is directed throughout the profile, either downwards from the surface or upwards from a shallow water table, an alternative method is needed. This is usually during a wet season or during winter in temperate climates. Even when a ZFP has become established, it can sometimes be destroyed by water infiltrating the profile following a heavy rainstorm or period of wet weather, before it is re-established.

Water content changes can still be measured, and so an estimate of either evaporation or drainage allows the other component to be determined.

Evaporation can be estimated by one of the methods described in Section 24.3.2 or by means of a lysimeter (van Bavel *et al.*, 1968) (see following section). Ehlers and van der Ploeg (1976) assumed a rate of $1\ \mathrm{mm\ d^{-1}}$, while Dreiss and Anderson (1985) assumed zero evaporation; several others used a meteorological estimate of evaporation,

Table 24.1 Past uses of the ZFP method

Authors	Water content	Water potential	Purpose	Non-ZFP period
Richards *et al.* (1956)	Gravimetric	Tensiometers	Unsaturated *K*	Not applicable
De Boodt *et al.* (1967)	Neutron probe	Tensiometers	Unsaturated *K*	Not applicable
Giesel *et al.* (1970)	Gamma absorption	Tensiometers	Water balance, unsaturated *K*	Darcy's law drainage
Renger *et al.* (1970)	Gamma absorption	Tensiometers	Water balance, unsaturated *K*	Darcy's law drainage
Daian and Vachaud (1971)	Neutron probe	Scanivalve PTs	Water balance	Estimated evaporation
Daian and Vachaud (1972)	Neutron probe	Tensiometers	Water balance	Estimated evaporation
Stammers *et al.* (1973)	Neutron probe	Neutron probe	Water balance	Not clear
Royer and Vachaud (1974)	Neutron probe	Scanivalve PTs	Water balance	Not clear
Arya *et al.* (1975a)	Tensiometers	Tensiometers	Unsaturated *K*	Not applicable
Ehlers and van der Ploeg (1976)	Gravimetric	Tensiometers	Water balance, unsaturated *K*	Assume 1 mm d^{-1} evaporation
Cooper (1979)	Neutron probe	Tensiometers	Water balance	Not applicable
Cooper (1980)	Neutron probe	Tensiometers	Water balance	Estimated evaporation
Wellings and Bell (1980)	Neutron probe	Tensiometers	Water and solute balance	Penman
Kreutzer *et al.* (1980)	Gamma absorption	Tensiometers	Water balance	Darcy's law
McGowan and Williams (1980)	Neutron probe	Tensiometers	Water balance	ET
Wellings and Cooper (1983)	Neutron probe	Tensiometers	Water balance	ET
Wellings (1984a)	Neutron probe	Tensiometers	Water balance	Penman
Wellings (1984b)	Neutron probe	Tensiometers	Solute balance	Penman
Sadeghi *et al.* (1984)	Tensiometers	Tensiometers	Evaporation	Not applicable
Cooper (1985)	Neutron probe	Tensiometers	Water balance	Estimated evaporation
Dreiss and Anderson (1985)	Neutron probe/ tensiometers	Tensiometers	Water balance	Darcy's law for saturated conditions, otherwise zero drainage
Hodnett and Bell (1986)	Neutron probe	Tensiometers	Water balance	Drainage estimated from baseflow
Rab *et al.* (1987)	Neutron probe	Tensiometers	Unsaturated *K*	Not applicable
Gardner *et al.* (1990)	Neutron probe	Tensiometers	Water balance	Estimated evaporation
Cooper *et al.* (1990)	Neutron probe	Tensiometers	Water balance, unsaturated *K*	Estimated evaporation
Hodnett and Bell (1990)	Neutron probe	Tensiometers	Water balance, unsaturated *K*	Estimated evaporation
Villegas and Morris (1990)	None	Tensiometers	ZFP depth as indicator of deep drainage	Not applicable
Payne *et al.* (1990)	Neutron probe	Tensiometers	Water balance	Not applicable
Gardner (1990)	Neutron probe	Tensiometers/ neutron probe	Water balance	Estimated evaporation
Sharma *et al.* (1991)	Neutron probe	Neutron probe	Water balance	Darcy's law/unit gradient
Kirsch (1993)	Neutron probe	Tensiometers	Evaporation measurement	None
Kengni *et al.* (1994)	Neutron probe	Tensiometers	Unsaturated *K*	Darcy's law drainage
Román *et al.* (1996)	Neutron probe	Tensiometers	Water balance	Not clear
Hosty and Mulqueen (1996)	Neutron probe	Tensiometers	Water balance	Not clear
Tang (1996)	None	Tensiometers	Qualitative process identification	None
Cuenca *et al.* (1997b)	Neutron probe	Neutron probe	Water balance	Not applicable
Normand *et al.* (1997)	Neutron probe	Tensiometers	Unsaturated *K*	Darcy's law drainage
Joshi *et al.* (1997)	Neutron probe	Tensiometers	Water balance	Not applicable
Jones and Cooper (1998)	Neutron probe	PTTs	Water flux partitioning	Estimated evaporation

Table 24.1 (*continued*)

Authors	Water content	Water potential	Purpose	Non-ZFP period
Román *et al.* (1999)	Neutron probe	Tensiometers	Water balance	Not clear
Diez *et al.* (2000)	Neutron probe	Tensiometers	Nitrate leaching	Not clear
Tsujimura *et al.* (2001)	None	Tensiometers	Age dating of unsaturated zone water	Not applicable
Mdaghri-Alaoui and Eugster (2001)	Neutron probe	PTTs	Water flow direction identification	Penman–Monteith, Primault (1962)
Kimura *et al.* (2004)	Gravimetric	Gravimetric	Water balance	Numerical model
Kimura *et al.* (2006)	ML2X to 1 m	ML2X	Water balance	Not applicable
Fernández-Gálvez *et al.* (2007)	ML2X and Profile Probe	Profile Probe	Water flux and water balance	Not clear
Schwärzel *et al.* (2009)	ML2X, TDR	ML2X, TDR	Water balance	Not clear
Evett *et al.* (2012)	Neutron probe	Neutron probe	Water balance	Not applicable
Wang *et al.* (2012)	Tensiometers	Tensiometers	Water balance	Eddy correlation

such as Penman ET (Section 24.3.2). Fernández-Gálvez *et al.* (2007) and Wang *et al.* (2012) estimated evaporation by the eddy correlation method (Section 24.3.2). Unless the absence of a ZFP is caused by its annihilation following heavy rainfall or irrigation during a period of strongly evaporative conditions, or the growing season coincides with a wet season, evaporation is expected to be relatively small compared with drainage from the profile during a non-ZFP period. Under these conditions, any errors in evaporation estimates should cause only a small error in the annual total. Drainage from the profile is likely to be the larger of the two components.

Alternatively, drainage can be estimated by an independent means, such as porous plates (Sections 20.2.4 and 23.3.3), wick samplers (Sections 20.2.5 and 23.3.4) or a lysimeter (Section 24.3.8). Alternatively, a Darcy's law solution (Sections 23.2 and 24.3.6) may be used (Giesel *et al.*, 1970; Renger *et al.*, 1970; Kreutzer *et al.*, 1980). Hodnett and Bell (1986) estimated drainage from baseflow in a catchment in India. Direct estimation of drainage is usually less robust than using an estimate of evaporation, since drainage flux when no ZFP can be identified is most often large and so any error in its estimation is likely also to be large.

24.3.8 Lysimeters

A lysimeter is (usually) a large container of soil from which drainage from the base can be measured. Its water content can normally also be measured, so that evaporation can be calculated by difference. The term 'lysimeter' is sometimes applied also to pan, vacuum and wick samplers. This is confusing terminology and will not be used here.

The variety of lysimeters is very large, as also is the range of sizes and uses to which they are put. Common features of many lysimeters are shown in Fig. 24.10. The principal variants are described in the following.

Repacked versus undisturbed

Repacked lysimeters Many lysimeters (probably most) are filled with soil repacked from the native soil surrounding it or from the pit dug to accommodate the lysimeter in the ground. With great care, the soil layers may be preserved, so that an approximation to the natural soil profile can be reconstructed. With even greater care, the soil may be repacked to a similar bulk density as exists in the natural soil profile. The act of digging out the soil and repacking it, however, destroys most of the soil structure, certainly at a scale larger than a few millimetres. Over several years, this may re-establish itself if the lysimeter is managed carefully and the soil fauna were replaced at the time of packing, but it is difficult, if not impossible, to check on this except, perhaps, at the end of an experiment when the soil can be removed.

Undisturbed monoliths Collection of undisturbed monoliths is possible and was described in Section 17.1. The largest size that has been reported is about 1.5 m long by 0.8 m diameter. This is larger than many repacked lysimeters.

'Natural' lysimeters Larger 'undisturbed' lysimeters may be constructed *in situ* by isolating a block of soil. This can be done by constructing a trench around the soil block, using polyethylene film, sprayed on resin and/or waterproofed concrete to isolate and support the contents (e.g. Kitching and Bridge, 1974; Kitching *et al.*, 1980). Alternatively, sheet steel interlocking piling can define an enclosed area. Mastic applied just before driving will waterproof the interlocking clutches between the piles (Kitching *et al.*, 1980; Kitching & Shearer, 1982). The main problem with such a 'natural' lysimeter is in ensuring a watertight bottom boundary. Where a sufficiently impermeable horizon occurs within a reasonable depth from the ground surface, the walls of the lysimeter may

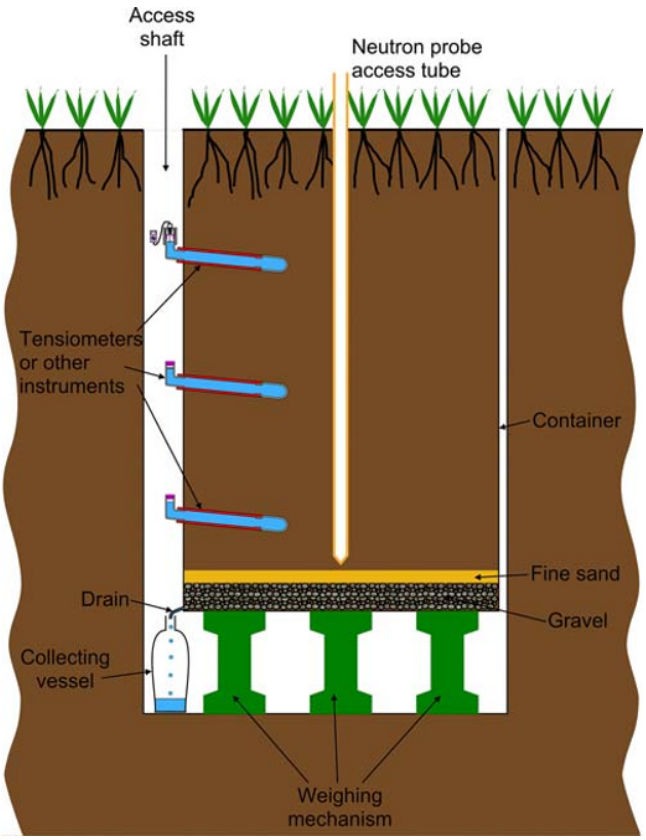

Fig. 24.10 Typical lysimeter features.

penetrate and be sealed into this, thereby creating a watertight box around the isolated soil block (e.g. Kitching & Bridge, 1974; Kitching *et al.*, 1980). Precautions may be needed to ensure that no leakage occurs around the bottom of the lysimeter walls. Kitching and Bridge (1974) installed their lysimeter into a layer of very low permeability clay, but a layer of hard, impermeable rock would be equally suitable, although presenting practical difficulties in implementation. Metering of the drainage water requires that the water table level inside and outside the lysimeter be kept equal. Kitching and Bridge (1974) and Kitching *et al.* (1977, 1980) used pumps connected to an automatic control system to both equalise water level and to meter the transfer of water to compute drainage from the lysimeter. For small volumes of water, cheap battery-powered pumps designed for emptying the bilge of leisure boats or for pumping drinking water in caravans are suitable. Where the subsurface flow of water is appreciable, the lysimeter can present a significant obstruction to groundwater flow, with a consequent higher level at the upstream edge outside the lysimeter and an artificially low level just below the downstream edge (Kitching & Bridge, 1974). This is undesirable, as leakage into or out of the lysimeter is minimised when the difference in water level across the wall is very small. Kitching and Bridge (1974) went to considerable lengths to equalise the water levels around the outside of their lysimeters.

Ingram *et al.* (2001) presented a neat passive solution to equalising the levels while measuring water transfer. They used a flexible plastic bag, partially filled with water and placed in a small pit next to the lysimeter. Changes in groundwater level would affect the pressure of water in the bag and so cause water to be transferred between the bag and the lysimeter to equalise the levels. Because the bag is impermeable, measuring the water in the bag allows the net amount of water transferred over the time between visits to be calculated. Another passive method was described by Huo *et al.* (2012), who used a Mariotte bottle to supply water when it was needed and a simple overflow system to collect excess water when drainage was positive.

Calder (1976) used a different approach in a forest area over a very shallow (~1 m) impermeable clay layer which had drainage ditches dug at intervals. By connecting two adjacent drainage ditches with trenches dug at right angles, he isolated a block of ground hosting several trees. Corrugated iron 'fences' driven into the underlying clay in the trenches, concreted in and sealed together, allowed the water seeping out of the isolated block to be led to a large tipping bucket flowmeter (Calder & Kidd, 1978) and measured.

Where no impermeable layer exists, an artificial base can be formed. Kitching *et al.* (1980) and Kitching and Shearer (1982) drove sheet piles under a sheet pile-isolated monolith well above the water table to collect drainage water from the monolith. The latter example was particularly ambitious, enclosing a $5 \times 5 \times 5$ m block of undisturbed chalk.

An alternative approach to providing a base for a natural lysimeter was described by Schwärzel and Bohl (2003). They isolated a block of peat of 0.9 m^2 area and 1 m deep by first digging a trench on opposite sides of the block and forming a tunnel underneath the block between the middle of each trench. The peat was then dug out from beneath by enlarging the tunnel horizontally to insert a plastic sheet underneath the block and down opposite sides. The void below the plastic sheet was filled with sand to support the block and the trench outside the plastic sheet refilled with peat. Then a trench along each of the two other sides was dug and lined with a plastic sheet sealed to the first one to enclose the complete block in plastic, except for the top. The second two trenches were refilled as for the first two. Operation was similar to that of Kitching and Bridge (1974).

Measuring drainage from the lysimeter

Drainage from the lysimeter may be by a simple drain, as shown in Fig. 24.10. On the other hand, it can incorporate a means of applying a tension to the bottom of the lysimeter by means of, for example, a hanging water column or wick sampler or attempt to match the matric potential at the base of the lysimeter to that of the surrounding soil in a similar way to that described in Section 20.2.4. If a suction is

applied to the base of the lysimeter, then it requires either a porous plate or a number of porous cups to prevent air entry (Dowdell *et al.*, 1984; Evett *et al.*, 2006c).

Drainage can be led to a collecting tank and measured periodically. If a finer timescale is needed, there are a number of options:

- The level in the collecting tank can be monitored by a float-operated recorder or a pressure transducer or the tank can be weighed using a load cell. Control software actuates an electrically operated valve to empty the tank when its level is near the top (Kitching & Shearer, 1982).
- The drainage is led to a large tipping bucket, similar to those used in rain gauges, but scaled up (Calder & Rosier, 1976; Calder & Kidd, 1978; Ziegler *et al.*, 2009; Meissner *et al.*, 2010).
- Where a pumping system is used to match the internal and external groundwater levels, the use of separate tanks for the water pumped into and out of the lysimeter, each with a pressure transducer in the base or on a load cell to measure the amount of water in the tank, allows the water transfers to be monitored (Proulx-McInnis *et al.*, 2011).

Monitoring water content

Change in water content of the lysimeter can be done in two ways: by weighing the lysimeter or by measuring soil water content by any of the methods described in Chapters 7–9. For accurate measurements, changes in the mass of crop growing on the lysimeter need to be taken into account.

Weighing the lysimeter Total change in water content of a lysimeter can be measured from its change in weight. The challenge is to obtain sufficient precision of the measurement to resolve a quite small change against a large fixed mass. A 1-m-diameter, 1.5-m-deep lysimeter contains about 2000 kg of soil, and the container and other parts of the lysimeter may add another few hundred kilograms, perhaps 500 kg. Against this, 1 mm of water has a mass of 0.785 kg, so that a resolution of 1 mm requires a precision of measurement of about 1 part in 3200 (i.e. 0.03%). The term precision is used here because a much lower level of absolute accuracy is acceptable, since only the change in mass need be measured to the required accuracy. Daily water balance changes usually result in a change in water content of the soil profile of a few millimetres of water, so that a resolution of 1 mm may be just about acceptable if daily water balance is required. If hourly changes need to be resolved, then the required precision will be closer to 1 part in 50,000 (i.e. 0.002%). This level of precision needs to be maintained over a temperature range of, typically, 10°C and over several years. Meissner *et al.* (2007, 2010) used three load cells and claimed a resolution of 30 g in a total lysimeter (1.13 m diameter, 2 m depth) mass of 4000–4500 kg, that is, 1 part in 150,000, which equates to 0.03 mm of water.

Achieving this level of precision is, however, very challenging in a straightforward weighing approach. An alternative approach is to counterbalance most of the weight of the lysimeter, so that only a small weight remains to be measured, which can be done with much lower precision. To resolve 0.1 mm over a range of 300 mm of water, for instance, requires a precision of 0.03%, which is about 15 times less demanding than if the full weight of the lysimeter is carried by the load cell. There are several ways in which counterbalancing can be achieved, but all require very low frictional forces to ensure that reversals of the lysimeter mass are correctly measured. Marek *et al.* (1988) described a system where the lysimeter load was transformed and counterbalanced by a series of levers, so that it could be measured by a 22 kg range load cell. Howell *et al.* (1995) and Evett *et al.* (2012) found that water storage in two replicate lysimeters could be resolved to 0.01 and 0.04 mm.

Weighing lysimeters are expensive to build. Counterbalancing systems also need regular maintenance to ensure their continued smooth operation. Load cells may be less demanding but nevertheless need regular checking and periodic recalibration.

Direct water content measurement Lysimeter water content can be measured by neutron probe, TDR, other dielectric methods or DPHP probes. A vertically installed TDR probe gives an integrated measure of water content along its length, although the maximum depth attainable may be much less than the total depth of the lysimeter. Measurement at discrete depths has the advantage that variations of water content by depth as well as time are measured, which gives more complete information. If parallel measurements in the surrounding soil are made, then any difference between the two can be assessed for its effect on the representivity of the lysimeter.

Other instrumentation

A lysimeter is a very well-controlled system, simple in concept and relatively easy to operate. With good attention to ensuring that the measuring system(s) works properly, they are adaptable to a wide variety of uses, not only to monitor the water and solute balance of its surroundings but also for more active experiments, for instance, by manipulating the environment or investigating the fate or effect of different agrochemicals. Such experiments may be performed in the field or under greenhouse or laboratory conditions.

Whether used in a monitoring or experimental role, a range of different instruments can be installed in a lysimeter, including (but not limited to) tensiometers, temperature probes and soil solution samplers. It is usually convenient to install these from the side of the lysimeter, thereby eliminating the possibility of water running down the side of the instrument or access tube as well as not disturbing the crop or micrometeorological environment and keeping the temperature regime more stable.

Limitations of lysimeters

Over many years, lysimeters have proved very useful in studying soil processes in a semi-natural environment with

much more control than is possible in an unconfined situation. There are, however, several aspects that make them unrepresentative of the natural field environment, which provide some limitation to their usefulness or need to be guarded against. Some of these have been touched on above, such as the possible effect of repacking soil.

Artificial base The bottom of the lysimeter is often a free draining boundary. This means that drainage occurs only when the matric potential rises to zero at the base (i.e. becomes saturated). The soil for some distance above this must also be at high matric potential. If the soil outside the lysimeter is dry, hydraulic conditions will be considerably different, particularly for a shallow lysimeter. On the other hand, once the matric potential at the base of the lysimeter falls below zero, drainage stops abruptly, while in the surrounding soil it may well be proceeding at a significant rate. If dry conditions persist, the ZFP outside the lysimeter may fall below the level of the lysimeter base and upward flow become established, providing an additional source of water for evaporation. In this case, the lysimeter soil may become significantly drier than that outside, leading to reduced evaporation from the lysimeter.

Of course, the deeper the lysimeter, the less effect its base will have. This does, however, have significant cost implications. An alternative solution is to apply a suction to the base of the lysimeter, as was discussed in connection with porous plates (Section 20.2.4). This could be a static or occasionally adjusted value or a tensiometer-controlled vacuum. Again, the latter option is expensive to implement and consumes significant power.

Runoff/runon The isolation of a vertical soil column precludes water running onto or off the surface of the lysimeter. In most cases, this component is difficult to measure and account for in the unconfined case, and so the use of a lysimeter where runoff/runon is forced to be zero may be an advantage, albeit at the expense of some artificiality.

Leakage down sides A gap between the soil at the edge of the lysimeter and the container wall is a possible route for water falling on or applied to the lysimeter to bypass the soil matrix. This may be even more important where solutes are the primary object of interest, as small amounts of pollutant appearing in groundwater soon after application are often a cause for considerable concern. The problem is likely to be greatest in soils which swell and shrink. The solution of Cameron *et al.* (1992) to seal off a gap was described in Section 17.1. Corwin (2000) built small rings around the inside of the container near the top to deflect flow away from the wall. The latter solution is applicable only for repacked lysimeters.

In most situations, regular inspection of the soil surface in the lysimeter to ensure good contact with the container wall and possible filling of any gaps as deeply as possible with a little soil should suffice, particularly if near-surface saturation is not important.

In soils which exhibit a significant amount of swelling and shrinking, a gap may be more of a problem. Petroleum jelly may fail, as shrinkage of the soil column would require a change in volume of the jelly to accommodate it.

Gap between lysimeter container and surrounding soil The container walls occupy a certain amount of area when viewed from above, which may not be negligible compared with the lysimeter's surface area. Where there is access to the base to collect drainage or the lysimeter is weighed, there is inevitably a gap between the outside of the container and an extra shaft in which it sits. This may affect the soil water dynamics through aerodynamic or other effects and may require some adjustment to the lysimeter's effective area if a closed canopy crop is grown (Evett *et al.*, 2012).

Aerodynamic disturbance If the crop within the lysimeter is not uniform in height and type from that of the surroundings, then an *oasis effect* is possible, which promotes enhanced or reduced evaporation from the crop inside the lysimeter through a change in the airflow across it. To be representative, the lysimeter should be surrounded by land growing the same crop for a distance several times the crop height.

Access shaft An access shaft is often required to allow access to the base of the lysimeter or to instruments installed within it. This should, ideally, be sited some distance away from the lysimeter, but this is often not practical. A metal or protruding roof to the shaft is likely to disturb the airflow or temperature regime significantly, leading to questionable results. The effects can be mitigated by:

- Having the top of the access shaft at the same level as the crop in the lysimeter.
- Covering the roof of the shaft with vegetation.
- Siting the shaft such that the prevailing wind is at right angles to the line between the lysimeter and shaft.

Cultivation It is difficult to treat the surface of a small lysimeter in exactly the same way as a surrounding field. This is especially the case for arable crops, which use machinery to cultivate the soil and sow the crop. Treatment of the lysimeter must be designed to mimic the farming operations in its surroundings as closely as possible. This may well extend to an appreciable distance around the lysimeter, since farm machinery has difficulty getting close to an obstruction.

24.4 Tracer Methods

As described in Section 19.2, there are a wide variety of tracers available, some which can be applied artificially

and some which are part of natural precipitation. The former are useful for plot-scale studies, while the latter may be applicable over a wider area. However, wider areas usually involve tracer investigations in groundwater or streams draining the area and hence integrate over the relevant catchment area as well as over a longer timescale. Deep unsaturated zone measurements are likely to integrate over increasingly large areas the deeper in the profile the samples are taken from, albeit that this area is not very well defined.

An important consideration is whether or not the tracer is *conservative*. That is, once applied to the soil, does it remain in the profile or is some of it removed (or added) in some way? Conservative tracers do not undergo chemical transformations, are not taken up by plant roots, are not evaporated back into the atmosphere and do not undergo radioactive decay. Very few tracers fulfil all these conditions completely, but several are usually regarded as being close enough to doing so, that they can be treated as such (e.g. Cl^-, Br^-, Li^+, provided that they do not occur in subsurface minerals). Nitrogen (usually used as the stable isotope ^{15}N) is taken up by plant roots and there may be some losses by volatilisation, but if plant material is also analysed for nitrogen, most of the tracer should be recovered. Radioactive isotopes have well-known half-lives. If, instead of using the actual input quantity, the amount left after decay up to the time of measurement is used, and if there are no other loss mechanisms, they can be treated as if they were conservative.

24.4.1 Principles of tracer methods to water balance estimation

There are two main ways in which tracers can be used to estimate a soil water balance. The appropriate route depends on whether the input varies over time (for instance, seasonally or was introduced at one time) and whether the tracer is sufficiently conservative or its losses can be estimated sufficiently well. For a time-varying input, identification of the peak movement can be used to estimate water flux, while for a conservative tracer, a *mass balance* approach is possible. In some cases, both methods may be used, providing an opportunity to cross-check the results. In both methods, the interpretation is complicated by diffusion, dispersion, adsorption or anion exclusion (see Section 19.1.2). The former induces *retardation* (i.e. slowing down) of the tracer relative to that of the water (Section 23.1), and the latter speeds it up.

24.4.2 Peak movement

The principles governing the movement of a slug of solute were described in Section 19.1. For a perfect tracer (i.e. conservative, non-diffusive or dispersive, which travels at the same speed as the water), a narrow slug of tracer would travel at a speed given by Equation 19.1.4, that is, at the instantaneous water flux divided by the volumetric water content. Under steady-state conditions, that is, constant water content and water flux over a time period, Δt, then the total displacement, Δz, of the slug would be

$$\Delta z = \frac{q}{\theta}\Delta t. \tag{24.4.1}$$

More generally, if the water flux and water content vary in time, then

$$\Delta z = \int_{t_1}^{t_2} \frac{q(t)}{\theta(t)} \mathrm{d}t, \tag{24.4.2}$$

where $\Delta t = t_2 - t_1$.

If water content varies with depth, things are a little more difficult, as there is no neat solution for an arbitrary variation of θ with z. Recourse must be made to using a simple model of the relationship or a numerical solution. Below the root zone, water content is often sufficiently constant that this provides a good enough approximation to allow robust estimates of peak movement to be made.

Artificial tracers

An artificial tracer is usually applied at one time, either dry on the surface or, more usually, dissolved in a small amount of water and irrigated evenly over the area to be covered. Uniformity of application is important to avoid erroneous conclusions – for instance, inferences of preferential flow may be drawn when in reality non-uniform surface application is responsible. To avoid unacceptable disturbance to the hydrological system, the amount of water should be the minimum necessary to achieve satisfactory application. The area used should be as large as practical compared with the depth to which samples will be taken.

Barraclough *et al.* (1994) irrigated a plot of 2×1 m with ^{15}N-enriched nitrate fertiliser and an adjacent 2×2 m plot with deuterium-enriched water and chloride tracer. Over 40 months, lateral spreading of the ^{15}N at 0.5 m and Cl^- at 0.35 m from the edge of the plot was not detectable to a depth of 6 m, with the peak at about 3 m. The deuterium, however, was detectable at 0.35 m from the plot edge, probably reflecting the greater self-diffusion coefficient for hydrogen. In other situations, a larger area may be necessary, particularly if preferential flow carrying water in a lateral direction occurs.

An artificial tracer applied as a single 'slug' allows a peak of concentration to be followed unambiguously. Vertical spreading of the peak also allows combined diffusion and dispersion to be assessed. Preferential flow often produces *forward tailing* of a peak, in which a long 'tail' of solute is observed well below the main part of the peak, usually reducing in concentration with depth. This is sometimes attributed to flow in fractures or interaggregate pores with diffusional interchange of solute with the rest of the soil matrix (van Genuchten & Wierenga, 1976; Foster & Smith-Carington, 1980). Or it may result directly from preferential flow either within the soil matrix (Simmonds & Nortcliff, 1998) or in macropores.

Environmental tracers

Tracers arriving in precipitation usually show either a seasonally varying concentration, as in the case of ^{2}H or ^{18}O, or a broad peak extending over several weeks, months or years where the input is the result of human activity, such as tritium or ^{36}Cl from nuclear bomb testing, chemical releases from industrial plants or the Chernobyl accident in 1986. Provided that mixing in the surface layers or dispersion is not too great, these peaks may be followed through the unsaturated zone in the same way as for a single application.

24.4.3 Mass balance methods

If a tracer is conservative, then in principle, it should remain in the soil profile indefinitely or at least until it is transported away laterally by groundwater flow. Loss of tracer, therefore, should reflect:

- Uptake by plant roots
- Volatilisation and evaporation from the ground surface
- (Bio)chemical transformation within the profile
- Lateral movement away from the area of sampling
- Preferential flow beyond the deepest depth of sampling
- Radioactive decay

In practice, even where there appears to be very little scope for these processes to occur, tracer recovery is usually in the range of 85–105%, with values less than 100% being more common. Mass balance is, therefore, an important technique in aiding the interpretation of solute profiles.

'Steady-state' mass balance

For tracers where there is no identifiable peak displacement, that is, if the input is relatively constant or there is effective mixing close to the ground surface, then a method based on a concentration principle and steady-state conditions can be employed.

The most common tracer for the purpose is Cl^{-}, which is commonly not present in the subsurface except *via* precipitation. Chloride in precipitation is normally derived from seawater and so is strongly dependent on distance from the ocean and the direction of the prevailing wind.

The basic principle is quite simple. Chloride is usually regarded as conservative and, averaged over a number of years, both precipitation and chloride input are assumed to be reasonably constant. Assume that the total quantity of chloride deposited annually per unit land area, either as 'dry' deposition or in precipitation, is M_{Cl}, the annual precipitation is P, annual evaporation is E and all precipitation is evaporated or infiltrates into the soil, that is, there is no runoff. The chloride below the root zone is, therefore, dissolved in a quantity of water, $P - E$, that is, the concentration of chloride in unsaturated zone water, C_{Cl}, is expected to be

$$C_{Cl} = \frac{M_{Cl}}{P-E}. \qquad (24.4.3)$$

$P - E$ is, in the absence of surface runoff, the average drainage, D, from the soil profile or, in most cases, equal to groundwater recharge. Hence

$$D = \frac{M_{Cl}}{C_{Cl}}, \qquad (24.4.4)$$

or

$$D = \frac{C_P}{C_{Cl}}P, \qquad (24.4.5)$$

since $M_{Cl} = PC_P$, where C_P is the concentration of chloride in precipitation (ignoring dry deposition).

The method is usually applied in arid or semi-arid regions, where most precipitation is evaporated, but has been tried with reasonable success in a temperate climate (e.g. De Silva, 1999). From Equation 24.4.5, it can be seen that where annual drainage, D, is low, the ratio C_P/C_{Cl} is also low, that is, the chloride concentration in the soil profile is high and so the method is better suited to arid and semi-arid areas, where analysis of higher concentrations is less prone to errors. These areas are also less easily accessible to other methods of water balance computation.

At many sites, particularly in developing countries, chloride concentration data in rainfall may be available for only a short period. In view of many other uncertainties connected with the method, this is not regarded as a major limitation. Edmunds and Gaye (1994) used a 3-year record, although there was considerable variability between years. Bromley *et al.* (1997) had only 1 year's data, albeit from 16 sites over a 60 km transect. Rainfall data is usually available over a longer period, albeit rarely at the specific site sampled, and the method depends on both temporal and spatial stability of inputs.

Small-scale variations of chloride concentration with depth are usually attributed to annual or decadal variations in climate and deposition. An average through these is taken to compute drainage. Larger-scale variations can be identified with climatic shifts. The low rates of recharge and the often deep unsaturated zone of many (semi-)arid areas mean that there is a very long time record preserved in the chloride profile. For instance, Bromley *et al.* (1997) estimated that a 70-m-deep profile in Niger contained a record going back 765 years, with a mean recharge rate of 13 mm $year^{-1}$. Even longer time series have been observed at some sites. Flint *et al.* (2002b) identified reduced chloride concentrations at depth with increased precipitation in the Pleistocene period.

The method depends on an assumption of there being no net runoff from the area under study, no preferential flow below the near surface and no artificial sources (or sinks) of chloride either at the surface or within the profile. These are often questionable, but in many situations, comparison with other techniques has been good (Scanlon *et al.*, 2006).

Mass balance of surface applied tracers

Where the tracer is applied over a fixed period of time, whether deliberately or as an environmental contaminant, such as tritium or ^{36}Cl from nuclear bomb testing or from an industrial accident, then the mass balance can be used as an alternative to peak tracing, provided that the input is known. Loss of tracer would indicate volatilisation of the tracer, uptake by plants, evaporation from the soil surface, preferential flow or lateral movement. If the tracer is conservative, then only the latter two mechanisms are expected. Even non-conservative tracers, for example, tritium, deuterium and nitrate (whether as normal fertiliser or labelled with ^{15}N), once they are beyond the root zone of any vegetation, are expected to behave as conservative. Once safely beyond this, the tracer remaining can be regarded as the starting quantity, and we would expect to find the same amount at a later sampling time. Roots often penetrate deeper than expected, however, and upward flow of water above the ZFP can bring solutes back into the root zone, so some care in interpretation is needed.

Checking the mass balance is, therefore, a powerful way to check for consistency in interpretation of peak movement data.

24.4.4 Combined peak movement and mass balances

Combining the two approaches can reveal unexpected behaviour and challenge the assumptions made.

For instance, Wellings (1984b) applied water equivalent to 10 mm rainfall at twice natural deuterium concentration to a small plot on chalk at a site in southern England, and Barraclough *et al.* (1994) applied a much more concentrated amount of deuterated water at another chalk site in southern England in 5 mm water, washed in with a further 5 mm. In the former case, a deuterium peak was detectable in the upper 3 m of the profile for about 18 months after application, consistent with concentrations of chloride applied in fertiliser. At the latter site, rainfall and deep drainage were smaller and deuterium, chloride (artificially applied with the deuterium) and ^{15}N peaks were observed clearly over 4 years, reaching a maximum of 4 m depth. Comparison with water balances and volumetric water content of the chalk suggested that only about 50% of the water contained in the chalk was active in transmitting the solutes.

24.5 Aquifer Recharge and Groundwater Pollution

In many areas, aquifer recharge is controlled principally by the soil water balance. The techniques described in this chapter are, therefore, of particular importance for estimation of sustainable groundwater extraction and pollution from soil-applied chemicals. These techniques are, however, appropriate only if:

- Recharge is predominantly *via* water movement through the soil profile.
- Sites can be monitored representing all of the main soil and land use classes in the area.

This is usually termed *diffuse recharge* as it is areally extensive. Pollution arising from this source is termed *diffuse* or *non-point source pollution*.

Other recharge mechanisms that are not amenable to soil water balance monitoring include:

- *Mountain front recharge* (recharge from rivers discharging from mountain ranges into alluvial fans at their base).
- *Focussed, indirect or localised recharge* occurring from riverbeds, lakes and ephemeral lakes.

Other techniques for estimation of aquifer recharge, mainly applicable to these other mechanisms, include:

- Estimation of river baseflow, where the river(s) is fed by groundwater from the aquifer of interest.
- Analysis of groundwater level records.
- Seepage meters, for lakebeds.
- Estimation of the gain of river flow over a reach.
- Heat flow tracing.
- Isotopic and chemical concentrations in groundwater.
- Numerical modelling.

It is important to appreciate that although drainage at a depth a few metres below ground level will probably recharge the aquifer, the flux at the bottom of the monitored profile is not usually that at the water table. Impermeable layers within the unsaturated zone may divert water flowing down the profile into nearby streams, and there is almost always a long delay between drainage occurring a little way below the soil surface and its appearance at the water table, often tens and sometimes hundreds of metres below. If the profile between the depth at which drainage is measured and the water table is close to saturation, then there may be only a small delay between the water flux at the latter from that occurring at the former. This is not, however, the same water. Piston displacement means that water is pushed ahead of that at the top of the profile, so that solutes do not appear at the water table until usually much later, often decades or even centuries. Where the unsaturated zone has low water content, with small values of both hydraulic conductivity and diffusivity, the water table response to increased recharge near the surface will also take a long time, perhaps being little faster than the physical movement of the water.

Preferential flow is often more significant for solute movement than for water resources assessment. Some solutes, such as pesticides, have toxic levels in drinking water which are only a few parts per billion. If concentration at the soil surface is in the parts per million range, then if only 1% were able to infiltrate rapidly to the aquifer over a large area, or by concentration into surface depressions, this could cause a major problem.

24.6 Conclusion

Significant progress in our ability to measure and understand the factors controlling both water and

solute movement in field soils has been made through the methods outlined in this chapter and through laboratory experiments and modelling efforts. As in most areas of environmental science, the understanding of solute transport lags some considerable way behind that of water flow. In view of the bewildering array of chemicals and the variety of interactions they may have with different soil constituents, this is readily understandable.

At the conceptual level, the principal mechanisms appear to be well understood, but translating these into practical application and reliable measurement or prediction is possible in some situations, but will require much more research in most others.

Part VIII Conclusion

25 Concluding Remarks

This book has set out to describe techniques for measuring relevant aspects of the relationship between soil and water. Where possible, detailed descriptions of methods have been given. The working principles of the main instruments and methods have also been described in as simple a manner as possible. With these two sets of information, it should be possible to apply and adapt the basic principles to other methods which have been omitted or will appear in the future.

The ready availability of cheap computing power, together with the development of low power electronics, has transformed the study of soil–water interactions over the past four decades in a number of ways:

- It has enabled automated data collection of ever greater volumes of data from sometimes very remote field sites.
- Manual data collection has become simpler, with recording direct to electronic media.
- Statistical analysis of data can be incorporated routinely, and in many cases automatically, into data processing procedures.
- Several options for telemetry mean that real-time data monitoring from remote sites is possible.
- Data processing can be automated, poor quality identified quickly and remedial action taken.
- Data processing can be carried out at the point of measurement using intelligent data loggers.
- Much larger data sets can be handled and analysed.
- Different data sets can be related to one another with comparative ease.
- Data can be transmitted easily around the world *via* the Internet, enabling collaboration between workers separated by large physical distances.
- Sophisticated numerical models have been developed to predict the behaviour of large environmental systems.
- Inverse modelling enables the identification of the parameters controlling the behaviour of a system from measurement of other, more easily determined quantities.

As with all advances, there are dangers inherent all of this. These include:

- The ability to collect and transmit data automatically can lead to false assumptions about the true nature of the data or the system behaviour. There is no substitute for going into the field in challenging weather conditions and observing the myriad interactions between water and the environment, as well as those unpredicted events, like the tree that has blown down and is causing unexplained readings.
- The seductive plausibility of model results without all the irregularities of real field data. There is a real danger that, with the falling costs of computer power and the increasing expense of running properly managed field experiments, the world will be reduced to a virtual system inside a computer and if the results don't fit the observations, then there must be something wrong with the measurements. Already, there is a mini-industry in generating synthetic data sets and the success of a model is being judged on how well it agrees with other models.

Remote and automated data collection enables us to do many things that were not possible in the past. Networks of sensors capable of communicating with one another are starting to become more common, so that data can be collected, processed and related both spatially and interactively in real time (e.g. Akyildiz *et al.*, 2002; Delin *et al.*, 2002; Cook *et al.*, 2004; Porter *et al.*, 2005; Collins *et al.*, 2006; Bogena *et al.*, 2010). Used wisely, with understanding of the likely pitfalls and backed up with first-hand observation, these developments can add a great deal to efforts to understand the world we live in and to control those facets that need management.

Similarly, models are indispensable to prediction of the future or exploring the effect of a proposed course of action. But unless these are grounded by comparison against real observations of the behaviour of the relevant system, instead of being a substitute for them, then no matter how clever the algorithms, they cannot provide a true description of the processes at work.

If this book encourages more people to get out and make more measurements in the field environment, then it will have done the job intended.

Soil Water Measurement: A Practical Handbook, First Edition. J. David Cooper.

References

Abdu, H, Robinson, D A & Jones, S B (2007) Comparing bulk soil electrical conductivity determination using the DUALEM-1S and EM38-DD electromagnetic induction instruments. *Soil Science Society of America Journal* 71, 189–196.

Abdu, H, Robinson, D A, Seyfried, M S & Jones, S B (2008) Geophysical imaging of watershed subsurface patterns and prediction of soil texture and water holding capacity. *Water Resources Research* 44, W00D18.

Absolom, J P, Young, S D & Crout, M J (1995) Radio-caesium fixation dynamics: Measurement in six Cumbrian soils. *Soil Use & Management* 46, 461–469.

Abu-Hamdeh, N H (2001) Measurement of the thermal conductivity of sandy loam and clay loam soils using single and dual probes. *Journal of Agricultural Engineering Research* 80, 209–216.

Agus, S S & Schanz, T (2005) Comparison of four methods for measuring total suction. *Vadose Zone Journal* 4, 1087–1095.

Ahuja, L R & El-Swaify, S A (1979) Determining soil hydrologic characteristics on a remote forest watershed by continuous monitoring of soil-water pressures, rainfall and runoff. *Journal of Hydrology* 44, 135–147.

Akyildiz, I F, Su, W, Sankarasubramaniam, Y & Cayirci, E (2002) Wireless sensor networks: A survey. *Computer Networks* 38, 393–422.

Al Majou, H, Bruand, A & Duval, O (2008a) Use of in situ volumetric water content to improve prediction of soil water retention properties. *Canadian Journal of Soil Science* 88, 533–541.

Al Majou, H, Bruand, A, Duval, O, Le Bas, C & Vautier, A (2008b) Prediction of soil water retention properties after stratification by combining texture, bulk density and the type of soil horizon. *Soil Use & Management* 24, 383–391.

Allen, R G, Pereira, L S, Raes, D & Smith, M (1998) Crop evapotranspiration. Guidelines for computing crop water requirements. FAO Irrigation and Drainage Paper 56. Food and Agriculture Organization of the United Nations, Rome, Italy, 300 pp.

Allmaras, R R, Nelson, W W & Voorhees, W B (1975a) Soybean and corn rooting in southwestern Minnesota: I. Water-uptake sink. *Soil Science Society of America Proceedings* 39, 764–777.

Allmaras, R R, Nelson, W W & Voorhees, W B (1975b) Soybean and corn rooting in southwestern Minnesota: II. Root distribution and related water inflow. *Soil Science Society of America Proceedings* 39, 771–777.

Amezketa, E (2007) Use of an electromagnetic technique to determine sodicity in saline-sodic soils. *Soil Use & Management* 23, 278–285.

Amoozegar, A (1992) Compact constant head permeameter: A convenient device for measuring hydraulic conductivity. In: *Advances in Measurement of Soil Physical Properties: Bringing Theory into Practice*, SSSA Special Publication 30 (Eds. G C Topp, W D Reynolds & R E Green), Soil Science Society of America, Madison, WI, 31–43.

Andraski, B J & Scanlon, B R (2002) Thermocouple psychrometry. In: *Methods of Soil Analysis: Part 4. Physical Methods* (Eds. J H Dane & G C Topp), Soil Science Society of America, Madison WI, 609–642.

Ankeny, M D, Kaspar, T C & Horton, R (1988) Design for an automated tension infiltrometer. *Soil Science Society of America Journal* 52, 893–896.

Ankeny, M D, Ahmed, M, Kaspar, T C & Horton, R (1991) Simple field method for determining unsaturated hydraulic conductivity. *Soil Science Society of America Journal* 55, 467–470.

Archie, G E (1942) The electrical resistivity log as an aid in determining some reservoir characteristics. *Transactions of the American Institute of Mining, Metallurgical, and Petroleum Engineers* 146, 54–62.

Arslan, A, Razzouk, A K & Al-Ain, F (1997) The performance and radiation exposure of some neutron probes in measuring the water content of the topsoil layer. *Australian Journal of Soil Research* 35, 1397–1407.

Arya, L M, Farrell, D A & Blake, G R (1975a) A field study of soil water depletion patterns in presence of growing soybean roots: I. Determination of hydraulic properties of the soil. *Soil Science Society of America Proceedings* 39, 424–444.

Arya, L M, Blake, G R & Farrell, D A (1975b) A field study of soil water depletion patterns in presence of growing soybean roots: II. Effect of plant growth on soil water pressure and water loss patterns. *Soil Science Society of America Proceedings* 39, 430–436.

Arya, L M, Blake, G R & Farrell, D A (1975c) A field study of soil water depletion patterns in presence of growing soybean roots: III. Rooting characteristics and root extraction of soil water. *Soil Science Society of America Proceedings* 39, 437–444.

ASTM (2009) Standard Test Methods for Laboratory Determination of Density (Unit Weight) of Soil Specimens. D7263-09, American Society for Testing and Materials, 7 pp.

Soil Water Measurement: A Practical Handbook, First Edition. J. David Cooper.

ASTM (2010) Standard Test Methods for Laboratory Determination of Water (Moisture) Content of Soil and Rock by Mass. D2216-10, American Society for Testing and Materials, 7 pp.

Baatz, R, Bogena, H R, Hendricks Franssen, H-J, Huisman, J A, Qu, W, Montzka, C & Vereecken, H (2014) Calibration of a catchment scale cosmic-ray probe network: A comparison of three parameterization methods. *Journal of Hydrology* 516, 231–244.

Baker, J M & Allmaras, R R (1990) System for automating and multiplexing soil moisture measurement by time-domain reflectometry. *Soil Science Society of America Journal* 54, 1–6.

Baker, T H W & Goodrich, L E (1987) Measurement of soil water content using the combined time-domain reflectometry–thermal conductivity probe. *Canadian Geotechnical Journal* 24, 160–163.

Baker, F G, Veneman, P L M & Bouma, J (1974) Limitations of the instantaneous profile method for field measurement of unsaturated hydraulic conductivity. *Soil Science Society of America Proceedings* 38, 885–888.

Bakker, G, van der Ploeg, M J, de Rooij, G H, Hoogendam, C W, Gooren, H P A, Huiskes, C, Koopal, L K & Kruidhof, H (2007) New polymer tensiometers: Measuring matric pressures down to the wilting point. *Vadose Zone Journal* 6, 196–202.

Barker, R & Moore, J (1998) The application of time-lapse electrical tomography in groundwater studies. *The Leading Edge* 17, 1454–1458.

Barraclough, D, Gardner, C M K, Wellings, S R & Cooper, J D (1994) A tracer investigation into the importance of fissure flow in the unsaturated zone of the British Chalk. *Journal of Hydrology* 156, 459–469.

Barzegar, A R, Herbert, S J, Hashemi, A M & Hu, C S (2004) Passive pan sampler for vadose zone leachate collection. *Soil Science Society of America Journal* 68, 744–749.

Basinger, J M, Kluitenberg, G J, Ham, J M, Frank, J M, Barnes, P L & Kirkham, M B (2003) Laboratory evaluation of the dual-probe heat-pulse method for measuring soil water content. *Vadose Zone Journal* 2, 389–399.

Bath, A H, Darling, W G & Brunsdon, A P (1982) The stable isotopic composition of infiltration moisture in the unsaturated zone of the English Chalk. In: *Stable Isotopes* (Eds. H-L Schmidt, H Förstel & K Heinzinger), Elsevier, Amsterdam, 161–166.

Baumgartner, N, Parkin, G W & Elrick, D E (1994) Soil water content and potential measured by a hollow time domain reflectometer. *Soil Science Society of America Journal* 58, 315–318.

Baumhardt, R L, Lascano, R J & Evett, S R (2000) Soil material, temperature, and salinity effects on calibration of multisensor capacitance probes. *Soil Science Society of America Journal* 64, 1940–1946.

Belcher, D J, Cuykendall, T R & Sack, H S (1950) The measurement of soil moisture and density by neutron and gamma-ray scattering. Technical Development Report 127, Civil Aeronautics Administration, Technical Development and Evaluation Center, Washington, DC, 20 pp.

Belford, R K (1979) Collection and evaluation of large soil monoliths for soil and crop studies. *Journal of Soil Science* 30, 363–373.

Bell, J P (1969) A new design principle for neutron soil moisture gages: The 'Wallingford' neutron probe. *Soil Science* 108, 160–164.

Bell, J P (1987) Neutron probe practice. Report 19, Institute of Hydrology, Wallingford, UK. Available at http://www.ceh.ac.uk/products/publications/hydrology.html (accessed on 8 August 2015).

Bell, R W & Schofield, N J (1990) Design and application of a constant head well permeameter for shallow high saturated hydraulic conductivity soils. *Hydrological Processes* 4, 327–342.

Bell, J P, Dean, T J & Hodnett, M G (1987) Soil moisture measurement by an improved capacitance technique: Part II. Field techniques, evaluation and calibration. *Journal of Hydrology* 93, 79–90.

Beven, K J & Germann, P (1982) Macropores and water flow in soils. *Water Resources Research* 18, 1311–1325.

Beven, K J & Germann, P (2013) Macropores and water flow in soils revisited. *Water Resources Research* 49, 3071–3092.

Biesheuvel, P M, Raangs, R & Verweij, H (1999) Response of the osmotic tensiometer to varying temperatures: Modeling and experimental validation. *Soil Science Society of America Journal* 63, 1571–1579.

Biesheuvel, P M, van Loon, A P, Raangs, R, Verweij, H & Dirksen, C (2000) A prototype osmotic tensiometer with polymeric gel grains. *European Journal of Soil Science* 51, 355–364.

Bilskie, J, Horton, R & Bristow, K L (1998) Test of a dual-probe heat-pulse method for determining thermal properties of porous materials. *Soil Science* 163, 346–355.

Binley, A, Cassiani, G, Middleton, R & Winship, P (2002a) Vadose zone flow model parameterisation using cross-borehole radar and resistivity imaging. *Journal of Hydrology* 267, 147–159.

Binley, A, Winship, P, Pokar, M, West, S & Middleton, R (2002b) Seasonal variation of moisture content in unsaturated sandstone inferred from borehole radar and resistivity profiles. *Journal of Hydrology* 267, 160–172.

Black, J H (1977) Polyurethane foam – a useful new borehole grout. *Journal of Hydrology* 32, 183–188.

Blackwell, P S & Elsworth, M J (1980) A system for automatically measuring and recording soil water potential and rainfall. *Agricultural Water Management* 3, 135–141.

Blaney, H F & Criddle, W O (1950) Determining water requirements in irrigated areas from meteorological and irrigation data. USDA Soil Conservation Service Report TP-96, United States Department of Agriculture, Washington, DC, 48 pp.

Blonquist, J M, Jones, S B & Robinson, D A (2005a) A time domain transmission sensor with TDR performance characteristics. *Journal of Hydrology* 314, 235–245.

Blonquist, J M, Jones, S B & Robinson, D A (2005b) Standardizing characterization of electromagnetic water content sensors: Part 2. Evaluation of seven sensing systems. *Vadose Zone Journal* 4, 1059–1069.

Blonquist, J M, Jones, S B & Robinson, D A (2006) Precise irrigation scheduling for turfgrass using a subsurface electromagnetic soil moisture sensor. *Agricultural Water Management* 84, 153–165.

Boast, C W & Kirkham, D (1971) Auger hole seepage theory. *Soil Science Society of America Proceedings* 35, 365–374.

Bocking, K A & Fredlund, D G (1979) Use of the osmotic tensiometer to measure negative pore water pressure. *Geotechnical Testing Journal* 2, 3–10.

Bogena, H R, Huisman, J A, Oberdorster, C & Vereecken, H (2007) Evaluation of low-cost electromagnetic water content sensors. *Journal of Hydrology* 344, 32–42.

Bogena, H R, Herbst, M, Huisman, J A, Rosenbaum, U, Weuthen, A & Vereecken, H (2010) Potential of wireless sensor networks for measuring soil water content variability. *Vadose Zone Journal* 9, 1002–1013.

Boll, J, Steenhuis, T & Selker, J (1992) Fiberglass wicks for sampling of water and solutes in the vadose zone. *Soil Science Society of America Journal* 56, 701–707.

Booltink, H W G, van Breemen, N, Bongers, N, Waringa, N, van Grinsven, J J M & Dirksen, C (1988) Automated *in situ* measurement of unsaturated soil water flux. *Soil Science Society of America Journal* 52, 1215–1218.

Bouma, J & Denning, J L (1972) Field measurement of unsaturated hydraulic conductivity by infiltration through gypsum crusts. *Soil Science Society of America Proceedings* 36, 846–847.

Bouma, J, Hillel, D, Hole, F D & Amerman, C R (1971) Field measurement of hydraulic conductivity by infiltration through artificial crusts. *Soil Science Society of America Proceedings* 35, 362–364.

Bouyoucos, G J (1953) More durable plaster of Paris blocks. *Soil Science* 76, 447–451.

Bouyoucos, G J & Mick, A H (1940) Electrical resistance methods for the continuous measurement of soil moisture under field conditions. Technical Bulletin, Michigan Agricultural Experiment Station, East Lansing, MI, 172, 38pp.

Bower, C A & Wilcox, L V (1965) Soluble salts. In: *Methods of Soil Analysis: Part 2. Chemical and Microbiological Methods* (Ed. C A Black), American Society of Agronomy, Madison, WI, 933–951.

Brandi-Dohrn, F M, Dick, R P, Hess, M & Selker, J (1996) Field evaluation of passive capillary samplers. *Soil Science Society of America Journal* 60, 1705–1713.

Bremer, D J (2003) Evaluation of microlysimeters used in turfgrass evapotranspiration studies using the dual-probe heat-pulse technique. *Agronomy Journal* 95, 1625–1632.

Bristow, K L (1998) Measurement of thermal properties and water content of unsaturated sandy soil using dual-probe heat-pulse probes. *Agricultural & Forest Meteorology* 89, 75–84.

Bristow, K L, Campbell, G S & Calissendorf, K (1993) Test of a heat-pulse probe for measuring changes in soil water content. *Soil Science Society of America Journal* 57, 930–934.

Bristow, K L, Kluitenberg, G J & Horton, R (1994a) Measurement of soil thermal properties with a dual-probe heat-pulse technique. *Soil Science Society of America Journal* 58, 1288–1294.

Bristow, K L, White, R D & Kluitenberg, G J (1994b) Comparison of single and dual probes for measuring soil thermal properties with transient heating. *Australian Journal of Soil Research* 32, 447–464.

Bristow, K L, Bilskie, J, Kluitenberg, G J & Horton, R (1995) Comparison of techniques for extracting soil thermal properties from dual-probe heat-pulse data. *Soil Science* 160, 1–7.

Bristow, K L, Kluitenberg, G J, Goding, C J & Fitzgerald, T S (2001) A small multi-needle probe for measuring soil thermal properties, water content and electrical conductivity. *Computers and Electronics in Agriculture* 31, 265–280.

Bromley, J, Edmunds, W M, Fellman, E, Brouwer, J, Gaze, S, Sudlow, J & Taupin, J-D (1997) Estimation of rainfall inputs and direct recharge to the deep unsaturated zone of southern Niger using the chloride profile method. *Journal of Hydrology* 188, 139–154.

Brooks, R H & Corey, A T (1964) Hydraulic Properties of Porous Media. Hydrology Paper No. 3, Colorado State University, Fort Collins, CO.

Bruand, A & Prost, R (1987) Effect of water content on the fabric of a soil material: An experimental approach. *Journal of Soil Science* 38, 461–472.

Bruce, R R & Klute, A (1956) The measurement of soil diffusivity. *Soil Science Society of America Proceedings* 20, 458–462.

Brummer, E & Mardock, E S (1945) A neutron method for measuring saturation in laboratory flow measurements. In: *Proceedings of the American Institute of Mining and Metal Engineering*, Dove Valley, CO.

Brye, K R, Norman, J M, Bundy, L G & Gower, S T (1999) An equilibrium tension lysimeter for measuring drainage through soil. *Soil Science Society of America Journal* 63, 536–543.

Buckingham, E (1907) Studies on the movement of soil moisture. USDA Bureau of Soils, Bulletin 38, United States Department of Agriculture, Washington, DC.

Burdine, N T (1953) Relative permeability calculations from pore size distribution data. *Transactions of the American Institute of Mining, Metallurgical, and Petroleum Engineers* 198, 71–77.

Burle Industries Inc. (1980) *Photomultiplier Handbook*. Burle Industries Inc., Lancaster, PA, 180 pp.

Byrne, G F, Drummond, J E & Rose, C W (1967) A sensor for water flux in soil: 1. 'Point source' instrument. *Water Resources Research* 3, 1073–1078.

Byrne, G F, Drummond, J E & Rose, C W (1968) A sensor for water flux in soil: 2. 'Line source' instrument. *Water Resources Research* 4, 607–611.

Calder, I R (1976) The measurement of water losses from a forested area using a 'natural' lysimeter. *Journal of Hydrology* 30, 311–325.

Calder, I R (1977) A model of transpiration and interception from a spruce forest in Plynlimon, central Wales. *Journal of Hydrology* 33, 247–265.

Calder, I R (1990) *Evaporation in the Uplands*. John Wiley and Sons, Ltd, Chichester, UK, 166 pp.

Calder, I R & Kidd, C H R (1978) A note on the dynamic calibration of tipping-bucket gauges. *Journal of Hydrology* 39, 383–386.

Calder, I R & Rosier, P (1976) The design of large plastic sheet net rainfall gauges. *Journal of Hydrology* 30, 403–405.

Calder, I R, Rosier, P, Prasanna, K T & Parameswarappa, S (1997) Eucalyptus water use greater than rainfall input – possible explanation from southern India. *Hydrology & Earth System Sciences* 1, 249–256.

Cameron, K C, Smith, N P, McLay, C D A, Fraser, P M, McPherson, R J, Harrison, D F & Harbottle, P (1992) Lysimeters without edge flow: An improved design and sampling procedure. *Soil Science Society of America Journal* 56, 1625–1628.

Campbell Scientific (2009) *CS229 Heat Dissipation Matric Water Potential Sensor Instruction Manual*. Campbell Scientific, Logan, UT, 30 pp.

Campbell, D I, Laybourne, C E & Blair, I J (2002) Measuring peat moisture content using the dual-probe heat pulse technique. *Australian Journal of Soil Research* 40, 177–190.

Campbell, D J & Henshall, J K (2001) Bulk density. In: *Soil and Environmental Analysis: Physical Methods* (Eds. K A Smith & C E Mullins), Marcel Dekker, New York, 315–348.

Campbell, G S (1979) Improved thermocouple psychrometers for measurement of soil water potential in a temperature gradient. *Journal of Physics E: Scientific Instruments* 12, 739–743.

Campbell, G S, Calissendorf, C & Williams, J H (1991) Probe for measuring soil specific heat using a heat-pulse method. *Soil Science Society of America Journal* 55, 291–293.

Campbell, G S & Anderson, R Y (1998) Evaluation of simple transmission line oscillators for soil moisture measurement. *Computers and Electronics in Agriculture* 20, 31–44.

Campbell, J E (1990) Dielectric properties and influence of conductivity in soils at one to fifty megahertz. *Soil Science Society of America Journal* 54, 332–341.

Cannell, G H & Asbell, C W (1964) Prefabrication of mold and construction of cylindrical electrode-type resistance units. *Soil Science* 97, 108–112.

Carneiro, C & De Jong, E (1985) *In situ* determination of the slope of the calibration curve of a neutron probe using a volumetric technique. *Soil Science* 139, 250–254.

Carslaw, H S & Jaeger, J C (1959) *Conduction of Heat in Solids*. Oxford University Press, Oxford, UK.

Cary, J W (1968) An instrument for *in situ* measurements of soil moisture flow and suction. *Soil Science Society of America Proceedings* 32, 3–5.

Cary, J W (1970) Measuring unsaturated soil moisture flow with a meter. *Soil Science Society of America Proceedings* 34, 24–27.

Cary, J W (1971) Calibration of soil heat and water flux meters. *Soil Science* 111, 399–400.

Casey, F X M & Derby, N E (2002) Improved design for an automated tension infiltrometer. *Soil Science Society of America Journal* 66, 64–67.

Cassiani, G, Binley, A & Ferré, P A (2006) Unsaturated zone processes. In: *Applied Hydrogeophysics* (Eds. H Vereecken, A Binley, G Cassiani, A Revil & K Titov), Springer, Dordrecht, The Netherlands, 75–116.

Castiglione, P & Shouse, P J (2003) The effect of ohmic cable losses on TDR measurements of electrical conductivity. *Soil Science Society of America Journal* 67, 414–424.

Chanasyk, D S & Naeth, M A (1988) Measurements of near-surface soil moisture content with a hydrogenously shielded neutron probe. *Canadian Journal of Soil Science* 68, 171–176.

Chandler, D G, Seyfried, M S, Murdock, M D & McNamara, J P (2004) Field calibration of water content reflectometers. *Soil Science Society of America Journal* 68, 1501–1507.

Childs, E C & Collis-George, N (1950) The permeability of porous media. *Proceedings of the Royal Society A* 201, 393–405.

Childs, E C & Poulovassilis, A (1960) An oscillating permeameter. *Soil Science* 90, 326–328.

Chong, S K & Green, R E (1983) Sorptivity measurement and its application. In: *Advances in Irrigation* (Ed. D Hillell), Academic Press, London, 82–91.

Chong, S K, Green, R E & Ahuja, L R (1981) Simple *in situ* determination of hydraulic conductivity by power function descriptions of drainage. *Water Resources Research* 17, 1109–1114.

Ciglash, H, Amelung, W, Totrakool, S & Kaupenjohann, M (2005) Water flow patterns and pesticide fluxes in an upland soil in northern Thailand. *European Journal of Soil Science* 56, 765–777.

Clark, I (1979) *Practical Geostatistics*. Applied Science Publishers, Barking, UK, 129 pp.

Clark, I & Harper, W V (2000) *Practical Geostatistics 2000*. Ecosse North America LLC, Columbus, OH, 342 pp.

Clothier, B E (2001) Infiltration. In: *Soil and Environmental Analysis: Physical Methods* (Eds. K A Smith & C E Mullins), Marcel Dekker, New York, 239–281.

Clothier, B E & White, I (1981) Measurement of sorptivity and soil water diffusivity in the field. *Soil Science Society of America Journal* 45, 241–245.

Collins, S L, Bettancourt, L M A, Hagberg, A, Brown, R F, Moore, D I, Bonito, G, Delin, K A, Jackson, S P, Johnson, D W, Burleigh, S C, Woodrow, R R & McAuley, J M (2006) New opportunities in ecological sensing using wireless sensor networks. *Frontiers in Ecology and the Environment* 4, 402–407.

Comegna, V, Coppola, A, Basile, A & Comegna, A (2012) A review of approaches for measuring soil hydraulic properties and assessing the impacts of spatial dependence on the results. In: *Hydrogeology – A Global Perspective* (Ed. G A Kazemi), Intech, Rijeka, Croatia, 79–140.

Conca, J L & Wright, J V (1998) The UFA method for rapid, direct measurement of unsaturated transport properties in soil, sediment, and rock. *Australian Journal of Soil Research* 36, 291–315.

Constantz, J & Murphy, F (1987) An automated technique for flow measurements from Mariotte reservoirs. *Soil Science Society of America Journal* 51, 252–254.

Cook, W M, Casagrande, D G, Hope, D, Groffman, P M & Collins, S L (2004) Learning to roll with the punches: Adaptive experimentation in human-dominated systems. *Frontiers in Ecology and the Environment* 2, 467–474.

Cooper, J D (1974) *Etude de flux vertical non saturé à Thetford Chase (Norfolk) (Study of vertical unsaturated flux at Thetford Chase (Norfolk))*. Section III, Bulletin du BRGM, Deuxième Série, 171–174.

Cooper, J D (1979) Water use of a tea estate from soil moisture measurements. *East African Agricultural & Forestry Journal* 43, 102–121.

Cooper, J D (1980) Measurement of moisture fluxes in unsaturated soil in Thetford Forest. Report 66, Institute of Hydrology, Wallingford, UK. 97 pp.

Cooper, J D (1985) Estimation of aquifer recharge in the area of Fleam Dyke Pumping Station by soil physics methods. Report to Department of the Environment, UK in fulfillment of Contracts DGR480/276 & PECD7/7/034, Institute of Hydrology, Wallingford, Oxon, UK, 92 pp.

Cooper, J D, Gardner, C M K & Mackenzie, N (1990) Soil controls on recharge to aquifers. *Journal of Soil Science* 41, 613–630.

Cooper, J D, Bell, J, Hodnett, M, Beven, K, Gilman, K, Haria, A, Gardner, C, Evans, J, Ward, H & Robinson, M (2015) Terrestrial hydrological processes. Chapter 4. In: *Progress in Modern Hydrology: Past, Present and Future* (Eds. J C Rodda & M Robinson), Wiley-Blackwell, Chichester, UK, 416 pp.

Corwin, D L (2000) Evaluation of a simple lysimeter-design modification to minimize sidewall flow. *Journal of Contaminant Hydrology* 42, 35–49.

Corwin, D L & Lesch, S M (2003) Application of soil electrical conductivity to precision agriculture: Theory, principle, and guidelines. *Agronomy Journal* 95, 455–471.

Corwin, D L & Plant, R E (2005) Applications of apparent soil electrical conductivity in precision agriculture. *Computers and Electronics in Agriculture* 46, 1–10.

Couchat, P (1967) Détermination de la courbe d'étalonage de l'humidimètre à neutrons à partir de l'analyse chimique des sols. In: *Isotope and Radiation Techniques in Soil Physics and Irrigation Studies*, International Atomic Energy Agency, Vienna, 67–82.

Couchat, P (1983) Les applications de la méthode neutronique dans la recherche agronomique. In: *Isotope and Radiation Techniques in Soil Physics and Irrigation Studies*, International Atomic Energy Agency, Vienna, 509–531.

Couchat, P, Carré, C, Marcesse, J & Le Ho, J (1975) The measurement of thermal neutron constants of the soil: Application to the calibration of neutron moisture gauges and to the pedological study of the soil. In: *Proceedings of the Conference on Nuclear Data Cross Sections on Technology* (Eds. R A Schrack & C D Bowman), National Bureau of Standards Special Publication 425, National Bureau of Standards, Washington, DC, 516–519.

Cresswell, H P (1993) Evaluation of the portable pressure transducer technique for measuring field tensiometers. *Australian Journal of Soil Research* 31, 397–406.

Cross, R C (1983) Evaluation of the soil density measuring Nuclear Enterprises backscatter gamma probe. B.Sc. dissertation, Department of Geography, Coventry (Lanchester) Polytechnic. 61 pp.

Cuenca, R H, Brouwer, J, Chanzy, A, Droogers, P, Galle, S, Gaze, S, Stricker, H, Angulo-Jaramillo, R, Boyle, S A, Bromley, J, Chebhouni, A G, Cooper, J D, Dixon, A J, Fies, J C, Gandah, M, Gaudu, J C, Laguerre, L, Soet, M, Steward, H J, Vandervaere, J P & Vauclin, M (1997a) Soil measurements during the HAPEX-Sahel intensive observation period. *Journal of Hydrology* 188, 224–266.

Cuenca, R H, Stangel, D E & Kelly, S F (1997b) Soil water balance in a boreal forest. *Journal of Geophysics Research Atmospheres* 102(D24), 29355–29365.

Cui, Y J, Tang, A M, Mantho, A & De Laure, E (2008) Monitoring field soil suction using a miniature tensiometer. *Geotechnical Testing Journal* 31, 95–100.

Daian, J-F & Vachaud, G (1971) Méthode d'évaluation du bilan hydrique *in situ* à partir de la mésure des teneurs en eau et des pressions interstitielles. In: *Proceedings of the Symposium 'L'étude des infiltrations dans les sols en milieux non saturés*, XIV Congres AIRH, Paris. 5, 429–439.

Daian, J-F & Vachaud, G (1972) Méthode d'évaluation du bilan hydrique *in situ* à partir de la mésure des teneurs en eau et des succions. In: *Isotopes and Radiation in Soil-Plant Relationships Including Forestry*, International Atomic Energy Agency, Vienna, 649–660.

Daily, W, Ramirez, A, Binley, A & LaBrecque, D (2004) Electrical resistance tomography. *The Leading Edge* 23, 438–442.

Dalton, F N & van Genuchten, M Th (1986) The time-domain reflectometry method for measuring soil water content and salinity. *Geoderma* 38, 237–250.

Dane, J H (1980) Comparison of field and laboratory determined hydraulic conductivity values. *Soil Science Society of America Journal* 44, 228–231.

Dane, J H & Hruska, S (1983) *In-situ* determination of soil hydraulic properties during drainage. *Soil Science Society of America Journal* 47, 619–624.

Dane, J H & Topp, G C (2002) *Methods of Soil Analysis: Part 4. Physical Methods*. Soil Science Society of America, Madison, WI.

Daniels, D J (2004) *Ground Penetrating Radar*, Vol. 1, 2nd edn. The Institution of Engineering and Technology, London, 734 pp.

Darcy, H (1856) *Les Fontaines Publiques de la Ville de Dijon*. Dalmont, Paris.

Dashtaki, S G, Homaee, M & Khodaverdiloo, H (2010) Derivation and validation of pedotransfer functions for estimating soil water retention curve using a variety of soil data. *Soil Use & Management* 26, 68–74. doi: 10.1111/j.1475-2743.2009.00254.x.

Davis, J L & Annan, A P (2002) Ground penetrating radar to measure soil water content. In: *Methods of Soil Analysis: Part 4. Physical Methods* (Eds. J H Dane & G C Topp), Soil Science Society of America, Madison, WI, 446–463.

Day-Lewis, F D, Singha, K & Binley, A (2005) On the limitations of applying petrophysical models to tomograms: A comparison of correlation loss for cross-hole electrical-resistivity and radar tomography. *Journal of Geophysics Research* 110, B08206.

De Boodt, M, Hartmann, R & De Meester, P (1967) Determination of soil-moisture characteristics for irrigation purposes by neutron-moisture meter and air-purged tensiometers. In: *Isotope and Radiation Techniques in Soil Physics and Irrigation Studies, Proceedings of the Symposium in Istanbul, 1967*, International Atomic Energy Agency, Vienna, 147–160.

De Neve, S, Van de Steene, J, Hartmann, R & Hofman, G (2000) Using time domain reflectometry for monitoring mineralization of nitrogen from soil organic matter. *European Journal of Soil Science* 51, 295–304.

De Silva, R P (1999) Estimating the rate of recharge to the groundwater table using environmental chloride as a tracer. *Tropical Agriculture Research and Extension* 2, 44–50.

Dean, T J (1994) The IH capacitance probe for measurement of soil water content. Report 125, Institute of Hydrology, Wallingford, UK, 39 pp.

Dean, T J, Bell, J P & Baty, A J B (1987) Soil moisture measurement by an improved capacitance technique: Part 1. Sensor design and performance. *Journal of Hydrology* 93, 67–78.

Deka, R N, Wairu, M, Mtakwa, P W, Mullins, C E, Veenendaal, E M & Townend, J (1995) Use and accuracy of the filter paper technique for measurement of soil matric potential. *European Journal of Soil Science* 46, 233–238.

Delin, K A, Jackson, S P, Johnson, D W, Burleigh, S C, Woodrow, R R, McAuley, J M, Dohm, J M, Ip, F, Ferré, P A, Rucker, D F & Baker, V R (2002) Environmental studies with the sensor web: Principles and practice. *Sensors* 5, 103–117.

Delta-T (2005) Augering Manual for PR2 and PR1. Manual Version AUG-UM-2.2 July 2005, Delta-T Devices, Cambridge, UK, 25 pp.

Delta-T (2013) User Manual for the ML3 ThetaProbe. Manual Version ML3-UM-1.0 April 2013, Delta-T Devices, Cambridge, UK, 47 pp.

Desilets, D & Zreda, M (2013) Footprint diameter for a cosmic-ray soil moisture probe: Theory and Monte Carlo simulations. *Water Resources Research* 49, 3566–3575.

Desilets, D, Zreda, M & Ferré, T P A (2010) Nature's neutron probe: Land surface hydrology at an elusive scale with cosmic rays. *Water Resources Research* 46, W11505.

Diez, J A, Caballero, R, Román, R, Tarquis, A M, Cartagena, M C & Vallejo, A (2000) Integrated fertilizer and irrigation management to reduce nitrate leaching in Central Spain. *Journal of Environmental Quality* 29, 1539–1547.

Dirksen, C (1975) Determination of soil water diffusivity by sorptivity measurements. *Soil Science Society of America Proceedings* 39, 1012–1013.

Dirksen, C (1991) Unsaturated hydraulic conductivity. In: *Soil Analysis: Physical Methods* (Eds. K A Smith & C E Mullins), Marcel Dekker, New York, 209–269.

Dirksen, C (1999) *Soil Physics Measurements*. Catena-Verlag, Reiskirchen, Germany.

Dirksen, C (2001) Unsaturated hydraulic conductivity. In: *Soil and Environmental Analysis: Physical Methods* (Eds. K A Smith & C E Mullins), Marcel Dekker, New York, 183–237.

Dirksen, C & Matula, S (1994) Automatic atomized water spray system for soil hydraulic conductivity measurements. *Soil Science Society of America Journal* 58, 319–325.

Doering, E J (1965) Soil-water diffusivity by the one-step method. *Soil Science* 99, 322–326.

Dolman, A J, Stewart, J B & Cooper, J D (1988) Predicting forest transpiration from climatological data. *Agricultural & Forest Meteorology* 42, 339–353.

Dowdell, R J, Webster, C P, Hill, D & Mercer, E R (1984) A lysimeter study of the fate of fertilizer nitrogen in spring barley crops grown on shallow soil overlying Chalk: Crop uptake and leaching losses. *Journal of Soil Science* 35, 169–181.

Dreiss, S J & Anderson, L D (1985) Estimating vertical soil moisture flux at a land treatment site. *Ground Water* 23, 503–511.

Edmunds, W M & Gaye, C B (1994) Estimating the spatial variability of groundwater recharge in the Sahel using chloride. *Journal of Hydrology* 156, 47–59.

Edmunds, W M, Lovelock, P E R & Gray, D A (1973) Interstitial water chemistry and aquifer properties in the Upper and Middle Chalk of Berkshire, England. *Journal of Hydrology* 19, 21–31.

Ehlers, W & van der Ploeg, R R (1976) Evaporation, drainage and unsaturated hydraulic conductivity of tilled and untilled fallow soil. *Zeitschrift für Pflanzenernährung und Bodenkunde* 139, 373–386.

Elder, A N & Rasmussen, T C (1994) Neutron probe calibration in unsaturated tuff. *Soil Science Society of America Journal* 58, 1301–1307.

Elrick, D E, Reynolds, W D & Tan, K A (1989) Hydraulic conductivity measurements in the unsaturated zone using improved well analyses. *Ground Water Monitoring Review* 9, 184–193.

Enfield, C G, Hsieh, J J C & Warrick, A W (1973) Evaluation of water flux above a deep water table using thermocouple psychrometers. *Soil Science Society of America Proceedings* 37, 968–970.

Ernst, F (1950) Een nieuwe formule voor de berekening van de doorlaatfactor met de boorgatenmethode. Report Landbouwproefsta. En Bodemkundig, TNO Institute, Groningen, Netherlands.

Evett, S R (2000a) The TACQ program for automatic time domain reflectometry measurements: I. Design and operating characteristics. *Transactions of the American Society of Agricultural Engineers* 43, 1939–1946.

Evett, S R (2000b) The TACQ program for automatic time domain reflectometry measurements: II. Waveform interpretation methods. *Transactions of the American Society of Agricultural Engineers* 43, 1947–1956.

Evett, S R (2000c) Some aspects of time domain reflectometry, neutron scattering, and capacitance methods for soil water content measurement. In: *Comparison of Soil Water Measurement using the Neutron Scattering, Time Domain Reflectometry and Capacitance Methods*. International Atomic Energy Agency, Vienna, 5–49.

Evett, S R (2007) Soil water and monitoring technology. In: *Irrigation of Agricultural Crops*, Agronomy Monograph 30, 2nd edn., ASA-CSSA-SSSA, Madison, WI. 25–84.

Evett, S R, Tolk, J A & Howell, T A (2005) TDR laboratory calibration in travel time, bulk electrical conductivity and effective frequency. *Vadose Zone Journal* 4, 1020–1029.

Evett, S R, Tolk, J A & Howell, T A (2006a) Soil profile water content determination: Sensor accuracy, axial response, calibration, temperature dependence, and precision. *Vadose Zone Journal* 5, 894–907.

Evett, S R, Tolk, J A & Howell, T A (2006b) Response to 'Comments on "TDR laboratory calibration in travel time, bulk electrical conductivity, and effective frequency"'. *Vadose Zone Journal* 5, 1073–1075.

Evett, S R, Ruthardt, B B & Copeland, K S (2006c) External full-time vacuum lysimeter drainage system. *Applied Engineering in Agriculture* 22, 875–880.

Evett, S R, Heng, L, Moutonnet, P & Nguyen, M L (2008) *Field Estimation of Soil Water Content: A Practical Guide to Methods, Instrumentation, and Sensor Technology*. IAEA-TCS-30. International Atomic Energy Agency, Vienna, Austria, 131 pp.

Evett, S R, Schwartz, R C, Howell, T A, Baumhardt, R L & Copeland, K S (2012) Can weighing lysimeter ET represent surrounding field ET well enough to test flux station measurements of daily and sub-daily ET? *Advances in Water Resources* 50, 79–90.

Fawcett, R G & Collis-George, N (1967) A filter-paper method for determining the moisture characteristic of soil. *Australian Journal of Experimental Agriculture* 7, 162–167.

Feng, W, Lin, C-P, Deschamps, R J & Drnevich, V P (1999) Theoretical model of a multisection time domain reflectometry measurement system. *Water Resources Research* 35, 2321–2331.

Fernández-Gálvez, J, Verhoef, A & Barahona, E (2007) Estimating soil water fluxes from soil water records obtained using dielectric sensors. *Hydrological Processes* 21, 2785–2793.

Ferré, P A, Rudolph, D L & Kachanoski, R G (1996) Spatial averaging of water content by time domain reflectometry: Implications for twin rod probes with and without dielectric coatings. *Water Resources Research* 32, 271–279.

Ferré, P A, Knight, J H, Rudolph, D L & Kachanoski, R G (1998) The sample areas of conventional and alternative time domain reflectometry probes. *Water Resources Research* 34, 2971–2979.

Fityus, S G, Wells, P A & Huang, W (2011) Water content measurement in expansive soils using the neutron probe. *Geotechnical Testing Journal* 34, 1–10.

Flint, A L, Flint, L E & Richards, K A (1994) Evaluation of measurement scale using imbibition experiments in volcanic tuffs. *Soil Science Society of America Journal* 58, 94–102.

Flint, A L, Campbell, G S, Ellett, K M & Calissendorf, C (2002a) Calibration and temperature correction of heat dissipation matric potential sensors. *Soil Science Society of America Journal* 66, 1439–1445.

Flint, A L, Flint, L E, Kwicklis, E M, Fabryka-Martin, J M & Bodvarsson, G S (2002b) Estimating recharge at Yucca Mountain, Nevada, USA: Comparison of methods. *Hydrogeology Journal* 10, 180–204.

Flühler, H, Ardakani, M S & Stolzy, L H (1976) Error propagation in determining hydraulic conductivities from successive water content and pressure head profiles. *Soil Science Society of America Journal* 40, 830–836.

Foster, S S D & Smith-Carington, A (1980) The interpretation of tritium in the Chalk unsaturated zone. *Journal of Hydrology* 46, 343–365.

Fourt, D F & Hinson, W H (1970) Water relations of tree crops: I. A comparison between Corsican Pine and Douglas Fir in south-east England. *Journal of Applied Ecology* 7, 295–309.

Franz, T E (2012) *Installation and Calibration of the Cosmic-Ray Soil Moisture Probe*. University of Arizona,Tucson, AZ, 12 pp.

Franz, T E, King, E G, Caylor, K K & Robinson, D A (2011) Coupling vegetation organization patterns to soil resource heterogeneity in a central Kenyan dryland using geophysical imagery. *Water Resources Research* 47, W07531.

Franz, T E, Zreda, M, Ferré, T P A, Rosolem, R, Zweck, C, Stillman, S, Zeng, X & Shuttleworth, W J (2012) Measurement depth of the cosmic ray soil moisture probe affected by hydrogen from various sources. *Water Resources Research* 48, W08515.

Franz, T E, Zreda, M, Rosolem, R & Ferré, T P A (2013) A universal calibration function for determination of soil moisture with cosmic-ray neutrons. *Hydrology & Earth System Sciences* 17, 453–460. doi: 10.5194/hess-17-453-2013.

Frede, H-G, Weinzierl, W & Meyer, B (1984) Kurzmitteilung Ein tragbares elektronisches Einstich-Tensiometer (A portable electronic puncture tensiometer). *Zeitschrift für Pflanzenernährung und Bodenkunde* 147, 131–134.

Friel, R & Or, D (1999) Frequency analysis of time-domain reflectometry (TDR) with application to dielectric spectroscopy of soil constituents. *Geophysics* 64, 707–718.

Furman, A, Warrick, A W & Ferré, T P A (2002) Electrical potential distributions in a heterogeneous subsurface in response to applied current. *Vadose Zone Journal* 1, 273–280.

Furman, A, Ferré, T P A & Warrick, A W (2003) A sensitivity analysis of electrical resistivity tomography array types using analytical element modeling. *Vadose Zone Journal* 2, 416–423.

Furman, A, Ferré, T P A & Warrick, A W (2004) Optimization of ERT surveys for monitoring transient hydrological events using perturbation sensitivity and genetic algorithms. *Vadose Zone Journal* 3, 1230–1239.

Garambois, S, Sénéchal, P & Perroud, H (2002) On the use of combined geophysical methods to assess water content and water conductivity of near-surface formations. *Journal of Hydrology* 259, 32–48.

Gardner, C M K (1990) *Recharge in Lincolnshire: Estimates from Soil Water Measurements*. Institute of Hydrology, Wallingford, UK, 76 pp.

Gardner, C M K, Cooper, J D, Wellings, S R, Bell, J P, Hodnett, M G, Boyle, S A & Howard, M J (1990) Hydrology of the unsaturated zone of the Chalk of south east England. In: *Chalk* (Eds. J B Burland, R N Mortimore, L D Roberts, D L Jones & B O Corbett), Thomas Telford, London, 611–618.

Gardner, W R (1958) Some steady-state solutions of the unsaturated moisture flow equation with application to evaporation from a water table. *Soil Science* 85, 228–232.

Gaskin, G J & Miller, J D (1996) Measurement of soil water content using a simplified impedance measuring technique. *Journal of Agricultural Engineering Research* 63, 153–160.

Gee, G W & Hillel, D (1988) Groundwater recharge in arid regions: Review and critique of estimation methods. *Hydrological Processes* 2, 255–266.

Germán-Heins, J & Flury, M (2000) Sorption of brilliant blue FCF in soils affected by pH and ionic strength. *Geoderma* 97, 87–101.

Giesche, H (2006) Mercury porosimetry: A general (practical) overview. *Particle & Particle Systems Characterization* 23, 1–11.

Giese, K & Tiemann, R (1975) Determination of the complex permittivity from a thin sample time-domain reflectometry, improved analysis of the step response waveform. *Advances in Molecular Relaxation Processes* 7, 45–59.

Giesel, W, Lorch, S, Renger, M & Strebel, O (1970) Water-flow calculations by means of gamma-absorption and tensiometer field measurements in the unsaturated soil profile. In: *Isotope Hydrology 1970*, International Atomic Energy Agency, Vienna, 663–672.

Gieske, A & de Vries, J J (1990) Note on the analysis of moisture–depth curves obtained by the hot-air method for the determination of soil moisture diffusivity. *Journal of Hydrology* 115, 261–268.

Glenn, D M, Henderson, R L & Bolton, F E (1980) A retractable, neutron-probe access tube. *Agronomy Journal* 72, 1067–1068.

Glubrecht, H & Kühn, W (1971) Additional paper, 4th UN International Conference on the Peaceful Uses of Atomic Energy, Geneva, September 1971. Report AED-CONF-71-100-45, Zentralstelle für Atomkernenergie—Dokumentation, Leopoldshafen.

Gooddy, D C, Shand, P, Kinniburgh, D G & Van Riemsdijk, W H (1995) Field-based partition coefficients for trace elements in soil solutions. *European Journal of Soil Science* 46, 265–285.

Gorden, D S & Veneman, P L M (1995) Soil water pressure measurements in subzero air temperatures. *Soil Science Society of America Journal* 59, 1242–1243.

Goss, M J & Youngs, E G (1983) The use of horizontal piezometers for *in situ* measurements of hydraulic conductivity below the water table. *Journal of Soil Science* 34, 659–664.

Granier, A (1987) Evaluation of transpiration in a Douglas-fir stand by means of sapflow measurements. *Tree Physiology* 3, 309–320.

Grant, D R (1975) Measurement of soil moisture near the surface using a neutron moisture meter. *Journal of Soil Science* 26, 124–129.

Greacen, E L (1981) *Soil Water Assessment by the Neutron Method*. CSIRO Publishing, Collingwood, VIC.

Greacen, E L & Hignett, C (1979) Sources of bias in the field calibration of a neutron meter. *Australian Journal of Soil Research* 17, 405–415.

Greacen, E L & Schrale, G (1976) The effect of bulk density on neutron meter calibration. *Australian Journal of Soil Research* 14, 159–169.

Green, R E & Corey, J C (1971) Calculation of hydraulic conductivity: a further evaluation of some predictive methods. *Soil Science Society of America Proceedings* 35, 3–8.

Green, R E, Ahuja, L R & Chong, S K (1986) Hydraulic conductivity, diffusivity and sorptivity of unsaturated soils: Field methods. In: *Methods of Soil Analysis: Part 1. Physical and Mineralogical Methods*, 2nd edn. (Ed. A Klute), American Society of Agronomy, Madison, WI, 771–798.

Greenwood, K L & Daniel, H (1996) A double-puncture technique for improving the accuracy of puncture tensiometer measurements. *Australian Journal of Soil Research* 34, 153–159.

Grossmann, J & Udluft, P (1991) The extraction of water by the suction-cup method: A review. *Journal of Soil Science* 42, 83–93.

Gunston, H M & Eeles, C W O (1979) Operational experience with neutron moisture meter equipment in Kenya. *East African Agricultural & Forestry Journal* 43, 308–311.

Hallett, P D & Young, I M (1999) Changes to water repellance of soil aggregates caused by substrate-induced microbial activity. *European Journal of Soil Science* 50, 35–40.

Ham, J M & Benson, E J (2004) On the construction and calibration of dual-probe heat capacity sensors. *Soil Science Society of America Journal* 68, 1185–1190.

Hamamatsu (2006) *Photomultiplier Tubes – Basics and Applications*. Hamamatsu Photonics K. K., Electron Tube Division, Hamamatsu City, Shizuoka, 309 pp.

Hamblin, A P (1981) Filter-paper method for routine measurement of field water potential. *Journal of Hydrology* 53, 355–360.

Hanna, L W & Siam, N (1980) The estimation of moisture in the top 10 cm of soil using a neutron probe. *Journal of Agricultural Science* 94, 251–253.

Harris, W (1973) A method for improving the accuracy of measuring soil moisture near the soil surface with a neutron meter. Agricultural Research Council Letcombe Laboratory Annual Report, 1973, Letcombe Regis, Oxfordshire, UK, 56–58.

Haverkamp, R, Vauclin, M & Vachaud, G (1984) Error analysis in estimating soil water content from neutron probe measurements: 1. Local standpoint. *Soil Science* 137, 78–90.

Haverkamp, R, Ross, P J, Smettem, K R J & Parlange, J-Y (1994) Three-dimensional analysis of infiltration from the disc infiltrometer: 2. Physically-based infiltration equation. *Water Resources Research* 30, 2931–2935.

Healy, R W (1989) Seepage through a hazardous-waste trench cover. *Journal of Hydrology* 108, 213–241.

Healy, R W & Mills, P C (1991) Variability of an unsaturated sand unit underlying a radioactive-waste trench. *Soil Science Society of America Journal* 55, 899–907.

Heimovaara, T J (1994) Frequency domain analysis of time domain reflectometry waveforms: 1. Measurement of the complex

dielectric permittivity of soils. *Water Resources Research* 30, 189–199.

Heimovaara, T J (2001) Frequency domain modeling of TDR waveforms in order to obtain frequency-dependent dielectric properties of soil samples: A theoretical approach. In: *Proceedings of the 2nd International Symposium & Workshop on Time Domain Reflectometry for Geotechnical Applications*, September 5–7 2001. Available at www.iti.northwestern.edu/tdr/tdr2001/proceedings/Final/TDR2001.pdf.

Heimovaara, T J & Bouten, W (1990) A computer-controlled 36-channel time-domain reflectometry system for monitoring soil water contents. *Water Resources Research* 26, 2311–2316.

Heimovaara, T J & de Water, E (1993) A computer controlled TDR system for measuring water content and bulk electrical conductivity of soils. Report 41, Laboratory of Physical Geography and Soil Science, University of Amsterdam, Netherlands.

Heimovaara, T J, Huisman, J A, Vrugt, J A & Bouten, W (2004) Obtaining the spatial distribution of water content along a TDR probe using the SCEM-UA Bayesian inverse modeling scheme. *Vadose Zone Journal* 3, 1128–1145.

Heitman, J L, Basinger, J M, Kluitenberg, G J, Ham, J M, Frank, J M & Barnes, P L (2003) Field evaluation of the dual-probe heat-pulse method for measuring soil water content. *Vadose Zone Journal* 2, 552–560.

Hendrickx, J M H, Nieber, J L & Siccama, P D (1994) Effect of tensiometer cup size on field soil water tension variability. *Soil Science Society of America Journal* 58, 309–315.

Herrero, J, Robinson, D A & Nogués, J (2007) A regional soil survey approach for upgrading from flood to sprinkler irrigation in a semi-arid environment. *Agricultural Water Management* 93, 145–152.

Hignett, C, Correll, R L & Klem, D J (1980) A field calibration of neutron moisture meter and gamma ray density probe in a duplex soil profile. CSIRO Divison of Soils Report 46, Adelaide, Australia, 9 pp.

Hillel, D (2004) *Introduction to Environmental Soil Physics*. Elsevier Academic Press, San Diego, CA, 494 pp.

Hillel, D & Benyamini, Y (1974) Experimental comparison of infiltration and drainage methods for determining unsaturated hydraulic conductivity of a soil profile *in situ*. In: *Isotope and Radiation Techniques in Soil Physics and Irrigation Studies*, International Atomic Energy Agency, Vienna, 271–275.

Hillel, D & Gardner, W R (1970) Measurement of unsaturated conductivity and diffusivity by infiltration through an impeding layer. *Soil Science* 109, 149–153.

Hodnett, M G & Bell, J P (1986) Soil moisture investigations of groundwater recharge through black cotton soils in Madhya Pradesh, India. *Hydrological Sciences Journal* 31, 361–381.

Hodnett, M G & Bell, J P (1990) Processes of water movement through a Chalk Coombe deposit in southeast England. *Hydrological Processes* 4, 361–372.

Hodnett, M G & Bell, J P (1991) Neutron probe standards: Transport shields or a large drum of water? *Soil Science* 151, 113–120.

Holder, M, Brown, K W, Thomas, J C, Zabcik, D & Murray, H E (1991) Capillary-wick unsaturated zone soil pore water sampler. *Soil Science Society of America Journal* 55, 1195–1202.

Hook, W R, Livingston, N J, Sun, Z J & Hook, P J (1992) Remote diode shorting improves measurement of soil water by time domain reflectometry. *Soil Science Society of America Journal* 56, 1384–1391.

Hopmans, J W & Dane, J H (1986) Temperature dependence of soil hydraulic properties. *Soil Science Society of America Journal* 50, 4–19.

Hopmans, J W, Šimůnek, J & Bristow, K L (2002a) Indirect estimation of soil thermal properties and water flux from heat pulse measurements: Geometry and dispersion effects. *Water Resources Research* 38, 1006.

Hopmans, J W, Šimůnek, J, Romano, N & Durner, W (2002b) Simultaneous determination of water transmission and retention properties. Inverse methods. In: *Methods of Soil Analysis: Part 4. Physical Methods* (Eds. J H Dane & G C Topp), Soil Science Society of America, Madison, WI, 963–1008.

Hornbuckle, B K, Irvin, S, Franz, T E, Rosolem, R & Zweck, C (2012) The potential of the COSMOS network to be a source of new soil moisture information for SMOS and SMAP. In: *Proceedings of the IEEE International Geoscience & Remote Sensing Symposium*, Munich, Germany, 1243–1246.

Hosty, M & Mulqueen, J (1996) Soil moisture and ground water drawdown in a dry grassland soil. *Irish Journal of Agricultural and Food Research* 35, 17–24.

Howell, T A, Schneider, A D, Dusek, J, Marek, T H & Steiner, J L (1995) Calibration and scale performance of Bushland weighing lysimeters. *Transactions of the American Society of Agricultural Engineers* 38, 1019–1024.

Howse, K R (1981) A technique for using permanent neutron meter access tubes in cultivated soils. *Experimental Agriculture* 17, 265–269.

Huang, W & Fityus, S G (2008) Numerical study of neutron probe measurement of water content in expansive soils. In: *Proceedings of the 12th International Conference of the International Association for Computer Methods and Advances in Geomechanics*, 1–6 October 2008, Goa, India. Curran Associates, Red Hook, NY, 1420–1427.

Hubbell, J M & Sisson, J B (1996) Portable tensiometer use in deep boreholes. *Soil Science* 161, 376–381.

Hubbell, J M & Sisson, J B (1998) Advanced tensiometer for shallow or deep water potential measurements. *Soil Science* 163, 271–277.

Hubbell, J M, Nicholl, M J, Sisson, J B & McElroy, D L (2004) Application of a Darcian approach to estimate liquid flux in a deep vadose zone. *Vadose Zone Journal* 3, 560–569.

Huisman, J A, Hubbard, S S, Redman, J D & Annan, A P (2003) Measuring soil water content with ground penetrating radar: A review. *Vadose Zone Journal* 2, 476–491.

Huo, Z, Feng, S, Dai, X, Zheng, Y & Wang, Y (2012) Simulation of hydrology following various volumes of irrigation to soil with different depths to the water table. *Soil Use & Management* 28, 229–239.

IAEA (2012) *Regulations for the Safe Transport of Radioactive Material*, 2012 edn. IAEA Safety Standards Series No. SSR-6, International Atomic Energy Agency, Vienna, Austria, 168 pp.

ICRP (2007) *Recommendations of the International Commission on Radiological Protection*. ICRP Publication 103, International Commission on Radiological Protection, Ottawa, ON.

IMKO (2013a) User Manual for TRIME®-PICO IPH. IMKO Micromodultechnik GmbH, D-76275 Ettlingen, Germany, 35 pp.

IMKO (2013b) Manual for TRIME®-PICO 64/32. IMKO Micromodultechnik GmbH, D-76275 Ettlingen, Germany, 53 pp.

Ingram, H A P, Coupar, A M & Bragg, O M (2001) Theory and practice of hydrostatic lysimeters for direct measurement of net seepage in a patterned mire in north Scotland. *Hydrology & Earth System Sciences* 5, 693–709.

Ireson, A M, Wheater, H S, Butler, A P, Mathias, S, Finch, J & Cooper, J D (2006) Hydrological processes in the Chalk unsaturated zone – insights from an intensive field monitoring programme. *Journal of Hydrology* 330, 29–43.

Irmak, S & Haman, D Z (2001) Performance of the Watermark® granular matrix sensor in sandy soils. *Applied Engineering in Agriculture* 17, 787–795.

ISO (1995) Soil quality—Determination of water content in the unsaturated zone—Neutron depth probe method. ISO 10573:1995. International Standards Organisation, 13 pp.

ISO (1998a) Soil quality—Determination of dry bulk density. ISO 11272:1998. International Standards Organisation, 10 pp.

ISO (1998b) Soil quality—Determination of particle density. ISO 11508:1998. International Standards Organisation, 5 pp.

ISO (2001) Soil quality—Determination of soil water content as a volume fraction using coring sleeves—Gravimetric method. ISO 11461:2001. International Standards Organisation, 6 pp.

ISO (2003) Soil quality—Determination of soil water content as a volume fraction on the basis of known dry bulk density—Gravimetric method. ISO 16586:2003. International Standards Organisation, 7 pp.

Iwata, Y & Hirota, T (2005) Monitoring over-winter soil water dynamics in a freezing and snow-covered environment using a thermally insulated tensiometer. *Hydrological Processes* 19, 3013–3019.

Jacobsen, O H & Schjønning, P (1993) A laboratory calibration of time domain reflectometry for soil water measurement including effects of bulk density and texture. *Journal of Hydrology* 151, 147–157.

Jarvis, N J, Leeds-Harrison, P B & Dosser, J M (1987) The use of tension infiltrometers to assess routes and rates of infiltration in a clay soil. *Journal of Soil Science* 38, 633–640.

Jayawickreme, D H, Van Dam, R L & Hyndman, D W (2008) Subsurface imaging of vegetation, climate, and root-zone moisture interactions. *Geophysical Research Letters* 35, L18404.

Jewell, D E (1990) Soil water movement in glacial till. In: *Irrigation and Drainage* (Ed. S C Harris), American Society of Civil Engineers, New York, 315–322.

Jol, H M (2009) *Ground Penetrating Radar: Theory and Applications*. Elsevier, Amsterdam.

Jones, H K & Cooper, J D (1998) Water transport through the unsaturated zone of the Middle Chalk: A case study from Fleam Dyke lysimeter. In: *Groundwater Pollution, Aquifer Recharge and Vulnerability* (Ed. N S Robins), Special Publication 130, Geological Society, London, 117–128.

Jones, S B & Or, D (2001) Extending TDR measurement range in saline soils using frequency domain methods. In: *Proceedings of the 2nd International Symposium & Workshop on Time Domain Reflectometry for Geotechnical Applications*, 5–7 September 2001. Available at www.iti.northwestern.edu/tdr/tdr2001/proceedings/Final/TDR2001.pdf, 140–148.

Jones, S B, Wraith, J M & Or, D (2002) Time domain reflectometry measurement principles and applications. *Hydrological Processes* 16, 141–153.

Joshi, B, Maule, C & De Jong, E (1997) Subsurface hydrologic regime and estimation of diffuse soil water flux in a semi arid region. *Electronic Journal of Geotechnical Engineering* 2. Available at www.ejge.com (accessed on 27 August 2015).

Journel, A G & Huijbregts, Ch J (1978) *Mining Geostatistics*. Academic Press, New York, 600 pp.

Jung, W K, Kitchen, N R, Sudduth, K A, Kremer, R J & Motavalli, P P (2005) Relationship of apparent soil electrical conductivity to claypan soil properties. *Soil Science Society of America Journal* 69, 883–892.

Jury, W A & Horton, R (2004) *Soil Physics*, 6th edn. Wiley, Hoboken, NJ, 384 pp.

Karunarathna, A K, Chhoden, T, Kawamoto, K, Komatsu, T, Møldrup, P & de Jonge, L W (2010) Estimating hysteretic soil-water retention curves in hydrophobic soil by a mini tensiometer-TDR coil probe. In: *Transactions of the 19th World Congress of Soil Science*, 1–6 August 2010, Brisbane, Australia. International Union of Soil Sciences, Vienna, Austria.

Kawanishi, H (1983) A soil-water flux sensor and its use for field studies of transfer processes in surface soil. *Journal of Hydrology* 60, 357–365.

Kelleners, T J, Soppe, R W G, Robinson, D A, Schaap, M, Ayars, J E & Skaggs, T H (2004a) Calibration of capacitance probe sensors using electric circuit theory. *Soil Science Society of America Journal* 68, 430–439.

Kelleners, T J, Soppe, R W G, Ayars, J E & Skaggs, T H (2004b) Calibration of capacitance probe sensors in a saline silty clay soil. *Soil Science Society of America Journal* 68, 770–778.

Kelleners, T J, Seyfried, M S, Blonquist, J M, Bilskie, J & Chandler, D G (2005) Improved interpretation of water content reflectometer measurements in soils. *Soil Science Society of America Journal* 69, 1684–1690.

Keller, B R, Everett, L G & Marks, R J (1990) Effect of access tube material and grout on neutron probe measurements in the vadose zone. *Ground Water Monitoring Review* 10, 96–100.

Kengni, L, Vachaud, G, Thony, J L, Laty, R, Garino, B, Casabianca, H, Jame, P & Viscogliosi, R (1994) Field measurements of water and nitrogen losses under irrigated maize. *Journal of Hydrology* 162, 23–46.

Kessler, J & Oosterbaan, R J (1974) Determining hydraulic conductivity of soils. In: *Drainage Principles and Applications. III: Surveys and Investigations*, ILRI Publication 16, International Institute for Land Reclamation and Improvement, Wageningen, 253–296.

Khanzode, R M, Vanapalli, S K & Fredlund, D G (2002) Measurement of soil-water characteristic curves for fine-grained soils using a small-scale centrifuge. *Canadian Geotechnical Journal* 39, 1209–1217.

Kimura, R, Kamichika, M, Takayama, N, Matsuoka, N & Zhang, X (2004) Heat balance and soil moisture in the Loess Plateau. *Journal of Agricultural Meteorology (Japan)* 60, 103–113.

Kimura, R, Fan, J, Zhang, X, Takayama, N, Kamichika, M & Matsuoka, N (2006) Evapotranspiration over the grassland field in the Liudaogou basin of the Loess Plateau, China. *Acta Oecologica* 29, 45–53.

Kinniburgh, D G & Miles, D L (1983) Extraction and chemical analysis of interstitial water from soils and rocks. *Environmental Science & Technology* 17, 362–368.

Kirsch, S W (1993) A field test of a soil-based measure of evapotranspiration. *Soil Science* 156, 396–404.

Kirsch, R (2009) *Groundwater Geophysics: A Tool for Hydrogeology*, 2nd edn. Springer-Verlag, Berlin & Heidelberg, 493 pp.

Kitanidis, P K (1997) *Introduction to Geostatistics: Applications to Hydrogeology*. Cambridge University Press, Cambridge, UK, 272 pp.

Kitching, R & Bridge, L R (1974) Lysimeter installations in sandstone at Styrrup, Nottinghamshire. *Journal of Hydrology* 23, 219–232.

Kitching, R & Shearer, T R (1982) Construction and operation of a large undisturbed lysimeter to measure recharge to the Chalk aquifer, England. *Journal of Hydrology* 58, 267–277.

Kitching, R, Shearer, T R & Shedlock, S L (1977) Recharge to Bunter Sandstone determined from lysimeters, *Journal of Hydrology* 33, 217–232.

Kitching, R, Edmunds, W M, Shearer, T R, Walton, N R G & Jacovides, J (1980) Assessment of recharge to aquifers. *Hydrological Sciences Bulletin* 25, 217–235.

Kizito, F, Campbell, C S, Campbell, G S, Cobos, D R, Teare, B L, Carter, B & Hopmans, J W (2008) Frequency, electrical conductivity and temperature analysis of a low-cost capacitance soil moisture sensor. *Journal of Hydrology* 352, 367–378.

Klaij, M C & Vachaud, G (1992) Seasonal water balance of a sandy soil in Niger cropped with pearl millet, based on profile moisture measurements. *Agricultural Water Management* 21, 313–330.

Kluitenberg, G J & Philip, J R (1999) Dual thermal probes near plane interfaces. *Soil Science Society of America Journal* 63, 1585–1591.

Kluitenberg, G J, Ham, J M & Bristow, K L (1993) Error analysis of the heat pulse method for measuring soil volumetric heat capacity. *Soil Science Society of America Journal* 57, 1444–1451.

Kluitenberg, G J, Bristow, K L & Das, B S (1995) Error analysis of the heat pulse method for measuring soil heat capacity, diffusivity and conductivity. *Soil Science Society of America Journal* 59, 719–726.

Klute, A & Peters, D B (1966) Hydraulic and pressure head measurements with strain gauge pressure transducers. In: *Water in the Unsaturated Zone*, Vol. 1 (Eds. P E Rijtema & H Wassink), IASH Publication 82, International Association for Scientific Hydrology-UNESCO, Gentbrugge, Belgium, 156–165.

Knight, J H (1992) Sensitivity of time domain reflectometry measurements to lateral variations in soil water content. *Water Resources Research* 28, 2345–2352.

Knight, J H & Kluitenberg, G J (2004) Simplified computational approach for dual-probe heat-pulse method. *Soil Science Society of America Journal* 68, 447–449.

Knight, J H, Jin, W & Kluitenberg, G J (2007) Sensitivity of the dual-probe heat-pulse method to spatial variations in heat capacity and water content. *Vadose Zone Journal* 6, 746–758.

Knutson, J H, Lee, S B, Zhang, W Q & Selker, J (1993) Fiberglass wick preparation for use in passive capillary wick soil porewater samplers. *Soil Science Society of America Journal* 57, 1474–1476.

Kool, J B & Parker, J C (1987) Development and evaluation of closed-form expressions for hysteretic soil hydraulic-properties. *Water Resources Research* 23, 105–114.

Kosugi, K & Katsuyama, M (2004) Controlled-suction period lysimeter for measuring vertical water flux and convective chemical fluxes. *Soil Science Society of America Journal* 68, 371–382.

Kreutzer, K, Strebel, O & Renger, M (1980) Field measurement of seepage and evapotranspiration rate for a soil under plant cover: A comparison of soil water balance and tritium labeling procedure. *Journal of Hydrology* 48, 137–146.

Kutilek, M & Nielsen, D R (1994) *Soil Hydrology*. Catena-Verlag, Reiskirchen, Germany, 370 pp.

Lal, R & Shukla, M (2004) *Principles of Soil Physics*. Marcel Dekker, New York.

Lassabatère, L, Angulo-Jaramillo, R, Soria Ugalde, J M, Cuenca, R H, Braud, I & Haverkamp, R (2006) Beerkan estimation of soil transfer parameters through infiltration experiments – BEST. *Soil Science Society of America Journal* 70, 521–532.

Lawrence, G P (1977) Measurement of pore sizes in soils: A review of existing techniques. *Journal of Soil Science* 28, 527–540.

Lawrence, G P, Payne, D & Greenland, D J (1979) Pore size distribution in critical point and freeze dried aggregates form clay subsoils. *Journal of Soil Science* 30, 499–516.

Lax, P D (1972) The formation and decay of shock waves. *American Mathematical Monthly* 79, 227–241.

Ledieu, J, de Ridder, P, de Clerck, P & Dautrebande, S (1986) A method of measuring soil moisture by time domain reflectometry. *Journal of Hydrology* 88, 319–328.

Leeds-Harrison, P B & Youngs, E G (1997) Estimating the hydraulic conductivity of soil aggregates conditioned by different tillage treatments from sorption measurements. *Soil & Tillage Research* 41, 141–147.

Leeds-Harrison, P B, Youngs, E G & Uddin, B (1994) A device for determining the sorptivity of soil aggregates. *European Journal of Soil Science* 45, 269–272.

Leibundgut, Ch, Maloszewski, P & Külls, C (2009) *Tracers in Hydrology*. Wiley, Chichester, UK, 432 pp.

Lentz, R D & Kincaid, D C (2003) An automated vacuum extraction control system for soil water percolation samplers. *Soil Science Society of America Journal* 67, 100–106.

Lesch, S M, Corwin, D L & Robinson, D A (2005) Apparent soil electrical conductivity mapping as an agricultural tool for arid zone soil. *Computers and Electronics in Agriculture* 46, 351–378.

Li, J, Smith, D W, Fityus, S G & Sheng, D (2003a) Numerical analysis of neutron moisture probe measurements. *International Journal of Geomechanics* 3, 11–20.

Li, J, Smith, D W & Fityus, S G (2003b) The effect of a gap between the access tube and the soil during neutron probe measurements. *Australian Journal of Soil Research* 41, 151–164.

Libardi, P L, Reichardt, K, Nielsen, D R & Biggar, J W (1980) Simplified field methods for estimating the unsaturated hydraulic conductivity. *Soil Science Society of America Journal* 44, 3–7.

Lin, C-P (2003) Frequency domain versus travel time analyses of TDR waveforms for soil moisture measurements. *Soil Science Society of America Journal* 67, 720–729.

Logsdon, S D (2009) CS616 calibration: Field versus laboratory. *Soil Science Society of America Journal* 73, 1–6.

Loke, M H (2012) Tutorial: 2-D and 3-D electrical imaging surveys. Available at http://www.geotomosoft.com/downloads.php (accessed on 8 August 2015).

Lourenço, S D N, Gallipoli, D, Toll, D G, Augarde, C E, Evans, F D & Medero, G M (2008) Calibrations of a high-suction tensiometer. *Geoderma* 58, 659–668.

Luckner, L, van Genuchten, M Th & Nielsen, D R (1989) A consistent set of parametric models for the two-phase flow of immiscible fluids in the subsurface. *Water Resources Research* 25, 2187–2193.

Mahler, C F & Dienne, A A (2007) Tensiometer development for high suction analysis in laboratory lysimeters. In: *Experimental Unsaturated Soil Mechanics* (Ed. T Schanz), Vol. 112, Springer, Berlin, 103–105.

Mahmood-ul-Hassan, M & Gregory, P J (2002) Dynamics of water movement on Chalkland. *Journal of Hydrology* 257, 27–41.

Malicki, M A, Plagge, R & Roth, C H (1996) Improving the calibration of dielectric TDR soil moisture determination taking into account the solid soil. *European Journal of Soil Science* 47, 357–366.

Marcesse, J (1967) Détermination *in situ* de la capacité de rétention d'un sol au moyen de l'humidimètre à neutrons. In: *Isotope and Radiation Techniques in Soil Physics and Irrigation Studies*, International Atomic Energy Agency, Vienna, 137–146.

Marek, T H, Schneider, A D, Howell, T A & Ebeling, L L (1988) Design and construction of large weighing monolithic lysimeters. *Transactions of the American Society of Agricultural Engineers* 31, 477–484.

Marquardt, D W (1963) An algorithm for least-squares estimation of non-linear parameters. *Journal of the Society for Industrial & Applied Mathematics* 11, 431–441.

Marshall, T J (1958) A relation between permeability and size distribution of pores. *Journal of Soil Science* 9, 1–8.

Marshall, T J, Holmes, J W & Rose, C W (1996) *Soil Physics*. Cambridge University Press, Cambridge, UK, 472 pp.

Marthaler, H P, Vogelsanger, W, Richard, F & Wierenga, P J (1983) A pressure transducer for field tensiometers. *Soil Science Society of America Journal* 47, 624–627.

Matzdorf, K D, Cassel, D K, Worcester, B K & Malo, D D (1975) *In situ* hydraulic conductivity at four hillslope locations in a closed drainage system. *Soil Science Society of America Proceedings* 39, 508–512.

McCulloch, D B & Wall, T (1976) A method of measuring the neutron absorption cross-sections of soil samples for calibration of the neutron moisture meter. *Nuclear Instruments & Methods* 137, 577–581.

McElroy, D L & Hubbell, J M (2004) Evaluation of the conceptual flow model for a deep vadose zone system using advanced tensiometers. *Vadose Zone Journal* 3, 170–182.

McGowan, M (1974) Depths of water extraction by roots. Application to soil-water balance studies. In: *Isotope and Radiation Techniques in Soil Physics and Irrigation Studies*, International Atomic Energy Agency, Vienna, 435–445.

McGowan, M & Williams, J B (1980) The water balance of an agricultural catchment: I. Estimation of evaporation from soil water records. *Journal of Soil Science* 31, 217–230.

McNeill, J D (1980) Electromagnetic terrain conductivity measurement at low induction numbers. Technical Note TN-6, Geonics Ltd, Mississauga, ON. Available at http://www.geonics.com/html/technicalnotes.html (accessed on 8 August 2015).

McQueen, I S & Miller, R F (1968) Calibration and evaluation of a wide-range gravimetric method for measuring stress. *Soil Science* 106, 225–231.

Mdaghri-Alaoui, A & Eugster, W (2001) Field determination of the water balance of the Areuse River delta, Switzerland. *Hydrological Sciences Journal* 46, 747–760.

Meilani, I, Rahardjo, H, Leong, E C & Fredlund, D G (2002) Mini suction probe for matric suction measurements. *Canadian Geotechnical Journal* 39, 1427–1432.

Meissner, R, Seeger, J, Rupp, H, Seyfarth, M & Borg, H (2007) Measurement of dew, fog and rime with a high-precision gravitation lysimeter. *Journal of Plant Nutrition & Soil Science* 170, 335–344.

Meissner, R, Rupp, H, Seeger, J, Ollesch, G & Gee, G W (2010) A comparison of water flux measurements: Passive wick-samplers versus drainage lysimeters. *European Journal of Soil Science* 61, 609–621.

Melville, J G, Molz, F J & Guven, O (1985) Laboratory investigation and analysis of a ground-water flowmeter. *Ground Water* 23, 486–495.

Mendes, J, Gallipoli, D, Toll, D G, Augarde, C E & Evans, F D (2008) A system for field measurement of suctions using high capacity tensiometers. In: *Unsaturated Soils: Advances in Geo-Engineering* (Eds. D G Toll, C E Augarde, D Gallipoli & S Wheeler), Taylor and Francis, London, 219–225.

Merrill, S D & Rawlins, S L (1972) Field measurement of soil water potential with thermocouple psychrometers. *Soil Science* 113, 102–109.

Miller, J D & Gaskin, G J (1999) ThetaProbe ML2x: Principles of operation and applications. Technical Note (2nd edn.), Macaulay Land Use Research Institute. 20 pp. Available from http://www.macaulay.ac.uk/MRCS/pdf/tprobe.pdf (accessed on 8 August 2015).

Miller, E E & Salehzadeh, A (1993) Stripper for bubble-free tensiometry. *Soil Science Society of America Journal* 57, 1470–1473.

Millington, R J & Quirk, J P (1959) Permeability of porous media. *Nature* 183, 387–388.

Millington, R J & Quirk, J P (1961) Permeability of porous solids. *Transactions of the Faraday Society* 57, 1200–1207.

Moffett, K B, Robinson, D A & Gorelick, S M (2010) Relationship of salt marsh vegetation zonation to spatial patterns in soil moisture, salinity, and topography. *Ecosystems* 13, 1287–1302.

Mojid, M A, Wyseure, G C L & Rose, D A (1997) Extension of the measurement range of electrical conductivity by time-domain reflectometry (TDR). *Hydrology & Earth System Sciences* 1, 175–183.

Mojid, M A, Rose, D A & Wyseure, G C L (2007) A model incorporating the diffuse double layer to predict the electrical conductivity of bulk soil. *European Journal of Soil Science* 58, 560–572.

Monteith, J (1965) Evaporation and the environment. *Symposia of the Society of Experimental Biology* 19, 205–234.

Mori, Y, Hopmans, J W, Mortensen, A P & Kluitenberg, G J (2003) Multifunctional heat pulse probe for simultaneous measurement of soil water content, solute concentration, and heat transport parameters. *Vadose Zone Journal* 2, 561–571.

Mori, Y, Hopmans, J W, Mortensen, A P & Kluitenberg, G J (2005) Estimation of vadose zone water flux from multi-functional heat pulse probe measurement. *Soil Science Society of America Journal* 69, 599–606.

Morris, E M & Cooper, J D (2004) Density measurements in ice boreholes using neutron scattering. *Journal of Glaciology* 49, 599–604.

Mortensen, A P, Hopmans, J W, Mori, Y & Šimůnek, J (2006) Multifunctional heat pulse probe measurements of coupled vadose zone flow and transport. *Advances in Water Resources* 29, 250–267.

Moutonnet, P, Pluyette, N, El Mourabit, N & Couchat, P (1988) Measuring the spatial variability of soil hydraulic conductivity using an automatic neutron moisture gauge. *Soil Science Society of America Journal* 52, 1521–1526.

Mualem, Y (1976) A new model for predicting the hydraulic conductivity of unsaturated porous media. *Water Resources Research* 12, 513–522.

Mualem, Y & Friedman, S P (1991) Theoretical prediction of electrical conductivity in saturated and unsaturated soil. *Water Resources Research* 27, 2771–2777.

Mullins, C E (2001) Matric potential. In: *Soil and Environmental Analysis: Physical Methods* (Eds. K A Smith & C E Mullins), Marcel Dekker, New York, 65–93.

Mullins, C E & Smith, K A (Eds.) (2001) *Soil and Environmental Analysis: Physical Methods*. Marcel Dekker, New York, 637 pp.

Nadler, A & Frenkel, H (1980) Determination of soil solution conductivity from bulk soil electrical conductivity measurements by the four-electrode method. *Soil Science Society of America Journal* 44, 1216–1221.

Nichol, C, Beckie, R & Smith, L (2002) Evaluation of uncoated and coated time domain reflectometry probes for high electrical conductivity systems. *Soil Science Society of America Journal* 66, 1454–1465.

Nicolls, K D, Hutton, J T & Honeysett, J L (1977) Gadolinium in soils and its effect on the count rate of the neutron moisture meter. *Australian Journal of Soil Research* 15, 287–291.

Nimmo, J R, Akstin, K C & Mello, K A (1992) Improved apparatus for measuring hydraulic conductivity at low water content. *Soil Science Society of America Journal* 56, 1758–1761.

Nimmo, J R, Stonestrom, D A & Akstin, K C (1994) The feasibility of recharge rate measurements using the steady state centrifuge method. *Soil Science Society of America Journal* 58, 49–56.

Nimmo, J R, Perkins, K S & Lewis, A M (2002a) Steady-state centrifuge. In: *Methods of Soil Analysis: Part 4. Physical Methods* (Eds. J H Dane & G C Topp), Soil Science Society of America, Madison, WI, 903–916.

Nimmo, J R, Deason, J A, Izbicki, J A & Martin, P (2002b) Evaluation of unsaturated-zone water fluxes in heterogeneous alluvium at a Mojave Basin site. *Water Resources Research* 38, 1215.

Nissen, H H, Møldrup, P & Henriksen, K (1998) High-resolution time domain reflectometry coil probe for measuring soil water content. *Soil Science Society of America Journal* 62, 1203–1211.

Nissen, H H, Møldrup, P, Olesen, T & Rasmark, P (1999) Printed circuit board time domain reflectometry probe: Measurements of soil water content. *Soil Science* 164, 454–466.

Nissen, H H, Ferré, T P A & Møldrup, P (2003a) Time domain reflectometry developments in soil science: I. Unbalanced two-rod probe spatial sensitivity and sampling volume. *Soil Science* 168 77–83.

Nissen, H H, Ferré, T P A & Møldrup, P (2003b) Sample area of two- and three-rod time domain reflectometry probes. *Water Resources Research* 39, 1289.

Norikane, J H, Prenger, J J, Rouzan-Wheeldon, D T & Levine, H G (2005) A comparison of soil moisture sensors for space flight applications. *Applied Engineering in Agriculture* 21, 211–216.

Noborio, K, Horton, R & Tan, C S (1999) Time domain reflectometry probe for simultaneous measurement of soil matric potential and water content. *Soil Science Society of America Journal* 63, 1500–1505.

Normand, B, Recous, S, Vachaud, G, Kengni, L & Garino, B (1997) Nitrogen-15 tracers combined with tensio-neutronic method to estimate the nitrogen balance of irrigated maize. *Soil Science Society of America Journal* 61, 1508–1518.

Ølgaard, P L (1965) On the Theory of the Neutronic Method for Measuring the Water Content in Soil. Report No. 97, Danish Atomic Energy Commission, Risø, Denmark, 97 pp.

Or, D, Hartwell, T, Fisher, B, Hubscher, R A & Wraith, J M (1998) *WinTDR99 – Users Guide*. Utah Agricultural Experiment Station Research, Logan, UT, http://soilphysics.usu.edu/wintdr/english/doc/html (accessed on 8 August 2015).

Oschner, T E, Horton, R & Ren, T (2003) Use of the dual-probe heat-pulse technique to monitor soil water content in the vadose zone. *Vadose Zone Journal* 2, 572–579.

Oschner, T E, Horton, R, Kluitenberg, G J & Wang, Q (2005) Evaluation of the heat pulse ratio method for measuring soil water flux. *Soil Science Society of America Journal* 69, 757–765.

Pachepsky, Y A & Rawls, W J (2003) Soil structure and pedotransfer functions. *European Journal of Soil Science* 54, 443–451.

Paltineanu, I C & Starr, J L (1997) Real-time soil water dynamics using multisensor capacitance probes: Laboratory calibration. *Soil Science Society of America Journal* 61, 1576–1585.

Papritz, A & Webster, R (1995a) Estimating change in soil monitoring: I. Statistical theory. *European Journal of Soil Science* 46, 1–12.

Papritz, A & Webster, R (1995b) Estimating change in soil monitoring: II. Sampling from simulated fields. *European Journal of Soil Science* 46, 13–27.

Parkes, M E & Siam, N (1979) Error associated with the measurement of soil moisture change by the neutron probe. *Journal of Agricultural Engineering Research* 24, 87–93.

Patterson, D E & Smith, M W (1981) The measurement of unfrozen water content by time domain reflectometry: Results from laboratory tests. *Canadian Geotechnical Journal* 18, 131–144.

Payne, W A, Wendt, C W & Lascano, R J (1990) Bare fallowing on sandy fields of Niger, West Africa. *Soil Science Society of America Journal* 54, 1079–1084.

Peck, A J & Rabbidge, R M (1966) Soil-water potential: Direct measurement by a new technique. *Science* 151, 1385–1386.

Peck, A J & Rabbidge, R M (1969) Design and performance of an osmotic tensiometer for measuring capillary potential. *Soil Science Society of America Proceedings* 33, 196–202.

Pelowitz, D B (Ed.) (2005) MCNPX user's manual, version 5. Report LA-CP-05-0369, Los Alamos National Laboratory, Los Alamos, NM.

Penman, H L (1948) Natural evaporation from open water, bare soil and grass. *Proceedings of the Royal Society A* 193, 120–146.

Perrier, E & Marsh, A W (1958) Performance characteristics of various electrical resistance units and gypsum materials. *Soil Science* 86, 140–147.

Perroux, K M & White, I (1988) Designs for disc permeameters. *Soil Science Society of America Journal* 52, 1205–1215.

Phene, C J, Hoffman, G J & Rawlins, S L (1971a) Measuring soil matric potential *in situ* by sensing heat dissipation within a porous body: I. Theory and sensor construction. *Soil Science Society of America Proceedings* 35, 27–33.

Phene, C J, Rawlins, S L & Hoffman, G J (1971b) Measuring soil matric potential *in situ* by sensing heat dissipation within a porous body: II. Experimental results. *Soil Science Society of America Proceedings* 35, 225–229.

Philip, J R (1957) The theory of infiltration: 4. Sorptivity and algebraic infiltration equations. *Soil Science* 84, 257–264.

Philip, J R (1973) On solving the unsaturated flow equation: 1. The flux-concentration relation. *Soil Science* 116, 328–335.

Philip, J R (1985) Reply to 'Comments on steady infiltration from spherical cavities'. *Soil Science Society of America Journal* 49, 788–789.

Philip, J R & de Vries, D A (1957) Moisture movement in porous materials under temperature gradients. *Transactions of the American Geophysical Union* 38 222–232.

Philip, J R & Kluitenberg, G J (1999) Errors of dual thermal probes due to soil heterogeneity across a plane interface. *Soil Science Society of America Journal* 63, 1579–1585.

Philip, J R & Knight, J H (1974) On solving the flow equation: 3. New quasi-analytical technique. *Soil Science* 117, 1–13.

Pieper, G F (1949) The measurement of soil moisture by the slowing down of neutrons. Ph.D. thesis, Cornell University, Ithaca, NY.

Pierpont, G (1966) Measuring surface soil moisture with the neutron depth probe and a surface shield. *Soil Science* 101, 189–192.

Pirie, E, Lin, K & Taylor, D (1968) Soil density measurements with gamma rays. *Soil Science* 106, 411–414.

van der Ploeg, M J, Gooren, H P A, Bakker, G & de Rooij, G H (2008) Matric potential measurements by polymer tensiometers in cropped lysimeters under water-stressed conditions. *Vadose Zone Journal* 7, 1048–1054.

van der Ploeg, M J, Gooren, H P A, Bakker, G, Hoogendam, C W, Huiskes, C, Koopal, L K, Kruidhof, H & de Rooij, G H (2010) Polymer tensiometers with ceramic cones: Performance in drying soils and comparison with water-filled tensiometers and time domain reflectometry. *Hydrology & Earth System Sciences* 14, 1787–1799.

Porter, J, Arzberger, P & Braun, H-W (2005) Wireless sensor networks for ecology. *BioScience* 55, 561–572.

Poulovassilis, A, Krentos, V D, Stylianou, Y & Metochis, Ch (1974) Soil-water properties of layered soils determined *in situ*. In: *Isotope and Radiation Techniques in Soil Physics and Irrigation Studies*, International Atomic Energy Agency, Vienna, 205–224.

Prebble, R E, Forrest, J A, Honeysett, J L, Hughes, M W, McIntyre, D S & Schrale, G (1981) Field installation and maintenance. In: *Soil Water Assessment by the Neutron Method* (Ed. E L Greacen), CSIRO, Melbourne, Australia, 82–98.

Priestley, C H B & Taylor, R J (1972) On the assessment of surface heat flux and evaporation using large scale parameters. *Monthly Weather Review* 100, 81–82.

Primault, B (1962) Du calcul de l'évapotranspiration (On the calculation of evapotranspiration). *Archives for Meteorology, Geophysics, and Bioclimatology, Series B* 12, 124–150.

Proulx-McInnis, S, St-Hilaire, A, Rousseau, A N, Jutras, S, Carrer, G & Levrei, G (2011) Technical note: Development of an automated lysimeter for the calculation of peat soil actual evapotranspiration. *Hydrology & Earth System Sciences Discussions* 8, 5009–5033.

Rab, M A, Willatt, S T & Olsson, K A (1987) Hydraulic properties of a duplex soil from *in situ* measurements. *Australian Journal of Soil Research* 25, 1–7.

Ragab, R & Cooper, J D (1993) Variability of unsaturated zone water transport parameters: Implications for hydrological modelling: 2. Predicted vs. *in situ* measurements and evaluation of methods. *Journal of Hydrology* 148, 133–147.

Rajkai, K, Kabos, S & van Genuchten, M Th (2004) Estimating the water retention curve from soil properties: Comparison of linear, nonlinear and concomitant variable methods. *Soil & Tillage Research* 79, 145–152.

Reatto, A, Silva, E M, Bruand, A, Martins, E S & Lima, J E (2008) Validity of the centrifuge method for determining the water retention properties of tropical soils. *Soil Science Society of America Journal* 72, 1547–1553.

Redman, J D, Davis, J L, Galagedara, L W & Parkin, G W (2002) Field studies of GPR air launched surface reflectivity measurements of soil water content. In: *Proceedings of the SPIE 4758, Proceedings of the Ninth International Conference on Ground Penetrating Radar* (Eds. S Koppenjan & H Lee), University of Santa Barbara, Goleta, CA, 156–161.

Reece, C F (1996) Evaluation of a line heat dissipation sensor for measuring soil matric potential. *Soil Science Society of America Journal* 60, 1022–1028.

Reedy, R C & Scanlon, B R (2003) Soil water content monitoring using electromagnetic induction. *Journal of Geotechnical & Geoenvironmental Engineering* 129, 1028–1039.

Reicosky, D C, Doty, C W & Campbell, R B (1977) Evapotranspiration and soil water movement beneath the root zone of irrigated and nonirrigated millet (*Panicum miliaceum*). *Soil Science* 124, 95–101.

Ren, T, Noborio, K & Horton, R (1999) Measuring soil water content, electrical conductivity, and thermal properties with a thermo-time domain reflectometry probe. *Soil Science Society of America Journal* 63, 450–457.

Ren, T, Oschner, T E & Horton, R (2003a) Development of thermo-time domain reflectometry for vadose zone measurements. *Vadose Zone Journal* 2, 544–551.

Ren, T, Oschner, T E, Horton, R & Ju, Z (2003b) Heat-pulse method for soil water content measurement: Influence of the specific heat of the soil solids. *Soil Science Society of America Journal* 67, 1631–1634.

Ren, T, Ju, Z, Gong, Y & Horton, R (2005) Comparing heat-pulse and time domain reflectometry soil water contents from thermo-time domain reflectometry probes. *Vadose Zone Journal* 4, 1080–1086.

Renger, M, Giesel, W, Strebel, O & Lorch, S (1970) Erste Ergebnisse zur quantitativen Erfassung der Wasserhaushaltskomponenten in der ungesättigten Bodenzone (Quantitative determination of the water conservation equation components in the unsaturated soil zone: Preliminary results). *Zeitschrift für Pflanzenernährung und Bodenkunde* 126, 15–33.

Reynolds, W D (1986) The Guelph Permeameter method for *in situ* measurement of field-saturated hydraulic conductivity and matric flux potential. Ph.D. dissertation. University of Guelph, Guelph, ON, Canada.

Reynolds, W D & Elrick, D E (1986) A method for simultaneous *in situ* measurement in the vadose zone of field-saturated hydraulic conductivity, sorptivity and the conductivity-pressure relationship. *Ground Water Monitoring Review* 6, 84–95.

Reynolds, W D & Elrick, D E (1990) Ponded infiltration from a small ring: Part 1. Analysis of steady flow. *Soil Science Society of America Journal* 54, 1233–1241.

Reynolds, W D, Elrick, D E & Clothier, B E (1985) The constant head well permeameter: Effect of unsaturated flow. *Soil Science* 139, 172–180.

Rhoades, J D (1996) Salinity: Electrical conductivity and total dissolved solids. In: *Methods of Soil Analysis: Part 3. Chemical Methods* (Ed. D L Sparks), American Society of Agronomy, Madison, WI, 417–435.

Rhoades, J D, Raats, P A C & Prather, R J (1976) Effects of liquid-phase electrical conductivity, water content, and surface conductivity on bulk soil electrical conductivity. *Soil Science Society of America Journal* 40, 651–655.

Rhoades, J D, Manteghi, N A, Shouse, P J & Alves, W J (1989) Soil electrical conductivity and soil salinity: New formulations and calibrations. *Soil Science Society of America Journal* 53, 433–439.

Rice, R (1975) Diurnal and seasonal soil water uptake and flux within a Bermudagrass root zone. *Soil Science Society of America Proceedings* 39, 394–398.

Richards, L A (1931) Capillary conduction of liquids through porous media. *Physics* 1, 318–333.

Richards, L A & Ogata, G (1958) Thermocouple for vapor pressure measurement in biological and soil systems at high humidity. *Science* 128, 1089–1090.

Richards, L A, Gardner, W R & Ogata, G (1956) Physical processes determining water loss from soil. *Soil Science Society of America Proceedings* 20, 310–314.

Ridley, A M & Burland, J B (1993) A new instrument for the measurement of soil moisture suction. *Géotechnique* 43, 321–324.

Robinson, D A & Friedman, S P (2000) Parallel plates compared to conventional rods as TDR waveguides for sensing soil moisture. *Subsurface Sensing Technologies and Applications* 1, 497–511.

Robinson, D A, Gardner, C M K, Evans, J, Cooper, J D, Hodnett, M G & Bell, J P (1998) The dielectric calibration of capacitance probes for soil hydrology using an oscillation frequency response model. *Hydrology & Earth System Sciences* 2, 111–120.

Robinson, D A, Gardner, C M K & Cooper, J D (1999) Measurement of relative permittivity in sandy soils using TDR, capacitance and theta probes: Comparison including effects of bulk soil electrical conductivity. *Journal of Hydrology* 223, 198–211.

Robinson, D A, Jones, S B, Wraith, J M, Or, D & Friedman, S P (2003) A review of advances in dielectric and electrical conductivity

measurement in soils using time domain reflectometry. *Vadose Zone Journal* 2, 444–475.

Robinson, D A, Lebron, I, Lesch, S M & Shouse, P J (2004) Minimizing drift in electrical conductivity measurements in high temperature environments using the EM-38. *Soil Science Society of America Journal* 68, 339–345.

Robinson, D A, Schaap, M, Or, D & Jones, S B (2005) On the effective measurement frequency of time domain reflectometry in dispersive and nonconductive dielectric materials. *Water Resources Research* 41, W02007.

Robinson, D A, Abdu, H, Jones, S B, Seyfried, M S, Lebron, I & Knight, R (2008) Eco-geophysical imaging of watershed-scale soil patterns links with plant community spatial patterns. *Vadose Zone Journal* 7, 1132–1138.

Robinson, D A, Lebron, I, Kocar, B, Phan, K, Sampson, M, Crook, N & Fendorf, S (2009) Time-lapse geophysical imaging of soil moisture dynamics in tropical deltaic soils: An aid to interpreting hydrological and geochemical processes. *Water Resources Research* 45, W00D32.

Robinson, D A, Abdu, H, Lebron, I & Jones, S B (2012) Imaging of hill-slope soil moisture wetting patterns in a semi-arid oak savanna catchment using time-lapse electromagnetic induction. *Journal of Hydrology* 416, 39–49.

Rodda, J C (1967) The systematic error in rainfall measurement. *Journal of the Institution of Water Engineers* 21, 173–177.

Rojas, J C, Pagano, M C, Zingariello, M C, Mancuso, C, Giordano, G & Passeggio, G (2008) A new high capacity tensiometer. In: *Unsaturated Soils: Advances in Geo-Engineering* (Eds. D G Toll, C E Augarde, D Gallipoli & S Wheeler), Taylor and Francis, London.

Román, R, Caballero, R, Bustos, A, Diez, J A, Cartagena, M C, Ballejo, A & Caballero, A (1996) Water and solute movement under conventional corn in Central Spain: I. Water balance. *Soil Science Society of America Journal* 60, 1530–1536.

Román, R, Caballero, R & Bustos, A (1999) Field water drainage under traditional and improved irrigation schedules for corn in central Spain. *Soil Science Society of America Journal* 63, 1811–1817.

de Rooij, G H & Stagnitti, F (2000) Spatial variability of solute leaching: Experimental validation of a quantitative parameterization. *Soil Science Society of America Journal* 64, 499–504.

Rose, C W (2004) *An Introduction to the Environmental Physics of Soil, Water, and Watersheds*. Cambridge University Press, Cambridge, UK.

Rose, C W & Stern, W R (1967) Determination of withdrawal of water from soil by crop roots as a function of depth and time. *Australian Journal of Soil Research* 5, 11–19.

Rosolem, R, Shuttleworth, W J, Zreda, M, Franz, T E, Zeng, X & Kurc, S A (2013) The effect of atmospheric water vapor on the cosmic-ray soil moisture signal. *Journal of Hydrometeorology* 14, 1659–1671.

Royer, J-M & Vachaud, G (1974) Détermination direct de l'évapotranspiration et de l' infiltration par mésures des teneurs en eau et des succions. *Hydrological Sciences Bulletin* 19, 319–336.

Royer, J-M & Vachaud, G (1975) Field determination of hysteresis in soil-water characteristics. *Soil Science Society of America Proceedings* 39, 221–223.

Rubin, Y & Hubbard, S S (Eds.) (2005) *Hydrogeophysics*. Water Science and Technology Library Series, Springer, The Netherlands, 50, 523 pp.

Rubio, C M, Llorens, P & Gallart, F (2008) Uncertainty and efficiency of pedotransfer functions for estimating water retention characteristics of soils. *European Journal of Soil Science* 59, 339–347.

Rutter, H K, Cooper, J D, Pope, D, Smith, M & Gallagher, A (2012) New understanding of deep unsaturated zone controls on recharge in the Chalk: A case study near Patcham, SE England. *Quarterly Journal of Engineering Geology & Hydrogeology, London* 45, 487–495.

Sadeghi, A M, Scott, H D & Ferguson, J A (1984) Estimating evaporation: A comparison between Penman, Idso–Jackson, and zero-flux methods. *Agricultural & Forest Meteorology* 33, 225–238.

Sauer, T J, Moore, P A Jr., Ham, J M, Bland, W L, Prueger, J H & West, C P (2002) Seasonal water balance of an Ozark hillslope. *Agricultural Water Management* 55, 71–82.

Scanlon, B R, Healy, R W & Cook, P G (2002a) Choosing appropriate techniques for quantifying groundwater recharge. *Hydrogeology Journal* 10, 18–39.

Scanlon, B R, Healy, R W & Cook, P G (2002b) Erratum: Choosing appropriate techniques for quantifying groundwater recharge. *Hydrogeology Journal* 10, 347.

Scanlon, B R, Keese, K, Flint, A L, Flint, L E, Gaye, C B, Edmunds, W M & Simmers, I (2006) Global synthesis of groundwater recharge in semiarid and arid regions. *Hydrological Processes* 20, 3335–3370.

Schaap, M, Leij, F J & van Genuchten, M Th (2001) Rosetta: A computer program for estimating soil hydraulic parameters with hierarchical pedotransfer functions. *Journal of Hydrology* 251, 163–176.

Schaap, M, Robinson, D A, Friedman, S P & Lazar, A (2003) Measurement and modeling of the dielectric permittivity of layered granular media using time domain reflectometry. *Soil Science Society of America Journal* 67, 1113–1121.

Schindler, U, Durner, W, von Unold, G & Muller, L (2010) Evaporation method for measuring unsaturated hydraulic properties of soils: Extending the measurement range. *Soil Science Society of America Journal* 74, 1071–1083.

Scholl, D G (1976) Soil moisture flux and evapotranspiration determined from soil hydraulic properties in a Chaparral stand. *Soil Science Society of America Journal* 40, 14–18.

Scholl, D G (1978) A two-element ceramic sensor for matric potential and salinity measurements. *Soil Science Society of America Journal* 42, 429–432.

Schuh, W M, Meyer, R F, Sweeney, M D & Gardner, J C (1993a) Spatial variation of root-zone and shallow vadose-zone drainage on a loamy glacial till in a sub-humid climate. *Journal of Hydrology* 148, 1–26.

Schuh, W M, Klinkebiel, D L & Gardner, J C (1993b) Use of an integrated transient flow and water budget procedure to predict and partition components of local recharge. *Journal of Hydrology* 148, 27–60.

Schwärzel, K & Bohl, H P (2003) An easily installable groundwater lysimeter to determine water balance components and hydraulic properties of peat soils. *Hydrology & Earth System Sciences* 7, 23–32.

Schwärzel, K, Menzer, A, Clausnitzer, F, Spank, U, Häntzschel, J, Grünwald, T, Köstner, B, Bernhofer, C & Feger, K-H (2009) Soil water content measurements deliver reliable estimates of water fluxes: A comparative study in a beech and a spruce stand in the Tharandt forest (Saxony, Germany). *Agricultural & Forest Meteorology* 149, 1994–2006.

Scotter, D R, Clothier, B E & Harper, E R (1982) Measuring saturated hydraulic conductivity and sorptivity using twin rings. *Australian Journal of Soil Research* 20, 295–304.

Selker, J (2002) Passive capillary sampler. In: *Methods of Soil Analysis: Part 4. Physical Methods* (Eds. J H Dane & G C Topp), Soil Science Society of America, Madison, WI, 1266–1269.

Selker, J, Graff, L & Steenhuis, T (1993) Noninvasive time domain reflectometry moisture measurement probe. *Soil Science Society of America Journal* 57, 934–936.

Sentek (2003) *Access Tube Installation Guide*, Version 1.0. Sentek Pty Ltd., Stepney, South Australia, 54 pp.

Sentek (2011) *Moisture Calibration Manual* Ver. 2. Sentek Pty Ltd., Stepney, South Australia, 56 pp.

Seyfried, M S & Murdock, M D (2001) Response of a new soil water sensor to variable soil, water content, and temperature. *Soil Science Society of America Journal* 65, 28–34.

Sharma, M L, Bari, M & Byrne, J (1991) Dynamics of seasonal recharge beneath a semiarid vegetation on the Gnangara mound, Western Australia. *Hydrological Processes* 5, 383–398.

Sherlock, M D & McDonnell, J J (2003) A new tool for hillslope hydrologists: Spatially distributed groundwater level and soil water content measured using electromagnetic induction. *Hydrological Processes* 17, 1965–1977.

Siemens, J & Kaupenjohann, M (2004) Comparison of three methods for field measurement of solute leaching in a sandy soil. *Soil Science Society of America Journal* 68, 1191–1196.

Simmonds, L P & Nortcliff, S (1998) Small scale variability in the flow of water and solutes, and the implications for lysimeter studies of solute leaching. *Nutrient Cycling in Agroecosystems* 50, 65–75.

Sisodia, S & Helweg, O J (1998) Modeling the heat sense flowmeter. *Journal of Irrigation & Drainage Engineering* 124, 148–151.

Sisson, J B, Ferguson, A H & van Genuchten, M Th (1980) Simple method for predicting drainage from field plots. *Soil Science Society of America Journal* 44, 1147–1152.

Sisson, J B, Klittich, W M & Salem, S B (1988) Comparison of two methods for summarizing hydraulic conductivities of a layered soil. *Water Resources Research* 24, 1271–1276.

Slater, L, Zaidman, M D, Binley, A & West, L J (1997) Electrical imaging of saline tracer migration for the investigation of unsaturated zone transport mechanisms. *Hydrology & Earth System Sciences* 1, 291–302.

Smettem, K R J & Clothier, B E (1989) Measuring unsaturated sorptivity and hydraulic conductivity using multi-disc permeameters. *Journal of Soil Science* 40, 563–568.

Smiles, D E & Youngs, E G (1963) A mulitple-well method for determining the hydraulic conductivity of a soil *in situ*. *Journal of Hydrology* 1, 279–287.

Smiles, D E & Youngs, E G (1965) Hydraulic conductivity determinations by several field methods in a sand tank. *Soil Science* 99, 83–87.

Soilmoisture Equipment Corp. (2012) *2800 Guelph Permeameter Operating Instructions*. Soilmoisture Equipment Corporation, Santa Barbara, CA, 60 pp.

Song, Y, Ham, J M, Kirkham, M B & Kluitenberg, G J (1998) Measuring soil water content under turfgrass using the dual-probe heat-pulse technique. *Journal of the American Society for Horticultural Science* 123, 937–941.

Song, Y, Kirkham, M B, Ham, J M & Kluitenberg, G J (1999) Dual probe heat pulse technique for measuring soil water content and sunflower water uptake. *Soil & Tillage Research* 50, 345–348.

Song, Y, Kirkham, M B, Ham, J M & Kluitenberg, G J (2000) Root-zone hydraulic lift evaluated with the dual-probe heat-pulse technique. *Australian Journal of Soil Research* 38, 927–935.

Spaans, E J A & Baker, J M (1993) Simple baluns in parallel probes for time domain reflectometry. *Soil Science Society of America Journal* 57, 668–673.

Spanner, D C (1951) The Peltier effect and its use in the measurement of suction pressure. *Journal of Experimental Botany* 2, 145–168.

Stammers, W N, Igwe, O C & Whiteley, H R (1973) Calculation of evaporation from measurements of soil water and the soil water characteristic. *Canadian Journal of Agricultural Engineering* 15, 2–5.

Steenhuis, T, Jackson, C D, Kung, S K & Brutsaert, W (1985) Measurement of groundwater recharge in eastern Long Island, New York, USA. *Journal of Hydrology* 79, 145–169.

Stein, J & Kane, D L (1983) Monitoring the unfrozen water content of soil and snow using time domain reflectometry. *Water Resources Research* 19, 1573–1584.

Stephens, D B & Knowlton, R G Jr. (1986) Soil water movement and recharge through sand at a semiarid site in New Mexico. *Water Resources Research* 22, 881–889.

Stephens, D B, Lambert, K & Watson, D (1987) Regression models for hydraulic conductivity and field test of the borehole permeameter. *Water Resources Research* 23, 2207–2214.

Stone, L R, Horton, M L & Olson, T C (1973a) Water loss from an irrigated sorghum field: I. Water flux within and below the root zone. *Agronomy Journal* 65, 492–495.

Stone, L R, Horton, M L & Olson, T C (1973b) Water loss from an irrigated sorghum field: II. Evapotranspiration and root extraction. *Agronomy Journal* 65, 495–497.

Strebel, O (1970) Messung der Bodenwasserspannung mit Hg-Manometer-Tensiometern bei Lufttemperaturen unter 0°C (Mercury manometer-type tensiometers for use at temperatures below 0°C). *Zeitschrift für Pflanzenernährung und Bodenkunde* 126, 111–116.

Strebel, O, Renger, M & Giesel, W (1973) Soil suction measurements for evaluation of vertical water flow at greater depths with a pressure transducer tensiometer. *Journal of Hydrology* 81, 297–332.

Sun, Y, Ren, S, Ren, T & Minasny, B (2010) A combined frequency domain and tensiometer sensor for determining soil water characteristic curves. *Soil Science Society of America Journal* 74, 492–494. doi: 10.2136/sssaj2009.0047N.

Takamatsu, T, Koshikawa, M K, Watanabe, M, Hou, H & Murata, T (2007) Design of a meso-scale indoor lysimeter for undisturbed soil to investigate the behaviour of solutes in soil. *European Journal of Soil Science* 58, 329–334.

Take, W A & Bolton, M D (2003) Tensiometer saturation and the reliable measurement of soil suction. *Géotechnique* 53, 159–172.

Talsma, T (1969) *In situ* measurement of sorptivity. *Australian Journal of Soil Research* 7, 269–276.

Tang, C Y (1996) Interception and recharge processes beneath a *Pinus elliotii* forest. *Hydrological Processes* 10, 1427–1434.

Tarantino, A & Mongiovi, L (2001) Experimental procedures and cavitation mechanisms in tensiometer measurements. *Geotechnical & Geological Engineering* 19, 189–210.

Tarara, J M & Ham, J M (1997) Measuring soil water content in the laboratory and field with dual-probe heat-capacity sensors. *Agronomy Journal* 89, 535–542.

Telford, W M, Geldart, L P & Sheriff, R E (1990) *Applied Geophysics*, 2nd edn. Cambridge University Press, New York.

Theis, C V (1935) The relation between the lowering of the piezometric surface and the rate of duration of discharge of a well

using ground water storage. *Transactions of the American Geophysical Union* 16, 519–524.

Thony, J L, Vachaud, G & Vauclin, M (1989) Analyse critique de mésures tensiometriques par capteur de pression portatif. *Bulletin du GFHN* 25, 11–34.

Thony, J L, Vachaud, G, Clothier, B E & Angulo-Jaramillo, R (1991) Field measurements of the hydraulic properties of soil. *Soil Technology* 4, 111–123.

Thornthwaite, C W (1948) An approach toward a rational classification of climate. *Geographical Review* 38, 55–94.

Topp, G C & Davis, J L (1985) Measurement of soil water content using time-domain reflectometry (TDR): A field evaluation. *Soil Science Society of America Journal* 49, 19–24.

Topp, G C, Davis, J L & Annan, A P (1980) Electromagnetic determination of soil water content: Measurements in coaxial transmission lines. *Water Resources Research* 16, 574–582.

Triantafilis, J, Roe, J A E & Monteiro Santos, F A (2011) Detecting a leachate plume in an aeolian sand landscape using a DUALEM-421 induction probe to measure electrical conductivity followed by inversion modelling. *Soil Use & Management* 27, 357–366.

Tseng, P T & Jury, W A (1993) Simulation of field measurement of hydraulic conductivity in unsaturated heterogeneous soil. *Water Resources Research* 29, 2087–2099.

Tsujimura, M, Numaguti, A, Tian, L, Hashimoto, S, Sugimoto, A & Nakawo, M (2001) Behavior of subsurface water revealed by stable isotope and tensiometric observation in the Tibetan Plateau. *Journal of the Meteorological Society of Japan* 79, 599–605.

Tyner, J S, Arya, L M & Wright, W C (2006) The dual gravimetric hot-air method for measuring soil water diffusivity. *Vadose Zone Journal* 5, 1281–1286.

Vachaud, G, Royer, J-M & Cooper, J D (1977) Comparison of methods of calibration of a neutron probe by gravimetry or neutron-capture model. *Journal of Hydrology* 34, 343–356.

Vachaud, G, Passerat de Silans, P, Balabanis, P & Vauclin, M (1985) Temporal stability of spatially measured soil water probability density function. *Soil Science Society of America Journal* 49, 822–828.

Van Bavel, C H M & Stirk, G B (1967) Soil water measurement with an 241Am-Be neutron source and an application to evaporimetry. *Journal of Hydrology* 5, 40–46.

Van Bavel, C H M, Stirk, G B & Brust, K J (1968) Hydraulic properties of a clay loam soil and the field measurement of water uptake by roots: 1. Interpretation of water content and pressure profiles. *Soil Science Society of America Proceedings* 32, 310–317.

Van den Berg, G J & Louters, T (1986) An algorithm for computing the relationship between diffusivity and soil moisture content from the hot air method. *Journal of Hydrology* 83, 149–159.

Van der Velde, M, Green, S R, Gee, G W, Vanclooster, M & Clothier, B E (2005) Evaluation of drainage from passive suction and non-suction fluxmeters in a volcanic clay soil under tropical conditions. *Vadose Zone Journal* 4, 1201–1209.

van Genuchten, M Th (1980) A closed-form equation for predicting the hydraulic conductivity of unsaturated soils. *Soil Science Society of America Journal* 44, 892–898.

van Genuchten, M Th & Wierenga, P J (1976) Mass transfer studies in sorbing porous media: I. Analytical solutions. *Soil Science Society of America Journal* 40, 473–480.

Van Vuuren, W E (1984) Problems involved in soil moisture determinations by means of a neutron depth probe. In: *Recent Investigations in the Zone of Aeration*, (Eds. P Udluft, B Merkel & K-H Prüsl), Technical University of Munich, Munich, Germany 1, 271–280.

Vaz, C M P, Hopmans, J W, Macedo, A, Bassoi, L H & Wildenschild, D (2002) Soil water retention measurements using a combined tensiometer–coiled time domain reflectometry probe. *Soil Science Society of America Journal* 66, 1752–1759.

Vereecken, H, Binley, A, Cassiani, G, Revil, A & Titov, K (Eds.) (2006) *Applied Hydrogeophysics*. Springer, Netherlands, 383 pp.

Villegas, A N & Morris, R A (1990) Zero flux plane recession under monocropped and intercropped cowpea and sorghum. *Agronomy Journal* 82, 845–851.

Visconti, F, de Paz, J M & Rubio, J L (2010) An empirical equation to calculate soil solution electrical conductivity at 25°C from major ion concentrations. *European Journal of Soil Science* 61, 980–993.

Wagner, G H (1962) Use of porous ceramic cups to sample soil water within the profile. *Soil Science* 94, 379–386.

Wait, J R (1962) A note on the electromagnetic response of a stratified earth. *Geophysics* 27, 382–385.

Waldron, L J & Manbeian, T (1970) Soil moisture characteristics by osmosis with polyethylene glycol: A simple system with osmotic pressure data and some results. *Soil Science* 110, 401–404.

Wang, Q, Oschner, T E & Horton, R (2002a) Mathematical analysis of heat pulse signals for soil water flux determination. *Water Resources Research* 38, WR1089.

Wang, Q, Oschner, T E & Horton, R (2002b) Correction to 'Mathematical analysis of heat pulse signals for soil water flux determination' Quanjiu Wang, Tyson E. Oschner, and Robert Horton. *Water Resources Research* 38, WR0176.

Wang, P, Song, X, Han, D, Zhang, Y & Zhang, B (2012) Determination of evaporation, transpiration and deep percolation of summer corn and winter wheat after irrigation. *Agricultural Water Management* 105, 32–37.

Warrick, A W (Ed.) (2002) *Soil Physics Companion*. CRC Press, Boca Raton, FL, 400 pp.

Warrick, A W (2003) *Soil Water Dynamics*. Oxford University Press, New York, 416 pp.

Warrick, A W, Wierenga, P J, Young, M H & Musil, S A (1998) Diurnal fluctuations of tensiometric readings due to surface temperature changes. *Water Resources Research* 34, 2863–2869.

Watson, K K (1966) An instantaneous profile method for determining the hydraulic conductivity of unsaturated porous materials. *Water Resources Research* 2, 709–715.

Watson, K K, Reginato, R J & Jackson, R D (1975) Soil water hysteresis in a field soil. *Soil Science Society of America Proceedings* 39, 242–246.

Waxman, M & Smits, L (1968) Electrical conductivities in oil-bearing shaly sands. *Society of Petroleum Engineering Journal* 8, 107–122.

Webster, R (1966) The measurement of soil water tension in the field. *New Phytologist* 65, 249–258.

Webster, R & Oliver, M A (2007) *Geostatistics for Environmental Scientists*, 2nd edn. John Wiley & Sons Ltd, Chichester, 330 pp.

Weihermüller, L, Siemens, J, Deurer, M, Knoblauch, S, Rupp, H, Göttlein, A & Pütz, T (2007) *In situ* water extraction: A review. *Journal of Environmental Quality* 36, 1735–1748.

Wellings, S R (1984a) Recharge of the Upper Chalk aquifer at a site in Hampshire, England: 1. Water balance and unsaturated flow. *Journal of Hydrology* 69, 259–273.

Wellings, S R (1984b) Recharge of the Upper Chalk aquifer at a site in Hampshire, England: 2. Solute movement. *Journal of Hydrology* 69, 275–285.

Wellings, S R & Bell, J P (1980) Movement of water and nitrate in the unsaturated zone of Upper Chalk near Winchester, Hants, England. *Journal of Hydrology* 48, 119–136.

Wellings, S R & Cooper, J D (1983) The variability of recharge of the English Chalk aquifer. *Agricultural Water Management* 6, 243–253.

Wellings, S R, Bell, J P & Raynor, R J (1985) The use of gypsum resistance blocks for measuring soil water potential in the field. *Institute of Hydrology Report* 92, 32 pp.

Wendt, C W, Wilke, O C & New, L L (1978) Use of methanol–water solutions for freeze protection of tensiometers. *Agronomy Journal* 70, 890–891.

Whalley, W R (1993) Considerations on the use of time domain reflectometry (TDR) for measuring soil water content. *Journal of Soil Science* 44, 1–9.

Whalley, W R, Dean, T J & Izzard, P (1992) Evaluation of the capacitance technique as a method of dynamically measuring soil water content. *Journal of Agricultural Engineering Research* 52, 147–155.

Whalley, W R, Leeds-Harrison, P B, Joy, P & Hoefsloot, P (1994) Time domain reflectometry combined in an integrated soil water monitoring system. *Journal of Agricultural Engineering Research* 59, 141–144.

Whalley, W R, Watts, C W, Hilhorst, M A, Bird, N R A, Balendonck, J & Longstaff, D J (2001) The design of porous material sensors to measure the matric potential of water in soil. *European Journal of Soil Science* 52, 511–519.

Whalley, W R, Clark, L J, Take, W A, Bird, N R A, Leech, P K, Cope, R E & Watts, C W (2007) A porous-matrix sensor to measure the matric potential of soil water in the field. *European Journal of Soil Science* 58, 18–25.

Whalley, W R, Lock, G, Jenkins, M, Peloe, T, Burek, K, Balendonck, J, Take, W A, Tuzel, H & Tuzel, Y (2009) Measurement of low matric potentials with porous matrix sensors and water filled tensiometers. *Soil Science Society of America Journal* 73, 1796–1803.

Whisler, F D, Klute, A & Peters, D B (1968) Soil water diffusivity from horizontal infiltration. *Soil Science Society of America Proceedings* 32, 6–11.

White, I & Sully, M J (1987) Macroscopic and microscopic capillary length and time scales from field infiltration. *Water Resources Research* 23, 1514–1522.

White, I, Knight, J H, Zegelin, S & Topp, G C (1994) Comments on 'Considerations on the use of time domain reflectometry (TDR) for measuring soil water content'. *European Journal of Soil Science* 45, 503–508.

Wierenga, P J, Hills, R G & Hudson, D B (1991) The Las Cruces Trench site: Characterization, experimental results, and one-dimensional flow predictions. *Water Resources Research* 27, 2695–2705.

Wiessler, F (1996) Membrane contactors: An introduction to the technology. *Ultrapure Water*, May/June 1996, 27–31.

Wiessler, F & Sodaro, R (1996) Degasification of water using novel membrane technology. *Ultrapure Water*, September 1996, 53–56.

Wind, G P (1968) Capillary conductivity data estimated by a simple method. In: *Water in the Unsaturated Zone*, Vol. 1 (Eds. P E Rijtema & H Wassink), IASH Publication 82, International Association for Scientific Hydrology-UNESCO, Gentbrugge, Belgium, 181–191.

Winfield, K A & Nimmo, J R (2002) Water retention and storage – controlled liquid volume. In: *Methods of Soil Analysis: Part 4. Physical Methods* (Eds. J H Dane & G C Topp), Soil Science Society of America, Madison WI, 698–703.

Wooding, R A (1968) Steady infiltration from a shallow circular pond. *Water Resources Research* 4, 1259–1273.

Yang, C Y, Sakai, M & Jones, S B (2013) Inverse method for simultaneous determination of soil water flux density and thermal properties with a penta-needle heat pulse probe. *Water Resources Research* 49, 5851–5864. doi: 10.1002/wrcr.20459.

Yanuka, M, Topp, G C, Zegelin, S & Zebchuk, W D (1988) Muliple reflection and attenuation of TDR pulses: Theoretical considerations for applications to soil and water. *Water Resources Research* 24, 939–944.

Youngs, E G (1968) An estimation of sorptivity for infiltration studies from moisture moment considerations. *Soil Science* 106, 157–163.

Youngs, E G (1983) Soil physical theory and heterogeneity. *Agricultural Water Management* 6, 145–159.

Youngs, E G (1987) Estimating hydraulic conductivity values from ring infiltrometer measurements. *Journal of Soil Science* 38, 623–632.

Youngs, E G (1991) Hydraulic conductivity of saturated soils. In: *Soil Analysis: Physical Methods* (Eds. K A Smith & C E Mullins), Marcel Dekker, New York, 161–207.

Youngs, E G (2001) Hydraulic conductivity of saturated soils. In: *Soil and Environmental Analysis: Physical Methods* (Eds. K A Smith & C E Mullins), Marcel Dekker, New York, 141–181.

Zhang, Z F, Groenvelt, P H & Parkin, G (1998) The well shape-factor for the measurement of soil hydraulic properties using the Guelph Permeameter. *Soil & Tillage Research* 49, 219–221.

Zhu, Y, Fox, R H & Toth, J D (2002) Leachate collection efficiency of zero-tension pan and passive capillary fiber wick lysimeters. *Soil Science Society of America Journal* 66, 37–43.

Ziegler, A D, Giambelluca, T W, Nullet, M A, Sutherland, R A, Tantasarin, C, Vogler, J B & Negishi, J N (2009) Throughfall in an evergreen-dominated forest stand in northern Thailand: Comparison of mobile and stationary methods. *Agricultural & Forest Meteorology* 149, 373–384.

Zreda, M, Desilets, D, Ferré, T P A & Scott, R L (2008) Measuring soil moisture content non-invasively at intermediate spatial scale using cosmic-ray neutrons. *Geophysical Research Letters* 35, L21402.

Zreda, M, Shuttleworth, W J, Zeng, X, Zweck, C, Desilets, D, Franz, T E & Rosolem, R (2012) COSMOS: The COsmic-ray Soil Moisture Observing System. *Hydrology & Earth System Sciences* 16, 4079–4099.

Zur, B (1966) Osmotic control of the matric soil-water potential: I. Soil-water system. *Soil Science* 102, 394–398.

Index

Soil Water Measurement: A Practical Handbook, First Edition. J. David Cooper.

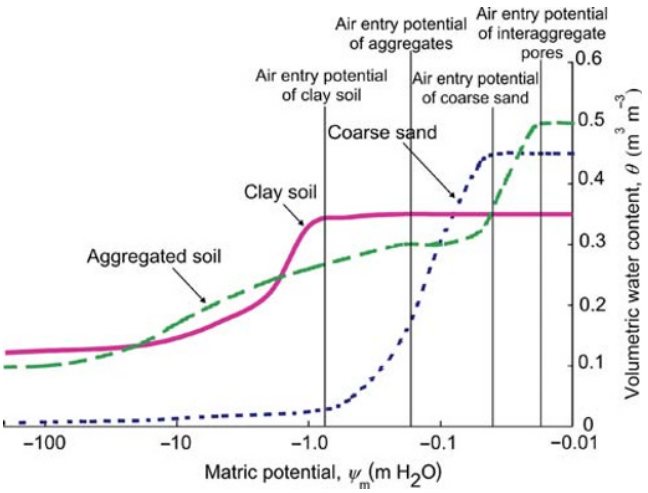

Fig. 2.2 Soil water characteristic curves for three different soils.

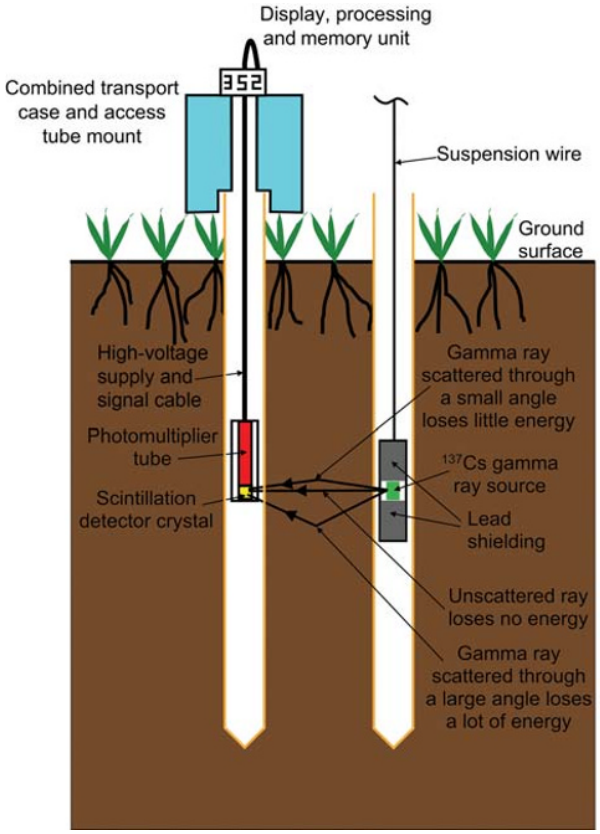

Fig. 6.5 Schematic of a gamma ray transmission gauge.

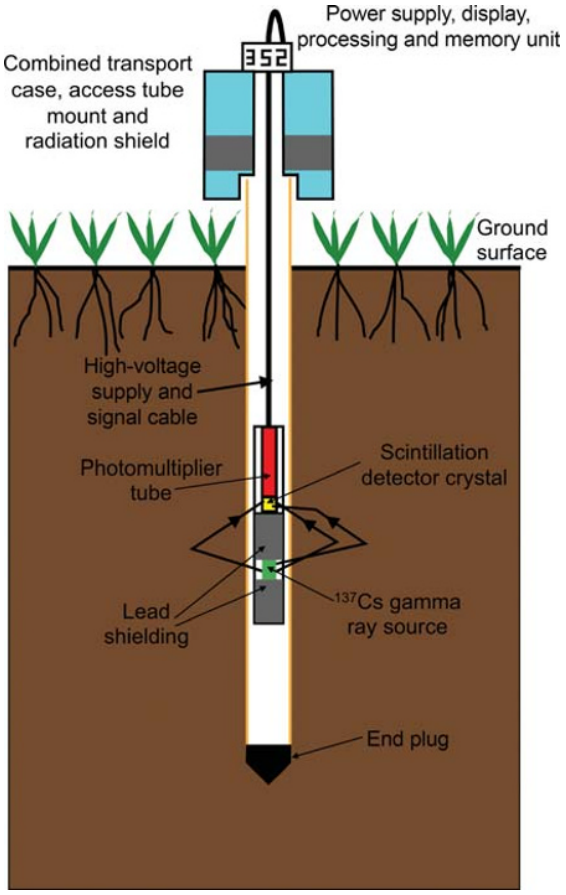

Fig. 6.7 Schematic diagram of a gamma ray backscatter gauge.

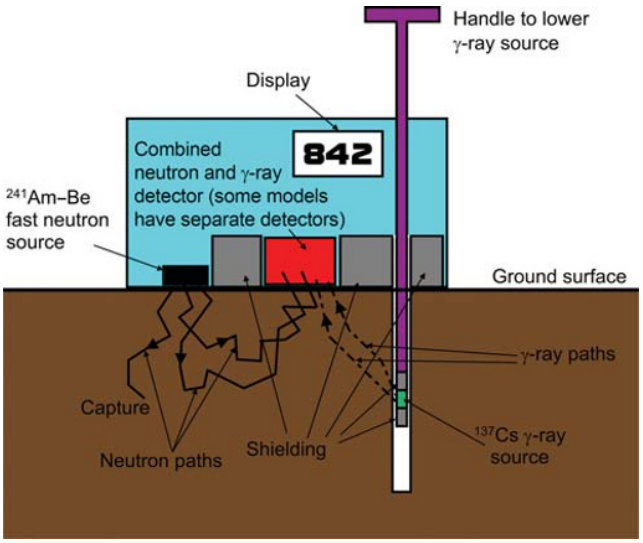

Fig. 7.3 Combined neutron water content and gamma density probe for surface measurement.

Soil Water Measurement: A Practical Handbook, First Edition. J. David Cooper.

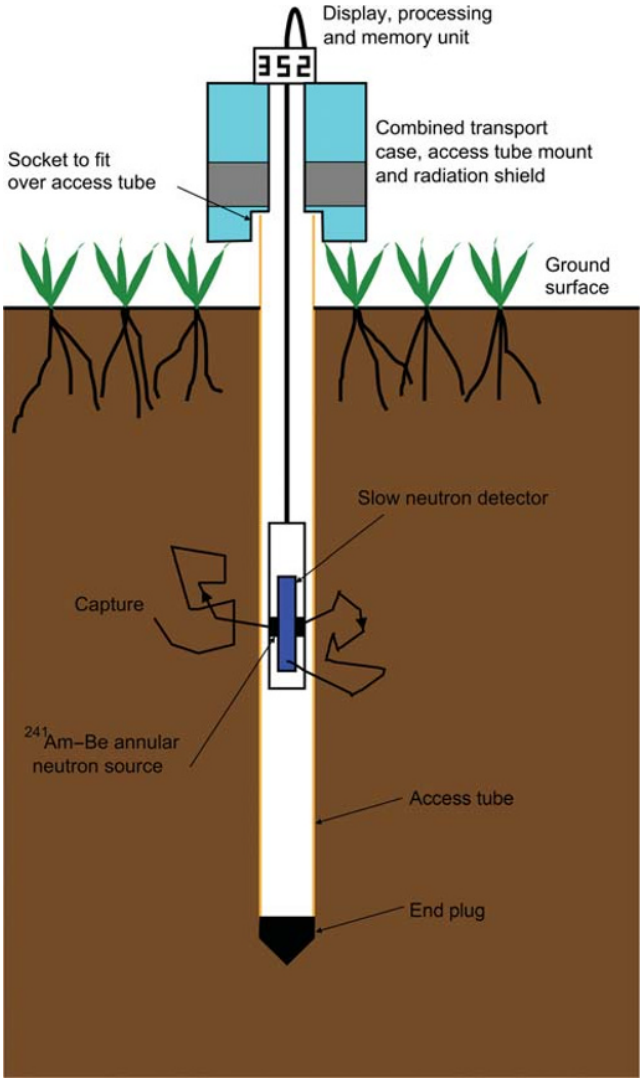

Fig. 7.4 Schematic diagram of depth neutron probe. Hypothetical paths for a neutron which returns to the detector and one captured in the soil are shown.

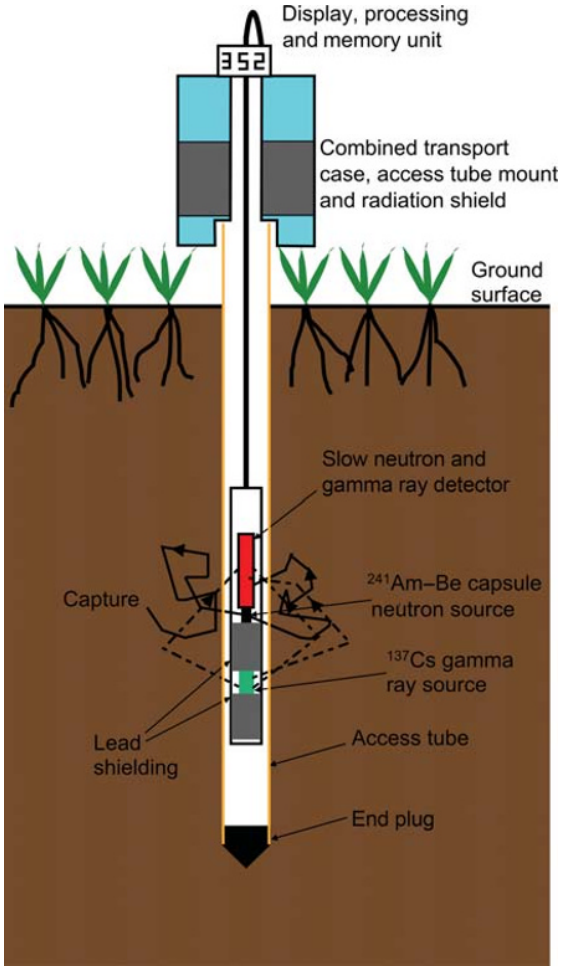

Fig. 7.7 Combined neutron and gamma density backscatter probe.

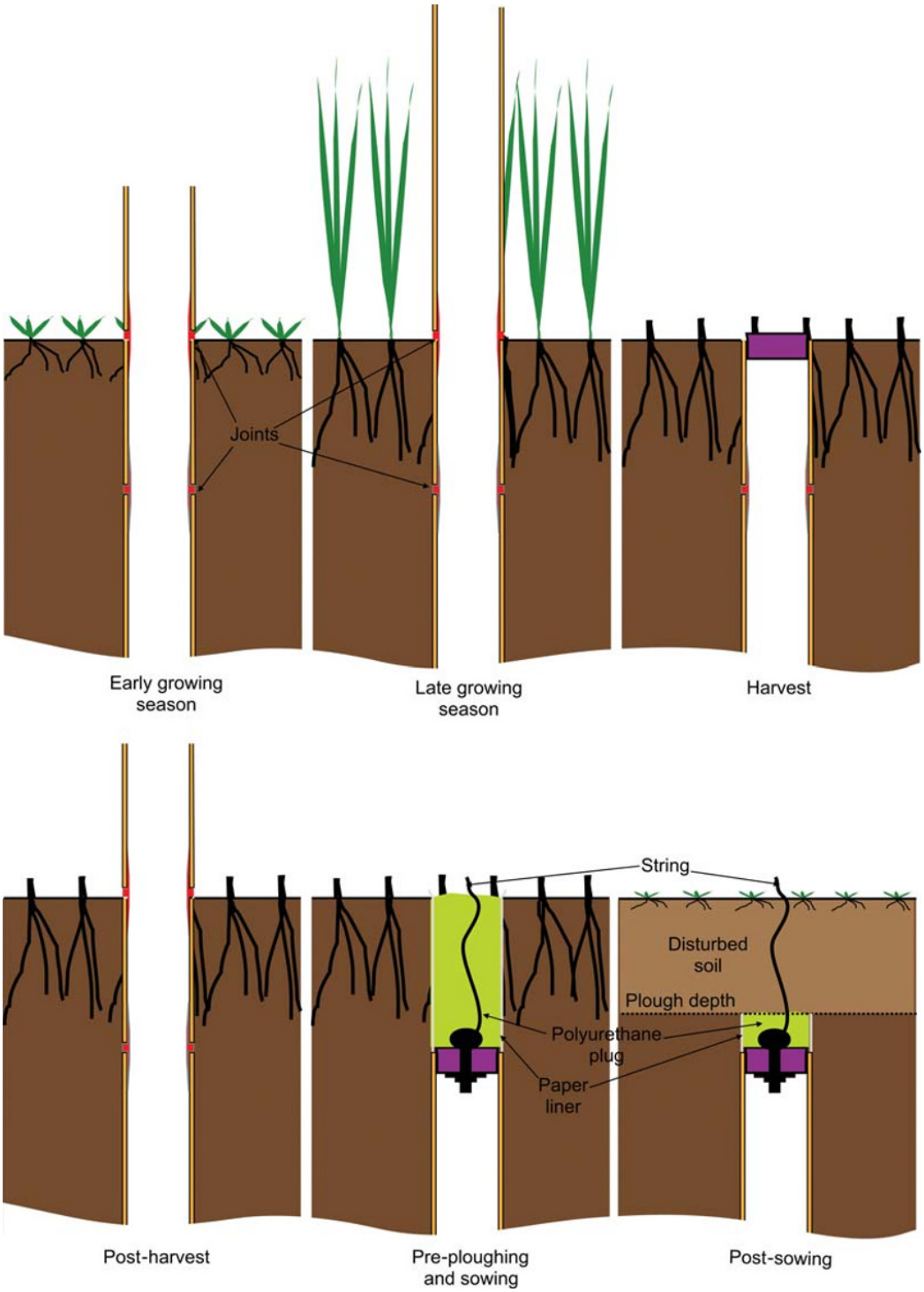

Fig. 7.17 Access tube arrangement to accommodate farming operations.

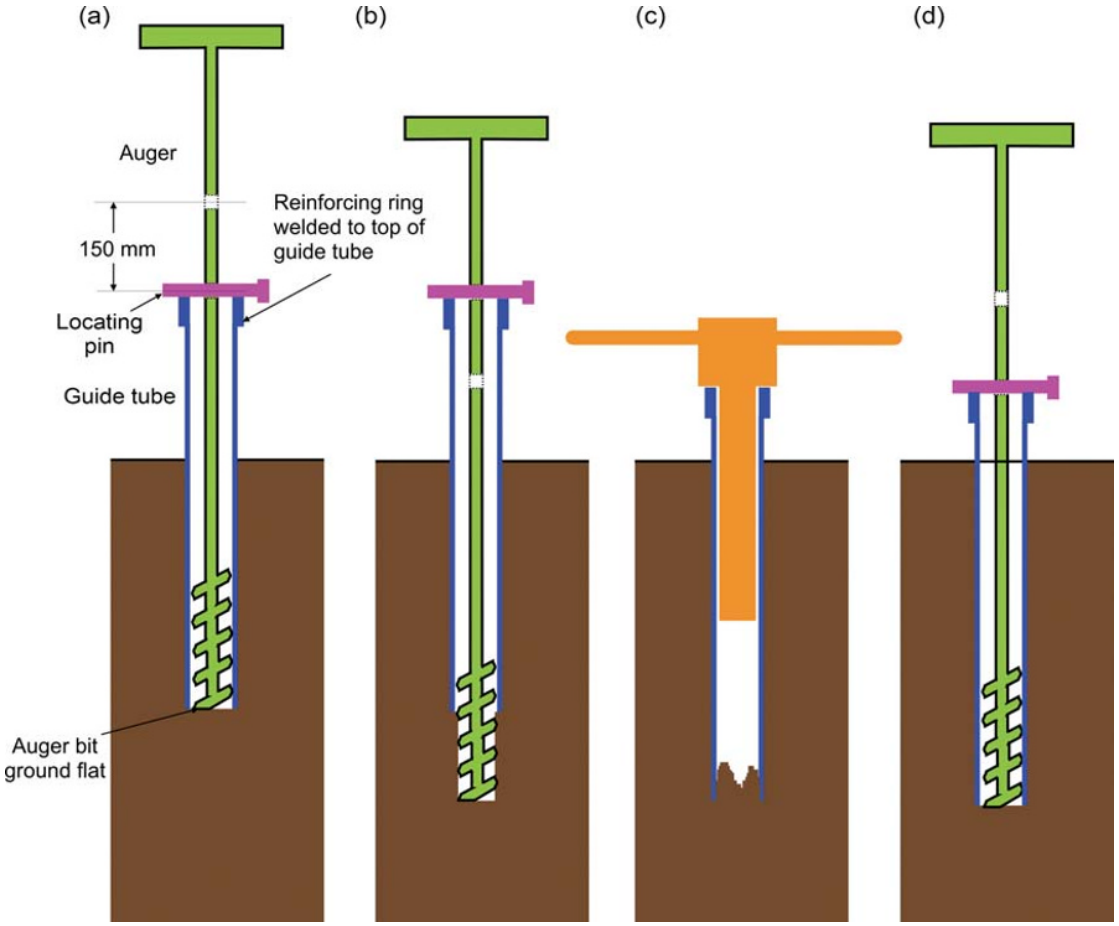

Fig. 7.23 Calibration by removing constant volume samples during access tube installation. (a) The hole is cleared to the bottom of the guide tube using an auger ground to have a flat bottom surface. A pin through a hole in the auger stem locates the bottom of the auger with the bottom of the guide tube. (b) The hole is deepened by 150 mm, using the pin in a second hole in the auger stem to define it. The soil removed is collected. (c) The guide tube is knocked to the bottom of the pre-drilled hole, collecting the soil shaved from the sides inside it. Marks on the guide tube indicate the correct depth. (d) The auger again clears the hole to the bottom of the guide tube and the soil from the bottom is collected.

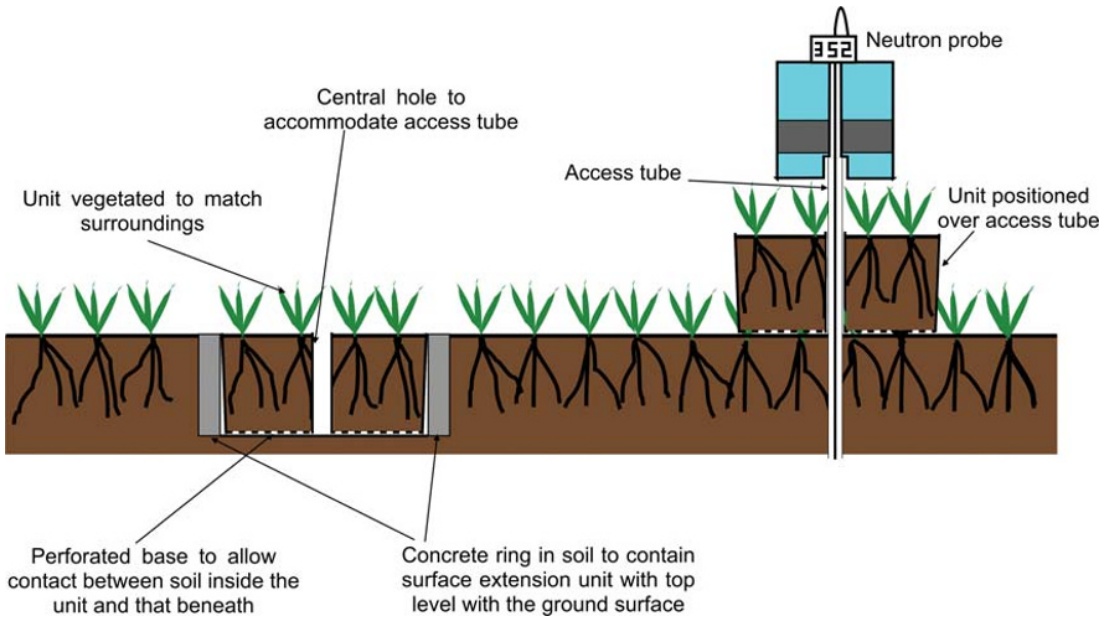

Fig. 7.26 Surface extension unit. Left – in the ground between reading occasions. Right – in use over an access tube.

Fig. 7.30 COSMOS probe in centre foreground at Tonzi Ranch, California (USA). AmeriFlux eddy covariance tower is seen in background at left and NASA AirMOSS soil profile monitoring station is shown in background at right. Photograph by Richard Cuenca.

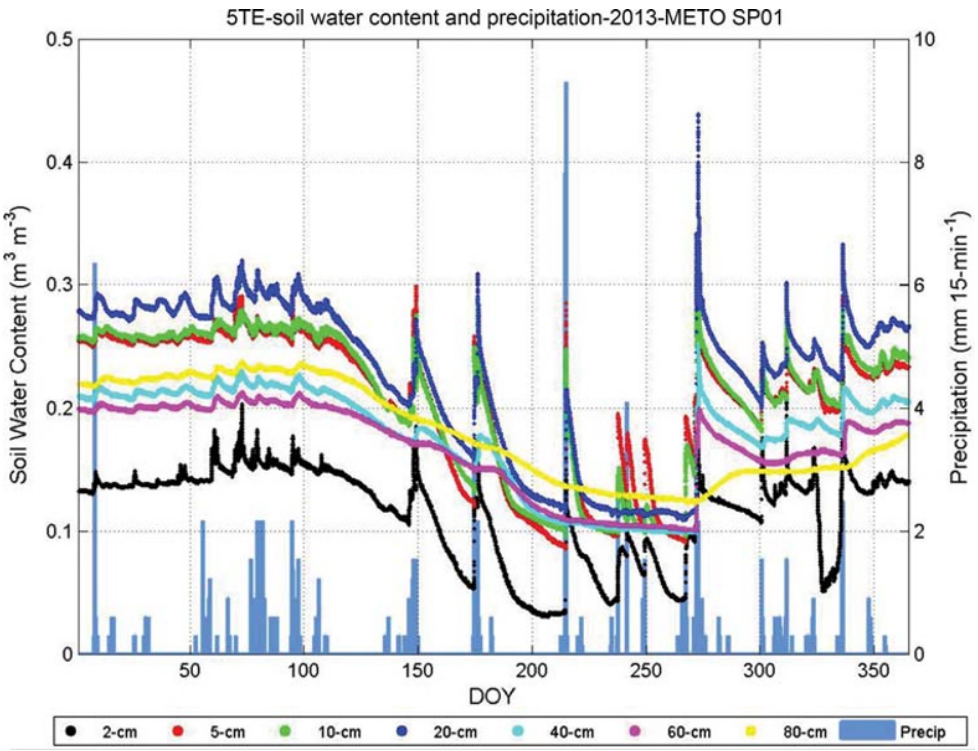

Fig. 7.33 Volumetric soil water content for seven depth layers from NASA AirMOSS soil profile monitoring station (using Decagon 5-TE dielectric probe) at AmeriFlux Metolius site, Oregon (USA) for 2013. Precipitation captured in 15-min intervals on right-hand side *y*-axis.

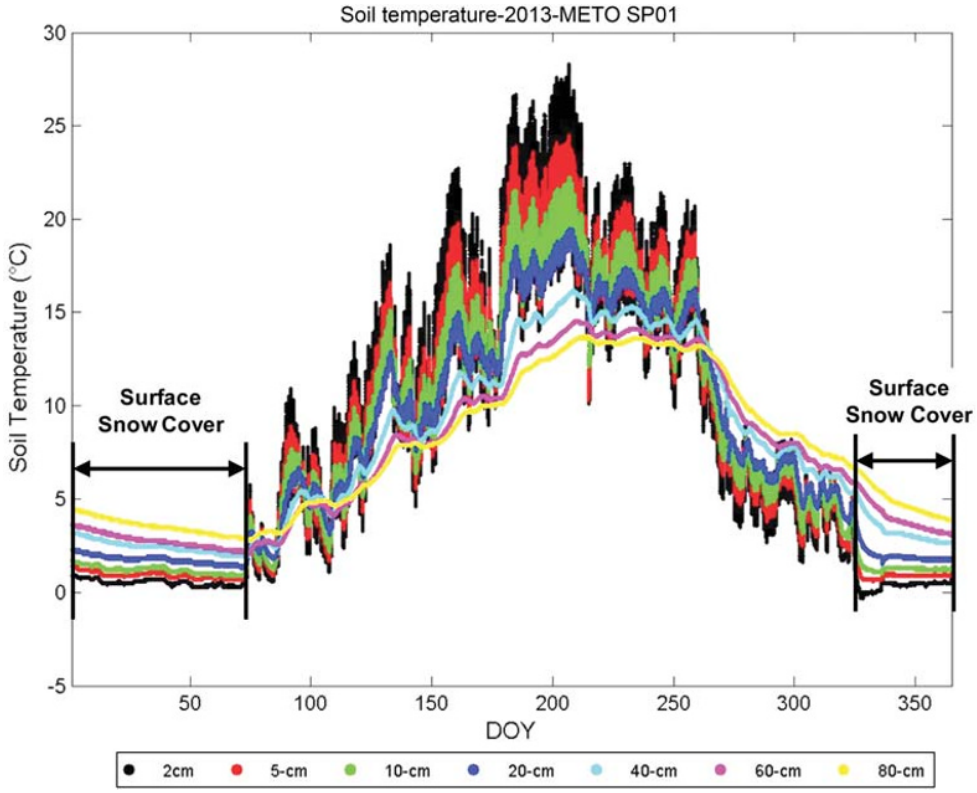

Fig. 7.34 Soil temperature for seven depth layers from NASA AirMOSS soil profile monitoring station (using Decagon 5-TE dielectric probe) at AmeriFlux Metolius site, Oregon (USA) for 2013. Periods of dampened diurnal fluctuation are evidence of snow cover over the soil profile.

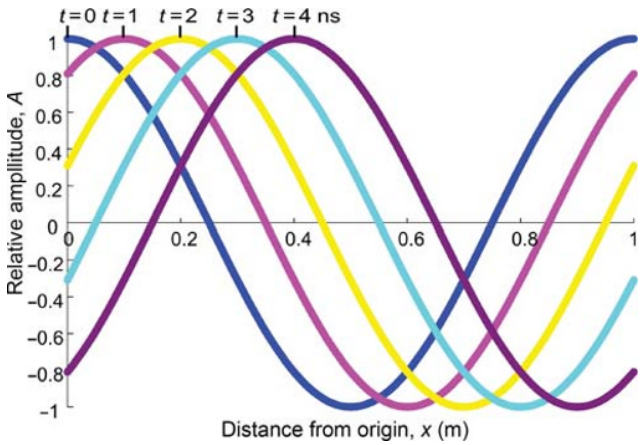

Fig. 8.15 Wave propagation along a 1 m length of transmission line. The wave has a frequency of 100 MHz and a speed, v, of 10^8 m s^{-1}, so that it travels 0.1 m in 1 ns. The curves have the equation $A = \cos\omega(t - {}^{x}/_{v})$, where $\omega = 2\pi \times 10^8$ s^{-1}.

Fig. 8.39 Sentek *EnviroScan* capacitance probe system showing the two cylindrical electrodes of each sensor unit. The printed circuit board of each unit is located inside the rings, with the main control board at the top. The ribbon cable connecting each sensor's printed circuit board to the main control board runs behind the plastic partition between the sensors. In operation, the complete assembly is placed inside the plastic access tube, the top of which can be seen protruding above the ground surface. Photograph reproduced with permission of Sentek Pty, Australia.

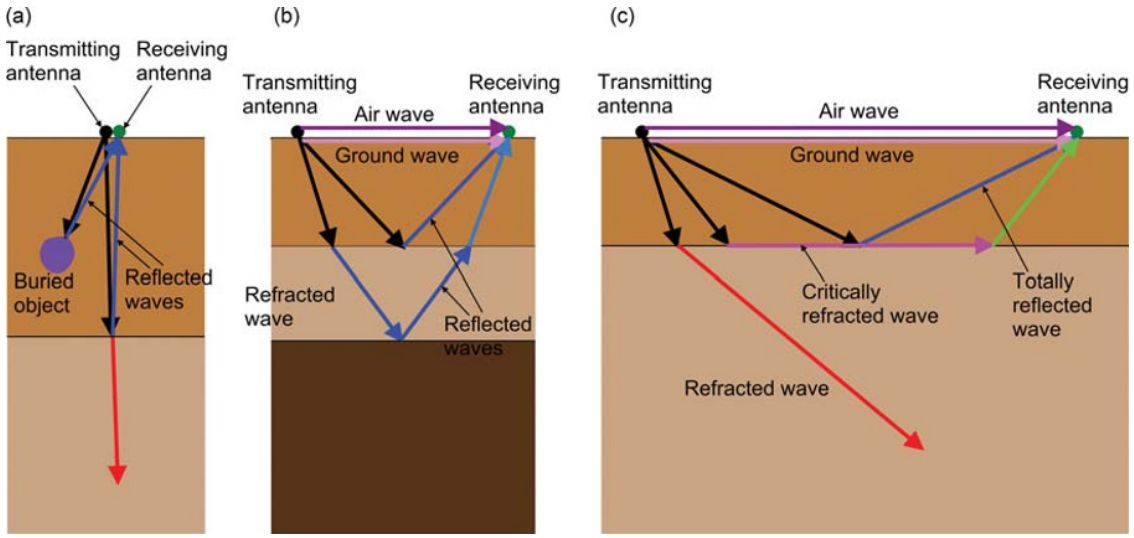

Fig. 8.57 Ray paths for GPR-generated waves in a layered medium. (a) Reflection from an interface and a buried object with no separation between antennae. (b) Reflections and refractions at interfaces with separated antennae The permittivity of the lighter-coloured layer is lower than that of the darker one, and so the speed of the wave is greater and it is refracted towards the interface in the lighter-coloured material. (c) At greater antenna separation, a critically refracted wave can travel through the faster medium and may reach the receiving antenna before the ground wave.

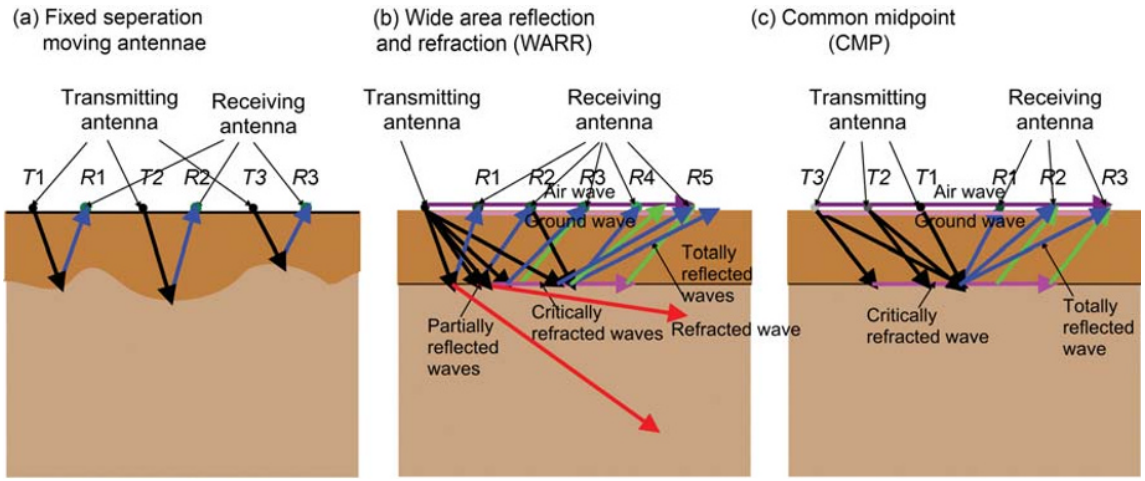

Fig. 8.58 Common configurations for separated antenna measurements using GPR at the ground surface.

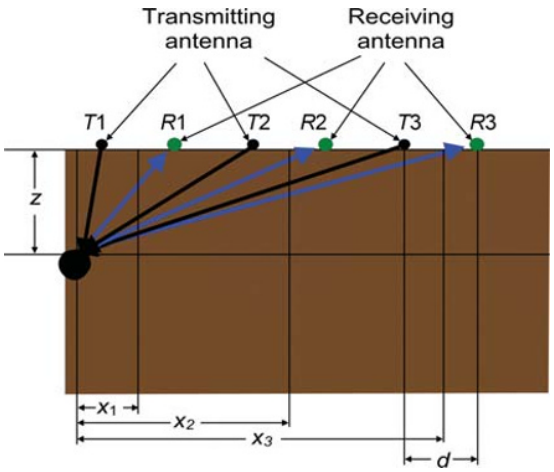

Fig. 8.59 Estimating depth of a buried object and permittivity using moving antennae.

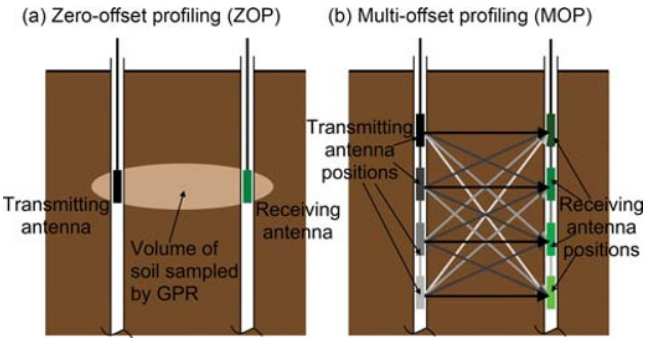

Fig. 8.60 Borehole GPR configurations.

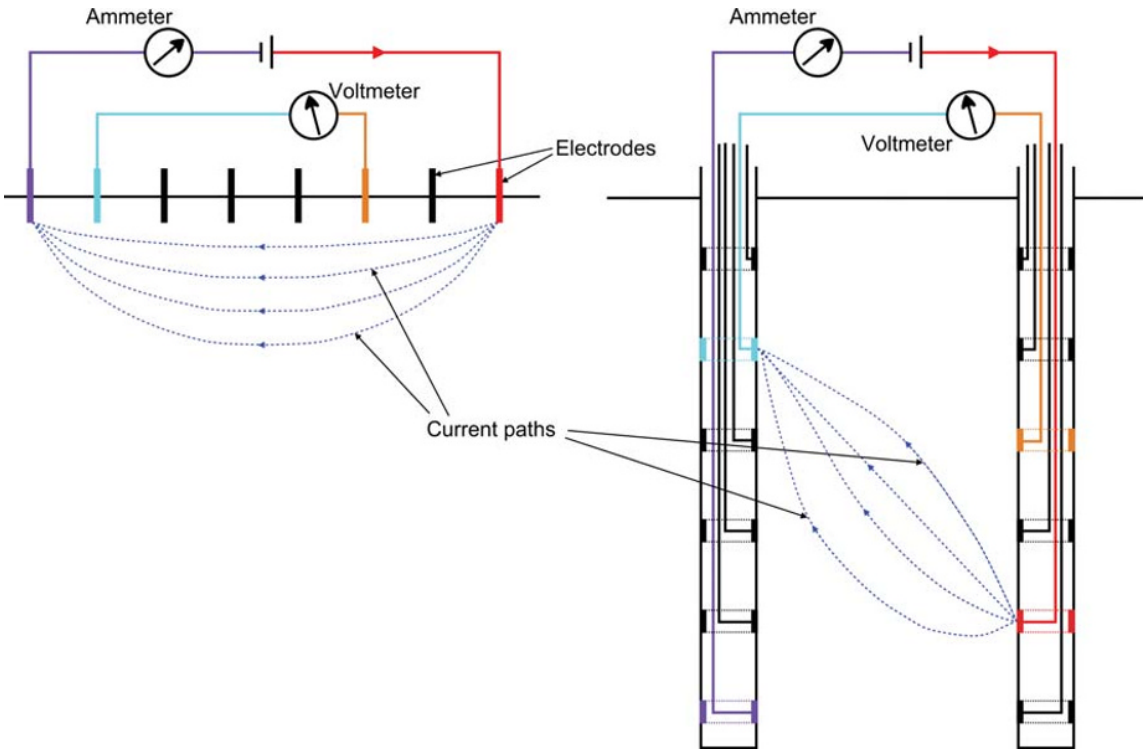

Fig. 10.3 Two possible arrays of electrodes for performing ERI measurements, one set measuring from the surface, whereas the other between two boreholes. The four-electrode array with separate current and voltage electrodes minimises errors resulting from poor contact between the electrodes and the ground.

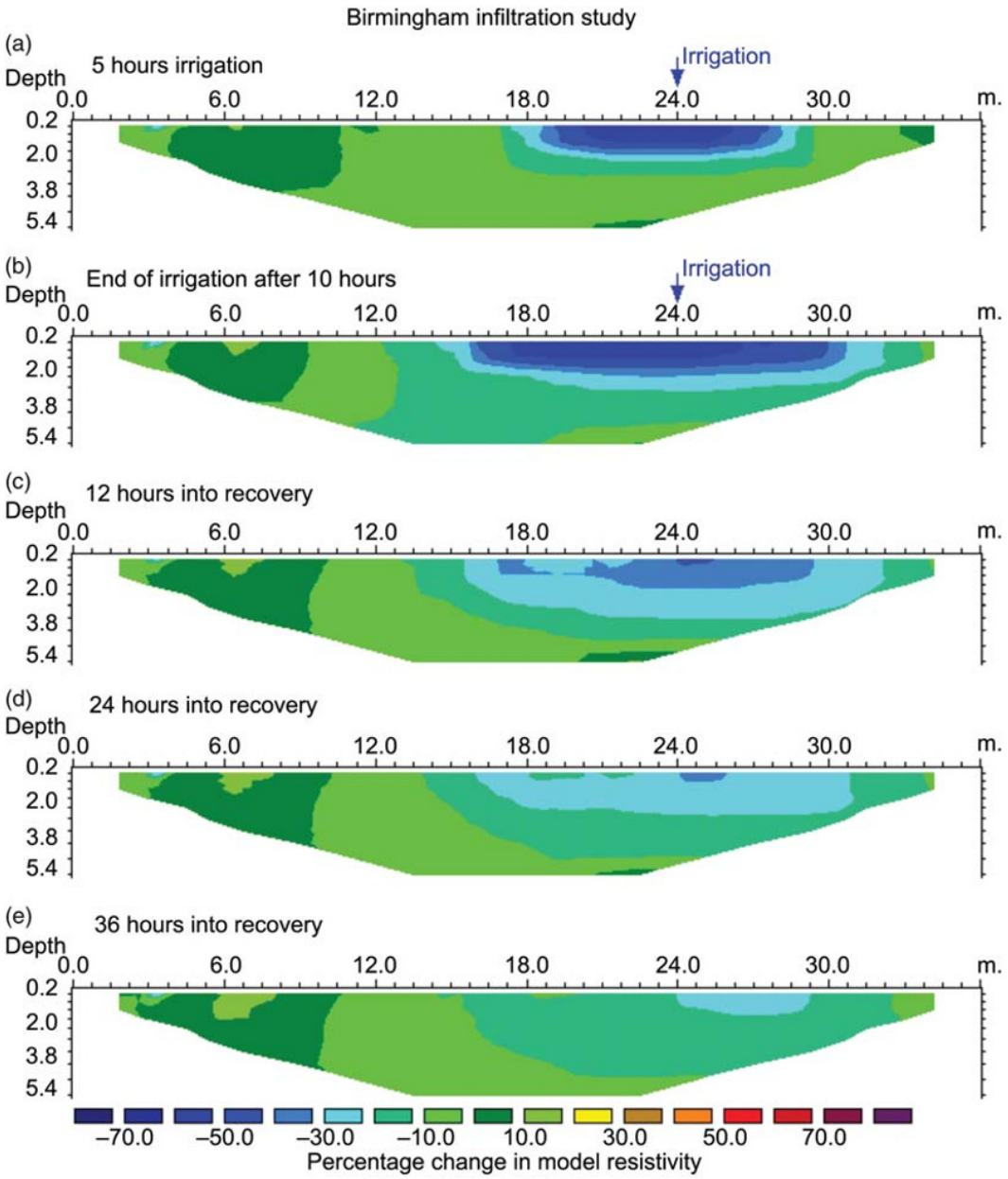

Fig. 10.6 Example of a two-dimensional resistivity survey tracking irrigation from a hosepipe in one section of the area and the subsequent redistribution (Loke, 2012 from data of Barker and Moore, 1998). Reproduced with permission of Dr. M H Loke.

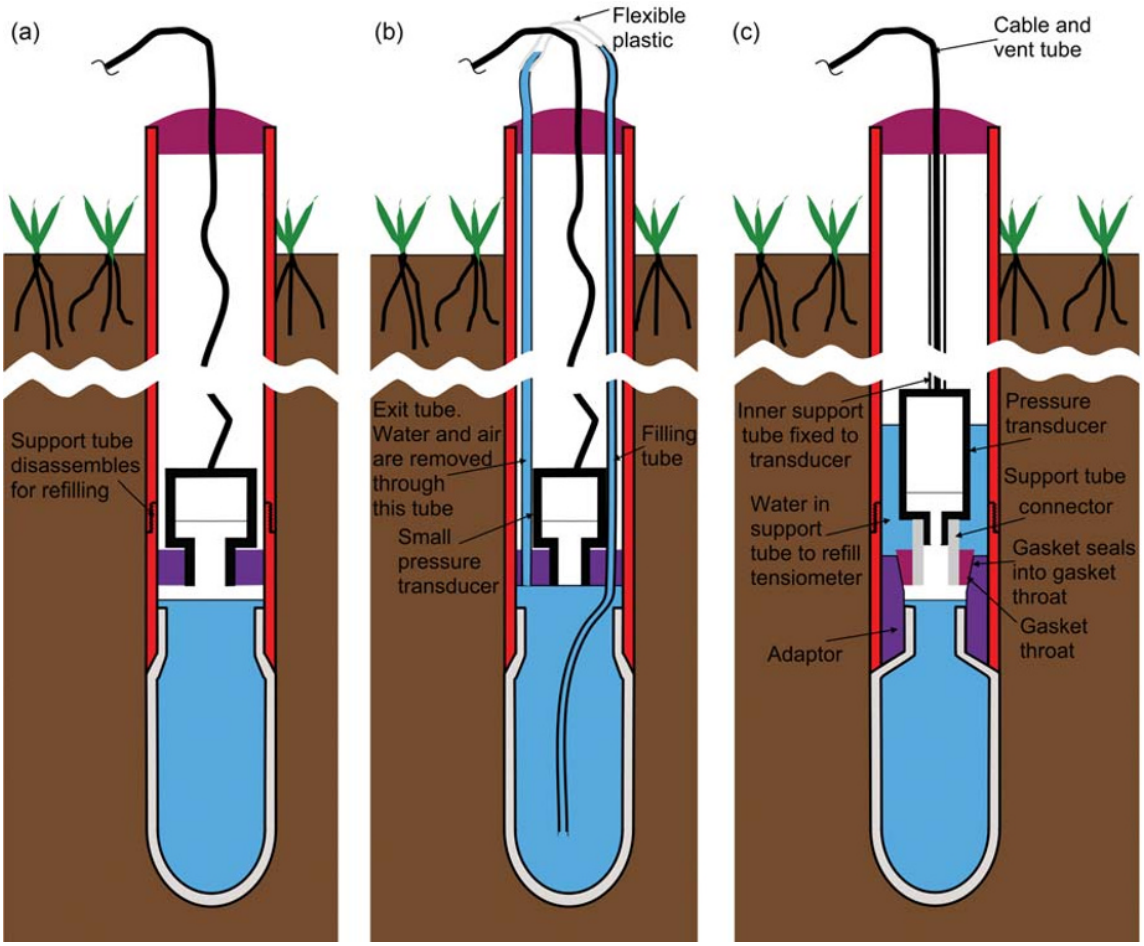

Fig. 12.9 Three designs of tensiometer with the pressure transducer mounted close to the porous cup below ground level. (a) A simple design that must be removed and disassembled to refill. (b) A design devised by UMS GmbH, which can be purged and refilled *in situ* using two hypodermic tubes. (c) A design incorporating the principles of the 'advanced tensiometer' (Hubbell & Sisson, 1998). The transducer and gasket can be lifted out of the gasket throat by the inner support tube, allowing water in the outer support tube to refill the tensiometer.

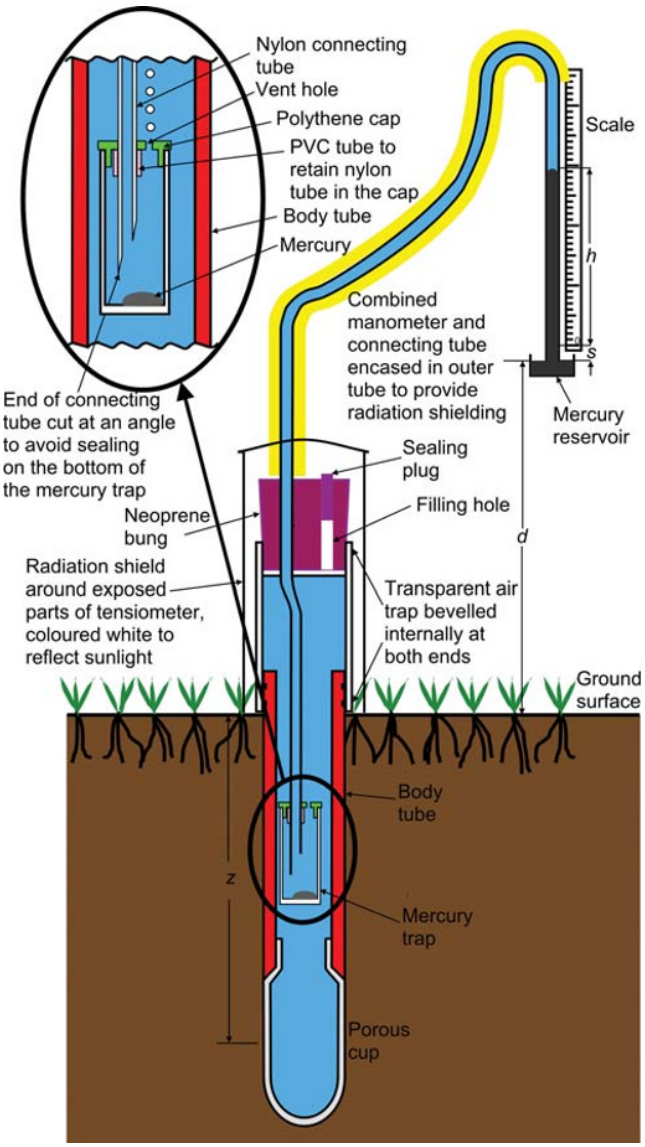

Fig. 12.13 A mercury manometer tensiometer.

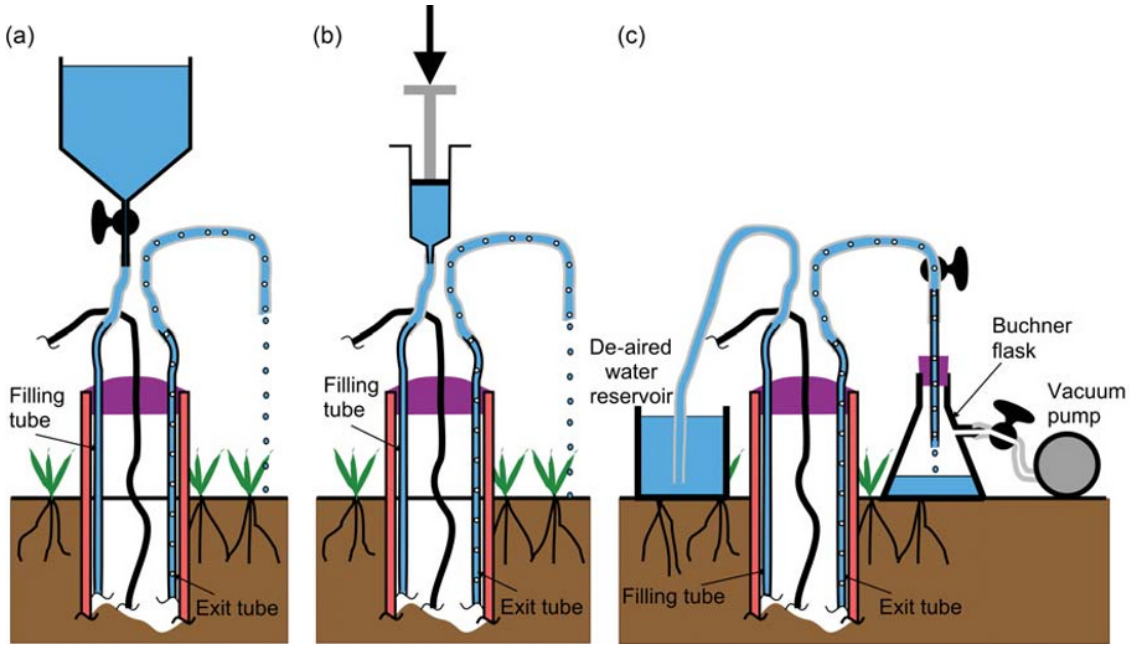

Fig. 12.21 Three ways to fill a purgeable pressure transducer tensiometer. (a) Gravity filling from a water reservoir. (b) Injection of water from a syringe. (c) The preferred method – filling by application of a suction.

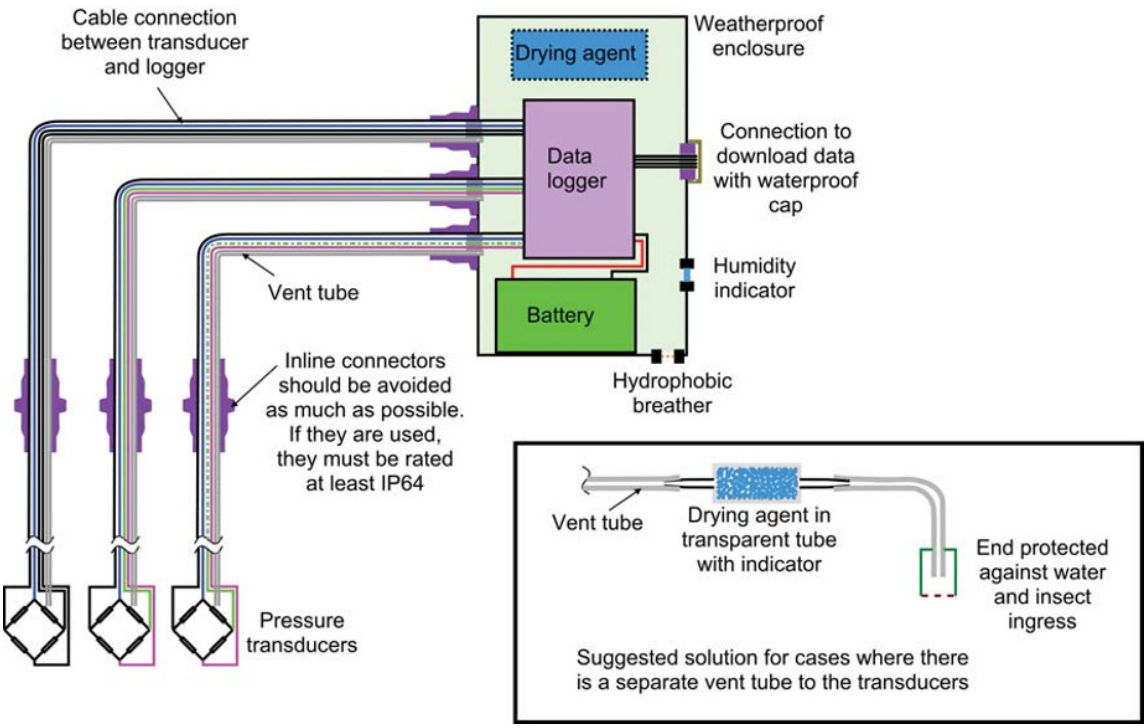

Fig. 12.23 A data logger setup for recording readings of pressure transducer tensiometers. Three transducers are shown, but usually there will be more, together with other instruments (e.g. raingauge, dielectric soil water sensors), a solar panel, etc. All should be connected using waterproof connectors rated to at least IP64. An unobstructed atmospheric pressure reference to the transducers is important while maintaining dry conditions to avoid spurious data and electronics malfunctions. An alternative arrangement for transducers with a separate vent tube is also shown.

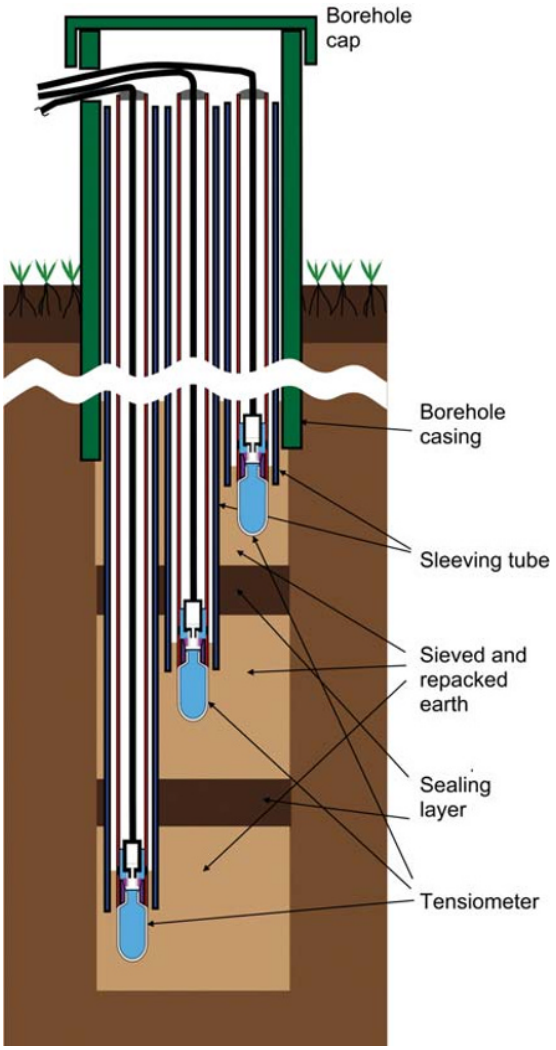

Fig. 12.32 Arrangement for installation of several embedded tensiometers in one borehole.

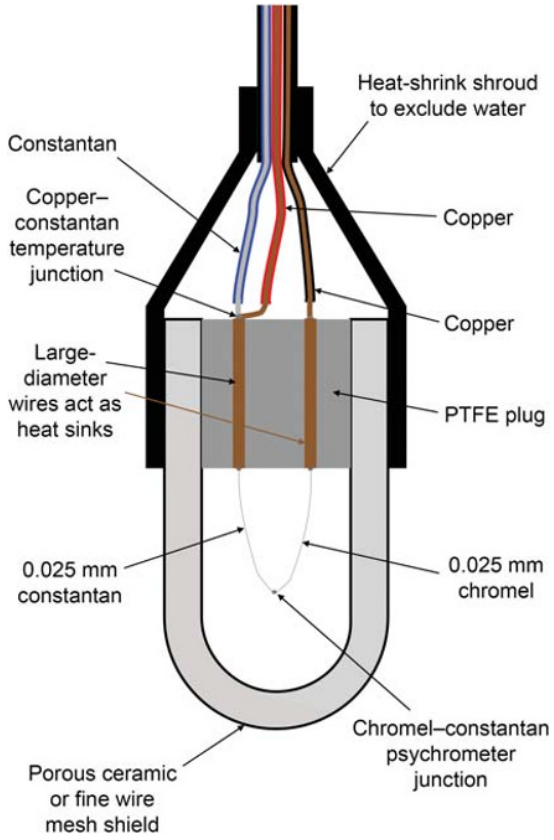

Fig. 14.1 Components of a soil psychrometer.

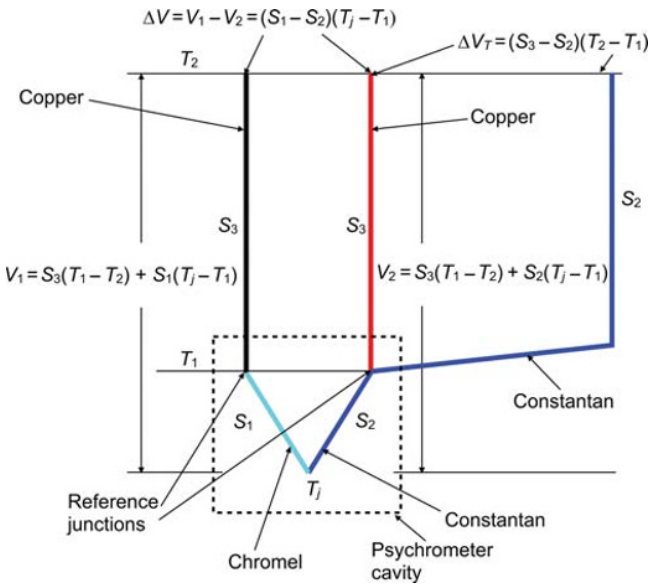

Fig. 14.6 Arrangement of thermocouples in a soil psychrometer. Copper leads from the primary thermocouple to the measuring instrument eliminate voltage differences caused by the leads. The measured voltage is proportional to the difference in temperature between the primary thermocouple junction and the reference junctions with the copper leads. The auxiliary copper–constantan thermocouple measures the difference in temperature between the measuring instrument and the thermocouple cavity.

Fig. 18.3 Guelph Permeameter. Photograph reproduced with permission from Soilmoisture Equipment Corporation.

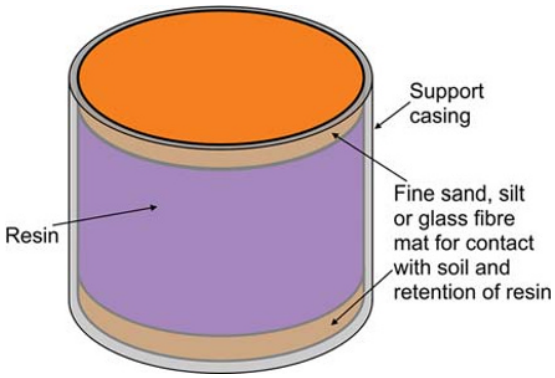

Fig. 20.6 Schematic of a resin box sampler. The resin may be of a single type, mixed anionic and cationic or in layers of different kinds.

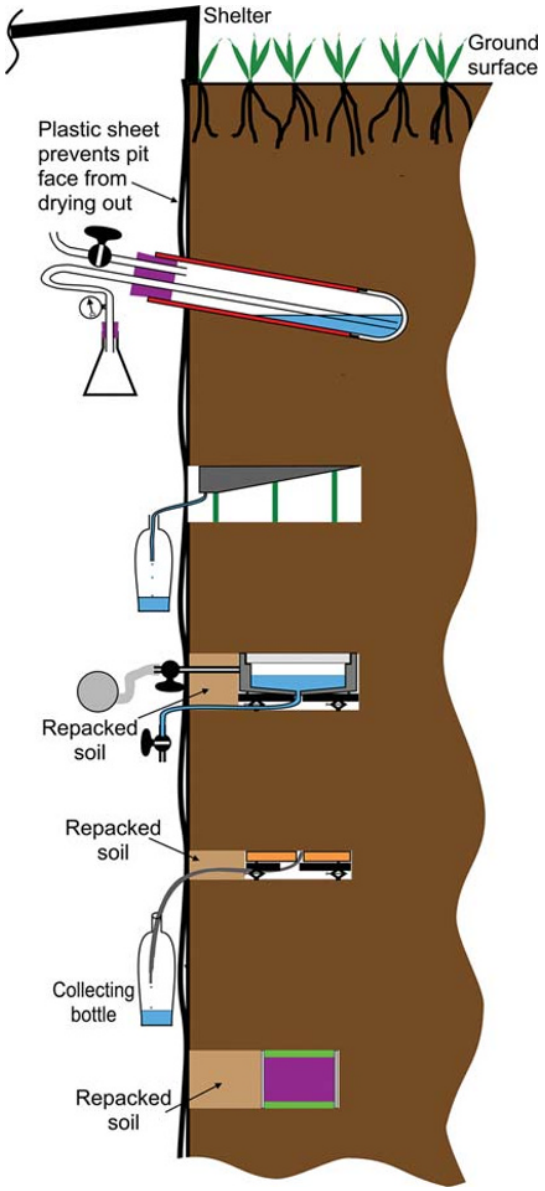

Fig. 20.7 Installation arrangements for different solute samplers from an access pit. From top, suction sampler, pan sampler, porous plate, wick sampler and resin box.

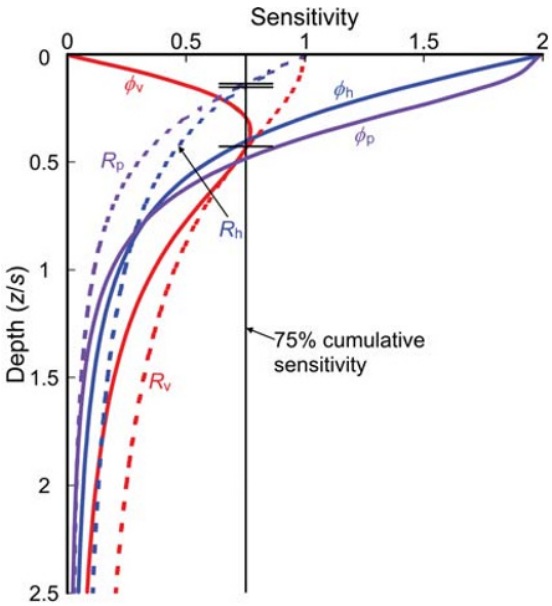

Fig. 21.5 Sensitivity of measurement with depth for EMI dipole orientations vertical (ϕ_v – horizontal coils), horizontal (ϕ_h – vertical coils) and perpendicular (ϕ_p – horizontal transmitter and vertical receiver coil), with cumulative upward values, R_v, R_h and R_p. Note that depth is expressed as the ratio of depth below the coil plane to the spacing between the coils.

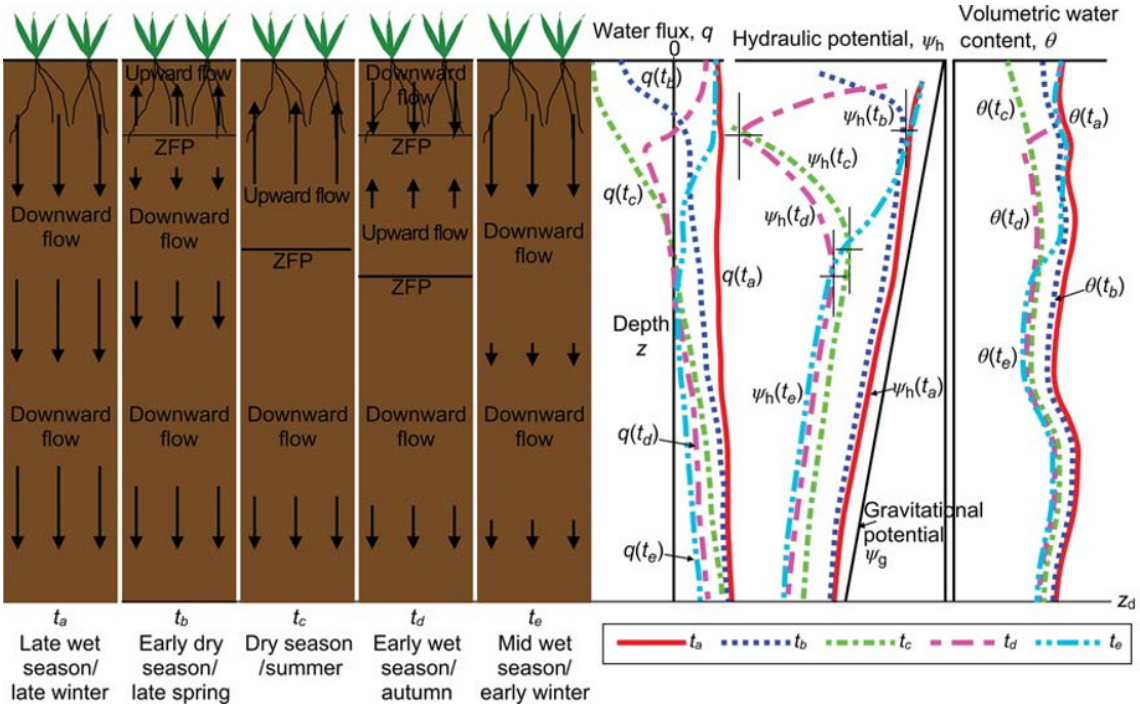

Fig. 24.7 Evolution of the water balance of a soil profile over the course of a year. ZFP positions, where the gradient with depth is zero, are indicated on the hydraulic potential graphs by horizontal lines.

WILEY END USER LICENSE AGREEMENT

Go to www.wiley.com/go/eula to access Wiley’s ebook EULA.